LEABHARLANN CHOLÁISTE NA TRÍONÓIDE, BAILE ÁTHA CLIATH | TRINITY COLLEGE LIBRARY DUBLIN
Ollscoil Átha Cliath | The University of Dublin

Terms and Conditions of Use of Digitised Theses from Trinity College Library Dublin

Copyright statement

All material supplied by Trinity College Library is protected by copyright (under the Copyright and Related Rights Act, 2000 as amended) and other relevant Intellectual Property Rights. By accessing and using a Digitised Thesis from Trinity College Library you acknowledge that all Intellectual Property Rights in any Works supplied are the sole and exclusive property of the copyright and/or other IPR holder. Specific copyright holders may not be explicitly identified. Use of materials from other sources within a thesis should not be construed as a claim over them.

A non-exclusive, non-transferable licence is hereby granted to those using or reproducing, in whole or in part, the material for valid purposes, providing the copyright owners are acknowledged using the normal conventions. Where specific permission to use material is required, this is identified and such permission must be sought from the copyright holder or agency cited.

Liability statement

By using a Digitised Thesis, I accept that Trinity College Dublin bears no legal responsibility for the accuracy, legality or comprehensiveness of materials contained within the thesis, and that Trinity College Dublin accepts no liability for indirect, consequential, or incidental, damages or losses arising from use of the thesis for whatever reason. Information located in a thesis may be subject to specific use constraints, details of which may not be explicitly described. It is the responsibility of potential and actual users to be aware of such constraints and to abide by them. By making use of material from a digitised thesis, you accept these copyright and disclaimer provisions. Where it is brought to the attention of Trinity College Library that there may be a breach of copyright or other restraint, it is the policy to withdraw or take down access to a thesis while the issue is being resolved.

Access Agreement

By using a Digitised Thesis from Trinity College Library you are bound by the following Terms & Conditions. Please read them carefully.

I have read and I understand the following statement: All material supplied via a Digitised Thesis from Trinity College Library is protected by copyright and other intellectual property rights, and duplication or sale of all or part of any of a thesis is not permitted, except that material may be duplicated by you for your research use or for educational purposes in electronic or print form providing the copyright owners are acknowledged using the normal conventions. You must obtain permission for any other use. Electronic or print copies may not be offered, whether for sale or otherwise to anyone. This copy has been supplied on the understanding that it is copyright material and that no quotation from the thesis may be published without proper acknowledgement.

Monitoring and Prediction of Traffic-Related Urban Air Pollution

Dawn-Marie Keating

Submitted in fulfilment of the requirements for the award of the degree of Doctor of Philosophy to the University of Dublin, Trinity College, 31st October 2000.

The work presented in this thesis was conducted at the Department of Civil, Structural and Environmental Engineering, University of Dublin, Trinity College, Ireland.

TRINITY COLLEGE
06 JUN 2001
LIBRARY DUBLIN
Thesis
6190

DECLARATION

I declare that the present work has not been submitted as an exercise for a degree at any other university. This thesis consists entirely of my own work except where references indicate otherwise.

I agree that the library of the University of Dublin, Trinity College, Dublin, may lend or copy this thesis upon request.

Dawn-Marie Keating

Dawn-Marie Keating

ACKNOWLEDGEMENTS

I would like to express sincere gratitude to Dr. Brian Broderick and Mr. Bruce Misstear, my supervisors, for their advice and guidance throughout the course of researching and writing this thesis.

I wish to thank Professor Simon Perry for making available the full facilities of the Department of Civil, Structural and Environmental Engineering.

I am grateful to all the technical staff, including Messrs. Chris O' Donovan, George Jones, Dave McAuley, and particularly Ms. Anne Desmond, for all their help and friendship over the years.

I also wish to acknowledge the contribution of data by Mr. Ciaran O'Donnell of the EPA and Mr. George Ebrill of the ESB.

I would like to thank my fellow postgraduate students with whom I shared my time in Trinity, especially, Andrew, Anthony, Cathy, Samir, Sarah and Toman. My heartfelt thanks are due to Ian for his friendship, encouragement, and company in the office. Special thanks are due to John for everything, from his support, to my computer.

The final word goes to my family, to whom I owe everything.

ABSTRACT

This research project involved the investigation of urban air quality with a view to (a) adding to the limited information on the state of the atmospheric environment in Dublin, Ireland and (b) formulating a methodology to maximise the efficiency of air monitoring equipment and programmes through the commissioning and use of the Trinity College Mobile Air Monitoring Unit.

Real-time concentrations of CO, NO_2 and PM_{10} were recorded at a city centre intersection site and roadside site, for thirteen months and three months, respectively. Hourly concentrations of 27 VOCs recorded over one month are discussed. Data recorded by the EPA (CO, NO_x, SO_2, particulates, benzene, toluene and xylene) at the intersection site and by the ESB (NO_x) at a nearby street canyon are also analysed.

The results of a statistical analysis of the data are presented. The potential of CO, NO_2 and PM_{10} to act as tracer compounds for VOCs is analysed. The measured frequency distributions of CO, NO_2 and PM_{10} for varying averaging intervals are characterised. The relationships between the chief air pollutants associated with vehicular sources, and the influence on ambient concentrations of meteorological and temporal factors are investigated and quantified.

Adjustment factors are determined using these observed relationships, enabling the prediction of monthly averages based on three days of short-term monitoring (1 hour to 24 hours) at intervals throughout the month. A methodology for the prediction of 1-hour, 8-hour and 24-hour peak concentrations is also formulated. This employs a theoretical frequency distribution, and the estimated standard deviation of ambient concentrations, combined with either the predicted monthly average or a long-term average measured with simple sampling equipment.

This prediction algorithm was evaluated through comparison with actual concentration measurements. It was found to be effective for urban intersection, roadside and street canyon sites and a wide range of pollutants and required only 1 week of data for calibration purposes.

Table of Contents

DECLARATION I

ACKNOWLEDGEMENTS II

ABSTRACT III

NOMENCLATURE XI

1. Introduction 12

1.1 RATIONALE FOR STUDY 12

1.2 SCOPE, OBJECTIVES AND NOVEL ASPECTS OF THE PROJECT 13

1.3 FORMAT OF THESIS 15

1.4 HISTORICAL PERSPECTIVE 17

1.5 URBAN AIR POLLUTION 19

2. Literature Review 22

2.1 BACKGROUND 22

2.1.1 Pollutant Descriptions 24

2.1.2 Urban Air Pollutant Formation 26

2.1.3 Pollutant Impacts 31

2.1.4 The Role of Weather and Topography 33

2.1.5 Personal Exposure 37

2.1.6 Prediction of Air Pollution Levels 37

2.1.7 Persistence Factors 39

2.2 POLICIES AND STANDARDS 41

2.2.1 European Policies 42

2.2.2 Irish Legislation 42

2.2.3 International Agreements on Pollution Control 46

2.3 SUMMARY OF IRISH STUDIES 48

2.3.1 Review of Air Quality Information in Dublin 48

2.3.2 Carbon Monoxide 49

2.3.3 Nitrogen Dioxide 49

2.3.4 PM_{10} 50

2.3.5 Smoke 51

2.3.6 Sulphur Dioxide 52

2.3.7 Lead 52

2.3.8 Independent Studies 53

3. Description of Monitoring Sites and Apparatus 55

3.1 MONITORING PROGRAMME 55

3.2 SITE DESCRIPTIONS 57

3.3 Traffic Flow Characteristics 60
3.4 Description of Monitoring Equipment 62
3.4.1 Carbon Monoxide Monitoring Equipment 62
3.4.2 Nitrogen Dioxide Monitoring Equipment 62
3.4.3 Particulate Monitoring Equipment 63
3.4.4 VOC Monitoring Equipment 63
3.4.5 Meteorological Equipment 64
4. Monitoring Results 65
4.1 Data Summary 65
4.1.1 Site A (Pearse Street/Westland Row Junction) – Phase 1 65
4.1.2 Site A (Pearse Street/Westland Row Junction) – Phase 2 71
4.1.3 Site B (Pearse Street) 73
4.1.4 Site C – (Westland Row) 75
4.2 Comparison of Results at Site A 76
4.2.1 Analysis of Carbon Monoxide Data 76
4.2.2 Analysis of Nitrogen Dioxide Data 81
4.2.3 Analysis of PM_{10} Data 84
4.2.4 Summary of Results 87
4.3 Statistical Analysis of Data 87
4.3.1 Candidate Frequency Distributions 87
4.3.2 Goodness-of-Fit Tests 92
4.3.3 Frequency Distribution of Carbon Monoxide Data 94
4.3.4 Frequency Distribution of Nitrogen Dioxide Data 96
4.3.5 Frequency Distribution of PM_{10} Data 97
4.4 Conclusions 98
5. Pollutant Relationships 99
5.1 Temporal Variability of Pollutant Concentrations 99
5.1.1 Diurnal Trends in Carbon Monoxide Concentrations 100
5.1.2 Diurnal Trends in Nitrogen Dioxide Concentrations 102
5.1.3 Diurnal Trends in PM_{10} Concentrations 104
5.1.4 Comparison of Daily Profiles 106
5.1.5 Weekly Trends in Carbon Monoxide Concentrations 107
5.1.6 Weekly Trends in Nitrogen Dioxide Concentrations 108
5.1.7 Weekly Trends in PM_{10} Concentrations 109
5.1.8 Seasonal Trends in Carbon Monoxide Concentrations 110
5.1.9 Seasonal Trends in Nitrogen Dioxide Concentrations 111
5.1.10 Seasonal Trends in PM_{10} Concentrations 112

5.2 Variation in Pollutant Concentrations with Meteorological Factors 113
5.3 Variation in Pollutant Concentrations with Wind Speed 114
5.3.1 Carbon Monoxide 114
5.3.2 Nitrogen Dioxide 116
5.3.3 PM_{10} 118
5.4 Variation in Pollutant Concentrations with Wind Direction 120
5.4.1 Carbon Monoxide 120
5.4.2 Nitrogen Dioxide 122
5.4.3 PM_{10} 124
5.5 Variation in Pollutant Concentrations with Temperature 126
5.5.1 Carbon Monoxide 126
5.5.2 Nitrogen Dioxide 127
5.5.3 PM_{10} 127
5.6 Variation in Pollutant Concentrations with Relative Humidity 128
5.6.1 Carbon Monoxide 128
5.6.2 Nitrogen Dioxide 128
5.6.3 PM_{10} 129
5.7 Variation in Pollutant Concentrations with Sunshine Duration 130
5.8 Spatial Variability 131
5.8.1 Carbon Monoxide 131
5.8.2 Oxides of Nitrogen 131
5.8.3 PM_{10} 134
5.9 Inter-Compound Relationships 134
5.9.1 Oxides of Nitrogen 134
5.9.2 PM_{10} and other Particulate Matter 139
5.9.3 VOC's and Carbon Monoxide, Nitrogen Dioxide and PM_{10} 142
5.9.4 Sulphur Dioxide and Carbon Monoxide, Nitrogen Dioxide and PM_{10} 148
5.10 Conclusions 149
6. Pollutant Concentration Prediction Algorithm 151
6.1 Algorithm Description 151
6.2 Flow Chart 152
6.3 Prediction Equations 154
6.4 Calculation of Adjustment Factors for Time of Sampling 155
6.4.1 Carbon Monoxide 155
6.4.2 Nitrogen Dioxide 158
6.4.3 PM_{10} 160
6.5 Adjustment of Wind Speed Measurements 162

6.6 Adjustment of Data for Wind Speed 164
6.6.1 Carbon Monoxide *164*
6.6.2 Nitrogen Dioxide *167*
6.6.3 PM_{10} *169*
6.7 Adjustment of Pollutant Data for Wind Direction 173
6.7.1 Carbon Monoxide *173*
6.7.2 Nitrogen Dioxide *177*
6.7.3 PM_{10} *178*
6.8 Adjustment of Pollutant Data for Temperature 179
6.9 Adjustment of Pollutant Data for Relative Humidity 179
6.10 Adjustment of Prediction for Average Monthly Wind Speed 180
6.10.1 Carbon Monoxide *180*
6.10.2 Nitrogen Dioxide *182*
6.10.3 PM_{10} *183*
6.11 Rates of Convergence of Factors 184
6.11.1 Convergence of Time-of-Sampling Factors *185*
6.11.2 Convergence of Wind Speed Factors *188*
6.11.3 Convergence of Wind Direction Factors *191*
6.11.4 Summary of Rates of Convergence of Factors *196*
6.12 Prediction of Extreme events 196
6.12.1 Estimation of Population Variance and Standard Deviation *197*
6.12.2 Calculation of Confidence Intervals for Standard Deviation *198*
6.12.3 Terminology *201*
6.12.4 Exceedances of Critical Levels *202*
6.12.5 Expected Return Period or Waiting Time *204*
6.13 Conclusions 205
7. Algorithm Evaluation and Verification 207
7.1 Prediction of Monthly Averages – Site A (Pearse Street/Westland Row Intersection) Phase 1 209
7.1.1 Carbon Monoxide *210*
7.1.2 Nitrogen Dioxide *217*
7.1.3 PM_{10} *220*
7.2 Indicative Monitoring – Worst Case Scenario 223
7.2.1 Carbon Monoxide *223*
7.2.2 Nitrogen Dioxide *227*
7.2.3 PM_{10} *229*
7.3 Estimation of Standard Deviation 231

7.3.1 Carbon Monoxide *231*
7.3.2 Nitrogen Dioxide and PM_{10} *231*
7.4 Frequency Distributions of Hourly, 8-Hourly and 24-Hourly Data 232
7.4.1 Carbon Monoxide *232*
7.4.2 Nitrogen Dioxide *235*
7.4.3 PM_{10} *237*
7.5 Extreme Event Prediction 240
7.5.1 24-Hour Averages– Carbon Monoxide *240*
7.5.2 24-Hour Averages – Nitrogen Dioxide *244*
7.5.3 24-Hour Averages – PM_{10} *244*
7.5.4 8-Hour Averages – Carbon Monoxide *245*
7.5.5 8-Hour Averages – Nitrogen Dioxide *248*
7.5.6 8-Hour Averages – PM_{10} *248*
7.5.7 1-Hour Averages – Carbon Monoxide *248*
7.5.8 1-Hour Averages – Nitrogen Dioxide *251*
7.5.9 1-Hour Averages – PM_{10} *252*
7.6 Prediction of Exceedences 252
7.6.1 Carbon Monoxide *252*
7.6.2 Nitrogen Dioxide *253*
7.6.3 PM_{10} *254*
7.7 Application of Existing Persistence Factors 255
7.8 Summary of Site A, Phase 1 Concentration Predictions 259
7.8.1 Summary of Site A, Phase 1 Carbon Monoxide Predictions *259*
7.8.2 Summary of Site A, Phase 1 Nitrogen Dioxide Predictions *261*
7.8.3 Summary of Site A, Phase 1 PM_{10} Predictions *263*
7.9 Prediction of Monthly Averages Site A (Pearse Street/Westland Row Intersection) Phase 2 265
7.9.1 Calculation of Monthly Averages – Carbon Monoxide *266*
7.9.2 Calculation of Monthly Averages – Nitrogen Dioxide *267*
7.9.3 Calculation of Monthly Averages – PM_{10} *268*
7.10 Extreme Event Prediction – Phase 2 270
7.10.1 24-Hour Averages – Carbon Monoxide *270*
7.10.2 24-Hour Averages – Nitrogen Dioxide *271*
7.10.3 24-Hour Averages – PM_{10} *271*
7.10.4 8-Hour Averages – Carbon Monoxide *272*
7.10.5 8-Hour Averages – Nitrogen Dioxide *273*
7.10.6 8-Hour Averages – PM_{10} *273*
7.10.7 1-Hour Averages – Carbon Monoxide *274*

7.10.8 1-Hour Averages – Nitrogen Dioxide 275
7.10.9 1-Hour Averages – PM_{10} 275
7.11 PREDICTION OF EXCEEDENCES 275
7.12 CONCLUSIONS ON MODEL EVALUATION AT PEARSE STREET/WESTLAND ROW INTERSECTION 276
8. Extension And Application of Algorithm to Other Sites and Pollutants 280
8.1 INTRODUCTION 280
8.2 APPLICATION OF ALGORITHM TO ROADSIDE SITE 281
8.2.1 Calculation of Monthly Averages 281
8.2.2 24-Hour Averages – Carbon Monoxide 283
8.2.3 24-Hour Averages – Nitrogen Dioxide 284
8.2.4 24-Hour Averages – PM_{10} 284
8.2.5 8-Hour Averages – Carbon Monoxide 285
8.2.6 8-Hour Averages – Nitrogen Dioxide 286
8.2.7 8-Hour Averages – PM_{10} 286
8.2.8 1-Hour Averages – Carbon Monoxide 286
8.2.9 1-Hour Averages – Nitrogen Dioxide 288
8.2.10 1-Hour Averages – PM_{10} 288
8.2.11 Prediction of Exceedences 288
8.2.12 Conclusions of Application of Algorithm to Roadside Site 289
8.3 APPLICATION OF ALGORITHM TO STREET CANYON (WESTLAND ROW) 290
8.3.1 Calculation of Adjustment Factors for Nitrogen Dioxide 290
8.3.2 Calculation of NO_2 Monthly Averages 290
8.3.3 24-Hour Averages– Nitrogen Dioxide 291
8.3.4 8-Hour Averages – Nitrogen Dioxide 292
8.3.5 1-Hour Averages – Nitrogen Dioxide 294
8.3.6 Prediction of Exceedences 295
8.3.7 Conclusions on Application of Algorithm to Street Canyon. 295
8.4 APPLICATION OF MODEL TO OTHER POLLUTANTS (AT ORIGINAL LOCATION – SITE A) 296
8.4.1 24-Hour Averages – Acetylene 296
8.4.2 24-Hour Averages – 1,3,5-Trimethylbenzene 298
8.4.3 8-Hour Averages – Acetylene 298
8.4.4 8-Hour Averages – 1,3,5-Trimethylbenzene 299
8.4.5 1-Hour Averages – Acetylene 299
8.4.6 1-Hour Averages – 1,3,5-Trimethylbenzene 301
8.4.7 Prediction of Benzene Concentrations 301
8.4.8 Prediction of Exceedences 302

8.4.9 Conclusions of Application of Algorithm to New Compounds at Pearse Street/Westland Row Junction 303

8.5 APPLICATION OF ALGORITHM TO NEW COMPOUND AT STREET CANYON LOCATION 305

8.5.1 Calculation of Factors 305

8.5.2 Calculation of Monthly Averages 305

8.5.3 24-Hour Averages – Nitrogen Monoxide 306

8.5.4 8-Hour Averages – Nitrogen Monoxide 308

8.5.5 1-Hour Averages – Nitrogen Monoxide 309

8.5.6 Prediction of Exceedences 310

8.6 CONCLUSIONS ON TRANSFERABILITY OF METHODOLOGY WITH RESPECT TO LOCATIONS AND COMPOUNDS 310

9. Discussion 312

9.1 INTRODUCTION 312

9.2 CATEGORIES OF AIR QUALITY MODELS 312

9.2.1 Empirical/Statistical Models 314

9.2.2 Deterministic Models 316

9.3 DISCUSSION OF ALGORITHM 321

9.4 CONCLUSIONS 323

10. Conclusions 324

10.1 SUMMARY 324

10.2 CONCLUSIONS 325

10.3 RECOMMENDATIONS FOR FURTHER RESEARCH 328

11. Appendices 330

11.1 APPENDIX A 330

11.2 APPENDIX B 331

11.3 APPENDIX C 333

11.4 APPENDIX D 346

1-HOUR AVERAGES – ROADSIDE SITE (PEARSE ST.) 348

12. References 352

NOMENCLATURE

Abbreviation

CO	Carbon monoxide
CO_2	Carbon dioxide
EPA	Environmental Protection Agency
ESB	Electricity Supply Board
GC	Gas chromatograph
HCs	Hydrocarbons
MAE	Mean average error
NO	Nitrogen monoxide
NO_2	Nitrogen dioxide
NO_x	Oxides of nitrogen
PM_{10}	Particulate matter with a mass median aerodynamic diameter less than 10 μm
$PM_{2.5}$	Particulate matter with a mass median aerodynamic diameter less than 2.5 μm
PM_1	Particulate matter with a mass median aerodynamic diameter less than 1 μm
RMSE	Root mean square error
RPM	Roadside pollution monitor
SO_2	Sulphur dioxide
TEOM	Tapered element oscillating microbalance
VOCs	Volatile organic compounds
WS	Wind speed

1. INTRODUCTION

1.1 RATIONALE FOR STUDY

Air quality monitoring is a crucial part of an air quality management strategy. However, the commissioning of a dedicated, continuous air monitoring facility involves a large investment of capital, as each site requires a secure air-conditioned room with a power supply, to house the instruments. This constraint and its associated costs reduce the number of potential monitoring sites. There is currently no inexpensive method of accurately measuring pollutant concentrations at a large number of sites simultaneously, and diffusion tubes can only provide single point measurements of long-term averages. There is also substantial uncertainty associated with the ability of a single air monitoring site to accurately and satisfactorily represent the surrounding neighbourhood and city. It is, therefore, of prime importance that the available funding and equipment be used to the maximum efficiency. This research project involves the design of a methodology to use short-term measurements to predict peak 1-hour, 8-hour and 24-hour concentrations over longer periods and to predict possible exceedences of ambient air quality limit values. This methodology also allows long-term average concentration data recorded by inexpensive passive sampling techniques to be combined with short periods of monitoring at a higher temporal resolution to estimate peak 1-hour, 8-hour and 24-hour concentrations and be related to ambient air quality legislation. The ability of pollutants that can be monitored relatively cheaply to act as tracer compounds for volatile organic compounds is also investigated, as, at present, the monitoring of such compounds can be both labour intensive and expensive.

1.2 Scope, Objectives and Novel Aspects of the Project

Scope

The research project involved the commissioning and use of the Trinity College Mobile Air Monitoring Unit for the investigation of urban air quality with a view to (a) adding to the limited information on the state of the atmospheric environment in Dublin, and (b) formulating a methodology to maximise the efficiency of both air monitoring equipment and programmes.

Following the collection of the data from a number of monitoring sites, the data are analysed to ascertain the theoretical distribution which best characterises the observed distribution for different averaging periods. The relationships between the concentrations of individual compounds, time of sampling and meteorological factors are then investigated. These relationships are then used to calculate adjustment factors that compensate for conditions at the time of sampling. Using these adjustment factors, short-term monitoring data are used to predict the mean monthly concentration. From the appropriate theoretical frequency distribution, the predicted monthly concentration and the estimated standard deviation, short-term peak concentrations over the course of the month are predicted. This information is then compared to the limit values defined under EU Framework Directive 96/62/EC on Ambient Air Quality Assessment and Management (CEC, 1996).

Objectives

The specific objectives of this project were to:

i) Characterise the ambient air quality impacts of vehicular sources at an urban intersection in Dublin;

ii) Investigate the relationships between the chief air pollutants associated with vehicular sources;

iii) Investigate the relationships between urban air pollutants and meteorological variables;

iv) Investigate the temporal variability of the air pollutants;

v) Investigate the potential of carbon monoxide, nitrogen dioxide and PM_{10} to act as tracer compounds for volatile organic compounds;

vi) Develop and evaluate an effective methodology for predicting long-term air pollution concentration averages from limited short-term monitoring data;

vii) Develop and evaluate a methodology for using diffusion tubes to estimate short-term peak concentrations with the aid of short periods of real-time monitoring thereby maximising the efficiency of the available technology;

viii) Develop and evaluate an effective methodology for predicting peak short-term air pollution concentrations over long periods, based on short-term monitoring alone, and evaluate the ability of this methodology to contribute to local air quality assessments as required under the EU Framework Directive 96/62/EC on Ambient Air Quality Assessment and Management (CEC, 1996).

Novel Aspects

The novel aspects of this study include the following:

i) An extensive monitoring programme was carried out at two previously uninvestigated sites, significantly adding to the state of knowledge on urban air pollution in Dublin.

ii) Air pollution is highly location-specific; this is the most extensive study of urban air pollution at a high temporal resolution, and its influencing factors, in Ireland.

iii) The use of short periods of real-time monitoring combined with diffusion tubes or passive sampling to estimate short-term (1-hour, 8-hour and 24-hour) peak concentrations has not previously been investigated.

iv) Most studies of VOCs at other urban sites in Ireland have measured long-term average concentrations as opposed to the hourly averages considered in this study, as indeed have the majority of studies carried out globally. Where short-term averages were measured, generally only a limited range of VOCs was analysed.

v) A new methodology for the prediction of air pollution concentrations, both short- and long-term, based on very short monitoring periods, was designed and evaluated.

vi) Very little information on relating concentrations over differing averaging periods to each other is available; this work examines the relationships between monthly averages, 24-hour, 8-hour and 1-hour averages.

vii) This is the first study to develop a methodology for relating such short-term measurements to legislation, such as EU Framework Directive 96/62/EC on Ambient Air Quality Assessment and Management (CEC, 1996).

1.3 Format of Thesis

The remaining chapters of the thesis are structured as follows:

♦ Chapter 2 outlines the background to this study of air pollution. Urban air pollutants are discussed in relation to their properties, impacts and the factors influencing urban air quality. Policies and standards dealing with ambient air quality, both nationally and internationally, are summarised. Finally, other studies and surveys on ambient air quality in Dublin are described.

♦ Chapter 3 describes the sites at which monitoring was carried out, and the equipment used during the monitoring programme.

♦ Chapter 4 presents and summarises the data recorded during the monitoring program at each site. For one site, measurements recorded using two different sets of equipment are compared. The recorded data are then tested for goodness-of-fit to a selection of theoretical distributions.

♦ Chapter 5 includes an investigation of the temporal variability of the pollutants. The effects of meteorological variables on ambient pollutant concentrations are then analysed. Finally, inter-compound relationships are examined.

♦ Chapter 6 presents the formulation of a methodology to predict long-term concentration averages from short-term pollutant concentration, using carbon monoxide, nitrogen dioxide and PM_{10} data collected at Pearse Street/Westland Row intersection, in Dublin. The methodology for predicting absolute peak and percentile concentration values over 1-hour, 8-hour and 24-hour periods is then discussed.

♦ Chapter 7 discusses the results of the prediction algorithm with respect to long-term averages and short-term peaks for carbon monoxide, nitrogen dioxide and PM_{10} data collected at the Pearse Street/Westland Row intersection.

♦ Chapter 8 evaluates the performance of the prediction algorithm at two different types of urban site: a roadside site, and a street canyon site. The transferability of the prediction algorithm to other compounds is then examined, by application to nitrogen monoxide and three VOC compounds; acetylene, 1,3,5-trimethylbenzene and benzene.

♦ Chapter 9 presents the main findings and conclusions from this study, along with recommendations for future work in this area.

1.4 Historical Perspective

Ambient air quality has only become a concern relatively recently in the history of mankind. Only when social evolution reached the husbandry stage, involving the association of family units into fixed communities, could human activities impact upon the occupied neighbourhood. References to blackened buildings have been cited as evidence that smoke nuisance has existed for thousands of years (Stern, 1976), although prior to the industrial revolution the repercussions of the available metallurgical and industrial processes, with respect to air pollution, would have been limited. Although historical accounts of deaths caused by toxic atmospheres have survived, such as the suffocation of Pliny the Elder by volcanic fumes in 79 AD, as recorded by Tacitus, these serve only to demonstrate that the human species was, as it is now, physiologically responsive to anoxia or poisonous gases (Stern, 1976).

Before the Eighteenth Century

With the transition to coal as a common source of fuel, which began in 13th century medieval England and had spread world-wide by the 19th century, came the advent of a form of air pollution that commonly characterised city atmospheres until recent times (Brimblecombe, 1996).

One of the first formal protests against air pollution was recorded in England in the reign of Edward I (1272-1307) when the nobility of the time protested against the use of 'sea-coal'. This was followed in the reign of Edward II (1307-1327), by one of the first official penalties for polluting the atmospheric environment, when a man was put to torture for filling the air with a 'pestilential odour' through the use of coal (Stern, 1976).

The Industrial Revolution

The Industrial Revolution saw a significant deterioration of air quality in the burgeoning industrial towns. By 1878, the first legislation concerning air pollution had been introduced in Ireland, and the first municipal ordinances and regulations limiting emissions in the United States appeared in the 1880's. In addition to increased air pollution sources, the nineteenth

century saw significant developments in pollution control technology. Chief among these were the stoker for mechanical firing of coal, the scrubber for removing acid gases from effluent gas streams, cyclone and bag house dust collectors, and the introduction of physical and chemical principles into process design (Boubel, 1994).

1900-1950

Before World War I, public opinion in relation to air pollution was in general ambivalent, it being regarded by many as evidence of wealth and growth. Advertisements of the time could feature fuming smokestacks and cars with visible exhausts – something that is unlikely to be seen in present day campaigns.

Air quality in general in developed countries throughout the first quarter of the twentieth century worsened with the growth of cities and factories, despite changes in the technology of both the production of air pollution and its engineering control, such as the development of the electrostatic precipitator.

By 1950, the building of natural gas pipelines in western Europe began a rapid displacement of coal and oil as home heating fuels where gas was available, bringing a drastic improvement in air quality (Boubel, 1994).

1950-1980

Between 1950 and 1980 almost every country in Europe, as well as Japan, Australia and New Zealand, enacted national air pollution control legislation as a result of significant air pollution problems. In the United States, Los Angeles' smog problem continued to worsen, and in Pittsburgh in 1947 smog was so bad that streetlights were kept on all day (Freedomchannel, 2000).

In this period, the study of air pollution saw advances such as the mathematical modelling of atmospheric pollution; inroads were made into understanding the photochemistry of air pollution, and air quality monitoring systems became operational world-wide.

The 1980's

During the 1980's, the 'Greenhouse Effect' became the target of serious attention and study. Pollution controls also began to be imposed on new emission sources, with a preventative, rather than remedial mindset being adopted.

The 1990's

The 1990's saw the emergence of two distinct, but closely linked global environmental crises: uncontrolled global climate changes and stratospheric ozone depletion.

1.5 Urban Air Pollution

Cities are by nature concentrations of humans, materials and activities. They therefore combine both the highest levels of pollution with the largest targets of impact. Impacts of air pollution, however, are not confined to local effects, but are enacted on all geographical and temporal scales, with the capacity to change conditions for man and nature across the entire globe.

The scale of the urban air pollution problem is affected both by changing land use due to increasing urban areas, caused by drift to the cities, and the excess of births over deaths in the cities themselves, particularly in developing countries (Mayer, 1999). Migration to the cities is rooted in a fundamental structural change, especially in non-industrialised countries, caused by economic opening-up, new trading partners, and changing political conditions such as democratisation. Tiger economies are characterised by a high degree of structural change, and this tends to bring with it increased levels of emissions (Mayer, 1999).

After the Second World War the world population was about 2.5 billion. Between 1945 and 1988, the global population more than doubled to 5.9 billion, with the more developed countries accounting for 1.2 billion, and China alone accounting for another 1.2 billion. In that same 50-year period, the global urbanisation, defined as the fraction of people living in settlements above 2000 inhabitants, has risen from below 30% to above 44% (73% in more developed countries and 36% in the less developed). There is no indication of this trend

changing, with estimates of the population reaching 10 billion by the middle of this century, with the sharpest rise in the now developing countries (Fenger 1999).

In cities, the most important source of air pollution tends to be motor traffic (Osborn, 1989; Mayer, 1999; Palmgren *et al.*, 1999) with the global number of vehicles having increased by a factor of ten since 1950 to above 600 million (Fenger, 1999). Again, as with population growth, much of the expected future growth in vehicle numbers is likely to occur in developing countries, and in Eastern Europe. As cities expand, more people will also drive more vehicles over greater distances and for longer time, causing increased emissions (Mayer, 1999).

From experience, as cities develop, the tendency is for the air pollution trends to show a repeated pattern. Initially, the environmental quality is linked to the average income of the inhabitants. With an increase in average per capita earnings, comes an improvement in the availability of safe water and adequate sanitation, as does an increase in the municipal waste. The air pollution also increases to a certain point and then the trend reverses. For air pollution, and most other forms of pollution, this turning point occurs before a per capita income of USD 8000 is reached (Fenger, 1999).

Before rapid industrial development takes place, air pollution arises mainly from domestic sources and light industry; concentrations of pollutants are low and generally increase in proportion to the population increase. Air quality then shows an accelerated deterioration with increasing industrial development, leading to air pollution becoming a health concern (as illustrated in Figure 1.1). As a result, emission controls are then introduced, stabilising the situation, although it is possible for serious air pollution to exist for some time (Mayer, 1999).

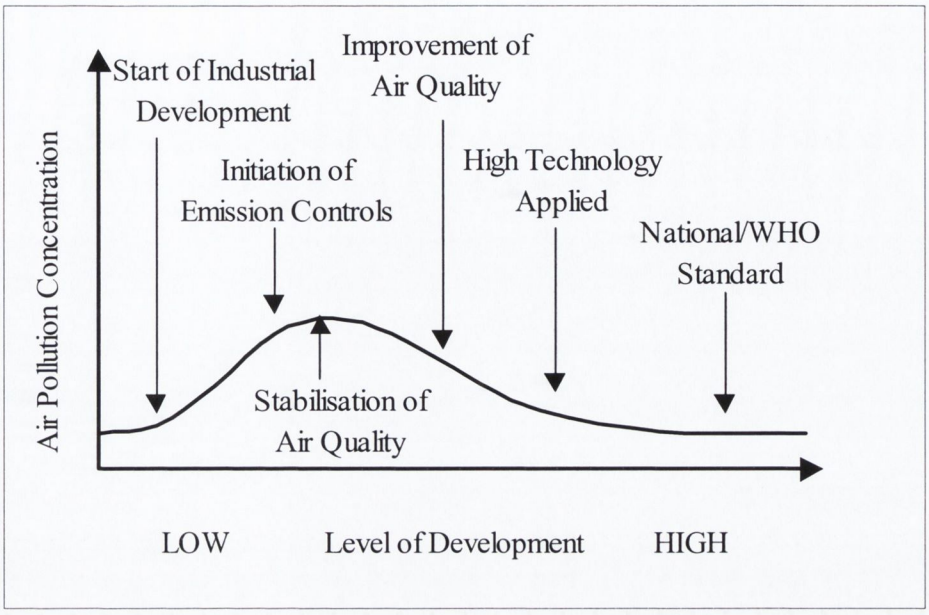

Figure 1.1 Pattern of ambient air pollutant concentrations (Mage *et al.*, 1996)

Europe is a highly urbanised continent, with more than 70% of the population living in cities. The general air quality in European cities has improved in recent decades, in spite of an increase in population density and standard of living. Despite this, air pollution is still considered an important issue, with far-reaching impacts (Fenger 1999), hence the recent European Framework Directive on ambient air quality assessment and management (discussed in Section 2.2.3).

2. LITERATURE REVIEW

This chapter is divided into three main sections: firstly, an overview of pollutants emitted from vehicles is presented, then the policies and standards governing air pollution are discussed, followed by a comprehensive state-of-the-art review of work carried out on air pollution, paying special attention to studies of the air quality in Ireland.

2.1 BACKGROUND

Urban air pollutants fall into a number of categories, shown in Table 2.1.

Table 2.1 Classifications of pollutants (Straub, 1989)

Major Classes	Subclasses	Typical Members
Inorganic gases	Oxides of nitrogen	Nitrogen dioxide, nitric oxide
	Oxides of sulphur	Sulphur dioxide, sulphuric acid
	Other inorganics	Carbon monoxide, ammonia, ozone
Organic gases	Hydrocarbons	Benzene, butadiene, butene, ethylene
	Aldehydes/Ketones	Acetone, formaldehyde
	Other organics	Acids, chlorinated hydrocarbons, polynuclear aromatics
Aerosols	Solid particulates	Dust, smoke
	Liquid particulates	Fumes, oil mists, polymeric reaction products

Ambient air quality is dependent not only on quantities of emissions, but also on external factors subsequent to the moment of emission. Factors such as mixing induced by vehicle motion, wind speed and direction, turbulence, chemistry and rate of pollutant removal, and the geometry of buildings and roads, all affect the ambient concentration (Samson, 1988; Theurer, 1999). A schematic diagram of the air pollution processes in the atmosphere is given in Figure 2.1.

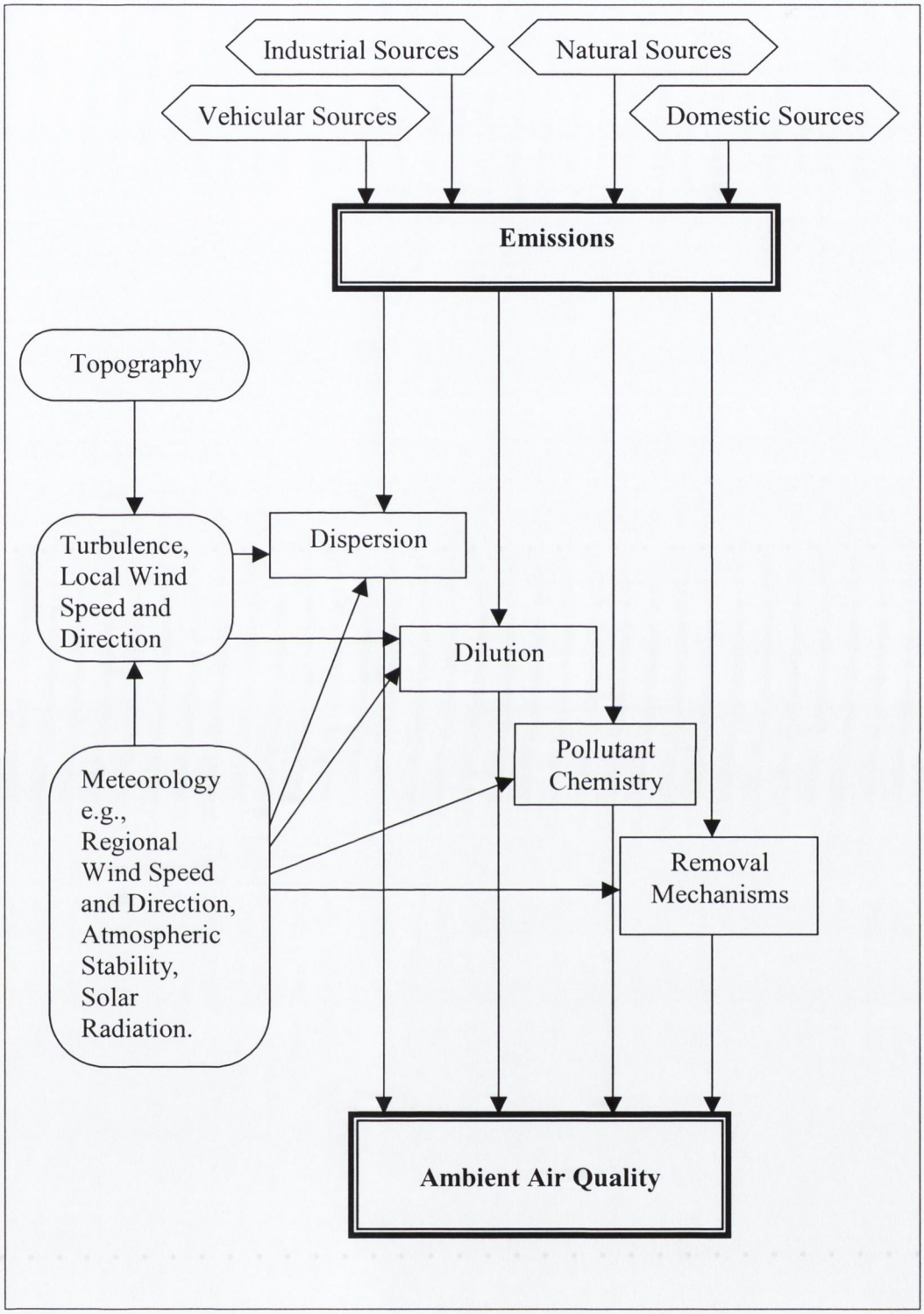

Figure 2.1 Schematic pathway for emissions to ambient air quality

2.1.1 Pollutant Descriptions

Carbon Monoxide

Carbon monoxide (CO) is a colourless, odourless and tasteless gas, and is slightly less dense than air. As carbon monoxide is not highly reactive, and almost solely emitted by vehicular sources, it is sometimes used as a tracer for other vehicle related pollutants (Stein and Toselli, 1996).

Oxides of Nitrogen

Nitrogen dioxide (NO_2) is a reddish-brown gas, which is soluble in water. It has a strong odour, and is corrosive, toxic and a strong oxidant.

Particulate Matter

Individual particulates are aggregates of similar and dissimilar molecules (Boubel, 1994; Dye *et al.*, 1998), differing in sources, size ranges, formation mechanisms and chemical composition (Casimiro, 1996; El-Fadel and Massoud, 2000). It is possible for airborne particulate matter to contain every compound existing, or produced on earth, that is solid or liquid at ambient temperatures. The extreme diversity of chemical species that can become airborne makes an analysis of particulate reactions and chemistry extremely difficult (Lodge *et al.*, 1981).

A typical schematic size distribution of atmospheric particulate matter is shown in Figure 2.2, although the size distribution tends to depend on the particulate source (Morawska *et al.*, 1999). In the atmosphere, the actual size spectra show quantitative differences with more pronounced mass peaks for fine particles in urban and suburban sites and larger peaks for coarse particles near seacoasts (Fenger, 1999), although the sub-micron particles exhibit a bi-modal size distribution (Kleeman and Cass, 1998; Morawska *et al.*, 1999). The mode with the 0.2 μm maximum results from coagulation and condensation of gases and vapours in the atmosphere. The mode with the 10 μm maximum comprises mainly of particles introduced to the air as solids, and particles from the coagulation/condensation mode which have grown larger and have crossed the saddle between the mode sizes (Boubel, 1994). It should be borne

in mind when measuring particulate concentrations, that if two particles, one 10 μm and one 0.1 μm, have the same density, the smaller has one-millionth the weight of the larger.

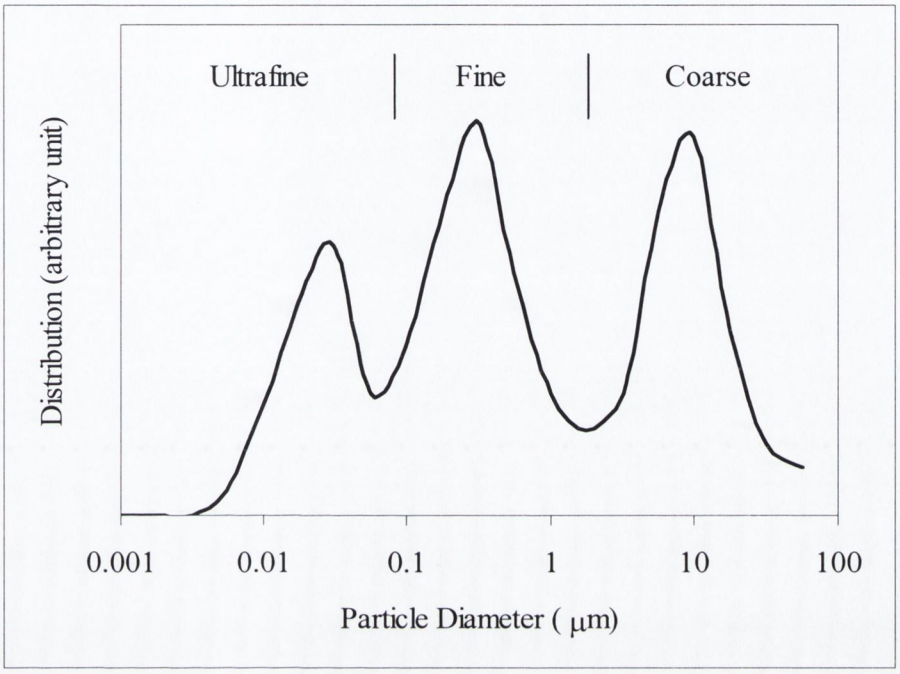

Figure 2.2 Schematic size distribution of particulate matter in the atmosphere (Fenger, 1999)

Volatile Organic Compounds

The term Volatile Organic Compounds (VOCs) is used to describe organic material in the vapour phase, excluding methane. Hydrocarbons (HCs) form a significant fraction of petrol and other fuel oils (Singh *et al.*, 1985). VOCs in the ambient air can be due to both combustion and non-combustion sources, and include the use of solvents, including those released from paints, and vehicular emissions. Evaporative losses of petrol during storage and distribution are also significant (Harrison, 1999). In urban air, the most important compounds are benzene and the polyaromatic hydrocarbons, although 1,3-butadiene, ethene, propene and the aldehydes have also received attention lately, as reported in Fenger (1999).

Other Compounds

Sulphur Dioxide (SO_2) is primarily associated with sulphur in fossil fuels. By using fuels with a low sulphur content, such as natural gas or oil, these emissions can be successfully reduced. On large plants, in industrialised countries, desulphurisation of fuels is an established alternative (Fenger, 1999). SO_2 is a pungent, colourless gas, is readily soluble in water, and can also be oxidised within moisture in the atmosphere to a fine particulate which can travel considerable distances (Murray, 1997). Classified as an irritant gas, it exacerbates bronchitis and other respiratory conditions and leads to excess mortality among those with previous respiratory or cardiac problems. Sulphate in the air also affects visibility, as well as being an important factor in the creation of acid rain (Martin and Barber, 1985).

Lead (Pb) as an additive to petrol has been phased out in the major part of the industrial world, including Ireland, but it is still used in many developing countries, and economies in transition, where emissions from industries also play a role (Fenger, 1999). Lead, in high enough concentrations, can affect almost every major body function, and has been particularly associated with neurological and behavioural problems in children (Lipfert, 1994; O'Regan, 1996).

2.1.2 Urban Air Pollutant Formation

The most significant source of anthropogenic air pollution is the combustion of fuels. The most familiar fuels are carbon or hydrocarbon compounds. These fuels are rapidly oxidised by atmospheric oxygen at high temperature yielding a large amount of energy as heat, together with the products of combustion, which are usually stable gaseous oxides (Brimblecombe, 1996).

Carbon compounds

The primary source of oxides of carbon is combustion. During complete combustion hydrocarbons are oxidised to carbon dioxide and water (Watkins, 1981). The anthropogenic creation of water is not significant, as the natural fluxes of water are very much larger than those due to human activities. On the other hand, carbon dioxide is released in large enough

quantities to affect the natural balance of atmospheric gases, causing the greenhouse effect (Brimblecombe, 1996).

In practice, however, combustion rarely results in carbon dioxide and water alone, with many other combustion products being formed. Of the gaseous carbon compounds released, it is carbon monoxide that is the most significant pollutant, with automobiles being the predominant source of carbon monoxide in urban areas. As an example, carbon monoxide emissions, by sector, in the UK in 1990 are shown in Figure 2.3.

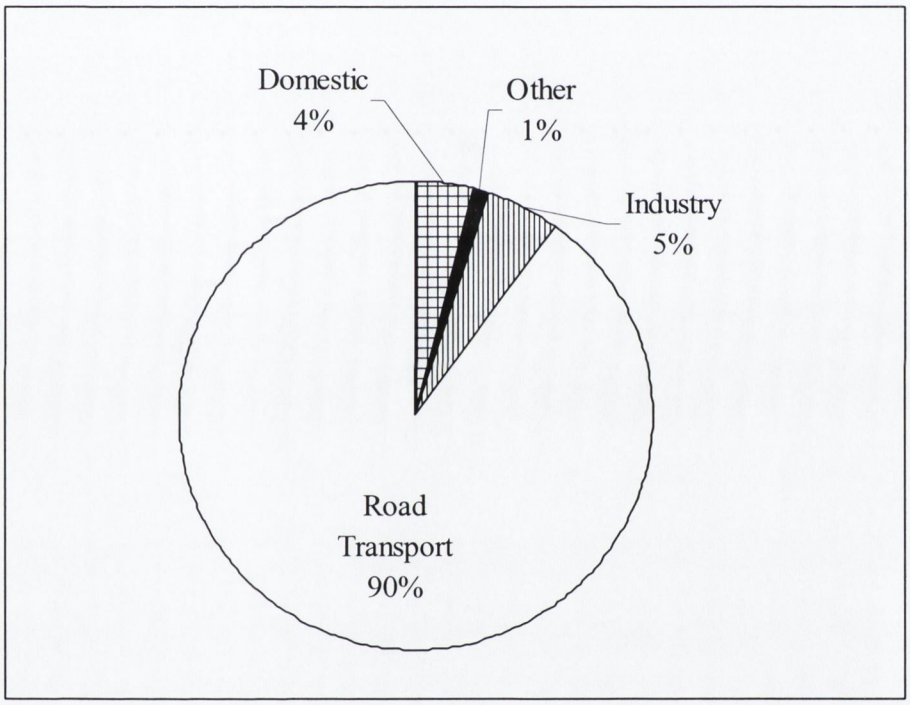

Figure 2.3 Sources of carbon monoxide emissions (Brimblecombe, 1996).

'Lean burn' engines, with increased air-to-fuel ratios help to reduce CO emissions, as more oxygen helps to oxidise all the fuel to carbon dioxide and water (Brimblecombe, 1996). The effect of the fuel-air ratio on engine emissions of carbon monoxide, hydrocarbons and nitrogen oxides is shown in Figure 2.4 (where parts per hundred thousand is abbreviated to ppht).

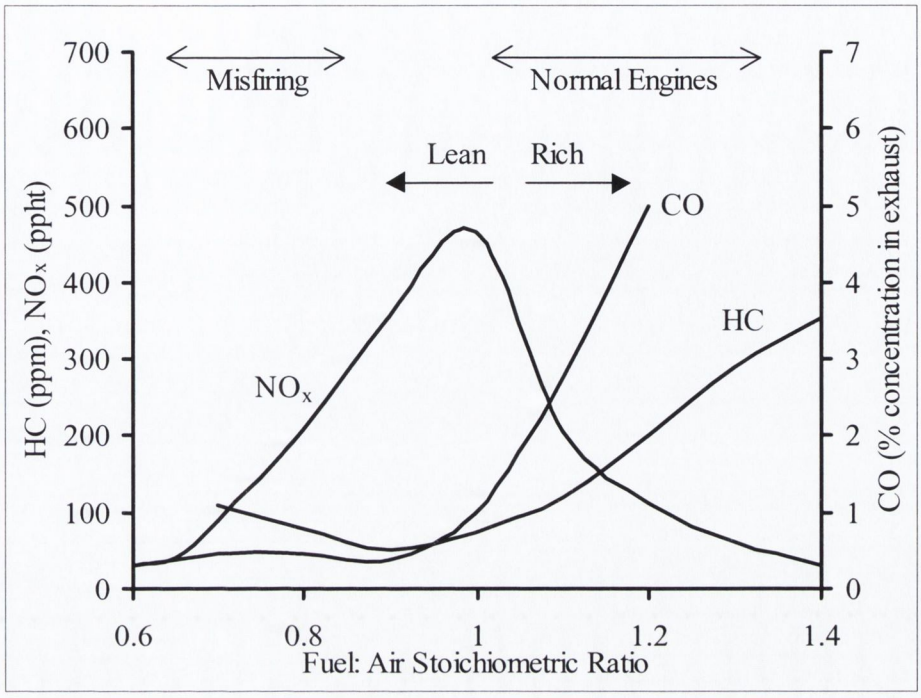

Figure 2.4 Concentrations of pollutant gases in automobile exhausts (Brimblecombe, 1996).

As well as the fuel-air ratio, the driving mode also affects the engine emissions. Carbon monoxide and hydrocarbon emissions are greatest for a decelerating vehicle (Strauss and Mainwaring, 1984).

The unburned hydrocarbons found in the exhaust gas are formed from carbon even less oxidised than carbon monoxide. Hydrocarbons of low molecular weight are probably formed in the much cooler layers of gas that exist against the wall of the engine cylinder (Brimblecombe, 1996). Typically, 60% of the total hydrocarbons emitted pass out through the exhaust pipe, 20% are lost through the crankcase, and the remaining 20% are lost equally from the fuel tank and the carburettor (Strauss and Mainwaring, 1984).

Nitrogen compounds

Combustion in the engine also takes place in the presence of nitrogen, as well as carbon. The combustion process causes the formation of oxygen atoms, which can enter chain reactions with nitrogen, as detailed in Equation 2.1 to Equation 2.3.

$O + N_2 \rightarrow NO + N$ Equation 2.1

$N + O_2 \rightarrow NO + O$ Equation 2.2

This can be summed to give the overall process

$N_2 + O_2 \rightarrow 2NO$ Equation 2.3

Because of the nature of the chemical equilibrium, the high temperatures encourage the formation of nitric oxide, although equilibrium rates of nitric oxide production are not reached. There are also more rapid routes to produce nitric oxide during the combustion of fuels. In the combustion of hydrocarbons, the presence of the CH radical can lead to rapid formation of HCN:

$CH + N_2 \rightarrow HCN + N$ Equation 2.4

This is then converted to CN, and the atomic nitrogen is oxidised first to NO and then to NO_2. The transformation rate of NO into NO_2 depends on emission characteristics, meteorological conditions, solar radiation, local environment and background concentrations of various pollutants (NO, NO_2, O_3, and hydrocarbons) (Seinfeld, 1986; Pisano *et al.*, 1997; Härkönen *et al.*, 1998).

Oxides of nitrogen also play an important part in many other atmospheric reactions, including the formation of tropospheric ozone (Härkönen, 1998). This reaction with ozone is the other main pathway for the production of NO_2 in urban air.

$NO + O_3 \rightarrow NO_2 + O_2$ Equation 2.5

This reaction can reach equilibrium in a matter of minutes. During the day the reaction is reversible, as NO_2 absorbs solar radiation and dissociates into nitric oxide and an oxygen atom, as a result. The oxygen atom combines rapidly with atmospheric oxygen to regenerate ozone (O'Keefe, 1997).

One difficulty in controlling nitrogen oxides from automobiles is that the conditions that reduce the formation of nitrogen oxides enhance the formation of carbon monoxide and hydrocarbons and vice versa, as indicated in Figure 2.4. Whereas carbon monoxide and hydrocarbon emissions are greatest for a decelerating vehicle, the opposite is true for oxides of nitrogen, which are greatest under accelerating and cruising conditions (Strauss and Mainwaring, 1984).

Particulates

Motor vehicles, in particular diesel vehicles, are known to be important sources of particulate matter (Weingartner *et al.*, 1996). Particulate material from vehicular sources ranges in size from large flakes to submicron particles and varies in consistency from hard and brittle particulate to oil mists (O'Regan, 1996). Mass and composition tend to fall into two groups: coarse particles greater than 2.5 μm in aerodynamic diameter and smaller fine particles.

Some of the particulate matter is generated in the engine combustion chamber and nucleated and agglomerated in the vehicle exhaust system before it passes out the exhaust pipe. Particulate matter formed in the engine can also settle on interior surfaces, to flake off at a later stage and be emitted with the exhaust gas (O'Regan, 1996). Re-entrained road dust is also a source of particulate matter (Wolff and Korsog, 1985). The larger particles usually comprise of earth crust materials and fugitive dust from roads and industries. The smaller particles are the secondarily formed aerosols (by nucleation and growth from gas to particles), and are composed mainly of sulphate, nitrate, ammonium, hydrogen ions, organic compounds, metals and particle bound water. The acid component of particulate matter, and the majority of its mutagenic activity, is generally contained in the fine fraction (Lodge, 1981; O'Regan 1996; Wilson and Suh, 1997). Particulates emitted from petrol-powered vehicles tend to be composed primarily of organic compounds, whereas for diesel-powered vehicles the particulate matter is composed of roughly equal parts of organic compounds and elemental carbon (Kleeman et al., 2000).

Figure 2.5 shows a shell model (in cross section) of a combustion particle (diameter about 35nm); species of low volatility are adsorbed on a carbonaceous core (diameter about 15nm)

with $PbBR_2$ islands (if operated with leaded fuel), covered by highly volatile species (Steiner *et al.*, 1992).

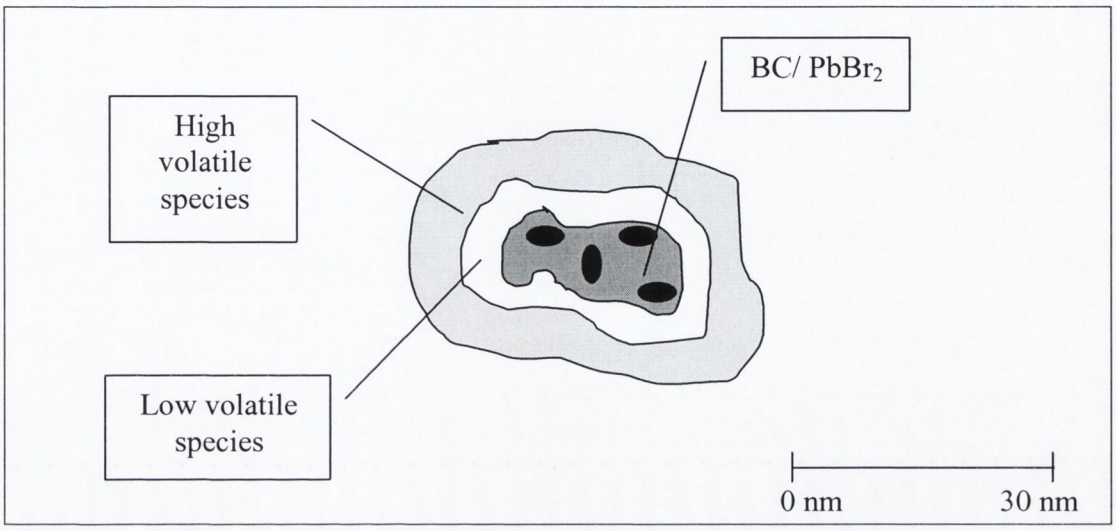

Figure 2.5 Shell model of a combustion particle (Steiner *et al.*, 1992).

2.1.3 Pollutant Impacts

In the 1960's, the main concern, particularly with particulate matter, was soiling; now visibility, material damage and especially health effects are considered more important (Tombach, 1985; Viles 1997). The effects of pollution on human health can be classified into four main categories, as shown in Table 2.2.

Table 2.2 Classification of pollutant health effects

Effect Classification	**Examples**
Irritation	Lachrymation due to smog, higher rates of bronchitis
Acute, direct, toxological	Deaths, e.g. Bhopal, 1984 and London, 1991 (details in Table 2.3)
Long-term, indirect	Absorption into food chain, acid rain
Carcinogenic, mutagenic	Cancer, genetic changes

The exact health and environmental impacts of various pollutant levels are still uncertain (Boddy, 1999). Air quality is affected by a large number of different pollutants, both gases

and suspended solids and liquids. As the relative percentages of these pollutants are constantly varying (British Lung Foundation, 1996), evaluation of the effect of any one pollutant or a particular mixture of pollutants is extremely difficult, and hence the health effects of various pollutant combinations in the short and long-term are unknown. Reports suggest that health hazards due to individual pollutants are increased by the combined pollution in the environment (Fukino *et al.*, 1994).

Carbon monoxide binds with the haemoglobin in the blood to form carboxyhaemoglobin, thereby reducing the capacity of the blood to carry oxygen round the body. First symptoms are headaches, blurry vision, difficulty in concentrating and confusion (Atimtay *et al.*, 2000). In lower concentrations, it may affect higher cerebral function, heart function and exercise capacity, all of which are sensitive to lowered blood oxygen content. In very high concentrations it is fatal due to cerebral and cardiac hypoxia (Lipfert, 1994).

Nitrogen dioxide can trigger biochemical reactions at relatively low concentrations due to its oxidising properties and has been found to induce three main types of respiratory effects:

- altered respiratory mechanics, such as localised constriction of the airways, resulting in uneven distribution of air and increased effort needed to breathe,
- increased incidence of human respiratory illness,
- ageing and chronic disease of the lung (Lipfert, 1994).

Suspended particulate matter is viewed as the most important air pollutant in terms of health (El-Fadel and Massoud, 2000). Individual particles can vary widely in composition and toxicity (Lipfert, 1994). The depth of penetration into the lungs depends on particle size. Individual health effects of various components of particulate matter are only now being defined (Moser *et al.*, 1996). However, there is consistent evidence from the United States and Europe that hospital admissions and emergency room attendances for respiratory complaints and asthma are related to the ambient levels of particulates (Harrison, 1996). There is also good evidence that short-term changes in mortality are also related to ambient particulate levels (Harrison, 1996; Ostro *et al.*, 1999), especially in countries with high

cardiovascular mortality (Nevalainen and Pekkanen, 1998), such as Ireland. Figure 2.6 shows the deposition of particulate matter in the respiratory system with respect to particle size.

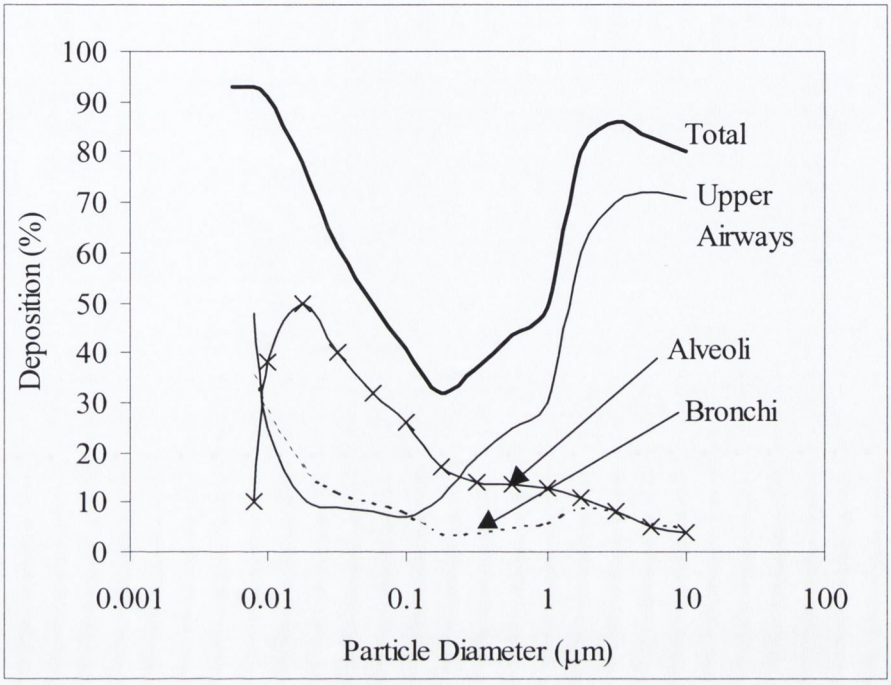

Figure 2.6 Deposition in the human respiratory system, with respect to particle size (Fenger, 1999)

2.1.4 The Role of Weather and Topography

While infrastructure and town planning determine emission patterns, meteorology and topography determine the extent of dispersion and transformation. Weather has a critical effect on pollutant concentrations in the air (Croxford *et al.*, 1995; Kassomenos *et al.*, 1995). The air pollution disasters detailed in Table 2.3 are all seen to be associated with calm conditions, with the Meuse Valley, Donora, and London (1952) episodes all featuring almost non-existent surface air motion and surface inversions caused by the condensation of fog, which persisted even through midafternoon (Boubel, 1994).

Table 2.3 Air pollution disasters (Brimblecombe, 1996)

Location					
Meuse Valley, Belgium, 1930	Donora, Pennsylvania, 1948	Pozo Rico, Mexico, 1950	London, UK, 1952	Bhopal, India, 1984	London, UK, 1991
Weather					
Anticyclonic inversion and fog	Anticyclonic inversion and fog	Nocturnal inversion, low winds	Anticyclonic inversion and fog	Nocturnal low winds	Anticyclonic inversion and fog
Mortality and Morbidity					
60 dead 6000 ill	15 dead 5900 ill	60 dead 6000 ill	22 dead	4000 dead >20000 ill	160 dead
Age Groups Affected					
Elderly	Elderly	All ages	Elderly at first		Patients with Respiratory illness
Sources					
Steel and zinc manufacture	Steel and zinc manufacture	Sulphur recovery (accident)	Domestic coal Burning	Fracturing of tank (accident)	Vehicles
Pollutants					
SO_2, smoke	SO_2, smoke	H_20	SO_2, smoke	Methyl-isocyanide	NO_2, particles

The weather can affect vehicular pollutant concentrations in three ways:

(i) by affecting rates of reaction and dispersion,

(ii) by causing a change in the modal split,

(iii) by changing individual driving patterns. A change in driving pattern, such as increased acceleration and deceleration will cause a change in emissions (O'Regan, 1996).

Wind

Wind speed is one of the most important meteorological parameters controlling pollutant concentrations, because the wind speed and its direction control the volume and dilution of the polluted air (Kartal and Özer, 1998). In general, low wind speeds result in high concentrations and vice versa (Harrison, 1999).

The initial transportation of pollutants from their source is determined by the wind direction at the source; therefore, the people most affected by air pollution are those who are downwind of major sources (Harrison, 1999). If the wind is blowing from a point source directly to a receptor, a change in wind direction of as little as 5° causes a reduction in concentrations at the receptor of about 10% under unstable conditions, 50% under neutral conditions and 90% under stable conditions (Boubel, 1994).

According to Croxford and Penn (1998), the majority of urban airborne pollution studies carried out to date have neglected to include full consideration of various meteorological factors. Through this lack of meteorological data, the effect of the prevailing wind direction on pollutant concentrations has been missed.

Wind can also play a role other than mixing and dispersal with respect to PM_{10} concentrations, as wind under certain conditions can cause recirculation and resuspension of particulate matter (Lam *et al.*, 1999).

Ireland and the rest of western Europe are influenced by a predominant south-westerly wind which brings moist air from the sea and favours long-range transport. In the northern part of Europe, the small amount of sunlight favours persistent inversions with poor dispersion conditions. In central and eastern Europe, high pressures with air stagnation and accumulation of local pollution are frequent. The Mediterranean region also suffers from this problem, although, in winter, large-scale wind systems are more frequent (Fenger, 1999).

Relative Humidity and Precipitation

For gaseous pollutants, relative humidity and precipitation do not have as significant an influence on ambient concentrations as wind. Precipitation reduces PM_{10} concentrations by 'washout' through agglomeration with the raindrops (Harrison, 1996). Differing opinions exist on the sensitivity of particle size to relative humidity (McMurray and Stolzenberg, 1989). Some studies have indicated that PM_{10} concentration in the ambient air is affected by the relative humidity (Monn *et al.*, 1997); whereas, in others, such as Lam *et al.* (1999), very little correlation was found.

Temperature

The most obvious significance of ambient temperature as an air pollution climatic factor is with respect to its influence on space heating requirements and the attendant discharge of pollutants into the atmosphere.

Ordinarily, cities are warmer than their nearby rural surroundings, particularly at night during light winds and clear skies, and this is known as the heat-island effect. Such conditions favour the formation of wind patterns in which the air near ground level converges towards the centre of the heat island. Furthermore, as the air moves across the city and is warmed, it becomes less stable. Thus, the urban heat island can have a profound effect on the transport and dilution of pollutants (Stern, 1976).

Atmospheric Stability

The relationship between pollutant concentrations and atmospheric stability is well known and has been reported in the literature by many authors (e.g., Benarie, 1980; Boubel, 1994), with more stable atmospheric conditions promoting the buildup of pollutants. Atmospheric stability is dependent on many factors such as the time of day, the synoptic weather conditions, and the nature of the earth's surface (Harrison, 1999).

Solar Radiation and Cloud Cover

The amount of solar radiation is not considered a significant parameter by many investigators as it has no direct physical influence on diffusion controls, although it does affect stability class. It could be also considered an indirect factor by influencing the amount of fuel consumed for space heating (Kartal and Özer, 1998). Solar radiation primarily affects the photochemistry of ozone, hydrocarbons, and oxides of nitrogen.

Topography

It is a common misconception that the presence of a valley or bowl is necessary for pollution build-up. Unfavourable topography is not a necessary condition for extreme pollutant

concentrations, provided the pollutant source strength is great enough compared with the total dispersal rate at the time (Wanta and Lowry, 1976).

Urban areas have different roughness and thermal characteristics to their rural surrounds. The increased roughness affects vertical wind and temperature profiles, although the effects due to the thermal features are dominant (Boubel, 1994).

2.1.5 Personal Exposure

As the majority of people's time is spent either at home or at work, these two environments are of particular importance. Studies have shown that the levels of pollution experienced while commuting by road to and from work are higher than those experienced at work or home (Flachsbart and Yo, 1987, as reported in Clifford *et al.*, 1997). The air inside a car acts as a buffer, damping out peaks in the external concentrations. Although the internal concentrations over a suitably long time-scale tend towards the external concentrations, the time taken to reach equilibrium is dependent upon the car ventilation, varying from 10 seconds with a window open, to ten minutes with windows and air vents closed. However, the presence of a 'dirty' vehicle in front of the driver has a significant effect on the levels of pollution inside the car (Clifford *et al.*, 1997). A similar situation exists with respect to indoor air quality, which is primarily dependent upon ambient pollution levels (Baek *et al.*, 1997).

2.1.6 Prediction of Air Pollution Levels

Air pollution models can be either physical (e.g. model in a wind tunnel) or mathematical. A mathematical model is an assembly of concepts or phenomena in the form of one or more mathematical equations, which approximate the behaviour of a natural system (Sivacoumar and Thanasekaran, 1999).

The spatial and temporal resolution of a model is determined by the structure of the model and the input data. Statistical models generally rely on several years of hourly or daily pollutant concentration data. The resolution of analytical models is limited by the spatial and temporal

resolution of the emissions inventory, meteorological fields and grid size chosen for the model implementation.

The accuracy of a model also depends on:
i) knowledge of the source strength;
ii) adequate definition of the meteorological parameters;
iii) reliable method for the calculation of dispersion from inputs (i) and (ii);
iv) adequate knowledge of pollutant losses (Benarie, 1980).

These factors can be further subdivided, so in predicting ambient concentrations from source estimates, 10 to 20 elementary individual processes must be estimated. Only a few of these can be calculated free of error, and many can only be estimated approximately, so that each model prediction may be tainted by large theoretical or instrumental uncertainties.

Different types of empirical/statistical and deterministic air pollution models are discussed in more detail in Section 9.

Another drawback with the use of models is that most dispersion models give predicted concentrations as 1-hourly averages, as the effect of meteorological variability over longer periods of time is difficult to model (Reynolds, 2000). It is therefore difficult to use most models for the purposes of estimating compliance with standards and legislation, as standards are defined over varying time periods.

Another less frequently used approach is to treat air pollution as a stochastic process, and derive a probability distribution for air pollutant concentration, by relating emission level to pollutant level (Morel *et al.*, 1999). The fundamental assumption underlying this approach is that concentrations of air pollutants are the combined results of pollutant emissions and stochastic effects, such as meteorological conditions. This technique can be used to obtain information on the degree by which existing emission levels may have to be decreased to achieve ambient air pollution targets (Morel *et al.*, 1999).

Frequency distributions can be used in a predictive capacity, although the distribution parameters must first be estimated. A hybrid deterministic-statistical approach is described in Jakeman *et al.* (1991) and Miles *et al.* (1991). The hybrid approach can be summarised in four steps:

i) Identify, from a range of alternatives, the appropriate probability distribution.
ii) Select an appropriate deterministic model to predict the properties of the probability distribution over the relevant period.
iii) Fit the predictions of the deterministic model in (ii) to the parametric form identified in (i) so that its parameters can be estimated.
iv) Calculate the desired extremes of the probability distribution for each period.

The disadvantages with this approach is that it is subject to many of the inaccuracies and errors of the deterministic models, as well as the time and expense of development and calibration. This thesis discusses a new method of using frequency distributions for the prediction of extreme events, based on the use of limited periods of short term monitoring rather than input from a deterministic model. The theoretical distribution is characterised by both the predicted monthly average (based on three days, or parts thereof, of short term monitoring, adjusted for relevant factors at the time of sampling) and the estimated standard deviation. This is then used to estimate peak 1-hour, 8-hour and 24-hour concentrations over longer periods.

2.1.7 Persistence Factors

Empirical relationships or 'persistence factors' can be used to convert estimated or measured concentrations over any specific time period to a different averaging period (Cooper, 1988; 1989). The US EPA (United States Environmental Protection Agency) recommends that a persistence factor for the estimation of 8-hour average concentrations from predicted 1-hour concentrations be calculated using data measured over three seasons (from October to April), although one or two can be used if three seasons of data is not available (US EPA, 1992). Factors should be calculated for each of the ten highest non-overlapping 8-hour concentrations and averaged. If less than three months of CO data are available then a default factor of 0.7 is

recommended. Cooper et al. (1992) recommend a factor of 0.55 for the conversion of 1-hour averages to 8-hour averages in Orlando, Florida, based on a statistical analysis of 10 years of data, coupled with modelling results. The problem with the estimation of concentrations in this manner is that, initially, the 1-hour average must be predicted using a model, and then the persistence factor applied. This involves two separate sources of error; firstly, in the 1-hour average concentration and secondly, in the application of the persistence factor. Another drawback is that if the recommended method of calculating the persistence factor is used, a considerable period of high temporal resolution concentration data is required. The results of the application of these persistence factors to the concentration data recorded in this study are discussed in Section 7.7.

Similarly, the US EPA (1992) recommends using a persistence factor of 0.08 to convert 1-hour PM_{10} concentrations to annual concentrations.

In the UK, the UK DETR (United Kingdom Department of the Environment, Transport and the Regions) state that the maximum 8-hour average for carbon monoxide is unlikely to exceed 10 ppm if the maximum 1-hour average does not exceed 12 ppm (UK DETR, 1998). This is equivalent to an upper bound persistence factor of 0.83. Similarly, the DETR states that the air quality objective of 50 $\mu g/m^3$ as the 99^{th} percentile of running 24-hour averages is unlikely to be exceeded where the annual mean concentration is less than 18 $\mu g/m^3$ (UK DETR, 1998).

The use of persistence factors to estimate peak values possesses a number of inherent disadvantages. Firstly, the use of peak values can be problematic as the maximum is the most difficult parameter to estimate (Miles *et al.*, 1991). Secondly, many of the standards and guidelines are expressed in terms of a certain permissible number of exceedences, and most work on persistence factors has dealt with the estimation of maximum values. Finally, as monitoring at high temporal resolution is generally more expensive than measuring longer-term averages using methods such as passive diffusion tubes, the use of 1-hour concentrations to predict long term or even annual concentrations is not the most efficient use of resources.

2.2 Policies and Standards

2.2.1 Basis for Ambient Air Quality Limits

The setting of standards depends on the risk management strategy adopted, which, in turn, is affected by the socio-political considerations and international agreements pertaining to the country in question (CEC, 1996)

Decisions can be based purely on health, cultural and environmental consequences with little weight to economic efficiency. This approach would have the effect of reducing the risk of adverse effects to a socially acceptable level. The second approach is based on a formal cost-effectiveness or cost-benefit analysis, with the objective of identifying the control action that achieves greatest net economic benefit or is the most economically efficient (WHO, 2000)

In setting air quality standards, it is necessary to define both the population and the effects from which the population is to be protected. The population at risk is that part of the population that is exposed to enhanced concentrations of air pollution. Each population has vulnerable sub-populations, which are then at a higher risk of developing adverse effects following exposure to pollutants, such as those suffering from concurrent diseases, or those with physiological limitations such as infants and the elderly. The sensitive groups in a population may vary across countries according to variables such as differences in medical care, nutritional status, lifestyle or prevalent diseases. Health effects range from temporary physiological or psychological changes through to acute illness and death. When health effects are either temporary and reversible or involve biochemical or functional changes with uncertain clinical significance, a judgement is required as to whether unknown or less serious effects should be taken into account.

When setting standards, the personal exposure of the population must be considered in conjunction with the pollutant concentrations in ambient air. The total exposure of individuals to pollutants is dependent on variables such as the time spent in polluted environments, outdoors, indoors, in-vehicle etc., and the various routes of intake of pollutants into the body

such as tobacco smoking. In deriving standards, the size of the population at risk is also an important factor to consider. Models of exposure estimates should be used in addition to ambient and indoor concentration monitoring.

Exposure response relationships are also of importance in the calculation of air quality limits. The percentage change of various health endpoints, such as daily mortality and hospital admissions can be derived. Assuming linearity, quantitative assessment of the unit risks provides an approximate estimate of responses at different concentrations. In the setting of standards, the definition of an acceptable risk is related to risk perception and economic and social circumstances (WHO, 2000).

The acceptability of risk may vary among countries because of differences in social norms, the degree of adversity and risk perception in the general population and because of the influences of various stakeholders. Risk acceptability is also influenced by how the risks associated with air pollution compare with risks from other pollution sources or human activities (WHO, 2000).

2.2.2 European Policies

In the European Union, the definition of limit values for ambient air quality is a multi-step process, with a system of EC Directives, the first being adopted in 1980. Since 1996, a Framework Directive (96/62/EU) provides a basic structure, and Daughter Directives lay down limit values and proscribe dates for attainment, methods for measurements and so on.

2.2.3 Irish Legislation

Prior to the introduction of the Air Pollution Act, 1987, in Ireland, there was no uniform legal system for the control of air pollution from emissions from domestic, vehicular, or industrial sources, although the following were in force:

♦The Alkali, etc. Works Regulation Act, 1906

This was in force until it was repealed under the Air Pollution Act, 1987 (Commencement) Order 1998, on 1st November 1998, and concerned the registration on an annual basis of all defined alkali, fertiliser, cement and smelting works.

♦The Public Health (Ireland) Act, 1878-1907

The Public Health (Ireland) Act, 1878 provided for the punishment of a number of statutory nuisances, including those arising from air pollutants. These were determined by two criteria: 1) if unlawful interference is caused with a person's use or enjoyment of land or of some right over and in connection with this; or 2) if the nuisance is injurious to health.

♦Local Government (Planning and Development) Act, 1963

Through the Local Government (Planning and Development) Act, 1963, planning authorities controlled, through their Development Plans, the location of developments likely to cause air pollution. It was also possible to attach conditions to permissions granted, in an attempt to prevent or limit air pollution, such as the height of stack and emission standards.

♦Local Government (Sanitary Services) Act, 1962

Two sets of regulations were made under Section 10 of the Local Government (Sanitary Services) Act, 1962: the Control of Atmospheric Pollution Regulations, 1970, and the Control of Atmospheric Pollution (Licensing) Regulations, (1985), both of which were later repealed under the Air Pollution Act, 1987. The Control of Atmospheric Pollution Regulations, 1970, prohibited the emission of smoke, dust, grit or fumes, from any premises other than a private dwelling, in such quantities as to be a nuisance to persons in any premises in the neighbourhood. The Control of Atmospheric Pollution (Licensing) Regulations, (1985), established a licensing system for the extraction or recovery of aluminium, zinc, copper, or lead by any process involving the application of heat.

♦Regulations under the European Communities Act, 1972

The regulations relating to air pollution made under the European Communities Act, 1972 were:

♦The European Communities (Sulphur Content of Gas Oil) Regulations, 1982, as amended by the European Communities (Sulphur Content of Gas Oil) (Amendment) Regulations, 1985,

♦The European Communities (Lead Content of Petrol) Regulations, 1980,

♦The European Communities (Lead Content of Petrol) (Amendment) Regulations, 1982,

♦The European Communities (Lead Content of Petrol) Regulations, 1985,

♦The European Communities (Lead Content of Petrol) Regulations, 1986.

The European Communities (Sulphur Content of Gas Oil) Regulations, 1982 limited the sulphur content of gas oil being used in the State. The European Communities (Lead Content of Petrol) Regulations set values for the lead and benzene content of petrol.

♦EU Directives

Prior to the Air Pollution Act, 1987, there also existed several other EU Directives relating to air pollution:

♦*Council Directive 80/779/EEC* on air quality limit values and guide values for sulphur dioxide and suspended particulates,

♦*Council Directive 82/884/EEC* on a limit value for lead in air,

♦*Council Directive 85/203/EEC* on air quality standards for nitrogen dioxide.

These were superseded by the Air Pollution Act, 1987, which provided a comprehensive legislative framework for the control of atmospheric pollutants. This was divided into six parts as follows:

Part I deals with matters of definition, administration and organisation, as well as matters relating to commencement and appeals,

Part II deals with general provisions relating to air pollution, and contains the general obligation of any premises (other than a private dwelling) to limit and to prevent emissions to the atmosphere,

Part III deals with the licensing of industrial plants,

Part IV deals with special control areas,

Part V deals with Air Quality Management Plans and Standards,

Part VI is a miscellaneous section.

Ambient air quality is currently regulated by EU Council Directive 96/62/EC of 27th September 1996 (CEC, 1996) on ambient air quality assessment and management. The objectives of this directive are to:

- define and establish objectives for ambient air quality in the European Community that will avoid, prevent and reduce harmful effects on human health and environment,
- assess ambient air quality in Member States on the basis of common methods and criteria,
- obtain adequate information on ambient air quality and ensure that it is made available to the public by means of, *inter alia,* alert thresholds,
- maintain ambient air quality where it is good and improve it in other cases.

Individual compound limit concentrations are set out in daughter directives (CEC,1999; EC, 1998) as detailed in Table 2.4, and are discussed in relation to the measured concentrations in Sections 4.1.1 to 4.1.4.

The main relevant current acts and statutory instruments relating to ambient air pollution are:

- Air Pollution Act, 1987 (Commencement) Order, 1987 (S.I. No. 201 of 1987)

This order brought the majority of the sections of the Act into operation on 1 September, 1987.

- Air Pollution Act, 1987 (Commencement) No. 2 Order, 1987 (S.I. No. 243 of 1987)

This order brought sections 50 and 52 relating to air quality standards into operation on 1st October, 1987.

- Air Pollution Act, 1987 (Air Quality Standards) Regulations, 1987 (S.I. No. 244 of 1987)

These regulations specify air quality standards for sulphur dioxide, suspended particulates, lead and nitrogen dioxide.

The implementation of the individual daughter directives under Council Directive 96/62/EC for CO, NO_2, and PM_{10} commence with PM_{10} Stage 1 in 2005.

Table 2.4 EU limit values for sulphur dioxide, nitrogen oxides, particulate matter, lead, carbon monoxide (proposed) and benzene (proposed)

Pollutant	Limit Value Objective	Averaging Period	Limit Value	Basis of Application of the Limit Value
SO_2	Protection of human health	1 hour	350 $\mu g/m^3$	Not to be exceeded more than 24 times/calendar year
SO_2	Protection of human health	24 hours	125 $\mu g/m^3$	Not to be exceeded more than 3 times/calendar year
SO_2	Protection of vegetation	Calendar Year	20 $\mu g/m^3$	Annual mean
SO_2	Protection of vegetation	1 Oct-31 Mar	20 $\mu g/m^3$	Winter mean
NO_2	Protection of human health	1 hour	104.6 ppb	Not to be exceeded more than 18 times/calendar year
NO_2	Protection of human health	Calendar Year	21 ppb	Annual mean
$NO+NO_2$	Protection of vegetation	Calendar Year	15.7 ppb	Annual mean
PM_{10} (Stage 1-2005)	Protection of human health	24 hours	50 $\mu g/m^3$	Not to be exceeded more than 35 times/calendar year
PM_{10} (Stage 1-2005)	Protection of human health	Calendar Year	40 $\mu g/m^3$	Annual mean
PM_{10} (Stage 2-2010)	Protection of human health	24 hours	50 $\mu g/m^3$	Not to be exceeded more than 7 times/calendar year
PM_{10} (Stage 2-2010)	Protection of human health	Calendar Year	20 $\mu g/m^3$	Annual mean
Lead	Protection of human health	Calendar Year	0.5 $\mu g/m^3$	Annual mean
CO (proposed)	Protection of human health	8 hours	8.7 ppm	Rolling 8-hour mean
Benzene (proposed)	Protection of human health	Calendar Year	5 ig/m^3	Annual mean

2.2.4 International Agreements on Pollution Control

The convention on Long-Range Transboundary Air Pollution was signed in Geneva in 1979 by 33 countries and was also signed and ratified by the EEC in 1989. It is a framework convention, under which states recognise the transnational problems of air pollution, and

accept their general responsibility to move towards a solution to these problems. It requires countries to gradually reduce and prevent air pollution and to exchange information on significant changes in air pollution levels, control technologies and approaches, and also to take account of the transboundary effect when authorising any new pollutant sources. The convention came into force in March 1983, after ratification by 24 of the signatories (Torvela, 1994).

The Executive Body of the Convention first met in June 1983 and agreed the necessity of developing abatement programmes to reduce SO_2 emissions by the mid-1990's. This led to the Helsinki Protocol, the legally binding commitment to reduce SO_2 levels by 30% by 1993. Twenty-five countries signed the equally binding Sofia Protocol, freezing NO_x emissions at 1987 levels, or those of any year before 1985. The protocol came into force on 14th February 1991, after ratification by 16 of the signatory countries. This was followed by a further agreement, called the NO_x Declaration, to reduce NO_x levels by 30% compared to 1987 levels.

A general agreement for the protection of the ozone layer was signed in Vienna, in 1985. Associated with this agreement, a protocol on the compounds associated with ozone layer depletion was signed, in Montreal, in 1987.

In June 1992, 120 heads of State attended the United Nations Conference on Environment and Development in Rio de Janeiro, Brazil, better known as 'The Earth Summit'. Among the agreements reached was Agenda 21. Agenda 21 is a comprehensive action plan to achieve more sustainable development for the twenty-first century, by incorporating environmental concerns into a wide range of activities. It recognises the need for both national and international actions and calls upon governments to prepare national strategies for sustainable development. The plan takes into consideration the needs of both developed and developing countries, especially the need to provide both financial and technological support in assisting developing countries to achieve these aims.

The United Nations Framework Convention on Climate Change was also signed in July 1992, in Rio de Janeiro. This Agreement is aimed at stabilising atmospheric concentrations of greenhouse gases at a level that would prevent harmful influence on climate.

The second Earth Summit was held in New York in June 1997 to review progress following the first Earth Summit. No major new developments were made, although commitment to sustainable development was renewed. A third summit is planned for 2002.

2.3 Summary of Irish Studies

Dublin Corporation is the main body responsible for ambient air quality monitoring in Dublin, although independent monitoring programmes have also been carried out. Dublin Corporation has a limited monitoring network at various sites around the city. SO_2 is measured at 14 sites, smoke at 14 sites, NO_x at one site, CO at one site, PM_{10} at five sites and $PM_{2.5}$ at one site (Reynolds, 2000). The EPA (Environmental Protection Agency) also measures NO_x at Rathmines and College Street and ozone at Pottery Road in Dun Laoghaire.

2.3.1 Review of Air Quality Information in Dublin

Recorded accounts of air quality in Dublin date back to World War II (Leonard *et al.*, 1940, 1941, 1950). During the 1960's, the Department of Local Government (Dawson, 1963, 1964, 1966) published reports on air pollution. Since 1974, yearly reports on air pollution in Dublin have been produced by the Air Quality Monitoring and Noise Control Unit of Dublin Corporation. The EPA (formerly the Environmental Research Unit) publishes reports on NO_x measurements at one site in Dublin. The publications reviewing air quality and emissions in Dublin are listed in Table 2.5.

Table 2.5 Publications reviewing air quality and emissions in Dublin

Year	Publications
1975 - 1979	McManus, 1975; McManus and Reilly, 1976; Bailey *et al.*, 1978; Nolan 1979; Walsh, 1976
1980 - 1984	Bailey and Walsh, 1980; Bailey, 1981; Bailey, 1983; Williams *et al.*, 1983; Bailey, 1984
1985 – 1989	Cabot, 1985; Bailey *et al.*, 1986; Reilly, 1986; Bailey, 1988; Dean, 1988; Delaney and Dowling, 1988; Flanagan *et al.*, 1988; Walsh, 1988
1990 – 1994	Sweeney, 1991; ENFO, 1992; Kelly, 1993; Spanton and McInnes, 1993
1991 – 1995	Envirocon, 1995; McGettigan and O'Donnell, 1995;
1996 – present day	Stapleton, 1996; McManus, 1998; Tarrant, 1999

Studies have been carried out to draw links between air pollution and health in Dublin by Chapman, 1965; De Wytt and Kevany, 1971; Kevany *et al.*, 1975; Ward *et al.*, 1978; Dean, 1988; Sinclair *et al.*, 1997; Kelly and Clancy, 1984; Dockery, 1999; Goodman *et al.*, 1999.

2.3.2 Carbon Monoxide

Dublin Corporation made measurements of CO levels in a once-off study in 1975. Urban ambient levels of CO have been measured since 1996. The annual average CO concentrations recorded during 1996, 1997 and 1998 were 1.95 ppm, 2.00 ppm and 1.72 ppm respectively.

2.3.3 Nitrogen Dioxide

Measurements of NO_2 were made in a single study by Dublin Corporation in 1975, although ongoing monitoring has only been carried out at a city centre site since 1988. The measured annual average NO_2 concentration in 1988 was 31 ppb. By 1990, this level had fallen marginally to 30 ppb. This trend then reversed, and by 1995 the level had risen to 47.8 ppb. The annual average during 1997 was 44.1 ppb. Passive sampling of NO_2 has been undertaken for the past number of years at various locations in the Greater Dublin Area by the three Dublin County Councils (Dublin County, 1999), and the results are summarised in Table 2.6.

Two concentrations in excess of 21 ppb (the new limit for NO_2 under EU Directive 1999/30/EC to be achieved by 2010, (CEC, 1999)) were recorded. In 1995, the annual average recorded by the EPA along one of the main commuter routes into the city was 20.2 ppb. This level remained fairly constant up until 1998, when the annual average was recorded as 9.6 ppb (significantly lower than the average readings recorded by Dublin County listed in Table 2.6) with monthly averages ranging from 7 ppb to 12 ppb. This decrease was caused by the monitoring equipment being moved back from the roadside, and up to a height of approximately 12 m, and as such did not represent a genuine decrease in ambient concentrations.

Table 2.6 NO_2 concentrations measured by passive sampling at various stations in Dublin (Dublin County, 1999)

	Average (ppb)		
	1996/1997	**1997/1998**	**1998/1999**
Balbriggan	21	18	18
Blanchardstown	18	16	18
Lissenhall	18	13	15
Clondalkin	14	12	
Naas Road	20	20	18
Rathfarnham	17	17	17
Lucan			22
Templeogue			23
Dun Laoghaire			10
Foxrock			13
Dundrum			7

2.3.4 PM_{10}

PM_{10} is currently being monitored at five sites throughout the city, two urban, two suburban, and one background. Annual averages are given in Table 2.7 for 1998. The concentrations at the urban sites are seen to be significantly higher than the suburban site, which is in turn higher than the background site. These concentrations are also significant from a legislative point of view as 49 $\mu g/m^3$ is higher than both Stage 1 and 2 of the Framework Directive

96/62/EC, to be attained by 2005 and 2010, respectively, and 38 $\mu g/m^3$ is above the value quoted for Stage 2.

Table 2.7 Annual concentrations of PM_{10} for 1998 (McGettigan, 2000)

Urban Sites	Suburban Sites	Background Site
49 $\mu g/m^3$ (Centre city)	19 $\mu g/m^3$ (Commercial)	14 $\mu g/m^3$ (Park)
38 $\mu g/m^3$ (Commercial)		

2.3.5 Smoke

Smoke levels have been measured extensively in Dublin. Mean annual concentrations of smoke showed a general downward trend from an average annual concentration of 128 $\mu g/m^3$ in 1963 to an average annual concentration of 27 $\mu g/m^3$ in 1978 (Figure 2.7). With the international oil crisis in the 1980's, there was a switch to coal for purposes of domestic heating, causing an increase in smoke levels. Since 1990, smoke levels have significantly decreased for two reasons, the banning of 'smokey' coal in 1990, and the switch to gas from solid fuel for domestic heating. The average annual concentration in 1998 was 12 $\mu g/m^3$.

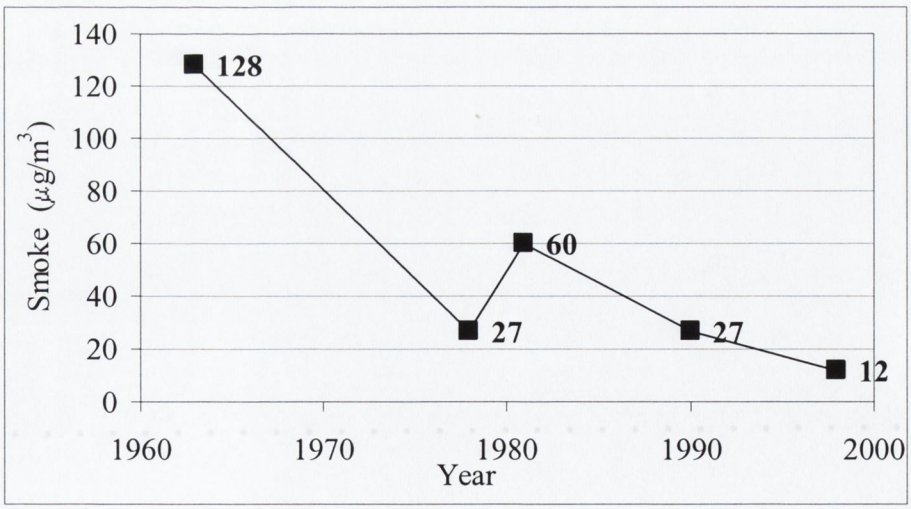

Figure 2.7 Long-term trends for smoke levels in Dublin (data from publications Table 2.5)

2.3.6 Sulphur Dioxide

The general trend for SO_2 levels in Dublin has also been downward, as shown in Figure 2.8. In 1971, annual average concentrations reached the highest value since records began of 100 $\mu g/m^3$. By 1984, the annual average level had fallen to 45 $\mu g/m^3$. Levels continued to decline in the late 1980's and early 1990's. This may be partly attributed to the change from oil to natural gas usage by the ESB (Electricity Supply Board) Poolbeg power plant, and by some factories and hospitals (Reynolds, 2000). Levels in the late 1990's rose slightly to 26 $\mu g/m^3$ in 1998.

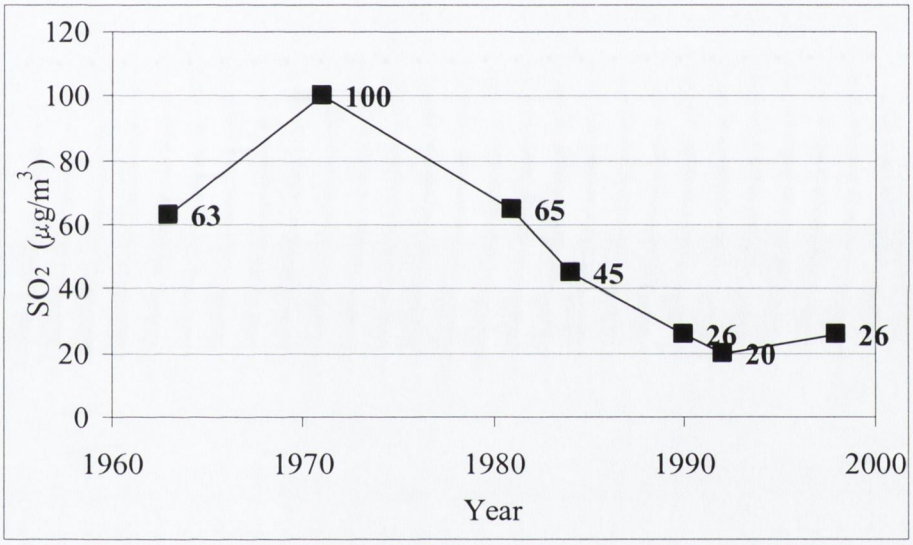

Figure 2.8 Long-term trends for SO_2 levels in Dublin (data from publications in Table 2.5)

2.3.7 Lead

Monitoring of lead in the ambient air in the city centre began in 1974. Again, there has been a downward trend in concentrations as shown in Figure 2.9, from between 2.2 $\mu g/m^3$ and 3.1 $\mu g/m^3$ in the late 1970's, to 0.5 $\mu g/m^3$ in 1988 and 0.13 $\mu g/m^3$ in 1997. This decrease in ambient lead levels can be attributed initially to a number of reductions in the level of lead in petrol, and subsequently to an increase in the proportion of sales of unleaded petrol since 1989, culminating in the banning of leaded petrol in January 1999.

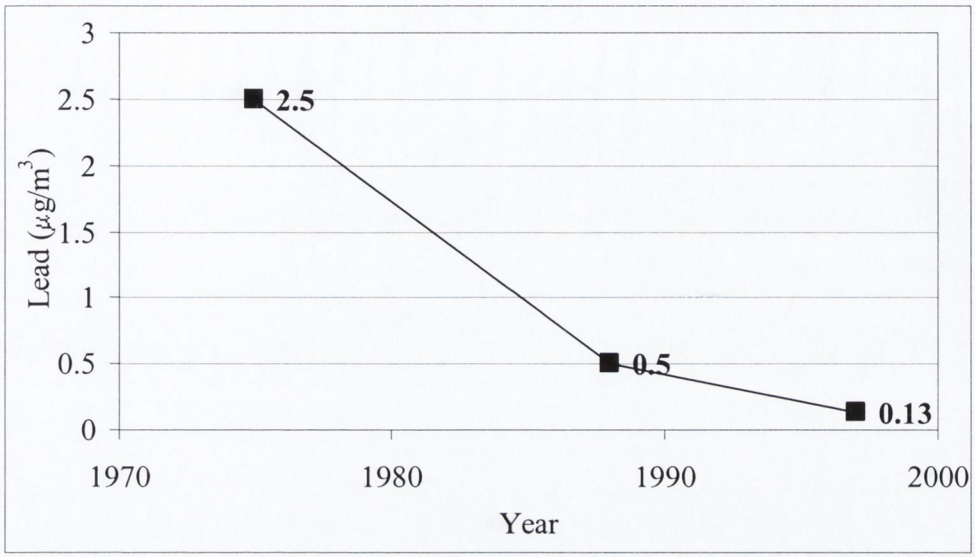

Figure 2.9 Long-term trends for lead levels in Dublin (data from publications Table 2.5)

2.3.8 Independent Studies

Several independent studies have been carried out in the past five years, the main findings of which are summarised below.

Concentrations of PM_{10} and certain VOCs (benzene, toluene and xylene) were measured over a 13-month period, from January 1996 to January 1997, as part of an EPA research study (Henderson *et al.*, 1997; Keary *et al.*, 1998). Results of the PM_{10} monitoring study are discussed in Keary (1997) and results of the VOC monitoring study are discussed in Shanahan *et al.*, (1997). PM_{10} concentrations were found to be higher in winter than summer, with daily maxima occurring between 8:00 and 10:00. PM_{10} concentrations were also found to be correlated with traffic counts. Passive diffusion tubes were used to measure benzene, toluene, and xylene levels over a 42-week period. The average annual concentrations were found to be 5.0 $\mu g/m^3$, 11.7 $\mu g/m^3$, 11.8 $\mu g/m^3$, and 14.9 $\mu g/m^3$ for benzene, toluene, p-xylene and m-,o-xylene respectively.

Healy and Dowling (1997, 1998), in conjunction with the Environmental Research Unit, investigated the level of PM_5 in Dublin, using a monitor attached to a bicycle. A particulate matter cyclone sampling head attached to a portable pump was used. The study confirmed that people in traffic experienced higher levels of PM_5 than average background values.

Envirocon (1996) measured roadside concentrations of NO_2 using passive diffusion tubes intermittently at one hundred locations between 1994 and 1996. Results are summarised in Table 2.8 and suggest exceedences of the EU limit value (21 ppb) given in Table 2.4. Maximum concentrations of 75.9 ppb to 84.3 ppb were recorded on Fleet Street, a street canyon with a high number of buses traversing it and idling on it, daily. Benzene, toluene and xylene were also measured at 51 sites, in conjunction with the NO_2 monitoring. The concentration ranges are shown in Table 2.9.

Table 2.8 Typical results for NO2 concentrations from Envirocon (1996)

Site Classification	Minimum	Maximum
Heavily trafficked	40 ppb	50 ppb
Pedestrian/Background	20 ppb	30 ppb

Table 2.9 VOC results measured by Envirocon (1996)

Compound	Average Minimum	Average Maximum
Benzene	1.5 ppb	5.0 ppb
Toluene	13.0 ppb	13.0 ppb
Xylene	7.8 ppb	7.8 ppb

3. DESCRIPTION OF MONITORING SITES AND APPARATUS

This chapter describes the ambient air quality monitoring carried out in this project. In Section 3.1, the monitoring programmes completed are discussed in relation to the compounds sampled and the periods of monitoring involved. The characteristics of each of the monitoring sites are then outlined in Section 3.2. Section 3.3 describes the traffic flow at each of the monitoring sites. Finally, Section 3.4 presents the equipment in the Trinity College Mobile Monitoring Unit.

3.1 MONITORING PROGRAMME

Monitoring of air pollutant concentrations was carried out at three sites in Dublin:

- Site A – the intersection of Pearse St. and Westland Row (Site A),
- Site B – Pearse St. (Site B),
- Site C – Westland Row (Site C).

The positions of the three monitoring sites in the city are shown in Figure 3.1

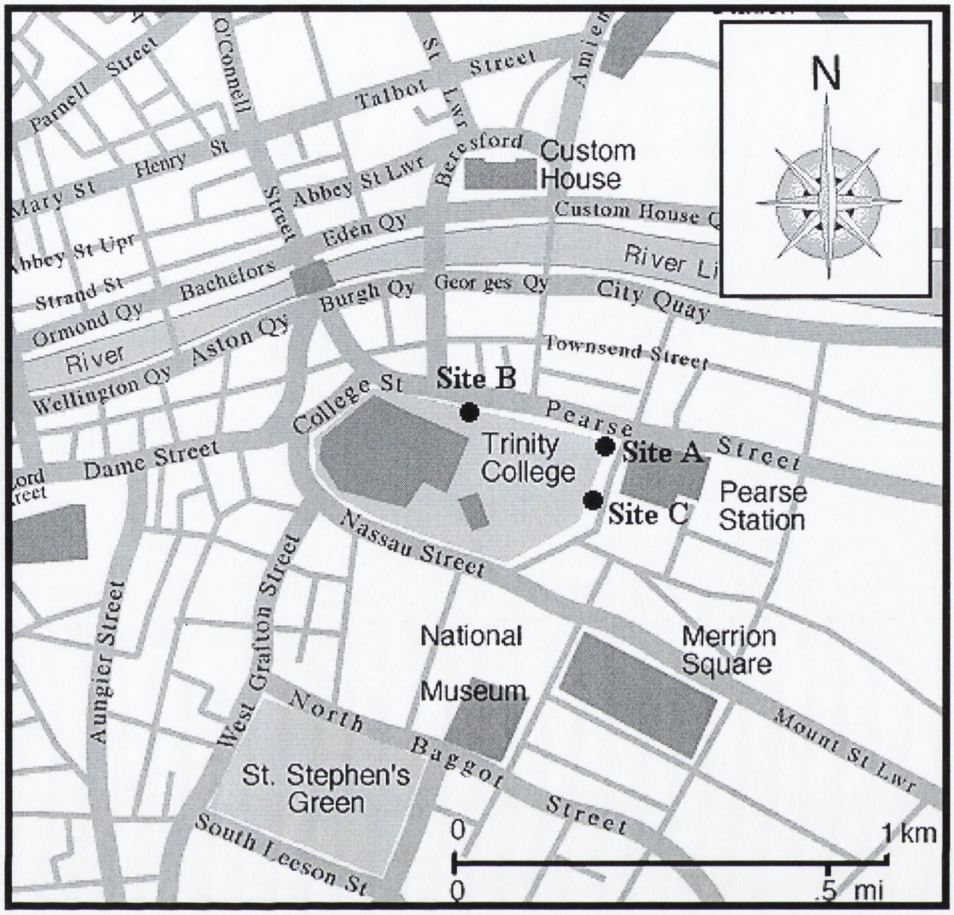

Figure 3.1 Positions of monitoring sites in Dublin city centre (map adapted from Magellan Geographix (2000))

Concentrations of CO, NO_2, PM_{10} and 27 VOCs were measured at the Pearse St./Westland Row Intersection, (Site A), using the Trinity College mobile monitoring unit, from December 1997 to January 1999. Concentrations of CO, NO_2, PM_{10} were then measured at Pearse St., (Site B), again using the Trinity College mobile monitoring unit, from February 1999 to April 1999. Further monitoring of CO, SO_2, NO_2, NO and NO_x, PM_{10}, $PM_{2.5}$ and PM_1, plus benzene, toluene and xylene was carried out at the Pearse St./Westland Row intersection, (Site A), by the EPA, from June 1999 to December 1999. Finally, NO and NO_2 concentrations were measured by the ESB (in collaboration with the Department of Civil, Structural and Environmental Engineering, TCD) at Westland Row, (Site C), from July 1999 to November 1999 and are also analysed. A schematic diagram of the calendar of monitoring is given in Figure 3.2.

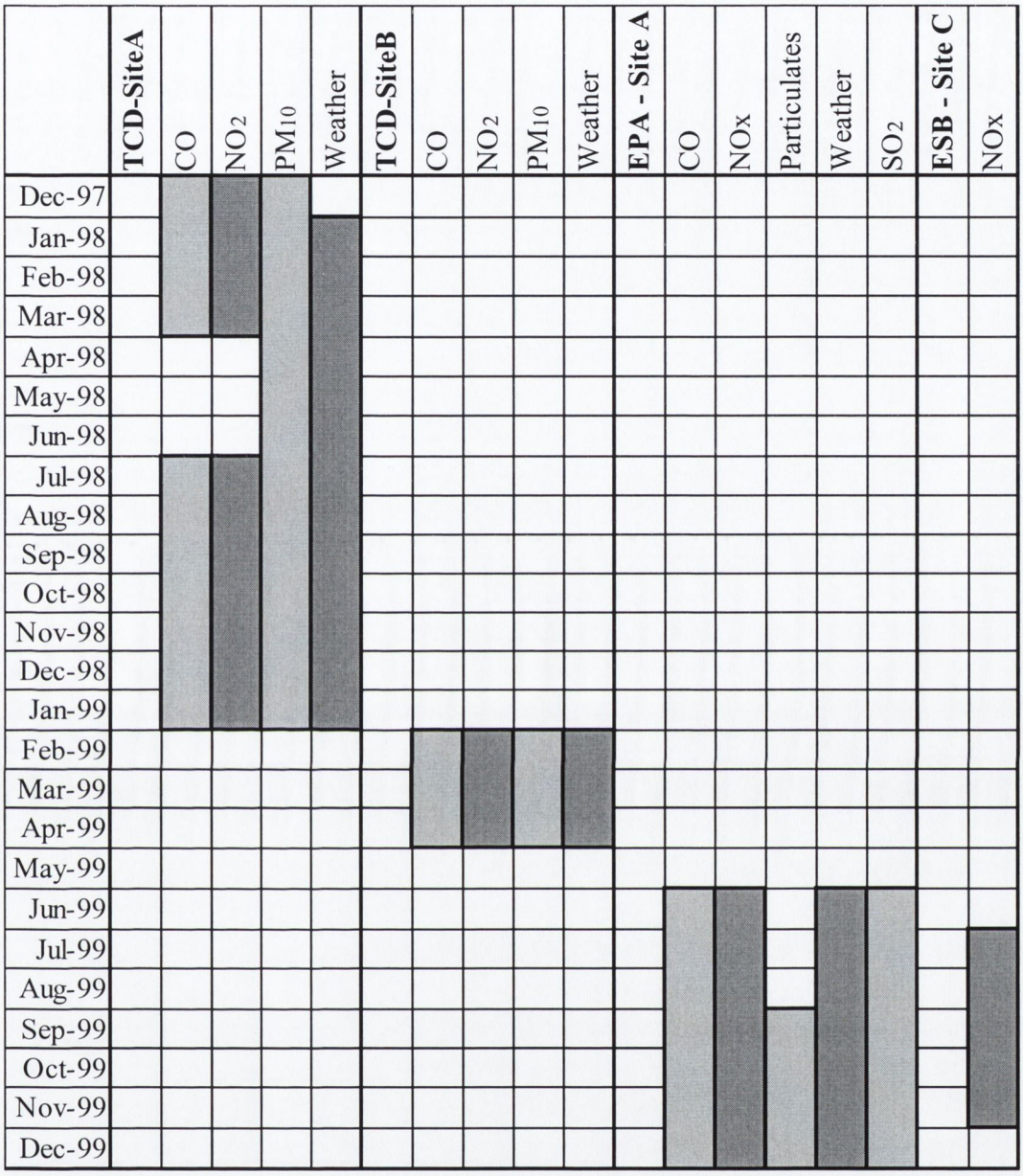

Figure 3.2 Timetable of monitoring carried out by TCD, EPA and ESB.

3.2 Site Descriptions

Analysis of ambient air quality measured at three different sites was carried out. The monitoring sites were chosen to represent a cross section of typical urban sites, with a junction site (Site A), typical urban street (not canyon) with nearby junctions (Site B) and an urban

canyon site (Site C), conforming to EU regulations on the location of sites for compliance with legislative limits.

The Pearse St./Westland Row monitoring site, (Site A), was located at an arterial four-way signalised junction in the heart of Dublin City, which is characterised by high local congestion. It is one of the busiest signalised intersections in the city, with over thirty-five thousand vehicles crossing the junction on weekdays. The junction geometry is depicted in Figure 3.3, with arrows indicating the direction of traffic lanes, and the broken arrows indicating bus lanes. Lombard Street is a one way street with three lanes; Pearse Street is also one way, with four lanes; and Westland Row has one lane travelling in each direction. Traffic flow characteristics for the sites are discussed in Section 3.3.

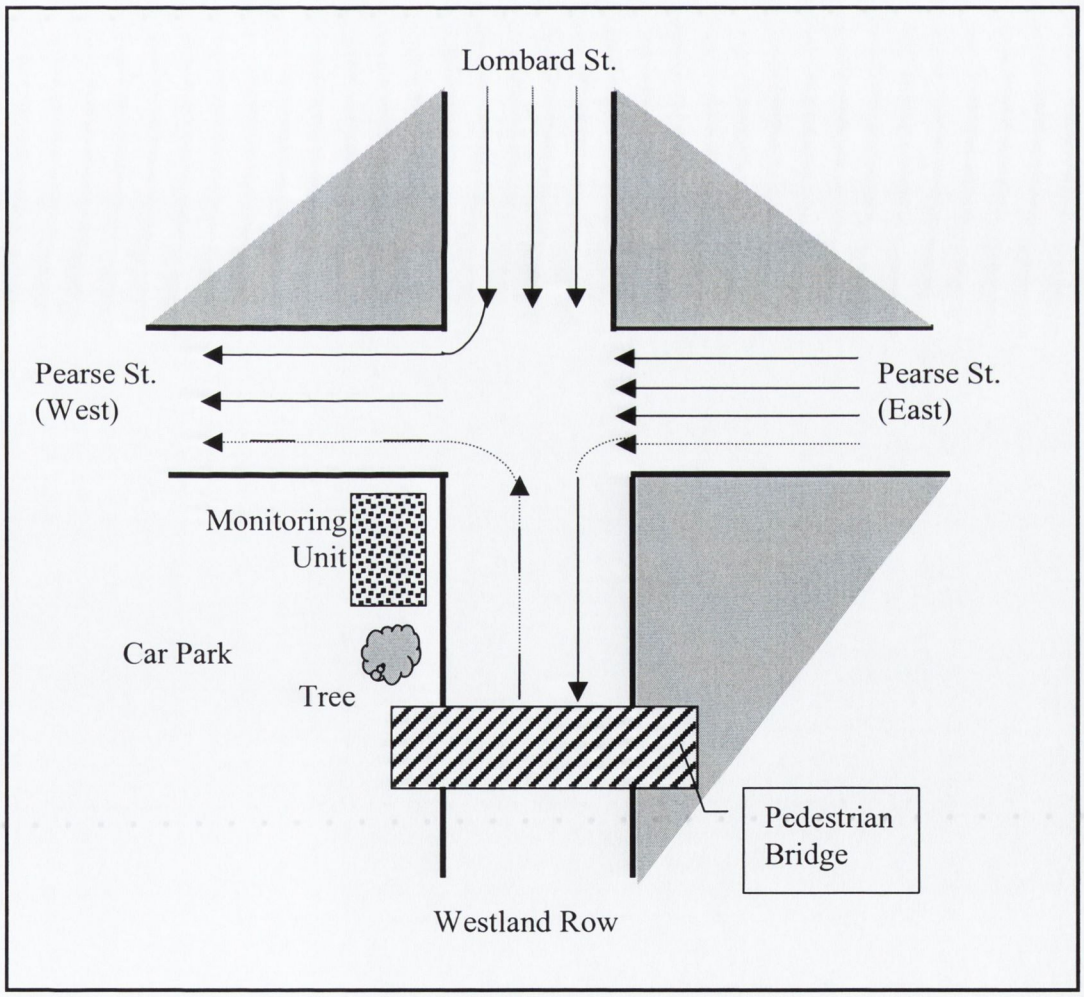

Figure 3.3 Schematic representation of intersection at Site A

The inlet of the CO and NO_2 analyser was situated 3 m away from the edge of the road at a height of 1.5 m. The PM_{10} monitoring inlet and meteorological equipment were located on top of the mobile monitoring unit, 3 m from the edge of the roadside and at a height of 3 m and 4.5 m respectively. The location did not fulfil the EU requirements for sampling locations due to the proximity of the junction.

For Phase 2 of the monitoring, the same site was used, although the EPA meteorological equipment was not raised above the roof of the its mobile monitoring unit, and was located at the back of the unit closer to a tree and a pedestrian bridge crossing Westland Row.

The second monitoring site was located at Pearse St., (Site B). Approximately 35,000 vehicles pass the monitoring site on weekdays (the break-down of vehicle types is discussed in Section 3.3). Pearse St. is one of the main arterial routes in the city, and as a result is congested during rush-hours. An important feature of the site is its close proximity to a number of bus stops, with a high number of buses idling or passing from early morning to late evening. The section of the street where monitoring was carried out is moderately open, and unlike Westland Row, (Site C), could not be classified as a street canyon.

At Site B, the CO and NO_2 inlet was located at a height of 1.25 m above pavement level and 2m from the roadside. As the mobile monitoring unit was situated on a level below that of the pavement level, the monitor inlet heights differ from Site A. The particulate inlet and weather equipment was located 1.3 m above pavement level, at a distance of 3.5 m from the roadside. Again the site did not fulfil the EU requirements for sampling locations due to the proximity of a junction.

Monitoring was also carried out on Westland Row, (Site C). Approximately 12,000 vehicles pass the monitoring site each working day. The street may be classified as a street canyon, as it is relatively narrow, and lined with tall buildings on either side. Traffic flow characteristics for the site are discussed in Section 3.3.

At Site C, the inlet for the analyser was situated 4 m above pavement level and approximately 7 m above basement level. The inlet was 3 m from the edge of the road, 1 m out from the wall of the building, and 0.7 m away from the nearest obstruction (balcony). These parameters fulfil the requirements for sampling locations defined in the EU Directive 96/62/EC on ambient air quality assessment and management (CEC, 1996).

3.3 Traffic Flow Characteristics

Traffic counts were carried out, both manually and using induction loops embedded beneath each road lane. Sample traffic flows are shown for Wednesday, 28th January 1998, for Sites A and C, in Figure 3.4. Sample traffic flows for Site B are shown in Figure 3.5.

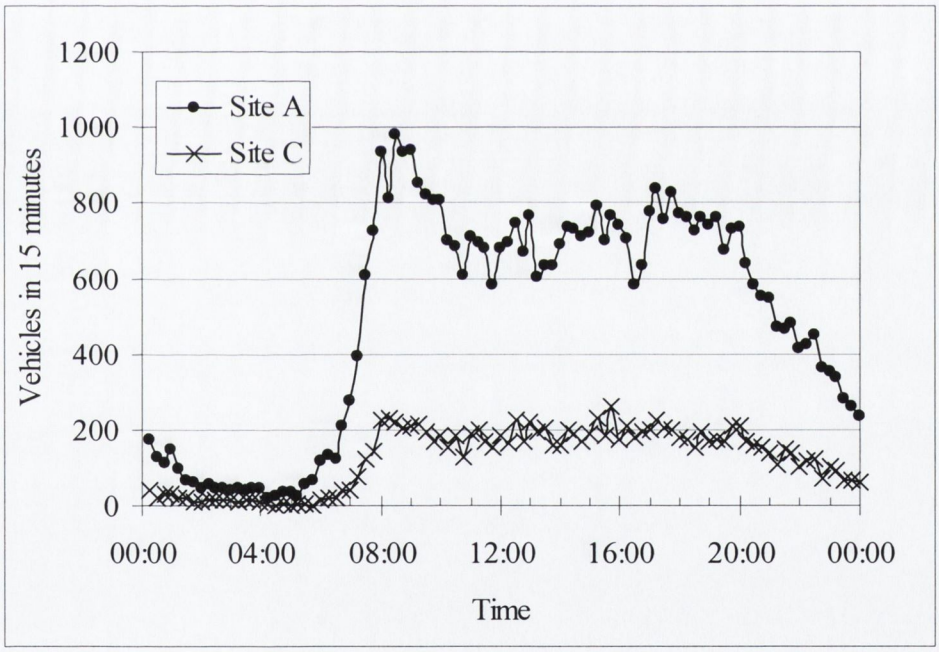

Figure 3.4 Traffic flow past monitoring sites A and C on Wednesday 28th January, 1998

Using a video camera set up at the junction, morning peak hours (8:00 – 9:00) and off-peak hours (14:00 – 15:00) were recorded to investigate fleet characteristics. Vehicles were split into five categories: passenger cars, light goods vehicles (LGVs), heavy goods vehicles (HGVs), buses and motorcycles (MCs). The vehicle mixes for peak and off-peak hours are

given in Table 3. 1. The number of cars as a proportion of the total number of vehicles is seen to drop at off-peak hours. Not evident from the categorisation of vehicles is that buses spend a significant amount of time idling in the vicinity of Site B, waiting to pick up passengers and subsequently accelerating on departure.

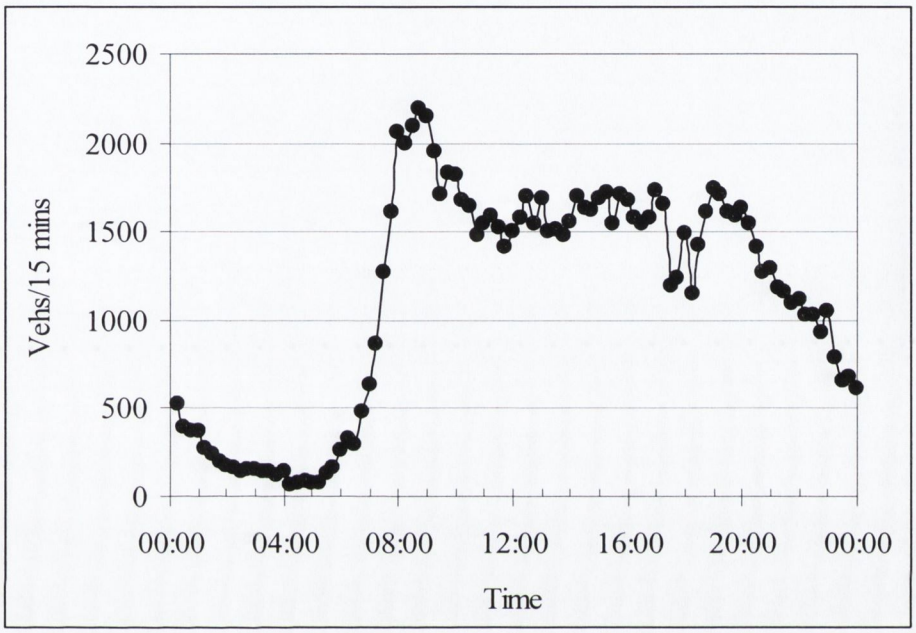

Figure 3.5 Sample traffic flow for Site B

Table 3. 1 Categorisation of traffic at monitoring sites A and C during peak hour (08:00 – 09:00) and off-peak hour (14:00 – 15:00)

Time	Site	Cars (%)	LGVs (%)	HGVs (%)	Buses (%)	MCs (%)
Peak	Site A	86.3	7.0	2.4	2.1	2.1
	Site C	84.7	7.7	1.9	3.4	2.4
Off-Peak	Site A	73.8	17.0	4.3	1.0	4.0
	Site C	73.2	12.2	4.1	7.2	3.3

3.4 Description of Monitoring Equipment

3.4.1 Carbon Monoxide Monitoring Equipment

CO levels were measured using a Siemens Roadside Pollution Monitor (RPM). The RPM uses electro-chemical cell technology. A pump is used to pull air through a filter and humidity exchanger and then over the cells at approximately 2 l/m. Each cell outputs an analogue signal, which is automatically converted into pollutant concentration using specified conversion formulae which take into account temperature, cross-sensitivity, and the degradation of the cells over time. Prior to installation, the cells are calibrated in the laboratory, and no other recalibration is required until the refurbishment of the equipment, approximately every 18 months.

Boddy (1999) found CO concentrations recorded using the RPM to be well correlated with on-street levels, with an R^2 value of 0.9 (R^2, the coefficient of determination, is defined in Appendix A). A maximum discrepancy of 1 ppm was calculated between the RPM and on-street concentrations.

3.4.2 Nitrogen Dioxide Monitoring Equipment

NO_2 concentrations were also measured using the RPM. However, the electrochemical cells for NO_2 are more unstable than those for CO, and regular recalibration is required. This is done automatically on-street at night when NO_2 levels should be low. NO_2 is removed from a sample using an internal scrubber, and that sample is then used to reset the baseline.

Boddy (1999) found the NO_2 data to be less well correlated with on-street concentrations of NO_2, with an R^2 value of between 0.5 and 0.7, although readings were generally within $\pm$ 20 ppb of the on-street concentration.

3.4.3 Particulate Monitoring Equipment

Concentrations of PM_{10} were measured using a Rupprecht and Pataschnick TEOM (**T**apered **E**lement **O**scillating **M**icrobalance), which is a designated US EPA equivalent method (Allen *et al.*, 1997). The TEOM measures the accumulation of mass on a heated filter attached to the tip of a hollow, tapered, oscillating, glass rod. The resulting change in the oscillation frequency is used to make a direct measurement of the accumulation of mass on the filter over time, with none of the assumptions used by all other non-inertial or non-gravimetric methods (Patashnick, 1998a). The flow through the filter is measured with a mass flow meter. Concentrations of PM_{10} are measured every 2 seconds from those two measurements, and the chosen averaging period dictates how rapidly mass change is displayed to the user (Patashnick, 1998b). The TEOM is fully described in Patashnick and Rupprecht (1991).

Unfortunately, some components of motor vehicle related particulate matter, such as ammonium nitrate, will be volatilised to varying degrees during residence on the filter. Hence TEOM reported concentrations in areas where there is a high volatilisable fraction in the particulate matter may produce readings that are lower than the true values (Allen *et al.*, 1997; Salter and Parsons, 1999); the extent of this underestimation is dependent on location.

3.4.4 VOC Monitoring Equipment

Monitoring of VOC concentrations was carried out using a Perkin-Elmer system comprising of an Autosystem GC (gas chromatograph) and an ATD thermal desorption unit. Ambient air is drawn in to the system at a flow rate of 15 ml/min for 40 minutes, and dried before entering the cold trap, where it is cooled to -30°C to retain any VOCs other than methane, before being heated to 400°C and flushed with hydrogen. The autosystem GC is equipped with BP1 and PLOT capillary columns connected to a flame ionisation detector. Analysis of the sample takes 20 minutes, at which point the next air sample starts to be collected. The VOC monitoring equipment is described in detail in Marnane (2000).

3.4.5 Meteorological Equipment

Wind direction and wind speed are measured by a wind vane and anemometer, respectively, attached to a telescopic pole on the roof of the mobile unit. In addition, two probes measure relative humidity and temperature. All are connected to a data logger within the mobile unit.

4. MONITORING RESULTS

This chapter presents the monitoring results for each site and statistical analysis of the concentration data. Section 4.1 summarises the recorded concentrations. Data recorded by TCD from January 1998 to January 1999 at the Pearse St./Westland Row Intersection is compared with the data recorded by the EPA at the same site from July 1999 to December 1999, in Section 4.2. In Section 4.3, the recorded data is analysed to determine the theoretical distribution that best fits the observed distribution, which, as will be discussed at a later stage, in Section 6.12, is important for the prediction of 1-hour, 8-hour and 24-hour peak concentrations. Conclusions to this chapter are in Section 4.4.

4.1 Data Summary

In the following sections, data capture rates are presented for each compound and monitoring period, as are the averages, minima, maxima and selected percentile values of the measured concentration data. The validity of the measurements is then evaluated by considering the values recorded by two different sets of monitoring equipment at the same site.

4.1.1 Site A (Pearse Street/Westland Row Junction) – Phase 1

Monitoring was carried out from January 1998 to January 1999, at the junction of Pearse Street and Westland Row. The percentage data capture rate is given in Table 4.1. No CO or NO_2 data were recorded during May 1998 and June 1998, and very little during April 1998 and July 1998, due to problems with the recalibration of the RPM, and possible damage done to the instrument in transit. Data capture rates for the TEOM were, in general, very high, with only two months (May 1998 and December 1998) below 50%. The data capture rates for the weather equipment were consistently high, with only May 1998 below 50%.

Table 4.1 Percentage data capture rates for variables measured during monitoring, Phase 1.

	NO_2 (%)	CO (%)	PM_{10} (%)	Weather Data (%)
Jan-98	99	99	88	100
Feb-98	99	99	99	100
Mar-98	99	48	98	100
Apr-98	12	11	90	70
May-98	0	0	44	45
Jun-98	0	0	89	100
Jul-98	32	32	97	100
Aug-98	99	99	95	100
Sep-98	62	63	94	74
Oct-98	98	97	94	96
Nov-98	98	98	91	95
Dec-98	95	95	48	100
Jan-99	96	96	73	100

The average pollutant concentrations measured at the Pearse St./Westland Row intersection are given in Table 4.2. The measured hourly concentrations did not exceed the limit value of 104.6 ppb under EU Directive 1999/30/EC (CEC, 1999) (detailed in Table 2.4), to be achieved by 2010. All monthly NO_2 averages were below 40 ppb, although higher than the majority of urban NO_2 average concentrations measured by Dublin Corporation in 1998 (Section 2.3.3), and lower than the typical concentrations at heavily trafficked sites measured by Envirocon (1996).

The monthly CO average for January 1998 was significantly higher than the other monthly averages. This was not reflected by particularly high CO concentrations during January at the Dublin Corporation roadside monitoring site on College Green (at the junction of College St. and Dame St., as seen in Figure 3.1). This would seem to indicate that elevated concentrations were not experienced throughout the city. CO concentrations measured at Site A are, in general, lower than the Dublin Corporation measured concentrations.

The CO and NO_2 concentrations measured during January 1998, February 1998 and March 1998 were significantly higher than the concentrations measured after the recalibration of the monitor. (The monitor was recalibrated due to the decrease of the measured CO concentrations to close to zero over the course of several days.) This raises severe doubts as to the validity of the absolute concentrations, when the significant , especially in view of the fact that elevated concentrations were not measured at the nearby College Green site. However, the relative concentrations displayed the same temporal patterns as the

concentrations measured after the recalibration, indicating that the concentrations could still be used to investigate the relative relationships of these compounds to other variables.

PM_{10} monthly averages ranged between 13.63 $\mu g/m^3$ and 28.26 $\mu g/m^3$. The annual average concentration recorded at Site A was 35% and 46% of the two annual urban PM_{10} concentrations measured by the EPA, listed in Table 2.7.

Table 4.2 Average pollutant concentrations measured at Pearse St./Westland Row Intersection

	Average NO_2 (ppb)	**Average CO (ppm)**	**Average PM_{10} ($\mu g/m^3$)**
Jan-98	39.8	2.67	22.10
Feb-98	34.8	1.58	16.72
Mar-98	38.8	1.56	20.21
Apr-98	Insufficient Data	Insufficient Data	18.79
May-98	Insufficient Data	Insufficient Data	21.95
Jun-98	Insufficient Data	Insufficient Data	16.69
Jul-98	27.4	0.45	11.90
Aug-98	28.1	0.51	14.70
Sep-98	24.5	0.75	21.05
Oct-98	24.4	0.69	13.63
Nov-98	25.5	1.02	15.29
Dec-98	25.6	1.01	19.61
Jan-99	25.0	0.74	28.26

The maximum and 95th percentile values for averaging periods of 1-hour, 8-hours and 24-hours for CO, NO_2 and PM_{10} are given in Table 4.3, Table 4.4 and Table 4.5, respectively. The 95th percentile is given as a more robust indicator of high concentrations compared to the maximum concentration, which exhibits a high degree of variability.

With respect to CO, the highest concentrations in each category occurred in January 1998. However, at no time were the measured concentrations higher than the proposed limit value under EU Directive 96/62/EC. Although, as mentioned before, the significantly higher CO concentrations recorded prior to the recalibration of the instrument raise doubts as to the accuracy of these readings, although relative concentrations were found to follow the same patterns as those measured after the recalibration. Outside this period the highest concentrations recorded were in December 1998. High concentrations were recorded over the course of 6th December, coinciding with particularly low wind speeds from the direction of the junction. The lowest concentrations in all categories were recorded in either July 1998 or August 1998.

The majority of the highest NO_2 values were also recorded in January 1998. The peak 1-hour average was recorded during March 1998, with a value of 132.5 ppb, although this was an isolated peak concentration, with elevated concentrations lasting only for approximately one hour. Disregarding the period before the recalibration of the instrument, the highest concentrations occurred during August 1998. High NO_2 concentrations were measured on the 21st August, peaking in the early afternoon. Although wind speed was not lower than average, the wind was blowing from the direction of the junction during the course of the day. The majority of the lowest values were recorded during January 1999, indicating the lack of a consistent seasonal trend.

Conversely, the majority of the highest PM_{10} concentrations were recorded during January 1999, with particularly high concentrations measured on the 10th, 30th and 31st of January, all days with a low average wind speed (less than 1 m/s), although the wind speed was not blowing consistently from the direction of the junction. Most of the lowest average concentrations were recorded in July 1998 and August 1998, generally coinciding with periods of above average wind speed.

Table 4.3 Maximum and 95th percentile values for CO

	Maximum Values (ppm)			**95th Percentiles (ppm)**		
	1 hour	**8 hours**	**24 hours**	**1 hour**	**8 hours**	**24 hours**
Jan-98	19.11	9.19	6.10	7.79	7.13	5.21
Feb-98	13.63	7.32	4.28	4.40	3.61	3.18
Mar-98	12.70	4.66	3.41	4.14	3.51	3.08
Apr-98	Insufficient Data			Insufficient Data		
May-98	Insufficient Data			Insufficient Data		
Jun-98	Insufficient Data			Insufficient Data		
Jul-98	3.47	2.02	0.90	1.04	1.06	0.79
Aug-98	2.82	1.84	1.17	1.48	1.37	1.06
Sep-98	4.42	2.50	1.60	1.99	1.91	1.43
Oct-98	3.87	2.31	1.40	1.74	1.50	1.24
Nov-98	8.02	5.15	3.22	3.51	3.44	2.84
Dec-98	9.68	7.57	4.35	2.65	2.53	2.05
Jan-99	7.05	3.04	1.70	2.04	1.80	1.47

Table 4.4 Maximum and 95th percentile values for NO_2

	Maximum Values (ppb)			95th Percentiles (ppb)		
	1 hour	**8 hours**	**24 hours**	**1 hour**	**8 hours**	**24 hours**
Jan-98	90.0	63.4	52.5	57.5	54.4	49.7
Feb-98	60.0	50.9	42.8	50.0	45.5	41.0
Mar-98	132.5	60.0	46.8	52.5	49.4	44.7
Apr-98	Insufficient Data			Insufficient Data		
May-98	Insufficient Data			Insufficient Data		
Jun-98	Insufficient Data			Insufficient Data		
Jul-98	65.0	50.0	33.1	40.0	35.9	32.0
Aug-98	67.5	55.6	45.1	45.0	41.6	36.6
Sep-98	45.0	33.8	29.5	32.5	31.3	27.4
Oct-98	45.0	36.3	31.1	32.5	30.9	29.2
Nov-98	60.0	44.1	34.1	40.0	35.2	31.0
Dec-98	60.0	43.1	36.0	35.0	31.9	31.0
Jan-99	45.0	32.5	30.4	30.0	30.6	29.1

Table 4.5 Maximum and 95th percentile values for PM_{10}

	Maximum Values ($\mu g/m^3$)			95th Percentiles ($\mu g/m^3$)		
	1 hour	**8 hours**	**24 hours**	**1 hour**	**8 hours**	**24 hours**
Jan-98	100.25	59.21	43.78	53.20	48.57	39.51
Feb-98	91.75	61.33	40.51	37.80	32.23	28.95
Mar-98	73.10	46.45	38.35	41.32	37.31	33.62
Apr-98	73.30	50.77	39.54	42.29	38.58	33.09
May-98	64.55	41.41	37.83	40.70	38.10	33.98
Jun-98	145.25	51.22	38.54	40.13	39.09	33.92
Jul-98	44.80	31.96	24.31	25.25	21.22	17.91
Aug-98	52.20	34.65	28.70	31.35	26.98	25.26
Sep-98	70.40	53.18	45.92	46.65	42.74	40.42
Oct-98	107.55	61.19	32.94	29.07	25.36	23.72
Nov-98	79.10	61.76	42.26	40.97	38.46	33.62
Dec-98	81.30	52.62	39.10	42.15	37.51	31.00
Jan-99	141.30	97.84	65.87	65.05	60.37	52.80

Meteorological Data

The prevailing wind at the monitoring station came from the south-west. As shown in Figure 4.1, this meant that for the majority (74%) of the time, the wind was not blowing directly from the junction.

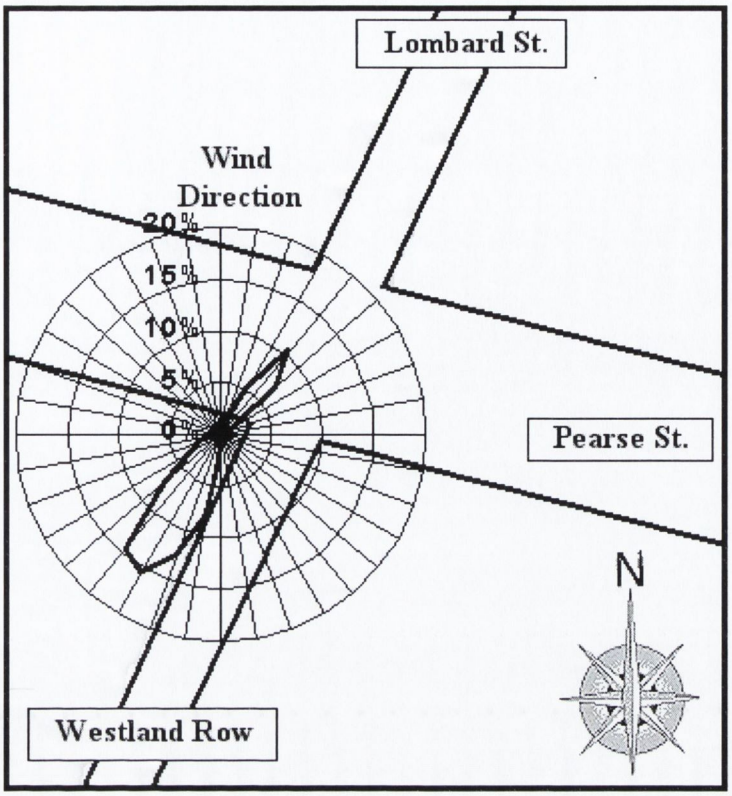

Figure 4.1 Wind rose superimposed on a schematic diagram of Pearse St./Westland Row intersection

Figure 4.2 shows the average monthly wind speeds recorded at the Pearse St./Westland Row intersection monitoring site. The average wind speed recorded at the site was 1.93 m/s.

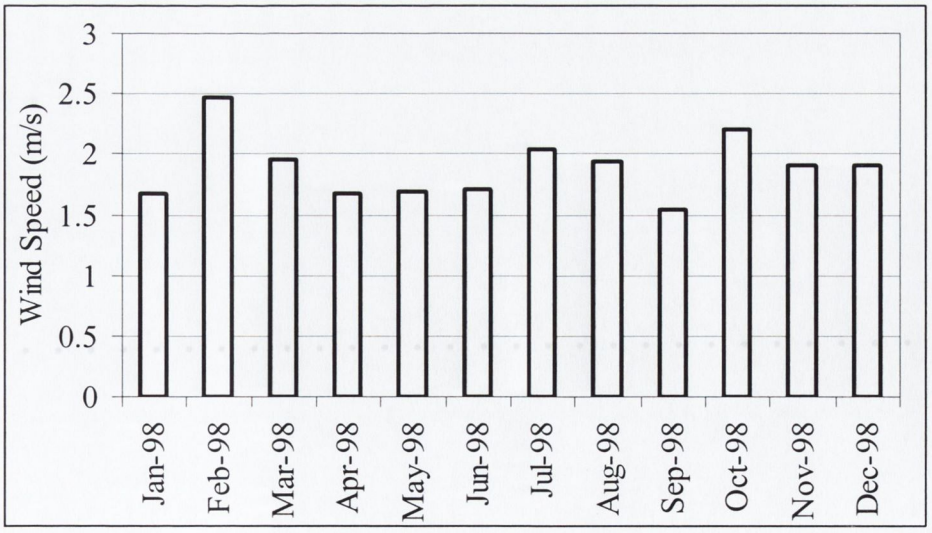

Figure 4.2 Average monthly wind speed at Pearse St./Westland Row intersection.

4.1.2 Site A (Pearse Street/Westland Row Junction) – Phase 2

Levels of CO, NO_2, and PM_{10} were recorded hourly from 17th July to 15th December 1999, by the EPA. A detailed comparison of these results with the TCD results is carried out in Section 4.2. Percentage data capture rates are given in Table 4.6. Data capture rates for CO and NO_2 during July 1999 and December 1999 are low as the monitoring programme began and ended during these months.

Table 4.6 Percentage data capture rates for monitoring conducted at Pearse Street – Westland Row Intersection (Phase 2)

	NO_2 (%)	CO (%)	PM_{10} (%)
Jul-99	51	51	0
Aug-99	88	100	0
Sep-99	94	78	90
Oct-99	86	87	75
Nov-99	100	100	100
Dec-99	46	47	46

The monthly average pollutant levels are given in Table 4.7. EU limit values were not exceeded for any pollutant. Average CO concentrations ranged between 0.51 ppm and 0.96 ppm, with three months between 0.70 ppm and 0.80 ppm. The higher average concentration measured during October 1999 may be partially due to the slightly lower than average wind speeds measured during this month.

Again, all NO_2 monthly average concentrations were below 40 ppb, ranging between 22.4 ppb and 36.8 ppb, with all but one average concentration between 22 ppb and 29 ppb. However, the average concentration measured during July 1999 was markedly higher than those measured during other months. As the average wind speed during this month was not below average and the wind direction readings unreliable due to local turbulence, this cause of this elevated concentration can not be pinpointed.

Average PM_{10} concentrations exhibited a large range with average concentrations between 23.8 $\mu g/m^3$ and 54.4 $\mu g/m^3$. The peak concentration of 54.4 $\mu g/m^3$ was recorded during October 1999. This high average could not be attributed to a single pollution episode as PM_{10} concentrations remained consistently high during this month. This can not be explained by reason of wind speed, as the monthly wind speed was not below average.

However, the lowest average concentration recorded during December 1999 did coincide with a higher than average monthly wind speed.

Table 4.7 Average pollutant readings measured at Pearse Street – Westland Row Intersection (Phase 2)

	Average NO_2 (ppb)	Average CO (ppm)	Average PM_{10} ($\mu g/m^3$)
Jul-99	36.8	0.51	No Data
Aug-99	25.4	0.78	No Data
Sep-99	25.6	0.78	40.6
Oct-99	28.4	0.96	54.4
Nov-99	29.4	0.70	37.8
Dec-99	22.4	0.61	23.8

The maximum and 95th percentile values for averaging periods of 1 hour, 8 hours and 24 hours for CO, NO_2 and PM_{10} are given in Table 4.8, Table 4.9, and Table 4.10, respectively. The high average CO value recorded in October 1999, (Table 4.7), is reflected in significantly higher maximum 1-hour, 8-hour and 24-hour concentrations during October than during the other months when measurement was carried out. The 95th percentiles (Table 4.8) followed the same trend. This was not due to any one episode, but consistently high concentrations during the month. As measured wind speed values at the monitoring site were not significantly below average, the elevated CO concentrations could not be explained by reason of wind speed.

Table 4.8 Maximum and 95th percentile values for CO, measured at Pearse Street/Westland Row Intersection (Phase 2)

	Maximum Values (ppm)			95th Percentiles (ppm)		
	1 hour	**8 hours**	**24 hours**	**1 hour**	**8 hours**	**24 hours**
Jul-99	2.40	1.61	1.17	1.30	1.01	1.00
Aug-99	3.40	2.16	1.43	1.80	1.69	1.29
Sep-99	4.20	2.64	1.56	2.00	1.71	1.37
Oct-99	5.00	3.19	2.30	2.50	2.15	1.97
Nov-99	3.20	2.11	1.39	1.60	1.56	1.28
Dec-99	3.90	2.78	1.29	1.20	1.14	1.18

In contrast, the highest NO_2 concentrations occurred in July 1999 (as can be seen in Table 4.9). This was due to a particularly high episode between 24th July 1999 and 2nd August, peaking on the 28th July. Slightly lower wind speeds than average were recorded during this period, which are likely to have contributed to the elevated concentration levels.

Table 4.9 Maximum and 95th percentile values for NO_2, measured at Pearse Street/Westland Row Intersection (Phase 2)

	Maximum Values (ppb)			95th Percentiles (ppb)		
	1 hour	**8 hours**	**24 hours**	**1 hour**	**8 hours**	**24 hours**
Jul-99	162.1	120.9	105.2	95.5	96.4	95.0
Aug-99	74.6	56.1	42.3	51.2	46.9	38.3
Sep-99	73.4	59.6	43.9	48.4	44.2	38.1
Oct-99	74.0	63.3	49.3	57.3	51.3	45.5
Nov-99	78.3	62.7	51.9	56.0	54.6	49.4
Dec-99	63.0	51.2	34.8	41.0	35.8	30.9

The PM_{10} concentrations during December were consistently significantly lower than those measured during previous months, with only five measured exceedences of $50\mu g/m^3$. As the average wind speed was almost 150% of the average wind speed recorded during this phase of monitoring in total, the high wind speeds are likely to be a significant factor in explaining the low PM_{10} concentrations measured.

Table 4.10 Maximum and 95th percentile values for PM_{10}, measured at Pearse Street/Westland Row Intersection (Phase 2)

	Maximum Values ($\mu g/m^3$)			95th Percentiles ($\mu g/m^3$)		
	1 hour	**8 hours**	**24 hours**	**1 hour**	**8 hours**	**24 hours**
Sep-99	207.5	109.7	67.9	79.1	75.3	64.1
Oct-99	237.1	135.9	104.1	107.8	99.0	91.1
Nov-99	793.2	132.1	75.7	86.0	79.6	68.7
Dec-99	67.1	49.3	41.2	48.9	44.3	32.9

4.1.3 Site B (Pearse Street)

Monitoring was carried out using the TCD mobile monitoring unit at a site on Pearse Street, from 10th February to 7th of April 1999. The percentage data capture rates are given in Table 4.11, and are consistently high for each compound.

Table 4.11 Percentage data capture rates for monitoring at Pearse Street between 10th February 1999 to 7th April 1999.

	NO_2 (%)	CO (%)	PM_{10} (%)
Feb 10th – Feb 28th 1999	73	70	99
March 1999	99	99	93
April 1st – April 7th 1999	79	79	91

The average pollutant concentrations recorded are given in Table 4.12. CO concentrations are at the lower end of the range of monthly concentrations measured at the Pearse St./Westland Row intersection (Site A). NO_2 concentrations were within the range of those measured at Site A during Phase 1, but lower than the typical measurements recorded at heavily trafficked sites by Envirocon (1996). Average PM_{10} concentrations are 1.6 times the measured average concentration at the Pearse St./Westland Row site (Site A). This is likely to be due to the proximity of a number of bus stops, with buses idling and waiting to pick up passengers. PM_{10} concentrations are, however, still lower than the urban annual concentrations measured by the EPA in 1998 (McGettigan, 2000).

Table 4.12 Average pollutant concentrations recorded at Pearse Street site between February 10th and April 7th.

	NO_2 (ppb)	CO (ppm)	PM_{10} ($\mu g/m^3$)
Feb 10th – Feb 28th 1999	28.3	0.64	28.2
March 1999	29.1	0.80	28.1
April 1st – April 7th 1999	30.1	0.77	25.4

The maximum concentrations and 95th percentiles recorded for 1-hour, 8-hour and 24-hour averaging periods for CO, NO_2 and PM_{10}, between February 10th and April 7th, are given in Table 4.13, Table 4.14 and Table 4.15 respectively. In general, these concentrations are within the range measured previously at the Pearse St./Westland Row by TCD, although the maximum 1-hour PM_{10} concentration of 162.80 $\mu g/m^3$ was higher than the maximum recorded at the intersection site.

Table 4.13 Maximum and 95th percentile values for CO (Pearse Street)

	Maximum Values (ppm)			95th Percentiles (ppm)		
	1 hour	8 hours	24 hours	1 hour	8 hours	24 hours
Feb 10th – Feb 28th 1999	5.20	3.25	1.78	1.68	1.58	1.64
March 1999	4.91	3.11	2.12	1.83	1.61	1.66
April 1st – April 7th 1999	2.94	1.95	1.27	1.65	1.68	1.26

Table 4.14 Maximum and 95th percentile values for NO_2 (Pearse Street)

	Maximum Values (ppb)			95th Percentiles (ppb)		
	1 hour	8 hours	24 hours	1 hour	8 hours	24 hours
Feb 10th – Feb 28th 1999	52.5	38.1	32.5	37.5	34.1	30.7
March 1999	50.0	37.2	32.8	40.0	35.3	31.5
April 1st – April 7th 1999	50.0	42.5	33.8	42.5	38.3	33.1

Table 4.15 Maximum and 95th percentile values for PM_{10} (Pearse Street)

	Maximum Values (μg/m³)			95th Percentiles (μg/m³)		
	1 hour	**8 hours**	**24 hours**	**1 hour**	**8 hours**	**24 hours**
Feb 10th – Feb 28th 1999	83.05	68.86	46.30	60.00	51.37	41.49
March 1999	162.80	64.99	51.35	54.20	49.31	43.73
April 1st – April 7th 1999	70.05	58.79	42.91	52.20	49.71	40.65

4.1.4 Site C – (Westland Row)

Monitoring was carried out at by the ESB, at the Westland Row site and data collected between June 1999 to November 1999 for NO_x, NO and NO_2 is analysed in this thesis. This site was the only site of the three monitoring sites to follow all E.U. guidelines for the siting of urban air monitoring stations. The measured hourly concentrations did not exceed the limit value of 21 ppb under EU Directive 1999/30/EC (CEC, 1999), to be achieved in 2010.

The percentage data capture rates are given in Table 4.16.

Table 4.16 Percentage data capture rates for Westland Row site.

	NO_x (%)	NO (%)	NO_2 (%)
Jun-99	42	95	42
Jul-99	100	100	100
Aug-99	100	100	100
Sep-99	98	98	98
Oct-99	66	66	66
Nov-99	65	65	65

Measured NO_x, NO and NO_2 concentrations are given in Table 4.17. NO_2 concentrations recorded at the Westland Row site were observed to be lower than the averages recorded at the other sites (as shown in Table 4.2, Table 4.7 and Table 4.12) and significantly lower than the typical concentrations measured in the Envirocon (1996) study. The average concentration was 66% and 71% of the concentrations measured at the Pearse St./Westland Row site by TCD and the EPA, respectively, and 68% of the concentration measured at the Pearse St. site.

Table 4.17 Summary of hourly concentrations of nitrogen oxides at Westland Row

	NO_x			NO			NO_2		
Month	**Ave. (ppb)**	**Max. (ppb)**	**95^{th} %ile (ppb)**	**Ave. (ppb)**	**Max. (ppb)**	**95^{th} %ile (ppb)**	**Ave. (ppb)**	**Max. (ppb)**	**95^{th} %ile (ppb)**
Jun-99	71.5	423.5	173.1	53.7	327.0	144.3	24.6	96.5	41.0
Jul-99	57.4	257.0	131.5	36.4	215.5	99.9	21.1	58.0	37.4
Aug-99	54.6	285.5	136.5	35.3	254.5	106.0	19.4	45.0	34.0
Sep-99	71.1	320.5	179.1	51.2	280.5	141.5	20.0	59.0	36.0
Oct-99	68.0	520.0	193.7	48.6	478.5	156.1	19.5	60.0	36.5
Nov-99	82.3	261.0	186.8	60.2	225.5	151.3	22.3	54.0	37.5

4.2 Comparison of Results at Site A

4.2.1 Analysis of Carbon Monoxide Data

Hypothesis testing is often used as a basis for comparing two populations, processes or treatments (Devore and Farnum, 1999). A t-test was used to investigate whether or not pollutant concentrations measured by TCD and the EPA at Site A belong to the same population, and is described in the following subsection.

t-testing of Both Populations

Let

μ_1 = mean of population 1 (TCD data)

μ_2 = mean of population 2 (EPA data)

Inferences about the value of μ_1 relative to μ_2 are based on two independently obtained random samples, one from the first population, one from the second. Let

n_1 = number of observations in the first sample

$\bar{x}_1$ = sample mean of these n_1 observations

s_1^2 = sample variance of these n_1 observations

n_2, $\bar{x}_2$, s_2^2 are defined analogously with respect to the second sample. As the sample sizes are large ($n > 30$) then the Central Limit Theorem implies that the normality assumption inherent in the t-test is no longer necessary.

Lévy's Central Limit Theorem states if the elements, X_i, of a set of n independent random variables have the same distribution function with mean μ and variance σ^2, then the larger n is, the more nearly will the random variable

$$z_n = \frac{\frac{1}{n}\sum_{i=1}^{n} X_i - \mu}{\sigma}\sqrt{n} \qquad \text{Equation 4.1}$$

be normally distributed. It follows that the means, $\bar{X}_i$, of a sequence of independent random variables which are identically distributed, (the original distribution of the $\bar{X}_i$'s being arbitrary to a great extent) are asymptotically distributed. In other words, the larger the sample size, the better is the approximation to the normal distribution.

A confidence interval for the difference $\mu_1 - \mu_2$ is based on the fact that the standardised variable t, where,

$$t = \frac{\bar{x}_1 - \bar{x}_2 - (\mu_1 - \mu_2)}{\sqrt{\frac{s_1^2}{n_1} + \frac{s_2^2}{n_2}}} \qquad \text{Equation 4.2}$$

has approximately a t distribution

A smaller sample from a normally distributed population follows a t distribution. Properties of t distributions include:

- The t distribution is specified by the number of degrees of freedom;
- The density curve corresponding to any particular t distribution is bell shaped and centred at 0, just like the normal distribution z curve;
- Any t curve is spread out more than the z curve, (Devore and Farnum, 1999)

The degrees of freedom (df) are calculated using Equation 4.3.

$$df = \frac{\left(\frac{s_1^2}{n_1} + \frac{s_2^2}{n_2}\right)^2}{\frac{\left(\frac{s_1^2}{n_1}\right)^2}{n_1 - 1} + \frac{\left(\frac{s_1^2}{n_2}\right)^2}{n_2 - 1}}$$

Equation 4.3

For this case, when the means of the two samples under consideration could be above or below each other, a two tailed test is involved:

$H_0 : \mu_1 - \mu_2 = 0$

$H_a : \mu_1 - \mu_2 \neq 0$

where

H_0 is the null hypothesis, that there is no difference between the population means

H_a is the alternative hypothesis, that there is a difference between the population means.

The P-value or observed significance level is the calculated probability, assuming H_0 is true, of obtaining a test statistic value at least as contradictory to H_0 as the value that actually resulted. (The test statistic is the function of the data that is of interest, in this case, the mean). The smaller the P-value, the more contradictory the data is to H_0. The null hypothesis should then be rejected if the P-value is sufficiently small. In particular, the following decision rule specifies a test with the desired significance level α:

Reject H_0 if P-value $\leq \alpha$. ($\alpha = 0.05$)

Do not reject H_0 if P-value is $> \alpha$. ($\alpha = 0.05$)

Analysis of Concentration Data

Hourly CO concentrations were measured by the EPA monitoring unit from July 1999 to December 1999 using an infra-red based sampler, as discussed in Section 4.1.2. Figure 4.3 compares these readings with the hourly average readings measured using the TCD monitoring unit, at the same site, for the same period in 1998.

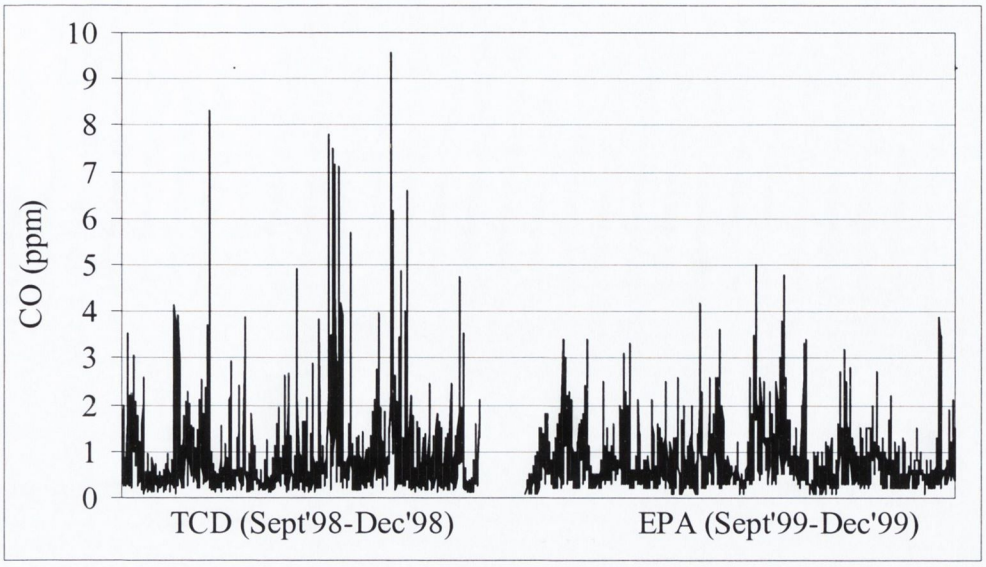

Figure 4.3 Comparison of TCD monitored hourly CO averages (September 1998 to December 1998) and EPA monitored hourly averages (September 1999 to December 1999)

The two data sets display similar mean concentrations (0.86 ppm and 0.75 ppm for the TCD and EPA data, respectively), and also similar minimum concentration values (0.07 ppm and 0.10 ppm). However, the data sets are seen to differ in terms of the maximum values; the EPA data on no occasion exceeds 5 ppm, which is exceeded by the TCD data on eleven occasions. A comparison of the statistical summaries is given in Table 4.18. A significant difference is that the maximum value in the TCD data is almost twice the EPA maximum value and the standard deviation is also larger (0.93 ppm compared to 0.57 ppm). This is likely to be due to characteristics of the different monitors; however, it may in part be due to the fact that maximum concentrations would be expected to differ, even for the same period in consecutive years.

Table 4.18 Comparison of TCD and EPA measurements of CO

	TCD data (ppm)	**EPA data (ppm)**
Average	0.86	0.75
Standard Deviation	0.93	0.57
Maximum	9.58	5.00
Minimum	0.07	0.10
95th percentile	2.35	1.90

For the CO concentration data recorded during Phase 1 and 2 at the Pearse St./Westland Row intersection, a t-statistic of 1.23 was calculated with 5923 degrees of freedom. This gives a P value of 0.21. As this is greater than α (where α is the significance level of

0.05), we cannot reject the null hypothesis that both populations have the same mean. In other words, it can be said at the 95% confidence level, that both samples come from the same population.

Both sets of data are shown in histogram format, in Figure 4.4. The histograms for both sets of data are similar in most respects, although the TCD data have a longer tail.

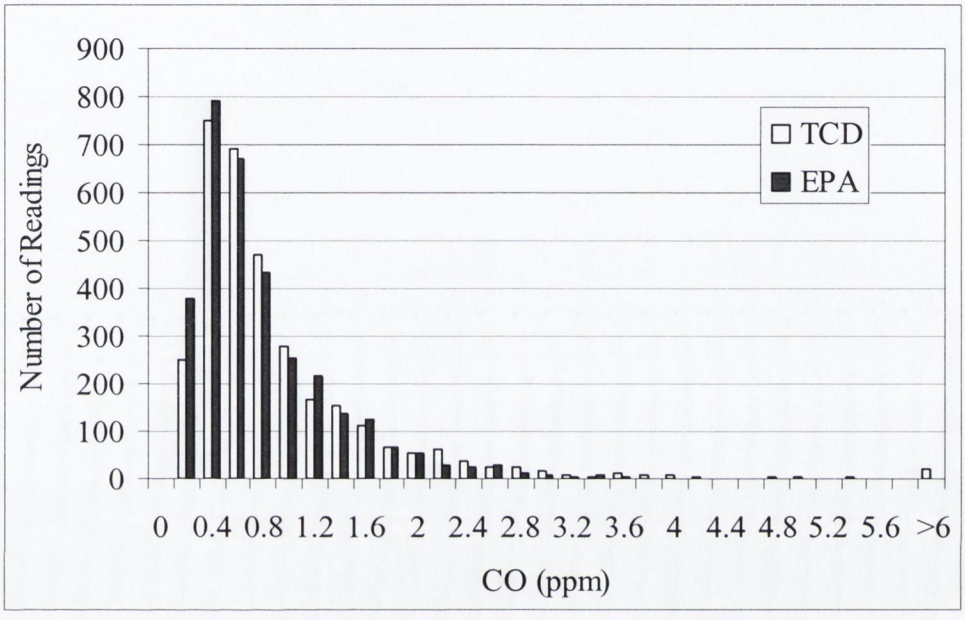

Figure 4.4 Comparison of histograms for hourly averages of TCD and EPA monitored CO data.

When the cumulative distribution of both data sets is examined (Figure 4.5), the similarity of the two data sets, but for the longer tail displayed by the TCD data, is highlighted. The cumulative distribution functions only begin to diverge at the 85th percentile level.

However, as the two data sets would be expected to differ to an extent, neither data set gives sufficient reason to doubt the monitoring accuracy of the other, especially as can be seen in Figure 4.4, the difference is concentrated in the tails of the concentration distributions.

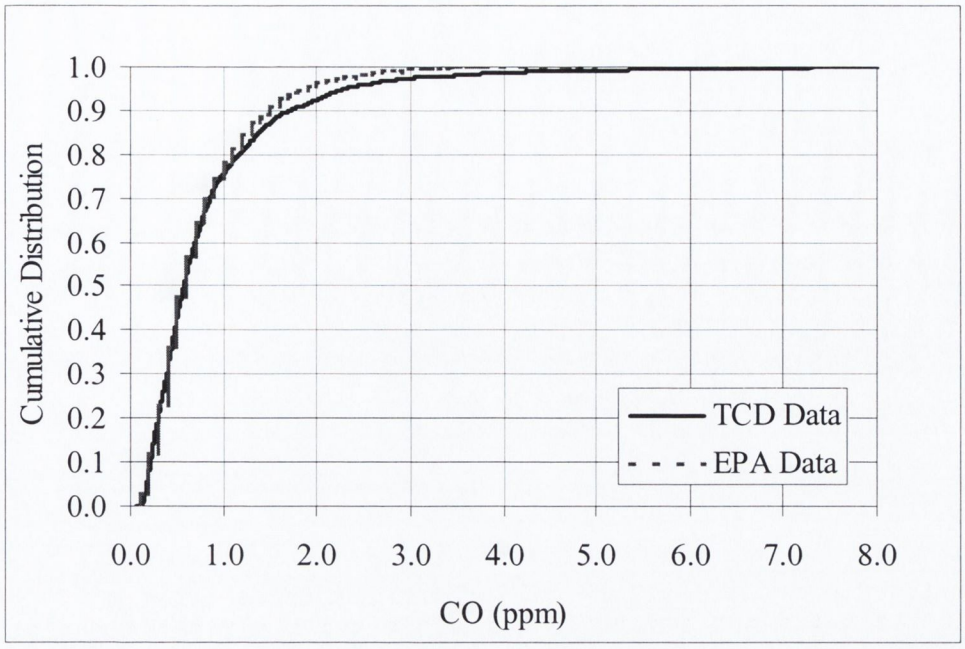

Figure 4.5 Comparison of cumulative frequency distributions of hourly averages of TCD and EPA monitored CO data.

4.2.2 Analysis of Nitrogen Dioxide Data

NO_2 concentrations were also measured by the EPA, using a chemiluminescence based sampler, at the same site as that used by the TCD monitoring unit, for the period from 15th July 1999 to 14th December 1999. A plot of the average hourly NO_2 concentrations, as measured by the EPA from 15th July 1999 to 14th December 1999, compared to the concentrations measured by the TCD monitoring unit for the same period in 1998, is given in Figure 4.6.

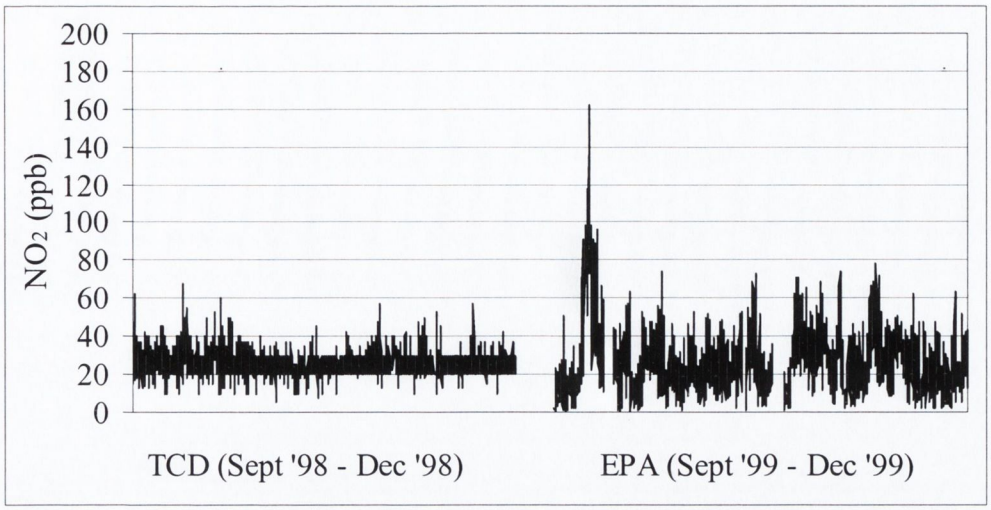

Figure 4.6 Comparison of TCD monitored NO_2 hourly averages (September 1998 to December 1998) and EPA monitored hourly averages (September 1999 to December 1999)

A statistical summary of both sets of data is given in Table 4.19. It can be seen from Figure 4.6 and Table 4.19, that both sets of readings have similar mean values. The poor resolution of the TCD NO_2 analyser may be partially responsible for the obvious absence of measured peaks in that data. With a 10 ppb resolution and a 12% level of accuracy, there is scope for measured values to be significantly lower than the on-street concentrations. The EPA data also frequently drop below 20 ppb, but the TCD data rarely do.

Table 4.19 Statistical summary hourly averages of TCD and EPA monitored NO_2 data

	Hourly NO_2 Readings (TCD-1998) (ppb)	**Hourly NO_2 Readings (EPA - 1999) (ppb)**
Average	25.77	27.97
Standard Deviation	7.09	17.00
Minimum	5.00	0.30
Maximum	67.50	162.10
95th percentile	40.00	58.56

When analysed using a t-test, the null hypothesis that there was no significant difference between the means of the two populations was rejected, i.e., the recorded concentrations are from populations with different means.

In the histogram shown in Figure 4.7, the greater scatter in the NO_2 concentrations measured by EPA is visible in the longer tail of the EPA data when compared to the TCD data.

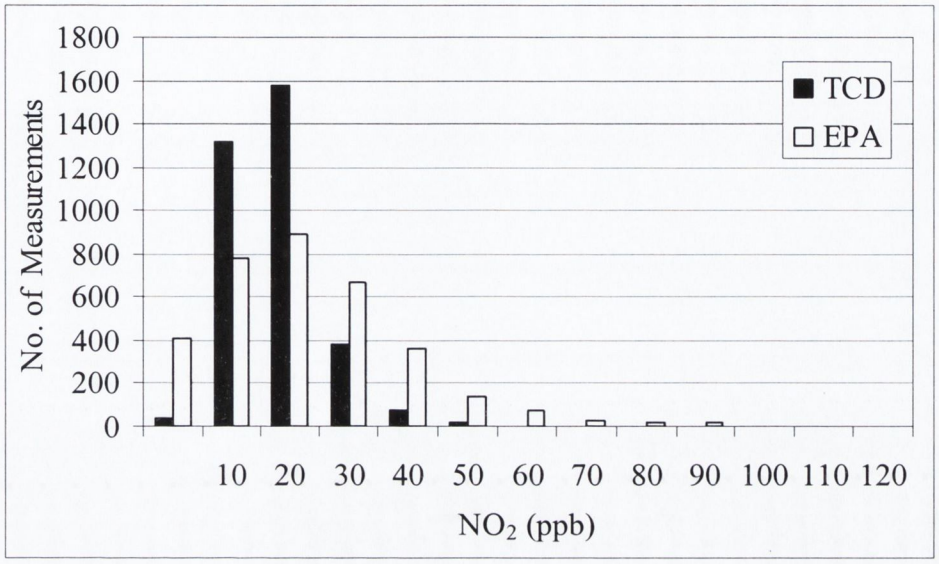

Figure 4.7 Comparison of histograms for hourly averages of TCD and EPA monitored NO_2 data.

The effect of the coarser resolution of the TCD data can be seen clearly in Figure 4.8. The two cumulative distributions are in close agreement in the middle of the range but then a step effect is visible at 20 ppb and 30 ppb, due to the predominance of those readings.

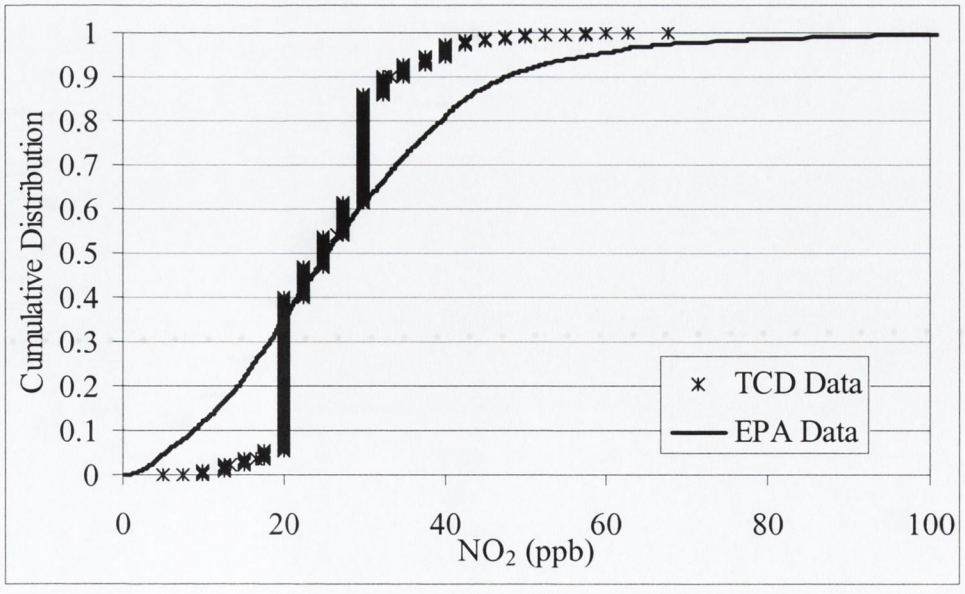

Figure 4.8 Comparison of cumulative frequency distributions of hourly averages of TCD and EPA monitored NO_2 data.

4.2.3 Analysis of PM_{10} Data

Concentrations of PM_{10} were measured by the EPA, at the Pearse St./Westland Row Intersection monitoring site, from 1st September 1999 to 14th December 1999. In Figure 4.9 and Figure 4.10, the average daily PM_{10} concentrations measured by the EPA during this period are compared to those measured by the TCD monitoring unit between the same dates in the two previous years.

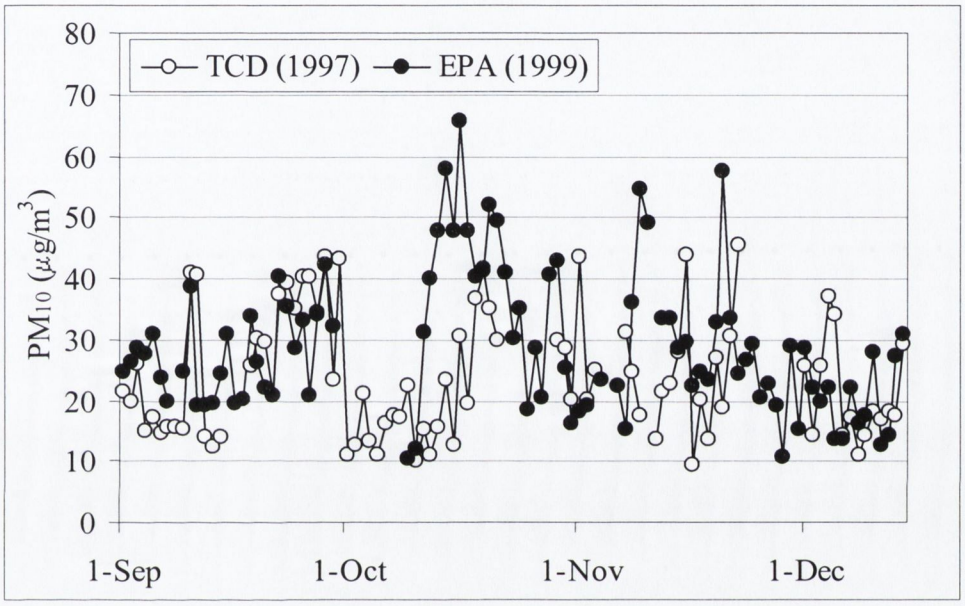

Figure 4.9 Comparison of TCD (1997) and EPA (1999) monitored daily PM_{10} averages

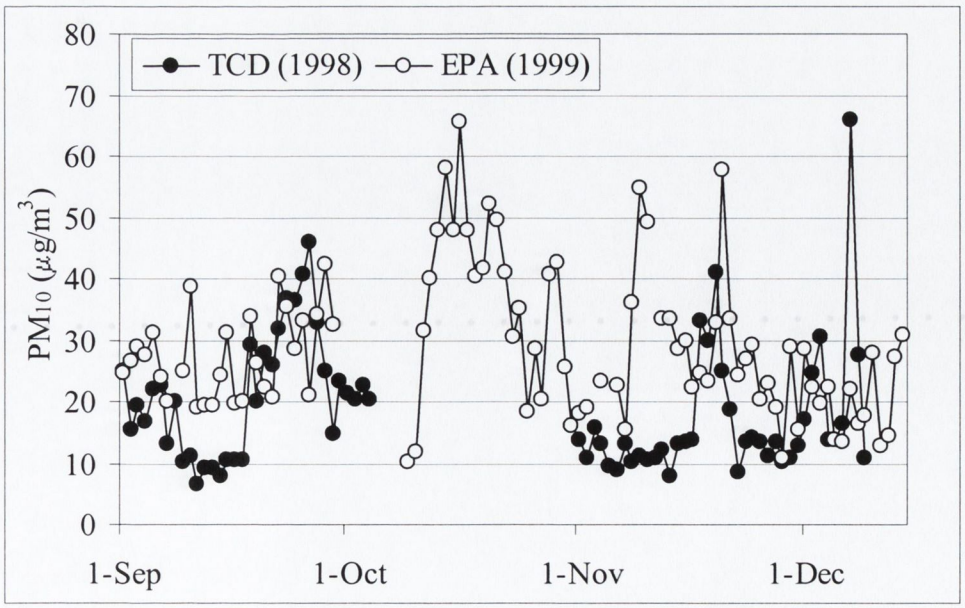

Figure 4.10 Comparison of TCD (1998) and EPA (1999) monitored daily PM_{10} averages

Summary statistics for the period from 1st Sept to 14th Dec in 1997, 1998 and 1999 are given in Table 4.20. As can be seen from the graphs, the mean daily concentration measured by the EPA is higher than the mean concentrations measured in the previous two periods by the TCD monitoring unit.

Table 4.20 Statistical summary hourly averages of TCD and EPA monitored PM_{10} data

	TCD 1997 ($\mu g/m^3$)	**TCD 1998 ($\mu g/m^3$)**	**EPA 1999 ($\mu g/m^3$)**
Average	23.84	18.89	28.88
Standard Deviation	10.11	10.67	11.61
95th Percentile	43.13	38.30	50.72
Maximum	45.56	66.02	65.56
Minimum	9.49	6.72	10.27

In each comparison (1997 and 1998; 1998 and 1999; 1997 and 1999), a P-value of close to zero is calculated, meaning that the null hypothesis, that there is no difference between the means, should be rejected.

In the histogram in Figure 4.11, the EPA data appear to be displaced to the right of the TCD data.

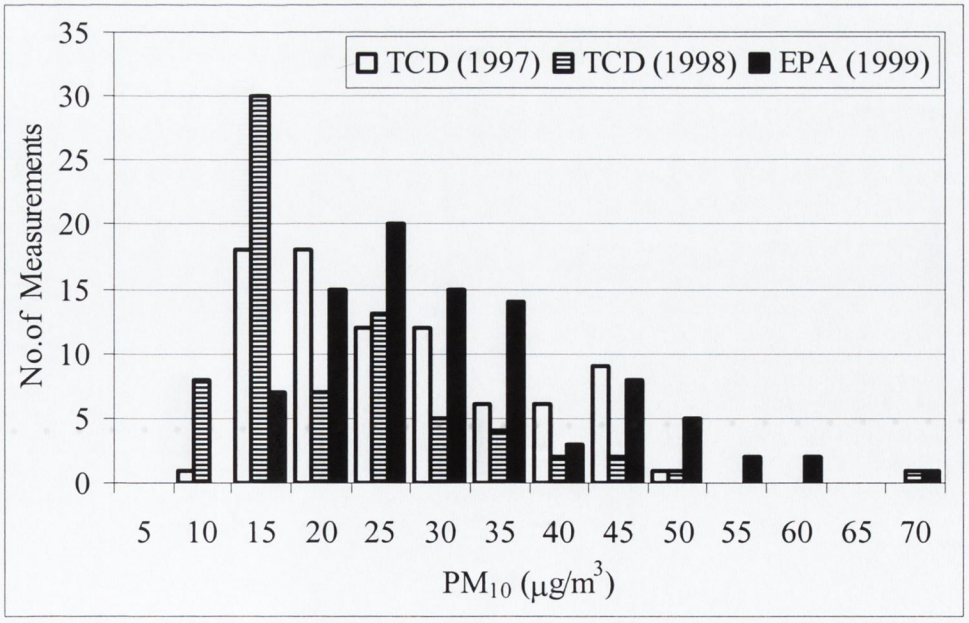

Figure 4.11 Comparison of histograms of 1-hour averages of PM_{10} data collected by TCD (1997) and EPA (1998, 1999)

This difference can be seen clearly when the cumulative distributions of all three data sets are compared (Figure 4.12). However, due to the variability present in the TCD data between the two years, it is not clear as to whether the difference is a function of the method of testing or the annual variability.

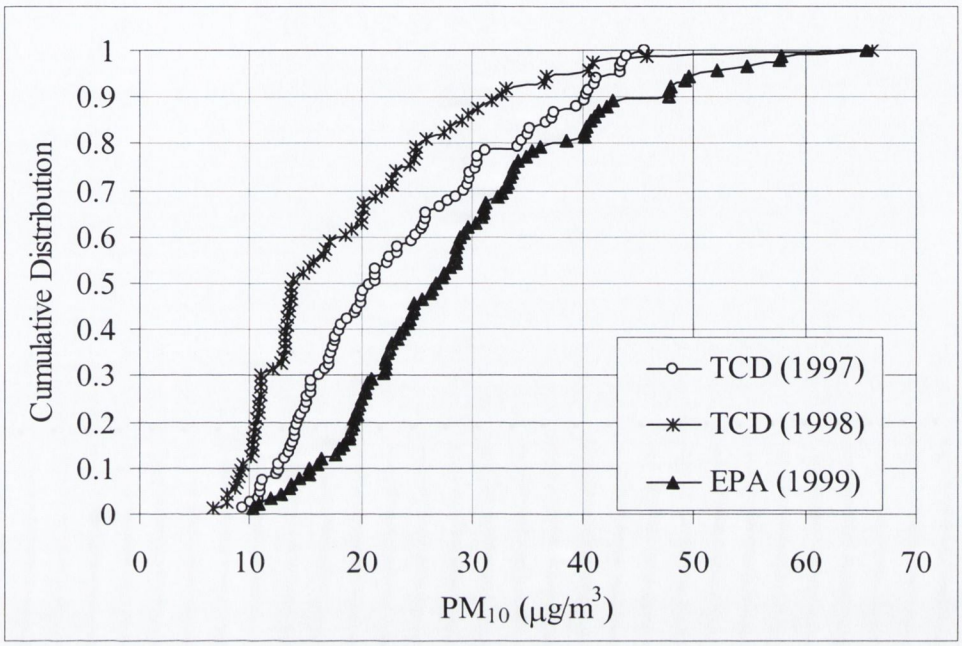

Figure 4.12 Comparison of cumulative distribution frequencies for 1-hour averages of PM_{10} data monitored by TCD (1997 and 1998) and EPA(1999)

The difference between the TCD data and the EPA data could be due to the different measurement methods. The EPA data were measured using a light scattering method, whereas the TCD data were sampled and measured with the TEOM, as described in Section 3.4.3. During operation of the TEOM instrument, some components of vehicle-related particulate matter, such as ammonium nitrate and similar volatiles will be partially volatilised during residence on the filter, as discussed in Section 3.4. Hence, in areas where there is a high volatilisable fraction in the particulate matter, readings lower than the true value may be recorded (Salter and Parsons, 1999). The measured concentrations should, therefore, more correctly be regarded as a lower bound of the actual concentration.

4.2.4 Summary of Results

The concentrations were seen not to breach any of the legislative standards introduced in Section 2.2. Good agreement was seen between the average CO concentrations measured by TCD and the EPA, although higher peak concentrations were measured by the TCD monitoring equipment. The poor resolution of the TCD NO_2 monitor was highlighted, compared with the EPA data. The PM_{10} data recorded by the TCD mobile air monitoring unit was also seen to have a slightly lower mean than the EPA data, possibly reflecting the volatilisation of compounds such as ammonium nitrate by the TEOM used in the TCD study. The PM_{10} data recorded by TCD should therefore be looked on as a lower bound of the ambient PM_{10} concentrations.

4.3 Statistical Analysis of Data

In Section 6.12, the theoretical frequency distribution of the recorded data is used in the estimation of extreme event pollutant concentrations. Simpson (1984) reported that if the frequency distribution of the concentrations was known, then it may be possible to use methods other than continuous monitoring to estimate mean concentrations of air pollutants, such as random sampling. Penn and Croxford (1998) found that the percentile plot could be a useful analytical tool for characterising locational variances in kerbside pollution.

It is therefore important to ensure that the chosen theoretical frequency distribution represents the actual frequency distribution as accurately as possible. In this section, various theoretical distributions are discussed, and the measured pollutant concentrations examined for the best-fit theoretical distribution.

4.3.1 Candidate Frequency Distributions

Frequency distributions applied in the field of air pollution include the Normal, Lognormal, Weibull, Gamma, and Beta distributions. These distributions are discussed below and their suitability analysed in the context of the measured pollution data. The

appropriate distribution form can be identified or assumed from historical observations and its parameter values inferred (Miles *et al.*, 1991). However, there are situations where several distributions may fit the data equally well (Morel *et al.*, 1999).

Candidate Distribution 1 – Normal Distribution

The normal distribution is an important example of a continuous distribution. It is also known as a "Gaussian Distribution". Many scientists assume that the distribution of pollutant concentrations follows a normal distribution (Nosal *et al.*, 2000). The normal probability density function is given by:

$$y = \frac{1}{\sigma\sqrt{2\pi}} \exp\left[\frac{-(x-\mu)^2}{2\sigma^2}\right] \qquad \text{Equation 4.4}$$

where μ is the population mean, σ is the standard deviation, and y is the probability density calculated at a value of x (e.g. Rohatgi, 1984).

Candidate Distribution 2 – Lognormal Distribution

However, because of the tendency of air pollution concentrations to be positively skewed, lognormal distributions have often been used to characterise air pollutant data. Data sets where negative values of a variable do not exist can often be characterised by lognormal distributions (Haynes, 1982). However, the assumption of lognormality with respect to air pollution data has been questioned by Berger *et al.*, (1982).

The lognormal probability density function is described by

$$y = \frac{1}{x\sigma(2\pi)^2} \exp\left\{-\frac{\left[\log(x/m)\right]^2}{2\sigma^2}\right\} \qquad \text{Equation 4. 5}$$

where

$m = \exp \mu$ and $\mu = \log m$ (e.g. Rohatgi, 1984)

After a study of CO daily maxima for different weather typology, Maffeis (1999) reported that the data was best represented by the lognormal distribution, due to the skewness of the

concentration values. Reynolds (1996) took measurements of urban CO concentrations and after analysis of the normal, the gamma, and the lognormal distributions found that the data was not statistically different from the lognormal distribution. Ott (1990) and Simpson (1984) reported that many investigators have found that distributions of pollution concentrations conform to a lognormal distribution.

Bower *et al.*, (1991) studied distributions of urban NO concentrations, which they found to be lognormally distributed. This observation is likely to be due, at least in part, to the strong dependence of primary pollutants on wind speeds, which are approximately lognormally distributed (Bower *et al.*, 1991).

Ott (1990) justified the use of the lognormal distribution to characterise air pollution concentrations by using a computer simulation of the dilution process. Ott generated data that was lognormally distributed; concluding that this was due to the successive random dilution that environmental pollution undergoes.

A rigorous proof of the applicability of the lognormal distribution to air pollution data would be very difficult due to the complexity of the emission-transport-receptor process. However, using Central Limit Theory, Kahn (1973) heuristically justified the use of the lognormal distribution, as reported in Reynolds (1996).

Kahn stated that air pollution concentration measured at regular time intervals constitute a positive, discrete random process, X_0, $X_1,\ldots,X_n$, where X_0 is the concentration at an arbitrary starting point, and X_n is the value of the *n*th observation. Kahn then assumed that the change in pollutant concentration from one observation to the next can be expressed as

$$X_j - X_{j-1} = p_j X_{j-1} \qquad \text{where } j = 1,\ldots,n \qquad \text{Equation 4.6}$$

which is the model for the "law of proportionate effect"

Equation 4.6 can rewritten as

$$\frac{X_j - X_{j-1}}{X_{j-1}} = p_j \qquad \text{where } j = 1,\ldots,n \qquad \text{Equation 4.7}$$

Then

$$\sum_{j=1}^{n} \frac{X_j - X_{j-1}}{X_{j-1}} = \sum_{j=1}^{n} p_j \qquad \text{Equation 4.8}$$

Assuming that the time interval and change between consecutive samples are small, then

$$\sum_{j=1}^{n} \frac{X_j - X_{j-1}}{X_{j-1}} \approx \int_{X_0}^{X_n} \frac{dx}{x} = \log X_n - \log X_0 \qquad \text{Equation 4.9}$$

therefore,

$$\log X_n \approx \log X_0 + p_1 + p_2 + \ldots + p_n \qquad \text{Equation 4.10}$$

Kahn then concluded that central limit theory states that log X_n is asymptotically normally distributed regardless of the distribution of the P_j and therefore X_n is asymptotically lognormally distributed.

Candidate Distribution 3 – Weibull Distribution

The Weibull distribution can be viewed as a generalised exponential distribution. It is formulated in terms of three parameters, and these allow it to approximate the normal distribution and a variety of asymmetric distributions.

The probability density of the Weibull distribution with parameters for location (α), scale (β) and form (γ) is

$$\mathrm{P}(x) = \frac{\gamma}{\beta}\left(\frac{x-\alpha}{\beta}\right)^{\gamma-1} \exp\left[-\left(\frac{x-\alpha}{\beta}\right)^{\gamma}\right] \qquad \text{Equation 4.11}$$

As reported by Sachs (1984), a nomogram for estimating the three parameters is given by Sen and Prabashanker (1980).

Candidate Distribution 4 – Beta Distribution

The beta distribution also offers a large amount of flexibility. The beta density function, with parameters α and β, is given in Equation 4.12.

$$f(x) = [B(\alpha,\beta]^{-1} x^{\alpha-1}(1-x)^{\beta-1}, \qquad 0 < x < 1 \qquad \text{Equation 4.12}$$

$$B(\alpha,\beta) = \int_0^1 x^{\alpha-1}(1-x)^{\beta-1}dx, \qquad where \alpha,\beta > 0. \qquad \text{Equation 4.13}$$

Candidate Distribution 5 – Gamma Distribution

The Gamma distribution is a modified form of the exponential model (Rohatgi, 1984) and has been used to characterise ambient pollutant concentrations with good results (Jakeman *et al.*, 1991; Bai *et al.*, 1995; Nosal *et al.*, 2000). However, the gamma distribution is more cumbersome, and is difficult to calculate in packages such as SPSS (Reynolds, 1996). Reynolds (1996) calculated and applied a distribution by hand, but was unable to prove that the measured CO data conformed to a gamma distribution.

The gamma probability density function with parameters α>0, β>0 and x>0 is given by:

$$f(x) = [x^{\alpha-1}\exp(-x/\beta)]/(\Gamma(\alpha)\beta^{\alpha}) \qquad x > 0, \alpha,\beta > 0 \qquad \text{Equation 4.14}$$

where

$$\Gamma(n) = \int_0^{\infty} x^{n-1}e^{-x}dx, \qquad n > 0$$

$$\alpha = \frac{\mu}{\beta}\ ,\ \beta = \frac{\sigma^2}{\mu}$$

The gamma density function takes on a wide variety of shapes depending on the values of α and β. The concentration data was tested for conforming to a gamma distribution rather than the Weibull and beta distributions, because of the flexibility of the distribution and

because of the results achieved by Jakeman *et al.* (1991), Bai *et al.* (1995) and Nosal *et al.* (2000).

4.3.2 Goodness-of-Fit Tests

A goodness-of-fit test is a statistical test or procedure to quantitatively analyse how well a data series, such as a series of pollutant concentration data, is represented by a theoretical probability distribution. Two distribution-free tests were employed to examine which of the above theoretical distributions best fit the measured concentration data.

The Chi-Squared Goodness-of-Fit Test

In a chi-squared (χ^2) test the observations are used to produce a frequency table of the data. The mean and standard deviation of the data are also calculated. Using the calculated mean and standard deviation, the expected number of observations in each category of the frequency table are determined using the formula for the trial distribution. The test statistic can then be calculated as shown below.

$$\chi^2 = \sum_{j-1}^{k} \frac{(O_j - E_j)^2}{E_j} \qquad \text{Equation 4.15}$$

where O is the observed value, E is the expected value calculated using the trial distribution and k is the number of categories. Values of χ^2 can then be compared to readily available tables of values to ascertain whether or not the sample conforms to the distribution for which it is being tested (Neave and Worthington, 1988).

Therefore, if H_0 (the hypothesis that the observed frequencies belong to the predicted distribution) is true, the observed frequencies will tend to be relatively close to the expected frequencies. This will result in a corresponding small value for χ^2. If there are large differences between the expected and observed frequencies, χ^2 will also be large, indicating that H_1 (the hypothesis that the data belongs to a distribution other than the predicted distribution) is true.

Samples of the data were analysed using the chi-squared test; however, this method has a number of drawbacks. It is best suited to discrete distributions, so data such as pollution concentrations must be split into arbitrary categories before analysis. Another problem is that the chi-squared approximation for the null distribution of χ^2 deteriorates when the expected frequencies are small. This can happen when there are a small number of values in individual categories or when the sample size is small. Hence, no more than one fifth of the categories should have less than five members, implying that categories at the upper and lower bound may have to be combined (Neave and Worthington, 1988).

Kolmogorov-Smirnov Goodness-of-Fit Test

Given the above problems with the application of the chi-squared test, it was therefore decided to use the Kolmogorov-Smirnov test for analysis of all data except 15-minute NO_2 concentrations. (This case is discussed in more detail in Section 4.3.4.) As the Kolmogorov-Smirnov test is specifically designed for analysing goodness-of-fit of continuous distributions, the splitting of the data into arbitrary categories, as in the chi-squared test, is unnecessary. The need to combine small frequencies at the lower and upper bound categories is also avoided.

The Kolmogorov-Smirnov procedure compares the sample cumulative distribution function with the hypothesised cumulative distribution function (Neave and Worthington, 1988).

A sample of size n is drawn from a population with cumulative distribution function $F_n(x)$. The empirical distribution function $F_n(x)$ is defined as the step function:

$$F_n(x) = \frac{k}{n} \quad \text{for} \quad x_i \le x \le x_{(i+1)}, \qquad \text{Equation 4.16}$$

where k is the number of observations not greater than x. ($x_{(1)}...,x_{(n)}$ denote the sample values arranged in ascending order.) Under the null hypothesis that the sample has been drawn from the specified distribution, $F_n(x)$ should be close to $F(x)$. The test statistic D is therefore defined as:

$$D = \max\left|F_n(x) - F(x)\right| \qquad \text{Equation 4.17}$$

The hypothetical distribution should be rejected if the calculated D exceeds the tabulated value. Large differences between $F_n(x)$ and $F(x)$ constitute evidence against H_0 in favour of H_1, the hypothesis that the data comes from a distribution other than the predicted distribution. (The measure of difference between the two cumulative distributions is simply the vertical distance between them (Neave and Worthington, 1988)).

4.3.3 Frequency Distribution of Carbon Monoxide Data

24-hour sets of 15-minute readings

15 minutes was chosen as the shortest time compatible with greatest accuracy and the logging capabilities of the instrument. The distribution of the 15-minute concentrations recorded each day at the Pearse St./Westland Row site were analysed for 240 days, using the Kolmogorov-Smirnov test. The normal, lognormal and gamma distributions were considered, as these are the distributions that have been used to represent urban air pollution data in previous studies, as discussed in Section 4.3.1. Of the 240 sets of data analysed, 148 were found to be the normal, 178 were found to be lognormal and 179 were found to fit the gamma distribution, at a confidence level of 95%. Therefore, the underlying daily distribution was characterised equally well by both the lognormal and gamma distributions. Table 4.21 summarises these classifications.

Table 4.21 Daily distributions of CO data measured at Site A.

Classification	Percentage of Days Tested
Normal	62
Lognormal	74
Gamma	75

Monthly sets of daily averages

The daily averages collected over monthly periods were also analysed using Kolmogorov-Smirnov tests. The observed distribution for each of the 17 months investigated was not statistically different to either the lognormal or gamma distributions, and seemed to be characterised equally well by either distribution. A sample monthly distribution is

compared with the theoretical normal, lognormal and gamma distributions in Figure 4.13, Figure 4.14 and Figure 4.15 respectively. The lognormal and gamma distributions follow the measured distribution more closely than the normal distribution, as is typical for the data set.

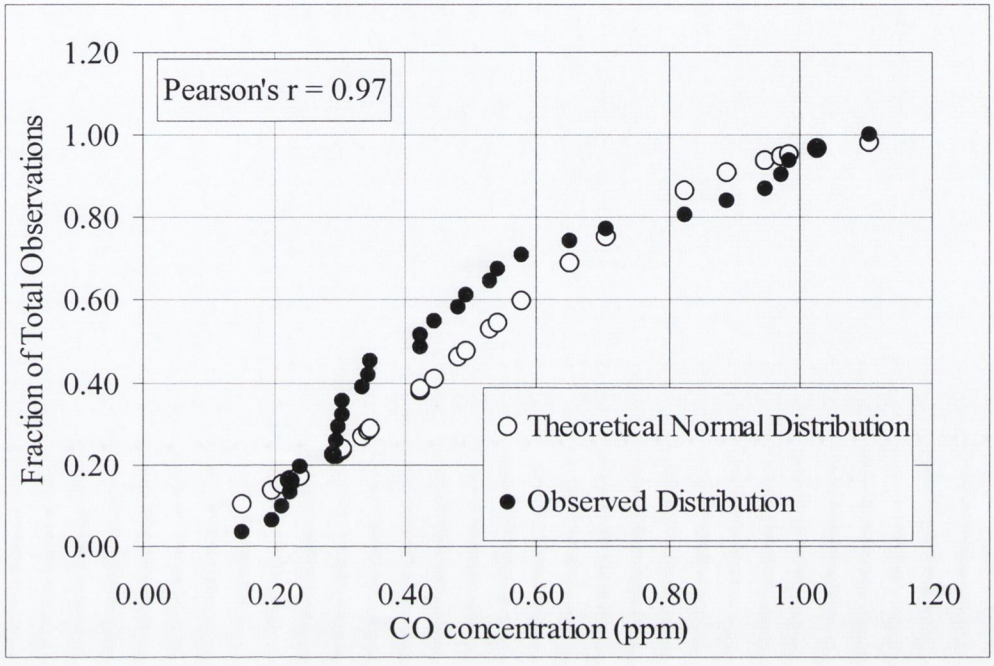

Figure 4.13 Sample monthly distribution of observed daily CO averages and theoretical normal distribution (August 1998)

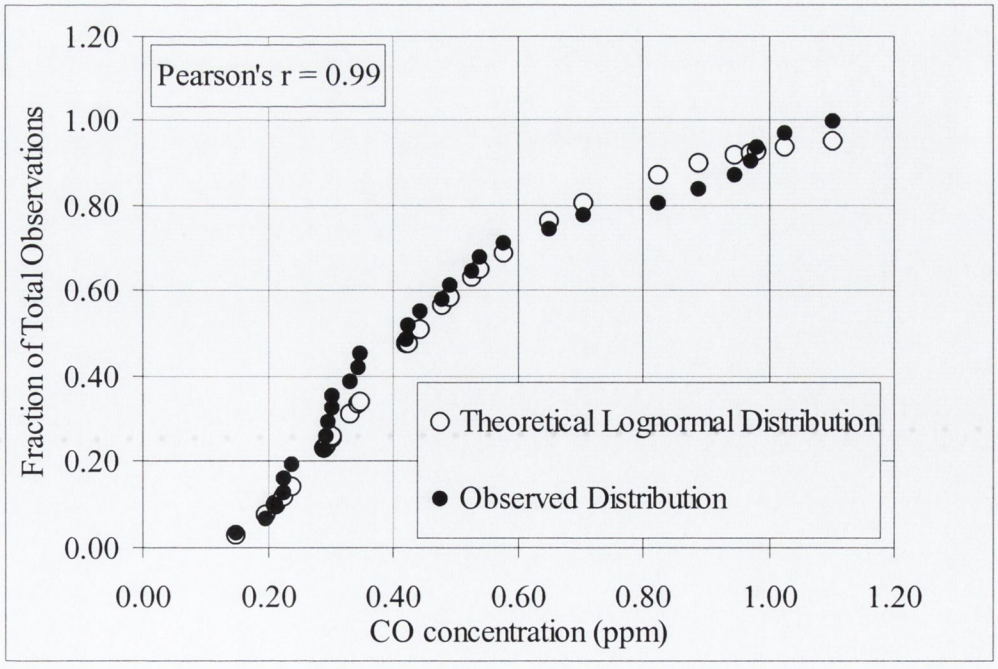

Figure 4.14 Sample monthly distribution of observed daily CO averages and theoretical lognormal distribution (August 1998)

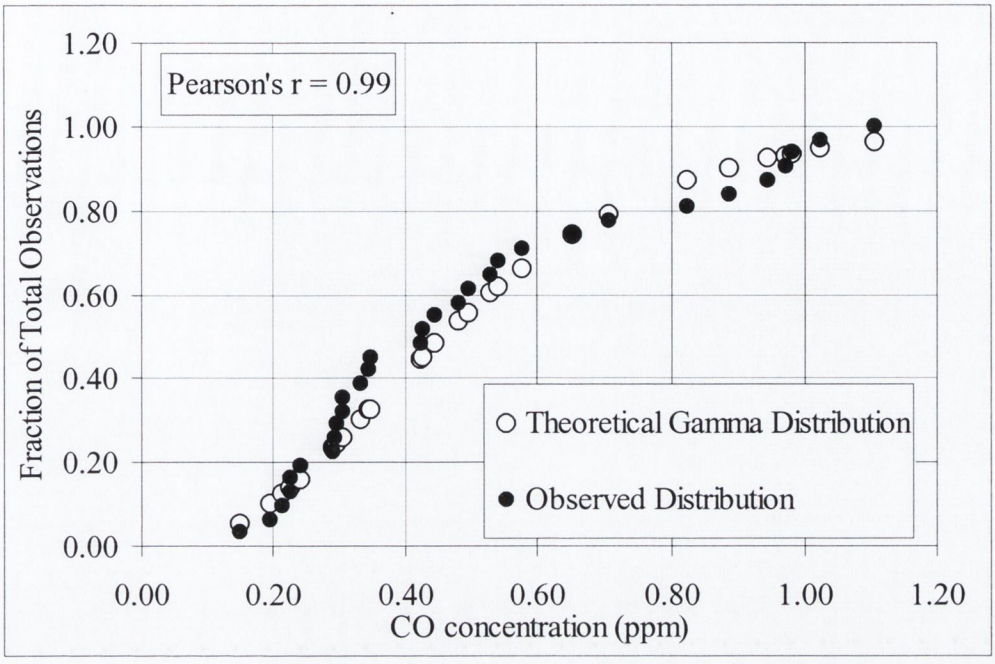

Figure 4.15 Sample monthly distribution of observed daily CO averages and theoretical gamma distribution (August 1998)

4.3.4 Frequency Distribution of Nitrogen Dioxide Data

24-hour sets of 15-minute readings

Due to the poor resolution of the TCD NO_2 monitor, it is not possible to analyse the underlying distribution of the measured 15-minute data using a Kolmogorov-Smirnov test, as all measurements taken on a particular day would fall into a small number of categories. This gives the data the appearance of a non-continuous or discrete data set, with on average only three to five categories, which is best analysed using a χ^2 test.

The χ^2 test with a 95% confidence level was therefore used instead. 40 days were randomly selected from the monitoring period and tested. Of these, 28 followed the normal distribution; none were classified as lognormal and only three were classified as having a gamma distribution.

As a secondary pollutant, NO_2 concentrations can be expected to display different patterns to those of primary pollutants such as CO. This is because in addition to wind speed, a multiplicity of other factors, such as precursor pollutant concentrations and meteorological

conditions, influence overall chemical reaction rates and physical scavenging mechanisms, and exert a strong influence on ambient concentrations (Bower *et al.*, 1991).

Monthly sets of daily averages

A different pattern was found for the data sets comprising of the 24-hour averages. Seventeen months were analysed, only one of which was found to be statistically different from either the normal, lognormal, or gamma distributions, at the 95% confidence level.

4.3.5 Frequency Distribution of PM_{10} Data

24-hour sets of 30-minute readings

The distribution of the recorded 30-minute concentrations of PM_{10} each day at the primary site were analysed for 244 days, using the Kolmogorov-Smirnov test. 30 minute intervals were recorded and analysed as was deemed to be the highest resolution compatible with the logging capabilities of the instrument. Of the 244 sets of data, 192 were found to be the normal, 228 were found to be lognormal and 232 were found to fit the gamma distribution. The underlying daily distribution was, therefore, characterised equally well by both the lognormal and gamma distributions. Table 4.22 summarises the classifications.

Table 4.22 Summary of daily distributions of PM_{10} data measured at Site A.

Classification	Percentage of Days Tested
Normal	79
Lognormal	93
Gamma	95

Monthly sets of daily averages

The distribution of the daily averages was investigated for 18 months of PM_{10} concentration data. For each month, the distribution was not statistically different to either a lognormal or gamma distribution. In only one case was the measured distribution different to the theoretical normal distribution, at a significance level of 95%.

4.4 Conclusions

Pollutant concentrations measured at each site were summarised in Section 4.1. The concentrations were seen not to breach any of the legislative standards introduced in Section 2.2.

Data recorded at the Pearse St./Westland Row Intersection by TCD and the EPA were compared in Section 4.2. The poor resolution of the TCD NO_2 monitor was highlighted, and hence, is not recommended for future urban ambient air pollution use, due to absence of short-term peaks recorded by the unit, compared with the EPA data. The PM_{10} data recorded by the TCD mobile air monitoring unit was also seen to have a slightly lower mean than the EPA data, possibly reflecting the volatilisation of compounds such as ammonium nitrate by the TEOM used in the TCD study. The PM_{10} data recorded by TCD should therefore be looked on as a lower bound of the ambient PM_{10} concentrations.

In Section 4.3, the underlying frequency distributions of the recorded concentration data were analysed. The observed distribution of the CO 15-minute averages and PM_{10} 30-minute averages was seen to be characterised similarly well by the lognormal and gamma distributions. The observed distribution of the NO_2 15-minute averages was seen to be best characterised by the normal and distribution. The monthly sets of 24-hour average concentrations for each compound were also found to conform to both the lognormal and gamma distributions. In Chapter 6, the frequency distributions are discussed with respect to their use in the prediction of short-term peak concentrations.

5. POLLUTANT RELATIONSHIPS

The measured level of air pollution is dependent upon many factors, such as background air pollution, specific emission conditions and general meteorological conditions (Mayer, 1999). If these variables can be quantified, then, as the geographic pattern of variation over time is essentially stable (Lebret *et al.*, 2000), they can be used in future characterisation of pollution at that site.

This chapter looks at the relationships between the measured pollutant concentrations and time of sampling in Section 5.1, and meteorological conditions in general in Section 5.2. The influence of wind speed and direction, relative humidity, and temperature on pollutant concentrations is investigated in Sections 5.3, 5.4, 5.5, and 5.6, respectively. In Chapter 6, these relationships are then used to develop a methodology for characterising air pollution conditions at a site from short-term measurements. The spatial variability of the individual compounds is assessed in Section 5.8. The inter-compound relationships are analysed in Section 5.9. Finally, conclusions to the chapter are presented in Section 5.10.

5.1 Temporal Variability of Pollutant Concentrations

The temporal variability of air pollutants can generally be characterised by time courses (annual, weekly and diurnal cycles) and by trends (Mayer, 1999). As it was not within the scope of the project to analyse trends, which by their nature require longer-term monitoring periods, the main emphasis in the analysis of temporal variation is on the effect of time courses. At a local level, signal timings and queuing have an effect on air pollution concentrations through the resulting acceleration, deceleration and idling. However, as the highest temporal resolution of the monitoring was 15-minutes, any effect on pollutant concentrations due to signal timing and queuing is masked by logging the data at a longer period than the signal timing cycles. As results from monitoring sites closer to the road display narrower seasonal fluctuations than sites further away (Hargreaves *et al.*, 2000), most of the temporal variation can be explained by diurnal and weekly patterns.

Diurnal Variation

The movement of people, as expressed in travel demand, is the most significant factor influencing the time variation of vehicle emissions (Hao *et al.*, 2000). Motor vehicle traffic is increasingly the most important source group for air pollution, especially in cities (Linkaritakis, 1988; Chan, 1985). Therefore, characterising the diurnal pattern is a fundamental part of understanding the temporal variability of ambient concentrations at a monitoring site.

Weekly Variation

It is important to analyse the weekly variation, as systematic differences tend to exist between the pollutant concentrations measured during the working week and during the weekend (Shi and Harrison, 1997).

Seasonal Variation

A marked seasonal cycle is typical of primary pollutants in urban areas, with highest concentrations observed during winter months and lowest concentrations in the summer months, for most climates (Derwent *et al.*, 1995). However, this effect can be offset by the proximity of the monitoring station to the road, as sites closer to the roadside tend to display smaller seasonal fluctuations (Bower *et al.*, 1991), due to decreased influence of dilution and dispersion.

5.1.1 Diurnal Trends in Carbon Monoxide Concentrations

In areas such as cities, where the majority of CO emissions are due to vehicular sources, the diurnal traffic patterns closely reflect CO emissions (Comrie and Diem, 1999). However, the effects of driving patterns may modify this relationship. When traffic flow decreases, CO emission rates drop proportionately further than the decrease in traffic flow, due to increased travel speed (Hao *et al.*, 2000). Concentrations also tend to be higher at intersections where queuing occurs because of the increased time spent accelerating or decelerating (Akeredolu *et*

al., 1994). Other studies do, however, show a quite repeatable CO trend, connected with the local traffic patterns (Maffeis, 1999).

Figure 5.1 shows the CO concentrations and the numbers of vehicles counted at the Pearse St./Westland Row intersection (see Section 3.3) on a sample day, 28th January 1998. The trend in CO concentrations is seen to follow closely the traffic patterns at the junction (wind speeds remained consistently low on this day).

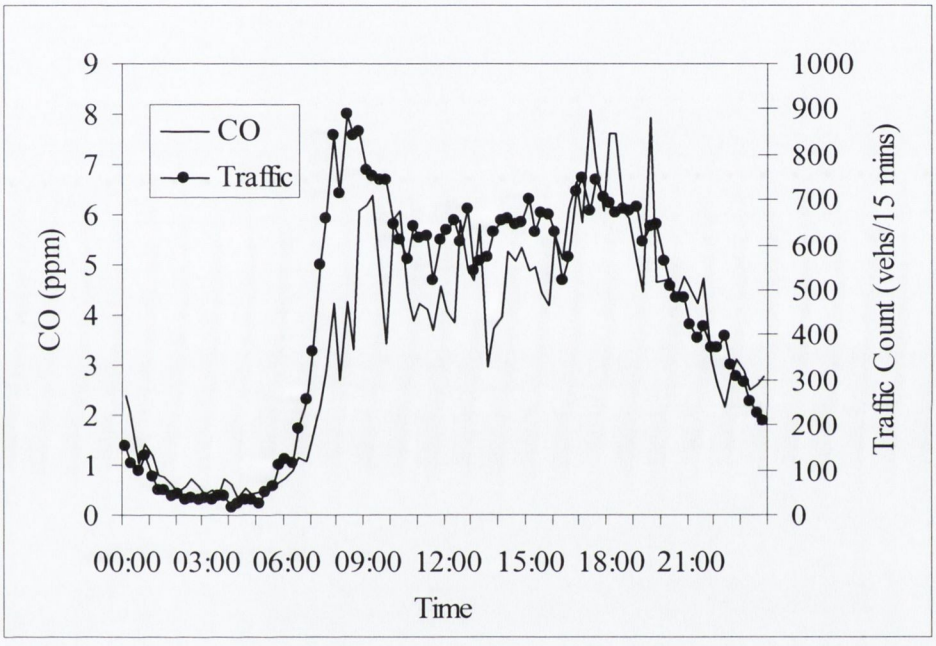

Figure 5.1 CO concentrations and numbers of vehicles through the junction. (Measurements taken at 15-minute intervals on 28th January 1998)

Figure 5.2 shows 15-minute average CO concentrations for one day, averaged over a one-month period to decrease the effect of short-term meteorological variables. Weekdays and weekends are seen to follow different patterns. This conforms to the tendency reported elsewhere for weekday CO levels to peak in the morning and evening rushhours, and fall to a minimum during the night (Nielson, 1996; Hao *et al.*, 2000). The weekend shows a gradual build-up of concentrations from the minimum values recorded overnight to a maximum at approximately 17:00.

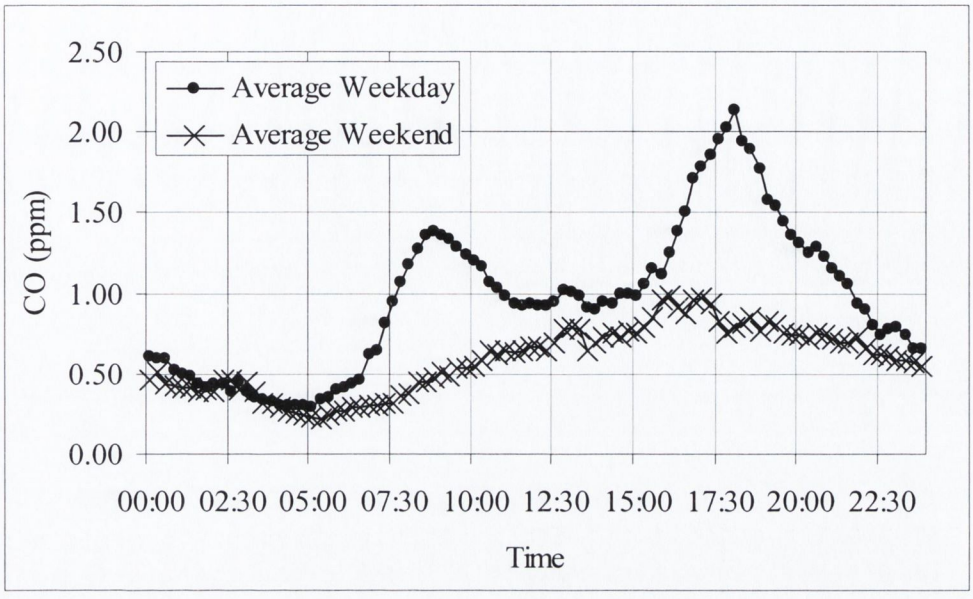

Figure 5.2 Sample diurnal pattern for CO (weekday and weekend) averaged over three months (October, November and December, 1998)

5.1.2 Diurnal Trends in Nitrogen Dioxide Concentrations

Explanation of the diurnal NO_2 patterns is more complex because this pollutant is a secondary compound. The transformation rate of NO into NO_2 depends on emission characteristics, meteorological conditions, solar radiation, local environment and background concentration of various pollutants (NO, NO_2, O_3, and hydrocarbons) (Härkönen *et al.*, 1998).

Variations in observed ambient NO_2 levels throughout the day are influenced by several factors:

a) Ambient NO levels, since most NO_2 arises from oxidation of this primary product;

b) The relative importance of the NO_2 formation and removal processes. These, in turn, will be dependent on insolation and temperature, as well as on ambient concentrations of NO, O_3 and reactive hydrocarbons;

c) Atmospheric stability and wind speed, which control dispersive processes;

d) The separation of the measurement site from major emission sources, determining the transit time of primary emissions and the consequent extent of oxidation;

e) The proportions of primary NO_2 emitted from sources: higher emissions may occur from idling engines (Bower *et al.*, 1991).

For this reason, correlations between NO_2 levels and traffic volumes are weaker than for CO, an observation also reported by Lam *et al.* (1999).

This effect is clear from the sample data in Figure 5.3. However, NO_2 levels do start to increase around 06:00, the same time that traffic levels begin to rise steeply. (The poor resolution of the NO_2 monitor, described in Section 3.4.2, is reflected in the stepped effect of the graph.)

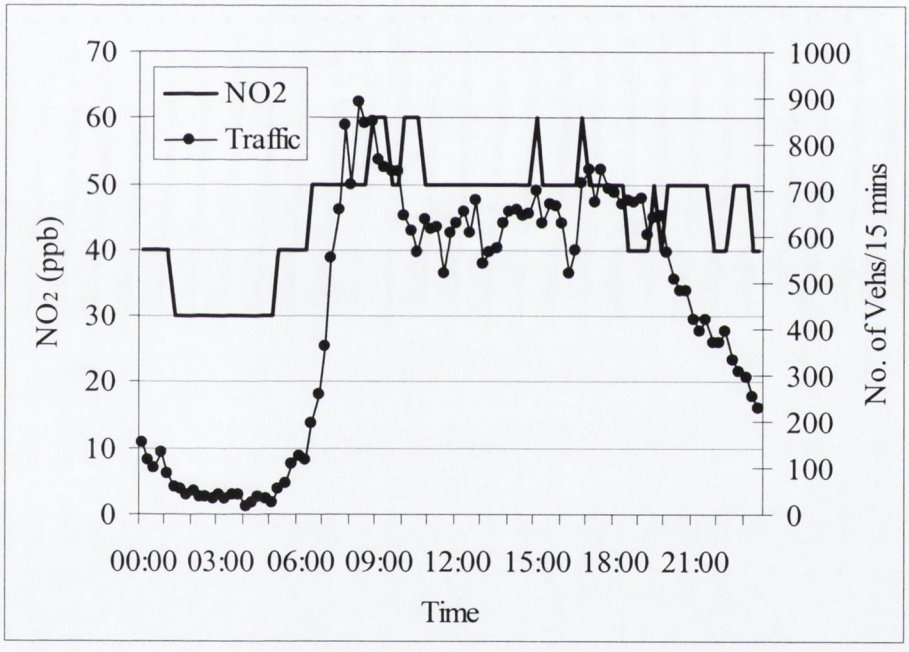

Figure 5.3 NO_2 concentrations and numbers of vehicles through the junction (Measurements taken at 15-minute intervals on 28th January 1998)

Due to greater traffic flows, the NO_2 levels are higher on weekdays than on weekends. Diurnal averages for both the weekdays and weekends show that NO_2 levels build up gradually during the day, due to oxidation of the limited primary emissions, and peak in the early evening (Figure 5.4). Concentrations decline gradually overnight due to dispersion and possible removal processes such as ozone scavenging (Bower *et al.*, 1991).

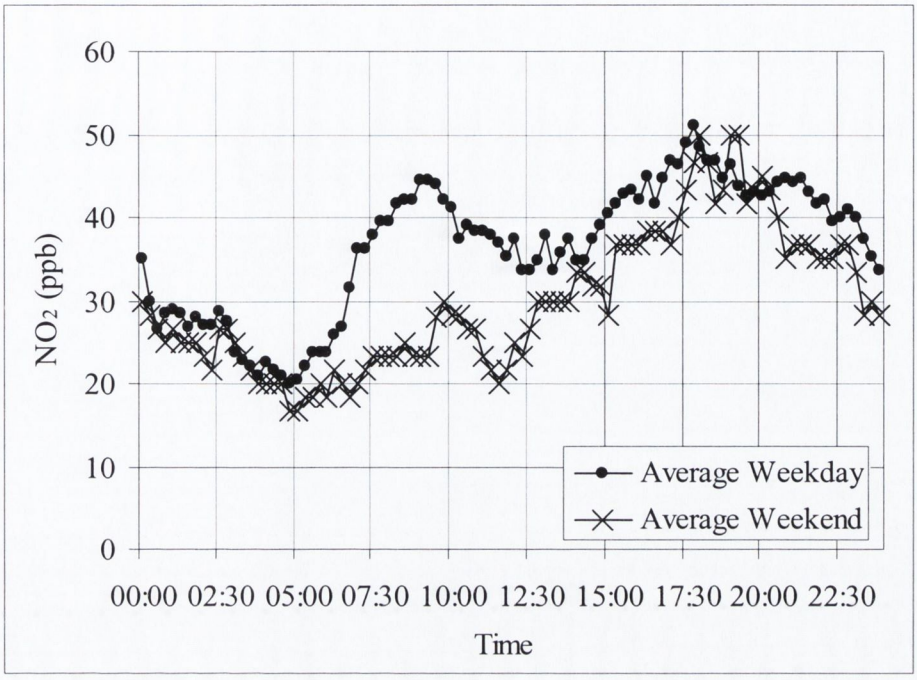

Figure 5.4 Sample diurnal patterns for NO_2 (weekday and weekend) averaged over three months (October, November and December, 1998)

5.1.3 Diurnal Trends in PM_{10} Concentrations

Diurnal variability in PM_{10} concentrations is influenced by the two separate processes, which give rise to primary and secondary particulates. Primary particulates are emitted from the exhaust. Secondary particulates are formed in the atmosphere. Secondary particulates can be formed through photochemical smog, produced by the action of sunlight on gaseous emissions (Lodge *et al.*, 1981), or through processes such as agglomeration. However, as the meteorological conditions in Dublin do not give rise to the formation of photochemical smog (Marnane, 2000), the PM_{10} concentrations (Figure 5.5), follow the traffic pattern more closely than would otherwise be the case. On weekdays, concentrations are seen to follow the trend in traffic flow, reaching a minimum in the early hours of the morning. Typical diurnal patterns for weekdays and weekends are shown in Figure 5.6.

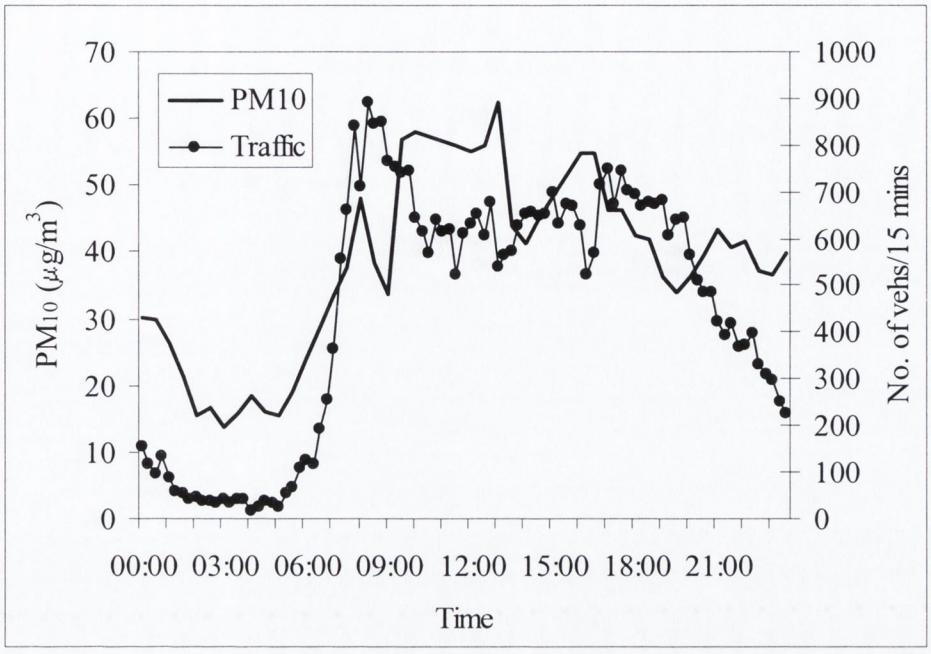

Figure 5.5 PM_{10} concentrations and numbers of vehicles through the junction. (Measurements taken at 15-minute intervals on 28th January 1998)

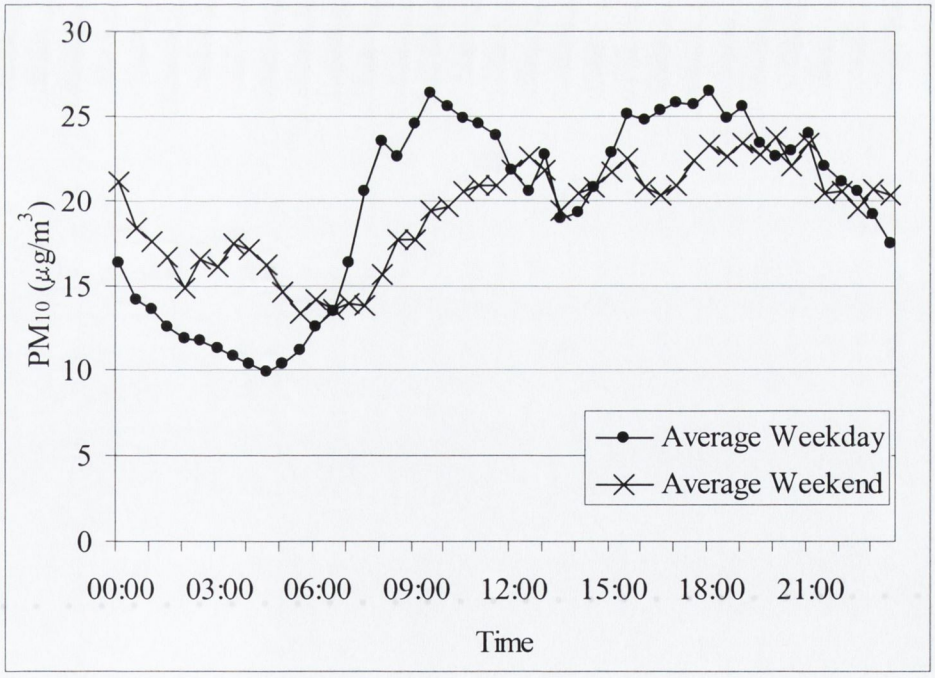

Figure 5.6 Sample diurnal pattern for PM_{10} (weekday and weekend) averaged over three months (January, February, March, 1998)

5.1.4 Comparison of Daily Profiles

The typical daily profiles calculated for weekdays and weekends in Sections 5.1.1, 5.1.2, and 5.1.3 are normalised and compared in Figure 5.7. The weekday profiles for NO_2 and PM_{10} are seen to agree very closely. The daily weekday profile for CO shows more exaggerated peaks and troughs, especially during the congested evening rush hour. On weekends, all three compounds show a similar daily profile; this may be due to the absence of congestion on these days.

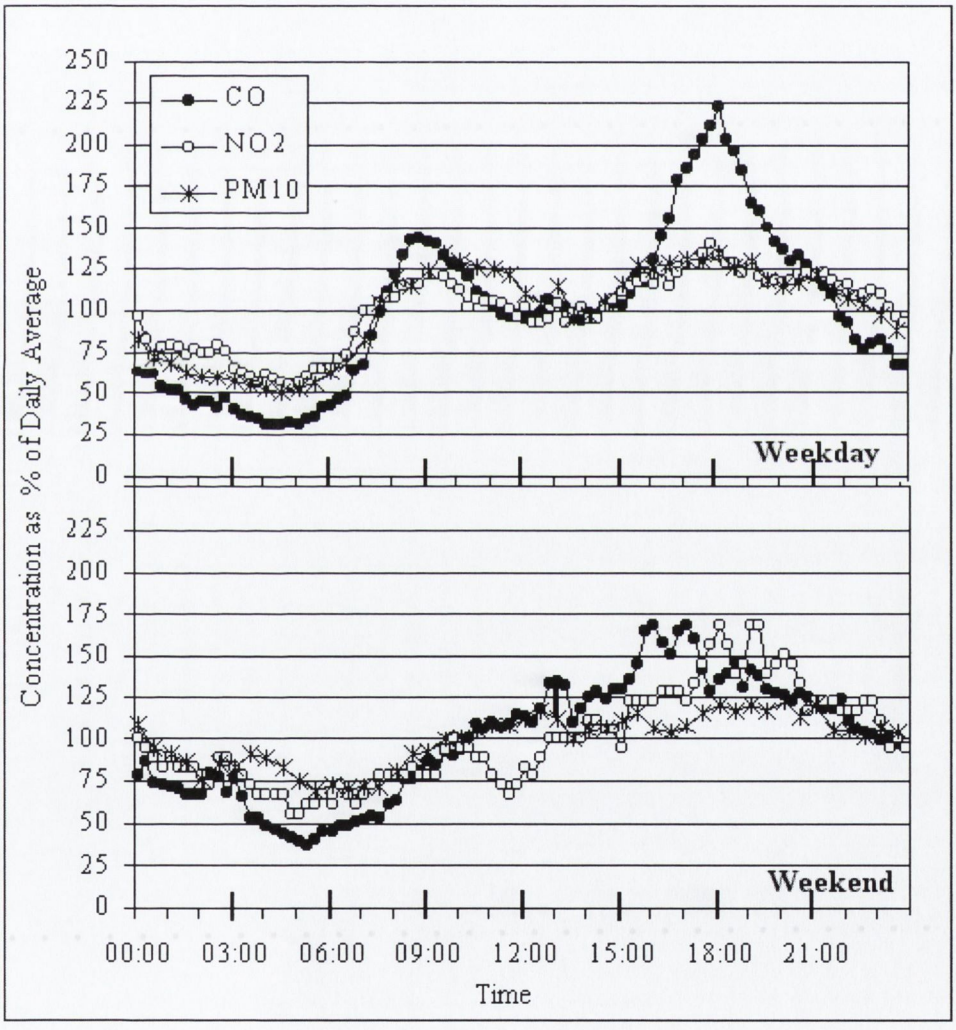

Figure 5.7 Comparison of daily (weekday) profiles for CO, NO_2, and PM_{10} calculated over three months

5.1.5 Weekly Trends in Carbon Monoxide Concentrations

In general, CO concentrations tend to exhibit a strong weekly cycle (Bogo *et al.*, 1999; Maffeis, 1999). Meteorological factors being equal, average weekday concentrations tend to be higher than weekend concentrations. The average ratio of weekend averages to weekday averages is 0.73 for the data measured at the Pearse St./Westland Row intersection. There tend to be no clear differences between the weekdays, all of which follow a very similar pattern. This is illustrated by sample days, averaged over the course of several months, in Figure 5.8. Both Saturday and Sunday follow a similar trend, which is clearly different to that of the weekdays.

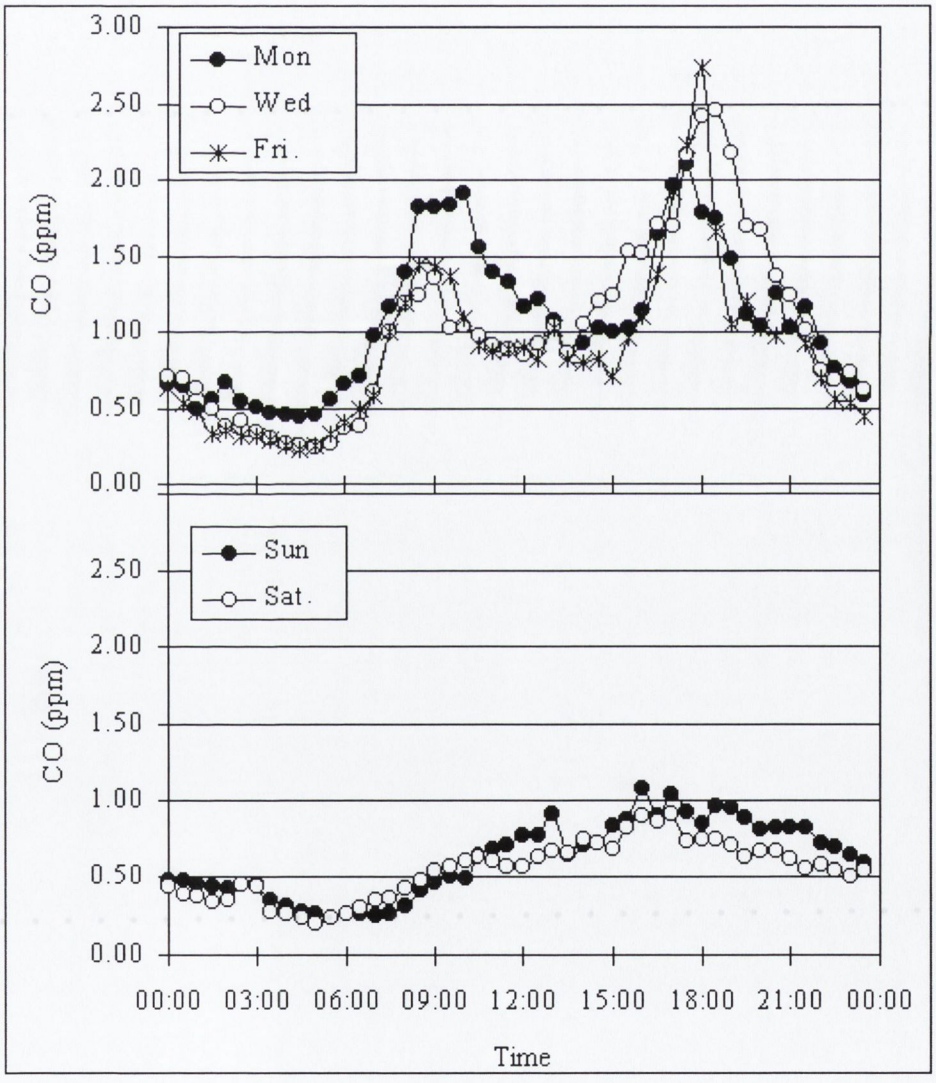

Figure 5.8 Sample diurnal trend sample days for CO averaged over three months (October, November and December, 1998)

5.1.6 Weekly Trends in Nitrogen Dioxide Concentrations

NO_2 concentrations are seen to exhibit similar trends to CO, as regards the similarity of days. Shi and Harrison (1997) also found real and systematic differences in NO_2 levels between weekdays and weekends, in London. At the Dublin site, the weekdays, as shown in Figure 5.9, tend to follow similar patterns, which are different to Saturday and Sunday, which in turn resemble each other.

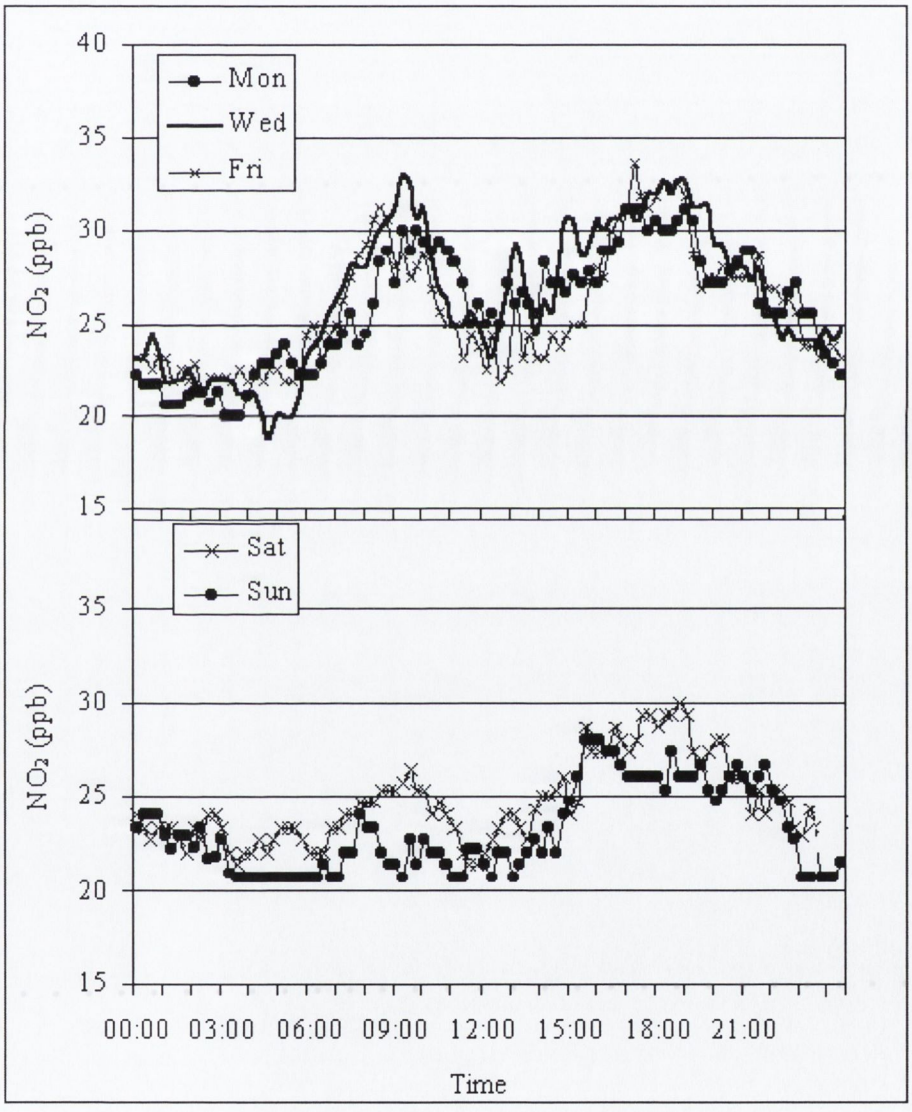

Figure 5.9 Sample diurnal trend for NO_2 averaged over three months (October, November and December, 1998)

5.1.7 Weekly Trends in PM_{10} Concentrations

The weekly trends for PM_{10} are presented in Figure 5.10 with typical profiles for weekdays and weekends illustrated. As can be seen, the weekdays and weekends follow different diurnal patterns, with a smaller peak during the day during Saturday and Sunday.

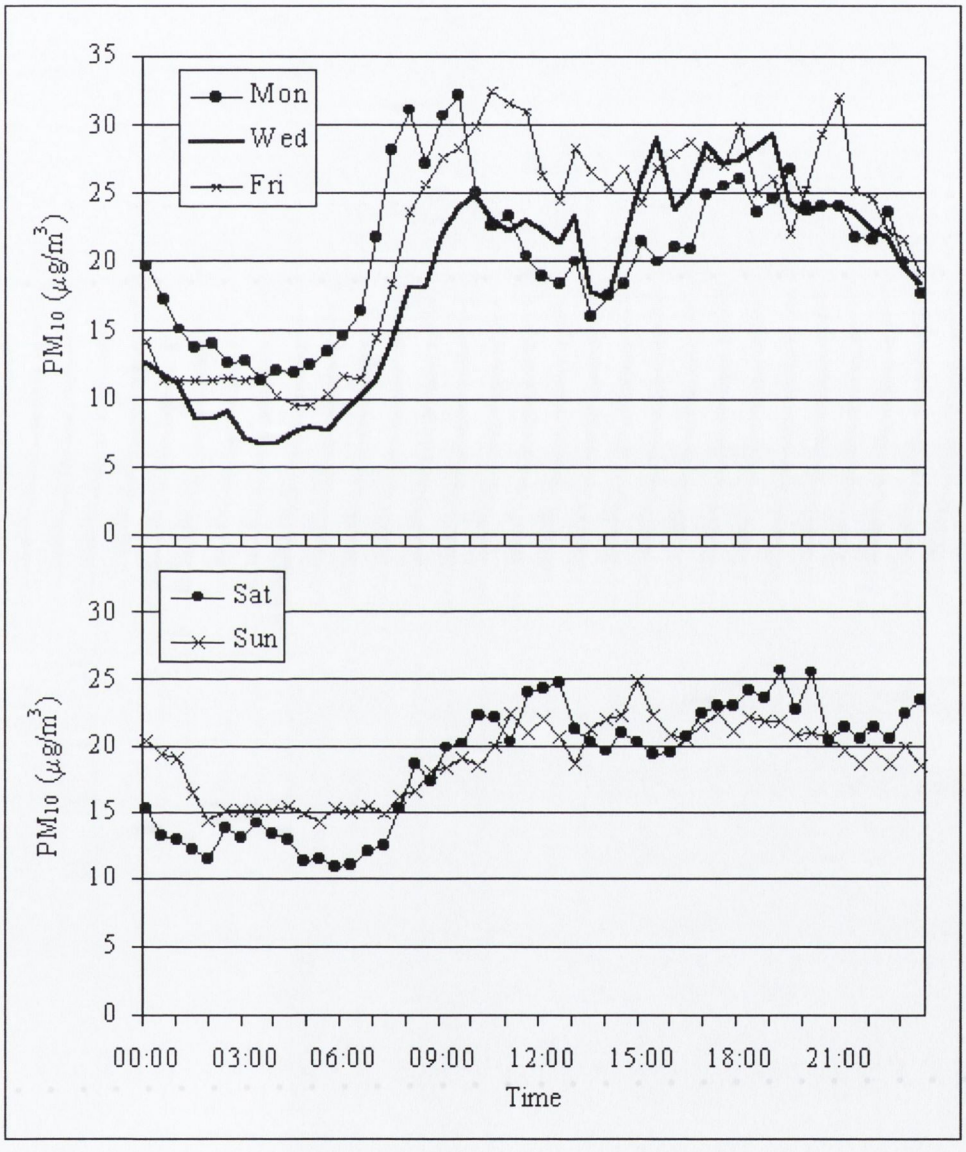

Figure 5.10 Sample diurnal trend for Monday, Tuesday and Wednesday for PM_{10} averaged over three months (January, February, March, 1998)

5.1.8 Seasonal Trends in Carbon Monoxide Concentrations

Studies elsewhere have shown that ambient CO concentrations often exhibit seasonal fluctuations (e.g. Glen *et al.*, 1996; Bogo *et al.*, 1999; Jo *et al.*, 2000). This is due to both the temperature dependence of CO emissions and varying atmospheric dispersion capability (Maffeis, 1999). However, as mentioned in the introduction to Section 5.1, these differences tend to be less noticeable at monitoring stations close to the roadside.

Figure 5.11 presents the monthly average concentrations of CO from January 1998 to January 1999. No readings were taken during May, June and July. With these months missing, recognition of the existence of a seasonal trend is difficult, although the lowest average was measured in August. It is also clear that significantly higher CO concentrations were measured during January 1998 to April 1998 (before recalibration of the instrument); this is discussed in further detail in Section 4.1.1. Due to the very significant difference in the magnitudes of the recorded CO concentrations before and after the recalibration of the RPM which was not reflected by higher concentrations at a nearby site on College Green, the magnitude of the recorded CO concentrations recorded during January to April 1998 must be regarded with a degree of scepticism.

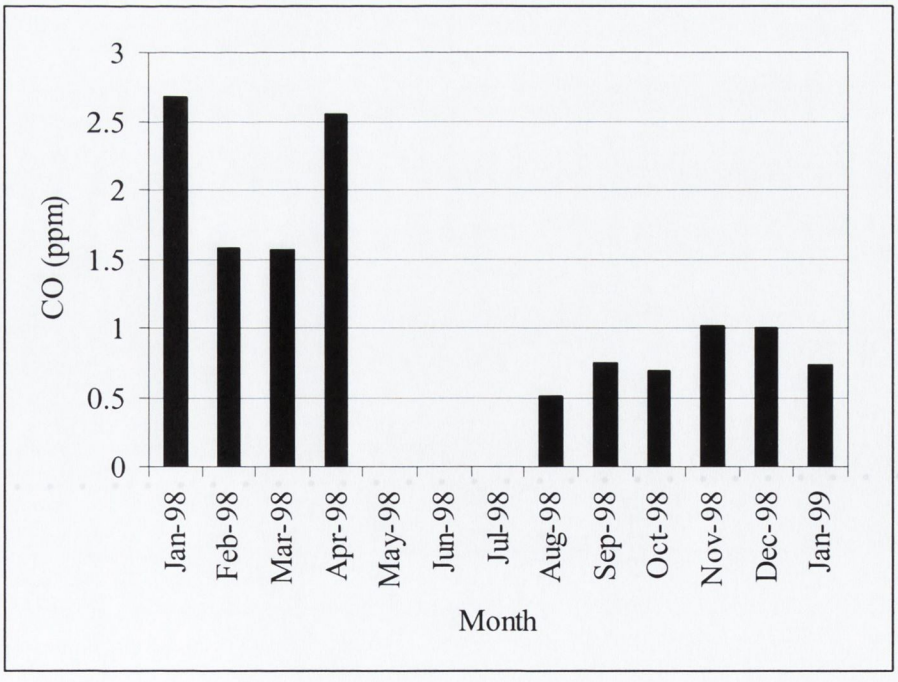

Figure 5.11 Monthly CO averages (Site A – Phase 1)

5.1.9 Seasonal Trends in Nitrogen Dioxide Concentrations

Differing views exist as to the nature of the seasonality of NO_2. Cadle (1985) comments that as urban NO_2 levels are largely dominated by motorvehicle sources, which would not be expected to show large seasonal variations, any seasonal variations would be due to seasonal changes in chemistry. Derwent *et al.*, (1995) reports in a study of London data that NO_2 concentrations peak in the summer, and that this probably reflects faster oxidation of NO to NO_2 in the summer and the greater extent of vertical mixing due to convection. Lebret *et al.* (2000) report in a study on a number of European areas, that concentrations tend to be highest in the winter months, possibly reflecting lower temperatures and mixing heights. Fukino *et al.* (1984), Mondal *et al.* (2000) and Karpinnen *et al.* (2000) also found concentrations of NO_2 to be higher in winter. Mayer (1999) reports that there is only slight variation in the annual cycle of NO_2 as this secondary substance is created mainly by chemical reactions. In relation to the monitoring undertaken in this research, the proximity of the monitoring station to the road mitigates against the observation of seasonal trends; increased summer oxidation rates exert less influence on measured NO_2/NO_x ratios at locations where sampling is undertaken close to the point of primary pollutant emissions (Bower *et al.*, 1991).

There are three mechanisms affecting ambient NO_2 concentrations:

- The effect of meteorological conditions on mixing;
- The influence of any possible seasonal change in the emissions of the pollutant, such as increased space heating in winter;
- The enhanced $NO \rightarrow NO_2$ oxidation process, due to increased ambient ozone levels together with higher temperatures and insolation rates which will tend to reduce overall NO levels.

These three mechanisms act in concert to reduce summer NO concentrations but increase average winter concentrations. For NO_2, however, the third mechanism opposes mechanisms

one and two and, in consequence, tends to reduce seasonal variability (Bower *et al.*, 1991). It is the balance of these three mechanisms that will determine the seasonal variability of NO_2.

Again, as for CO, no measurements were taken in the months of May, June or July. Despite missing these months, there would appear to be no seasonal trend in the NO_2 data (Figure 5.12). Concentrations of NO_2 are highest in the early part of 1998, but this was not reflected in higher NO_2 concentrations at the Dublin Corporation monitoring site in College Green.

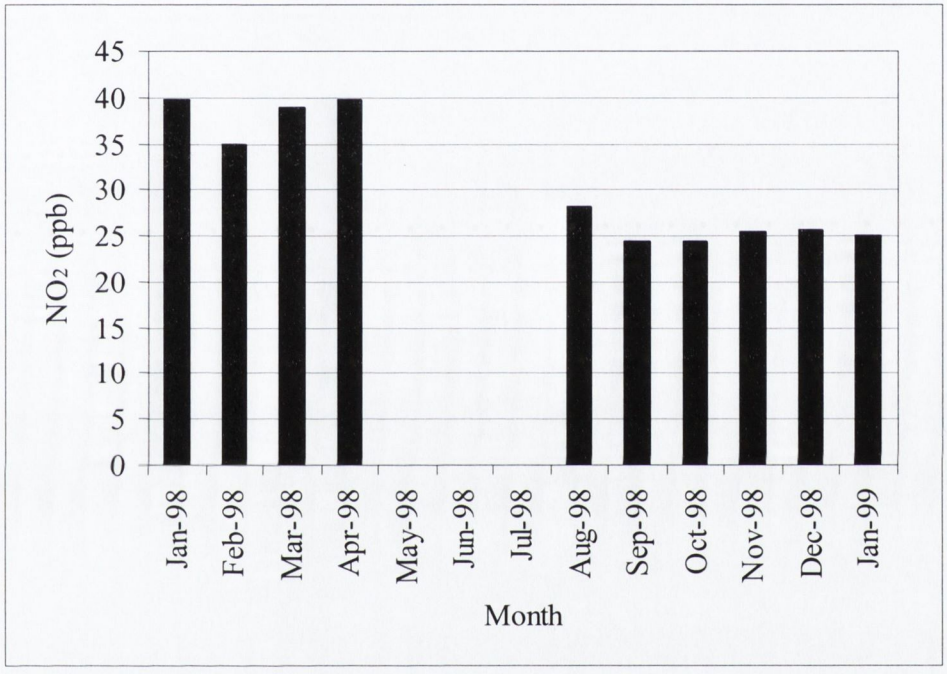

Figure 5.12 Monthly NO_2 averages (Site A – Phase 1)

5.1.10 Seasonal Trends in PM_{10} Concentrations

In winter, higher concentrations of PM_{10} have been reported (Romero *et al.*, 1999; Morel *et al.*, 1999). The major cause for this is not attributed to changes in emission patterns, but to the weather, and to the fact that the particulates are trapped in a smaller volume because the inversion temperature occurs at a lower elevation in winter (Morel *et al.*, 1999). Chow *et al.* (1992) found the primary motor vehicle contribution to PM_{10} to be similar from month to month.

In the current research, the length of the monitoring period makes the analysis of the data for a seasonal trend difficult. However, the lowest average measured was a summer month and the highest was a winter month, which could point towards PM_{10} concentrations being slightly seasonally influenced, although not at a significant level, as illustrated in Figure 5.13.

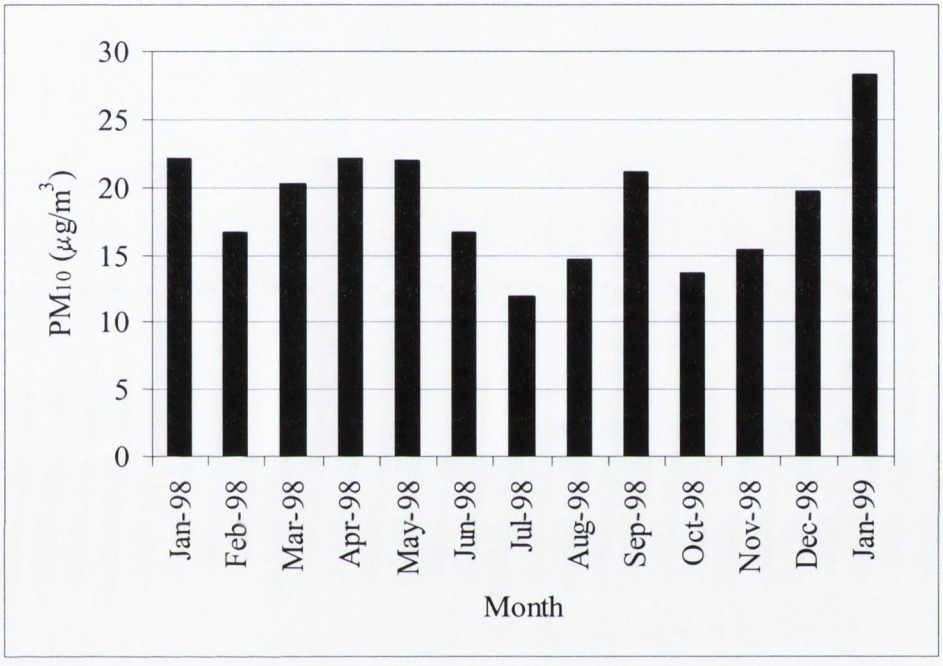

Figure 5.13 Monthly PM_{10} averages (Site A – Phase 1)

5.2 Variation in Pollutant Concentrations with Meteorological Factors

Most urban pollution studies that have been carried out to date have neglected to include full consideration of various meteorological parameters (Croxford and Penn, 1998). However, meteorological factors have been proven to significantly affect ambient urban pollutant concentrations (Kassomenos *et al.*, 1995); therefore, a good knowledge of the effects of meteorological factors on ambient pollution is necessary if a small number of pollutant measurements are to be used to predict the concentrations over longer timescales. It should be noted, also, that while stochastic effects like weather are unpredictable in the short-term, they do not change very much from one year to the next (Morel *et al.*, 1999; Owen *et al.*, 2000).

5.3 Variation in Pollutant Concentrations with Wind Speed

Wind speed increases dilution and diffusion of pollutants (Shi and Harrison, 1997); all other factors being equal, lower pollutant concentrations would be expected at higher wind speeds. However, the relationship between air pollution and wind depends on the physical form of built up area, as well as the wind speed itself (Demirci and Cuhadaroglu, 2000).

5.3.1 Carbon Monoxide

As expected, a negative association was found between CO and wind speed. A Pearson's sample correlation coefficient (r) of –0.75 was calculated for the data collected at the Pearse St./Westland Row intersection between January 1998 and January 1999 where r is calculated using:

$$r = \frac{\sum (x_i - \bar{x})(y_i - \bar{y})}{\sqrt{\sum (x_i - \bar{x})^2}\sqrt{\sum (y_i - \bar{y})^2}} \quad \text{where i} = 1 \ldots n \qquad \text{Equation 5.1}$$

where

(x_1,y_1), (x_2,y_2), …, (x_n,y_n) denote a sample of (x,y) pairs, and $\bar{x}, \bar{y}$ are the averages of the x samples and y samples.

In terms of pollutant concentrations (C) and wind speeds (U) Equation 5.1 is expressed as

$$r = \frac{\sum (C_i - \bar{C})(U_i - \bar{U})}{\sqrt{\sum (C_i - \bar{C})^2}\sqrt{\sum (U_i - \bar{U})^2}} \qquad \text{Equation 5.2}$$

By squaring r, R^2, the coefficient of determination is calculated; this gives the proportion of the variation that is attributable to the linear relationship between the two variables.

To compare the relationship between CO concentrations and wind speed over months with different average wind speeds, each daily average CO reading was expressed as a percentage of the average concentration recorded at a wind speed of 2 m/s (the average wind speed) that month. This allowed the data from all months to be included in the comparison. All CO data were then plotted against wind speed in Figure 5.14 (only weekdays being included.). A downward trend with increasing wind speed can be clearly observed.

When the CO concentrations are averaged in increments of 0.2 m/s wind speed, the data are seen to approximate closely the power series described in Equation 5.3 (R^2 = 0.97), and illustrated in Figure 5.15.

$$y = 154.34\ (x)^{-1.03} \qquad \text{Equation 5.3}$$

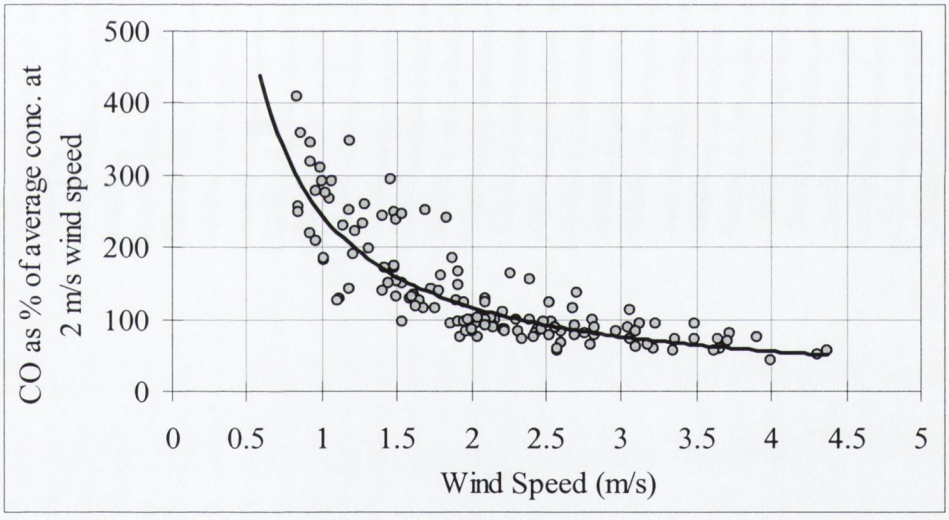

Figure 5.14 Average CO 24-hour concentrations (as a percentage of the average concentration at wind speed = 2 m/s) against wind speed.

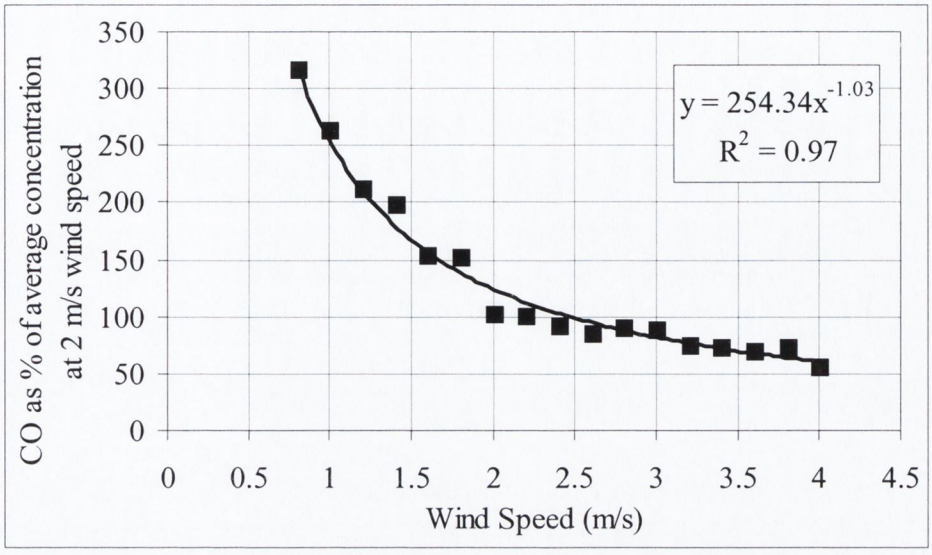

Figure 5.15 Average CO 24-hour concentrations as a percentage of the average monthly concentration at a wind speed of 2 m/s. Concentrations averaged over 0.2 m/s increments

5.3.2 Nitrogen Dioxide

A negative correlation between NO_2 concentrations and wind speed has been reported in studies elsewhere (Hargreaves *et al.*, 2000; Fenger 1999). However, the readings taken at the junction were found to be only slightly negatively correlated ($R^2 = -0.27$). Again, to avoid the calculations being influenced by possible seasonal factors, the NO_2 concentrations were expressed as a percentage of the average concentration for that month, at a wind speed of 2 m/s (the average wind speed). These NO_2 concentrations are shown plotted against wind speed in Figure 5.16.

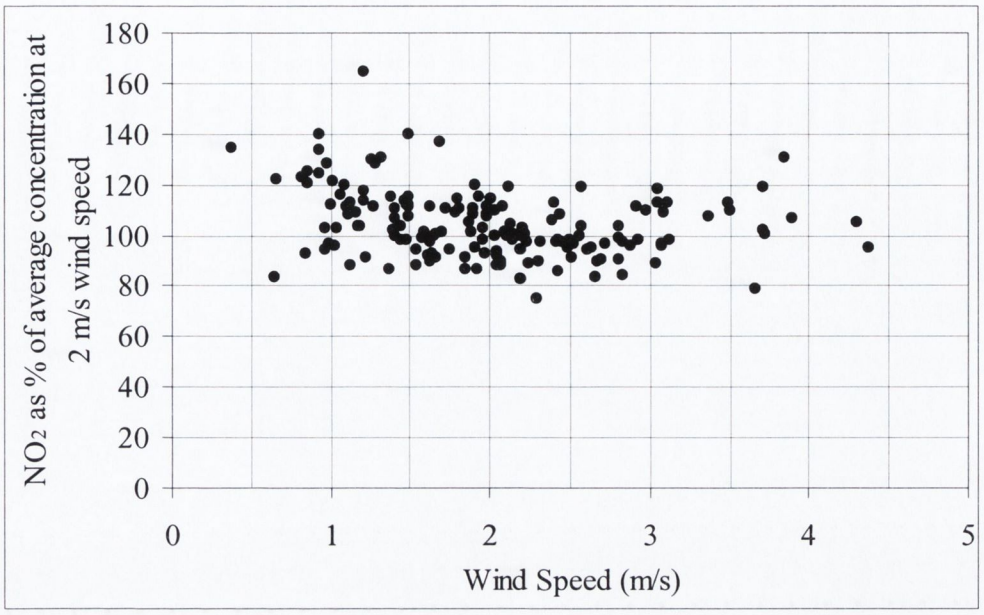

Figure 5.16 Variation of NO_2 24-hour concentrations (as a percentage of the average concentration at a wind speed of 2 m/s each month) with average daily wind speed.

This trend is highlighted in Figure 5.17, where the NO_2 concentrations are averaged for each 0.2 m/s wind speed increment. Concentrations are seen to decrease with increasing wind speed until the wind speed reaches 3 m/s, when concentrations increase again. Although the slight increase in NO_2 concentrations at 3 m/s is unexpected, the return of NO_2 concentrations to seasonal averages at particularly high wind speeds (4 m/s) has been reported before (Hargreaves *et al.*, 2000), although it was attributed to the effect of high wind speeds on diffusion tubes. Further investigation confirmed that this effect was not attributable to any particular episode, with data from every month but January 1998 included in the average.

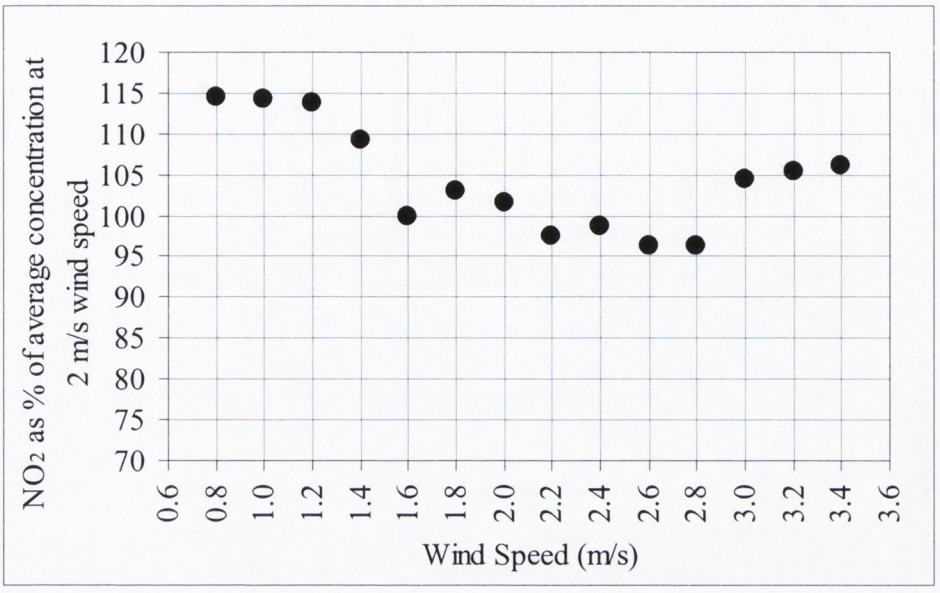

Figure 5.17 Average NO_2 24-hour concentrations (as a percentage of the average concentration at a wind speed of 2 m/s) plotted against 0.2 m/s increments of wind speed.

5.3.3 PM_{10}

Harrison *et al.* (1997) and Lam *et al.* (1999) both found PM_{10} concentrations to be slightly correlated with wind speed, albeit with low correlation coefficients. The data monitored at the junction was also found to be moderately negatively correlated with wind speed (as shown in Figure 5.18), with a correlation coefficient of –0.65. The effect of wind speed on PM_{10} concentrations becomes clearer when the average PM_{10} concentration is calculated for each 0.2 m/s wind speed increment (Figure 5.19). The data are seen to follow a power series with an R^2 value of 1.00.

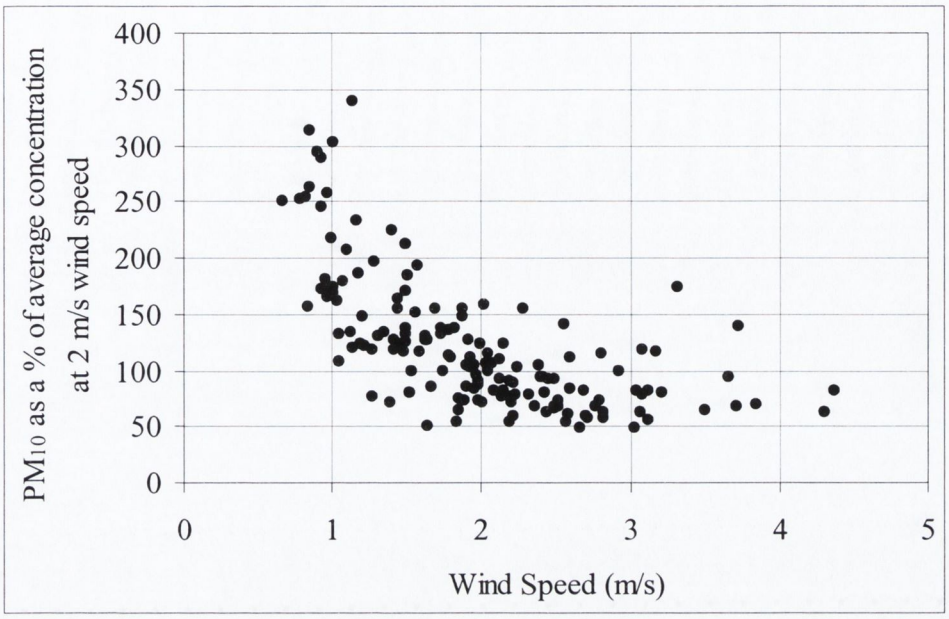

Figure 5.18 Variation of PM_{10} 24-hour concentrations (as a percentage of the average concentration at a wind speed of 2 m/s each month) with average daily wind speed.

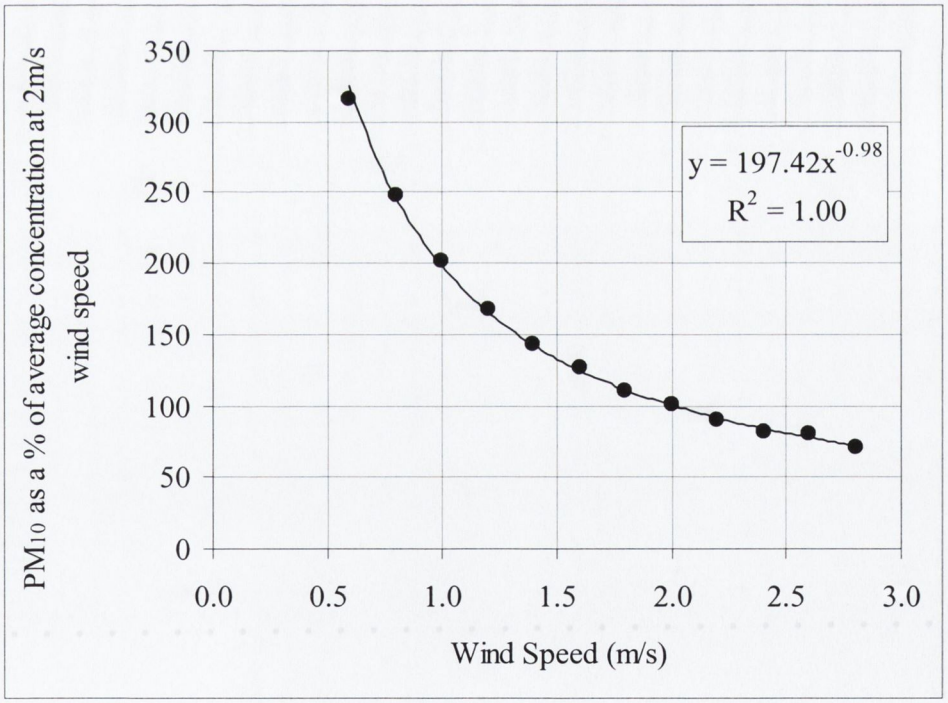

Figure 5.19 Average PM_{10} 24-hour concentrations (as a percentage of the average concentration at a wind speed of 2 m/s) plotted against 0.2 m/s increments of wind speed.

5.4 Variation in Pollutant Concentrations with Wind Direction

5.4.1 Carbon Monoxide

Croxford and Penn (1998) and Scaperdas and Colville (1999) reported that wind direction was a significant factor in the concentrations of CO measured. It was found that a change in wind direction could result in a difference in measured CO concentrations of up to 80% for a given level of traffic emissions and meteorological conditions (Scaperdas and Colville 1999). CO concentrations measured in the same study were also found to be dependent on wind speed.

In the present research, all CO concentrations measured were split into categories based on wind direction. The average concentration in each 45° direction category was calculated. Concentrations were found to follow the same pattern each month and the average results are shown in Figure 5.20. Concentrations are highest when the wind is blowing from the junction to the monitoring station, and lowest when the wind is blowing from the Trinity College campus; schematic diagrams of the monitoring site and the position of the site in the city centre are shown in Figure 3.3 and Figure 3.2, respectively. The ratio of the average concentration with a north-easterly wind to the average concentration with a south-westerly wind is 2.9.

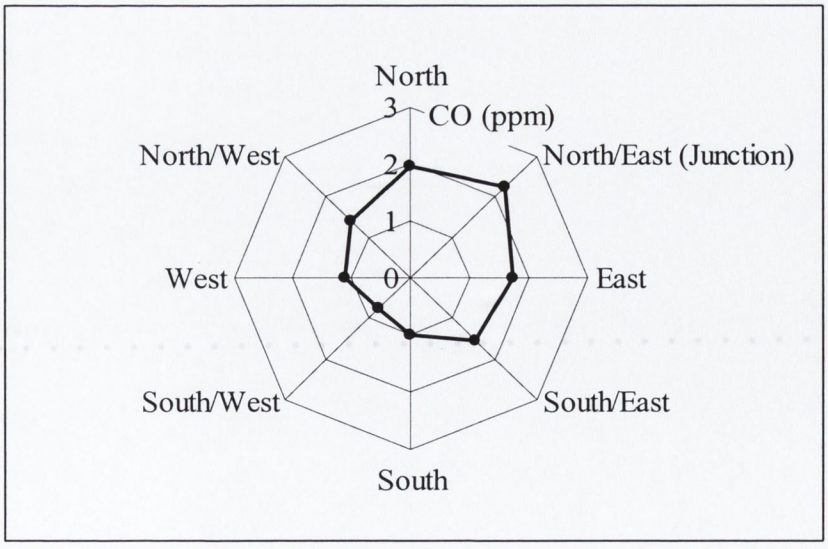

Figure 5.20 Graph of CO concentration with respect to wind direction

However, at the monitoring site, wind speeds from the north-east tend to be higher than those from the south-west, reducing the average CO concentration from that direction. Hence, the effect of wind direction alone is actually greater than that suggested in Figure 5.20. Using the power series Equation 5.3, in Section 5.3.1, average CO concentrations can be adjusted to estimate the equivalent concentration at 2 m/s wind speed. The results are shown in Figure 5.21 in which the effect of the wind direction is more pronounced. The ratio of the mean concentration when the wind is blowing from the junction (north-east) to that when the wind is blowing from the campus (south-west) has increased to 5.9.

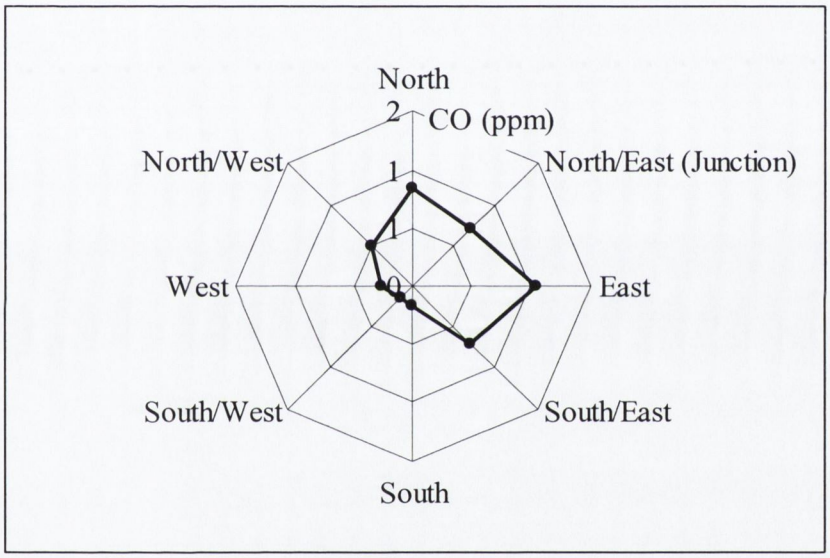

Figure 5.21 CO concentrations, adjusted for wind speed, with respect to wind direction

Figure 5.22 shows a radar diagram of CO concentrations with respect to wind direction, superimposed on a schematic map of the junction. It becomes clear that the highest CO readings are recorded when the wind blows from the North or East, transporting CO emissions from cars travelling on Pearse St. West and queuing at junction, directly to the monitor. The highest concentrations are observed when the wind blows from the queue at the end of Pearse St. East. Slightly lower concentrations are recorded when the wind blows from the centre of the junction, as dispersion and dilution have a greater effect with the increased distance.

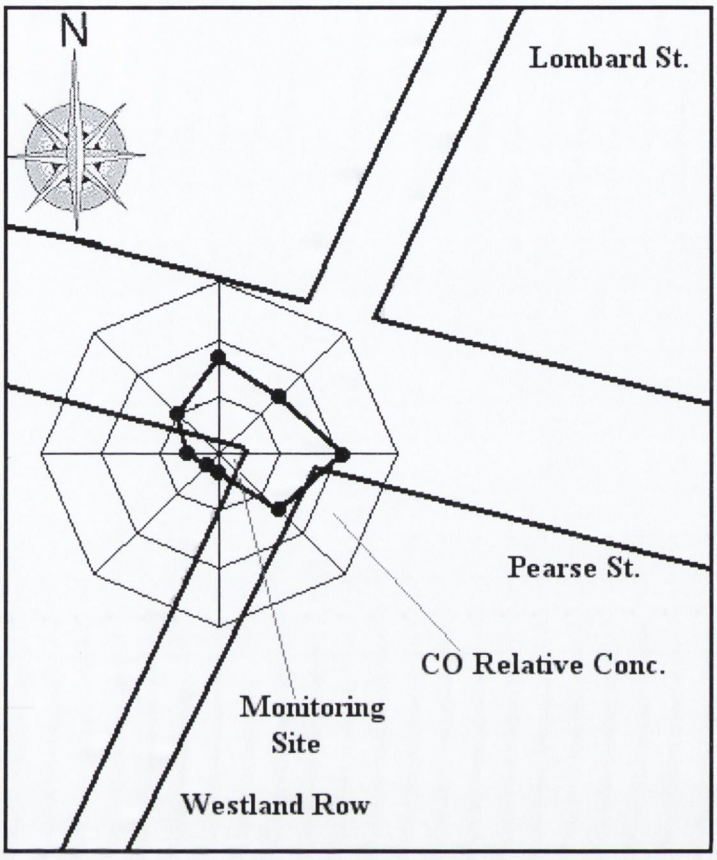

Figure 5.22 Radar diagram of relative CO concentrations with respect to wind direction superimposed on schematic map of monitoring site

5.4.2 Nitrogen Dioxide

Previous work suggests that the transformation of NO into NO_2 is most efficient when wind velocity is parallel to the road (Härkönen *et al.*, 1998). Berkowicz *et al.*, (1996) found NO_x concentrations to be dependent on wind direction. However, in this study, concentrations of NO_2 at the junction were found to be reasonably independent of wind direction, as shown in Figure 5.23. As for CO, the NO_2 data were divided into 8 directions and averaged. The ratio of the mean concentration with wind blowing from the north-east (junction) to that observed with wind blowing from the south-west (campus) is 1.2. Concentrations were then adjusted for wind speed according to Figure 5.17, in Section 5.3.2, and plotted against wind direction in Figure 5.24. Concentrations were found to still be largely independent of wind direction with

the ratio of the mean concentration with wind blowing from the north-east (junction) to that observed with wind blowing from the south-west (campus) being 1.1.

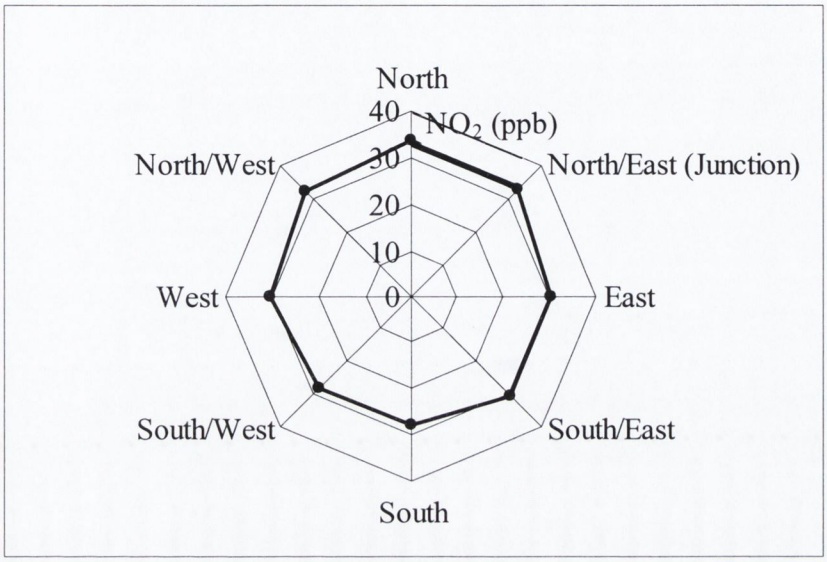

Figure 5.23 Graph of NO_2 concentration with respect to wind direction

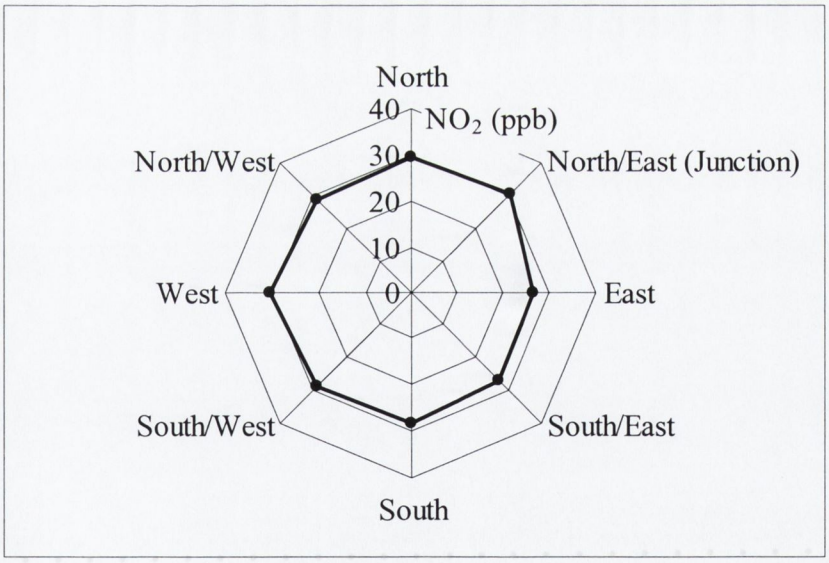

Figure 5.24 NO_2 concentrations, adjusted for wind speed, with respect to wind direction

5.4.3 PM_{10}

Urban concentrations of PM_{10} were found to be influenced by wind direction by Namdeo *et al.*, (1998). To investigate the influence of wind direction on PM_{10} concentrations at the junction, the same procedure as that used for CO and NO_2 was carried out for PM_{10}, using the data collected over 13 months. The concentrations before and after adjustment are shown in Figure 5.25 and Figure 5.26, respectively, which are representative of the individual monthly patterns. PM_{10} concentrations are seen to follow a similar pattern as CO, although with a slightly different magnitude, as the ratio of concentrations with the wind blowing from the north-east (junction) to those measured with the wind blowing from the south-west (campus), are 2.0 and 3.0 for the unadjusted and adjusted data, respectively.

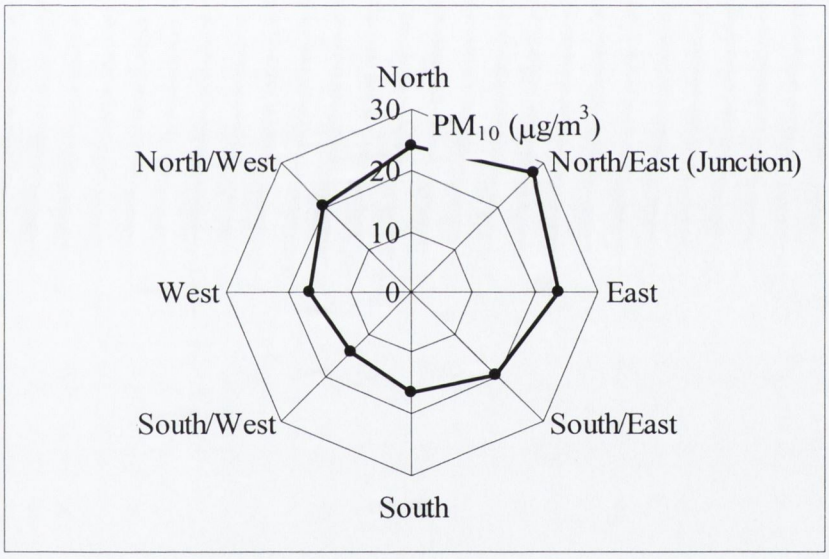

Figure 5.25 Graph of PM_{10} concentration with respect to wind direction

Figure 5.27 shows the radar graph from Figure 5.26 superimposed on a schematic map of the junction. The highest PM_{10} concentrations are seen to coincide with wind blowing from Pearse St. West and cars queuing at the traffic lights on Westland Row, as these directions represent the shortest travel distances and hence are the least affected by dilution and dispersion.

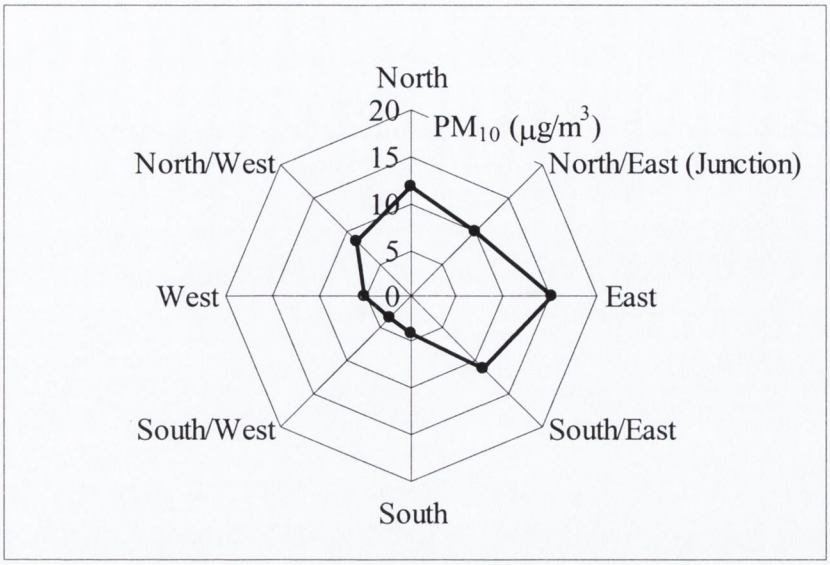

Figure 5.26 PM_{10} concentrations, adjusted for wind speed, with respect to wind direction

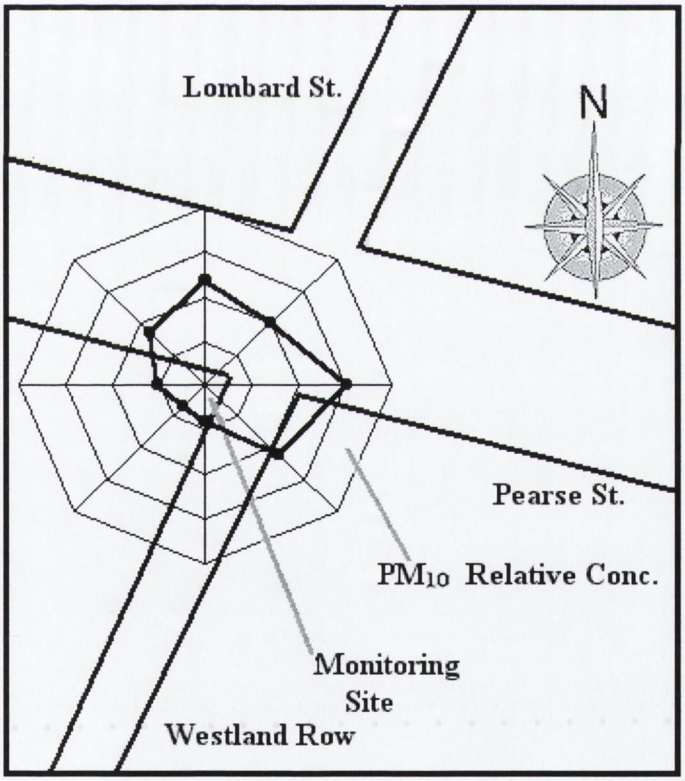

Figure 5.27 PM_{10} radar diagram (with respect to wind speed) superimposed on a schematic map of the Pearse St./Westland Row intersection

5.5 Variation in Pollutant Concentrations with Temperature

5.5.1 Carbon Monoxide

Motor vehicle emissions are reported to be sensitive to ambient temperature (Stump *et al.*, 1989) but Chang *et al.* (1980) reported that the temperature dependence of vehicle emissions did not have an effect on ambient atmospheric CO levels, based on an analysis of American cities. The CO concentrations measured at the Pearse Street/Westland Row junction were also found to be independent of the ambient temperature. Monthly values of Pearson's sample correlation coefficient, r, calculated using 24-hour averages, ranged between –0.31 and 0.34, averaging at –0.01. No stronger correlation was found when other averaging periods were analysed. Figure 5.28 is a scatter chart showing two consecutive months data.

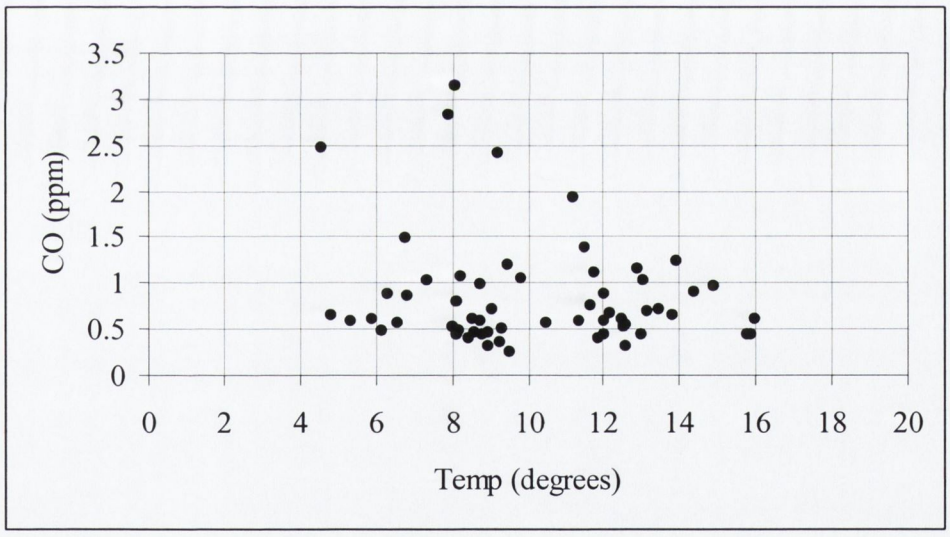

Figure 5.28 Sample scatter chart of 24-hour averages of CO and temperature recorded during November 1998 and December 1998

5.5.2 Nitrogen Dioxide

Although it has been reported elsewhere that the net production of NO_2 from NO increases with temperature (Härkönen *et al.*, 1998), concentrations of NO_2 observed at Site A were found to be independent of temperature. Values of Pearson's sample correlation, r, calculated monthly using 24-hour averages, ranged between –0.25 to 0.28, averaging at –0.03. Values of r remained insignificant with other averaging periods. A scatter chart of 24-hour average NO_2 concentrations and temperature values measured over six months is given in Figure 5.29.

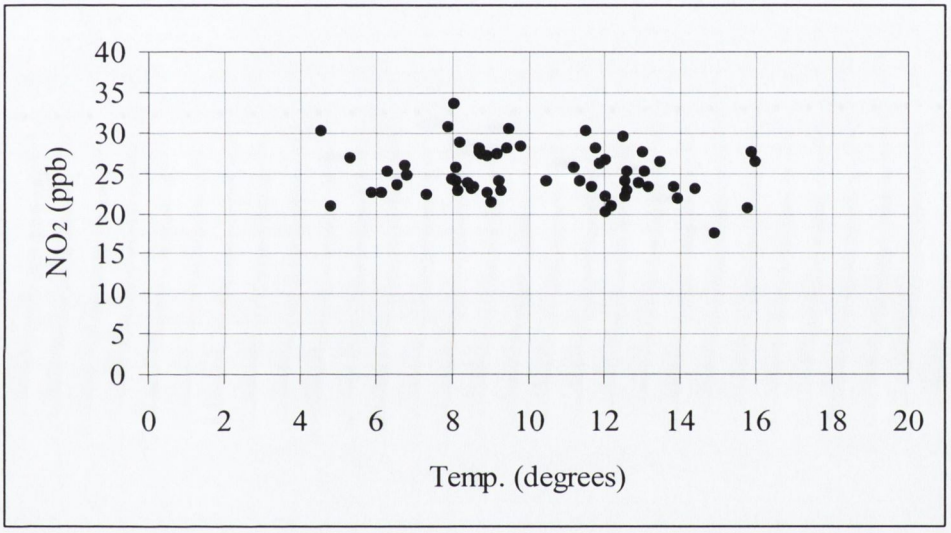

Figure 5.29 Sample scatter chart of 24-hour averages of NO_2 and temperatures recorded during November 1998 and December 1998

5.5.3 PM_{10}

Cuhadaroglu and Demirci (1996) found concentrations of suspended particulates increased with increasing temperature due to formation of inversion layers. However, in this study, measured PM_{10} concentrations were found to be independent of the ambient temperature. Monthly values of Pearson's sample correlation, r, calculated using 24-hour averages ranged between –0.08 and 0.28, averaging at 0.05. Values of the correlation coefficient, r, were no

more significant for other averaging periods. Figure 5.30 shows a scatter chart of 24-hour averages of PM_{10} against temperature measured over six months.

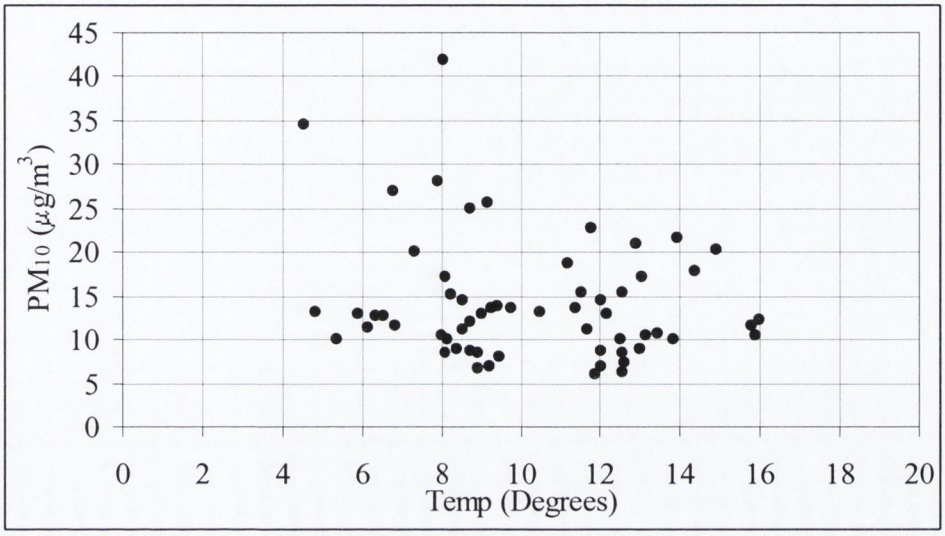

Figure 5.30 Sample scatter chart of 24-hour averages of PM_{10} and temperatures

5.6 Variation in Pollutant Concentrations with Relative Humidity

5.6.1 Carbon Monoxide

Concentrations of CO were not observed to have a significant level of correlation with relative humidity. A Pearson's sample correlation value of 0.31 was calculated for the 24-hour averages recorded over the six-month period graphed in Figure 5.31. However, when individual months were analysed, values of r fell below zero on a number of occasions.

5.6.2 Nitrogen Dioxide

Concentrations of NO_2 were also found not to have a significant level of correlation with relative humidity. A Pearson's sample correlation value of -0.24 was calculated for the sample six month period shown in Figure 5.32, indicating a slight negative association, but

when individual months were analysed separately, values of r varied between –0.4 and 0.09, averaging at –0.11 for all recorded data, suggesting very little correlation.

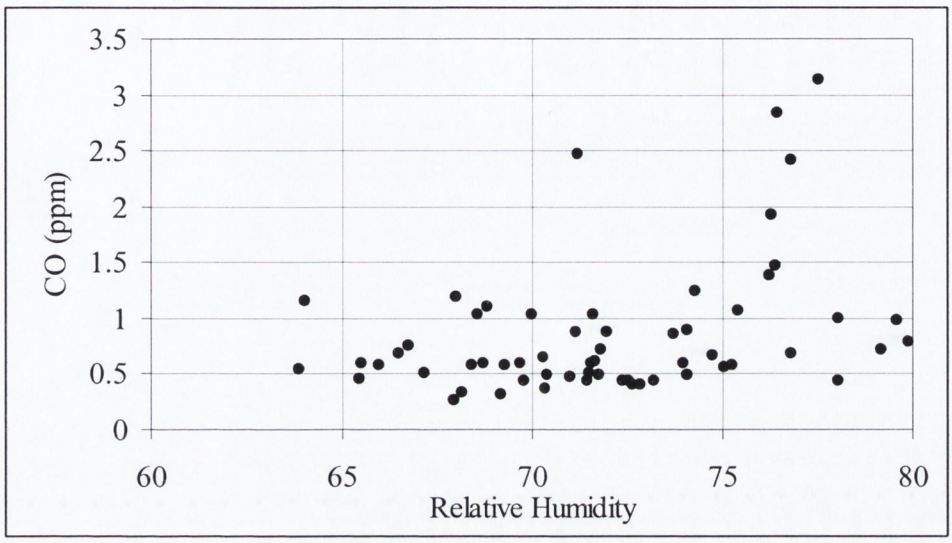

Figure 5.31 Sample scatter chart of 24-hour averages of CO and relative humidity

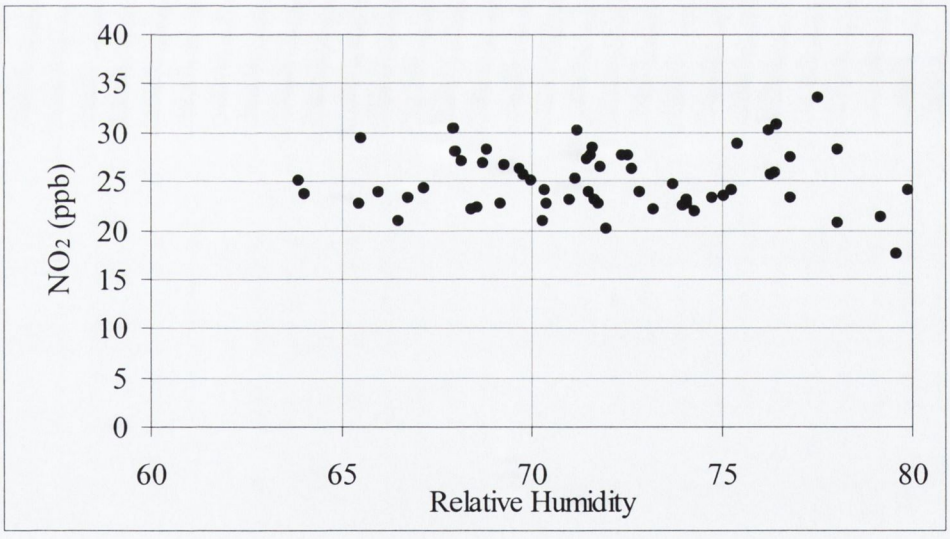

Figure 5.32 Sample scatter chart of 24-hour averages of NO_2 and relative humidity

5.6.3 PM_{10}

Differing opinions exist on the sensitivity of particle size distribution to relative humidity (McMurray and Stolzenburg, 1989). Some studies have indicated that PM_{10} concentrations in

the ambient air are affected by the relative humidity (Monn *et al.*, 1997). Although, in other cases (Lam *et al.*, 1999; Cuhadaroglu and Demirci, 1996), very little correlation was found.

A Pearson's correlation coefficient of 0.39 was calculated for a six-month sample graphed in Figure 5.33. Although this could be considered an indication of some degree of dependence, when the six individual months were analysed separately, the correlation coefficient ranged between –0.01 and 0.5, showing a high degree of variability, which appeared to be random and not seasonally dependent.

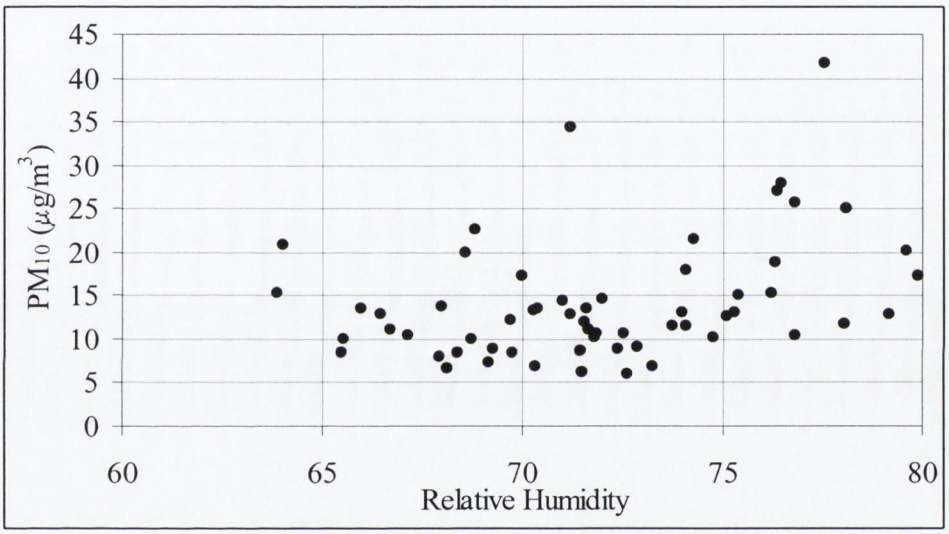

Figure 5.33 Sample scatter chart of 24-hour averages of PM_{10} and relative humidity

5.7 Variation in Pollutant Concentrations with Sunshine Duration

The amount of solar radiation is not considered a significant parameter by many investigators as it has no direct physical influence on diffusion controls (Kartal and Özer, 1998), although it does affect stability class and influences the photochemistry of ozone, hydrocarbons, and oxides of nitrogen.

No significant correlation was found between CO, NO_2 or PM_{10} concentrations and sunshine duration. Both hourly and daily pollutant averages and hourly and daily sunshine duration

were investigated using concentration data measured at Site A and sunshine data recorded at Dublin Airport by Met Eireann, between March 1998 and August 1998. Correlation coefficients of –0.20, -0.11, and -0.23 were calculated using daily average concentrations and total sunshine hours for CO, NO_2, and PM_{10}, respectively.

5.8 Spatial Variability

Spicer *et al.*, (1996) found that hazardous air pollutant measurements made in one neighbourhood could be reliably used to represent other locations in that neighbourhood, or even nearby neighbourhoods, so long as a sufficiently long averaging period is employed to smooth out temporal patterns. Therefore, pollutant characterisation at one site can give important information for that locality.

5.8.1 Carbon Monoxide

CO tends to exhibit a higher degree of spatial variability than some other compounds, such as ozone (McNair *et al.*, 1996). As, in this study, levels of CO were not measured at sites simultaneously, firm conclusions cannot be drawn on the extent of spatial variability; however, average levels measured at the Pearse St. monitoring station (Table 4.12) showed good agreement with those measured at the junction – Site A (Table 4.2). The CO readings measured at the junction in the uninterrupted period before monitoring at Pearse St. commenced (August 1999 to January 1999) averaged at 0.78 ppm, compared to an average of 0.76 ppm at the Pearse St. site. This could point towards the site at the junction being representative of the surrounding area, for CO concentrations.

5.8.2 Oxides of Nitrogen

Levels of NO, NO_2 and NO_x were measured simultaneously at the Westland Row site (by the ESB) and the Pearse Street/Westland Row intersection between 16th July 1999 and 20th

October 1999 (by the EPA). The two sites monitoring sites were within 150m of each other. Although both were roadside sites, the sampling intake for the monitoring equipment at Westland Row was at a height of 5m and the intake at the intersection was at a height of 3m.

The average recorded values are listed in Table 5.1. Concentrations of NO at both sites show a high level of agreement. As a secondary pollutant, NO_2 would be expected to have a lower level of spatial variability than the other primary pollutants (Fischer *et al.*, 2000) but NO_2 levels at the intersection are over one third higher than at the Westland Row site. This level of spatial variability would be expected to drop in the winter months, as the spatial coefficient of variation is thought to be seasonally dependent, with levels of horizontal and vertical variability decreasing in winter due to the slower oxidation process (Monn *et al.*, 1997). Monn *et al.*, (1997) and Hegner *et al.*, (1996) have also reported lower spatial variation in winter.

Table 5.1 Average concentrations of NO, NO_2, and NO_x measured simultaneously at Westland Row and Pearse St./Westland Row Intersection sites

	NO (ppb)	**NO_2 (ppb)**	**NO_x (ppb)**
Westland Row	42.62	19.68	62.16
Pearse St./Westland Row Intersection	44.96	27.94	72.90

Average concentrations of NO_2 measured at the Pearse St. monitoring site (Site B) are listed in Table 5.2. The average concentration measured at Site B is closer to the concentration measured at the junction (Site A) than to that measured at Westland Row (Site C). This could point towards a higher degree of mixing and lower coefficient of spatial variation horizontally than vertically, as the NO_2 inlets at both sites were at similar heights. The lack of dependence of NO_2 concentrations on wind direction may also point towards a lower coefficient of spatial variation. However, as the Site B measurements were not taken at the same time as those at Site A and Site C, no firm conclusions can be drawn.

It is also worth noting that although the NO concentrations are similar for both data sets (Site A, Phase2 and Site C), the NO_2 concentrations are approximately 30% higher at Site A. This

may indicate a steeper vertical concentration profile for NO_2 compared to NO, or differences in chemistry and dispersion caused by the differences in the physical characteristics in the site.

Table 5.2 Average concentrations of NO_2 measured at Pearse St. monitoring site.

Month	NO_2 (ppb)
Feb-99	28.28
Mar-99	29.11
Apr-99	30.13
Total Average	29.1

The Pearson's correlation coefficients between the compounds at each site were calculated (Table 5.3 and Table 5.4). The strongest correlations were observed between concentrations of NO and total NO_x (correlation coefficients of 0.98 and 0.99). Concentrations of NO_2 were also strongly correlated with concentrations of total NO_x (correlation coefficients of 0.86 and 0.82), and slightly less so with NO (correlation coefficients of 0.75 at both sites). The correlation coefficients are almost identical at both sites. The degree of association between the compounds would, therefore, appear to be reasonably spatially independent.

Table 5.3 Correlation coefficients for nitrogen oxides monitored at Pearse St./Westland Row Site (Site A – Phase 2)

	NO (Site A)	NO_2 (Site A)	NO_x (Site A)
NO (Site A)	1.00		
NO_2 (Site A)	0.75	1.00	
NO_x (Site A)	0.98	0.86	1.00

Table 5.4 Correlation coefficients for nitrogen oxides monitored at Westland Row (Site C)

	NO (Site C)	NO_2 (Site C)	NO_x (Site C)
NO (Site C)	1.00		
NO_2 (Site C)	0.75	1.00	
NO_x (Site C)	0.99	0.82	1.00

5.8.3 PM_{10}

There appears to be little consensus on the degree of spatial variability exhibited by ambient PM_{10} concentrations. Brook *et al.*, (1997) report substantial intersite correlation, due to the influence of synoptic-scale meteorology and the relatively long lifetime of fine particles. Van Curen (1999) reports that even minor sources very close to a sampler will overwhelm any regional component. This was concluded from a study in California, in which most coarse (PM_{10}) particles collected were less than 2 hours old, and most primary fine ($PM_{2.5}$) particles were less than 4 days old. Hence, even on days that were not truly 'stagnant', samples were strongly influenced by their immediate surroundings.

PM_{10} levels were not measured simultaneously at any of the monitoring sites. The concentrations measured at the Pearse St. site, listed in Table 4.12, were significantly higher than those measured at the junction (Table 4.2), with average concentrations of 27.90 $\mu g/m^3$ and 18.12 $\mu g/m^3$ respectively. This is likely to be due to the close proximity of a series of bus stops to the Pearse St. monitoring site. The high concentrations of PM_{10} measured would be explained by the high emissions of particulates from the diesel-engined buses compared to cars.

5.9 Inter-Compound Relationships

5.9.1 Oxides of Nitrogen

In conjunction with NO_2, levels of NO and NO_x were measured at hourly intervals from July 1999 to December 1999, by the EPA at the Pearse St./Westland Row Intersection, and from July 1999 to November 1999 by the ESB at Westland Row.

Temporal Variations

As NO_2 is a secondary compound formed mainly by the oxidation of NO, a primary compound, differences in the diurnal trends would be expected. The double peak characteristic of traffic-dependent pollutant concentrations on weekdays, already observed for NO_2 at the Pearse St./Westland Row Intersection in Figure 5.4, is again visible for the NO_2 in Figure 5.34 (showing concentration data measured by the ESB during August to November 1999). NO displays a more pronounced double peak then NO_2, as expected for a primary compound. The average diurnal variations on weekdays are greater for NO than for NO_2 because NO_2 has a longer lifespan than the more reactive NO (Mayer, 1999), the low NO concentrations in the early afternoon resulting mainly from the oxidation of NO to form NO_2 (Mayer, 1999).

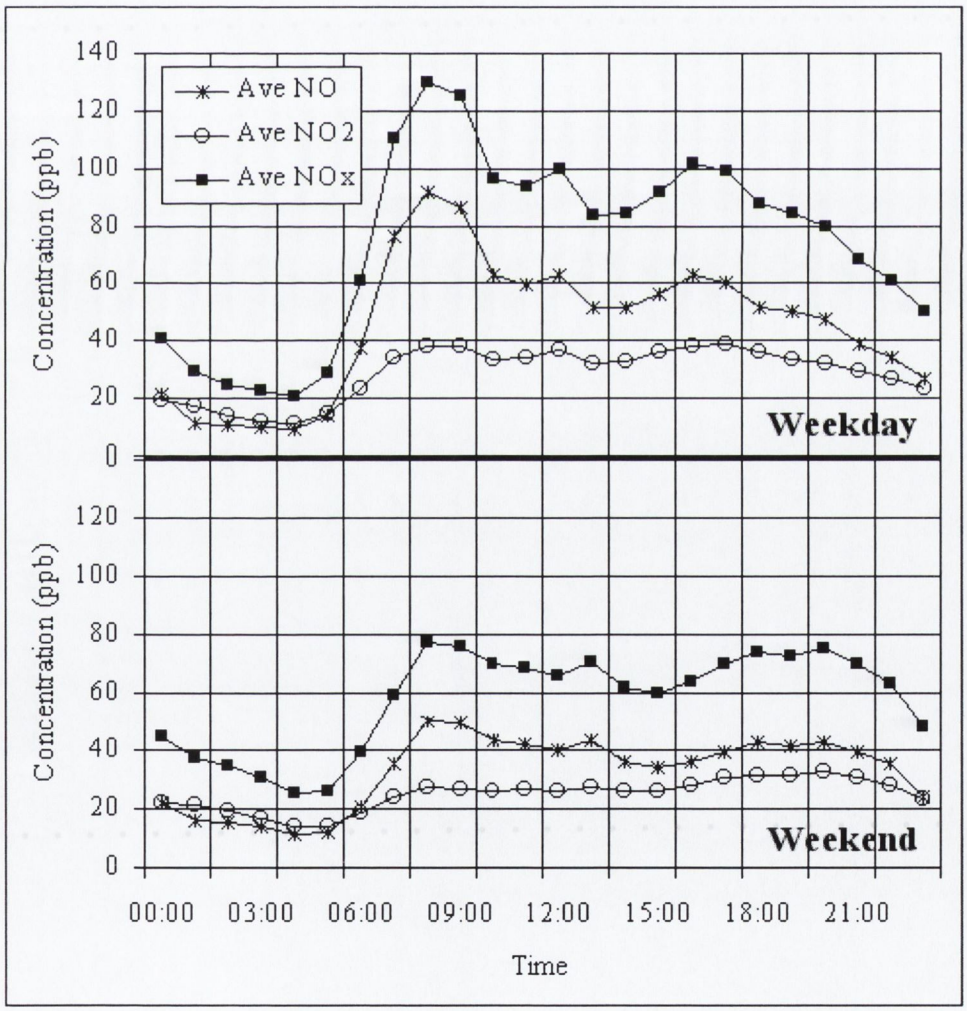

Figure 5.34 Weekday diurnal Pattern for NO, NO_2 and total NO_x averaged over August 1999 to November 1999

All oxides of nitrogen exhibit comparatively higher levels on the weekdays than on weekends, due to higher traffic density on weekdays. At the Pearse St./Westland Row intersection monitoring site, the ratios of weekend concentrations to weekday concentrations are 0.72, 0.87 and 0.78 for NO, NO_2 and NO_x respectively. Concentrations also tend to remain more constant over the course of the day on Saturdays and Sundays than during weekdays, falling to similar minima at night, as illustrated in Figure 5.34.

The average annual cycle of NO has been reported to display the lowest values in summer (Mayer, 1999); however, the NO concentrations measured at the intersection were not consistent with this behaviour (Figure 5.35). In general, the annual cycle of NO_2 shows only slight variation, as it is produced mainly by secondary chemical reactions (Mayer, 1999), as discussed in greater detail in Section 5.1.9; although, the highest concentration was measured in July and the lowest in December. NO_2 levels do show less variation than concentrations of NO, as expected. However, to fully analyse seasonal trends, a longer monitoring period is needed.

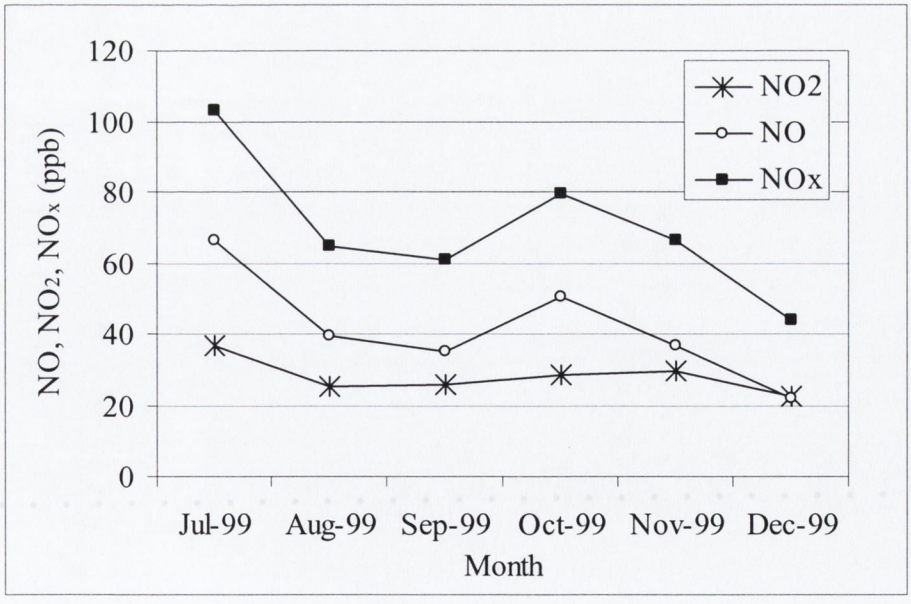

Figure 5.35 Average concentrations of NO, NO_2 and NO_x measured at Pearse St./Westland Row Junction from July 1999 to December 1999

Ratios of NO and NO_x to NO_2

The average daily ratio of NO to NO_2 is shown in Figure 5.36. Although the ratio shows a significant degree of variability, the value usually lies between 2 and 3. The ratio was found to be related to NO concentrations, with a correlation coefficient of 0.78. This differs from the typical assumed ratio of 1:5. A high level of NO resulted in a high ratio of NO to NO_2, due to the time lag before the NO was oxidised to NO_2. Figure 5.37 shows values of the ratio between NO and NO_2 plotted against the daily NO concentrations. Although, there is a degree of scatter (as seen in Figure 5.37), when average NO concentrations are plotted against the ratio of NO to NO_2 in increments of 0.2, the data can be seen to follow a power series with an R^2 value of 0.97 (as seen in Figure 5.38). In other words, 97% of the variation in the ratio of NO to NO_2 is attributable to the power relationship between the two variables. Therefore, given a 24-hour average NO concentration, the concentration of NO_2 can be estimated from Equation 5.4.

$$C_{NO} = 3.07 \times \left(\frac{C_{NO}}{C_{NO2}} \right)^{2.88} \qquad \text{Equation 5.4}$$

where

C_{NO} and C_{NO2} are the daily concentrations of NO and NO_2, respectively.

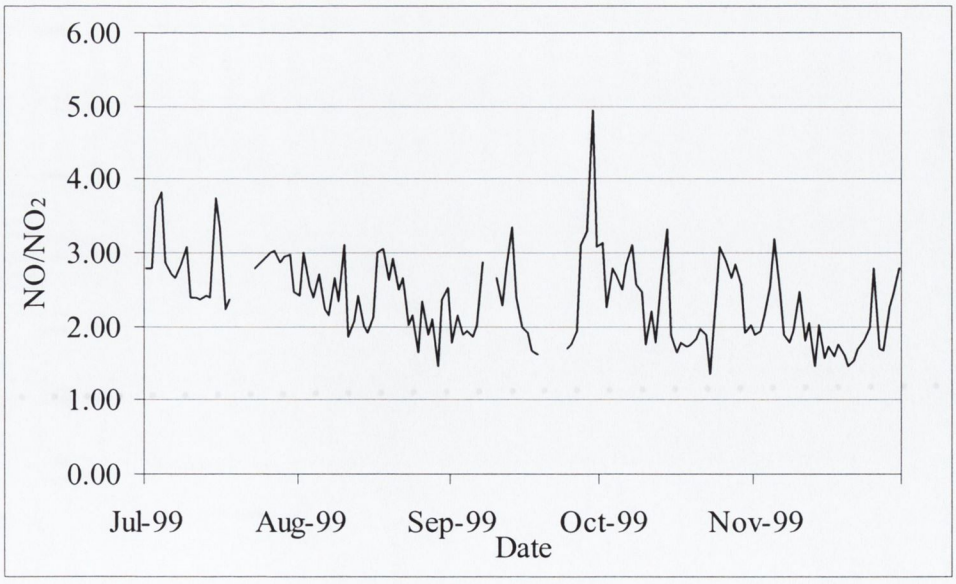

Figure 5.36 Daily variation in NO/NO_2 ratio

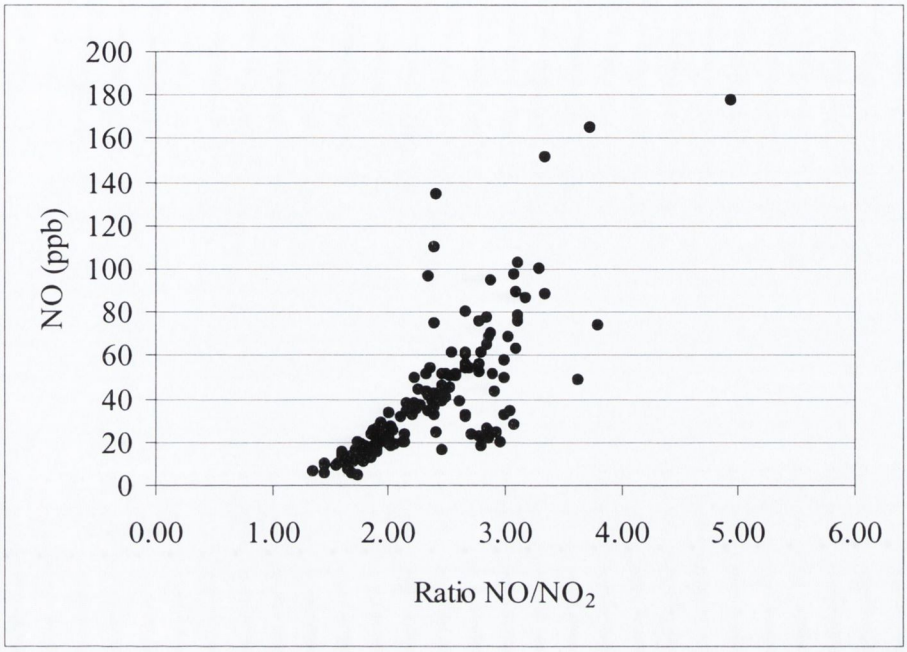

Figure 5.37 Ratio of NO/NO_2 plotted against NO concentrations (daily averages measured between July and December 1999, by the EPA)

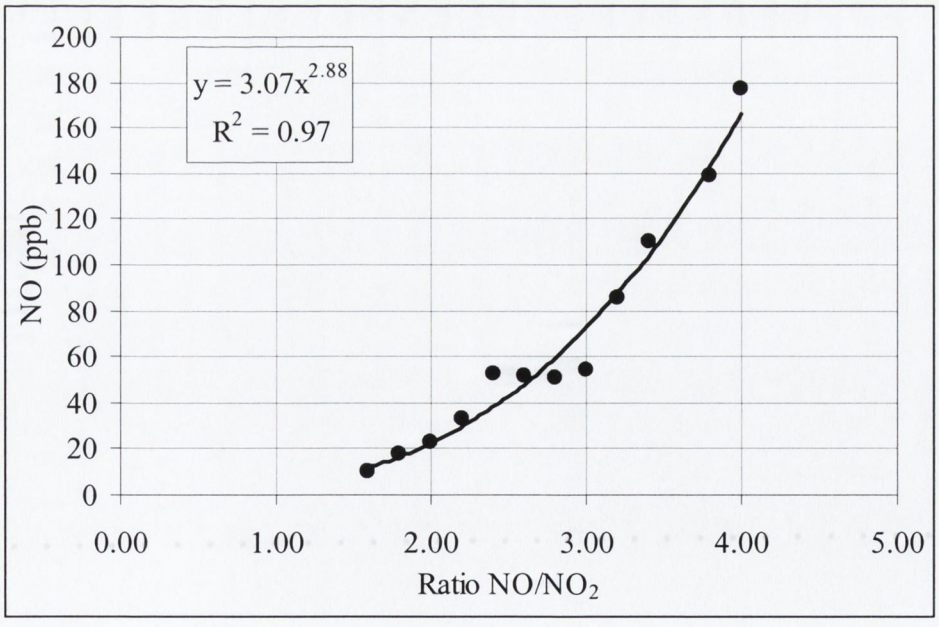

Figure 5.38 Power relationship between the (incremental) ratio of NO to NO_2 and concentrations of NO

Correlation Coefficients

Table 5.5 presents the correlation coefficients for concentrations of NO_2, NO and NO_x. There is a good correlation between all three, but particularly between NO and NO_x. The correlation with NO_2 is not as strong because, as a secondary compound, NO_2 is subject to different mechanisms, as discussed in Section 5.1.2.

Table 5.5 Correlation coefficients for NO_2, NO and NO_x

	NO_2	**NO_x**	**NO**
NO_2	1.00		
NO_x	0.87	1.00	
NO	0.77	0.98	1.00

5.9.2 PM_{10} and other Particulate Matter

Diurnal Pattern

Levels of PM_{10}, $PM_{2.5}$ and PM_1 were measured at hourly intervals from 1st September 1999 to 15th December 1999, by the EPA, at the Pearse St./Westland Row intersection. $PM_{2.5}$ follows a similar diurnal pattern to PM_{10} although the daily peak is less pronounced; whereas PM_1 concentrations remain almost constant throughout the day. The weekday and weekend average diurnal patterns for November 1999 are illustrated in Figure 5.39.

On average, both $PM_{2.5}$ and PM_1 exhibit comparatively higher levels on the weekdays than on weekends, due to higher traffic density on weekdays. The ratio of weekend concentrations to weekday concentrations are 0.90, 1.14 and 1.29 for PM_{10}, $PM_{2.5}$ and PM_1, respectively.

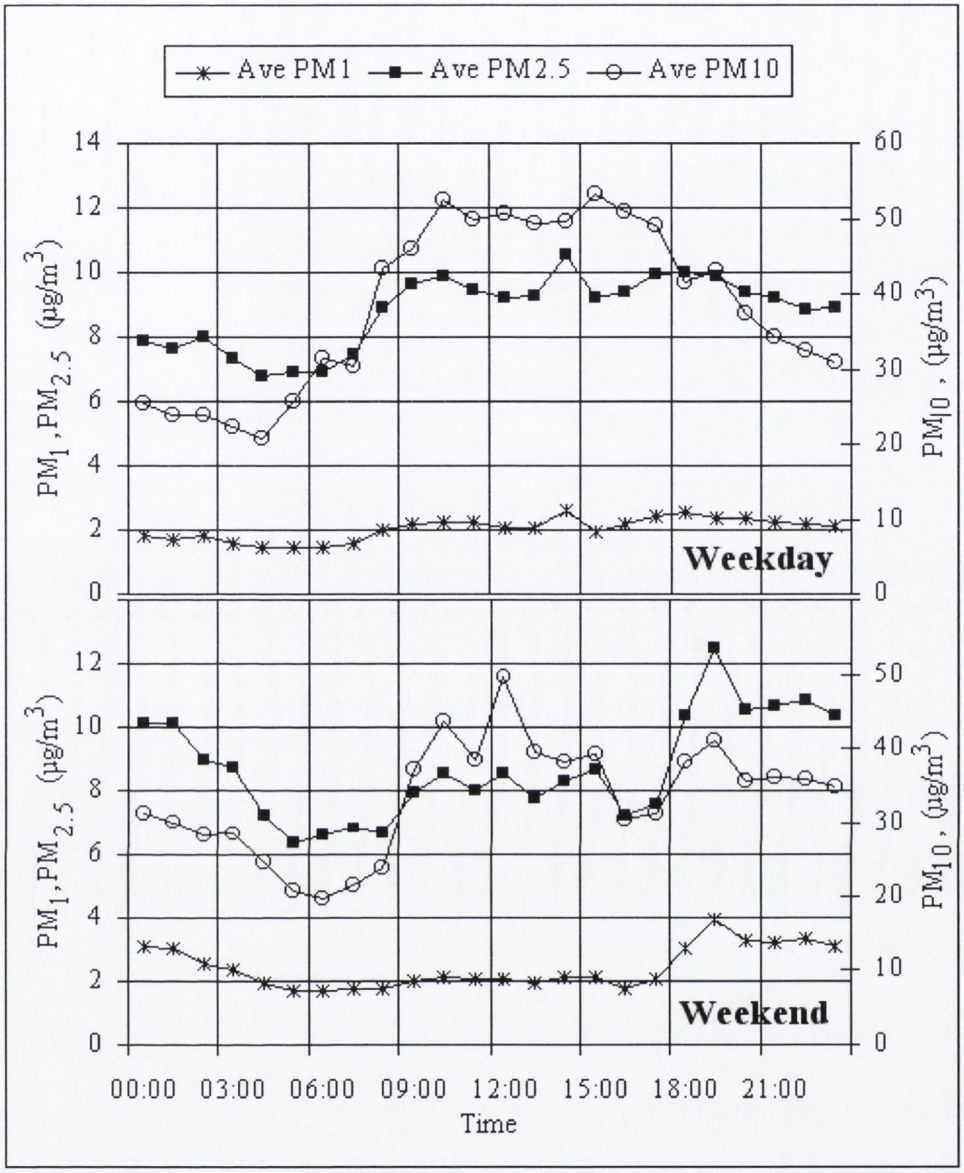

Figure 5.39 Weekday and weekend diurnal pattern for PM_{10}, $PM_{2.5}$ and PM_1 (November 1999)

Ratios of $PM_{2.5}$ and PM_1 to PM_{10}

Figure 5.40 shows the ratios of $PM_{2.5}$ and PM_1 to PM_{10}. A high level of variability is observable, with the majority of the values for $PM_{2.5}/PM_{10}$ between 0.175 and 0.4, and the PM_1/PM_{10} ratios lying between 0.04 and 0.1.

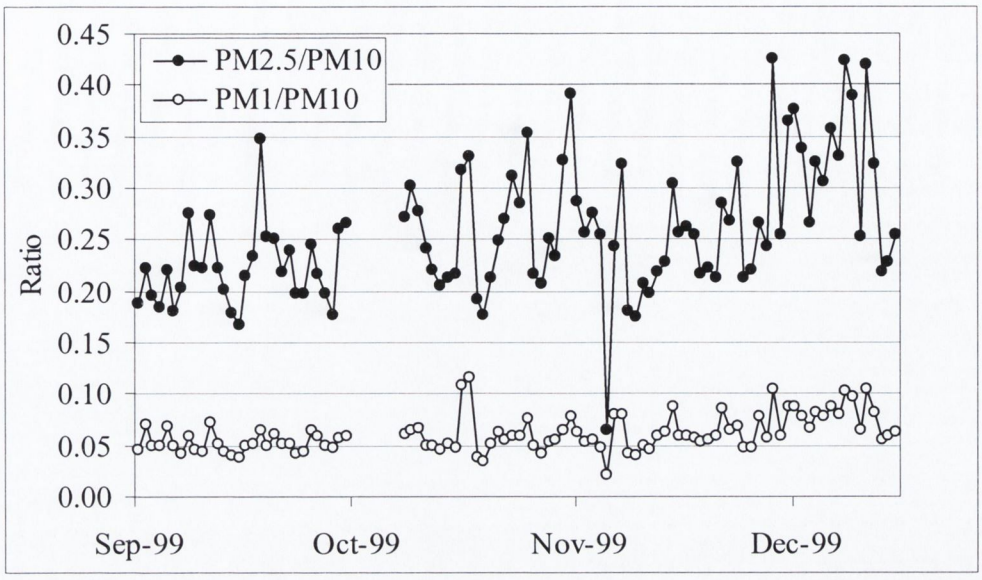

Figure 5.40 Ratios of $PM_{2.5}$ and PM_1 to PM_{10}

Correlation Coefficients

The Pearson's correlation coefficients for hourly averages of total particulates, PM_{10}, $PM_{2.5}$ and PM_1 are given in Table 5.6. PM_{10} is strongly correlated with total particulates, as might be expected as PM_{10} forms a high proportion of the total particulates. PM_1 and $PM_{2.5}$ are also highly correlated (r = 0.92). Particles between 0.1μm and 2μm have been reported to have similar lifetimes and be subject to the same mechanisms (Lodge *et al.*, 1981). The high correlation coefficient between PM_1 and $PM_{2.5}$ points towards $PM_{2.5}$ being included in this category also.

Table 5.6 Correlation coefficients for total particulates, PM_{10}, $PM_{2.5}$, PM_1

	Total Particles	**PM_{10}**	**$PM_{2.5}$**	**PM_1**
Total Particles	1.00			
PM_{10}	0.95	1.00		
$PM_{2.5}$	0.69	0.71	1.00	
PM_1	0.62	0.65	0.92	1.00

5.9.3 VOC's and Carbon Monoxide, Nitrogen Dioxide and PM_{10}

During March 1998, 27 VOCs (listed in Table 5.7) were measured at hourly intervals simultaneously with CO, NO_2 and PM_{10}. An in-depth analysis of these VOC results is performed in Marnane (2000).

Table 5.7 VOCs measured during March 1998

Ethane	Ethylene	Propane
Propylene	iso-Butane	n-Butane
Acetylene	Trans-2-Butene	1-Butene
Cis-2-Butene	Isopentane	n-Pentane
1,3-Butadiene	Trans-2-Pentene	Cis-2-pentene
2-Methylpentane	3-Methylpentane	Isoprene
n-Hexane	Benzene	n-Heptane
Toluene	Ethylbenzene	m+p-Xylene
o-Xylene	1,3,5-Trimethylbenzene	1,2,4-Trimethylbenzene

The Pearson's correlation coefficients for this range of VOCs and CO, NO_2 and PM_{10} were calculated. A summary of the r-values is in Table 5.8. As can be seen in Table 5.8, the correlations between CO and individual VOCs range from moderate for ethane, propane, and toluene ($r = 0.5 - 0.6$), to strong ($r > 0.8$) for the majority of compounds. Eight compounds including benzene and 1,3-butadiene have correlation coefficients higher than 0.9. A scatter chart of hourly concentrations of ethylene and CO is shown in Figure 5.41, highlighting the high degree of association between the compounds. This would indicate that for many hydrocarbons, CO can reasonably be used as an indicator of ambient concentrations, once the ratios have been accurately established. The strong correlation between benzene, toluene, xylene and CO was corroborated by Palmgren *et al.*, (1999), in a study on air quality measurements in Copenhagen.

Table 5.8 also shows that both NO_2 and PM_{10} are moderately correlated with the majority of the measured VOCs.

Table 5.8 Pearson's correlation coefficients between CO, NO_2, PM_{10} and VOCs

CO		NO_2		PM_{10}	
Pearson's r	**VOCs**	**Pearson's r**	**VOCs**	**Pearson's r**	**VOCs**
0.0 – 0.1	*No Compounds*	**0.0 – 0.1**	*No Compounds*	**0.0 – 0.1**	1-Butene
0.1 – 0.2	*No Compounds*	**0.1 – 0.2**	1-Butene	**0.1 – 0.2**	*No Compounds*
0.2 – 0.3	*No Compounds*	**0.2 – 0.3**	Ethane	**0.2 – 0.3**	*No Compounds*
0.3 – 0.4	*No Compounds*		Propane	**0.3 – 0.4**	*No Compounds*
0.4 – 0.5	*No Compounds*	**0.3 – 0.4**	*No Compounds*	**0.4 – 0.5**	2-Methylpentane
0.5 – 0.6	Ethane	**0.4 – 0.5**	2-Methylpentane		Ethane
	Propane		Cis-2-pentene		Propane
	Toluene	**0.5 – 0.6**	n-Heptane		Cis-2-pentene
0.6 – 0.7	Cis-2-pentene		Trans-2-Pentene		Toluene
0.7 – 0.8	1-Butene		Isoprene	**0.5 – 0.6**	Acetylene
0.8 – 0.9	iso-Butane		n-Hexane		n-Heptane
	n-Heptane		iso-Butane		n-Hexane
	Cis-2-Butene		Acetylene		3-Methylpentane
	n-Butane		n-Butane		Trans-2-Pentene
	Isoprene		1,2,4-Trimethylbenzene		Cis-2-Butene
	3-Methylpentane		Ethylene		Isoprene
	2-Methylpentane		Cis-2-Butene	**0.6 – 0.7**	m+p-Xylene
	n-Pentane		1,3,5-Trimethylbenzene		iso-Butane
	Isopentane		n-Pentane		1,3-Butadiene
	n-Hexane		Benzene		Ethylbenzene
	Trans-2-Pentene	**0.6 – 0.7**	o-Xylene		o-Xylene
	1,2,4-Trimethylbenzene		m+p-Xylene		Trans-2-Butene
	Trans-2-Butene		1,3-Butadiene		Benzene
	Acetylene		Ethylbenzene		Ethylene
0.9 –1.0	1,3,5-Trimethylbenzene		Isopentane		1,3,5-Trimethylbenzene
	Ethylbenzene		Toluene		n-Butane
	m+p-Xylene		Trans-2-Butene		Isopentane
	o-Xylene		3-Methylpentane		n-Pentane
	1,3-Butadiene	**0.7 – 0.8**	*No Compounds*		Propylene
	Propylene	**0.8 – 0.9**	*No Compounds*		1,2,4-Trimethylbenzene
	Benzene	**0.9 – 1.0**	*No Compounds*	**0.7 – 1.0**	*No Compounds*
	Ethylene			**0.8 – 0.9**	
				0.9 – 1.0	

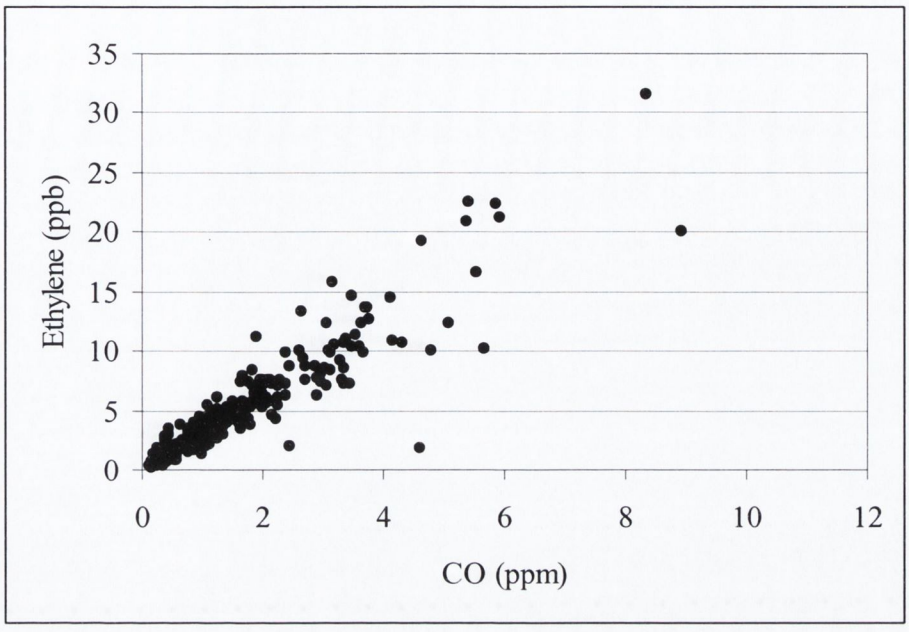

Figure 5.41 Scatter chart of hourly concentrations of ethylene and CO

The linear relationship as described in Equation 5. 5, between each VOC compound and carbon monoxide is summarised in Table 5. 9.

$$CO\ (ppm) = m\ VOC\ (ppb) + c \qquad \text{Equation 5. 5}$$

Table 5. 9 Relationship between VOC compounds and CO

VOC Compound	m	c	VOC Compound	m	c
Ethylene	3.09	0.01	Isopentane	1.28	0.01
Benzene	0.95	0	n-Pentane	0.43	0.08
Propylene	0.92	0.05	2-Methylpentane	0.35	-0.1
1,3-Butadiene	0.24	0.02	3-Methylpentane	0.23	0.03
o-Xylene	0.34	0.01	Isoprene	0.07	0.02
m+p-Xylene	0.88	0.06	n-Butane	0.169	0.48
Ethylbenzene	0.27	0.02	Cis-2-Butene	0.1	0.02
1,3,5-Trimethylbenzene	0.21	0.04	n-Heptane	0.07	0.03
Acetylene	1.91	0.07	iso-Butane	0.7	0.25
Trans-2-Butene	0.11	0.02	Cis-2-pentene	0.1	0.04
1,2,4-Trimethylbenzene	0.35	0.05	Toluene	1.78	0.19
Trans-2-Pentene	0.13	0.01	Propane	0.37	1.46
n-Hexane	0.18	0.05	Ethane	0.62	3.56

A regression analysis of one week of CO and VOC data was performed. Using the calculated regression equations, hourly VOC values for the following week were predicted from the measured CO concentrations. These are then compared with the actual hourly VOC concentrations. Sample graphs of the predicted and measured concentrations of ethylene, 1,3,5-trimethylbenzene, and o-xylene are shown in Figure 5.42, Figure 5.43, and Figure 5.44, respectively. It can be seen that there is the potential for certain traffic-related VOCs to be estimated reasonably accurately using ambient CO concentrations."

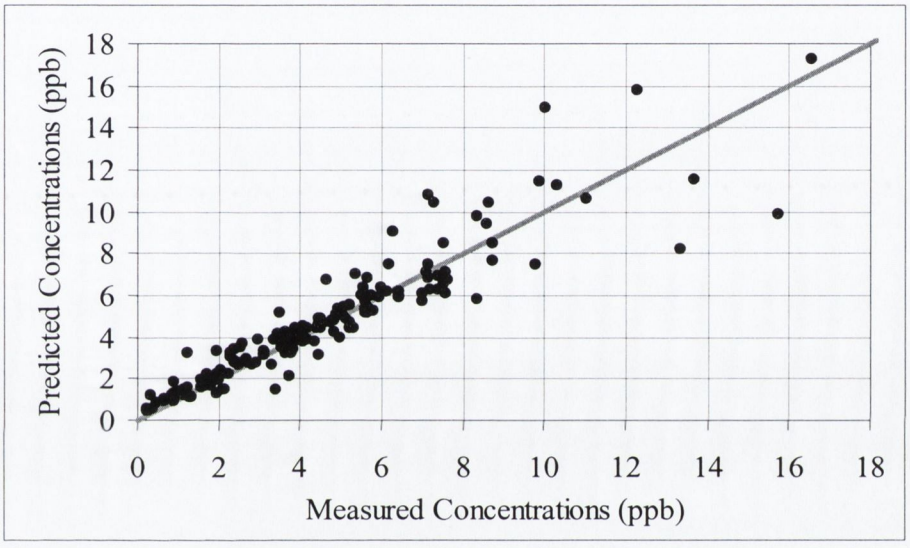

Figure 5.42 Predicted and measured hourly concentrations of ethylene

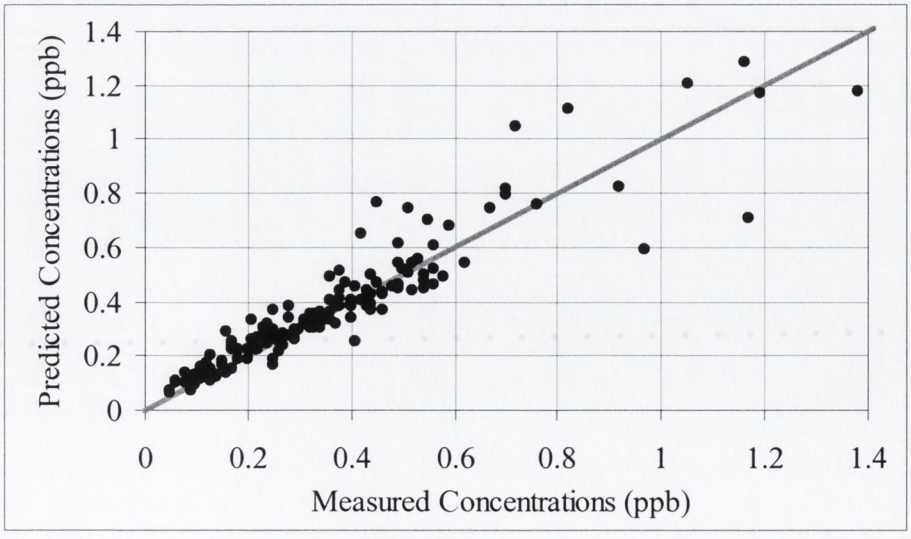

Figure 5.43 Predicted and measured hourly concentrations of 1,3,5-trimethylbenzene

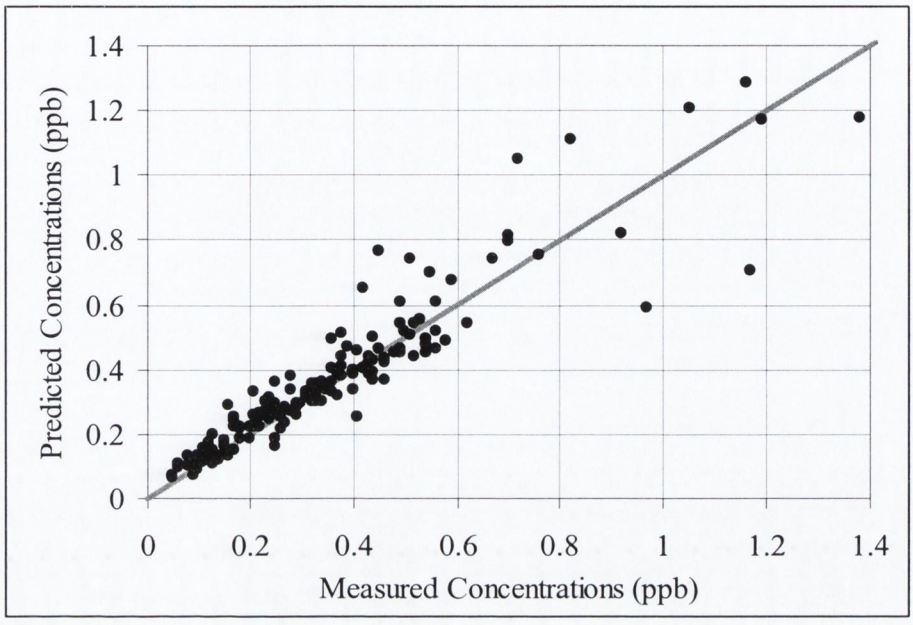

Figure 5.44 Predicted and measured hourly concentrations of o-xylene

To investigate the accuracy of this approach, the predictions for VOCs are expressed as a percentage of the recorded hourly averages and the standard deviations of the errors calculated. The average values and upper and lower limits (average ± twice the standard deviation) are shown in Figure 5.45 and Figure 5.46. As can be seen from the graphs, the average prediction error is quite small, although the spread of the data should be considered when predicting VOC concentrations. It seems that predictions of individual hourly hydrocarbon concentrations may be substantially in error, but that longer-term averages will be reasonably accurate. The exceptions to this include cis-2-butene and toluene. A significant point source of toluene has been identified in the vicinity of the monitoring site (Marnane, 2000).

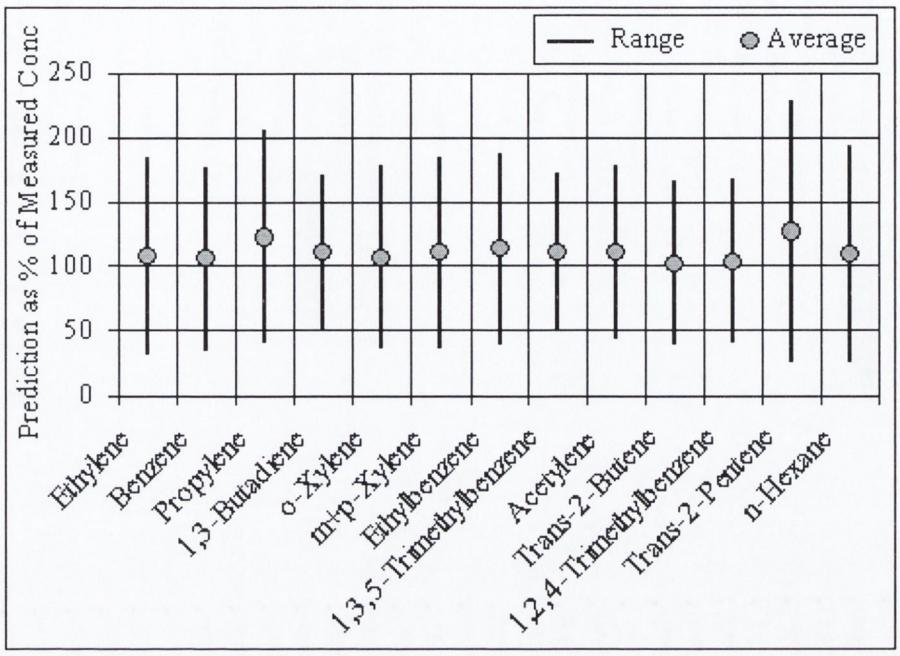

Figure 5.45 Predicted VOCs as a percentage of the measured concentration

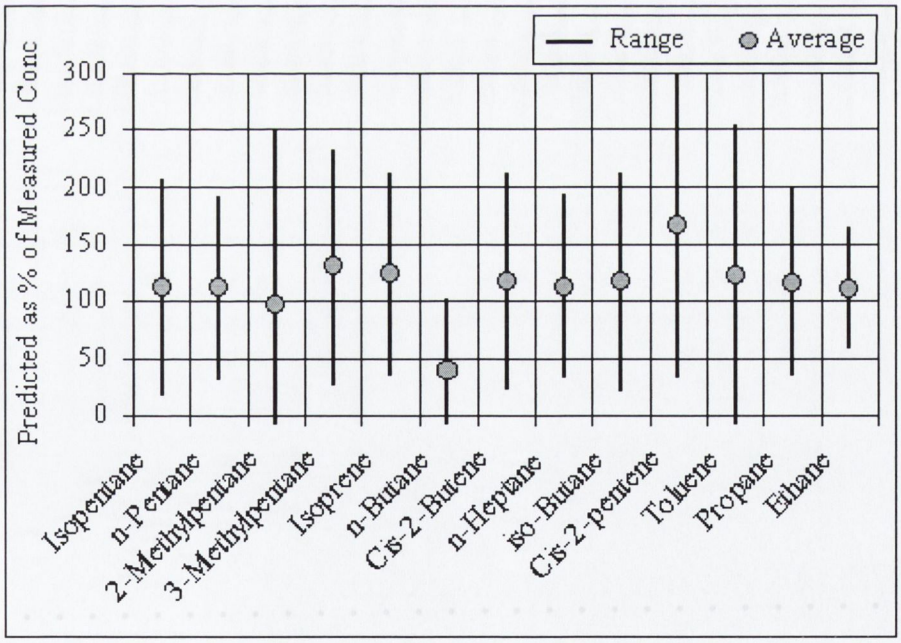

Figure 5.46 Predicted VOCs as a percentage of the measured concentration (cont.)

5.9.4 Sulphur Dioxide and Carbon Monoxide, Nitrogen Dioxide and PM_{10}

SO_2 is the product of fossil fuel combustion, usually coal and oil, with the majority of emissions coming from stationary sources (Kiely, 1997). As a result, the measured concentrations are only moderately correlated to CO, NO_2 and PM_{10}. The correlation coefficients calculated using hourly averages are listed in Table 5.10.

Table 5.10 Correlation coefficients between CO, NO_2, PM_{10}, SO_2.

	CO	**NO_2**	**PM_{10}**	**SO_2**
CO	1.00			
NO_2	0.66	1.00		
PM_{10}	0.52	0.53	1.00	
SO_2	0.63	0.58	0.42	1.00

The diurnal pattern of SO_2 does not display prominent double peaks, characteristic of primary pollutants emitted predominantly by traffic, and concentrations do not decrease until approximately 21:00, as illustrated in Figure 5.47.

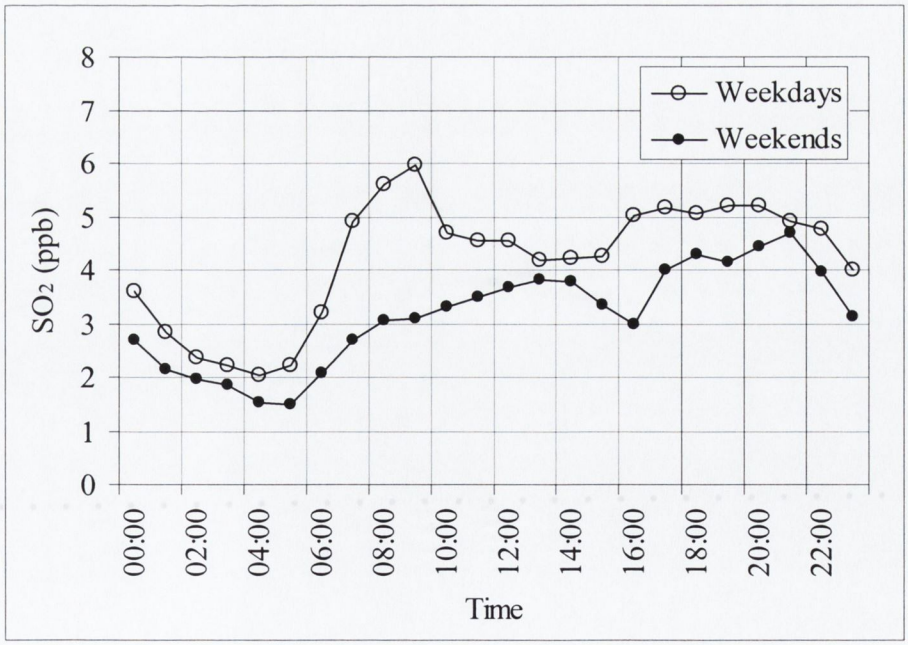

Figure 5.47 Average SO_2 concentrations for weekdays and weekends.

5.10 CONCLUSIONS

CO, NO_2 and PM_{10} were all found to have pronounced diurnal and weekly patterns (Section 5.1). When normalised, NO_2 and PM_{10} were seen to have very similar diurnal patterns during weekdays; whereas, CO displayed a more pronounced evening peak, due to congestion. All three compounds were seen to have similar diurnal patterns at weekends.

As mentioned in Section 5.2, studies of urban air quality have found pollutant concentrations to be significantly affected by meteorological factors. In this study, concentrations of CO, NO_2, and PM_{10} were found to be influenced by wind speed, as discussed in Section 5.3. The effects of wind direction on concentrations were analysed in Section 5.4. Concentrations of CO and PM_{10} were seen to be strongly affected by wind direction, unlike NO_2 concentrations, which were largely independent of wind direction. Pollutant concentrations were not significantly influenced by temperature, relative humidity or sunshine duration (Sections 5.5, 5.6, and 5.7, respectively).

The spatial variability of the individual compounds was assessed in Section 5.8. NO_2 displayed a higher degree of spatial variability than NO.

Inter-compound relationships were analysed in Section 5.9. CO was found to be very strongly correlated with 1,3,5-Trimethylbenzene, ethylbenzene, m+p-xylene, o-xylene, 1,3-butadiene, propylene, benzene and ethylene, with Pearson's correlation coefficients over 0.9 (Section 5.9.3). The strongest correlation between NO_2 and the measured VOCs was with 3-methylpentane, with a Pearson's correlation coefficient of 0.63. The strongest correlation between PM_{10} and the measured VOCs was with 1,2,4-trimethylbenzene, with a Pearson's correlation coefficient of 0.64. Correlation coefficients of 0.92, 0.60, and 0.62 were calculated for benzene with CO, NO_2 and PM_{10}, respectively.

In Section 5.9.3, the use of CO as a tracer compound for VOCs was discussed. Predictions of individual hourly concentrations display substantial errors, but a reasonable accuracy for

longer-term average predictions was observed, with the exceptions of cis-2-butene and toluene.

Diurnal variations for NO and NO_2 were found to be different, reflecting their natures as primary and secondary pollutants, respectively (Section 5.9.1). A correlation coefficient of 0.77 was calculated for NO and NO_2. NO_2 was found to have a stronger correlation with total NO_x, with a correlation coefficient of 0.87. A correlation coefficient of 0.98 was calculated for NO and NO_x.

The ratio of NO to NO_2 was found to be related to concentrations of NO. The increase in this ratio with NO concentrations was found to follow a power relationship.

Section 5.9.2 investigated the relationships between different particulate sizes (PM_{10}, $PM_{2.5}$ and PM_1). $PM_{2.5}$ and PM_1 were found to follow similar diurnal patterns to PM_{10}, with less pronounced peaks. PM_{10} concentrations were very strongly correlated with measured concentrations of total particulates ($r = 0.95$). PM_1 and $PM_{2.5}$ were also very strongly correlated ($r = 0.92$). PM_{10} was also correlated with $PM_{2.5}$ and PM_1, although to a slightly lesser degree, with correlation coefficients of 0.69 and 0.62, respectively.

SO_2 was moderately correlated with CO, NO_2, and PM_{10}, with correlation coefficients of 0.63, 0.58, and 0.42, respectively (Section 5.9.4).

6. POLLUTANT CONCENTRATION PREDICTION ALGORITHM

This chapter proposes a methodology to predict 30-day average concentrations 2and 1-hour, 8-hour and 24-hour peak concentrations over the course of one month, based on short-term periods of monitoring. Section 6.1 describes the rationale behind the algorithm. The steps of the algorithm are described in the form of a flow chart in Section 6.2. The algorithm equations for the prediction of monthly averages based on short-term monitoring are presented in Section 6.3. The calculation of adjustment factors for time-of-sampling is described in Section 6.4. Section 6.5 discusses the adjustment of wind speed measurements, to compensate for the lower wind speeds which occur at night. The calculation of adjustment factors for wind speed and wind direction at the time of sampling is detailed in Sections 6.6 and 6.7, respectively. Sections 6.8 and 6.9 cover adjustment of the measured data for temperature and relative humidity. The adjustment of the predicted monthly average pollutant concentration for average monthly wind speed is considered in Section 6.10. The rates of convergence of the adjustment factors are calculated in Section 6.11. Section 6.12 discusses a methodology for predicting the magnitude of extreme events using either the predicted or measured monthly with the theoretical frequency distribution and estimated standard deviation. Finally, conclusions to this chapter are in Section 6.13.

6.1 Algorithm Description

When sampling takes place over short periods of time, the conditions under which it takes place may not be representative of the typical conditions over the longer term; this can give rise to deceptively low or high measurements. For example, if the measurements were taken during a period with particularly high wind speeds, the concentrations would be lower than would usually be expected at that site. In this chapter, a method is derived to compensate for such atypical conditions during the time of sampling of CO, NO_2 or PM_{10}.

In this method, data are sampled for three or more partial or full days at intervals over the course of a month. By adjusting the measured pollutant concentrations to allow for the

conditions at the time of measurement, an improved estimate of the monthly concentration is arrived at. By using information on the statistical distribution of the data, the estimated monthly concentration can, in turn, be used to give information on extreme events, for comparison with air quality standards. The observations made during the monitoring programmes described in the previous chapters are used as the basis for the development of this method. The choice of three days per month as opposed to four was made to avoid the possibility of misrepresenting the typical concentrations by measuring concentrations on the same day each week.

6.2 Flow Chart

Figure 6. 1 shows a flow chart of the prediction algorithm discussed in detail in this chapter.

Figure 6. 1 Flow chart for prediction algorithm

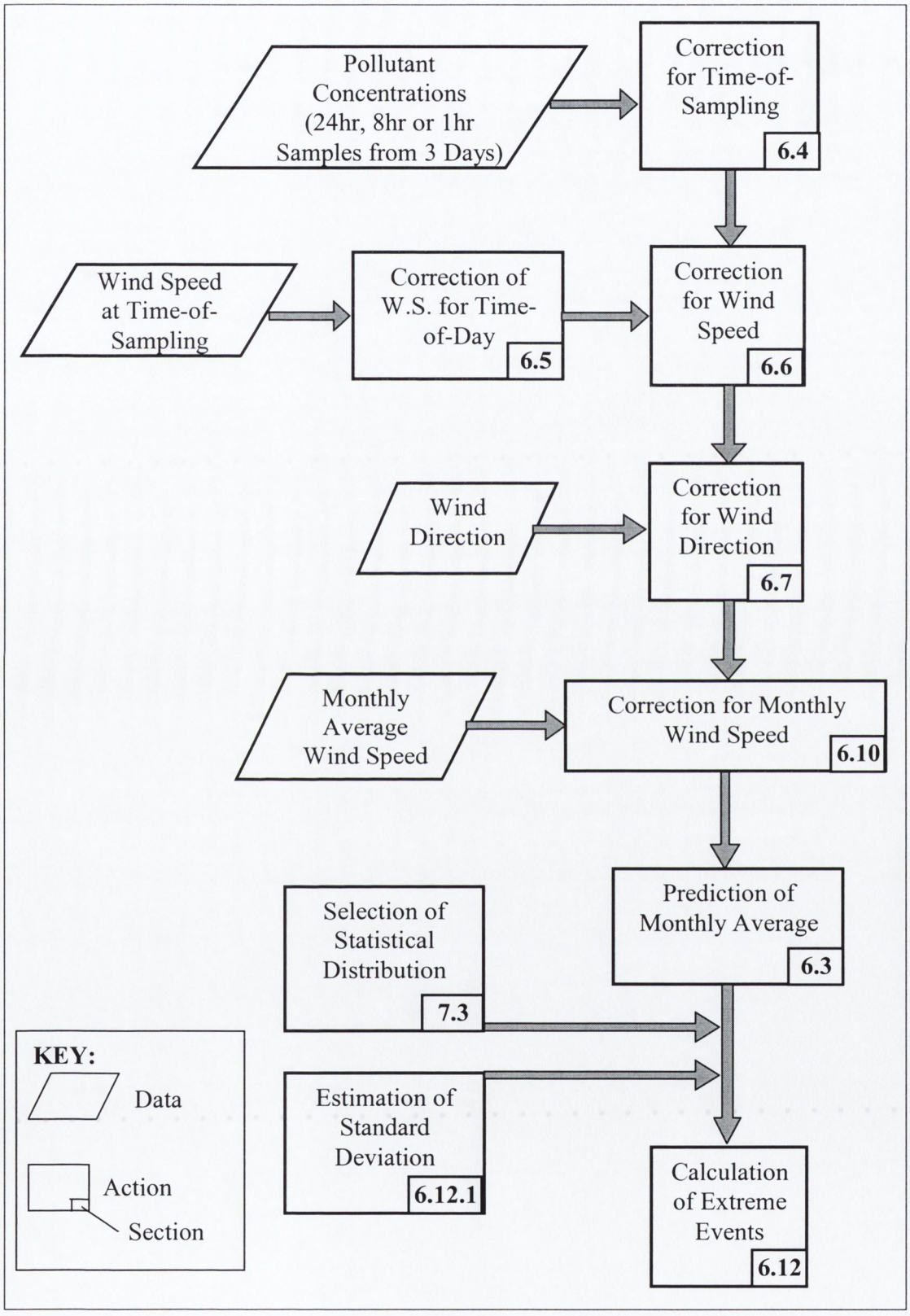

6.3 PREDICTION EQUATIONS

Equation 6.1 and Equation 6.4 are used to estimate the monthly average pollutant concentration.

Each individual concentration measurement is adjusted according to Equation 6.1.

$$C_{adj} = \bar{c} \times fac(t_c) \times fac(u_{adj}) \times fac(\theta) \times fac(temp) \times fac(rh) \qquad \text{Equation 6.1}$$

where

C_{adj} = the pollutant concentration adjusted for the conditions at the time of sampling

$\bar{c}$ = the measured pollutant concentration

$fac(t_c)$ = the concentration correction factor for time of sampling *(see Section 6.4)*

$fac(u_{adj})$ = the correction factor for wind speed *(see Section 6.6)*

$fac(\theta)$ = the correction factor for wind direction at time of sampling *(see Section 6.7)*

fac (temp) = the correction factor for temperature at time of sampling *(see Section 6.8)*

fac (rh) = the correction factor for relative humidity at time of sampling *(see Section 6.9)*

and

$$u_{adj} = \bar{u} \times fac(t_u) \qquad \text{Equation 6.2}$$

where

$\bar{u}$ is the measured wind speed

$fac(t_u)$ = the wind speed correction factor for time of day *(see Section 6.5)*.

These individual adjusted measurements are combined for each day according to Equation 6.3.

$$C_{adj}^{d} = \left(C_{adj(1)} + C_{adj(2)} + \ldots + C_{adj(m)}\right)/m \qquad \text{Equation 6.3}$$

where

C_{adj}^{d} = the average adjusted concentration for that (full or partial) monitored day, d,

$C_{adj(k)}$ = the k^{th} adjusted concentration, where k = 1,…,m

m = the number of pollutant concentrations measured on that full or partial day.

Finally, the values for each day are combined according to Equation 6.4.

$$C_{pred} = \left(C_{adj}^{d1} + C_{adj}^{d2} + \ldots + C_{adj}^{dn} \right) / n \times fac(u_{mth}) \qquad \text{Equation 6.4}$$

where

C_{pred} is the estimate of the monthly average concentration

n is the number of days or partial days on which sampling was undertaken

$fac(u_{mth})$ adjustment factor for the monthly wind speed *(see Section 6.10)*

6.4 Calculation of Adjustment Factors for Time of Sampling

6.4.1 Carbon Monoxide

As discussed in Section 5.1.1, CO concentrations exhibit a consistent daily pattern, as shown in Figure 5.2. One year's CO data were used to analyse the daily pattern.

The daily average for each day was calculated, and each 15-minute concentration expressed as a percentage of that average. Only weekdays were used as a different pattern is exhibited for weekends, as discussed in Section 5.1.5. The inverse of this value then forms the correction factor.

It is necessary to consider whether the concentration as a percentage of the daily average exhibited a seasonal dependence. To investigate this possibility, the above percentages were averaged over each month. In Figure 6.2, two typical summer months, August 1997 and 1998,

are shown as solid black lines against a selection of winter months. No consistent difference was seen between the summer months (solid lines) and the winter months (dotted lines).

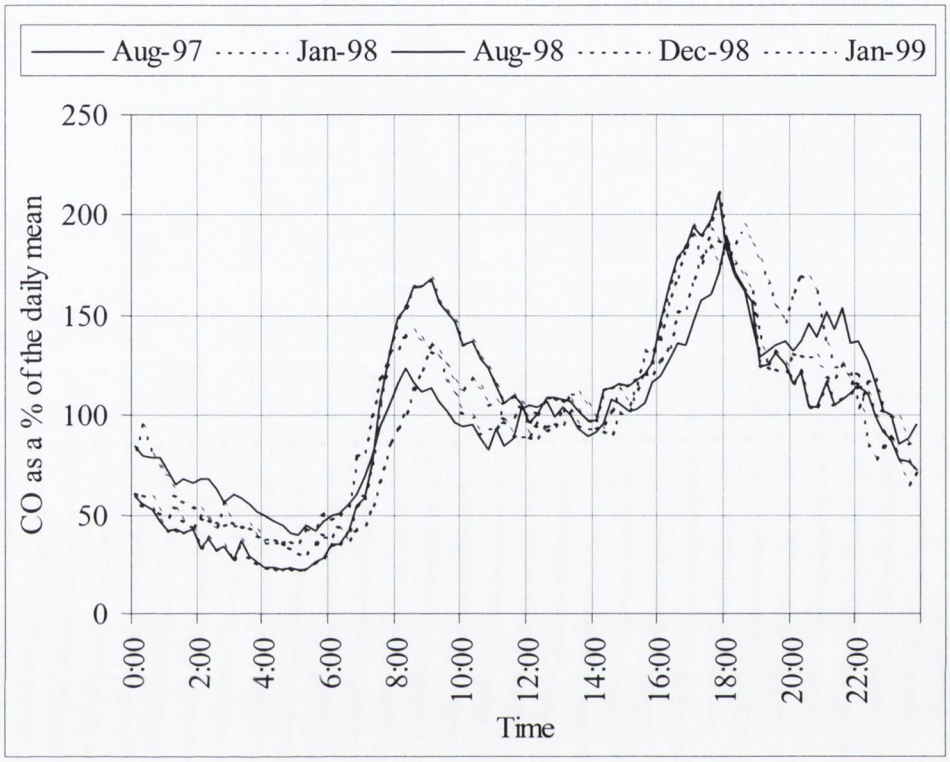

Figure 6.2 Comparison of seasonal factors

A paired two sample t-test was performed between average 15-minute values calculated for winter and summer. The hypothesis that there was no difference between the population means could not be rejected, at the 95% significance level.

As the summer values have no tendency to be either higher or lower than the winter months, seasonality was not considered in the calculation of the time correction factors. The average values for the year were, therefore, taken as the appropriate values to be used. The correction factors are listed in Table 6.1.

Table 6.1 Factors for the adjustment of CO concentrations for the time of sampling

Time	fac(t_c)	Time	fac(t_c)	Time	fac(t_c)	Time	fac(t_c)
0:00	1.47	6:00	2.50	12:00	1.04	18:00	0.49
0:15	1.52	6:15	2.33	12:15	1.04	18:15	0.52
0:30	1.61	6:30	2.17	12:30	1.01	18:30	0.55
0:45	1.79	6:45	1.79	12:45	1.01	18:45	0.59
1:00	1.92	7:00	1.54	13:00	0.98	19:00	0.68
1:15	2.08	7:15	1.20	13:15	0.99	19:15	0.70
1:30	2.22	7:30	0.97	13:30	1.05	19:30	0.72
1:45	2.33	7:45	0.84	13:45	1.06	19:45	0.74
2:00	2.38	8:00	0.75	14:00	1.05	20:00	0.74
2:15	2.44	8:15	0.69	14:15	1.02	20:15	0.75
2:30	2.56	8:30	0.68	14:30	0.96	20:30	0.76
2:45	2.63	8:45	0.67	14:45	0.93	20:45	0.77
3:00	2.86	9:00	0.67	15:00	0.93	21:00	0.77
3:15	2.86	9:15	0.72	15:15	0.88	21:15	0.81
3:30	2.94	9:30	0.76	15:30	0.83	21:30	0.83
3:45	3.13	9:45	0.79	15:45	0.80	21:45	0.85
4:00	3.33	10:00	0.85	16:00	0.74	22:00	0.91
4:15	3.33	10:15	0.88	16:15	0.67	22:15	0.97
4:30	3.45	10:30	0.93	16:30	0.61	22:30	1.04
4:45	3.45	10:45	0.97	16:45	0.57	22:45	1.09
5:00	3.57	11:00	1.00	17:00	0.53	23:00	1.14
5:15	3.33	11:15	0.01	17:15	0.52	23:15	1.23
5:30	3.13	11:30	0.01	17:30	0.51	23:30	1.32
5:45	2.70	11:45	1.04	17:45	0.50	23:45	1.35

By using the values above, each individual CO measurement can be adjusted to give a better indication of the daily average than the short-term reading alone would allow. This allows peak hours, or other times when concentrations would be atypical of the average concentration, to be used as an indicator of the average values. Similarly, peak concentrations can also be predicted from short-term measurements at non-peak hours.

Figure 6.3 shows a sample day of CO data, before and after application of the calculated factors. As can be seen from the chart, shorter time periods now reflect the 24-hour average with significantly increased accuracy, when compared to the unadjusted concentrations.

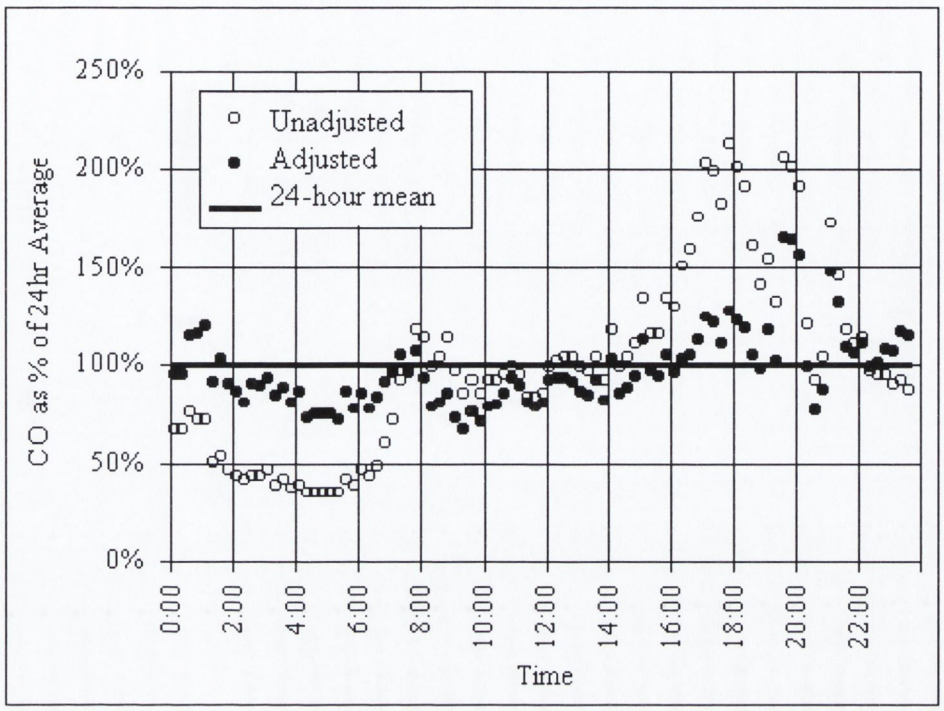

Figure 6.3 Comparison of CO data (27th October 1998) before and after correction for time-of-sampling

6.4.2 Nitrogen Dioxide

NO_2 also exhibits a consistent daily pattern as discussed in Section 5.1.2. Data measured over one year were used to calculate the adjustment factors for time-of-sampling, using the same method as for CO. The daily average for each day was calculated and then each 15-minute concentration expressed as a percentage of the daily average. Again, only weekdays were used as a different pattern is exhibited for weekends (as already discussed in Section 5.1.6).

As with CO, the data were analysed to investigate if the daily pattern had a seasonal element. A paired two sample t-test confirmed that the winter and summer averages belonged to the same population.

The average values for the year were therefore taken as the appropriate values to be used. The resultant factors are presented in Table 6.2.

Table 6.2 Factors for the adjustment of NO_2 concentrations for time of sampling

Time	fac(t_c)	Time	fac(t_c)	Time	fac(t_c)	Time	fac(t_c)
0:00	1.15	6:00	1.14	12:00	0.98	18:00	0.83
0:15	1.16	6:15	1.10	12:15	0.97	18:15	0.85
0:30	1.18	6:30	1.06	12:30	0.94	18:30	0.85
0:45	1.20	6:45	1.05	12:45	0.93	18:45	0.88
1:00	1.22	7:00	1.03	13:00	0.91	19:00	0.89
1:15	1.25	7:15	1.00	13:15	0.92	19:15	0.90
1:30	1.25	7:30	1.01	13:30	0.93	19:30	0.90
1:45	1.27	7:45	1.01	13:45	0.92	19:45	0.90
2:00	1.23	8:00	0.99	14:00	0.91	20:00	0.91
2:15	1.25	8:15	0.98	14:15	0.90	20:15	0.92
2:30	1.23	8:30	0.98	14:30	0.88	20:30	0.93
2:45	1.27	8:45	0.98	14:45	0.89	20:45	0.93
3:00	1.27	9:00	0.97	15:00	0.90	21:00	0.93
3:15	1.28	9:15	0.95	15:15	0.88	21:15	0.95
3:30	1.28	9:30	0.96	15:30	0.87	21:30	0.95
3:45	1.25	9:45	0.96	15:45	0.86	21:45	0.96
4:00	1.23	10:00	0.97	16:00	0.85	22:00	0.98
4:15	1.25	10:15	0.98	16:15	0.84	22:15	1.00
4:30	1.23	10:30	0.98	16:30	0.85	22:30	1.02
4:45	1.22	10:45	0.99	16:45	0.84	22:45	1.03
5:00	1.22	11:00	0.99	17:00	0.83	23:00	1.05
5:15	1.20	11:15	0.98	17:15	0.83	23:15	1.08
5:30	1.18	11:30	0.98	17:30	0.83	23:30	1.10
5:45	1.15	11:45	0.98	17:45	0.83	23:45	1.12

Figure 6.4 shows sample concentrations for January 1998 after application of the calculated factors. Average concentrations over the whole month are used to eliminate the step effect caused by the poor resolution of the equipment (see Section 3.4.2). It can be seen that, as with CO, shorter time periods now reflect the 24-hour average with increased accuracy.

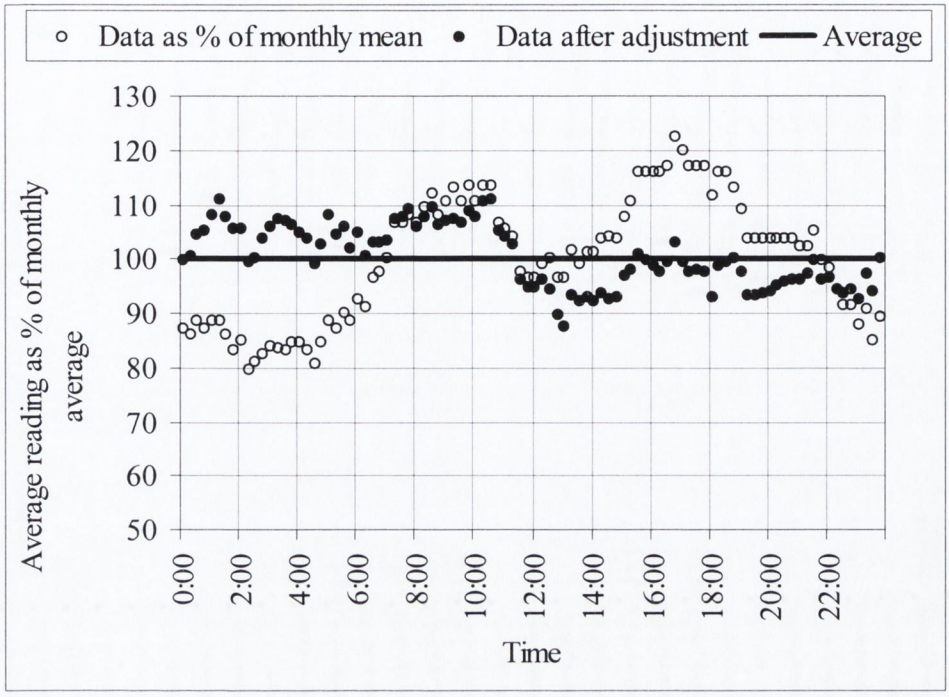

Figure 6.4 Comparison of NO_2 data (January 1999) before and after correction for time of sampling

6.4.3 PM_{10}

Ambient concentrations of PM_{10} also tend to exhibit a consistent daily pattern, as discussed in Section 5.1.3. As for CO and NO_2, using weekdays, each measurement was expressed as a percentage of the daily average. The winter concentrations were seen to take slightly longer to decrease in the evenings (Figure 6.5). A paired two sample t-test was used to investigate the possibility of seasonal dependence. The t-test confirmed that there was no statistically significant difference between winter and summer values during the day, and as the overall daily averages for winter and summer were within 5% of each other, it was decided to use the same factors throughout the year.

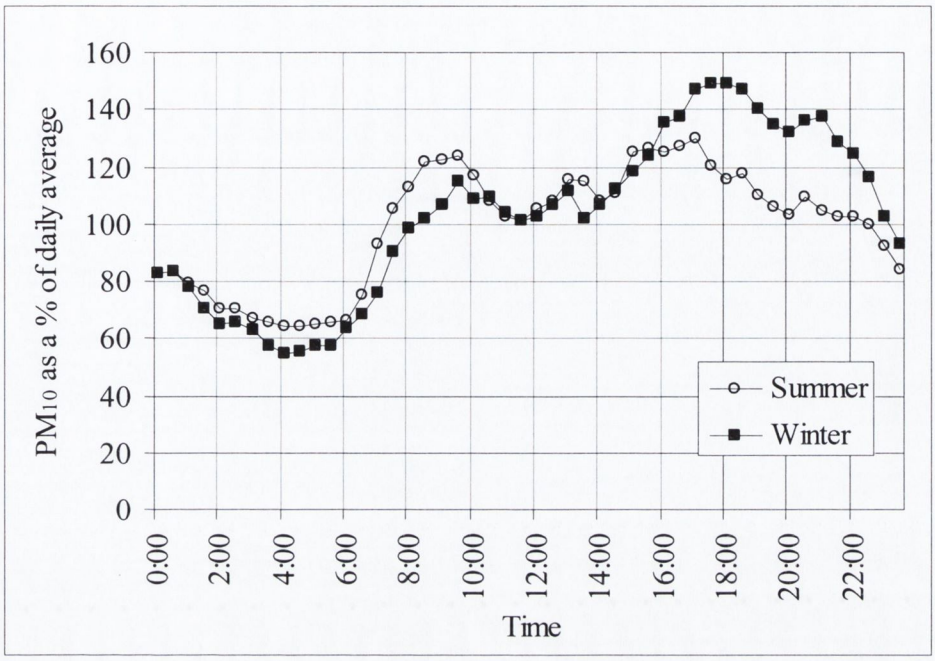

Figure 6.5 Average summer and winter 30-min PM_{10} concentrations expressed as a percentage of the daily average

The correction factors for time of sampling calculated using the both the summer and winter data sets are given in Table 6.3.

Table 6.3 PM_{10} correction factors for time of sampling

Time	fac(t_c)	Time	fac(t_c)	Time	fac(t_c)	Time	fac(t_c)
00:15	1.25	03:15	1.69	06:15	0.93	09:15	7.69
00:30	1.33	03:30	1.47	06:30	0.93	09:30	0.76
00:45	1.41	03:45	1.20	06:45	0.92	09:45	0.81
01:00	1.47	04:00	1.00	07:00	0.94	10:00	0.87
01:15	1.56	04:15	0.92	07:15	0.94	10:15	0.85
01:30	1.64	04:30	0.91	07:30	0.91	10:30	0.83
01:45	1.72	04:45	0.87	07:45	0.83	10:45	0.81
02:00	1.79	05:00	0.83	08:00	0.76	11:00	0.85
02:15	1.89	05:15	0.85	08:15	0.78	11:15	0.88
02:30	1.89	05:30	0.86	08:30	0.77	11:30	0.95
02:45	1.92	05:45	0.94	08:45	0.76	11:45	1.04
03:00	1.85	06:00	0.93	09:00	0.76	12:00	1.10

6.5 Adjustment of Wind Speed Measurements

If only a partial day's monitoring results are being used for longer-term predictions, it should be noted that the wind speed itself exhibits a daily pattern, tending to fall slightly at night (O'Regan, 1996). The diurnal variation of wind speed near ground level exhibits a maximum speed in the early to middle afternoon, when instability and the vertical eddy diffusion of momentum are at a maximum, and a minimum in the evening and early morning hours (Stern, 1976). Hence, using only daytime measurements could give rise to a slight error, in that the wind speed value would be unrepresentatively high.

Therefore, a method of correction similar to that used in the calculation of concentration adjustment factors for the time of sampling is applied. When the data collected over the course of the year are compiled, the wind speed is seen to display the daily pattern shown in Figure 6.6. When wind speed data supplied by Met Eireann and recorded at Dublin Airport during 1998 are examined a similar trend is visible.

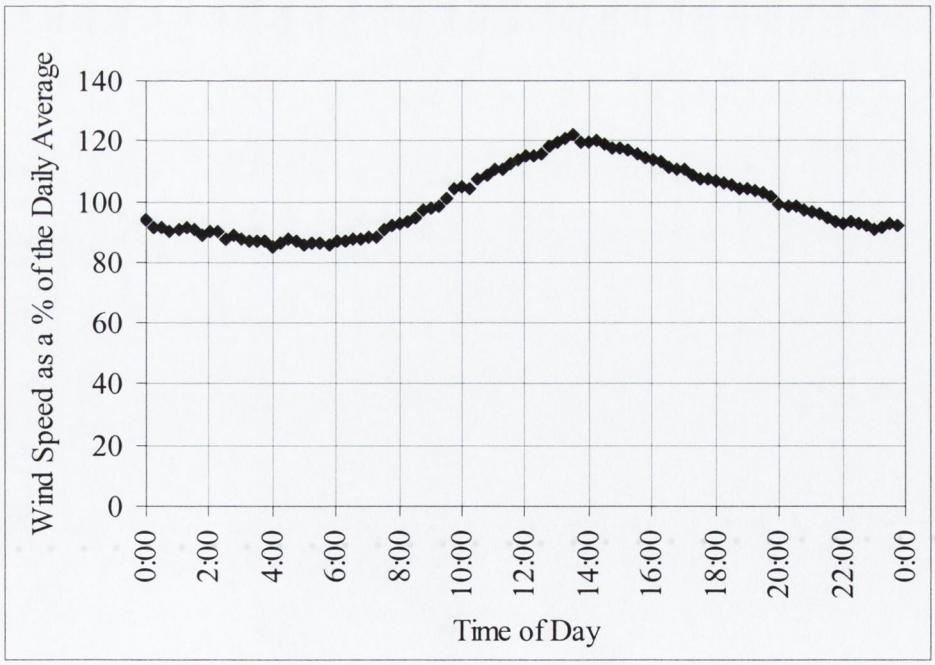

Figure 6.6 Wind speed at 15-minute intervals as a percentage of daily average

From this, the factors shown in Table 6.4 were determined. These are used to give a more representative value of wind speed, before correcting the measured concentrations to allow for the wind speed at the time of sampling, according to in Equation 6.2:

$$U_{adj} = \overline{u} \times fac(t_u) \qquad \text{Equation 6.2}$$

where

$\overline{u}$ = the measured wind speed

Table 6.4 Wind speed correction factors for time of sampling.

Time	fac(t_u)	Time	fac(t_u)	Time	fac(t_u)	Time	fac(t_u)
0:01	1.06	6:01	1.15	12:01	0.87	18:01	0.93
0:16	1.10	6:16	1.15	12:16	0.87	18:16	0.94
0:31	1.09	6:31	1.15	12:31	0.86	18:31	0.95
0:46	1.11	6:46	1.15	12:46	0.85	18:46	0.96
1:01	1.10	7:01	1.14	13:01	0.83	19:01	0.96
1:16	1.09	7:16	1.14	13:16	0.83	19:16	0.96
1:31	1.10	7:31	1.10	13:31	0.82	19:31	0.97
1:46	1.12	7:46	1.09	13:46	0.83	19:46	0.98
2:01	1.11	8:01	1.08	14:01	0.83	20:01	1.01
2:16	1.11	8:16	1.08	14:16	0.83	20:16	1.02
2:31	1.14	8:31	1.05	14:31	0.84	20:31	1.02
2:46	1.12	8:46	1.03	14:46	0.85	20:46	1.03
3:01	1.15	9:01	1.02	15:01	0.85	21:01	1.03
3:16	1.15	9:16	1.02	15:16	0.85	21:16	1.04
3:31	1.15	9:31	0.99	15:31	0.86	21:31	1.06
3:46	1.15	9:46	0.96	15:46	0.88	21:46	1.08
4:01	1.18	10:01	0.95	16:01	0.88	22:01	1.08
4:16	1.16	10:16	0.96	16:16	0.88	22:16	1.08
4:31	1.15	10:31	0.93	16:31	0.90	22:31	1.08
4:46	1.15	10:46	0.92	16:46	0.90	22:46	1.09
5:01	1.16	11:01	0.91	17:01	0.90	23:01	1.10
5:16	1.16	11:16	0.90	17:16	0.92	23:16	1.09
5:31	1.16	11:31	0.89	17:31	0.93	23:31	1.08
5:46	1.16	11:46	0.88	17:46	0.93	23:46	1.09

6.6 Adjustment of Data for Wind Speed

6.6.1 Carbon Monoxide

As would be expected, an increase in wind speed results in a decrease in pollutant concentration. Therefore, unless wind speed at the time of sampling is representative of typical long-term wind speed values, the measured concentration will not give an accurate indication of the local concentration.

Stochastic effects like weather are unpredictable but they do not change very much from one year to the next (Morel *et al.*, 1999, Owen *et al.*, 2000). Wind speed values tend to remain largely consistent all year round, with no marked seasonal variations. The average wind speed recorded at the Pearse St./Westland Row intersection is approximately 2 m/s.

The aim of applying a factor for wind speed is to calculate the equivalent pollutant concentration at 2 m/s by increasing or decreasing the concentration measured at lower or higher wind speeds.

Figure 6.7 is a scatter chart showing daily averages of CO and wind speed for two months. Only weekdays have been used. It can be seen that the decrease in CO with increased wind speed is reasonably consistent and predictable. Trendlines have been drawn using the data. One month displays higher concentrations of CO, but when either trendline is displaced along the y-axis, it is seen to match the other almost exactly.

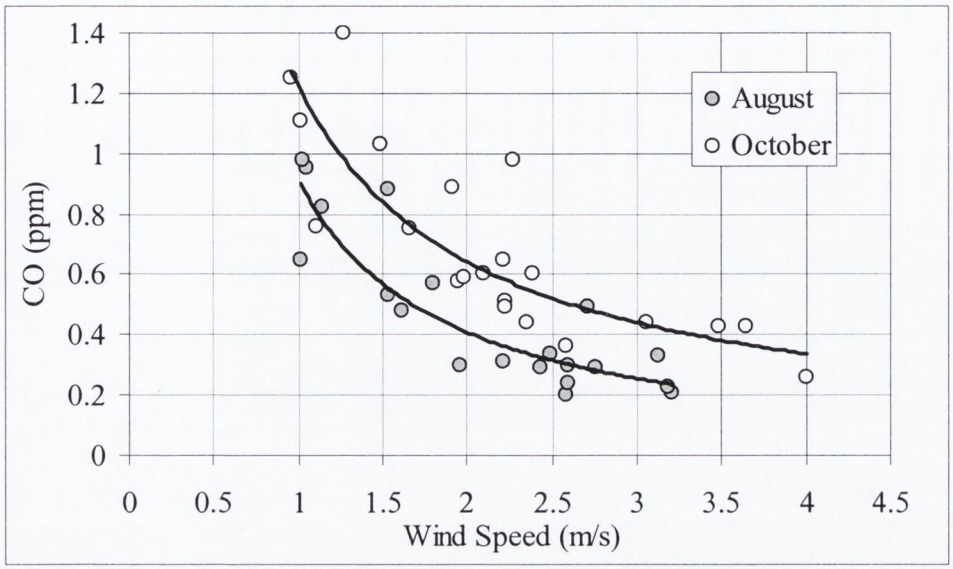

Figure 6.7 Graph of CO 24-hour averages against wind speed 24-hour averages for two months

A similar graph and trendline was produced for each month of available data. For each month, the CO concentration at a wind speed of 2 m/s is indexed as 100%. The CO concentrations at other wind speeds can then be expressed as a percentage of the concentration at a wind speed of 2 m/s, as for Figure 5.14. These data points were compiled and the trendline shown in Figure 6.8 fitted.

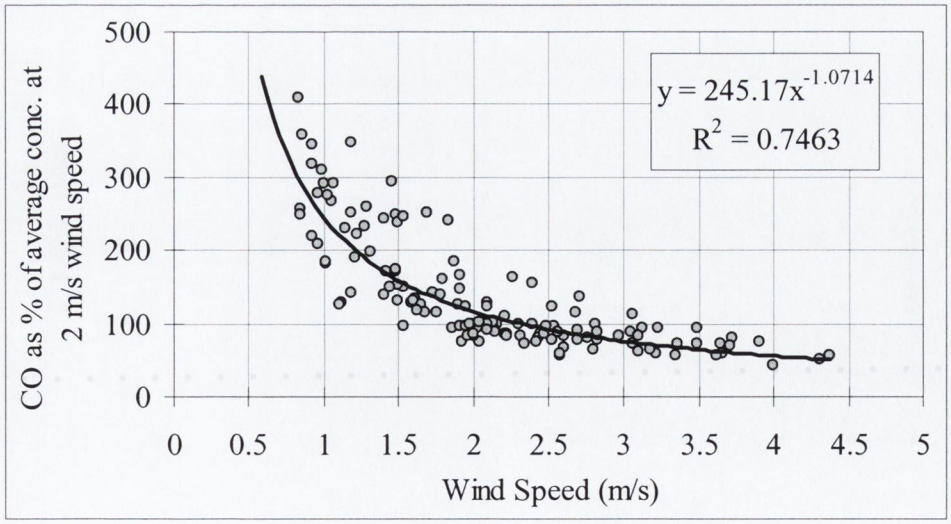

Figure 6.8 Graph of decrease in daily CO concentrations with increased daily average wind speed

The decrease in CO concentrations with wind speed is seen to approximate closely the power series in Equation 6.5.

$$y = 245.17 \times (x)^{-1.07} \qquad \text{Equation 6.5}$$

From this, Equation 6.6 for the wind speed concentration adjustment factor is derived,

$$fac\left(u_{adj}\right) = \frac{100}{245.17 \times \left(u_{adj}\right)^{-1.07}} \qquad \text{Equation 6.6}$$

where

$fac(u_{adj})$ is the wind speed concentration adjustment factor.

Using this factor, measurements of CO can be converted to what they would be at a wind speed of 2 m/s, under otherwise equivalent conditions. This removes the bias in measurements obtained during uncharacteristically high or low wind speeds.

However, the calculated power series becomes less accurate at very high or very low wind speeds. The power series diverges from the trend exhibited by the data at around 0.9 m/s at the lower end and 3.9 m/s at the upper end. Therefore, for wind speed values of 0.9m/s or less, a constant value of 318% is used, and for wind speed values of 3.9 m/s or higher, a constant value of 57% is used.

To illustrate how the data can be represented by a power series between wind speeds of 0.8 m/s and 4 m/s, the data were split into increments of 0.2 m/s, and all the CO values within that increment were averaged. The power series previously calculated is shown against these averages in Figure 6.9.

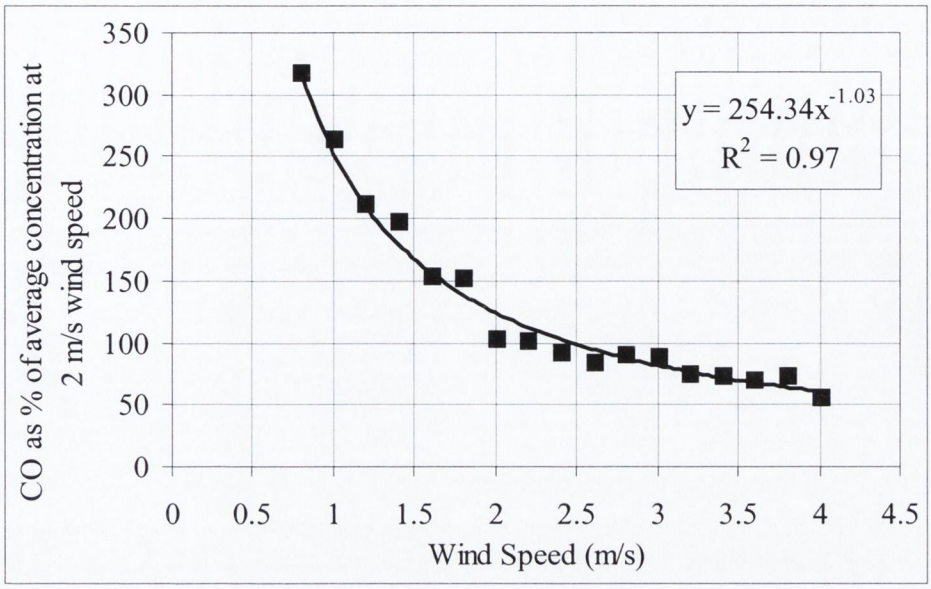

Figure 6.9 CO concentrations with respect to wind speed in increments of 0.2 m/s

From Figure 6.9, it can be seen that a similar result is obtained whether these average values are used to make the adjustment for wind speed or whether the power series of Equation 6.5 is employed. Use of these average values, however, removes the slight inaccuracy inherent in the use of this particular power series caused by the lack of fit, at 2 m/s wind speed.

6.6.2 Nitrogen Dioxide

For NO_2, as for CO, an adjustment factor is calculated to take account of the wind speed at the time of measurement. This allows measured NO_2 concentrations to be used to estimate concentrations under equivalent conditions, but at the average wind speed of 2 m/s.

Figure 6.10 shows the daily averages of NO_2 and wind speed plotted against each other for two months. It can be seen that the decrease in NO_2 with increased wind speed is reasonably consistent and predictable. Two different months are shown, with average daily NO_2 concentrations plotted against average wind speed. Trendlines have been drawn for each data set. As can be seen, one month has higher concentrations of NO_2, but when either trendline is displaced along the y-axis, it is seen to match the other closely.

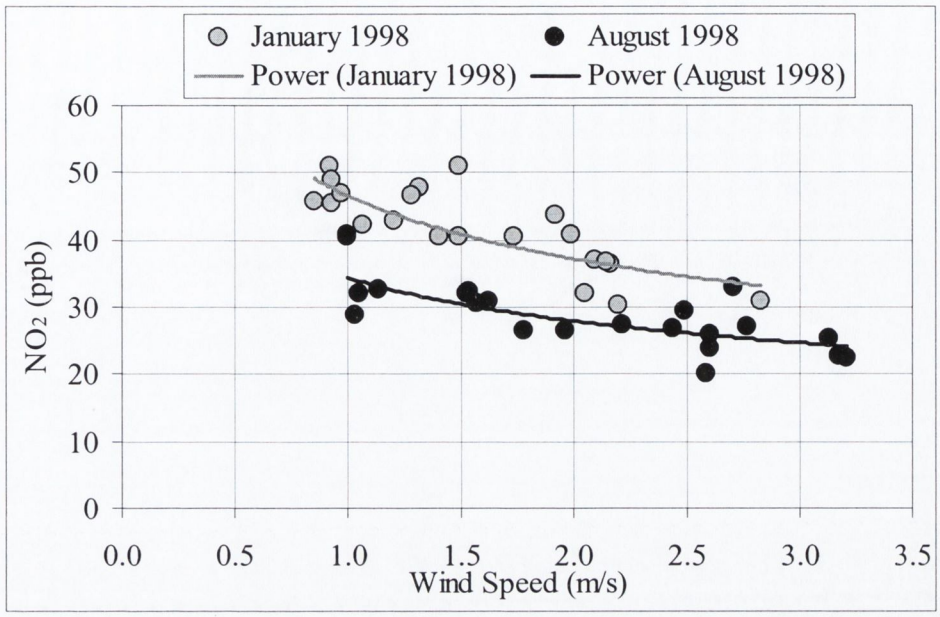

Figure 6.10 24-hour NO_2 average plotted against 24-hour wind speed average.

A similar graph and trendline was produced for each month of data available. Figure 6.11 shows the data points from Figure 5.17 averaged and expressed as a percentage of the average concentration at 2 m/s.

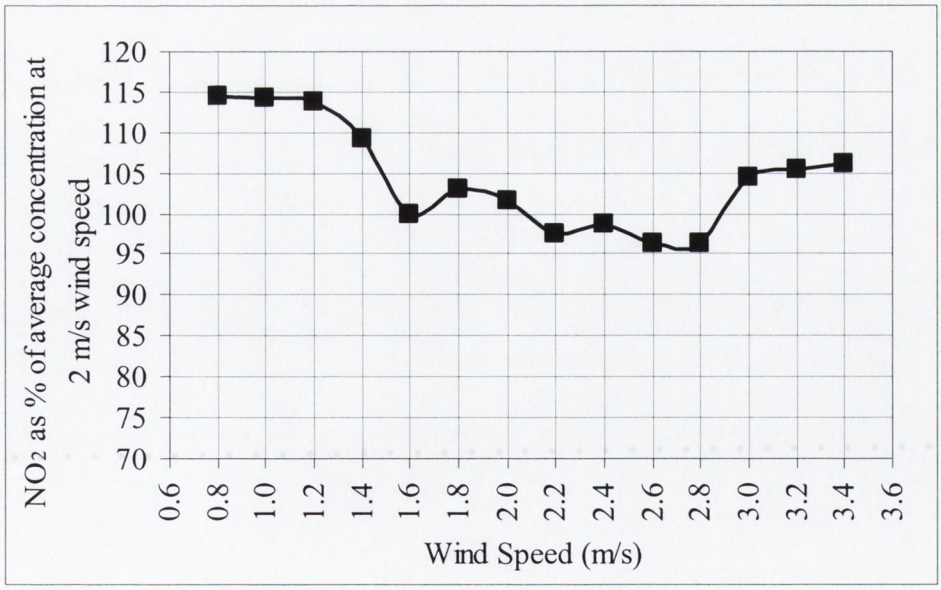

Figure 6.11 NO_2 concentration as a percentage of the concentration at a wind speed of 2 m/s plotted against wind speed.

The graph of concentration against wind speed is quite unlike the equivalent graph for CO, and cannot be characterised by a single power series. The concentration of NO_2 does not consistently decrease with wind speed, but at a wind speed of 3 m/s begins to rise again, as already discussed in Section 5.3.2.

For use in the prediction model, wind speed was split into 0.2 m/s increments, and the NO_2 concentrations expressed as a percentage of the monthly average for that increment. The NO_2 factors for each wind speed increment are tabulated in Table 6.5.

Table 6.5 Factors for the adjustment of NO_2 readings for wind speed.

WS Lower Limit (m/s)	WS Upper Limit (m/s)	Fac(u_t)
0	1.3	0.88
1.3	1.5	0.92
1.5	1.7	1.00
1.7	1.9	0.97
1.9	2.1	0.98
2.1	2.3	1.02
2.3	2.5	1.01
2.5	2.7	1.04
2.7	2.9	1.04
2.9	3.1	0.96
3.1	3.1 and above	0.94

6.6.3 PM_{10}

Figure 6.12 shows the daily averages of weekday PM_{10} concentrations and wind speed plotted against each other for two months. A power series is fitted to the data. The PM_{10} concentration shows a consistent reduction with increased wind speed.

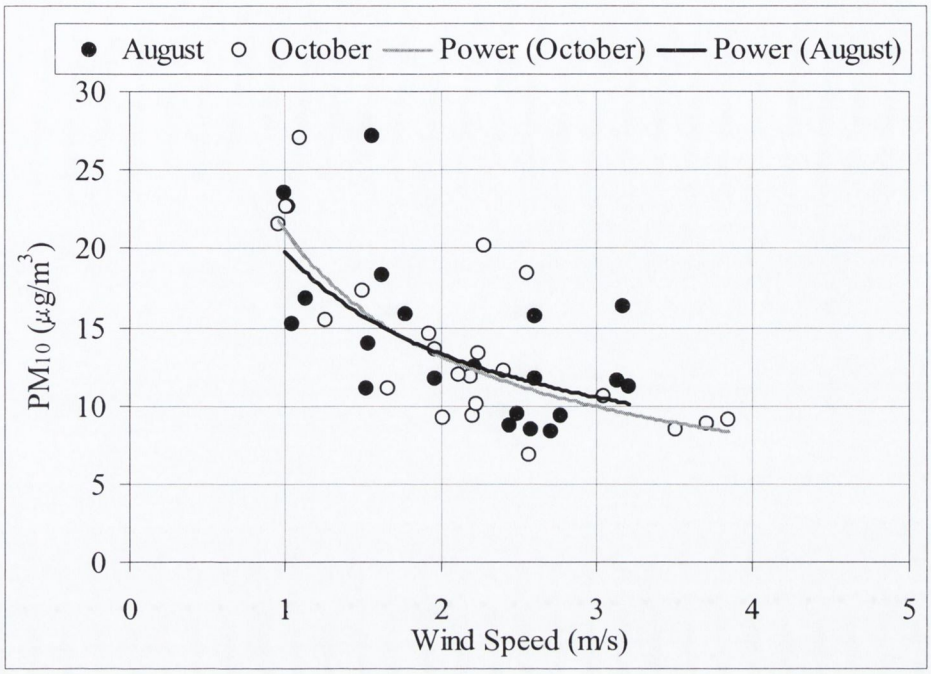

Figure 6.12 24-hour PM_{10} averages plotted against 24-hour wind speed averages

PM_{10} 24-hour concentrations are expressed as a percentage of the monthly average and plotted against daily wind speed averages in Figure 6.13.

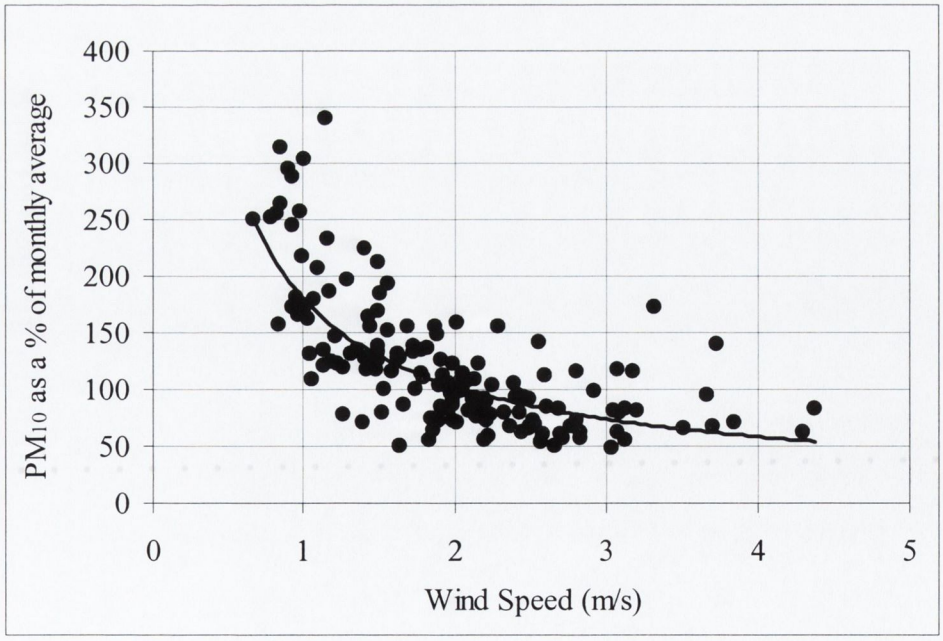

Figure 6.13 24-hour average PM_{10} concentrations as percentages of the average concentration at 2 m/s wind speed, plotted against 24-hour average wind speed for 8 months

The decrease in PM_{10} concentrations is seen to approximate the power series in Equation 6.7:

$$y = 180.00 \times (x)^{-0.81} \qquad \text{Equation 6.7}$$

From this, Equation 6.8 for the wind speed concentration adjustment factor is derived:

$$fac(u_{adj}) = \frac{100}{180 \times (u_{adj})^{-0.81}} \qquad \text{Equation 6.8}$$

where

$fac(u_{adj})$ is the wind speed concentration adjustment factor

Using this factor, measurements of PM_{10} can be converted to what they would be at a wind speed of 2 m/s, given the same conditions otherwise. Again, this eliminates any bias due to taking measurements during uncharacteristically high or low wind speeds.

To illustrate how the data can be represented by a power series, the wind speed values in Figure 6.13 were split into divisions of 0.2 m/s and expressed as a percentage of the average concentration at 2 m/s. The associated PM_{10} values for each category were calculated and graphed in Figure 6.14. A power series was fitted to the data, with a correlation coefficient of 0.998. For wind speed measurements less than 0.6 m/s, or greater than 4.0 m/s, the average PM_{10} values at these windspeeds are used, to avoid a loss of accuracy as the power series diverges from the measured data. However, these occasions would be relatively rare.

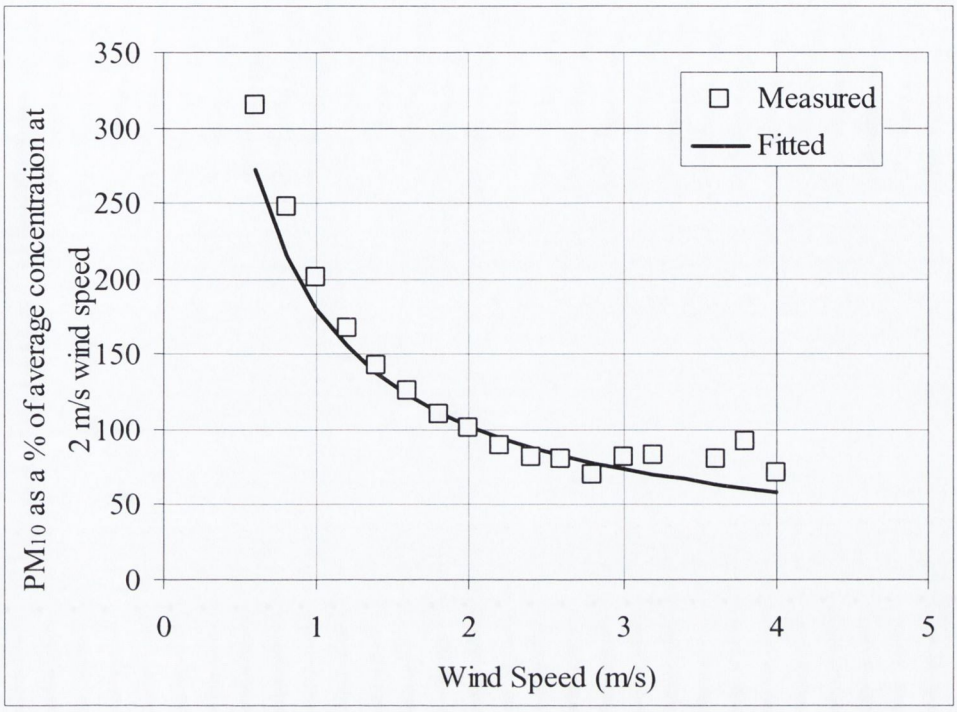

Figure 6.14 Wind speed (as a percentage of the average wind speed) plotted against PM_{10} (as a percentage of value at a wind speed of 2 m/s)

A summary of the wind speed concentration adjustment factor in each division is given in Table 6.6.

Table 6.6 Factors for the adjustment of PM_{10} readings for wind speed.

WS Lower Limit	WS Upper Limit	Fac(u_t)
m/s	m/s	
0	0.6	0.32
0.6	0.8	0.40
0.8	1	0.50
1	1.2	0.60
1.2	1.4	0.70
1.4	1.6	0.79
1.6	1.8	0.91
1.8	2	0.99
2	2.2	1.11
2.2	2.4	1.22
2.4	2.6	1.25
2.6	2.6 and above	1.43

Figure 6.15 compares the power series used to characterise the effect of wind speed on both CO and PM_{10}. The two power series are seen to diverge at lower wind speeds, with lower wind speeds having a greater effect on CO compared to PM_{10}.

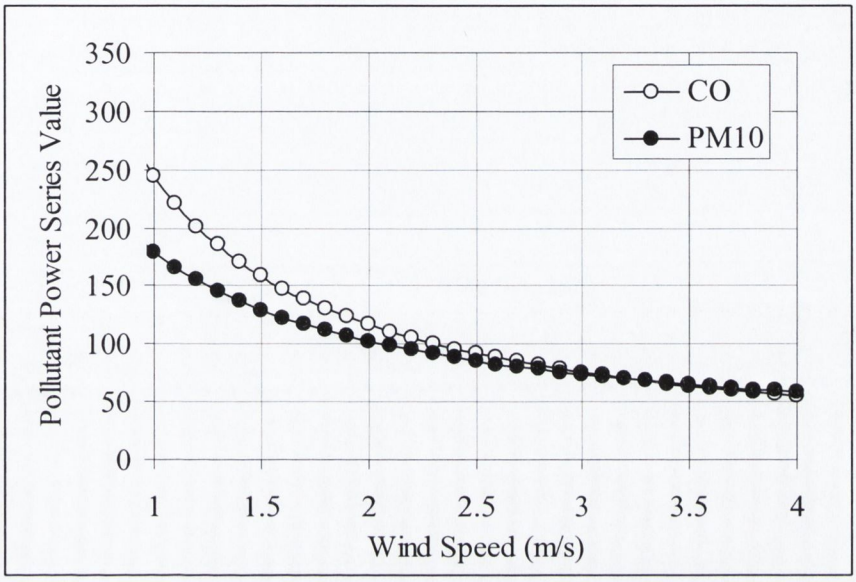

Figure 6.15 Comparison of power series characterising influence of wind speed in pollutant concentrations for CO and PM_{10}.

6.7 Adjustment of Pollutant Data for Wind Direction

6.7.1 Carbon Monoxide

As discussed in Section 5.4, wind direction can also affect pollutant concentrations. When the wind is blowing from the north or east CO measurements are higher than when the wind is blowing from other directions. Since the direction of the wind during a sampling period may not be representative of typical wind conditions, an adjustment factor must be introduced to adapt the measured concentrations to give an equivalent concentration under typical wind conditions.

For each month of recorded data, the data were split into eight classes according to the direction from which the wind was blowing at the time of sampling. These classes are shown in Table 6.7.

Table 6.7 Designation of wind direction categories

Designation	Street	Wind Direction
WR	Westland Row	0°-45°
WR/PW	Westland Row /Pearse St. (West)	46°-90°
PW	Pearse St. (West)	91°-135°
PW/L	Pearse St. (West)/Lombard St	136°-180°.
L	Lombard St.	181°-225°
L/PE	Lombard St./ Pearse St. (East)	226°-270°
PE	Pearse St. (East)	271°-315°
PE/WR	Pearse St. (East)/ Westland Row	316°-360°

For each class the average wind speed and CO concentration was calculated for each month. Any class with fewer than five samples was rejected. These values are shown in Table 6.8 and Table 6.9. (A sample calculation for February 1998 is given in Appendix B.)

Table 6.8 Average CO concentrations in each direction.

	WR (ppm)	WR/PW (ppm)	PW (ppm)	PW/L (ppm)	L (ppm)	L/PE (ppm)	PE (ppm)	PE/WR (ppm)
Jan-98	2.92	1.37	2.54	3.87	3.62	3.32		3.47
Feb-98	1.33	1.31	1.44	1.54	2.37	4.22	2.98	2.12
Jul-98	1.35	1.22	1.57	1.56	3.77	3.73	3.15	2.23
Aug-98	0.29	0.34	0.51	0.65	0.81	1.03	1.04	0.49
Sep-98	0.71	0.42	0.49	0.72	1.00	1.24	0.98	0.92
Oct-98	0.59	0.47	0.84	0.68	1.18	1.08	0.86	0.93
Nov-98	0.75	0.60	0.79	1.45	1.61	2.47	1.79	1.30
Dec-98	0.68	0.66	0.75	1.17	1.69	2.01	1.76	1.35
Jan-99	0.52	0.65	1.11	1.42	1.57	1.44	1.41	0.96

Table 6.9 Average wind speeds in each direction.

	WR (m/s)	WR/PW (m/s)	PW (m/s)	PW/L (m/s)	L (m/s)	L/PE (m/s)	PE (m/s)	PE/WR (m/s)
Jan-98	2.38	2.14	1.64	1.11	1.06	1.62	0.33	0.23
Feb-98	2.52	2.67	2.35	2.11	0.87	1.34	0.95	1.31
Jul-98	2.07	2.24	1.82	0.78	0.96	1.40	0.73	0.88
Aug-98	2.25	2.27	1.50	1.34	1.09	1.12	0.61	0.85
Sep-98	2.09	2.00	1.69	0.82	0.63	1.31	0.53	0.46
Oct-98	2.52	2.60	1.65	1.73	1.18	1.50	0.67	1.18
Nov-98	2.15	2.19	1.94	1.55	0.98	1.04	0.88	1.00
Dec-98	2.08	2.19	1.41	0.87	0.95	1.50	0.82	0.93
Jan-99	2.65	2.46	1.21	0.72	0.79	1.14	0.83	1.15

The average wind speed in certain directions was found to be higher than others, as discussed in Section 5.4.1, implying that concentration data should be corrected for wind speed before the factors for wind direction are determined. This ensures that subsequent measurements taken and adapted to take account of the conditions at the time of measurement would not be corrected twice for wind speed. For this purpose, the method of wind speed adjustment discussed in the previous section was used. The corrected data are shown in Table 6.10.

Table 6.10 Average CO concentrations in each direction, corrected for wind speed.

	WR (ppm)	WR/PW (ppm)	PW (ppm)	PW/L (ppm)	L (ppm)	L/PE (ppm)	PE (ppm)	PE/WR (ppm)
Jan-98	2.81	1.19	1.66	1.69	1.52	2.15		0.30
Feb-98	1.36	1.42	1.37	1.31	0.81	2.23	1.11	1.10
Jul-98	1.13	1.10	1.14	0.47	1.42	2.08	0.90	0.77
Aug-98	0.26	0.32	0.30	0.35	0.34	0.46	0.24	0.16
Sep-98	0.60	0.34	0.33	0.23	0.24	0.65	0.20	0.16
Oct-98	0.60	0.49	0.55	0.47	0.55	0.64	0.22	0.44
Nov-98	0.65	0.53	0.61	0.89	0.62	1.01	0.62	0.51
Dec-98	0.57	0.58	0.42	0.40	0.63	1.20	0.56	0.49
Jan-99	0.56	0.64	0.53	0.39	0.48	0.65	0.46	0.44

Using the corrected data, the concentrations in each direction are expressed as a percentage of the monthly average, allowing the effect of wind direction to be quantified. The annual average CO concentrations, as a percentage of the mean, are given in Table 6.11. The low arithmetic average of the values in all eight classes is explained when the frequency of

measurements in those classes is considered. Most of the readings fall into the 'L' or 'L/PE' classes, which therefore have more of an effect on the overall average than the other classes with the lower values.

Table 6.11 CO concentration in individual directions as a percentage of mean CO concentrations.

	WR (ppm)	WR/PW (ppm)	PW (ppm)	PW/L (ppm)	L (ppm)	L/PE (ppm)	PE (ppm)	PE/WR (ppm)
CO as %	63.30	71.66	59.37	58.85	103.22	105.06	39.58	45.17

However, when dealing with short periods of measurement, it is very unlikely that there will be a data entry in every direction, and to use only the directions recorded could give rise to inaccuracies. For this reason, the CO concentration as a fraction of the monthly average for each direction is also expressed in terms of the average concentration in the other directions. This is best expressed as a matrix, as shown in Table 6.12. The inverse of the individual entries is then used as the adjustment factor for that direction.

Table 6.12 CO concentrations for individual directions as a fraction of concentrations in other directions

	WR	WR/PW	PW	PW/L	L	L/PE	PE	PE/WR
WR	1.00	0.95	0.86	0.70	0.77	0.79	0.75	0.78
WR/PW	1.05	1.00	0.91	0.74	0.82	0.84	0.79	0.82
PW	1.16	1.10	1.00	0.82	0.90	0.92	0.87	0.91
PW/L	1.42	1.35	1.22	1.00	1.10	1.13	1.07	1.11
L	1.29	1.23	1.11	0.91	1.00	1.03	0.97	1.01
L/PE	1.26	1.20	1.08	0.89	0.97	1.00	0.94	0.98
PE	1.34	1.27	1.15	0.94	1.03	1.06	1.00	1.04
PE/WR	1.28	1.22	1.10	0.90	0.99	1.02	0.96	1.00

This is read as the column on the left in terms of the row on the top. To illustrate using the first column, the average concentration when the wind direction is 'WR' is obviously 100% of the concentration when the wind direction is 'WR' (or CO_{WR}=100% of CO_{WR}), but the average concentration when the wind direction is 'WR/PW' is 105% of the average concentration when the wind direction is 'WR' (or $CO_{WR/PW}$ = 105% of CO_{WR}). This allows the directions for which there are no data to be estimated in terms of the available data. To

ensure that the estimate is as accurate as possible, the algorithm spreadsheet uses the direction with the most entries as the basis from which to estimate the missing directions.

The final consideration for correcting the measured concentrations for wind direction is the influence of a prevailing wind, which leads to the concentrations in some directions having more of a bearing on the overall average than others. The eight wind direction classes are, therefore, weighted according to the percentage of time that the wind blows in each of the eight directions, as shown in Table 6.13. For example, even a very high average concentration when the wind is blowing from Pearse St. East ('PE') will have a small effect on the overall average.

Table 6.13 Sample of ratio of measurements in individual directions for one month

	WR	WR/PW	PW	PW/L	L	L/PE	PE	PE/WR
% of total entries	46	24	3	2	8	14	1	2
Ratio	0.46	0.24	0.03	0.02	0.08	0.14	0.01	0.02

To apply this weighting factor, the concentration in each direction is multiplied by the corresponding ratio, and all the resulting products are summed to give the estimate of the average concentration.

6.7.2 Nitrogen Dioxide

Wind direction factors for NO_2 were calculated in the same manner as for CO. For each month of recorded data the following calculations were carried out:

The average wind speed and NO_2 concentration were calculated for each month. These average NO_2 values were then corrected for the wind speed and expressed as fractions of the monthly average. These values are shown in Table 6.14.

Table 6.14 Average NO_2 and wind speed values for each direction

	WR	WR/PW	PW	PW/L	L	L/PE	PE	PE/WR
NO_2 (ppb)	28	28	30	32	34	33	30	30
WS (m/s)	2.30	2.31	1.69	1.22	0.95	1.33	0.71	0.89
$\overline{C}_{adj(\theta)}$ (ppb)	27	27	29	29	29	31	26	27
NO_2 as a fraction of average	0.95	0.96	1.01	1.04	1.02	1.07	0.97	0.94
fac(θ)	1.05	1.04	0.99	0.96	0.98	0.93	1.03	1.06

6.7.3 PM_{10}

For each month of recorded data the following calculations were carried out.

The average wind speeds and PM_{10} concentrations was calculated for each month, using the same methods as for CO. The average PM_{10} values were then adjusted for the wind speed and expressed as a fraction of the monthly average. These values are shown in Table 6.15 below.

Table 6.15 Average PM_{10}, wind speed, and corrected PM_{10} for each direction

	WR	WR/PW	PW	PW/L	L	L/PE	PE	PE/WR
PM_{10} ($\mu g/m^3$)	16.44	14.04	16.45	20.05	24.06	27.68	23.67	19.14
WS (m/s)	2.10	2.19	1.72	1.22	1.02	1.44	0.78	0.85
$\overline{C}_{adj(u)}$ ($\mu g/m^3$)	16.51	15.41	13.52	11.95	11.94	19.53	9.61	8.49
PM_{10} as fraction of average.	0.93	0.86	0.76	0.70	0.68	1.11	0.54	0.47
fac(θ)	1.07	1.16	1.31	1.42	1.47	0.90	1.85	2.12

Each PM_{10} percentage is then expressed in terms of the other directions to allow the average concentration to be estimated for a sample taken when the wind is blowing from any direction (Table 6.16). The inverse of each entry then forms the adjustment factor.

Table 6.16 Wind direction concentration adjustment matrix for PM_{10}

	WR	WR/PW	PW	PW/L	L	L/PE	PE	PE/WR
WR	1.00	1.09	1.22	0.89	1.32	0.81	1.54	1.84
WR/PW	0.91	1.00	1.11	0.81	1.21	0.74	1.41	1.68
PW	0.82	0.90	1.00	0.73	1.09	0.67	1.27	1.51
PW/L	1.12	1.23	1.37	1.00	1.48	0.91	1.73	2.07
L	0.76	0.83	0.92	0.67	1.00	0.62	1.17	1.39
L/PE	1.23	1.35	1.50	1.09	1.62	1.00	1.90	2.26
PE	0.65	0.71	0.79	0.58	0.86	0.53	1.00	1.19
PE/WR	0.54	0.59	0.66	0.48	0.72	0.44	0.84	1.00

6.8 Adjustment of Pollutant Data for Temperature

Monthly values of Pearson's sample correlation, r, for CO and temperature were calculated using 24-hour averages and ranged between –0.31 and 0.34, averaging at –0.01. As CO measurements were found not to be significantly correlated with temperature (as discussed in Section 5.5.1), the adjustment factor *fac(temp)* for CO is 1.

Pearson's sample correlation, r, calculated monthly using 24-hour averages ranged between –0.25 to 0.28, averaging at –0.03 for NO_2 and temperature data. NO_2 concentrations were found to be independent of temperature in Section 5.5.2, hence the adjustment factor *fac(temp)* for NO_2 is also 1.

PM_{10} concentrations were found to be independent of temperature in Section 5.5.3 with monthly values of Pearson's sample correlation, r, ranging between –0.08 and 0.28, averaging at 0.05. Therefore, the adjustment factor *fac(temp)* for PM_{10} is also 1.

6.9 Adjustment of Pollutant Data for Relative Humidity

As discussed in Sections 5.6.1 and 5.6.3, concentrations of CO and PM_{10} were found to be independent of relative humidity, therefore a value of 1 is used for the adjustment factor *fac(rh)*.

Although NO_2 showed a slight negative correlation with relative humidity on occasions, this was not consistent from month to month. Therefore, a value of one is also used for *fac(rh)* for the prediction of NO_2 levels.

Although the adjustment factor for relative humidity for CO, NO_2, and PM_{10} is 1, it is left in the initial equation to allow the expansion of the methodology to other compounds, which may be dependent on these factors.

6.10 Adjustment of Prediction for Average Monthly Wind Speed

6.10.1 Carbon Monoxide

In the calculation of the correction factors discussed so far, wind speed was expressed as a percentage of the monthly mean wind speed. The factors are, therefore, designed to give an estimate of the CO concentration at the mean wind speed. However, if the mean wind speed for the month in question varies from the assumed monthly average used in the calculation of the factors (in the case of the Westland Row/Pearse St. site, 2 m/s was assumed to be the mean), then that will introduce inaccuracies. If the wind speed at the site under investigation has been recorded, then this information can be used to further refine the estimate. If this is unavailable, then data from a suitable alternative site can be used instead, such as data for the nearest weather station. In this regard, wind speed data recorded at Dublin Airport were found to improve the prediction to a similar extent as the data recorded at the monitoring site.

As can be seen in Figure 6.16, there is a good correlation between wind speeds at both sites. A Pearson's correlation coefficient of 0.87 was calculated. However, because the absolute values of the wind speeds are different, they should be expressed as a percentage of the mean value, when calculating adjustment factors.

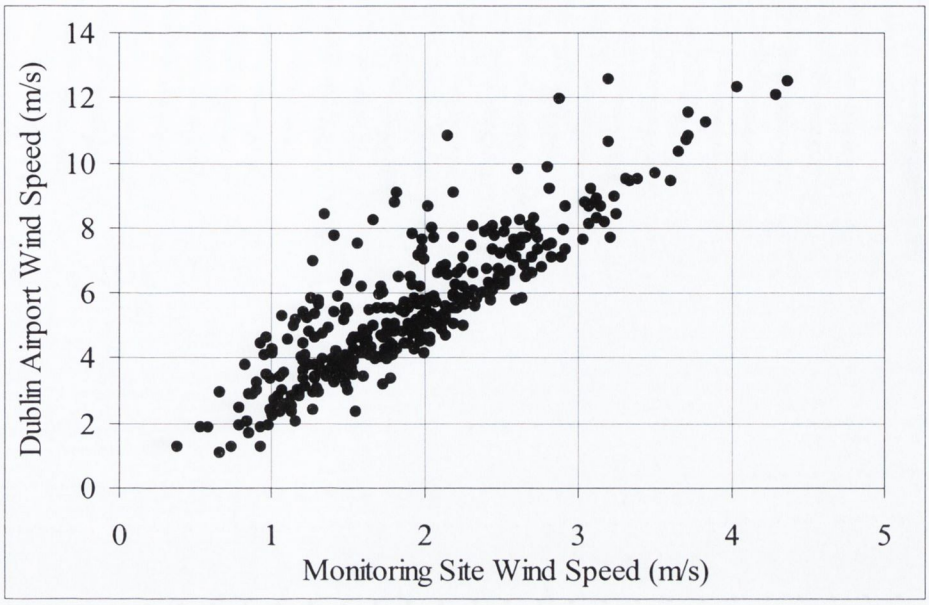

Figure 6.16 Wind speed measured at the TCD monitoring site against Met Eireann wind speed measurements from Dublin Airport

Using three complete days of data for each thirty day period, the average CO level (C_{adj}) was predicted. This predicted level was then expressed as a percentage of the correct (measured) value and plotted against wind speed. These values were found to have a linear relationship, as illustrated in Figure 6.17.

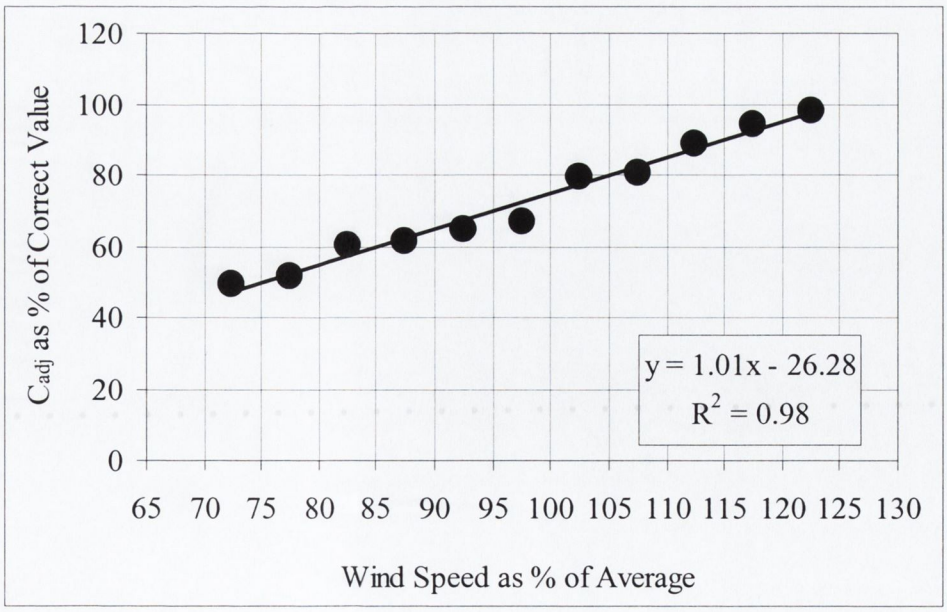

Figure 6.17 C_{adj} for CO as a percentage of the correct value, with respect to wind speed.

The trendline in Equation 6.9 was fitted to the data, with an R^2 value of 0.98:

$$y = 1.01(x) - 26.28 \qquad \text{Equation 6.9}$$

This linear relationship adjusts the prediction to take account of the average wind speed during the prediction period, which could be higher or lower than 2 m/s, the reference point for the prediction algorithm.

Either the monthly average wind speed at the site or that at Dublin Airport can be used in Equation 6.10 to calculate the adjustment factor.

$$fac(u_{mth}) = \frac{100}{1.01(u_{mth}) - 26.28} \qquad \text{Equation 6.10}$$

where

$fac(u_{mth})$ = the factor for the adjustment of the prediction for monthly wind speed

u_{mth} = the monthly average wind speed as a % of the long-term site average wind speed.

6.10.2 Nitrogen Dioxide

For NO_2, unlike CO, there is no clear correlation between the average monthly wind speed and the error in the prediction of the monthly concentration. Predictions of the monthly averages as percentages of the measured monthly concentrations are plotted against monthly average wind speed in Figure 6.18.

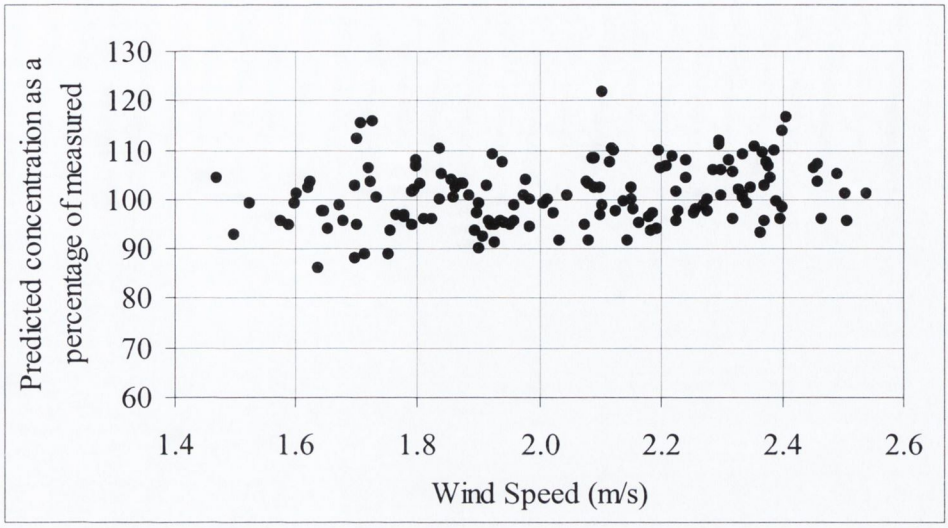

Figure 6.18 C_{adj} for NO_2 as a percentage of the correct value, with respect to wind speed.

As the accuracy of the NO_2 predictions is not dependent on the average monthly wind speed, $fac(u_{mth})$ for NO_2 is 1.0.

6.10.3 PM_{10}

As for CO, predictions of the monthly average PM_{10} concentrations (C_{adj}) were calculated for each 30-day period. These were then expressed as percentages of the measured averages and plotted against wind speed in Figure 6.19. The accuracy was seen to be linearly related to wind speed.

A trendline was fitted to the data (Equation 6.11), with a correlation coefficient of 0.91.

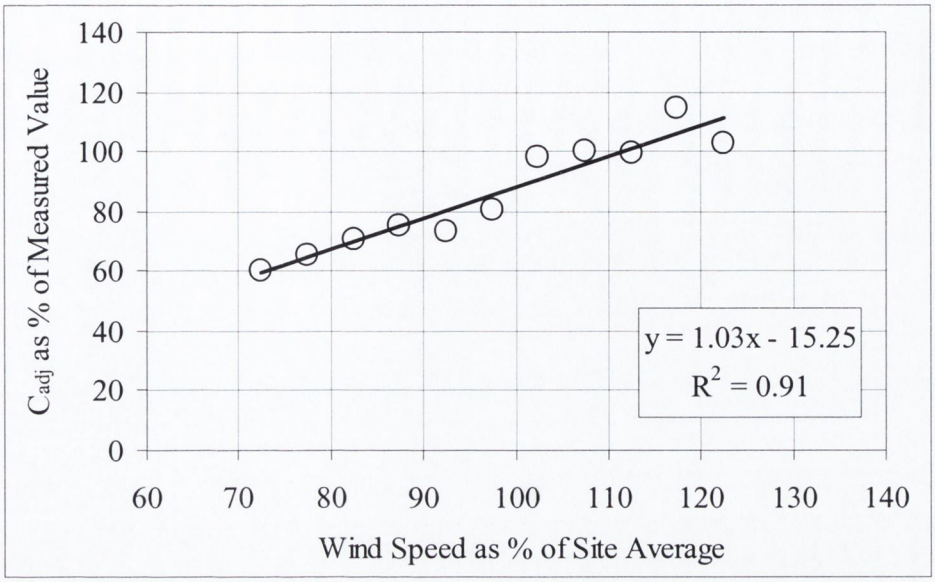

Figure 6.19 Predicted PM_{10} concentrations as percentages of the measured concentrations, plotted against wind speed.

$$y = 1.03(x) - 15.25 \qquad \text{Equation 6.11}$$

From Equation 6.11, Equation 6.12 for the adjustment of the prediction of the monthly average PM_{10} concentration is obtained.

$$fac(u_{mth}) = \frac{100}{1.03(u_{mth}) - 15.25} \qquad \text{Equation 6.12}$$

where

$fac(u_{mth})$ = the factor for the adjustment of the prediction for monthly wind speed

u_{mth} = the monthly average wind speed as a % of the long-term site average wind speed.

6.11 Rates of Convergence of Factors

The rate of convergence of a factor gives an indication of the period of time over which the data used in the calculation of that factor must be measured to give a reasonably accurate estimate. To investigate these rates of convergence, the adjustment factors were calculated

using increasing periods of measured data, and the resulting values of the factors compared. It is assumed that the monitoring period employed at Site A was sufficiently long to accurately define each adjustment factor. Hence, the error associated with using shorter monitoring periods can be evaluated through comparison with these accurate values. The rates of convergence of the factors are important for judging how long sampling should be carried out to ensure the calculation of reliable factors, and hence accurate predictions.

6.11.1 Convergence of Time-of-Sampling Factors

Carbon Monoxide

As discussed in Section 6.4, the time-of-sampling factors are used to adjust the concentration measured at a particular time of day to give an indication of the 24-hour average concentration. To examine the rate of convergence, these factors were calculated using increasing number of days from 1 to 160 (160 days being the longest uninterrupted monitoring period). The errors associated with a given number of days are expressed as a percentage of the final factor calculated using all the days. The rate of convergence over 160 days is shown in Figure 6.20.

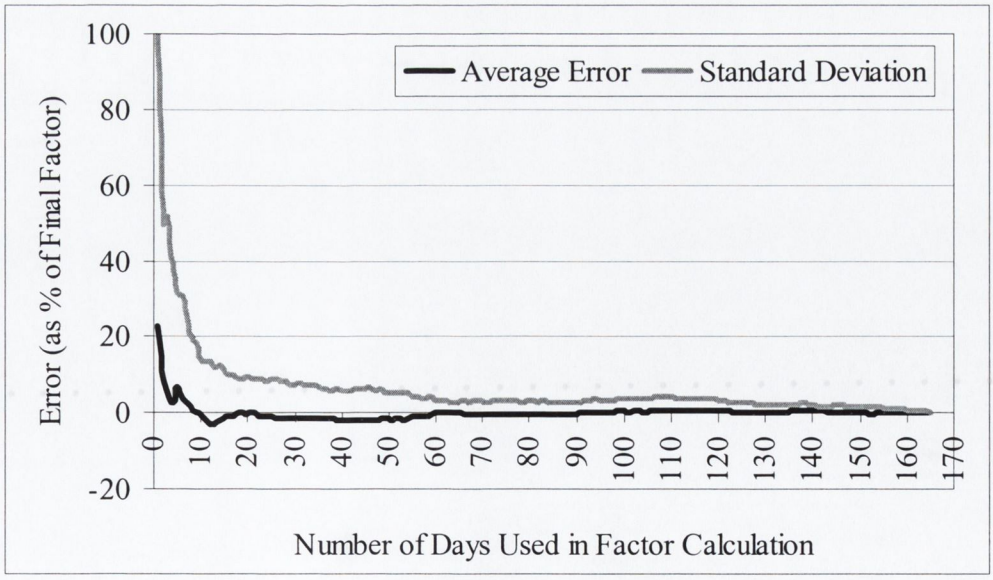

Figure 6.20 Rate of convergence of CO time-of-sampling factor

As can be seen, the average error over the 24-hours in the time-of-sampling factor falls to below 5% within four days. Hence, as the error averaged over the complete day drops to zero quickly for the factors based on the measured concentration data, the time-of-day factors show potential to be calculated using a relatively short measurement period.

The rate of convergence of the time-of sampling factor calculated using the measured concentration data is not very sensitive to the order of days in the calculation. Regardless of the order of days, the percentage error falls to close to zero within a similar number of days. This is illustrated in Figure 6.21, in which the days are arranged in a random order, as opposed to the sequential order used in Figure 6.20.

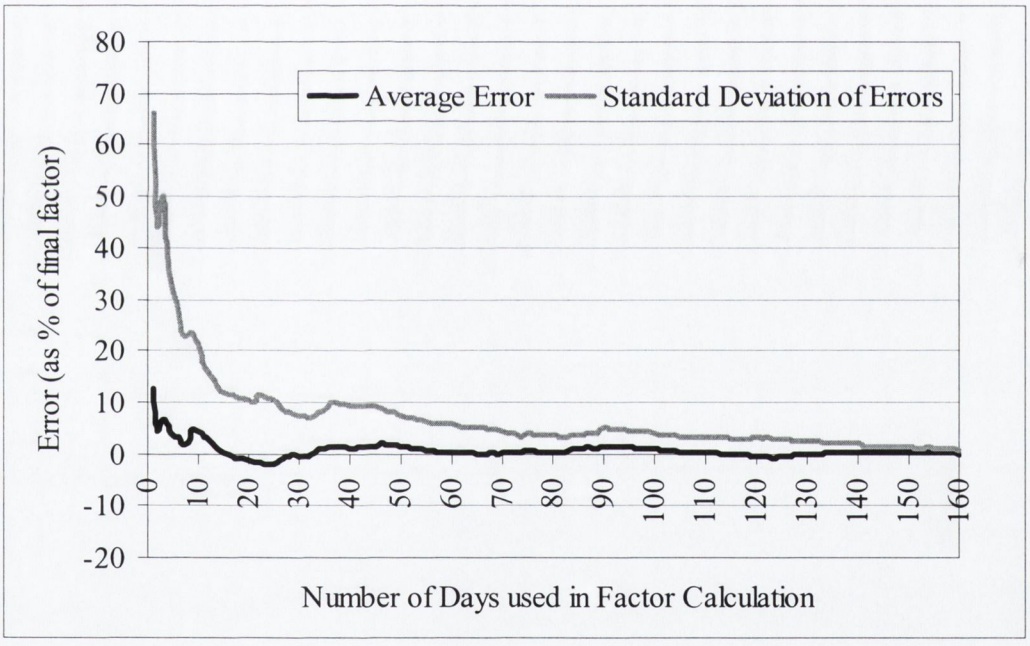

Figure 6.21 Sample rate of convergence of 'time-of-sampling' adjustment factors for CO, with days in random order.

Nitrogen Dioxide

As can be seen in Figure 6.22, the average error in the NO_2 time-of-sampling factor also converges to zero within several days.

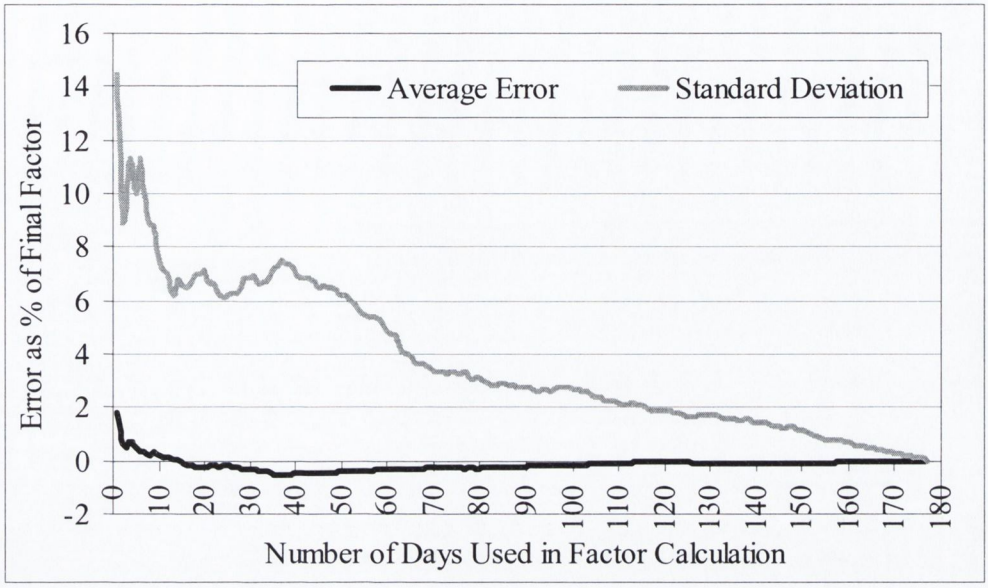

Figure 6.22 Rate of decrease in error for time-of-sampling adjustment factors for NO_2 with increasing numbers of days used in the calculation.

PM_{10}

As can be seen in Figure 6.23, the average error in the PM_{10} time-of-sampling factor for the measured concentration data also converges very quickly.

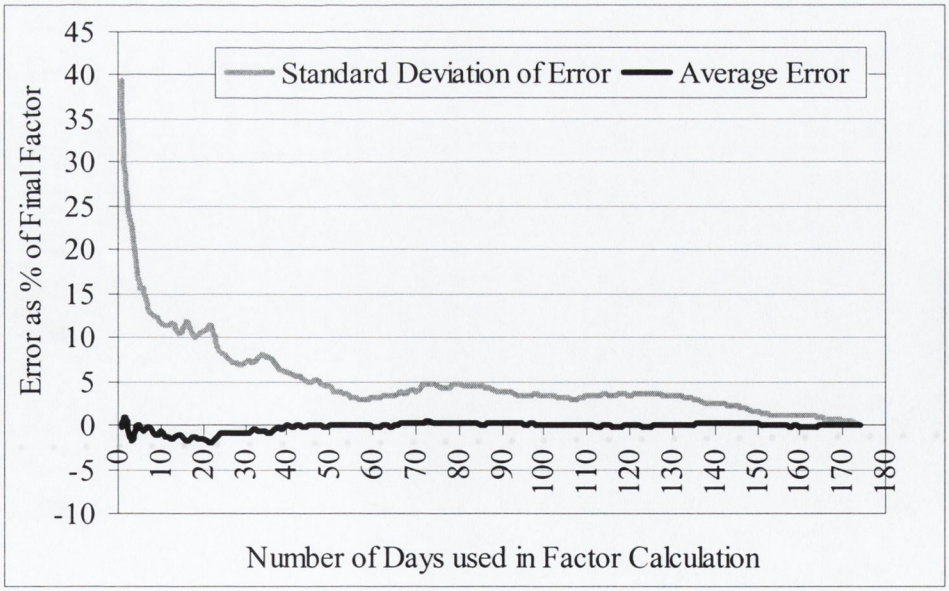

Figure 6.23 Rate of decrease in error for time-of-sampling adjustment factors for PM_{10} with increasing numbers of days used in the calculation.

6.11.2 Convergence of Wind Speed Factors

Carbon Monoxide

The decrease in CO concentrations with increased wind speed can be approximated as a power series, as already discussed (Section 5.3.1). To analyse the convergence of wind speed factors, different power series were calculated using varying sizes of data sets, from one month to eight months, giving eight different power series. (Several months were not included due to incomplete data collection). Figure 6.24 shows that each additional month results in only a small difference in the power series. This difference is evident mainly at low wind speeds.

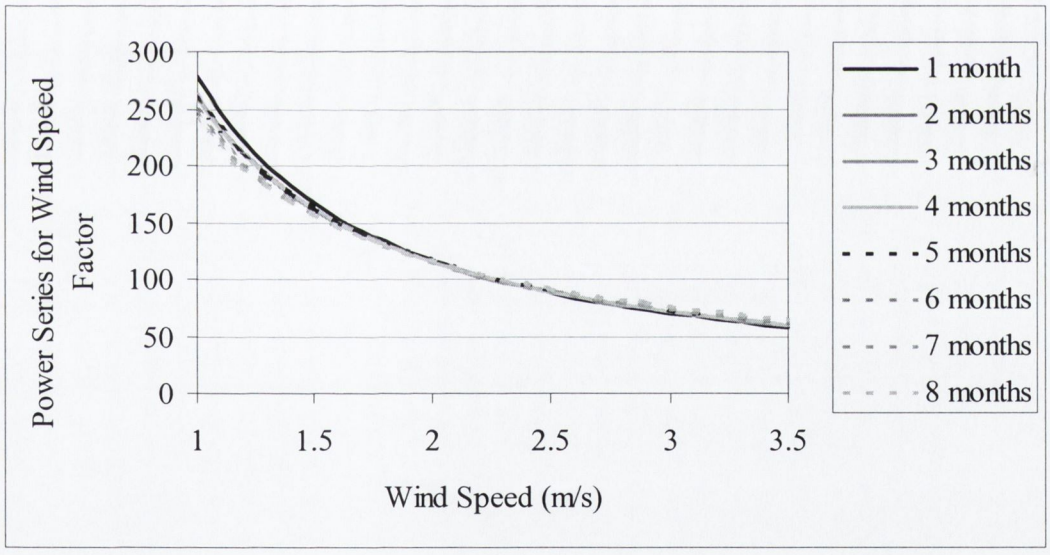

Figure 6.24 Wind speed factors for CO calculated using differing numbers of months

For each distinct power series calculated above, the magnitude of the error varies with the wind speed, so to quantify the average error, a range from 1 m/s to 3.5 m/s was chosen. The average error and the standard deviations of the errors within this range are expressed as a percentage of the final factor in Figure 6.25. As can be seen, the factors converge rapidly, with the standard deviation of the errors never larger than 8%.

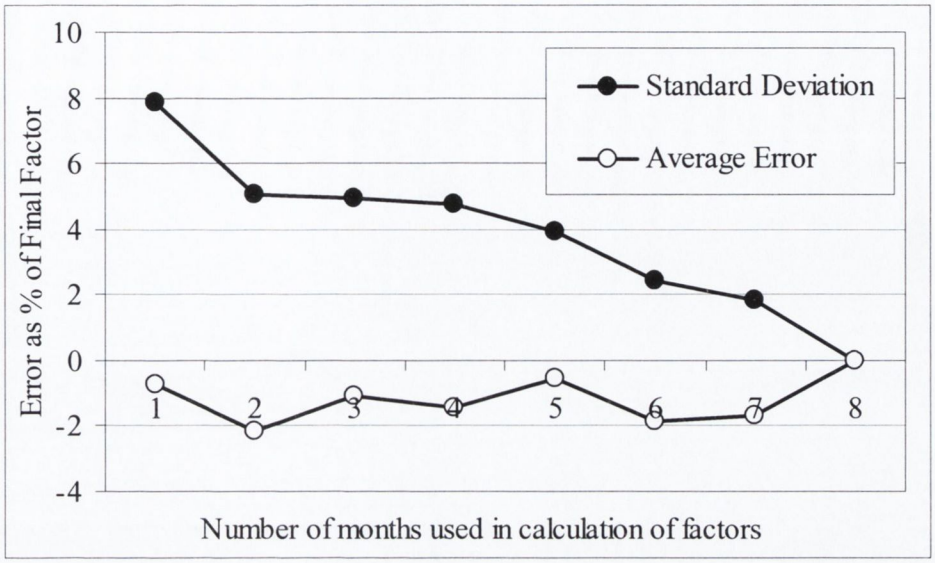

Figure 6.25 Average error in wind speed factors for CO with increasing numbers of months used in factor calculation.

Nitrogen Dioxide

As can be seen in Figure 6.26, the wind speed factors for NO_2 also converge on a stable value quickly, with the average error never exceeding 5%.

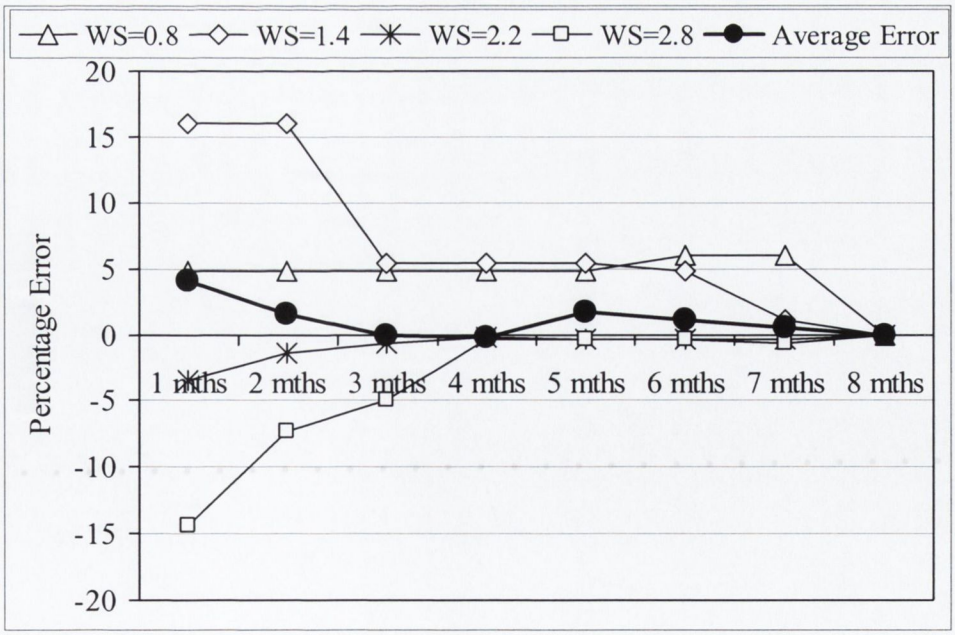

Figure 6.26 Decrease in percentage error of wind speed factors for NO_2 with increasing numbers of months used for calculation for average and sample wind speeds

PM_{10}

Figure 6.27 shows the wind speed factors from 1 m/s to 3.5 m/s, calculated using increasing monitoring periods, from 1 month to 8 months. The series of factors show good agreement with each other.

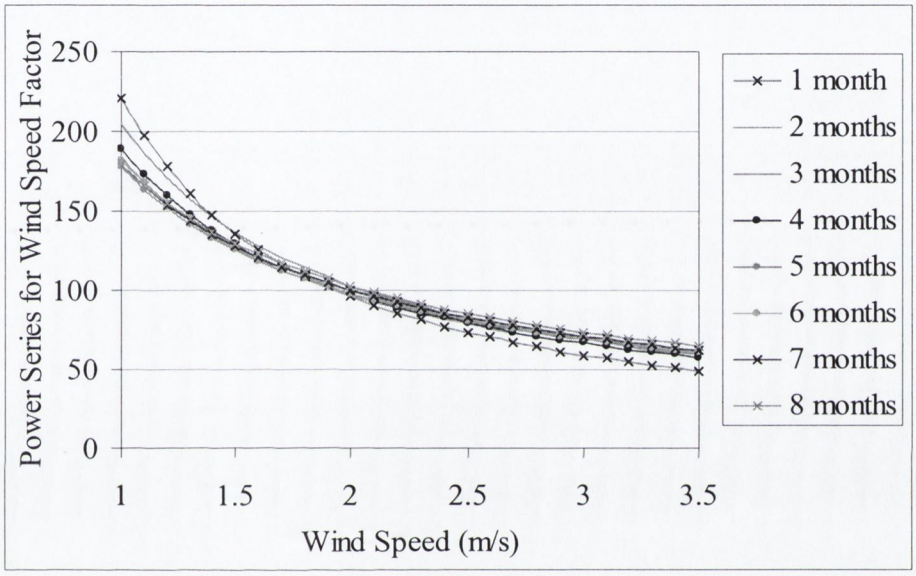

Figure 6.27 Wind speed factors for PM_{10} calculated using increasing numbers of months.

To quantify the average error, a range of 1 m/s to 3.5 m/s was again chosen. The average errors and standard deviations are graphed in Figure 6.28. As can be seen, even using one month for the calculation of the factors, the error is below 5%.

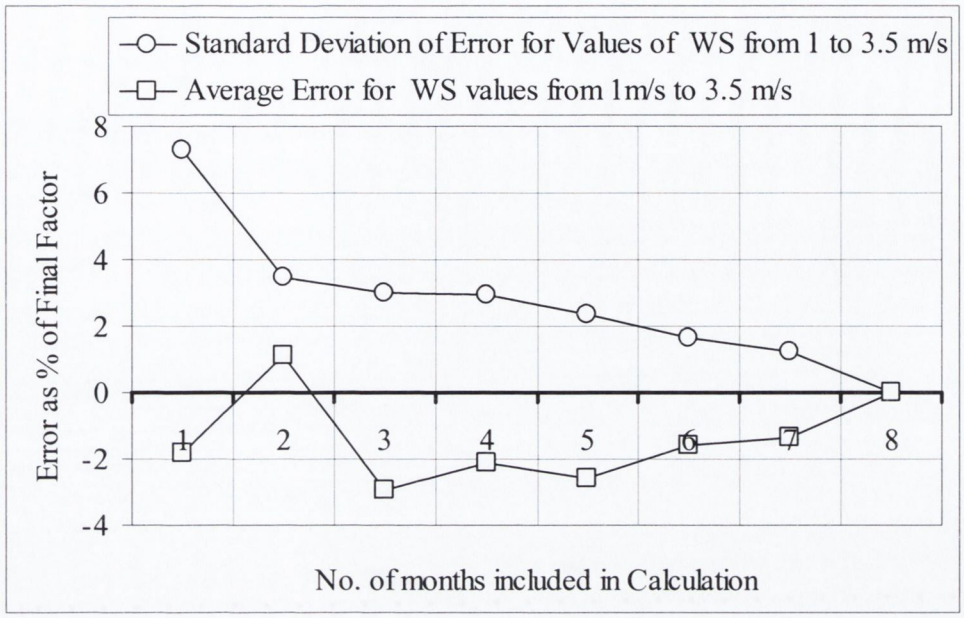

Figure 6.28 Average errors in wind speed factors for PM_{10} with increasing numbers of months used in factor calculation

6.11.3 Convergence of Wind Direction Factors

Carbon Monoxide

An analysis of the rate of convergence for wind direction factors is slightly more complex, as two separate sources of variation have to be combined. Errors could occur in calculating the ratio of measurements in each direction to the total number of measurements, and in expressing the concentration in that direction as a percentage of the mean. The magnitude of these errors will vary from direction to direction. As the ratio and concentration in each direction are multiplied and then summed (as described in Section 6.7), each error is expressed as a fractional error. The combined fractional error can then be calculated from the square root of the sum of the squares of the individual fractional errors, as described in Equation 6.13.

$$E = \sqrt{(e_1^2) + (e_2^2) + \ldots + (e_n^2)}$$ Equation 6.13

where

E is the total error;

e is the fractional error for each element of the calculation.

The calculated errors, as percentages of the final factor (calculated using all available data), are shown in Figure 6.29. As can be seen, the magnitude of the error term drops quickly, decreasing to less than 10% when more than one month of data are considered.

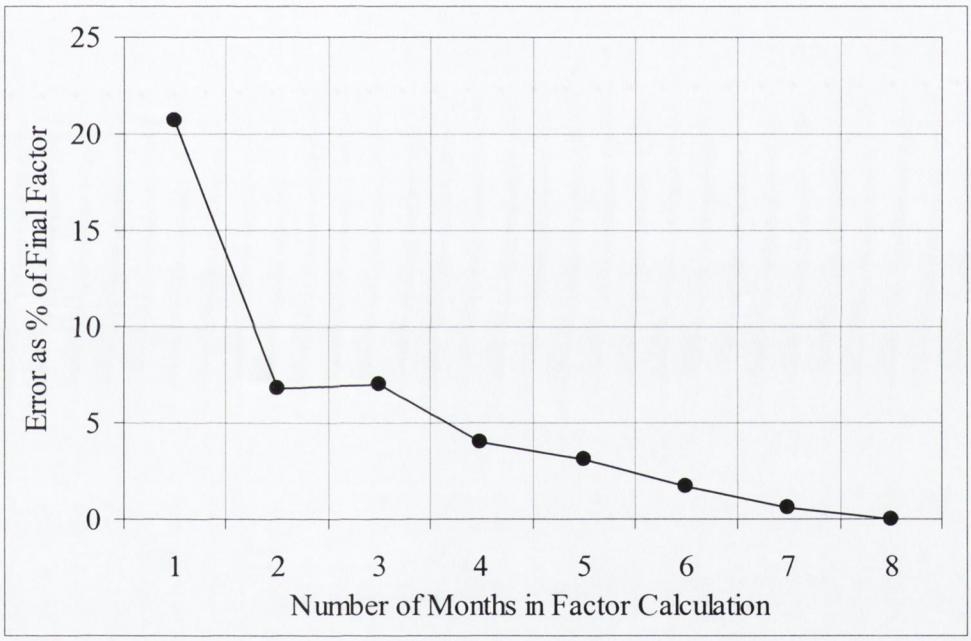

Figure 6.29 Error in wind direction factors for CO (as a percentage of final factor) with increasing numbers of months used in calculation of factors.

The sensitivity of the rate of convergence to the order of the months used in the calculations must also be considered. To this end, the same calculations, using increasing numbers of months, were carried out using 16 different arrangements of those months. The rate of convergence was seen to be comparable in each case. The maximum, minimum and average errors calculated from the 16 different arrangements of data are illustrated in Figure 6.30. The maximum error calculated for one month of data was 23%, although the average error was significantly smaller.

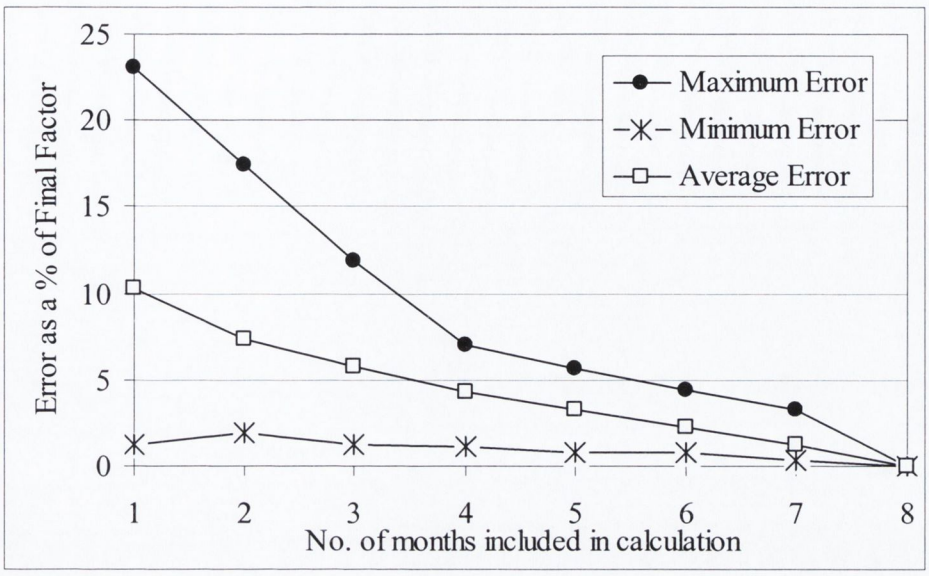

Figure 6.30 Maximum, minimum, and average errors in CO wind direction factors for 16 different arrangements of months with increasing numbers of months in calculation

Nitrogen Dioxide

The variation of the average percentage error in the NO_2 wind direction factors with length of monitoring period is shown in Figure 6.31. Errors, even using just one month of data, are under two percent (significantly less than for CO).

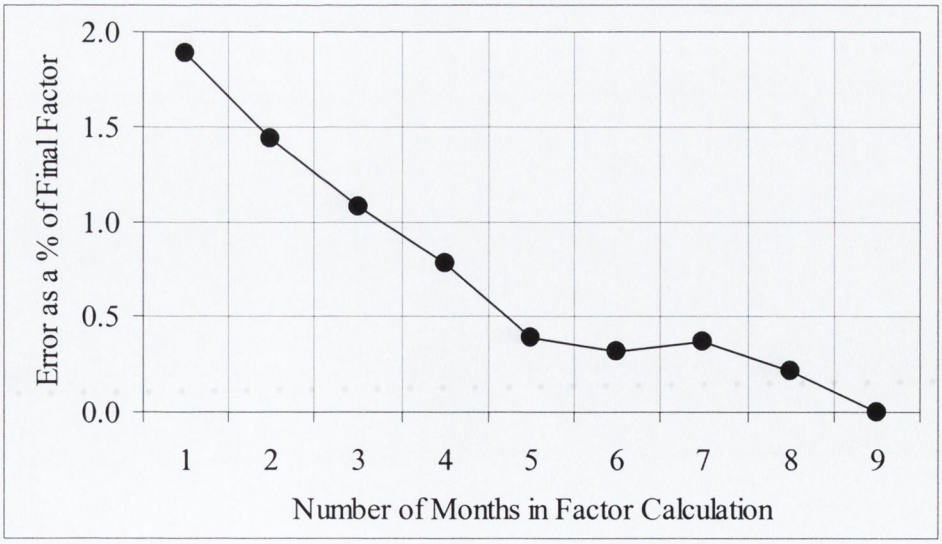

Figure 6.31 Error in wind direction factors for NO_2 (as a percentage of final factor) with increasing numbers of months used in calculation of factors.

As for CO, the sensitivity of the rate of convergence to the order of months used in the calculation was examined. Figure 6.32 shows the average, minimum and maximum errors calculated, using one month to eight months, for 16 different permutations of months. The largest error is exhibited by the calculation based on one month and ranges from just under 1.0% to just over 4.5%, dropping to close to 0% to 1% for calculations based on eight months.

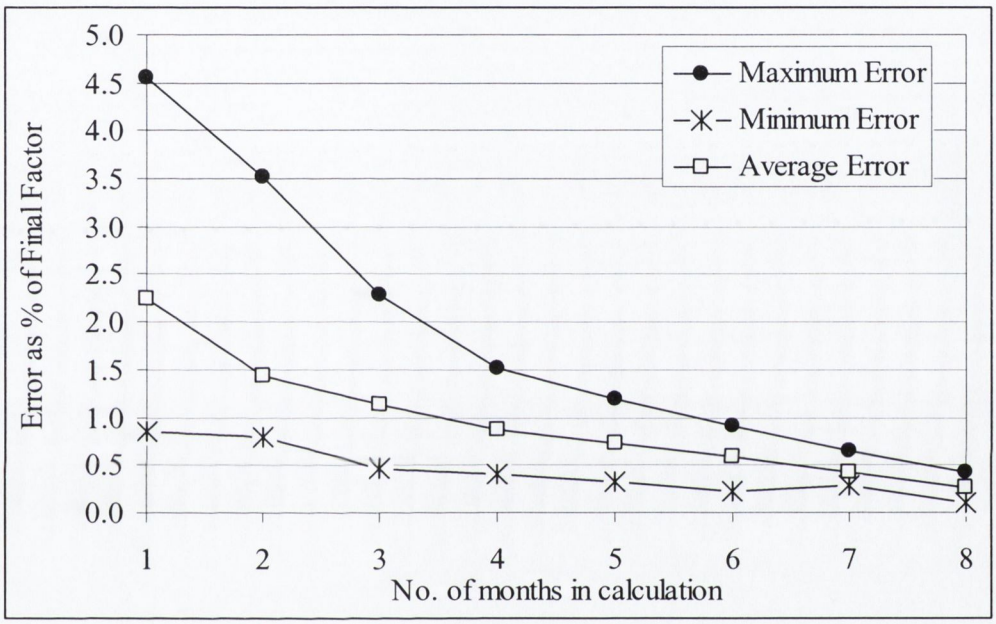

Figure 6.32 Maximum, minimum, and average errors in NO_2 wind direction factors for 16 different arrangements of months with increasing numbers of months in calculation

PM_{10}

The decrease in error in the wind direction adjustment factor with increasing numbers of months is shown in Figure 6.33. As for NO_2, even using just one month for the calculation of the wind direction factors results in a small error, in this case under 5%.

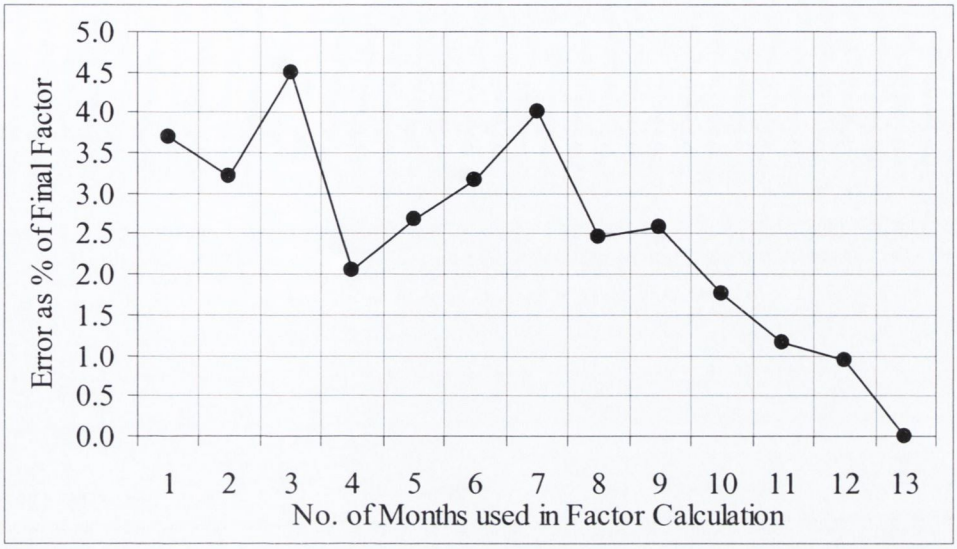

Figure 6.33 Error in wind direction factors for PM_{10} (as a percentage of final factor) with increasing numbers of months used in calculation of factors.

As before, the sensitivity of the rate of convergence to the order of months used in the calculation was examined. The maximum, minimum and average errors associated with the different numbers of months used in the calculation for all the permutations, are graphed in Figure 6.34. In no case is the error greater than 10%, and the average errors, even for factors based on one month of data, are significantly less than that.

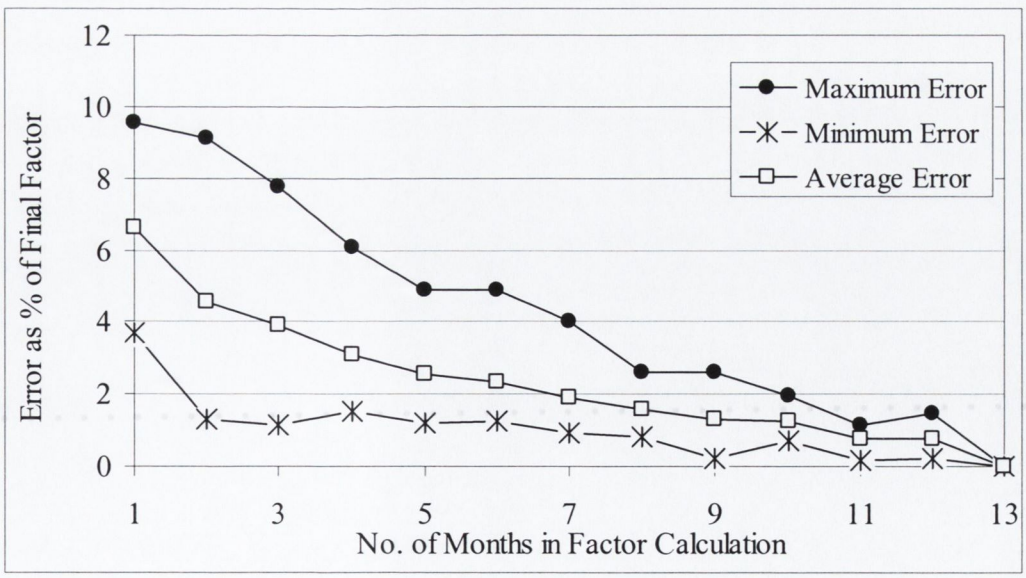

Figure 6.34 Maximum, minimum, and average errors in PM_{10} wind direction factors for 16 different arrangements of months with increasing numbers of months in calculation

6.11.4 Summary of Rates of Convergence of Factors

For the analysed concentration data, the convergence of the adjustment factors was found to be fast enough to allow factors to be calculated over a sufficiently short period to be of use in short-term monitoring programmes, with the error rapidly falling to below 5% rapidly in most cases. Combining these errors according to Equation 6.13, the total error in combining these factors should drop to less than 10% within one week.

6.12 Prediction of Extreme events

The population distribution function for each compound and selected averaging periods can be classified from a measured time series (as discussed in Section 4.3), and characterised using the mean and standard deviation. Using the prediction algorithm equations described in Section 6.3, the mean concentration can be estimated. Estimation of the population standard deviation is discussed in Section 6.12.1. The distribution function can then be used to provide information about pollution concentrations.

In this regard, a number of variables are of particular interest with respect to the characterisation of short-term concentrations at a monitoring site, such as:

- the highest (or, in general, the r-th highest) concentration in a finite sample of size m, where m is the number of 1-hour, 8-hour or 24-hour averaging periods over the period of interest;
- the number of exceedances of a given concentration level in a number of measurements taken within a given time period. This can be used to predict compliance or non-compliance with ambient air pollution legislation;
- the number of observations (waiting time or return period) between exceedances of a given concentration level.

6.12.1 Estimation of Population Variance and Standard Deviation

A point estimate of some parameter θ is a single number, calculated from sample data, that can be regarded as an educated guess for the value of θ. A point estimate is usually obtained by selecting a suitable statistic and calculating its value for the given sample data (Devore and Farnum, 1999).

If the population parameter is denoted generically by θ and any estimator of this parameter is denoted by $\hat{\theta}$ then $\hat{\theta}$ is an unbiased estimator if $\mu_{\hat{\theta}} = \mu_{\theta}$, where μ is the parameter mean. Otherwise, $\hat{\theta}$ is said to have a bias.

An estimator is said to be consistent if the probability that the estimator $\hat{\theta}$ falls close to the population parameter can be made as near to 1 as desired by increasing the sample size n.

The sample variance s^2 is an unbiased estimator of the population variance σ^2. However, the sample standard deviation s is a slightly biased estimator of the population standard deviation σ. For large samples this bias is negligible.

A point estimate, because it is a single number, provides no information about the precision and reliability of the estimate. For this reason, an interval estimate or confidence interval is of more use in attempting to estimate extreme concentrations.

Two methods were used to estimate the most likely value of standard deviation, as discussed below.

Estimation of the Population Standard Deviation: Method 1

The first method examined uses data from three entire monitoring days. If the sampling period during the three days is shorter than the averaging period under investigation, then method 2 below must be used.

In the first method the standard deviation is calculated using all the data collected during the three sampling days. Upper and lower bounds to this value are determined according to the number of time intervals taken into account, e.g., when calculating confidence intervals for standard deviations of 24-hour averages, a value of 3 would be used for n. For hourly and 8-hourly averages, the standard deviation should be calculated using a random sample of hourly values from the measured data. This is necessary because, as discussed in the next section, the use of the χ^2 distribution in the prediction of confidence intervals, requires that the variables are randomly selected.

Estimation of Population Standard Deviation: Method 2

The second method must be used when the monitoring periods are shorter than the averaging period of interest. For example, it is impossible to use the first method to estimate the standard deviation of the 24-hour averages, if monitoring was carried out over fewer hours. In this case a random sample of data from the week of monitoring used for the calculation of the adjustment factors is used to estimate the population standard deviation, in the manner discussed below.

6.12.2 Calculation of Confidence Intervals for Standard Deviation

As the standard deviation is proportional to the mean, the standard deviation of the data used to calculate the adjustment factors may not be representative of the standard deviation during the time period of interest. For example, if the concentrations measured during the period used for calculation of the adjustment factors are particularly low, then the standard deviation of these data will underestimate the standard deviation during periods with higher concentrations. For this reason, the standard deviation, and upper and lower bounds, of the initial monitoring period should be expressed as a percentage of the average concentration over that period. Then, from the predicted monthly average, the standard deviations and the upper and lower bounds of the population under consideration can be estimated.

Once the monthly average has been predicted using the equations in Section 6.3 and the point estimate of the standard deviation calculated, as described in Section 6.12.1, then confidence intervals for the standard deviation can be calculated. This provides the upper and lower bounds of short-term concentration predictions.

Let C be a normal random variable with mean *m* and variance s^2. From this population, a sample $C_1, C_2, \ldots, C_n$ of size n is taken. Let $\overline{C}$ be the sample mean and let S^2 be the sample variance. The following distribution is used to calculate a confidence interval for S^2 (the sample variance).

$$U = (n-1)\frac{S^2}{\sigma^2} \qquad \text{Equation 6.14}$$

(Rohatgi, 1984)

The distribution of U is known as the χ^2 distribution with n-1 degrees of freedom. Some of the useful properties of a χ^2 random variable are given below:

- The χ^2 random variables are all continuous random variables.
- A χ^2 random variable is always nonnegative.
- The graph of the probability density function of a χ^2 random variable is skewed to the right.
- If U is χ^2_v random variable then U has *v* degrees of freedom.
- For a number $0 < \alpha < 1$ and any positive integer *v*, we define a number $\chi^2_{v,\alpha}$ by the equation

$$P(U > \chi^2_{v,\alpha}) = \alpha \qquad \text{Equation 6.15}$$

(where P signifies probability)

where U has χ^2 distribution with degrees of freedom *v* (Rohatgi, 1984).

Therefore, from Equation 6.15,

$$P\left(\chi^2_{n-1,1-\alpha/2} < (n-1)S^2/\sigma^2 < \chi^2_{n-1,\alpha/2}\right) = 1-\alpha \qquad \text{Equation 6.16}$$

Equation 6.16 can be simplified to:

$P(L < \sigma^2 < U) = 1 - \alpha$ Equation 6.17

where

$L = (n-1)S^2/\chi^2_{n-1,\alpha/2}$

$U = (n-1)S^2/\chi^2_{n-1,1-\alpha/2}$

(Rohatgi, 1984)

As before, a $(1-\alpha)100$ percent confidence interval for the variance σ^2 is given by

$l < \sigma^2 < u$ Equation 6.18

where

$L = (n-1)s^2/\chi^2_{n-1,\alpha/2}$

$U = (n-1)s^2/\chi^2_{n-1,1-\alpha/2}$

or

$$\frac{(n-1)s^2}{\chi^2_{n-1,[\alpha/2]}} < \sigma^2 < \frac{(n-1)s^2}{\chi^2_{n-1,1-[\alpha/2]}}$$ Equation 6.19

(Rohatgi, 1984)

Taking the square root of the variance to calculate the standard deviation gives Equation 6.20 for the confidence intervals of the population standard deviation.

$$\sqrt{\frac{(n-1)s^2}{\chi^2_{n-1,[\alpha/2]}}} < \sigma < \sqrt{\frac{(n-1)s^2}{\chi^2_{n-1,1-[\alpha/2]}}}$$ Equation 6.20

where

n is the number of samples

s^2 is the sample variance

χ^2 is obtained from chi-squared tables

Using Equation 6.19, the confidence intervals for the population standard deviation can be calculated from the point estimate and sample size. In Sections 6.12.4 and 6.12.5, a method for using the estimated standard deviation in conjunction with the distribution function and predicted mean to estimate the extreme events is outlined.

6.12.3 Terminology

Air quality data are often available as sets of successive observations of concentrations measured sequentially in time, at some specific location, and averaged over successive equal non-overlapping time periods. These data form statistical time series of the discrete form:

$x_\tau(t_1), x_\tau(t_2), \ldots, x_\tau(t_n); \qquad t_1 < t_2 < \ldots t_n$

where $\tau = t_2-t_1=t_3-t_2=\ldots=t_n-t_{n-1}$ is the averaging time, and t_1 is the index for the time period arbitrarily set equal to the beginning of the period.

Consider the sample of m random unordered variates, $c_\tau(t_1), c_\tau(t_2),\ldots,c_\tau(t_m)$, taken from the population $x_\tau(t_1),\ldots, x_\tau(t_n)$ of available air quality data (c_τ is a subsection of x_τ). If this time series $\{x_\tau(t_i)\}$ is arranged in increasing order of magnitude, $x_{1;m} \geq x_{2;m} \ldots \geq x_{m;m}$, then a 'new' random sequence of ordered variates $c_{1;m} \geq c_{2;m} \ldots \geq c_{m;m}$, is formed, in which $c_{i;m}$ is the i-th highest order statistic or i-th extreme statistic.

The following assumptions are made:

- The concentration levels $x_\tau(t_i)$ are measured in successive, non-overlapping periods – and hence the unordered random variates $c_\tau(t_i)$ are independent of one another;
- The random variables $c_\tau(t_i)$ are identically distributed;
- The distribution function, $F(x)$, as well as the probability density function, $p(x)$, corresponding to the total number of available measurements, are known. They are called the parent (or initial) distribution and pdf respectively (Georgopoulos and Seinfeld, 1982).

6.12.4 Exceedances of Critical Levels

The probability that a particular concentration level, x, will be exceeded in a single observation is given by the complementary distribution function, $\overline{F}(x)$.

$$\overline{F}(x) = \text{Prob}\{c > x\} = 1 - F(x) \qquad \text{Equation 6.21}$$

where

$$F(x) = \text{Prob}\{c \leq x\}$$

The larger the concentration, x, the smaller is the complementary function. In other words, the higher the concentration, the smaller the probability that it will be exceeded in a single observation.

The number of exceedances, $N_x(m)$, of a given time-averaged, concentration level x_τ in a set of m successive observations (or averaging periods), $x_\tau(t_i)$, is itself a random function. Similarly, the number of averaging periods (or observations) between exceedances of the concentration level x_τ is another random function (the waiting time, or return time) of interest (Georgopoulos and Seinfeld, 1982).

In the case of independent, identically distributed variables, each one of the observations is a Bernoulli trial (outcome is either success or failure). Therefore the probability density function of $N_x(m)$ is, in terms of the parent distribution F(x):

$$\phi(N_x; m, x) = \left(\frac{m}{N_x}\right)\left[1 - F(x)\right]^{N_X} \times \left[F(x)\right]^{m - N_X} \qquad \text{Equation 6.22}$$

From Equation 6.22, it may be concluded that the expected number of exceedances, $E\{N_x(m)\}$, of the level x in a sample of m measurements is the following function of m:

$$\overline{N}_x(m) = E\left\{N_x(m)\right\} = m\left[1 - F(x)\right] = m\overline{F}(x) \qquad \text{Equation 6.23}$$

(Georgopoulos and Seinfeld, 1982)

(For clarity of the notation the subscript τ is left out, although all concentrations are based on a fixed averaging period). This allows the number of exceedences of a reference concentration to be predicted once the distribution function has been identified and characterised.

From the theory of order statistics comes a distribution free result concerning the distribution of exceedences (Georgopoulos and Seinfeld, 1982). The probability that n observations of a random variable X will result in N^*_r values of X that exceed the r-th highest value of m initial observations (and is independent of the r-th highest value and the form of the distribution of X) is:

$$\phi\left(N_r^*;r,m,n\right)=\frac{\binom{m}{r}r\binom{n}{N_r^*}}{(n+m)\binom{n+m-1}{N_r^*+r-1}} \qquad \text{Equation 6.24}$$

where

$$\sum_{N_r^*=0}^{n}\phi\left(N_r^*;r,m,n\right)=1 \qquad \text{Equation 6.25}$$

(Georgopoulos and Seinfeld, 1982)

Thus, for example, the probability of at least one exceedance of $c_{r;m}$ is:

$$\text{Prob}\left\{N_r^*\geq 1\right\}=1-\phi(0;r,m,n)=1-\frac{m!(m+m-r)}{(m-r)!(n+m)!} \qquad \text{Equation 6.26}$$

For r = 1 (the maximum concentration) the following equation is obtained:

$$\text{Prob}\left\{N_r^*\geq 1\right\}=\frac{n}{m+n} \qquad \text{Equation 6.27}$$

(Georgopoulos and Seinfeld, 1982)

Hence, if n = m, a probability if 0.5 is calculated. Equation 6.27 implies that as n (the number of successive averaging periods) increases with respect to m, the probability that the initial

maximum concentration (taken from m, the initial number of averaging periods) will be exceeded also increases (Georgopoulos and Seinfeld, 1982).

For example, the probability that the highest hourly concentration measured in one week (m = 168) will be exceeded in the following 3 weeks (n = 504) is 504/(168+504) or 0.75.

6.12.5 Expected Return Period or Waiting Time

The expected return period is defined as the average number of averaging periods (or observations) between exceedances of a given level, x. This level, x, must be calculated over the fixed average time τ.

The probability that the concentration will exceed x for the first time at observation n is:

$$f_n = \text{Prob}\{c \le x\}^{n-1}\ \text{Prob}\{c > x\} = [F(x)]^{n-1}[1 - F(x)] \qquad \text{Equation 6.28}$$

(Georgopoulos and Seinfeld, 1982)

By definition:

$$\text{E}\{n\} = \sum_{n=1}^{\infty} n f_n \qquad \text{Equation 6.29}$$

Using Equation 6.28 and Equation 6.29, the following equation is obtained:

$$\text{E}\{n\} = \sum_{n=1}^{\infty} n[F(x)]^{n-1}[1 - F(x)] = [1 - F(x)]\sum_{n=1}^{\infty} n[F(x)]^{n-1} \qquad \text{Equation 6.30}$$

(Georgopoulos and Seinfeld, 1982)

Since F(x) < 1, the following equation can be written

$$\sum_{n=1}^{\infty} n[F(x)]^{n-1} = 1 + 2F + 3F^2 + \ldots = \frac{1}{[1 - F(x)^2]} \qquad \text{Equation 6.31}$$

(Georgopoulos and Seinfeld, 1982)

Combining Equation 6.30 and Equation 6.31, the following equation for the waiting period is obtained

$$\mathrm{E}\{n\}\frac{1}{1-F(x)} = \left[\overline{F}(x)\right]^{-1} \qquad \text{Equation 6.32}$$

In other words, the waiting period to record a concentration 'x', is the inverse complementary distribution function evaluated at x (Georgopoulos and Seinfeld, 1982).

6.13 CONCLUSIONS

In this chapter, the formulation of a methodology for predicting monthly concentration averages based on short-term monitoring was described. The methodology was introduced in Sections 6.1 and 6.2. The algorithm equations are described in Section 6.3. The calculation of the required adjustment factors was described in Sections 6.4 to 6.10. The rates of convergence of these factors were calculated and discussed in Section 6.11. For the measured concentration data, the adjustment factors were found to be converge swiftly. This would indicate that the factors can potentially be calculated over a sufficiently short period to be of use in short-term monitoring programmes. A methodology for predicting 1-hour, 8-hour and 24-hour concentrations using the theoretical frequency distribution, and the estimated standard deviation combined with either the predicted monthly average or a long-term average measured with a diffusion tube or other passive sampling techniques, was then discussed in Section 6.12.

This model can be used to characterise air quality at a site using a shorter period of data than would otherwise be needed. One week of monitoring can be used to estimate adjustment factors and standard deviations, followed by three (full or partial) days each month, for the estimation of the monthly average and frequency distribution. It is not necessary for this week of monitoring to take place before the three indicative days of monitoring. Passive sampling can be used to measure the monthly average cost effectively and this eliminates the prediction of the mean as a source of error, resulting in a higher level of accuracy in the prediction of the short-term peak concentrations. In practice, an efficient monitoring strategy would be the use

of two sets of equipment operating simultaneously, one monitoring for the determination of the adjustment factors, and the other monitoring at a number of sites in rotation collecting data to be used in the prediction of monthly average and peak concentrations.

7. ALGORITHM EVALUATION AND VERIFICATION

In this chapter, the effectiveness and accuracy of the prediction algorithm developed in Chapter 6 are evaluated by predicting 30-day averages and peak short-term concentrations measured at the Pearse Street/Westland Row Junction.

Thirty-day average concentrations of CO, NO_2 and PM_{10} are predicted for Phases 1 and 2, based on short-term monitoring over a range of periods. The required adjustment factors are calculated from the monitoring data collected during Phase 1. These average values are then used to predict short-term peak values.

In Sections 7.1, 7.3, 7.4, and 7.5, the application of the prediction algorithm to Phase 1 of the monitoring at Site 1 (Pearse Street/Westland Row Intersection) is discussed. Predictions of monthly averages based on three days of monitoring during the month are compared to estimates calculated using the unadjusted data. Monitoring periods shorter than 24 hours (office hours, and a single hour of data at peak, off-peak and shoulder periods) are also used to predict the monthly average, and the results evaluated. In Section 7.6, the prediction of exceedences of limit values, as defined under Framework Directive 96/62/EC, is discussed. Section 7.2 compares measured and predicted pollutant monthly averages using data monitored during specific meteorological conditions. The prediction of monthly averages and short-term peaks in Phase 1 are summarised in Section 7.8.

In Sections 7.9, 7.10, and 7.11, this analysis is repeated for Phase 2 of monitoring, at the same site, but with the equations and factors based on the data collected during Phase 1, thereby investigating the reproducibilty of the results over time. Following this presentation of results, conclusions and a summary of the findings are presented in Section 7.12.

The sequence of prediction calculations is illustrated schematically in Figure 7.1.

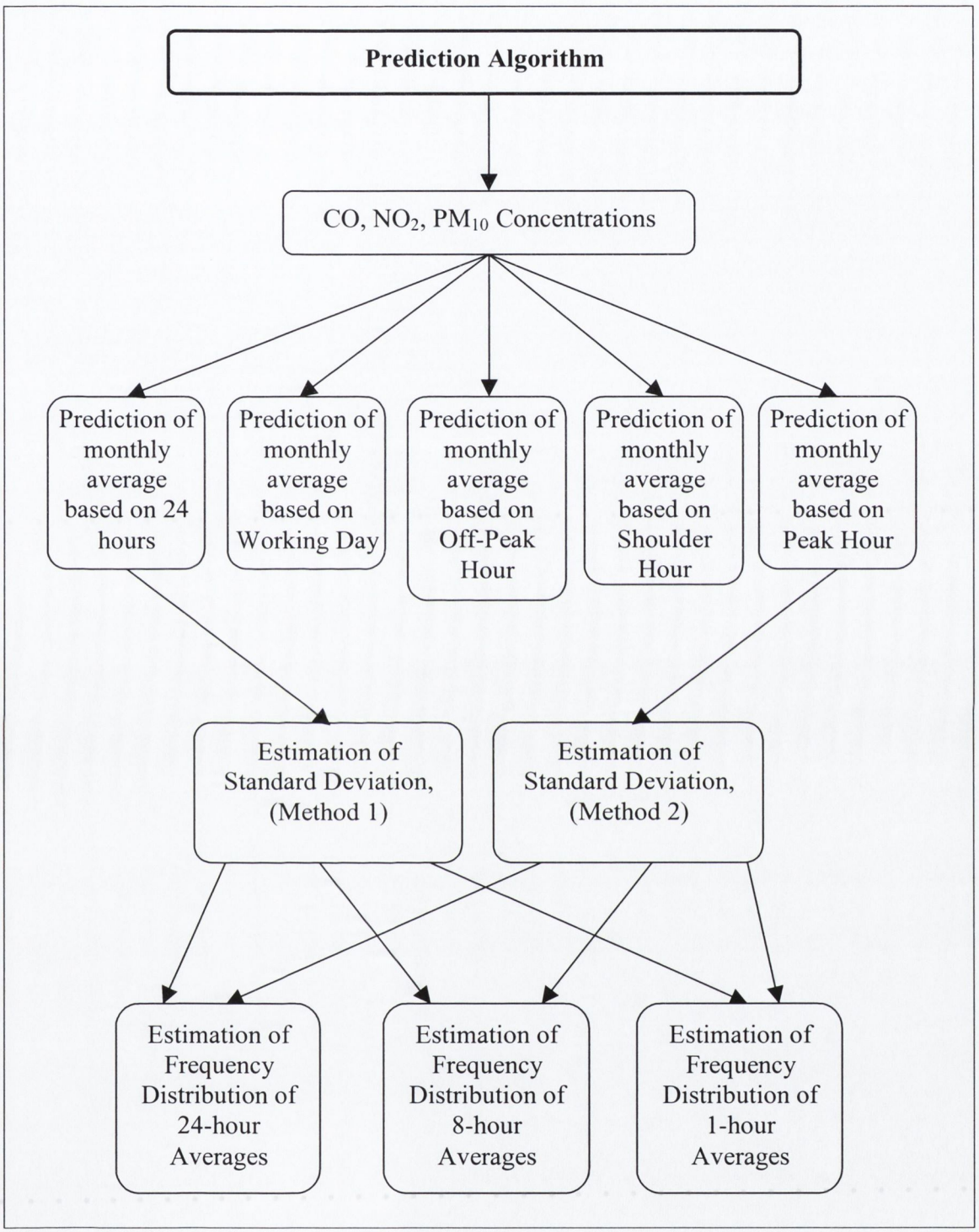

Figure 7.1 Schematic diagram of the calculations carried out in Chapter 7

The terminology used in this chapter is listed in Table 7.1 and defined in Equation 7.1 and Equation 7.2.

Table 7.1 Terminology for the evaluation of the prediction algorithm

r	Pearson's correlation coefficient. As already described in Equation 5.1, this describes how strongly the x and y values in a sample of pairs are related to one another.
R^2	Coefficient of determination, where (correlation coefficient)^2 = (coefficient of determination). This gives the proportion of variation that is attributable to the linear relationship between the two variables, as described in Appendix A.
MAE	Mean absolute error
σ_{MAE}	Standard deviation of the mean absolute error
RMSE	Root mean squared error
σ_{RMSE}	Standard deviation of the root mean square error

where

$$MAE = \frac{(|e_1| + |e_2| + ... + |e_n|)}{n} \qquad \text{Equation 7.1}$$

$$RMSE = \left(\frac{\sqrt{e_1^2 + e_2^2 + ...e_n^2}}{n} \right) \qquad \text{Equation 7.2}$$

where

e_i = error in a single concentration prediction

n = number of concentration predictions.

7.1 Prediction of Monthly Averages – Site A (Pearse Street/Westland Row Intersection) Phase 1

For each 30-day period, the average concentration is calculated. Using the algorithm discussed in Chapter 6, data from three separate monitoring days are used to estimate the monthly average. In each case, one of the monitoring days is at the beginning of the month (close to the 5th), one from the middle (close to the 15th), and one from the end (close to the 25th).

In practice, the collection of data for periods shorter than 24 hours is easier than full 24-hour monitoring, which would require a permanent or semi-permanent monitoring site. Such sites

require secure, air-conditioned rooms with power supply to house the instruments, and these constraints and the associated costs reduce the number of possible sites. In contrast, short-term monitoring at a site (in the order of hours) can be carried out with less preparatory work, using portable equipment. To investigate the usefulness and degree of accuracy that can be obtained using shorter monitoring periods, a range of sampling times were chosen as input for the prediction algorithm. The monitoring periods used are:

- 24 hours,
- 10:00 – 16:00,
- 10:00 – 11:00,
- 13:00 – 14:00,
- 17:00 – 18:00.

The period 10:00 – 16:00 was chosen to represent the working day, allowing time to get to and from the monitoring site within working hours. The period 10:00–11:00 was chosen to investigate the effect of inputting data from shoulder hours (neither peak nor off-peak) into the algorithm. The periods 17:00–18:00 and 13:00–14:00 represent peak and off-peak hours, respectively.

7.1.1 Carbon Monoxide

Monitoring 24 hours Each Day

The predictions throughout Chapters 7 and 8 are based on three days of monitoring data, obtained at intervals throughout the month. Table 7.2 summarises the results of the prediction based on 24 hours of monitoring data for each day. Three methods of prediction are compared: the arithmetic average of the measured data, the standard algorithm result employing the adjustment factors discussed in Chapter 6, and the algorithm result including a correction for average monthly wind speed. Pearson's r is the correlation coefficient calculated using Equation 5.1, and the MAE and RMSE are calculated using Equation 7.1 and Equation 7.2, respectively. Both the MAE and RMSE are expressions of the average error,

which cannot be calculated directly, as positive and negative values would cancel out. By definition, ninety-five per cent of the errors should be within MAE or RMSE ± 2(σ_{MAE} or σ_{RMSE}). From Table 7.2, the arithmetic average appears marginally more accurate than the algorithm result, if no correction is made for average monthly wind speed. However, when this correction is applied, the predictions are significantly more accurate than those obtained with the arithmetic average, as can be seen in the scatter graph in Figure 7.2, where wind speed is abbreviated to WS.

Table 7.2 Prediction of 30-day average CO concentrations calculated using three days of 24-hour monitoring

	Arithmetic Average	**Prediction**	**Prediction with Correction for Monthly Wind Speed**
Pearson's r	0.92	0.91	0.99
RMSE (%)	28.48	29.15	11.07
σ_{RMSE}(%)	33.72	27.06	13.82
MAE(%)	23.23	25.40	8.54
σ_{MAE}(%)	16.55	14.35	7.07

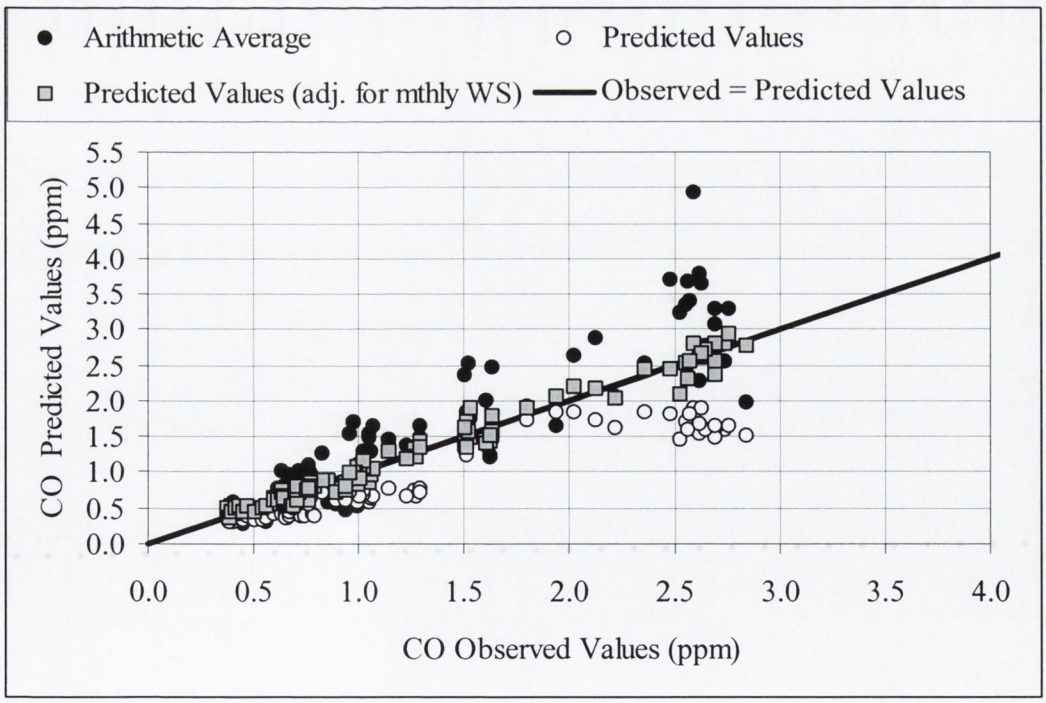

Figure 7.2 Graph of predicted and observed 30-day CO average concentrations (predictions calculated using 24-hour monitoring periods)

Monitoring 10:00–16:00 Each Day

The above predictions are repeated, assuming a reduced monitoring period of 10:00-16:00 only, on each of the three monitoring days. The results are shown in Table 7.3. Again, the prediction adjusted for average monthly wind speed performs best. In this case, however, the predicted value (unadjusted for average wind speed) outperforms the arithmetic average with respect to the average errors, although the correlation coefficients for both are the same. Predicted concentrations are plotted against observed 30-day averages in Figure 7.3. The values calculated using the prediction algorithm are again seen to follow the line of unity more closely than the arithmetic averages.

Table 7.3 Prediction of 30-day average CO concentrations calculated using three days of monitoring between 10:00 and 16:00

	Arithmetic Average	**Prediction**	**Prediction with Correction for Monthly Wind Speed**
Pearson's r	0.89	0.89	0.97
RMSE (%)	37.43	30.44	19.54
σ_{RMSE} (%)	48.81	30.80	25.03
MAE (%)	28.76	26.15	15.10
σ_{MAE} (%)	24.05	15.64	12.45

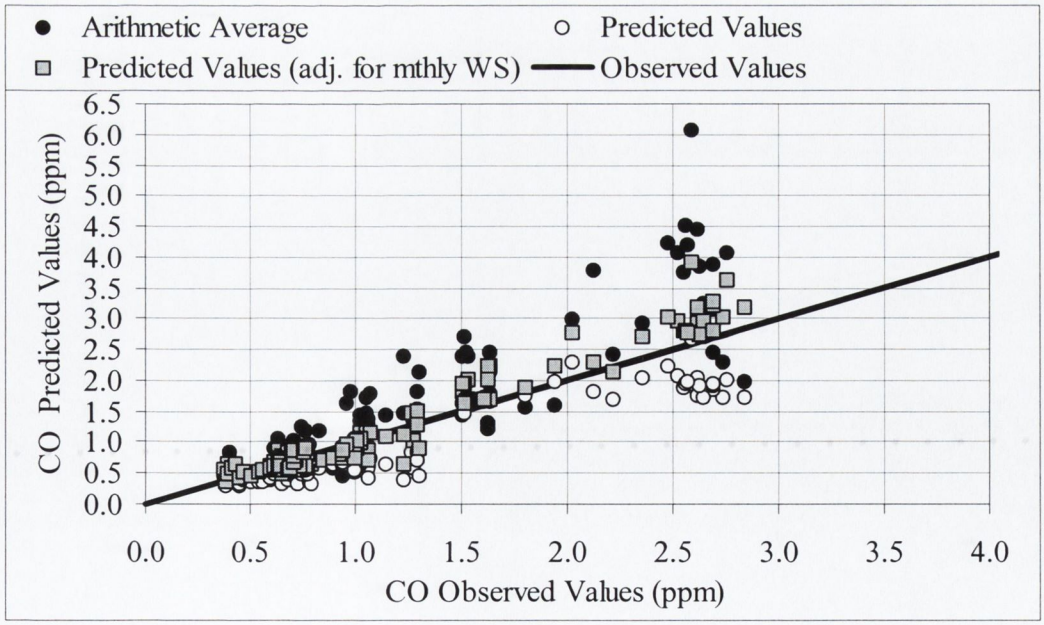

Figure 7.3 Graph of predicted and observed 30-day CO average concentrations (predictions calculated using monitoring periods from 10:00 to 16:00)

Monitoring 10:00–11:00 Each Day

The difference in accuracy between the arithmetic average and the algorithm prediction is more marked with this shorter averaging period (Table 7.4). The RMSE of the algorithm predictions, either with or without the monthly wind direction adjustment, is approximately half that of the arithmetic averages. This improvement is noticeable in the scatter chart of Figure 7.4. The predicted and observed values agree reasonable well at lower concentrations, but there is proportionately greater scatter at higher concentrations.

Table 7.4 Prediction of 30-day average CO concentrations calculated using three days of monitoring between 10:00 and 11:00

	Arithmetic Average	**Prediction**	**Prediction with Correction for Monthly Wind Speed**
Pearson's r	0.75	0.88	0.89
RMSE (%)	65.81	33.97	27.87
σ_{RMSE} (%)	110.43	32.53	46.50
MAE (%)	44.05	29.44	19.42
σ_{MAE} (%)	49.08	17.02	20.06

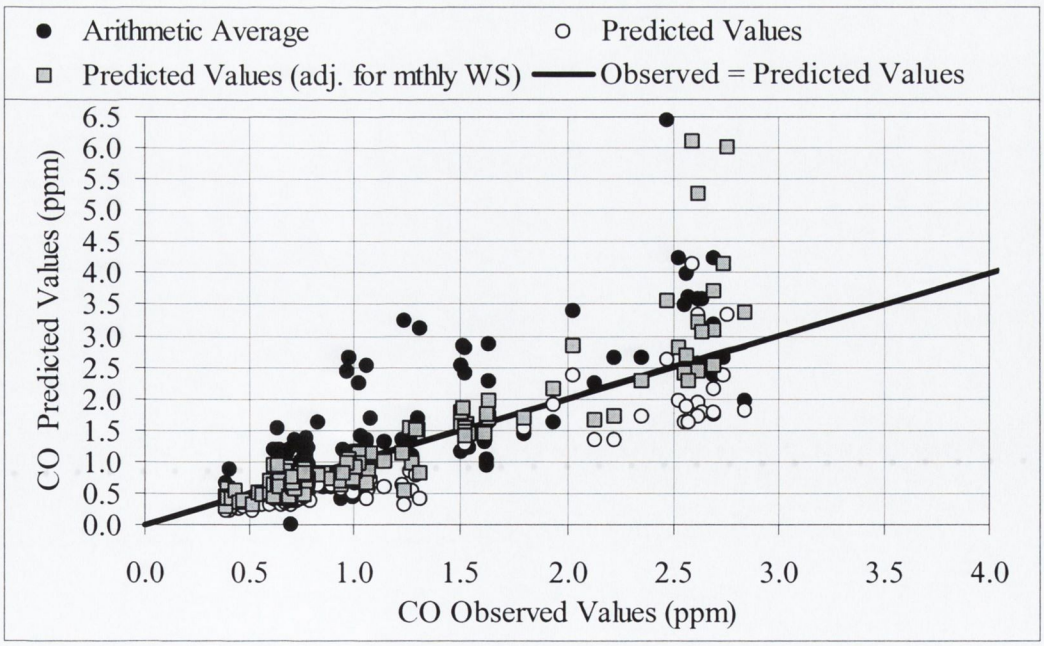

Figure 7.4 Graph of predicted and observed 30-day CO average concentrations (predictions calculated using monitoring periods from 10:00 to 11:00)

Monitoring 13:00–14:00 Each Day

Table 7.5 details statistics calculated for predictions based on monitoring between 13:00 and 14:00 only. Correlations between the predicted values and the observed values are strong, with the predicted values matching the observed values more closely than the arithmetic averages when the monthly wind speed correction is applied. The arithmetic averages match the observed 30-day average values more closely than when the 10:00 to 11:00 monitoring period is employed. The results are illustrated graphically in Figure 7.5.

Table 7.5 Prediction of 30-day average CO concentrations calculated using three days of monitoring between 13:00 and 14:00

	Arithmetic Average	**Prediction**	**Prediction with Correction for Monthly Wind Speed**
Pearson's r	0.86	0.82	0.95
RMSE (%)	38.85	32.13	23.62
σ_{RMSE} (%)	46.48	32.45	31.86
MAE (%)	32.01	27.83	16.99
σ_{MAE} (%)	22.09	16.12	16.48

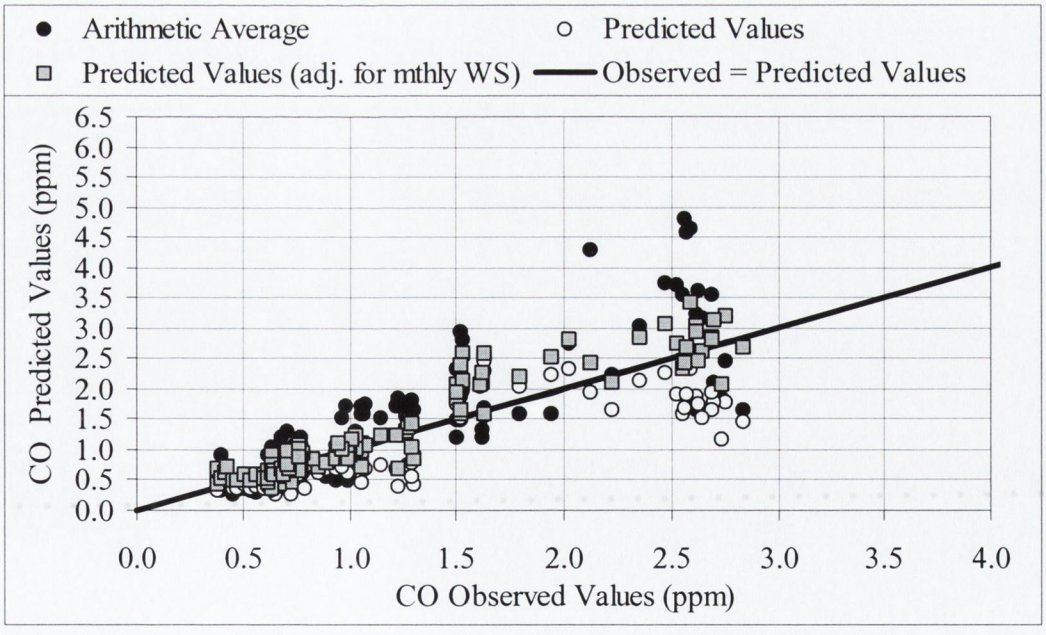

Figure 7.5 Graph of predicted and observed 30-day CO average concentrations (predictions calculated using monitoring periods from 13:00 to 14:00)

Monitoring 17:00–18:00 Each Day

Predictions calculated using data recorded between 17:00 and 18:00, only, are evaluated in Table 7.6. Correlations between the predicted values and the observed values are strong, and the errors of a similar magnitude to those observed using the 10:00-11:00 and 13:00-14:00 sampling periods. In contrast, the arithmetic average significantly overestimates the 30-day average concentration, with the RMSE calculated as 141.32% and the MAE as 112.61%. Figure 7.6 highlights the manner in which the arithmetic average overestimates the monthly average in comparison to the values calculated using the prediction algorithm.

Table 7.6 Prediction of 30-day average CO concentrations calculated using three days of monitoring between 17:00 and 18:00

	Arithmetic Average	**Prediction**	**Prediction with Correction for Monthly Wind Speed**
Pearson's r	0.89	0.90	0.96
RMSE (%)	141.32	32.80	24.67
σ_{RMSE} (%)	166.49	31.01	26.03
MAE (%)	112.61	28.74	20.71
σ_{MAE} (%)	85.74	15.89	13.47

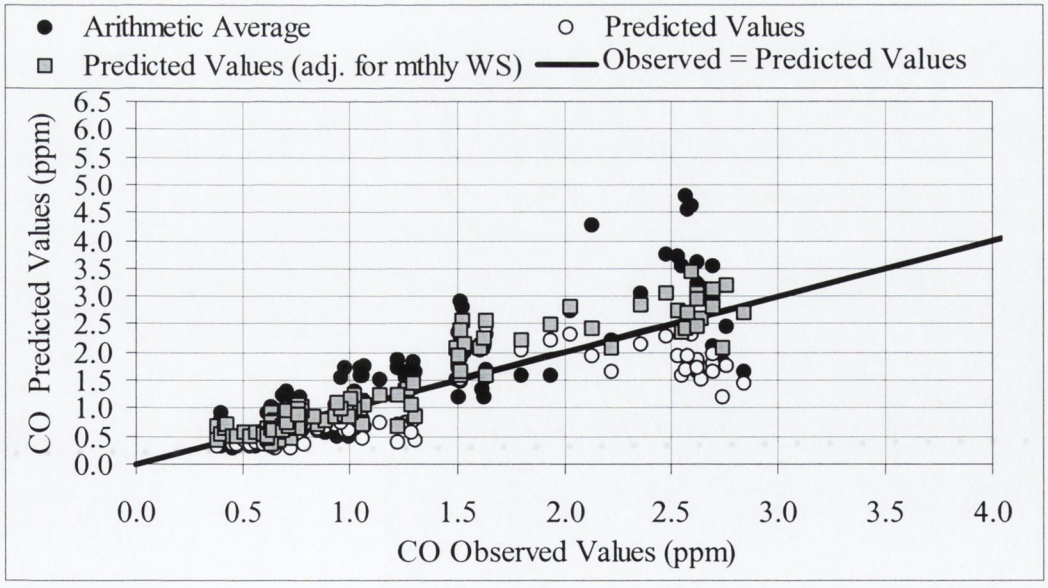

Figure 7.6 Graph of predicted and observed 30-day CO average concentrations (predictions calculated using monitoring periods from 13:00 to 14:00)

The choice of time period is seen to have a highly significant influence on the accuracy of the arithmetic average. Therefore, if unadjusted concentration data is being used, it is important that, for indicative monitoring, the conditions at the time of monitoring are representative of typical conditions at the monitoring site. The choice of time period, and conditions at the time of monitoring are not observed to be a significant factors when the prediction algorithm is used to estimate the monthly averages. The effect of the choice of time period is illustrated by comparison of the RMSEs in Figure 7.7. The algorithm is seen to provide a significantly more accurate prediction of the monthly average in all cases, with a similar RMSE for each monitoring period. In contrast, predictions based on the arithmetic average exhibit a high degree of sensitivity to the time and length of monitoring period, with the RMSE for predictions calculated using data collected between 17:00 and 18:00 over 140%. The errors for the arithmetic average and the prediction algorithm do not follow the same pattern and the algorithm errors are apparently independent of traffic flow characteristics. Section 7.2 considers the effect of conditions at the time of monitoring in further detail.

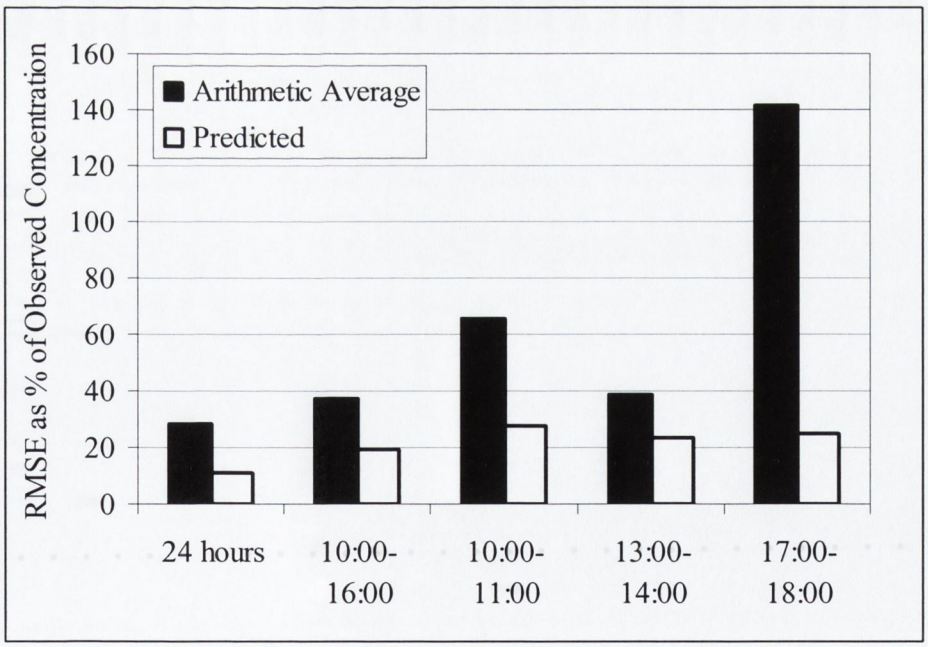

Figure 7.7 Comparison of RMSE of predictions of CO monthly average concentrations using the arithmetic average of data and algorithm

7.1.2 Nitrogen Dioxide

For each 30-day period, the average concentration is calculated. Using the algorithm discussed in Chapter 6, data from three days, one from the beginning, middle and end of the month, are used to estimate the monthly average. Table 7.7 summarises the results of the predictions of the monthly average based on different monitoring data inputs.

For predictions based on 24 hours of concentration data each day, the results produced by the prediction algorithm predict the average concentrations very well, although the arithmetic average also closely predicts the monthly averages. A very strong correlation between the predicted and observed data was found, with a Pearson's correlation coefficient of 0.96.

The algorithm also performs well with inputs from shorter-term monitoring periods. The correlation coefficient between the predicted and measured concentrations range between 0.94 (data collected between 17:00 and 18:00) and 0.80 (data collected between 13:00 and 14:00), and both the RMSE and MAE for each case are below 15%. The algorithm consistently outperforms the arithmetic average of the data.

A sample graph comparing predicted and arithmetic average NO_2 based on data collected between 17:00-18:00 with the observed 30-day average concentrations between August 1998 and January 1999 is given in Figure 7.8.

As for CO, the time at which monitoring is carried out affects the accuracy of the arithmetic average, as illustrated in Figure 7.9, with the highest RMSE associated with the peak hour, 17:00 to 18:00. Values calculated using the prediction algorithm are affected by the time of monitoring to a lesser degree; however, the improvement is not as great as that observed for CO.

Table 7.7 Summary of monthly NO_2 concentration predictions

Monitoring Period			Arithmetic Average	Prediction
24 hours	Pearson's r		0.95	0.96
	RMSE	%	6.78	5.91
	σ_{RMS}	%	9.00	6.86
	MAE	%	5.26	4.81
	σ_{MAE}	%	4.30	3.45
10:00 - 16:00	Pearson's r		0.88	0.91
	RMSE	%	14.35	9.69
	σ_{RMS}	%	16.80	10.93
	MAE	%	11.40	7.91
	σ_{MAE}	%	8.75	5.61
10:00 - 11:00	Pearson's r		0.84	0.88
	RMSE	%	18.97	13.74
	σ_{RMS}	%	27.07	18.28
	MAE	%	14.25	10.50
	σ_{MAE}	%	12.57	8.89
13:00 - 14:00	Pearson's r		0.77	0.80
	RMSE	%	16.61	13.43
	σ_{RMS}	%	20.97	15.64
	MAE	%	13.07	10.92
	σ_{MAE}	%	10.28	7.86
17:00 - 18:00	Pearson's r		0.92	0.94
	RMSE	%	28.00	8.60
	σ_{RMS}	%	25.93	9.29
	MAE	%	25.31	7.04
	σ_{MAE}	%	12.01	4.95

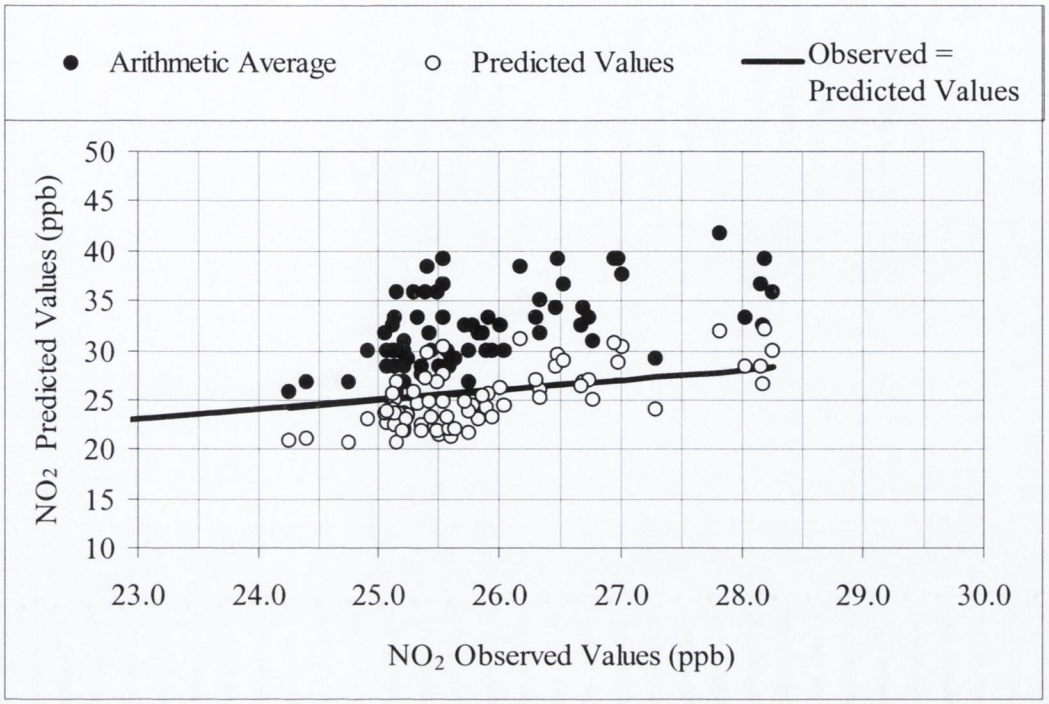

Figure 7.8 Scatter graph of predicted NO_2 concentrations using data collected between 17:00 and 18:00 plotted against observed 30-day average concentrations, between August 1998 and January 1999

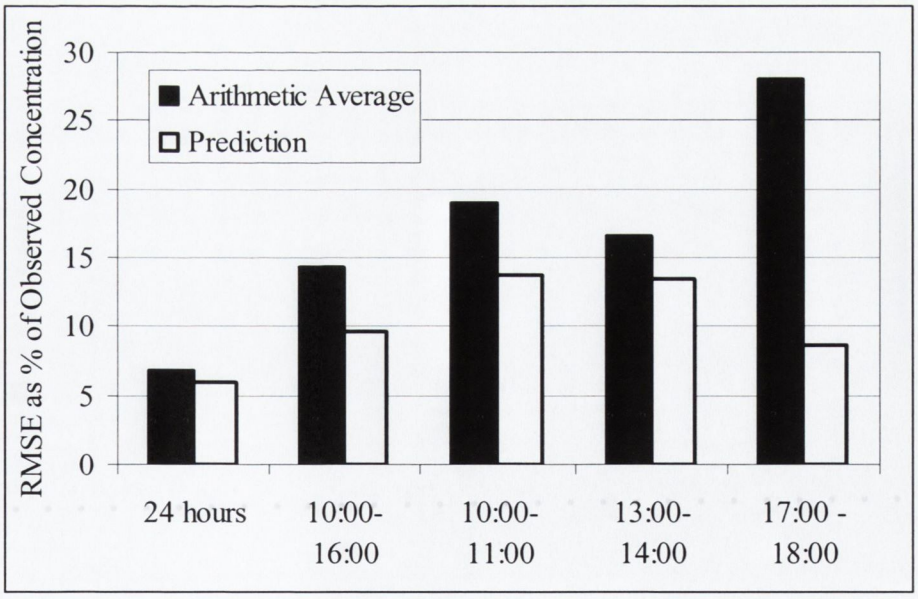

Figure 7.9 Comparison of RMSE of predictions of NO_2 monthly average concentrations using the arithmetic average of data and algorithm

7.1.3 PM_{10}

Table 7.8 details the correlation coefficients and errors in the prediction of the monthly average concentrations of PM_{10} from the algorithm and arithmetic average of the data. Predictions are not corrected for the average monthly wind speed, as that was found not to result in a consistent significant improvement in accuracy. For calculations based on 24 hours, the average PM_{10} values calculated using the arithmetic average are as accurate as those calculated with the prediction algorithm. However, using the arithmetic average as a predictor of the monthly average can lead to greater errors than using the prediction algorithm when monitoring is carried out on days with atypical meteorological conditions. In all other cases, the prediction algorithm results in smaller errors than using the arithmetic average of the data, although lower Pearson's r-values were calculated than for either CO or NO_2. Predictions based on concentrations recorded between 17:00 – 18:00 result in the largest errors for the arithmetic average, although the errors in the averages calculated using the prediction algorithm are similar to those calculated using other time periods. From this it can be seen that the choice of monitoring period is important for indicative monitoring where no adjustments are subsequently made to the data, but it has a negligible effect when the prediction algorithm is employed.

Figure 7.10 is a sample scatter chart of the observed 30-day average PM_{10} concentrations plotted against the arithmetic average and the results of the prediction algorithm, for data collected between 17:00 and 18:00. Although the results of the prediction algorithm show quite a high degree of scatter around the line of unity, they are centred on the correct values. This is not so for the arithmetic average, which consistently overestimates the observed values. Possible reasons for the large amount of scatter in the algorithm results are discussed in Section 7.8.3.

The effect of the choice of time period is illustrated graphically in Figure 7.11. Unlike the results calculated using the arithmetic average, the RMSE calculated using the prediction algorithm is similar, regardless of the chosen monitoring period. However, as seen in Figure 7.11, when a 24-hour monitoring period is used the RMSE for the arithmetic average is smaller than that associated with the prediction algorithm.

Table 7.8 Summary of predictions of monthly PM_{10} concentrations

Monitoring Period			Arithmetic Average	Prediction
24 hours	Pearson's r		0.73	0.60
	RMSE	%	19.96	21.56
	σ_{RMS}	%	22.08	24.25
	MAE	%	16.43	17.64
	σ_{MAE}	%	11.37	12.44
10:00 - 16:00	Pearson's r		0.66	0.54
	RMSE	%	33.79	23.29
	σ_{RMS}	%	41.61	26.12
	MAE	%	25.74	19.08
	σ_{MAE}	%	21.96	13.38
10:00 - 11:00	Pearson's r		0.65	0.58
	RMSE	%	40.04	26.18
	σ_{RMS}	%	46.26	32.46
	MAE	%	32.17	20.25
	σ_{MAE}	%	23.90	16.65
13:00 - 14:00	Pearson's r		0.53	0.47
	RMSE	%	42.46	30.18
	σ_{RMS}	%	62.36	34.19
	MAE	%	31.50	24.90
	σ_{MAE}	%	28.57	17.11
17:00 - 18:00	Pearson's r		0.57	0.47
	RMSE	%	47.60	26.17
	σ_{RMS}	%	61.36	29.32
	MAE	%	35.16	21.85
	σ_{MAE}	%	32.18	14.46

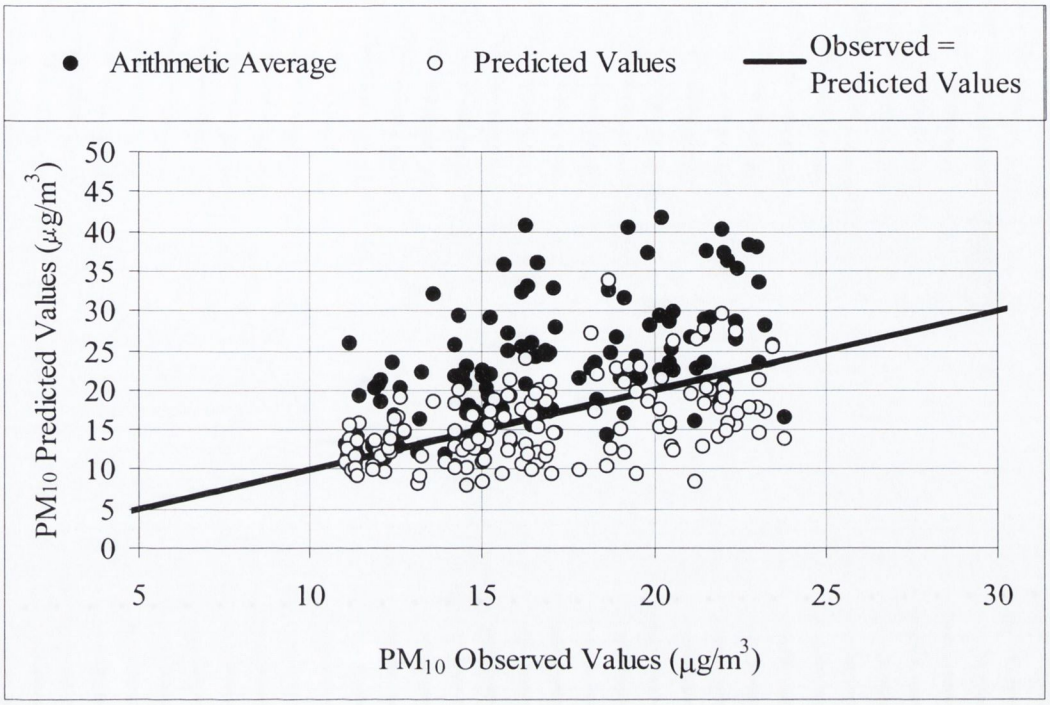

Figure 7.10 Graph of predicted and observed 30-day PM_{10} average concentrations (Predictions calculated using monitoring periods from 17:00 to 18:00)

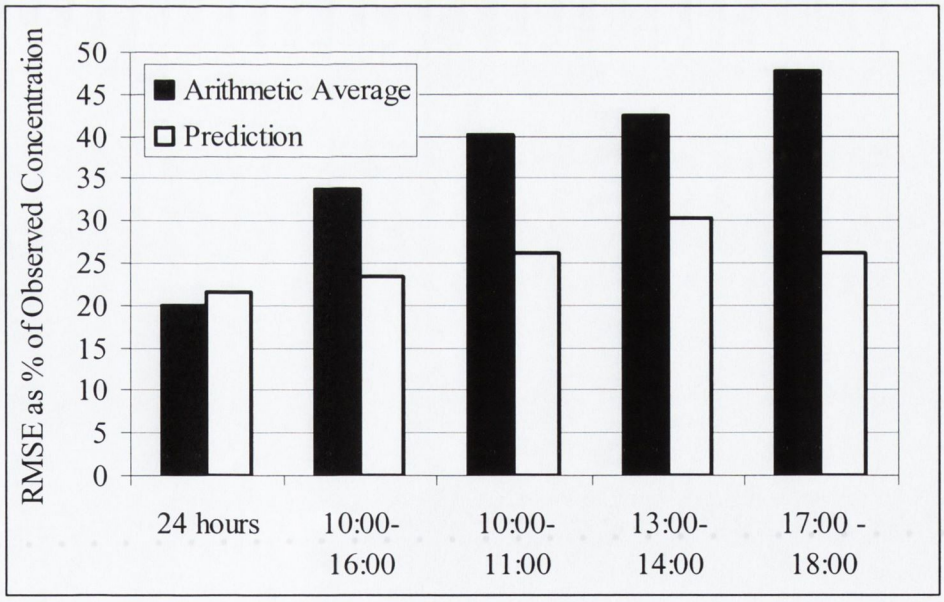

Figure 7.11 Comparison of RMSE of predictions of PM_{10} monthly average concentration predictions

7.2 Indicative Monitoring – Worst Case Scenario

Unadjusted concentrations recorded during short-term indicative monitoring only characterise the pollutant concentrations well if the conditions at the time of monitoring are typical of the prevailing conditions at the site. Adjusting the measured concentrations for conditions at the time of sampling is of particular importance under atypical conditions. Four scenarios are investigated in which the monitoring periods are not representative of general conditions at the site. These are:

(i) Low wind speed

(ii) High wind speed

(iii) Wind blowing consistently from the junction

(iv) Wind blowing consistently to the junction

Clearly, short-term indicative monitoring carried out under any of these conditions will result in the pollutant concentration conditions at the junction being misrepresented if only the arithmetic average of the measured data were examined.

7.2.1 Carbon Monoxide

Figure 7.12 shows the results of the prediction algorithm when the input days have lower than average wind speed. This low wind speed leads to the arithmetic average overestimating the monthly average. However, the algorithm is seen to function well, with the calculated predictions being close to the observed averages. The algorithm (when adjusted for monthly wind speed) results in a significant improvement over the arithmetic average in seven out of nine cases (78%). The unadjusted algorithm achieves an improvement in six cases (67%). On no occasion does the arithmetic average display a significant improvement over the prediction algorithm.

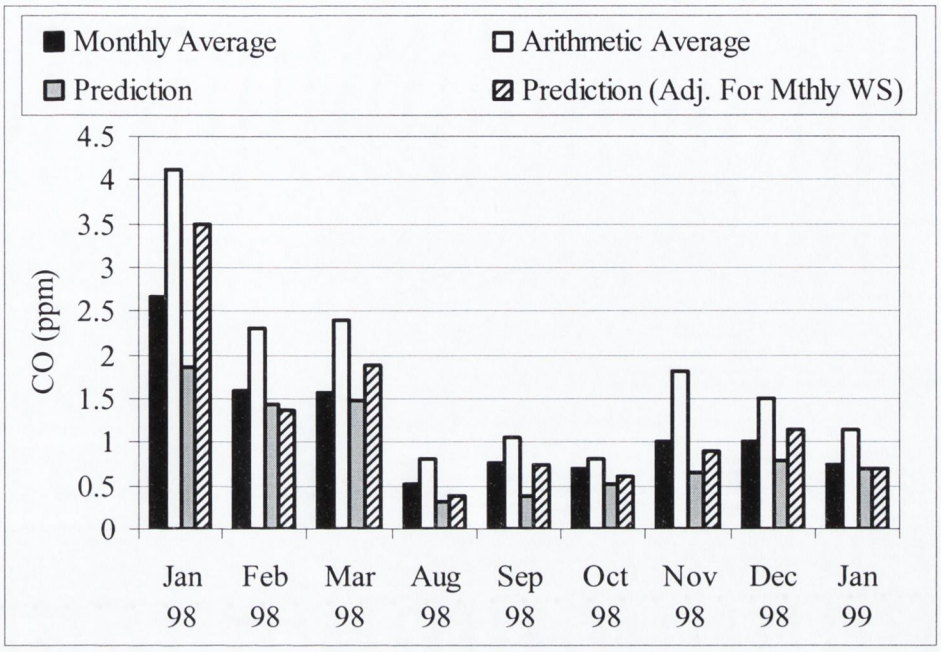

Figure 7.12 Predictions of monthly average CO concentrations from data collected during three whole days with low wind speeds

The effect of conditions at the time of monitoring is of particular importance for predictions based on short-term monitoring, as the decreased time of sampling can increase the degree to which the data misrepresents the typical concentrations at the site. Figure 7.13 compares the results of the algorithm and arithmetic averages based on data recorded between 17:00 and 18:00, during lower than average wind speed conditions. Most obvious from the chart is the degree to which short-term measurements can misrepresent the concentrations at the monitoring site. The results from the arithmetic average are, on average, three times the observed average concentration, and up to 5.3 times the observed concentration (November 1998). This is in contrast to the results of the prediction algorithm. The algorithm results, after adjustment for monthly wind speed, are on average 0.95 times the observed average; with the predicted average a maximum of 1.35 times the observed value (January 1998). The prediction algorithm limits the magnitude of the error, which is very similar in both cases. Even without an adjustment for monthly wind speed, use of the algorithm is seen to decrease the discrepancy between the measured and estimated concentrations. The average error in the algorithm predictions is 16% of the observed concentration, compared to an average of 205% for the arithmetic average; maximum errors of 29% and 425% are observed for the algorithm and arithmetic average, respectively.

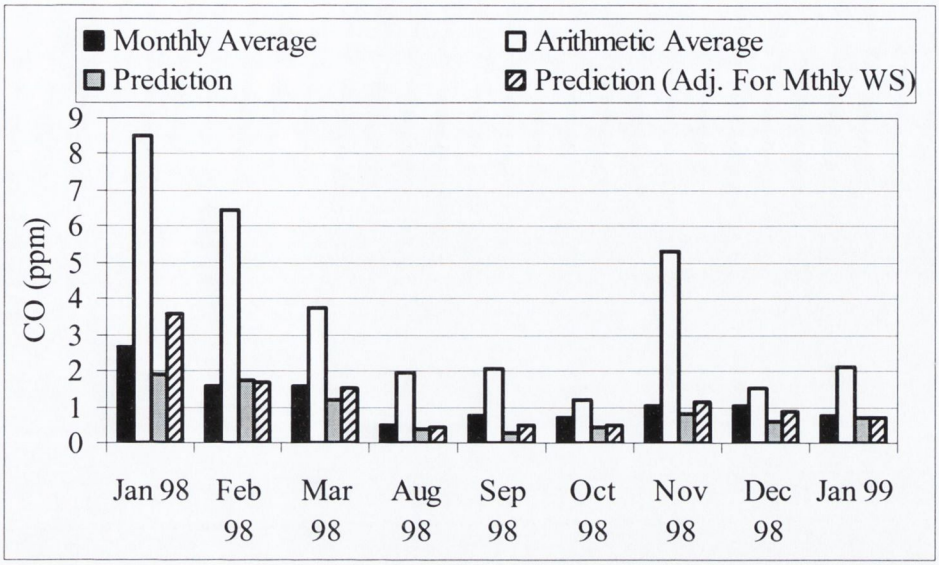

Figure 7.13 Predictions of monthly average CO concentrations from data collected between 17:00 and 18:00 during three days with low wind speeds

Figure 7.14 shows the results of the prediction algorithm for input days with higher than average wind speed. Although the arithmetic average is seen to underestimate the monthly average, the error is smaller than the equivalent error for lower than average wind speed. Again, the algorithm is seen to function well, with the predictions calculated being close to the observed averages, with similar magnitudes of errors as calculated for lower than average wind speeds. Unlike the concentration estimates calculated using the arithmetic average of the short term measurements, the prediction algorithm does not consistently either underpredict or overpredict the measured concentrations.

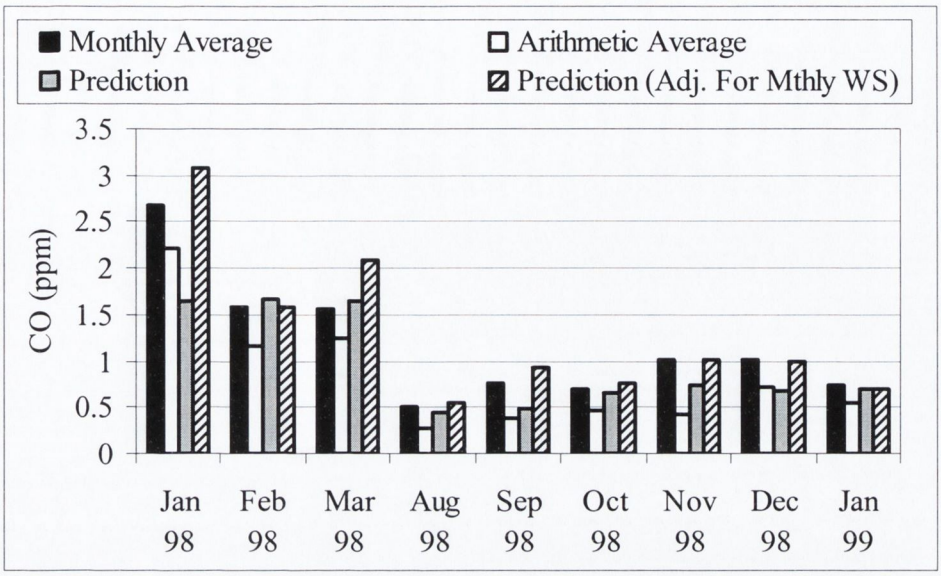

Figure 7.14 Predictions of monthly average CO concentrations from data collected during three days of high wind speeds

Figure 7.15 shows an equivalent comparison with wind blowing from the monitoring site to the junction. The arithmetic average shows a tendency to underestimate the monthly average, although with a smaller average error than those in Figure 7.13 and Figure 7.14. The predicted monthly averages are seen to closely estimate the measured values, and as before, the prediction algorithm does consistently underpredict or overpredict the concentrations.

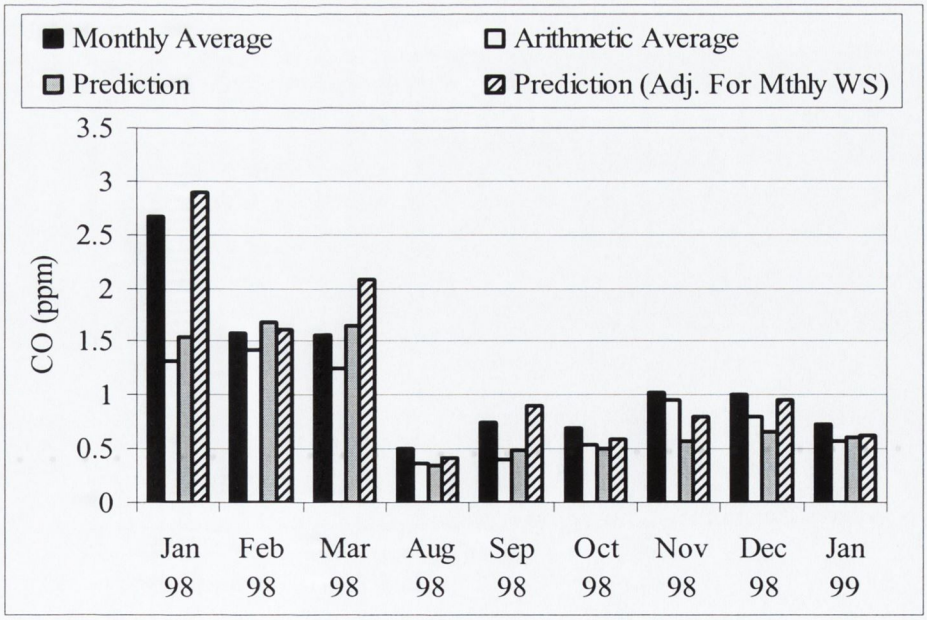

Figure 7.15 Predictions of monthly average CO concentrations from data collected during three days during which the wind was blowing from the monitoring site to the junction

Figure 7.16 shows the bar graph for wind blowing to the monitoring site from the junction. As would be expected, the arithmetic average overpredicts the monthly average concentration. The magnitude of the error caused by using the arithmetic average to estimate the average concentrations is approximately 60% on average for the analysed data. Conditions at the site are better represented by the predictions from the algorithm after correction for the average monthly wind speed, which display smaller errors, in comparison (on average approximately 15%). However, algorithm predictions not adjusted for monthly average wind speed also display smaller errors for the sample data than the estimates based on the arithmetic average. No predictions for January 1999 are shown, as the required conditions did not occur sufficiently often during this month.

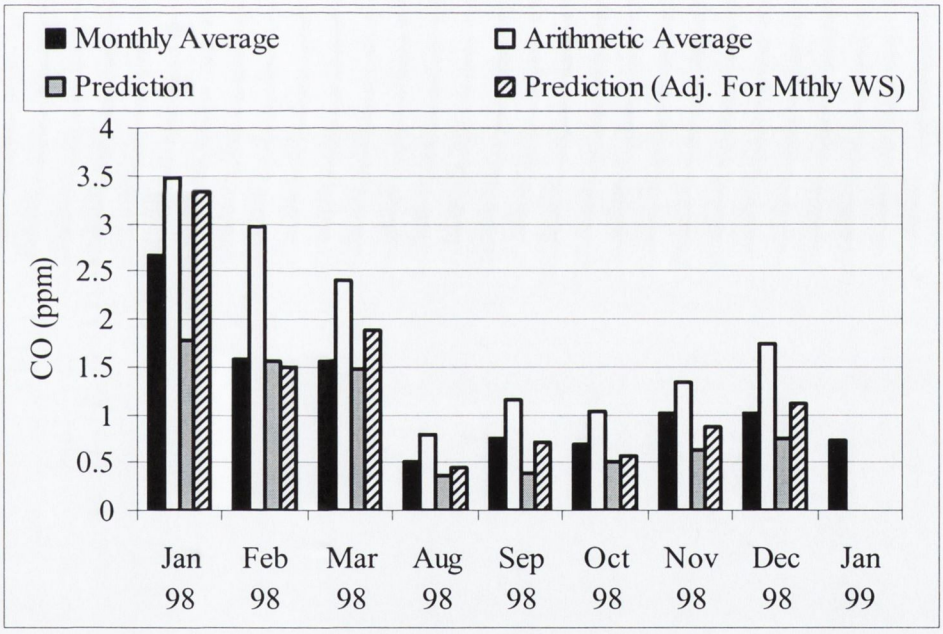

Figure 7.16 Predictions of monthly average CO concentrations from data collected during three days during which the wind was blowing to the monitoring site from the junction

7.2.2 Nitrogen Dioxide

Conditions at the time of monitoring also affect NO_2 concentrations, as seen in Figure 7.17. The effect of wind speed on the accuracy of NO_2 predictions is less marked than for CO.

However, the arithmetic average of concentration data measured under high wind speed conditions tends to underestimate the monthly concentrations. However, the errors associated with both the arithmetic average of the data and the prediction algorithm are of a similar magnitude for the sample data.

Conversely, the average of data measured under low wind speed conditions tends to overestimate concentrations. Figure 7.18 compares the algorithm results and arithmetic averages based on concentration data measured between 17:00 and 18:00, at low wind speeds. The accuracy of the arithmetic average is dependent on the conditions at the time of sampling; however, the algorithm is seen to limit the magnitude of the error to a maximum of 15%, compared to an error of 57% for the arithmetic average.

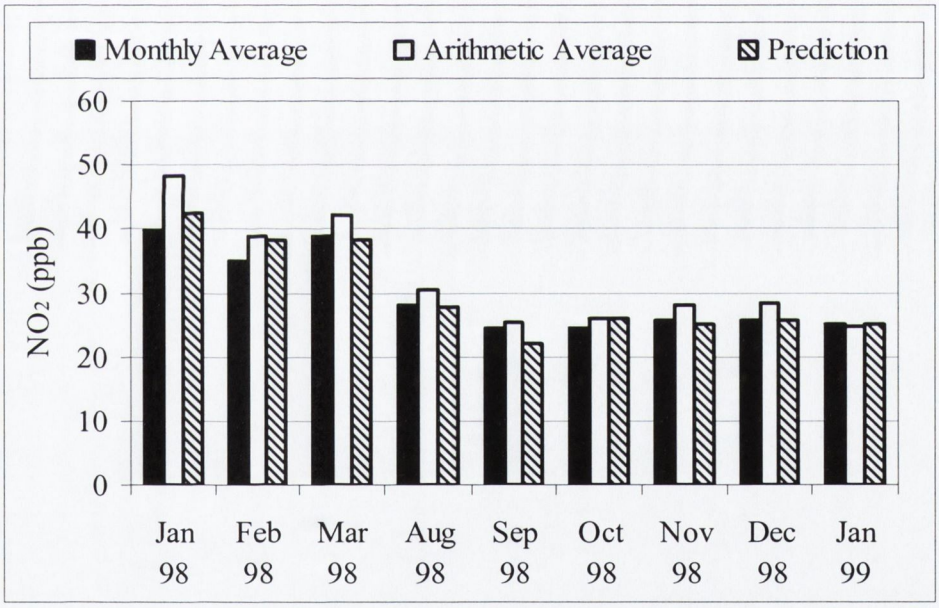

Figure 7.17 Predictions of monthly average NO_2 concentrations from data collected during three days with lower than average wind speed

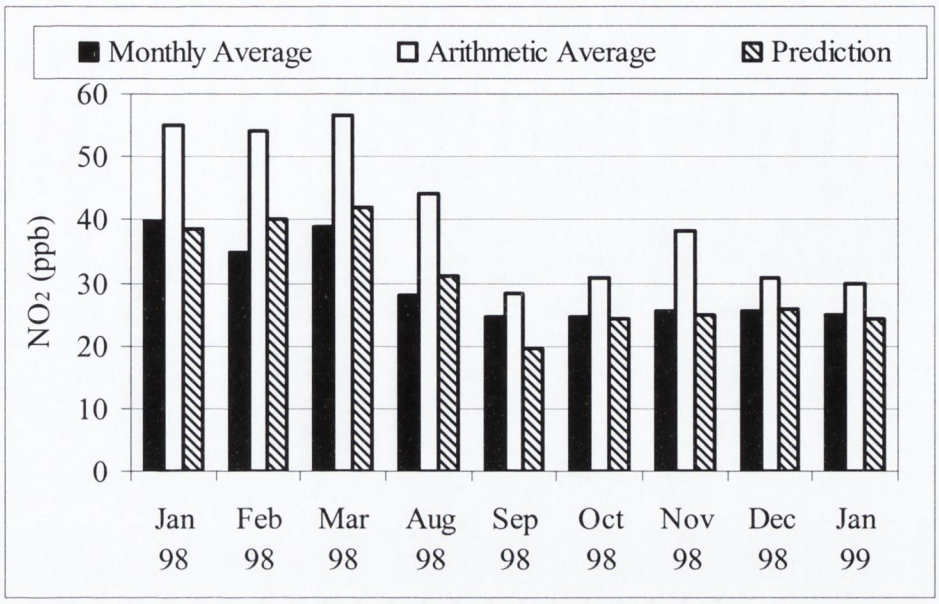

Figure 7.18 Predictions of monthly average NO_2 concentrations from data collected between 17:00 and 18:00 during three days with lower than average wind speed

7.2.3 PM_{10}

Figure 7.19 compares the results of the algorithm and the arithmetic average, with respect to PM_{10} concentrations, based on data collected during lower than average wind speed conditions. (Sufficient data was not available for April or May 1998). The arithmetic average overpredicts the observed concentrations in all cases, by an average of 23%, compared to an average error of 17% for the prediction algorithm. The effect of conditions at the time of sampling is visible to a greater extent in Figure 7.20 where the predictions are based on concentrations measured between 17:00 and 18:00, with average errors for the algorithm and arithmetic average of 30% and 74%, respectively. In this case, the two conditions that are most likely to cause an overestimation of the pollutant concentration (low wind speed and peak traffic) coincide causing the large error in the estimation using the arithmetic average.

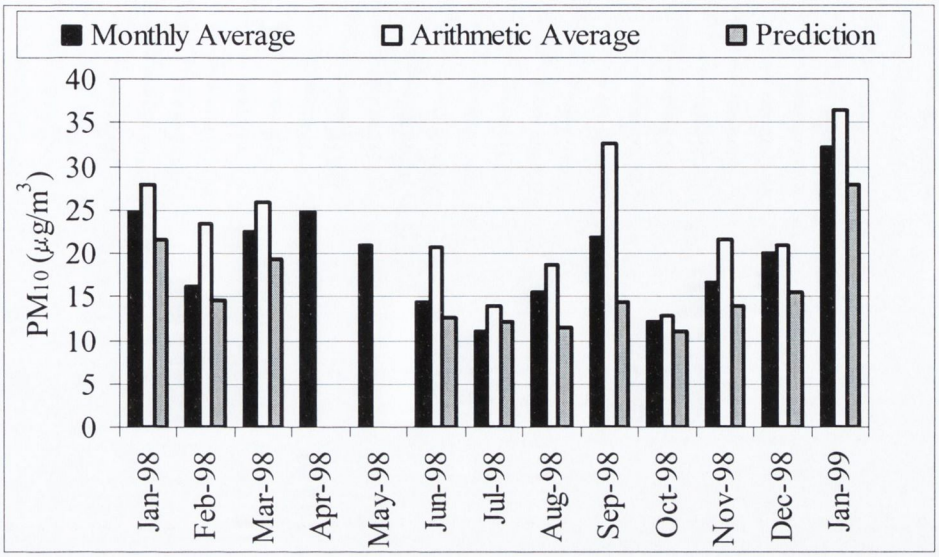

Figure 7.19 Predictions of monthly average PM_{10} concentrations from data collected during three days with lower than average wind speed

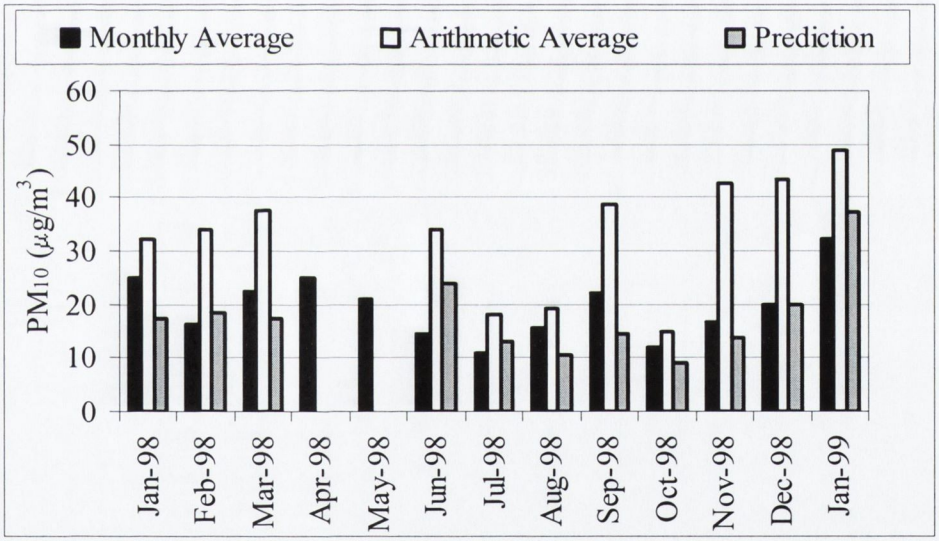

Figure 7.20 Predictions of monthly average PM_{10} concentrations from data collected between 17:00 and 18:00 during three days with lower than average wind speed

7.3 Estimation of Standard Deviation

7.3.1 Carbon Monoxide

Once the nature of the frequency distribution has been established, two parameters are still necessary to establish the shape of the distribution, i.e., the mean and standard deviation. The standard deviation may be estimated using the data collected in the initial monitoring period to establish the adjustment factors, in conjunction with Equation 6.20, to give upper and lower bounds of the desired confidence.

The performance of Equation 6.20 was tested using a sample period of six months (July 1998 – January 1999). The resulting sample estimates of standard deviation are given in Table 7.9. Using a confidence level of 95%, the upper and lower bounds of the standard deviations were calculated. Six measurements (either 24-hour averages, 8-hour averages, or 1-hour averages) were used for each sample (one from each month). In each case, the measured standard deviation falls within the estimated confidence intervals calculated using this reduced data set.

Table 7.9 Measured population standard deviations and estimated standard deviations for CO 24-hour averages, 8-hour averages and 1-hour averages.

	Measured σ	**Lower Bound of Estimate**	**Upper Bound of Estimate**	**Is measured Value within Estimate?**
24-hour ave.	0.536	0.155	0.608	Yes
8-hour ave.	0.802	0.244	0.957	Yes
1-hour ave.	0.666	0.282	1.107	Yes

7.3.2 Nitrogen Dioxide and PM_{10}

The methods of estimation of population standard deviations are the same as those used for CO prediction, and are detailed in Section 7.3.1 and Section 6.12.1, and the observed values were found to be within the predicted estimates.

7.4 Frequency Distributions of Hourly, 8-Hourly and 24-Hourly Data

7.4.1 Carbon Monoxide

In order to predict extreme events and estimate the likely highest pollutant concentrations, it is necessary to characterise the data set as completely as possible. To fully characterise a data set in terms of its statistical distribution, the parameters that uniquely determine that distribution must be known, as well as the form of the distribution itself. The normal, lognormal and gamma distributions, as described in Section 4.3.1, can all be determined using the mean and standard deviation. The mean concentration may be predicted using the algorithm described (or measured using passive sampling), while the estimation of the standard deviation is discussed in Section 7.3.1. In this section, the appropriate choice of distribution for three time periods of interest – 24-hourly, 8-hourly and 1-hourly – is discussed.

Frequency Distribution of 24-hour Average CO Concentrations

Following the analysis of the frequency distributions of the 15-minute CO concentrations in Section 4.3.3, the lognormal and gamma distributions were considered the most likely distributions for the 24-hourly data. For the purpose of extreme event prediction, the agreement between the hypothetical statistical distribution and the observed data at higher concentrations is of particular importance.

The absolute differences between both the lognormal and gamma distributions and the observed distributions, from the 85^{th} percentile and higher, were compared. For 60% of the months analysed, the sum of the differences was smaller for the gamma distribution. A sample month (November 1998) is shown in Figure 7.21. For this month, the observed distribution is matched quite equally well by both distributions at the 100^{th} percentile, although the observed distribution is matched slightly better by the lognormal distribution at lower percentiles.

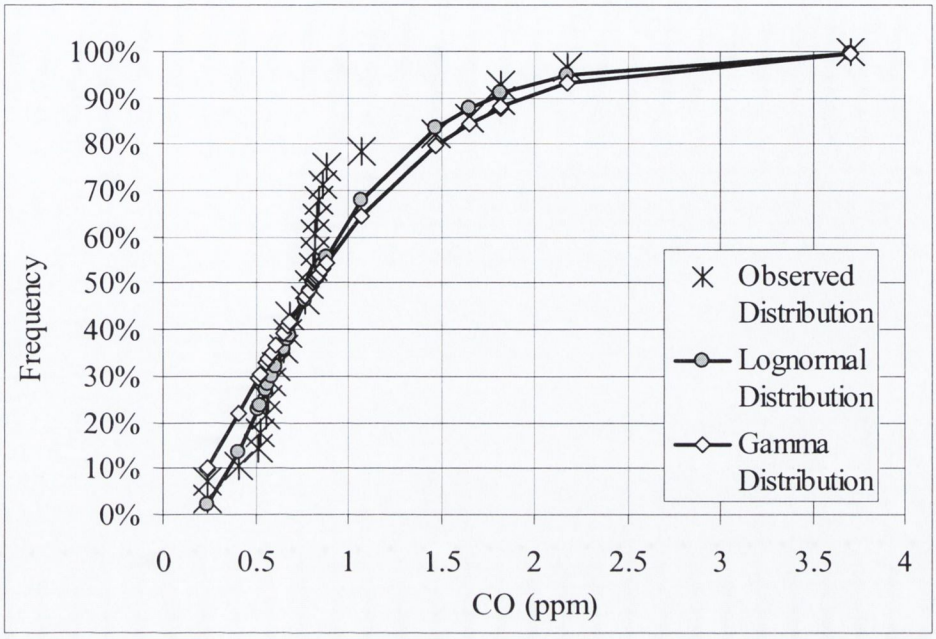

Figure 7.21 Lognormal and gamma distributions fitted to a sample month of data (November 1998) of 24-hour average CO concentrations

The gamma distribution was chosen to represent the 24-hour average CO concentrations, as the gamma distribution is more flexible and there was a tendency for the gamma distribution to represent the higher concentrations marginally better than the lognormal distribution. The theoretical distributions are calculated using the average and standard deviation of the recorded data (November 1998) and then plotted with the observed distributions in Section 7.5.

Frequency Distribution of 8-hour Average CO Concentrations

Both the lognormal and gamma distributions were also investigated with respect to the 8-hour averages. Again, the gamma distribution matched the observed distribution slightly better than the lognormal distribution for some data sets (60% of the analysed months), although for others there was no significant difference. As before, the gamma distribution was selected for use in extreme event prediction. A sample month (November 1998) is graphed in Figure 7.22. Here, the gamma distribution is seen to follow the observed distribution more closely than the lognormal distribution at high concentrations, although the converse is true at lower concentrations. However, it is not as important that the chosen distribution follows the

observed distribution at low concentrations, as it is high concentrations that are of concern when investigating limit value exceedences.

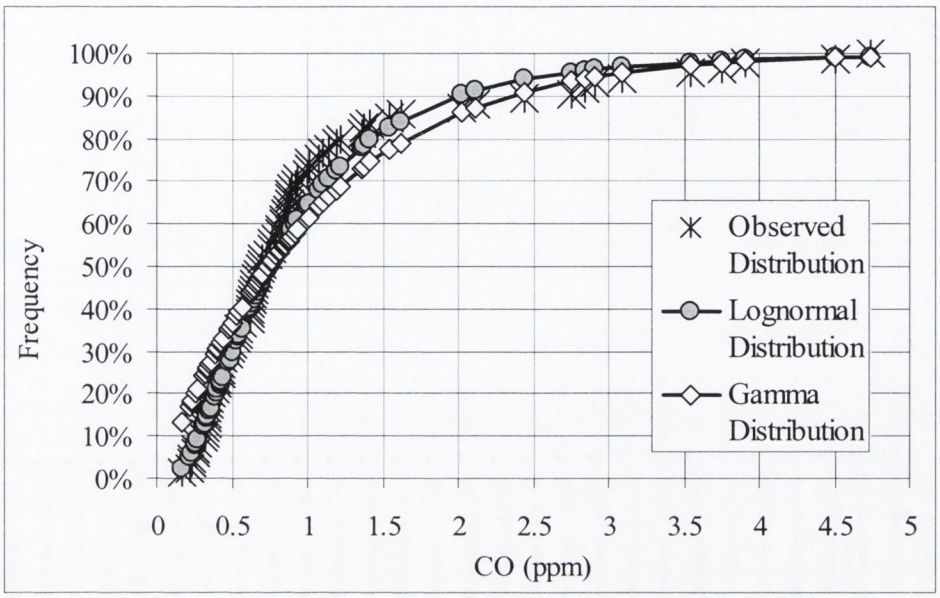

Figure 7.22 Lognormal and gamma distributions fitted to a sample month of data (November 1998) of 8-hour average CO concentrations

Frequency Distribution of 1-hour Average CO Concentrations

The gamma distribution was also selected for hourly CO concentrations, as when the differences above the 85th percentile were compared the gamma distribution resulted in smaller differences in 67% of the cases. In Figure 7.23 and Figure 7.24, both the lognormal and gamma distributions are plotted with the observed distribution for the sample month of November 1998. The gamma distribution better represents the observed distribution above the 90th percentile.

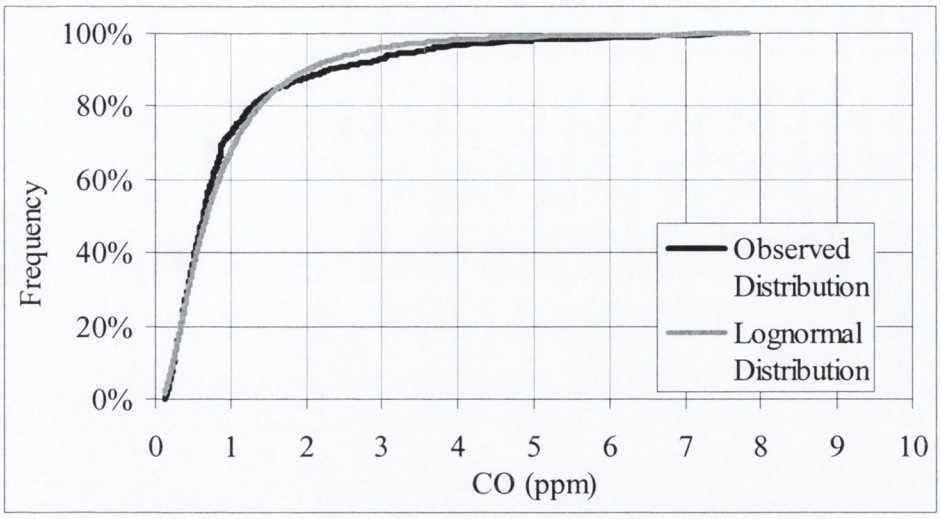

Figure 7.23 Lognormal distribution fitted to a sample month of data (November 1998) of 1-hour average CO concentrations

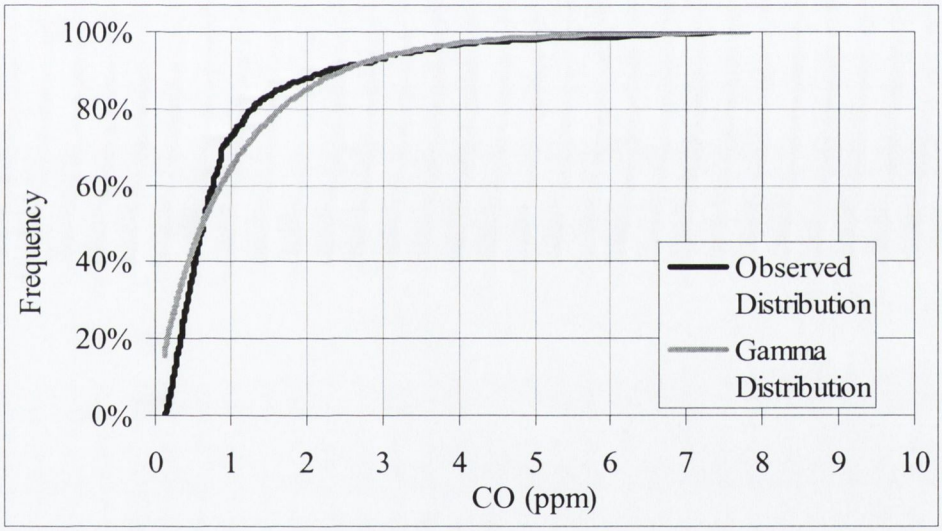

Figure 7.24 Gamma distribution fitted to a sample month of data (November 1998) of 1-hour average CO concentrations

7.4.2 Nitrogen Dioxide

Figure 7.25, Figure 7.26 and Figure 7.27 show lognormal and gamma distributions fitted to a sample month of data (August 1998) of 24-hour, 8-hour and 1-hour averages. Again, the stepped effect of the observed frequency distribution (due to the poor resolution of the NO_2 monitor) is visible in Figure 7.27. As illustrated in these figures, the lognormal and gamma

distributions in this case are similar, and therefore fit the data equally well. The gamma distribution was chosen to represent the data as it has the advantage of being more flexible in the forms of frequency distributions that it can represent, as described in Section 4.3.1.

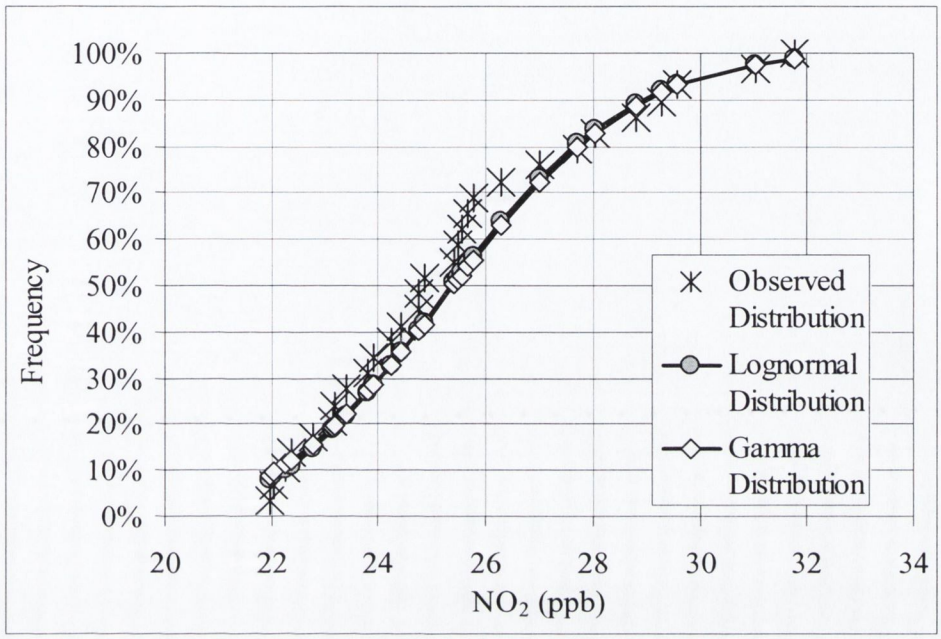

Figure 7.25 Lognormal and gamma distributions fitted to sample month (August 1998) of 24-hour NO_2 average concentrations

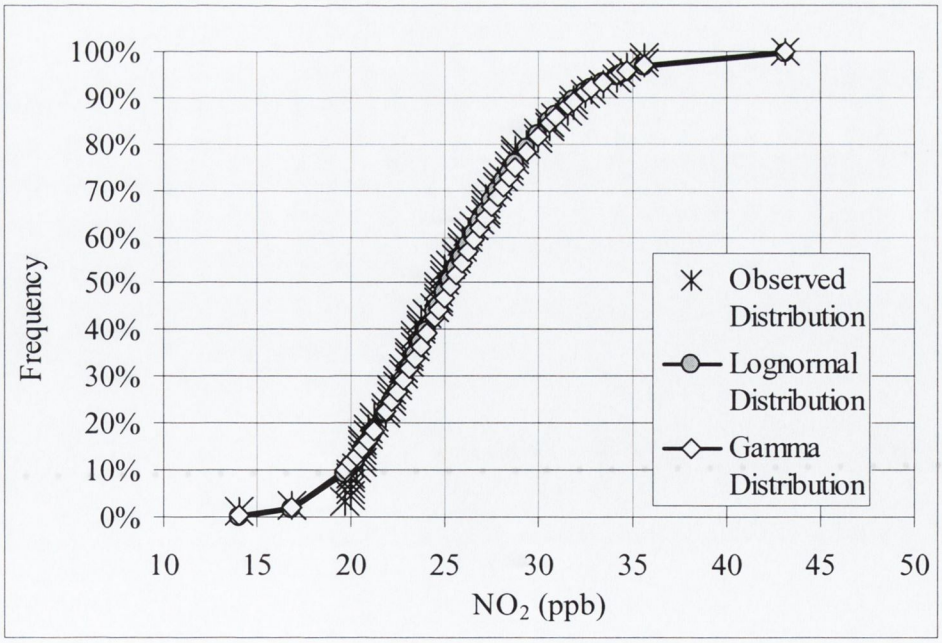

Figure 7.26 Lognormal and gamma distributions fitted to sample month (August 1998) of 8-hour average NO_2 concentrations

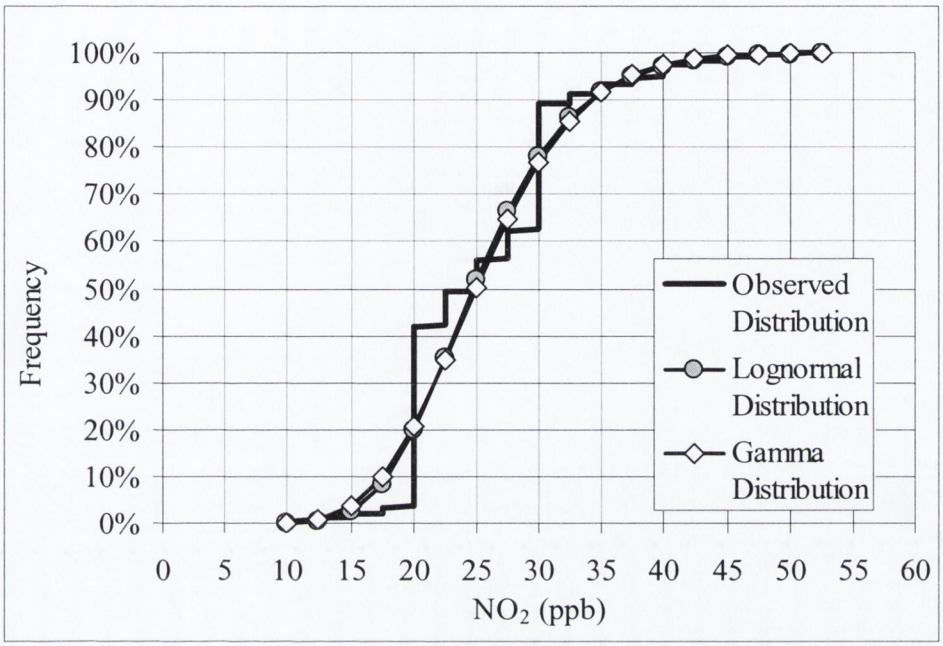

Figure 7.27 Lognormal and gamma distributions fitted to sample month (August 1998) of 1-hour average NO_2 concentrations

7.4.3 PM_{10}

The lognormal and gamma distributions were analysed for the best fit to the observed distributions of 24-hour, 8-hour and 1-hour averages. Lognormal and gamma distributions are fitted to a sample month of data (August 1998) in Figure 7.28 (24-hour averages), Figure 7.29 (8-hour averages) and Figure 7.30 and Figure 7.31 (1-hour averages). As for CO and NO_2, the observed distribution was well represented by both the lognormal and gamma distributions, although the gamma distribution was selected for use in the calculation of the estimated frequency distributions, as it was seen to perform marginally better at higher percentiles.

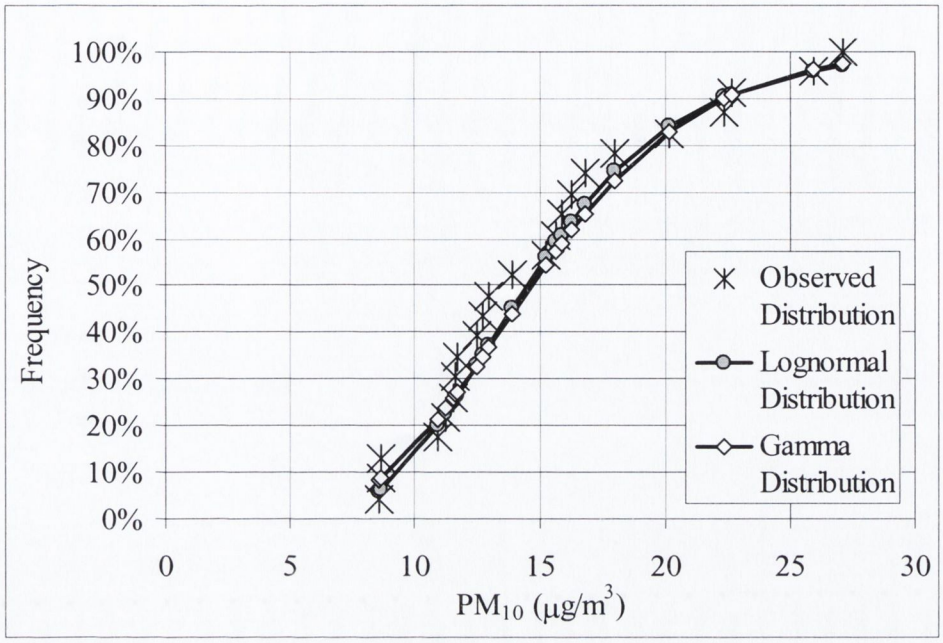

Figure 7.28 Lognormal and gamma distributions fitted to sample month (August 1998) of 24-hour average PM_{10} concentrations

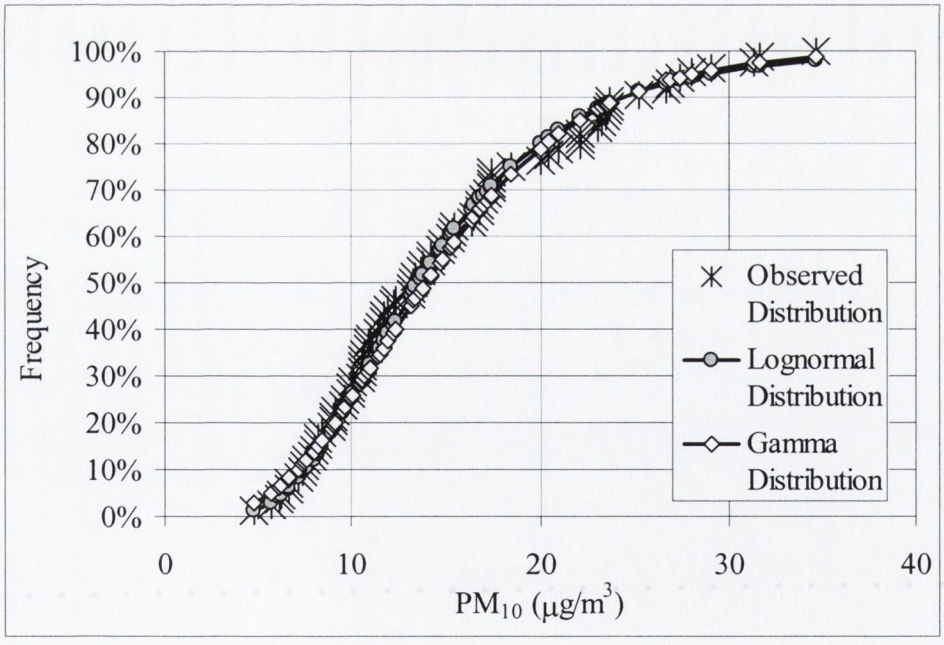

Figure 7.29 Lognormal and gamma distributions fitted to sample month (August 1998) of 8-hour average PM_{10} concentrations

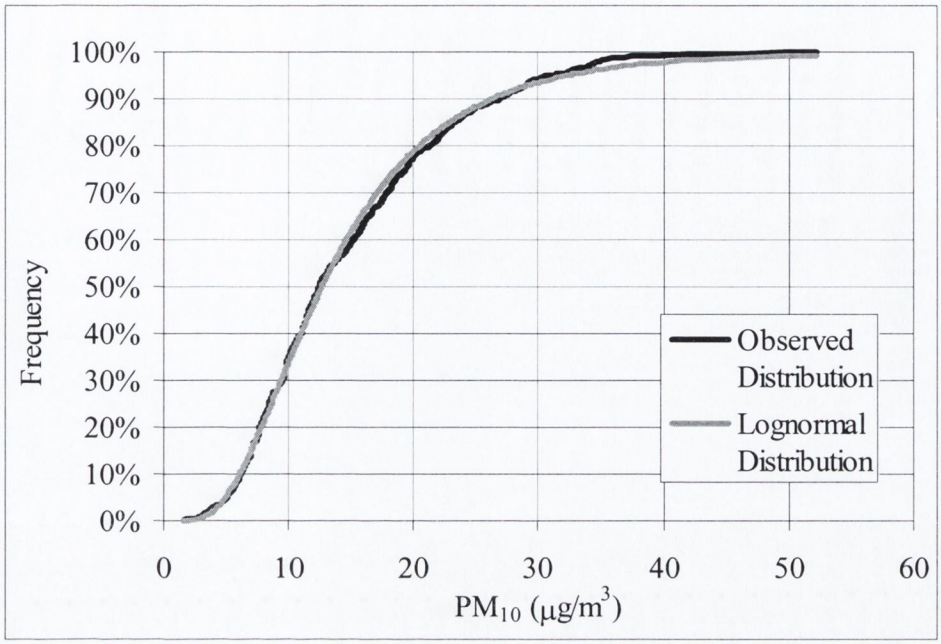

Figure 7.30 Lognormal distribution and observed frequency distribution for 1-hour PM_{10} averages (November 1998)

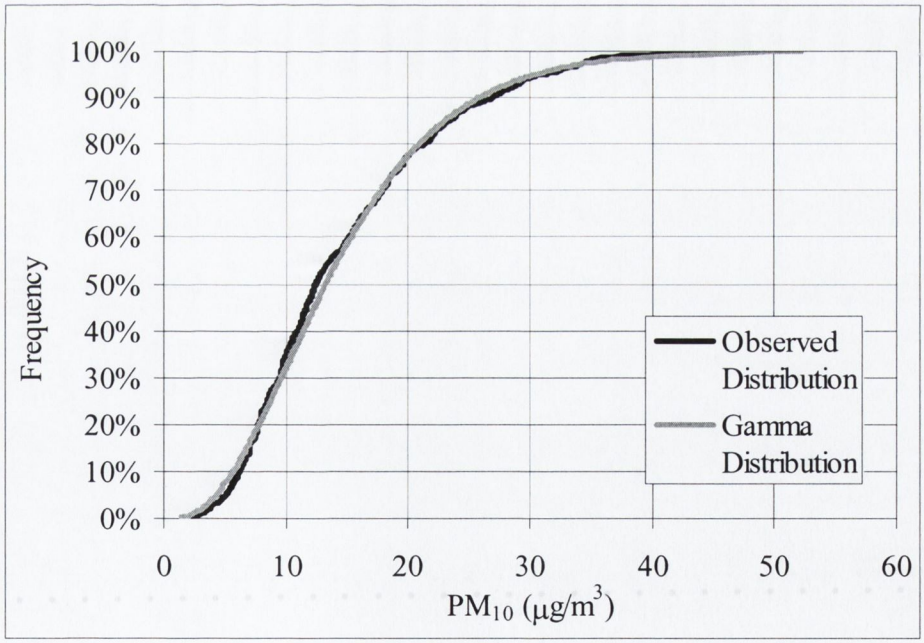

Figure 7.31 Gamma distribution and observed frequency distribution for 1-hour PM_{10} averages (November 1998)

7.5 Extreme Event Prediction

Short-term (24-hour, 8-hour, and 1-hour) peak concentrations are of more interest from the point of view of legislation and health, than long-term averages. However, once the concentration distribution has been characterised, using the mean and standard deviation, it is possible to estimate short-term concentrations over the longer term.

7.5.1 24-Hour Averages– Carbon Monoxide

Results based on two sets of input data are discussed in this section: results calculated using 24 hours of observed data on three separate input days, and results calculated using data collected during 17:00 and 18:00 only. The input days were selected as being the three weekdays with complete data collection closest to the 5th, 15th and 25th of each month; where the 5th, 15th, and 25th represent the most even intervals possible throughout the month. The time period 17:00 to 18:00 was chosen as a test of the accuracy of the algorithm, as unadjusted data collected during this period are the least representative of long-term concentrations at the monitoring site. Results for one summer and one winter month with high data capture rates are presented for each compound.

24-hour Average Concentration Predictions Calculated Using 3 x 24 hour s/day

The results for August 1998 and January 1999 are presented in this section. The population standard deviation is predicted using the first method described in Section 6.12.1. The prediction of the average monthly concentration for August was calculated using data measured on the 5th, 14th, and 25th August. (The 15th of August was not used as it fell on a Saturday). The prediction of the average monthly concentration for January was calculated using the 5th, 15th, and 25th January. The estimated frequency distributions were constructed using the gamma distribution, the estimated averages, and standard deviation confidence intervals. The predicted frequency distributions, showing the 95% confidence level upper and lower bounds, are plotted with the observed frequency distributions in Figure 7.32 (August

1998) and Figure 7.33 (January 1999). The frequency distribution calculated using the point estimate of the standard deviation is also shown.

Although the prediction calculated using the point estimate does not follow the observed frequency distribution closely, the observed distribution lies within the confidence intervals for both months. This accuracy is dependent on the prediction of the monthly average, however, as any error in the prediction will transform the upper and lower bounds along the x-axis by that amount. Measurement of the monthly average with a passive sampling would reduce this error.

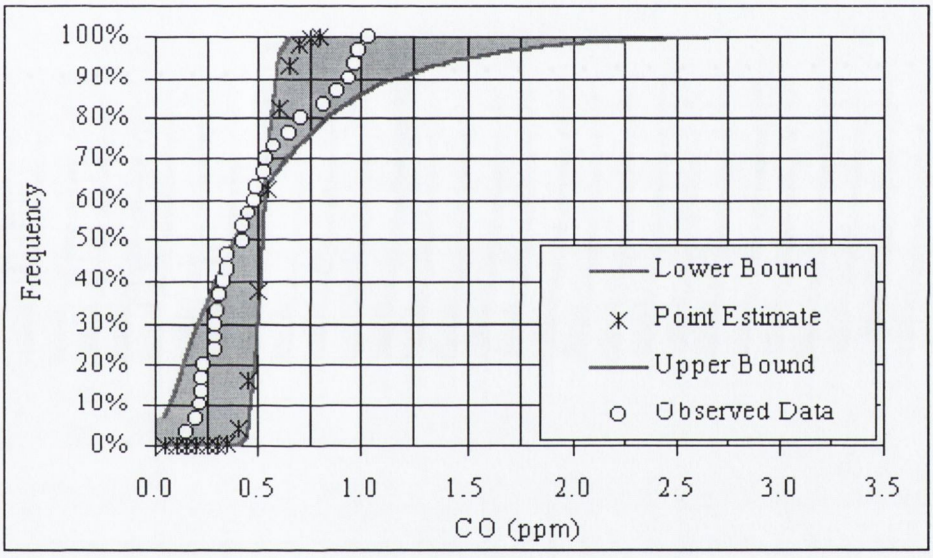

Figure 7.32 Predicted frequency distribution of 24-hour CO averages for August 1998, calculated using 3 complete days of monitoring.

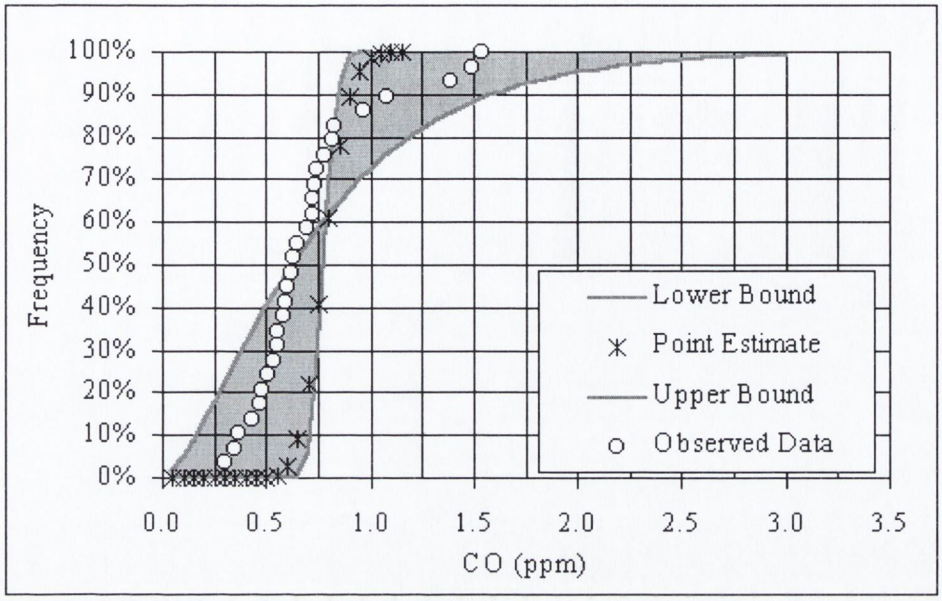

Figure 7.33 Predicted frequency distribution of 24-hour CO averages for January 1999, calculated using 3 complete days of monitoring.

24-hour Average Concentration Predictions Calculated using 3 x 1 hour/day (17:00-18:00)

A similar analysis was carried out for the same months using only monitoring data collected between 17:00 and 18:00. The first week of September 1998 was randomly chosen for the calculation of the relative standard deviations, which were then applied to the prediction of the monthly average for the calculation of the standard deviations.

The results for August 1998 and January 1999 are shown in Figure 7.34 and Figure 7.35, respectively. As can be seen, the observed frequencies are within the confidence intervals, and follow closely the prediction calculated with the point estimate of the standard deviation.

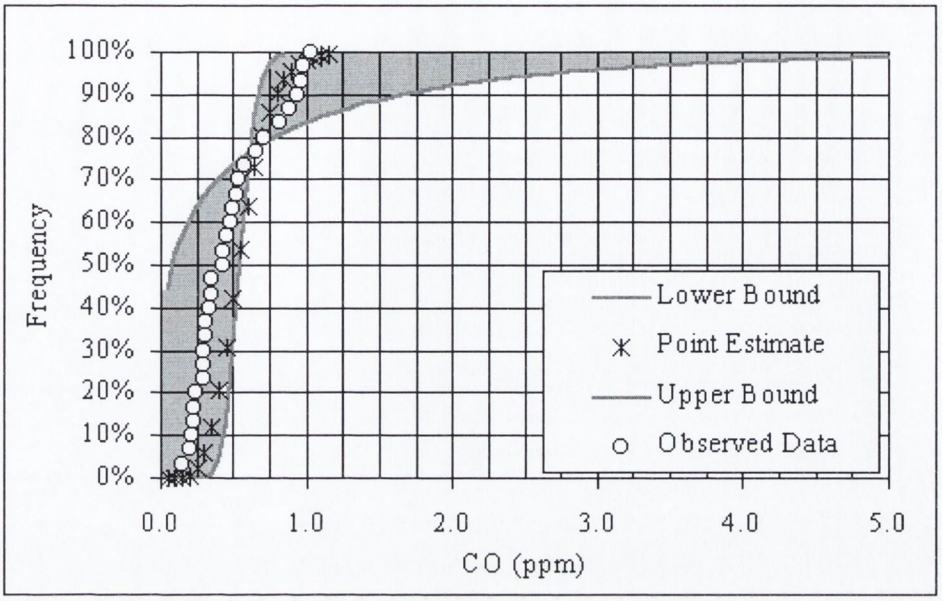

Figure 7.34 Predicted frequency distribution of 24-hour CO averages for August 1998, calculated using 3 days of monitoring data between 17:00 and 18:00

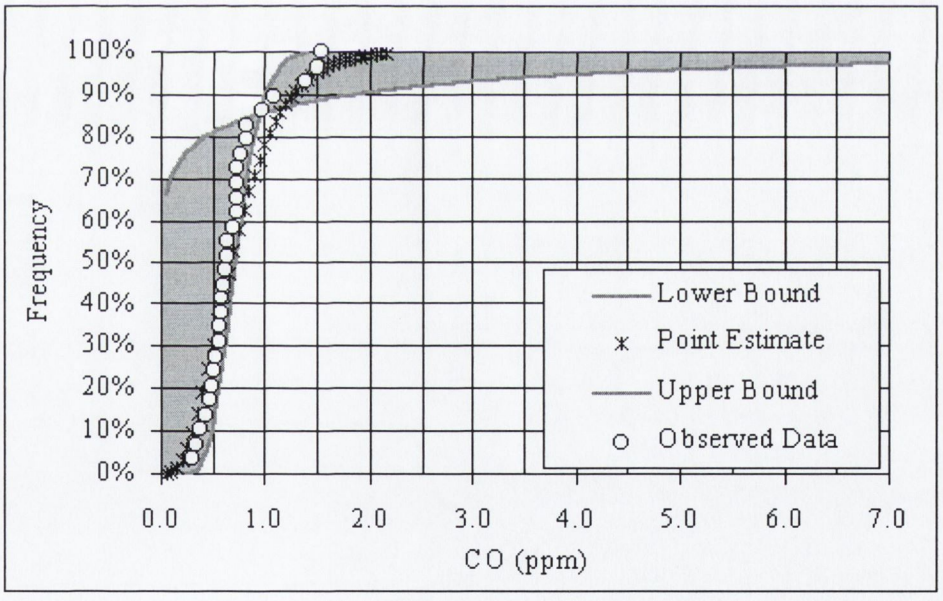

Figure 7.35 Predicted frequency distribution of 24-hour CO averages for January 1999, calculated using 3 days of monitoring data between 17:00 and 18:00

7.5.2 24-Hour Averages – Nitrogen Dioxide

As for CO, frequency distributions are calculated using the predicted average and standard deviation. Calculations are based on three days of data, taken from the beginning, middle and end of the month, with concentrations recorded over the full day and one hour between 17:00 and 18:00. Observed values for both August 1998 and January 1999 are well within the predicted confidence intervals for predictions based on both data sets, with the exception of the mid-range percentiles for January 1999 predictions based on 24-hour monitoring. The predicted and observed values are graphed in Figure 10.1 to Figure 10.4 in Appendix C.

7.5.3 24-Hour Averages – PM_{10}

As for CO and NO_2, results are presented for two representative sample months, February 1998 and August 1998. Predictions for February 1998 were calculated using data from 5th, 16th and 25th February. The 16th was used as the 15th fell on a weekend. Predictions for August 1998 were calculated using data from August 5th, 17th and 25th. (The 17th of August was used to avoid using data collected on a weekend)

Predictions were based on the same input periods as previously used for CO and NO_2. For predictions based on 24 hours of concentration data, the observed frequency distribution is within the predicted bounds for August 1998, but is fractionally underestimated at higher percentiles for February 1998. For predictions calculated using data collected between 17:00 and 18:00, the predicted confidence intervals bound the observed data for all percentiles, and the distribution calculated with the point estimate of the standard deviation also matches the observed distribution well. The predicted and observed frequency distributions are graphed in Figure 10.5 to Figure 10.8, in Appendix C.

7.5.4 8-Hour Averages – Carbon Monoxide

Using the same methodology and input data as for the 24-hour concentration maxima, the frequency distributions for 8-hour average concentrations were calculated.

8-hour Average Concentration Predictions Calculated using 3 x 24 hour s/day

Figure 7.36 shows the predicted upper and lower bounds of the frequency distribution for August 1998. The lower concentrations are overpredicted and the upper concentrations underpredicted. At the 95th percentile level the measured concentration is underpredicted by 0.25 ppm (20%) by the upper bound of the prediction estimate and by 0.75 ppm (40%) by the point estimate. The maximum concentration is underpredicted by 22% and 47% by the upper bound prediction and point estimate, respectively. In this case the estimated frequency distribution proves to be a poor representation of the measured frequency distribution resulting in considerable errors between the estimated and measured concentrations. The error is partially due to the average concentration being overpredicted. This error is then further compounded by an underprediction of the standard deviation.

The equivalent graph for January 1999 is shown in Figure 7.37. Here, the observed frequency distribution matches almost exactly the frequency distribution calculated with the point estimate of the standard deviation, and remains well within the estimated limits at both high and low concentrations.

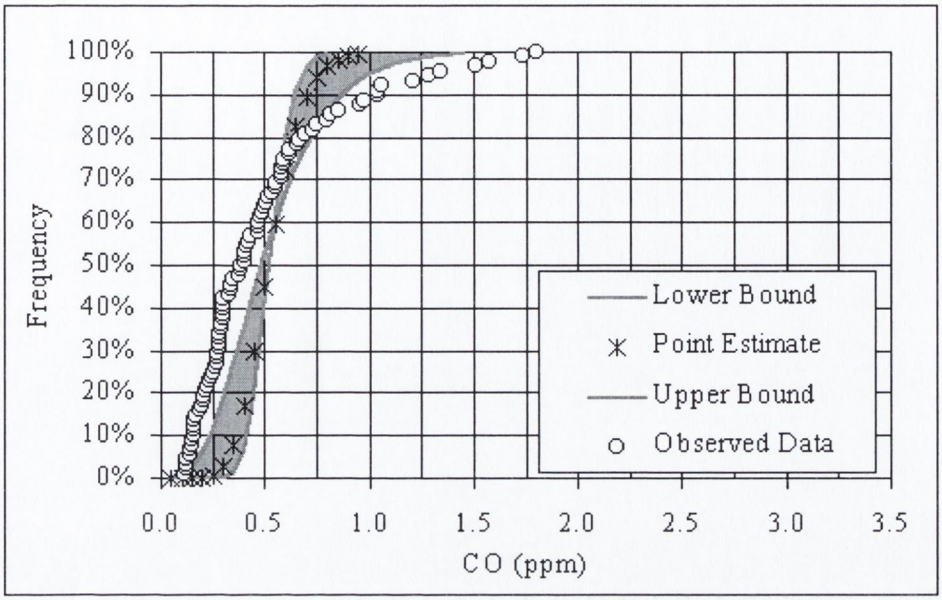

Figure 7.36 Predicted frequency distribution of 8-hour CO averages for August 1998, calculated using 3 complete days of monitoring.

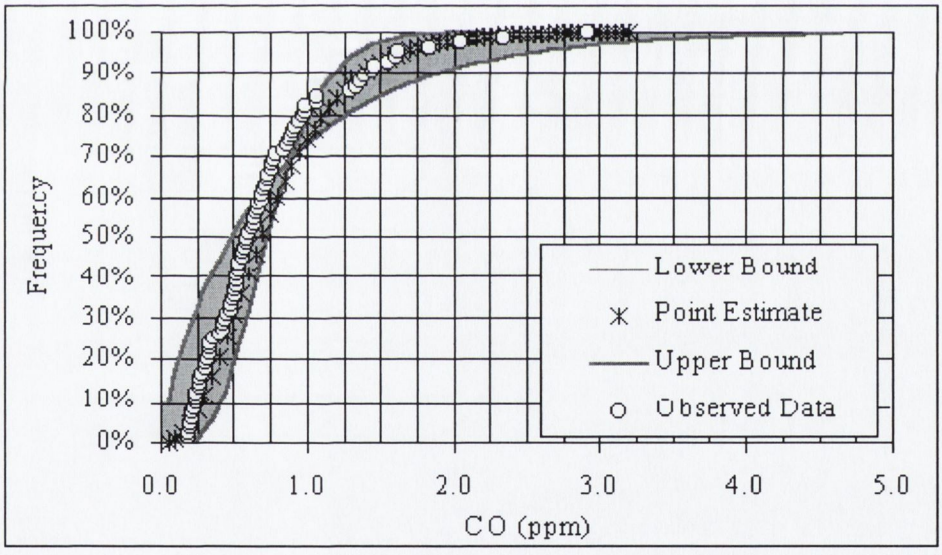

Figure 7.37 Predicted frequency distribution of 8-hour CO averages for January 1999, calculated using 3 complete days of monitoring.

8-hour Average Concentration Predictions Calculated using 3 x 1 hour/day (17:00-18:00)

The predicted frequency distribution using data collected between 17:00 and 18:00 matches the observed distributions very well for both August 1998 and January 1999, as seen in Figure

7.38 and Figure 7.39. In each case, the observed distribution follows the distribution calculated with the point estimate of the standard deviation closely.

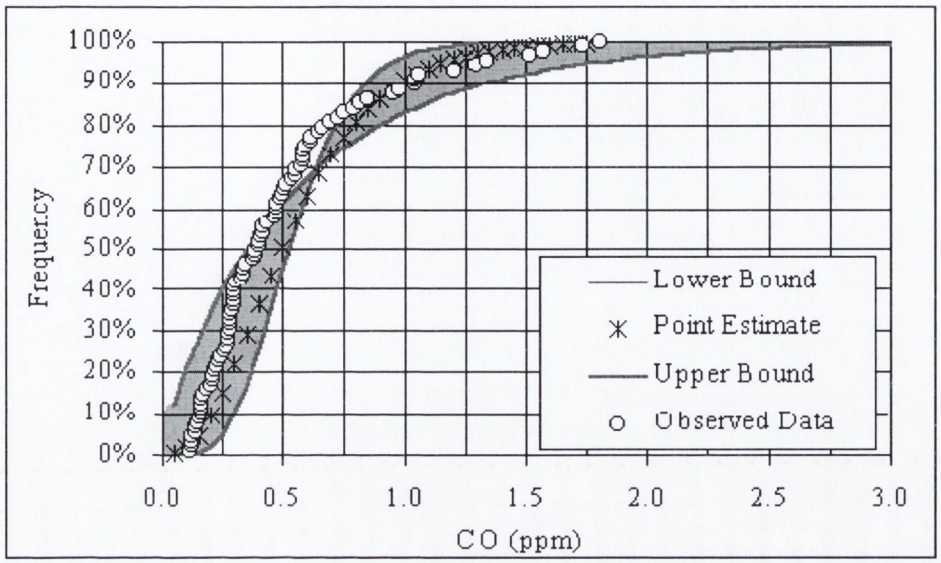

Figure 7.38 Predicted frequency distribution of 8-hour CO averages for August 1998, calculated using 3 days of monitoring data between 17:00 and 18:00

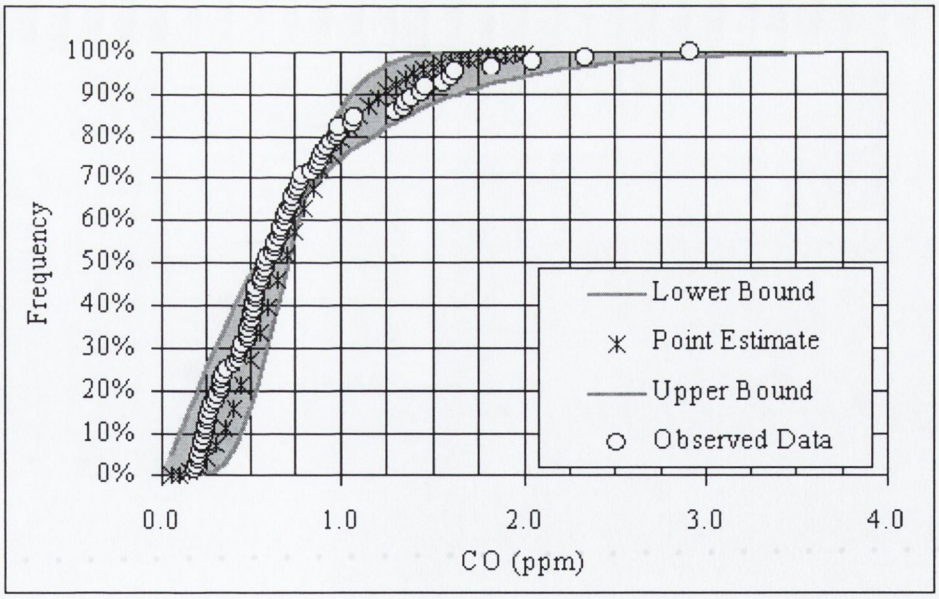

Figure 7.39 Predicted frequency distribution of 8-hour CO averages for January 1999, calculated using 3 days of monitoring data between 17:00 and 18:00

7.5.5 8-Hour Averages – Nitrogen Dioxide

Results of the frequency distribution estimation based on three days of data (24-hour/day and data collected between 17:00 and 18:00) for August 1998 and January 1999 are shown in Figure 10.9 to Figure 10.12, in Appendix C.

The observed concentrations are within the confidence intervals calculated using 24 hours of data for both August 1998 and January 1999, with the observed frequency distribution for August 1998 nearer the upper bound, and the observed frequency distribution for January 1999 nearer the lower bound. Estimated confidence intervals based on data collected between 17:00 and 18:00 for each of the three sampling days bound the observed frequency distribution for August 1998, but overestimate the 95^{th} to 100^{th} percentiles for January 1999.

7.5.6 8-Hour Averages – PM_{10}

The 8-hour average PM_{10} concentrations for August 1998 were found to be within the predicted confidence intervals. However, as with the 24-hour values, the higher percentiles for February 1998 are fractionally underpredicted. For predictions based on data collected between 17:00 and 18:00, the observed 8-hour concentrations for both August 1998 and February 1998 are within the predicted confidence intervals. The observed distribution is well matched by the predicted distribution calculated using the point estimate of the standard deviation. The observed and predicted frequency distributions are graphed in Figure 10.13 to Figure 10.16, in Appendix C.

7.5.7 1-Hour Averages – Carbon Monoxide

The equivalent analysis was repeated to predict the frequency distribution of the 1-hour concentrations recorded over each month. For the predictions using average 24-hour observed concentrations, a randomly chosen sample of 1-hour averages from the three days of recorded data was used to estimate the standard deviation. For the predictions based on the data

measured between 17:00 and 18:00, the standard deviations were calculated using the predicted mean and relative standard deviations calculated from 1 week of data, recorded previously.

1-hour Average Concentration Predictions Calculated using 3 x 24 hour s/day

Results for 1-hour averages were found to be similar to results for the 24-hour and 8-hour averages. High percentiles were slightly underpredicted for August 1998, although the observed frequency distribution for January 1999 was within the calculated limits, and are illustrated in Figure 7.40 and Figure 7.41, respectively.

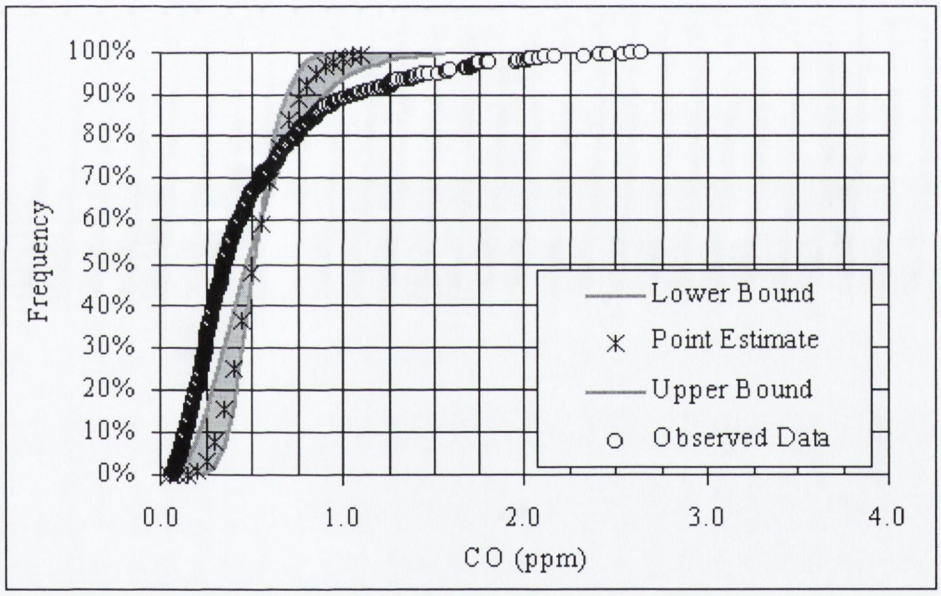

Figure 7.40 Predicted frequency distribution of 1-hour CO averages for August 1998, calculated using 3 complete days of monitoring.

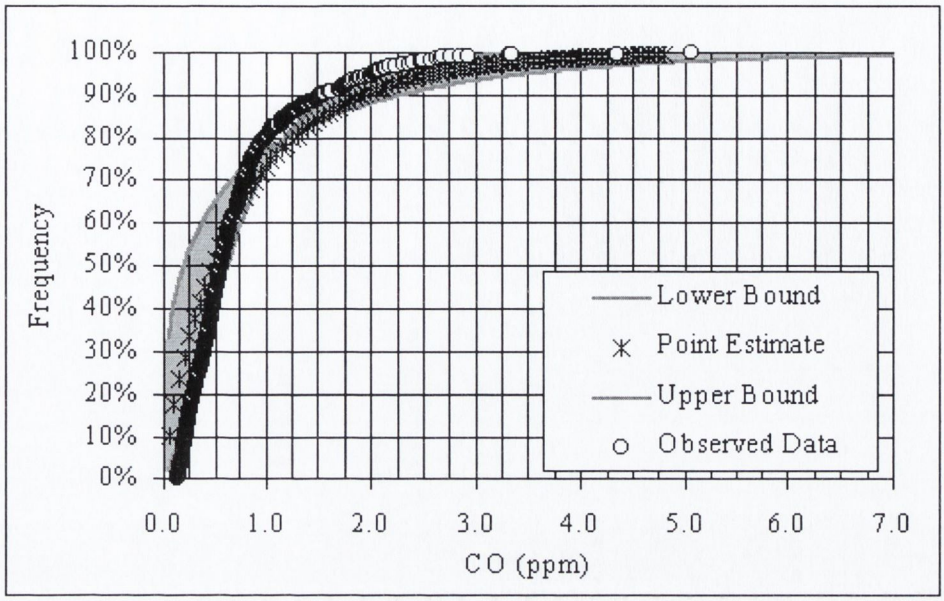

Figure 7.41 Predicted frequency distribution of 1-hour CO averages for January 1999, calculated using 3 complete days of monitoring.

1-hour Average Concentration Predictions Calculated using 3 x 1 hour/day (17:00-18:00)

The predicted frequency distributions of 1-hour concentrations are shown in Figure 7.42 and Figure 7.43. The recorded distributions are seen to be within the calculated confidence intervals, and match the distribution calculated with the point estimate of the standard deviation well.

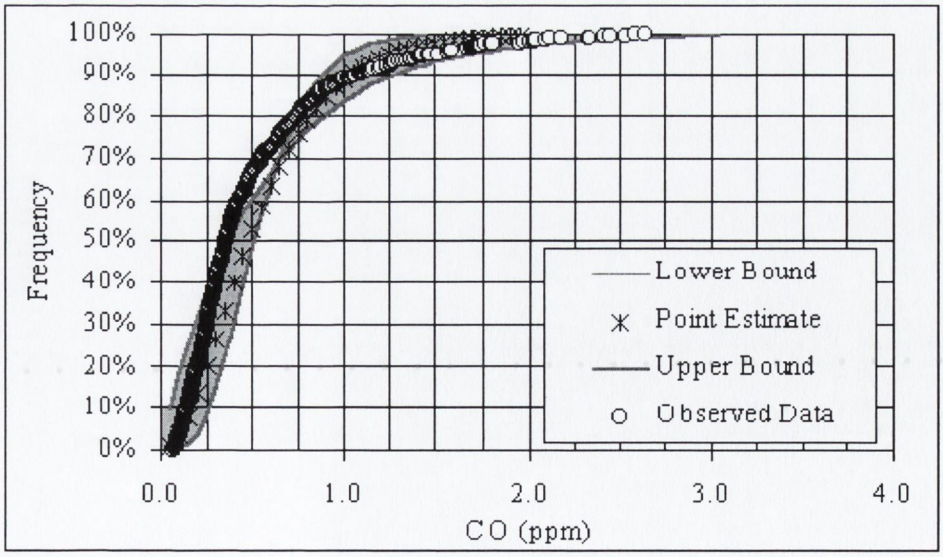

Figure 7.42 Predicted frequency distribution of 1-hour CO averages for August 1998, calculated using 3 days of monitoring data between 17:00 and 18:00

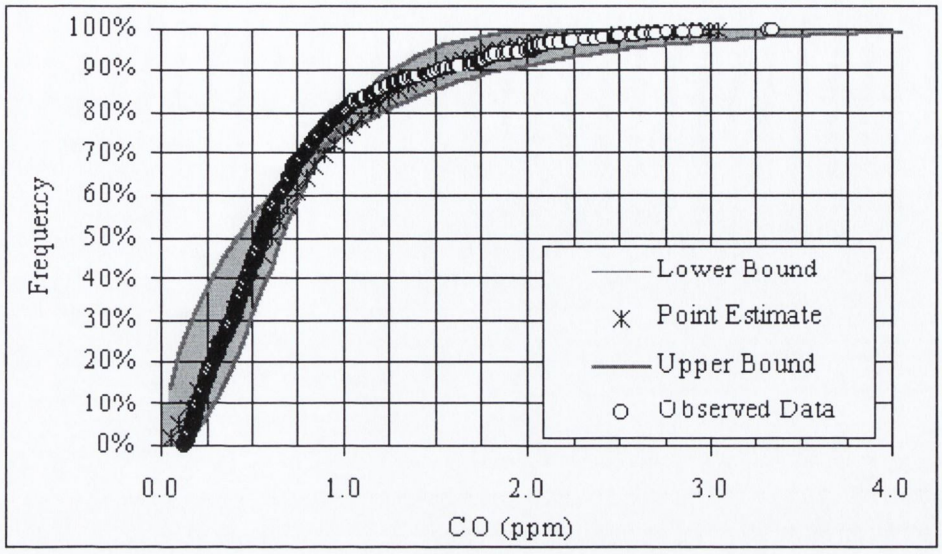

Figure 7.43 Predicted frequency distribution of 1-hour CO averages for January 1999, calculated using 3 days of monitoring data between 17:00 and 18:00

7.5.8 1-Hour Averages – Nitrogen Dioxide

The observed frequency distributions of the hourly NO_2 concentrations are distorted due to the poor resolution of the instrument, as already seen in Figure 4.8. This poor resolution means that during average conditions at this site, the instrument tends to read either 20 ppb or 30 ppb. This gives the frequency distribution a 'stepped' appearance.

Despite the lack of a smooth observed distribution curve, all values within the 80^{th} and 100^{th} percentiles are within the predicted confidence intervals for August 1998. The stepped appearance of the graph has a greater effect on the accuracy of the prediction for January 1999, when only the very highest percentiles fall within the confidence intervals. Predictions based on sampling between 17:00 and 18:00 are also affected. However, all values between the 80^{th} to 100^{th} percentiles are within the calculated confidence intervals for August 1998, as are those between the 96^{th} to 100^{th} percentiles for January 1999. The observed and predicted frequency distributions are graphed in Figure 10.17 to Figure 10.20 in Appendix C.

7.5.9 1-Hour Averages – PM_{10}

The results for hourly PM_{10} concentrations are graphed in Figure 10.21 to Figure 10.24 in Appendix C. The observed frequency distribution for August 1998 is within the confidence intervals, although for February 1998, the 90^{th} to 100^{th} percentiles are slightly underpredicted. For predictions based on 1 hour of sampling (17:00 – 18:00) during each of the three days, results are similar, with the observed frequency distribution for August lying within the calculated confidence intervals, and values for February 1998 slightly underpredicted.

7.6 Prediction of Exceedences

7.6.1 Carbon Monoxide

As the limit values for short-term concentrations specified in the EU Daughter Directives of 96/62/EC, are expressed in terms of the numbers of exceedences of each limit value, the number of times a certain concentration is exceeded within a given period is of particular importance. The number of exceedences of a reference concentration (e.g., legislative standard or guideline) can be estimated using the predicted frequency distribution parameters and Equation 6.23.

For 24-hour, 8-hour and 1-hour averages, the estimated numbers of exceedences of two reference values over the course of one month were calculated and compared to the observed number. Predictions are based on 24-hour and one-hour (17:00-18:00) sampling periods for each of three days in the 30-day period, as before.

As recorded concentrations at the monitoring site are less than limit values, lower reference values were also chosen for evaluation of the algorithm. Table 7.10 compares sample predicted and observed values for CO for August 1998 and January 1999. Exceedences are calculated for 8.7 ppm, as this is the rolling 8-hour concentration limit under 96/62/EC, and 2 ppm, as this is one of the higher concentrations measured during both months. No

exceedences of 8.7 ppm for any averaging period was either predicted or recorded. The numbers of exceedences of 2 ppm were within the calculated limits for all averaging periods.

Table 7.10 Predicted and measured number of exceedences of 8.7 ppm and 2 ppm CO during August 1998 and January 1999 at Pearse St./Westland Row Monitoring Site

	Conc ppm		Predictions based on 24 hours			Predictions based on 17:00-18:00			Measured
			Lower Bound	Point Estimate	Upper Bound	Lower Bound	Point Estimate	Upper Bound	
24hr Ave.	8.7	Aug 1998	0	0	0	0	0	0	0
		Jan 1999	0	0	0	0	0	0	0
	2.0	Aug 1998	0	0	1	0	0	2	0
		Jan 1999	0	0	1	0	0	3	0
8hr Ave.	8.7	Aug 1998	0	0	0	0	0	0	0
		Jan 1999	0	0	0	0	0	0	0
	2.0	Aug 1998	0	0	0	0	0	3	0
		Jan 1999	0	2	8	0	0	5	3
1hr Ave.	8.7	Aug 1998	0	0	0	0	0	0	0
		Jan 1999	0	0	3	0	0	0	0
	2.0	Aug 1998	0	0	0	0	3	21	14
		Jan 1999	35	65	85	7	28	64	39

7.6.2 Nitrogen Dioxide

For NO_2, exceedences of 104 ppb and 50 ppb were investigated (Table 7.11). The limit values for NO_2 under 96/62/EC are expressed in terms of hourly breaches of 104 ppb. No exceedences of this concentration were recorded or predicted during the months analysed. Exceedences of 50 ppb were then investigated, as this concentration was reached several times over the course of the two months. The recorded number of exceedences of 50 ppb were within the predicted upper and lower bounds for all averaging periods, using both sampling periods.

Table 7.11 Predicted and measured number of exceedences of 104 ppb and 50 ppb NO_2 during August 1998 and January 1999 at Pearse St./Westland Row Monitoring Site

	Conc ppb		Predictions based on 24 hours			Predictions based on 17:00-18:00			Measured
			Lower Bound	Point Estimate	Upper Bound	Lower Bound	Point Estimate	Upper Bound	
24hr Ave.	104	Aug 1998	0	0	0	0	0	0	0
		Jan 1999	0	0	0	0	0	0	0
	50	Aug 1998	0	0	2	0	0	0	0
		Jan 1999	0	1	4	0	1	4	0
8hr Ave.	104	Aug 1998	0	0	0	0	0	0	0
		Jan 1999	0	0	0	0	0	0	0
	50	Aug 1998	0	0	1	0	0	1	1
		Jan 1999	0	0	0	0	0	0	0
1hr Ave.	104	Aug 1998	0	0	0	0	0	0	0
		Jan 1999	0	0	0	0	0	0	0
	50	Aug 1998	0	2	23	0	4	32	10
		Jan 1999	0	0	6	0	0	10	0

7.6.3 PM_{10}

The equivalent calculations are carried out for PM_{10} for concentrations of 50 $\mu g/m^3$ and 40 $\mu g/m^3$. As the limit value for PM_{10} is defined in terms of exceedences of a daily average of 50 $\mu g/m^3$, this reference value was investigated. The recorded number of exceedences of 50 $\mu g/m^3$ were outside the predicted intervals for 1-hour averages recorded during August 1998, as were the 8-hour averages on one occasion (Table 7.12). The high number of exceedences (17) of 40 $\mu g/m^3$ for hourly averages recorded in August 1998 was also not predicted.

Table 7.12 Predicted and measured number of exceedences of 50 μg/m^3 and 40 μg/m^3 PM_{10} during August 1998 and January 1999 at Pearse St./Westland Row Monitoring Site

	PM_{10} μg/m^3		Predictions based on 24 hours			Predictions based on 17:00-18:00			Measured
			Lower Bound	Point Estimate	Upper Bound	Lower Bound	Point Estimate	Upper Bound	
24hr Ave.	50	Aug 1998	0	0	0	0	0	3	0
		Jan 1999	0	0	2	0	0	2	0
	40	Aug 1998	0	0	0	0	0	4	0
		Jan 1999	0	0	2	4	6	10	0
8hr Ave.	50	Aug 1998	0	0	0	0	0	1	1
		Jan 1999	0	0	1	0	0	1	0
	40	Aug 1998	0	0	0	0	0	4	1
		Jan 1999	0	0	1	2	5	10	0
1hr Ave.	50	Aug 1998	0	0	0	0	0	9	17
		Jan 1999	0	2	20	1	1	5	1
	40	Aug 1998	0	0	3	0	3	2	17
		Jan 1999	0	0	20	24	4	25	5

7.7 Application of Existing Persistence Factors

The persistence factors recommended by the US EPA (US EPA, 1992) and by Cooper et al. (1992) were used to estimate 8-hour CO concentrations for August 1998 and January 1999 at the Pearse St./Westland Row intersection (Site A). The persistence factors used are (a) 0.59 – calculated using the data recorded at the site, according to the US EPA guidelines, as discussed in Section 2.1.7; (b) 0.7 – the US EPA default value and (c) 0.55 – (Cooper, 1992). The maximum and average 8-hour concentrations were estimated using three days of data for August 1998 and January 1999 and are contrasted with the results calculated using the prediction algorithm, in Figure 7.44 and Figure 7.45, respectively. All three persistence factors give similar results, and displayed reduced accuracy when compared to the prediction algorithm, with the exception of the maximum CO concentration predicted for August 1998.

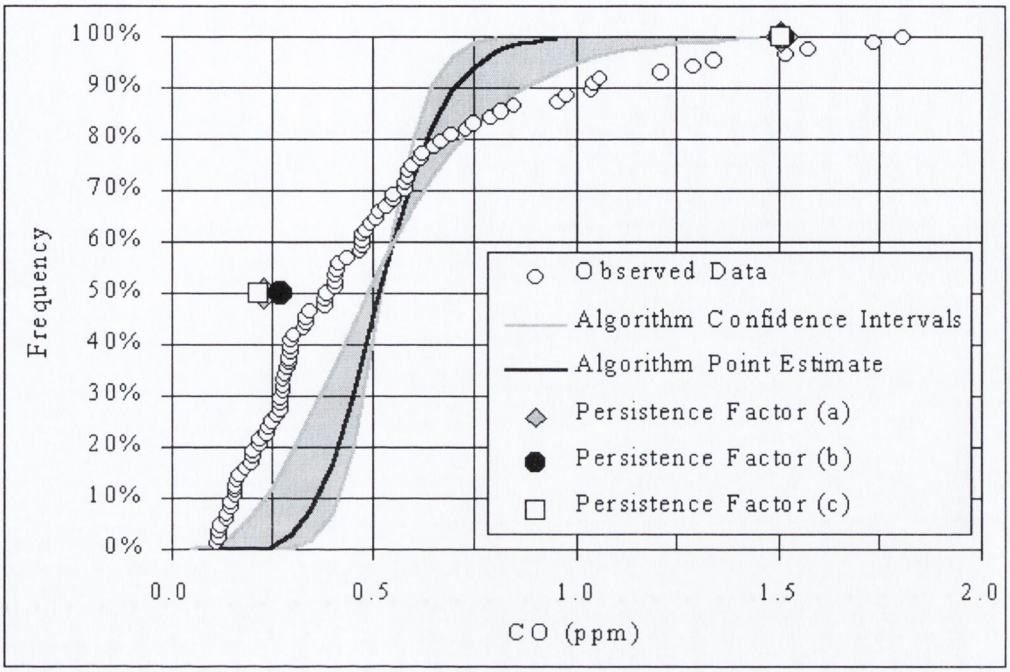

Figure 7.44 Comparison of persistence factor based 8-hour average and maximum CO predictions and algorithm results for August 1998

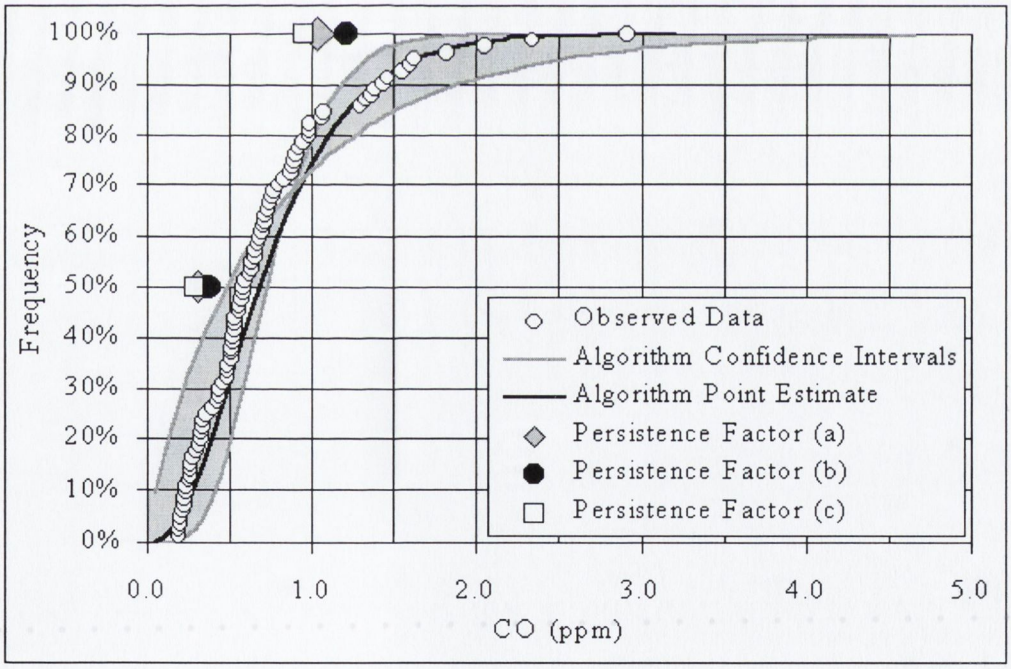

Figure 7.45 Comparison of persistence factor based 8-hour average and maximum CO predictions and algorithm results for January 1999

The performance of the US EPA factor recommended factor (a) is investigated in greater detail in Figure 7.46 to Figure 7.49. Using three complete days of monitoring, the frequency distribution of the 8-hour average concentrations was estimated by applying the persistence factor to the measured 1-hour concentrations for August 1998 and January 1999. This is contrasted with the results of the prediction algorithm in Figure 7.46 and Figure 7.47. The prediction algorithm is seen to perform significantly better, particularly in the 95% to 99% range, with the exception of the prediction of the maximum 8-hour concentration during August 1998.

The results of the equivalent predictions for August 1998 and November 1999 based on monitoring between 17:00 and 18:00 only, are shown in Figure 7.48 and Figure 7.49. The amount of information provided by the persistence factor calculation is less than that given by the algorithm prediction. The superiority of the prediction algorithm is highlighted further, as the performance of the persistence factors is seen to deteriorate with the decrease in input information.

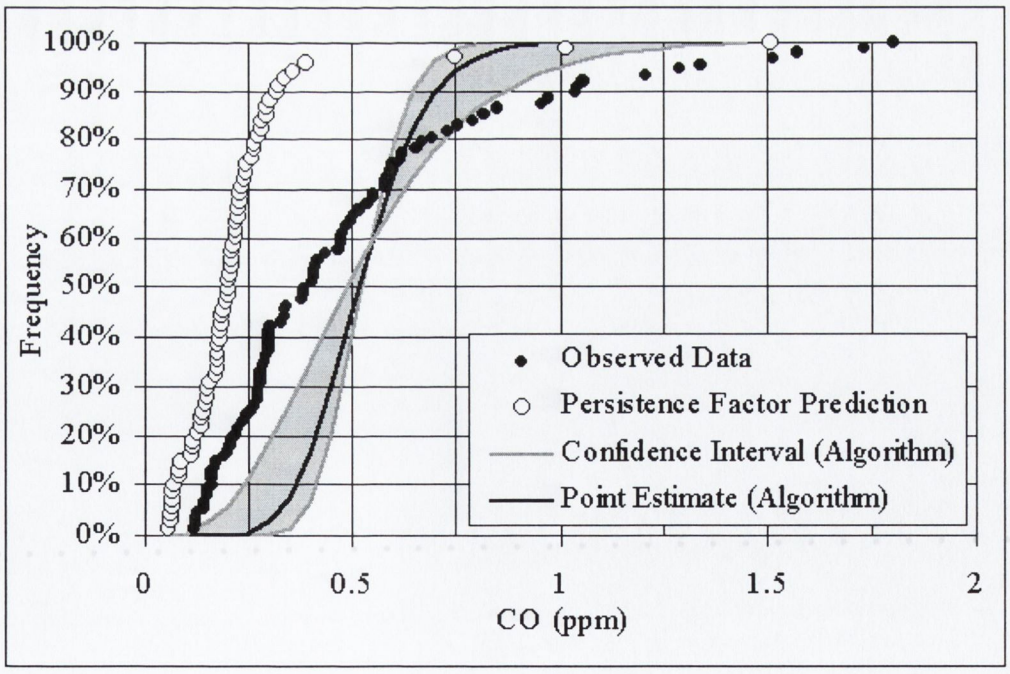

Figure 7.46 Comparison of US EPA persistence factor 8-hour CO predictions and algorithm results for August 1998, calculated using three complete days of monitoring

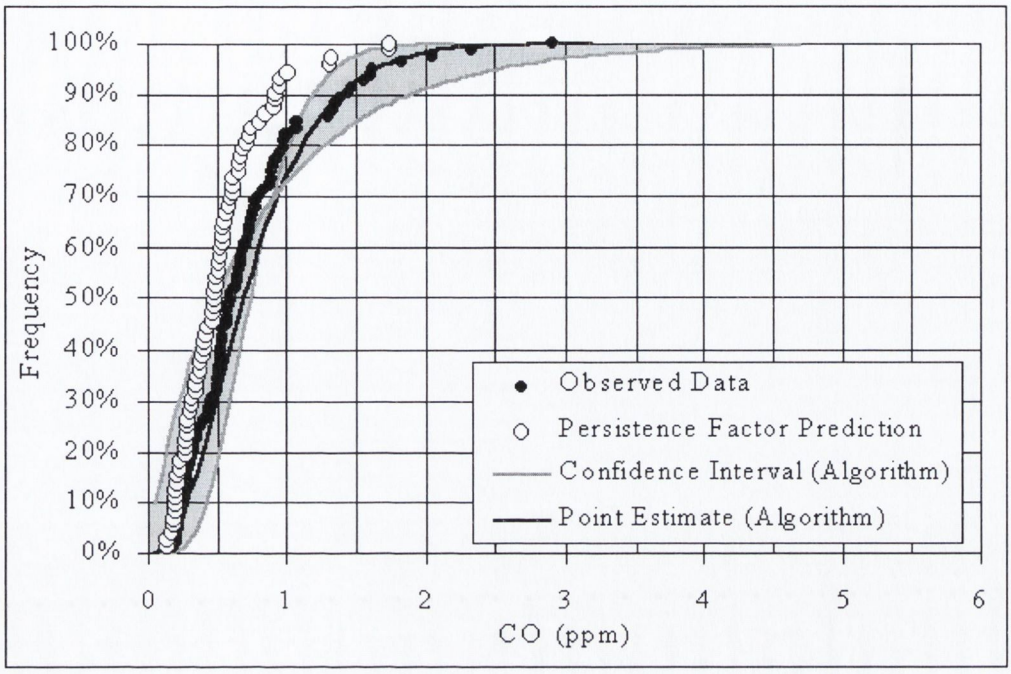

Figure 7.47 Comparison of US EPA persistence factor 8-hour CO predictions and algorithm results for January 1999, calculated using three complete days of monitoring

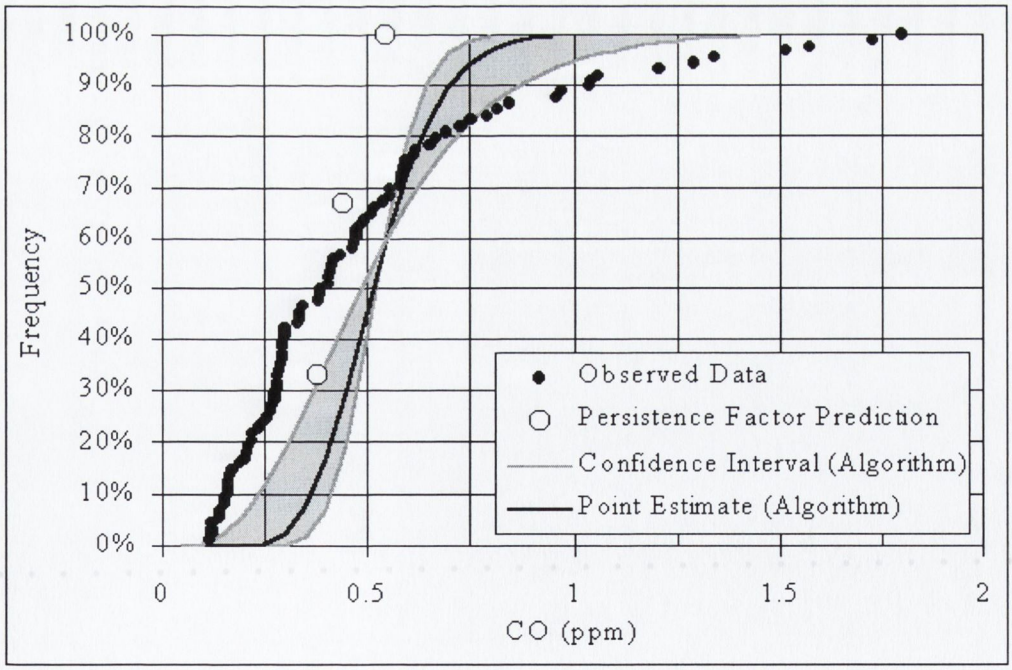

Figure 7.48 Comparison of US EPA persistence factor 8-hour CO predictions and algorithm results for August 1998 calculated using three days of monitoring between 17:00 and 18:00

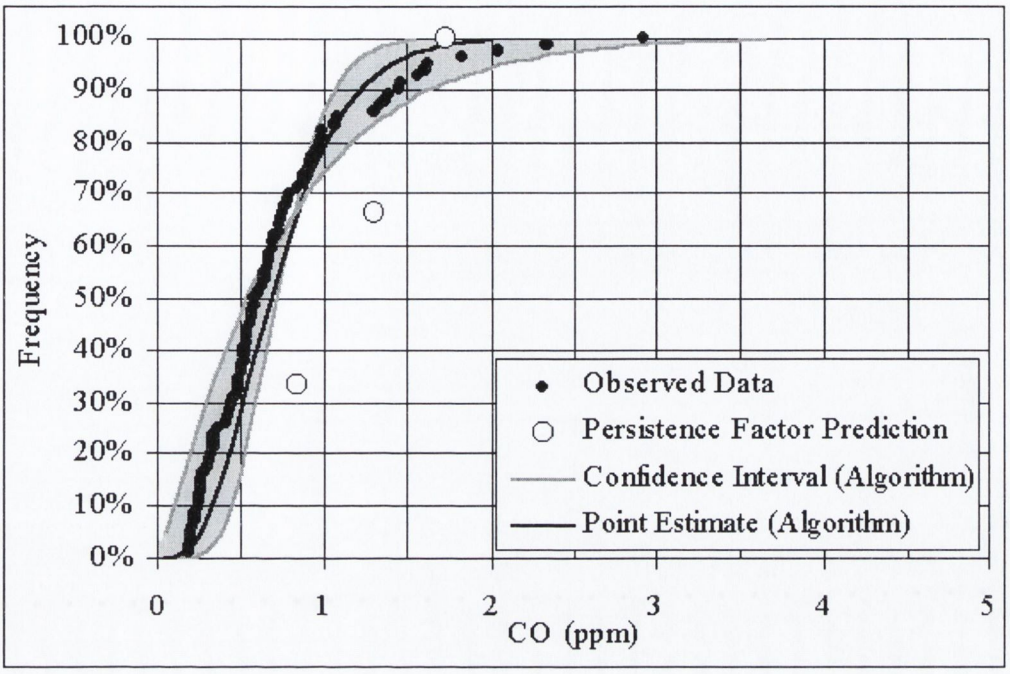

Figure 7.49 Comparison of US EPA persistence factor 8-hour CO predictions and algorithm results for January 1999 calculated using three days of monitoring between 17:00 and 18:00

7.8 Summary of Site A, Phase 1 Concentration Predictions

7.8.1 Summary of Site A, Phase 1 Carbon Monoxide Predictions

Table 7.13 summarises the sample results presented in Section 7.1. The predicted results have been assessed in 5 percentile increments from 70 to 100 to determine whether or not the observed data were within the predicted confidence intervals. The upper percentiles are important to investigate compliance with legislative guidelines and standards. As can be seen, only two cases were outside the predicted confidence intervals, the 70^{th} and 75^{th} percentile for January 1999, where 24 hours of monitoring data were used for the prediction interval. However, the same prediction using input data measured between 17:00 and 18:00 does fall within the confidence intervals. These sample results were seen to be representative of the complete data set. However, it should be borne in mind that the prediction of the monthly average is of crucial importance to the accuracy of the prediction method, as any under- or

over prediction transforms the predicted frequency distribution along the x-axis, resulting in errors in the extreme event prediction. A passive sampler, such as that described in Lee *et al.* (1992), could also be used to cheaply measure the long-term average, and thereby reduce possible errors encountered in the prediction process. The results could then be combined with short periods of monitoring at a higher resolution, and the peak 1-hour, 8-hour and 24-hour concentrations predicted in the manner outlined.

Table 7.13 Summary of prediction accuracy for upper percentiles for 24-hour CO averages

	August 1998		January 1999	
Percentile	**24 hours**	**17:00 - 18:00**	**24 hours**	**17:00 - 18:00**
70	Within Limits	Within Limits	*Outside Limits*	Within Limits
75	Within Limits	Within Limits	*Outside Limits*	Within Limits
80	Within Limits	Within Limits	Within Limits	Within Limits
85	Within Limits	Within Limits	Within Limits	Within Limits
90	Within Limits	Within Limits	Within Limits	Within Limits
95	Within Limits	Within Limits	Within Limits	Within Limits
100	Within Limits	Within Limits	Within Limits	Within Limits

Table 7.14 summarises the results of the frequency distribution calculation for 8-hour averages. A slightly reduced level of accuracy is visible. The August 1998 80^{th} to 100^{th} percentiles are not well predicted by the calculations using full days of 24-hours monitoring data for the calculation. However, for both months, the observed frequency distributions calculated using data recorded between 17:00 and 18:00 were within the calculated frequency intervals for almost all values, and were well matched by the frequency distribution calculated using the point estimate of the standard deviation.

Table 7.14 Summary of prediction accuracy for upper percentiles for 8-hour CO averages

	August 1998		January 1999	
Percentile	**24 hours**	**17:00 - 18:00**	**24 hours**	**17:00 - 18:00**
70	Within Limits	*Outside Limits*	*Outside Limits*	Within Limits
75	Within Limits	*Outside Limits*	*Outside Limits*	Within Limits
80	*Outside Limits*	Within Limits	Within Limits	Within Limits
85	*Outside Limits*	Within Limits	Within Limits	Within Limits
90	*Outside Limits*	Within Limits	Within Limits	Within Limits
95	*Outside Limits*	Within Limits	Within Limits	Within Limits
100	*Outside Limits*	Within Limits	Within Limits	Within Limits

The equivalent results for 1-hour CO concentrations are presented in Table 7.15. The accuracy of the prediction method has decreased further; however, the 90th, 95th and 100th percentiles are within the predicted intervals for three out of the four cases.

Table 7.15 Summary of prediction accuracy for upper percentiles for 1-hour CO averages

	August 1998		January 1999	
Percentile	**24 hours**	**17:00 - 18:00**	**24 hours**	**17:00 - 18:00**
70	Within Limits	*Outside Limits*	*Outside Limits*	*Outside Limits*
75	Within Limits	*Outside Limits*	*Outside Limits*	*Outside Limits*
80	Within Limits	Within Limits	Outside Limits	Within Limits
85	*Outside Limits*	Within Limits	Outside Limits	Within Limits
90	*Outside Limits*	Within Limits	Within Limits	Within Limits
95	*Outside Limits*	Within Limits	Within Limits	Within Limits
100	*Outside Limits*	Within Limits	Within Limits	Within Limits

Judging from the above results, the prediction methodology is seen, in many cases, to be a useful tool for characterising CO levels at an urban roadside site. CO levels can be predicted with a good degree of accuracy using a minimum of monitoring (as little as three hours a month) once an initial period of monitoring has been carried out to determine the adjustment factors. For the purpose of predicting extreme concentrations, monitoring for 24 hours did not result in a consistent improvement over monitoring for one hour. As seen in Section 7.6.1, the number of expected exceedences of legislative limits can also be calculated. The method is seen to eliminate the need for conditions at the time of short-term monitoring to be representative of long-term conditions at the site.

7.8.2 Summary of Site A, Phase 1 Nitrogen Dioxide Predictions

The results of the distribution prediction for 24-hour average NO_2 concentrations are tabulated in Table 7.16. As can be seen in the table, the observed frequency distributions are predicted with a good degree of accuracy for August 1998 by the calculations using both sets of input data. The observed concentrations for January 1999 are within the predicted confidence intervals for the predictions using the data collected between 17:00 and 18:00 for each percentile interval examined. For the predictions based on 24-hours of data each day, the 70th,

75th, 80th, and 85th percentile estimations are outside the predicted confidence intervals due to the monthly average concentration being underestimated. However, as mentioned before, the higher percentiles are of more importance.

Table 7.16 Summary of prediction accuracy for upper percentiles for 24-hour NO_2 averages

	August 1998		January 1999	
Percentile	**24 hours**	**17:00 - 18:00**	**24 hours**	**17:00 - 18:00**
70	Within Limits	*Outside Limits*	*Outside Limits*	Within Limits
75	Within Limits	Within Limits	*Outside Limits*	Within Limits
80	Within Limits	Within Limits	*Outside Limits*	Within Limits
85	Within Limits	Within Limits	*Outside Limits*	Within Limits
90	Within Limits	Within Limits	Within Limits	Within Limits
95	Within Limits	Within Limits	Within Limits	Within Limits
100	Within Limits	Within Limits	Within Limits	Within Limits

Table 7.17 summarises the accuracy of the average 8-hour NO_2 concentration frequency distribution calculations. The prediction algorithm and methodology are seen to perform very well with the observed frequency distributions within the calculated confidence intervals for all but two points.

Table 7.17 Summary of prediction accuracy for upper percentiles for 8-hour NO_2 averages

	August 1998		January 1999	
Percentile	**24 hours**	**17:00 - 18:00**	**24 hours**	**17:00 - 18:00**
70	Within Limits	Within Limits	Within Limits	Within Limits
75	Within Limits	Within Limits	Within Limits	Within Limits
80	Within Limits	Within Limits	Within Limits	Within Limits
85	Within Limits	Within Limits	Within Limits	Within Limits
90	Within Limits	Within Limits	Within Limits	Within Limits
95	Within Limits	Within Limits	Within Limits	*Outside Limits*
100	Within Limits	Within Limits	Within Limits	*Outside Limits*

The equivalent results for 1-hour average concentrations of NO_2 are presented in Table 7.18. Despite the distortion of the observed frequency distribution caused by the poor resolution of the instrument, the observed distribution for August 1998 lies within the predicted confidence intervals for all percentiles other than the 70th. In contrast, only the 100th percentile for

January 1999 is within the confidence intervals, as, in this case, the stepped shape of the graph does cause the lower percentile values to lie outside the calculated frequency distributions.

Table 7.18 Summary of prediction accuracy for upper percentiles for 1-hour NO_2 averages

	August 1998		January 1999	
Percentile	**24 hours**	**17:00 - 18:00**	**24 hours**	**17:00 - 18:00**
70	*Outside Limits*	*Outside Limits*	*Outside Limits*	*Outside Limits*
75	Within Limits	Within Limits	*Outside Limits*	*Outside Limits*
80	Within Limits	Within Limits	*Outside Limits*	*Outside Limits*
85	Within Limits	Within Limits	*Outside Limits*	*Outside Limits*
90	Within Limits	Within Limits	*Outside Limits*	*Outside Limits*
95	Within Limits	Within Limits	*Outside Limits*	Within Limits
100	Within Limits	Within Limits	Within Limits	Within Limits

As for CO, it is seen that there is a capacity for long-term NO_2 concentrations and extreme events to be estimated with a minimum of monitoring, and also the number of breaches of legislative guidelines in a certain period (Section 7.6.2). NO_2 levels, both long-term average and peak concentrations can be estimated on an ongoing basis using as little as three hours monitoring a month, the selection of these hours being of little relevance. However, as can be seen in Table 7.18 the measured concentrations can fall significantly outside the estimated interval.

7.8.3 Summary of Site A, Phase 1 PM_{10} Predictions

A summary of the accuracy of the prediction method for 24-hour PM_{10} concentrations for the two chosen sample months (August 1998 and February 1998) is given in Table 7.19. January 1999 was not used as a sample month, because no PM_{10} data was recorded between the 12^{th} and 19^{th} January 1999. As can be seen for August 1998, the observed concentration frequency distribution falls outside the predicted confidence intervals only once (the 70^{th} percentile for 24-hours monitoring input). For February 1998, the observed frequency distribution is outside the predicted bounds on three occasions: the 90^{th}, 95^{th}, and 100^{th} percentiles calculated using 24 hours of data for each of the three monitoring days.

Rainfall is known to decrease PM_{10} concentrations through washout (Harrison, 1996). However, rainfall data was not available at a sufficiently high resolution to be of use in the prediction algorithm. It is possible that the accuracy of the prediction algorithm for PM_{10} concentrations would therefore be improved by including a rainfall adjustment factor.

Table 7.19 Summary of prediction accuracy for upper percentiles for 24-hour PM_{10} averages

	August 1998		February 1998	
Percentile	**24 hours**	**17:00 - 18:00**	**24 hours**	**17:00 - 18:00**
70	*Outside Limits*	Within Limits	Within Limits	Within Limits
75	Within Limits	Within Limits	Within Limits	Within Limits
80	Within Limits	Within Limits	Within Limits	Within Limits
85	Within Limits	Within Limits	Within Limits	Within Limits
90	Within Limits	Within Limits	*Outside Limits*	Within Limits
95	Within Limits	Within Limits	*Outside Limits*	Within Limits
100	Within Limits	Within Limits	*Outside Limits*	Within Limits

For 8-hour average predictions, the observed frequency distribution falls within the calculated confidence intervals without exception, when one hour of data is used, as shown in Table 7.20. When the confidence intervals are predicted using 24 hours of data, the predictions are slightly less accurate, with the 80^{th} percentile for August 1998 being outside the predicted bounds, as well as the upper percentiles for February 1998. However, it was seen in Section 7.1.3 that the mean absolute error in the prediction of the monthly average could be almost as large as 25%. If the predictions of the short-term averages were based on a monthly average with a large error, then the accuracy of the short-term averages would also be affected.

Table 7.20 Summary of prediction accuracy for upper percentiles for 8-hour PM_{10} averages

	August 1998		February 1998	
Percentile	**24 hours**	**17:00 - 18:00**	**24 hours**	**17:00 - 18:00**
70	Within Limits	Within Limits	Within Limits	Within Limits
75	Within Limits	Within Limits	Within Limits	Within Limits
80	*Outside Limits*	Within Limits	Within Limits	Within Limits
85	Within Limits	Within Limits	*Outside Limits*	Within Limits
90	Within Limits	Within Limits	*Outside Limits*	Within Limits
95	Within Limits	Within Limits	*Outside Limits*	Within Limits
100	Within Limits	Within Limits	*Outside Limits*	Within Limits

The summary of the 1-hour average PM_{10} concentrations is presented in Table 7.21. Again, a high level of accuracy is seen, with the observed frequency distributions being outside the predicted bounds on a few occasions only.

Table 7.21 Summary of prediction accuracy for upper percentiles for 1-hour PM_{10} averages

	August 1998		February 1998	
Percentile	**24 hours**	**17:00 - 18:00**	**24 hours**	**17:00 - 18:00**
70	Within Limits	Within Limits	Within Limits	Within Limits
75	Within Limits	Within Limits	Within Limits	Within Limits
80	Within Limits	Within Limits	Within Limits	Within Limits
85	Within Limits	Within Limits	Within Limits	Within Limits
90	Within Limits	Within Limits	*Outside Limits*	Within Limits
95	Within Limits	Within Limits	*Outside Limits*	Within Limits
100	Within Limits	Within Limits	*Outside Limits*	*Outside Limits*

Similar observations can be made with respect to PM_{10} as already made for CO and NO_2. The methodology described allows measurements taken over very short periods of time to be used to estimate long-term averages, peak concentrations and the number of breaches of limits (Section 7.6.3).

7.9 Prediction of Monthly Averages Site A (Pearse Street/Westland Row Intersection) Phase 2

In this section, the stability of the adjustment factors with respect to time is analysed by applying the factors calculated during Phase 1 of the monitoring, to the data collected during Phase 2. If the adjustment factors are stable with regard to time then errors of similar magnitudes should be observed in the Phase 2 predictions. An absence of long-term stability in the adjustment factors would limit the applicability of the prediction methodology, and imply increased monitoring to calibrate the model regularly.

7.9.1 Calculation of Monthly Averages – Carbon Monoxide

During Phase 2 of the monitoring, the wind speed and direction monitoring apparatus was located in a slightly different position to that used in Phase 1, as mentioned in Section 3.2. When the resulting wind direction data were analysed, they were observed to have been significantly affected by local turbulence effects, caused by close proximity to a bridge and tree. Consequently, the wind direction readings are unrepresentative of the wind direction at the junction itself, as also reported by Marnane (2000). It was, therefore, impossible to correct the measured data for wind direction.

The average errors in the prediction (unadjusted for wind direction at the time of monitoring) of the 30-day average CO readings are given in Table 7.22. Despite not being able to correct for wind direction, average errors were still under 40%. In order to compare the magnitude of the Phase 2 errors to those calculated for Phase 1, the Phase 1 predictions were recalculated without an adjustment for wind direction. The wind direction adjustment was found to decrease the error by, on average, 37%. A similar improvement for Phase 2 data would result in the average errors being under 25%, which is similar to the magnitude of error in Phase 1 (Section 7.1.1).

Table 7.22 Summary of the 30-day CO concentration predictions errors (unadjusted for wind direction)

Monitoring Period			Arithmetic Average	Prediction (No Wind Direction Adjustment)
24 hours	Pearson's r		0.63	0.59
	RMSE	%	24.2	29.5
	σ_{RMS}	%	26.1	29.9
	MAE	%	20.3	24.7
	σ_{MAE}	%	13.3	16.2
10:00 -16:00	Pearson's r		0.53	0.39
	RMSE	%	37.2	31.4
	σ_{RMS}	%	43.0	30.5
	MAE	%	29.3	26.7
	σ_{MAE}	%	23.0	16.6
10:00 - 11:00	Pearson's r		0.58	0.59
	RMSE	%	38.9	37.6
	σ_{RMS}	%	47.8	32.7
	MAE	%	30.7	33.6
	σ_{MAE}	%	24.2	17.0
13:00 - 14:00	Pearson's r		0.47	0.37
	RMSE	%	41.4	31.1
	σ_{RMS}	%	51.1	34.4
	MAE	%	31.1	25.0
	σ_{MAE}	%	27.6	18.8
17:00 - 18:00	Pearson's r		0.35	0.52
	RMSE	%	109.2	32.3
	σ_{RMS}	%	100.1	33.1
	MAE	%	97.0	27.1
	σ_{MAE}	%	50.7	17.7

7.9.2 Calculation of Monthly Averages – Nitrogen Dioxide

The average errors of the prediction (unadjusted for wind direction) of the average 30-day NO_2 concentrations, for a range of input data, are detailed in Table 7.23. Although the average magnitude of the errors is slightly greater than those calculated for Phase 1, this is partly attributable to the wind data not being representative of conditions at the junction. The predicted values are still markedly more accurate than the simple arithmetic average of the monitored data. This indicates that the adjustment factors may be considered to be stable with respect to time.

Table 7.23 Summary of the 30-day NO_2 concentration predictions errors (unadjusted for wind direction)

Monitoring Period			Arithmetic Average	Prediction (No Wind Direction Adjustment)
24 hours	Pearson's r		0.71	0.72
	RMSE	%	18.6	17.5
	σ_{RMS}	%	22.0	21.1
	MAE	%	14.6	13.8
	σ_{MAE}	%	11.5	10.8
10:00 - 16:00	Pearson's r		0.66	0.65
	RMSE	%	32.1	24.6
	σ_{RMS}	%	34.8	28.8
	MAE	%	26.4	19.8
	σ_{MAE}	%	18.4	14.7
10:00 - 11:00	Pearson's r		0.64	0.66
	RMSE	%	35.4	22.3
	σ_{RMS}	%	37.2	24.4
	MAE	%	29.6	18.5
	σ_{MAE}	%	19.7	12.6
13:00 - 14:00	Pearson's r		0.58	0.56
	RMSE	%	34.0	30.6
	σ_{RMS}	%	41.6	39.2
	MAE	%	27.0	24.1
	σ_{MAE}	%	20.7	18.9
17:00 - 18:00	Pearson's r		0.54	0.53
	RMSE	%	41.0	20.5
	σ_{RMS}	%	43.8	26.3
	MAE	%	34.5	15.3
	σ_{MAE}	%	22.2	13.7

7.9.3 Calculation of Monthly Averages – PM_{10}

The average errors of the calculated predictions (unadjusted for wind direction) of the average 30-day PM_{10} concentrations, for a range of input data, are detailed in Table 7.24. When compared to the r-values calculated for Phase 1, similar values were seen for the arithmetic average, although the r-values of the predictions of the Phase 2 data are consistently significantly higher than those for Phase 1. However, the comparison of magnitudes of the

errors for both Phase 1 (Section 7.1.3) and 2 indicate that the calculated factors are stable with respect to time.

Table 7.24 Summary of the 30-day PM_{10} concentration predictions errors (unadjusted for wind direction)

Monitoring Period			Arithmetic Average	Prediction (No Wind Direction Adjustment)
24 hours	Pearson's r		0.74	0.82
	RMSE	%	23.7	23.4
	σ_{RMS}	%	28.3	24.4
	MAE	%	18.7	19.6
	σ_{MAE}	%	14.7	12.9
10:00 - 16:00	Pearson's r		0.48	0.70
	RMSE	%	55.5	22.4
	σ_{RMS}	%	69.7	29.0
	MAE	%	43.9	17.1
	σ_{MAE}	%	34.3	14.6
10:00 - 11:00	Pearson's r		0.61	0.80
	RMSE	%	61.5	23.8
	σ_{RMS}	%	69.8	23.6
	MAE	%	50.0	20.7
	σ_{MAE}	%	36.2	11.9
13:00 - 14:00	Pearson's r		0.42	0.66
	RMSE	%	49.4	23.0
	σ_{RMS}	%	63.7	24.8
	MAE	%	37.9	19.2
	σ_{MAE}	%	32.1	12.8
17:00 - 18:00	Pearson's r		0.56	0.81
	RMSE	%	39.2	35.1
	σ_{RMS}	%	45.2	31.0
	MAE	%	30.8	31.6
	σ_{MAE}	%	24.5	15.3

7.10 EXTREME EVENT PREDICTION – PHASE 2

7.10.1 24-Hour Averages – Carbon Monoxide

Compared to Phase 1 predictions, a similar degree of accuracy was observed in the predictions of the Phase 2 24-hour concentrations. The results for a representative sample month (August 1999) for calculations using 24 hours and 1 hour (17:00-18:00) of data are shown in Figure 7.50 and Figure 7.51. As for Phase 1, the predictions are based on the gamma distribution. The frequency distribution calculated using the point estimate of the standard deviation matches the observed frequency distribution well, for all percentiles except the highest, which are still within the estimated confidence intervals. This would suggest that once the necessary factors have been calculated for a site, they may remain valid for a significant period of time.

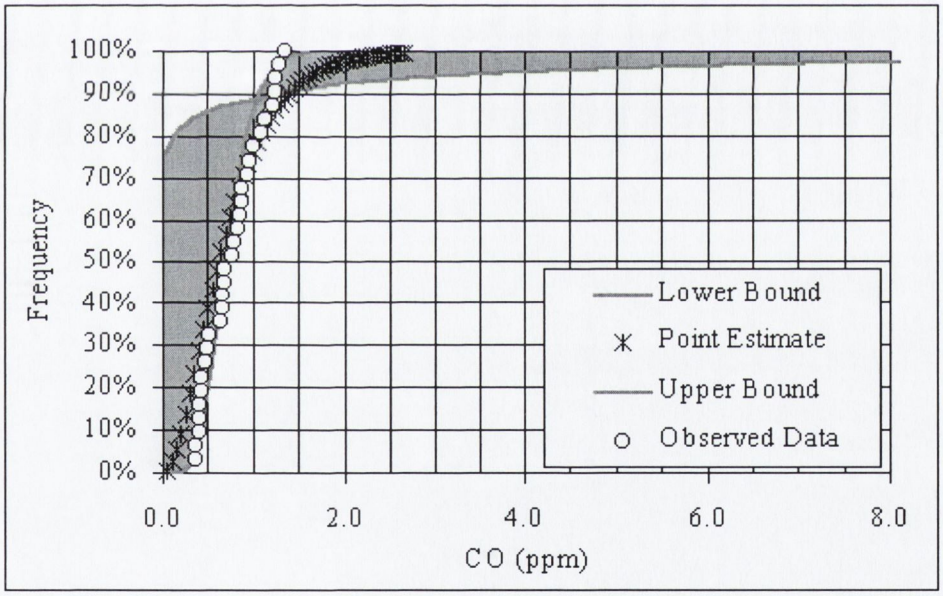

Figure 7.50 Predicted frequency distribution of 24-hour CO averages for August 1999, calculated using 3 complete days of monitoring.

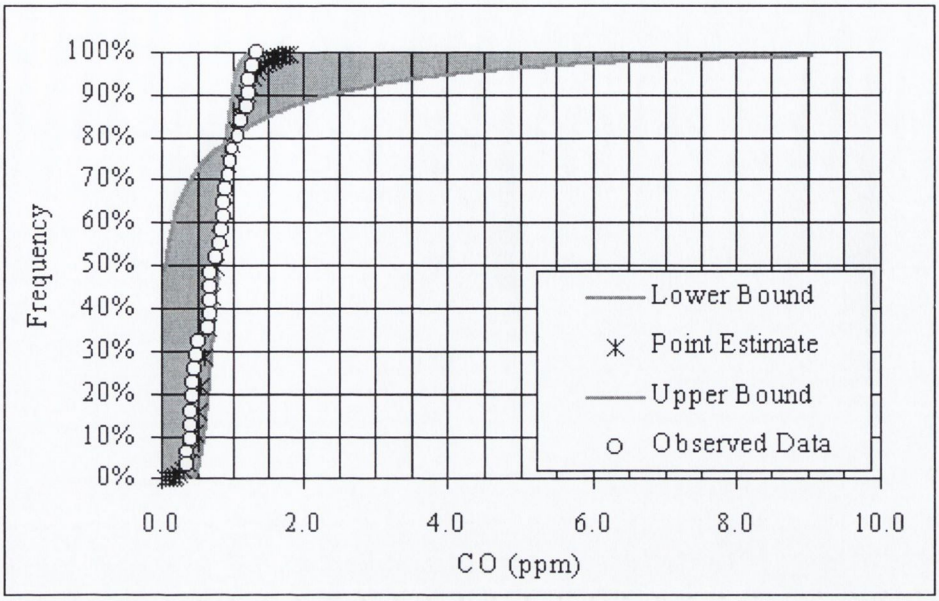

Figure 7.51 Predicted frequency distribution of 24-hour CO averages for August 1999, calculated using 3 days of monitoring data between 17:00 and 18:00

7.10.2 24-Hour Averages – Nitrogen Dioxide

As for CO, the accuracy of the NO_2 frequency distributions for August 1999 is similar to that of the Phase 1 predictions. The point estimate frequency distributions for both types of input (24 hours and 17:00 – 18:00) match the observed frequency distributions well for most percentiles, and the observed frequency distribution is within the estimated confidence intervals for all percentiles (Figure 10.25 and Figure 10.26 in Appendix C).

7.10.3 24-Hour Averages – PM_{10}

As PM_{10} levels were not recorded during August 1999, the results for November 1999 are presented. The observed distribution follows the point estimate standard deviation distribution (based on 24-hour sampling periods), closely up to the 80^{th} percentile. At this point, the two distributions diverge, with the predicted 100^{th} percentile overestimating the observed value by 10 $\mu g/m^3$. In this example, the upper bound significantly overestimates the upper percentiles.

The distributions calculated using data collected between 17:00 and 18:00 overestimate the observed distribution from the 85th percentile upwards, with the upper bound overestimating the highest percentiles very significantly. The results are graphed in Figure 10.27 and Figure 10.28 in Appendix C.

7.10.4 8-Hour Averages – Carbon Monoxide

Similar results were calculated for 8-hour CO averages (Figure 7.52 and Figure 7.53). The point estimate standard deviation prediction approximates the observed frequency well at all percentiles. Again, this would indicate time stability in the adjustment factors.

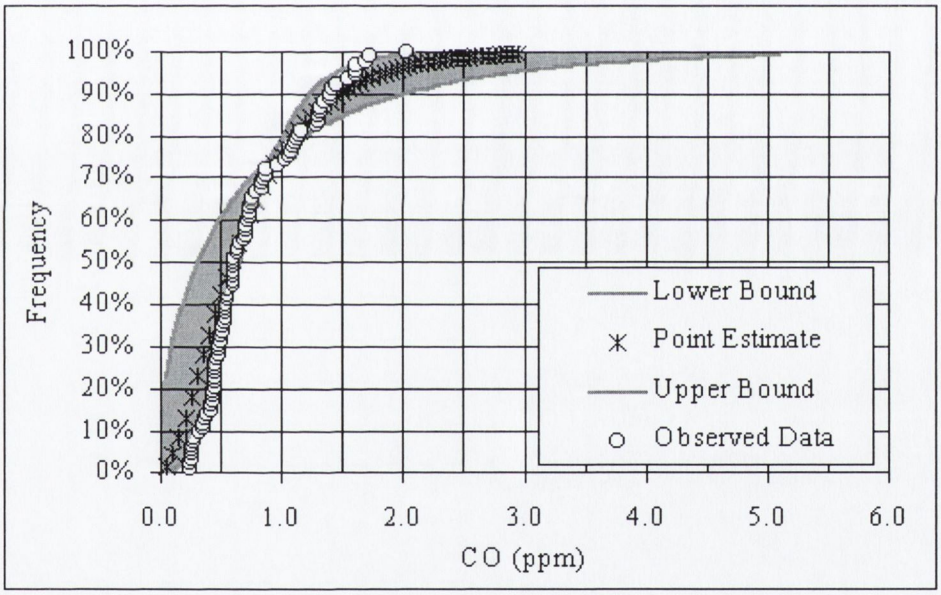

Figure 7.52 Predicted frequency distribution of 8-hour CO averages for August 1999, calculated using 3 complete days of monitoring.

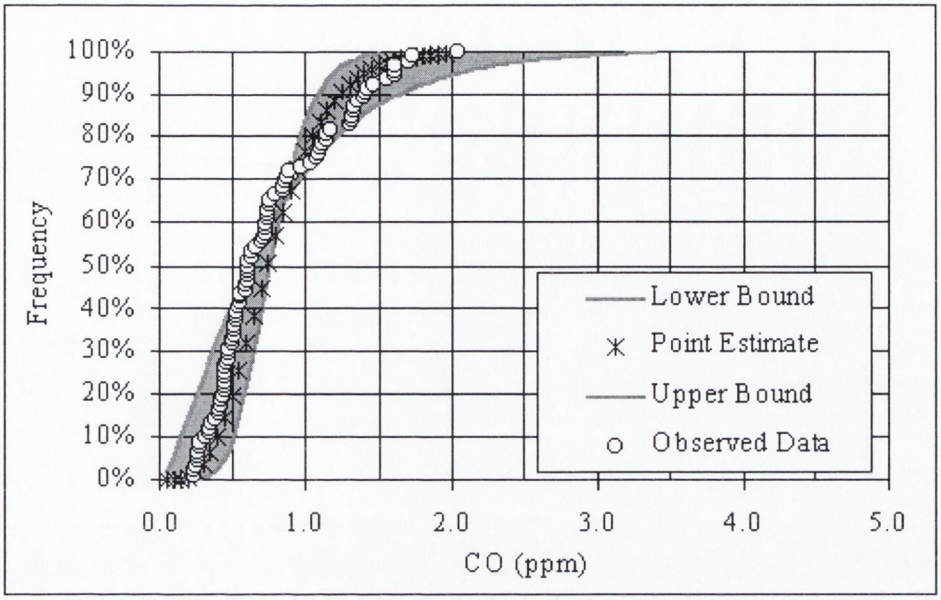

Figure 7.53 Predicted frequency distribution of 8-hour CO averages for August 1999, calculated using 3 days of monitoring data between 17:00 and 18:00

7.10.5 8-Hour Averages – Nitrogen Dioxide

For the sample month of August 1999, the observed frequency distributions of the 8-hour averages are within the predicted bounds (for both sampling periods) at all percentile levels, and are closely approximated by the point estimate frequency distribution, as seen in Figure 10.29 and Figure 10.30, in Appendix C.

7.10.6 8-Hour Averages – PM_{10}

The distribution of the 8-hour PM_{10} averages is approximated more closely by the predicted distributions then that for the 24-hour averages. For estimates calculated using 24 hours of data each day, the observed distribution is within the calculated confidence intervals at all times (Figure 10.31). For estimates calculated using data collected between 17:00 and 18:00, the observed distribution is within the confidence intervals from the 90^{th} percentile upwards, as well as at the lower percentiles (Figure 10.32).

7.10.7 1-Hour Averages – Carbon Monoxide

Again, as shown in Figure 7.54 and Figure 7.55, the frequency distribution predictions using the point estimate standard deviation approximate the observed frequency distributions well.

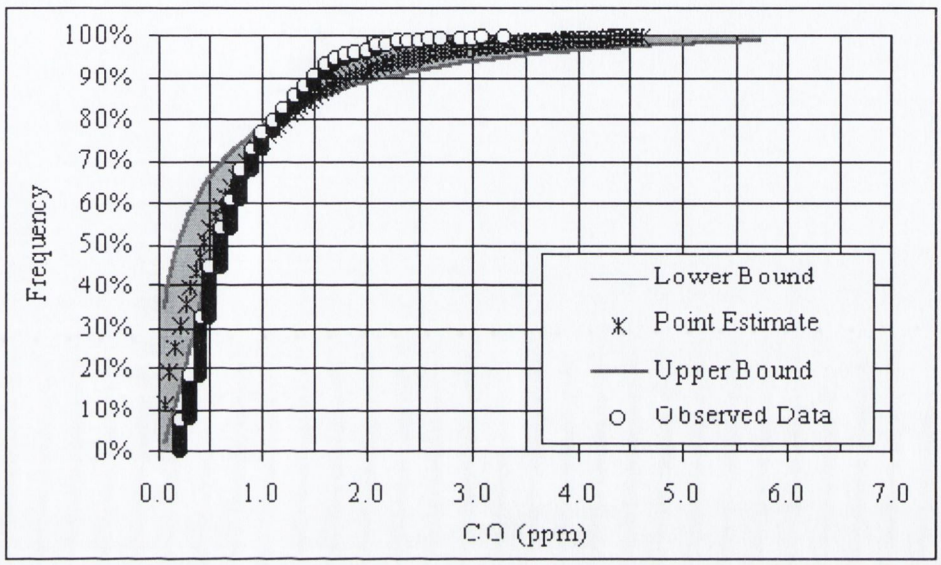

Figure 7.54 Predicted frequency distribution of 1-hour CO averages for August 1999, calculated using 3 complete days of monitoring.

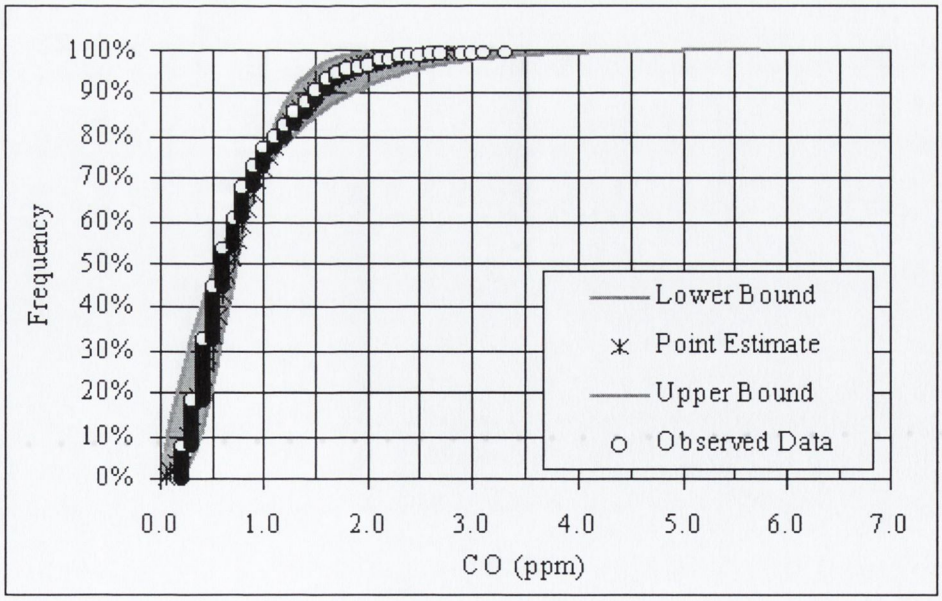

Figure 7.55 Predicted frequency distribution of 1-hour CO averages for August 1999, calculated using 3 days of monitoring data between 17:00 and 18:00

7.10.8 1-Hour Averages – Nitrogen Dioxide

The observed frequency distributions of the 1-hour NO_2 average concentrations are also predicted with a high degree of accuracy (as can be seen in Figure 10.33 and Figure 10.34 in Appendix C). The observed values follow the frequency distribution calculated with the point estimate of the standard deviation almost exactly. This indicates that for the 1-hour averages, as for the 8 hour and 24 hour averages, the frequency distribution can be predicted from a very small sample of data (3 hours of data per month) with a high degree of accuracy, and that the adjustment factors are stable with respect to time.

7.10.9 1-Hour Averages – PM_{10}

For the distribution estimation calculated using 24 hours of data per day, all observed percentiles except the 100^{th} lie within the confidence intervals (Figure 10.35). For the distribution estimates calculated using data collected between 17:00 and 18:00, the lower percentiles and the 90^{th} to 100^{th} percentiles are within the confidence intervals (Figure 10.36).

7.11 Prediction of Exceedences

Table 7.25 summarises the numbers of measured and predicted exceedences of limit values and reference values for CO, NO_2 (August 1999) and PM_{10} (November 1999). The measured number of exceedences of the CO and NO_2 values are within the predicted range on all but one occasion, when the observed number of hourly CO exceedences of 2.0 ppm is slightly overpredicted. The measured number of PM_{10} exceedences is outside the estimated range on five occasions (of twelve), although only by a small margin in most cases.

Table 7.25 Comparison of predicted and measured exceedences of sample values for CO and NO_2 (August 1999) and PM_{10} (November 1999)

	Ave. Period	Conc ppm	Predictions based on 24 hours			Predictions based on 17:00-18:00			Measured
			Lower Bound	Point Estimate	Upper Bound	Lower Bound	Point Estimate	Upper Bound	
CO	**24hr**	**8.7**	0	0	0	0	0	0	0
		2.0	0	1	2	0	0	4	0
	8hr	**8.7**	0	0	0	0	0	0	0
		2.0	1	3	9	0	0	5	1
	1hr	**8.7**	0	0	0	0	0	0	0
		2.0	29	58	79	4	21	59	25
NO_2	**24hr**	**104**	0	0	2	0	0	2	0
		35	0	1	4	0	1	4	0
	8hr	**104**	0	0	1	0	0	1	0
		35	0	3	11	0	3	11	4
	1hr	**104**	0	0	6	0	0	4	0
		35	10	38	84	8	35	83	40
PM_{10}	**24hr**	**50**	0	1	7	5	10	11	6
		40	5	8	9	5	15	18	10
	8hr	**50**	5	12	21	29	31	32	19
		40	27	30	32	36	46	52	33
	1hr	**50**	52	102	154	244	250	255	138
		40	221	245	255	327	380	425	239

7.12 Conclusions on Model Evaluation at Pearse Street/Westland Row Intersection

Short-term indicative monitoring under certain conditions can be problematic in that whenever the conditions at the time of monitoring are not representative of longer-term conditions at the site, then the measured concentrations will not be representative of the typical concentrations.

It was shown in Section 7.1, from data collected during Phase 1, that the effect of conditions at the time of sampling could be mitigated by applying adjustment factors, which improved the estimate of monthly averages. The adjustment factors calculated for the concentration data collected during Phase 1 were applied to Phase 2 with good results, as seen in Section 7.9, indicating that these factors remained stable with respect to time. The Pearson's correlation

coefficients for the predicted and measured monthly averages and the errors expressed as percentages of the measured values are compared in Table 7.26.

Predictions of the monthly CO average were observed to be more accurate for Phase 1 than Phase 2. This is partly attributable to the Phase 2 predictions not being corrected for the wind speed at the time of sampling. Predictions of NO_2 average monthly concentrations are unaffected as NO_2 concentrations were found to be largely independent of wind speed (Section 5.4.2), although the Phase 1 predictions are more accurate. Predictions of PM_{10} concentrations, on the other hand, are more accurate for Phase 2.

Table 7.27 summarises the accuracy of the predictions of the 24-hour, 8-hour and 1-hour concentrations at 5 percentile intervals from the 70^{th} percentile to the 100^{th} percentile, for two sample months for each compound. Results are presented for August 1998 and January 1999, for CO and NO_2, and August 1998 and February 1998 for PM_{10}, (abbreviated to A98, J99, and F98 respectively) for Phase 1, and August 1999 (A99) for Phase 2. The shaded area signifies where the measured concentration was within the predicted limits and the white area signifies where the measured concentration was outside the predicted limits. The algorithm is seen to perform well for all compounds, for both Phase 1 and Phase 2 of the monitoring programme.

In this chapter, predictions of monthly average concentrations and maximum 24-hour, 8-hour and 1-hour concentrations are presented. It has been demonstrated that in many cases predictions of these monthly averages, extreme concentrations and the numbers of exceedences of particular concentrations can be made with a high degree of accuracy, from short monitoring periods, once the recorded data is corrected for the time and conditions at the time of sampling. The adjustment factors calculations and frequency distribution calculation have been shown to be stable with respect to time. The next chapter discusses the extension of the model from an urban junction to urban roadside and canyon sites, and from CO, NO2 and PM_{10} to other pollutants.

Table 7.26 Summary of monthly average predictions for Phases 1 and 2

			CO		NO2		PM10	
Monitoring Period			**Phase 1**	**Phase 2**	**Phase 1**	**Phase 2**	**Phase 1**	**Phase 2**
24 hours	Pearson's r		0.99	0.59	0.96	0.72	0.60	0.72
	RMSE	%	11.1	29.5	5.9	17.5	21.6	17.5
	σ_{RMS}	%	13.8	29.9	6.9	21.1	24.3	21.1
	MAE	%	8.5	24.7	4.8	13.8	17.6	13.8
	σ_{MAE}	%	7.1	16.2	3.5	10.8	12.4	10.8
10:00-16:00	Pearson's r		0.97	0.39	0.91	0.65	0.54	0.65
	RMSE	%	19.5	31.4	9.7	24.6	23.3	24.6
	σ_{RMS}	%	25.0	30.5	10.9	28.8	26.1	28.8
	MAE	%	15.1	26.7	7.9	19.8	19.1	19.8
	σ_{MAE}	%	12.5	16.6	5.6	14.7	13.4	14.7
10:00-11:00	Pearson's r		0.89	0.59	0.88	0.66	0.58	0.66
	RMSE	%	27.9	37.6	13.7	22.3	26.2	22.3
	σ_{RMS}	%	46.5	32.7	18.3	24.4	32.5	24.4
	MAE	%	19.43	33.5	10.5	18.5	20.3	18.5
	σ_{MAE}	%	20.1	17.1	8.9	12.6	16.7	12.6
13:00-14:00	Pearson's r		0.95	0.37	0.80	0.56	0.47	0.56
	RMSE	%	23.6	31.1	13.4	30.7	30.2	30.6
	σ_{RMS}	%	31.9	34.4	15.6	39.2	34.2	39.2
	MAE	%	17.0	25.0	10.9	24.1	24.9	24.1
	σ_{MAE}	%	16.5	18.8	7.9	19.0	17.1	18.9
17:00-18:00	Pearson's r		0.96	0.52	0.94	0.53	0.47	0.53
	RMSE	%	24.7	32.3	8.6	20.5	26.2	20.5
	σ_{RMS}	%	26.0	33.1	9.3	26.3	29.3	26.3
	MAE	%	20.7	27.1	7.0	15.3	21.9	15.3
	σ_{MAE}	%	13.5	17.7	5.0	13.7	14.5	13.7

Table 7.27 Summary of predictions of short-term concentration predictions for Phase 1 and Phase 2 (P2), for August 1998 (A98), January 1999 (J99), August 1999 (A99) and February 1998 (F98).

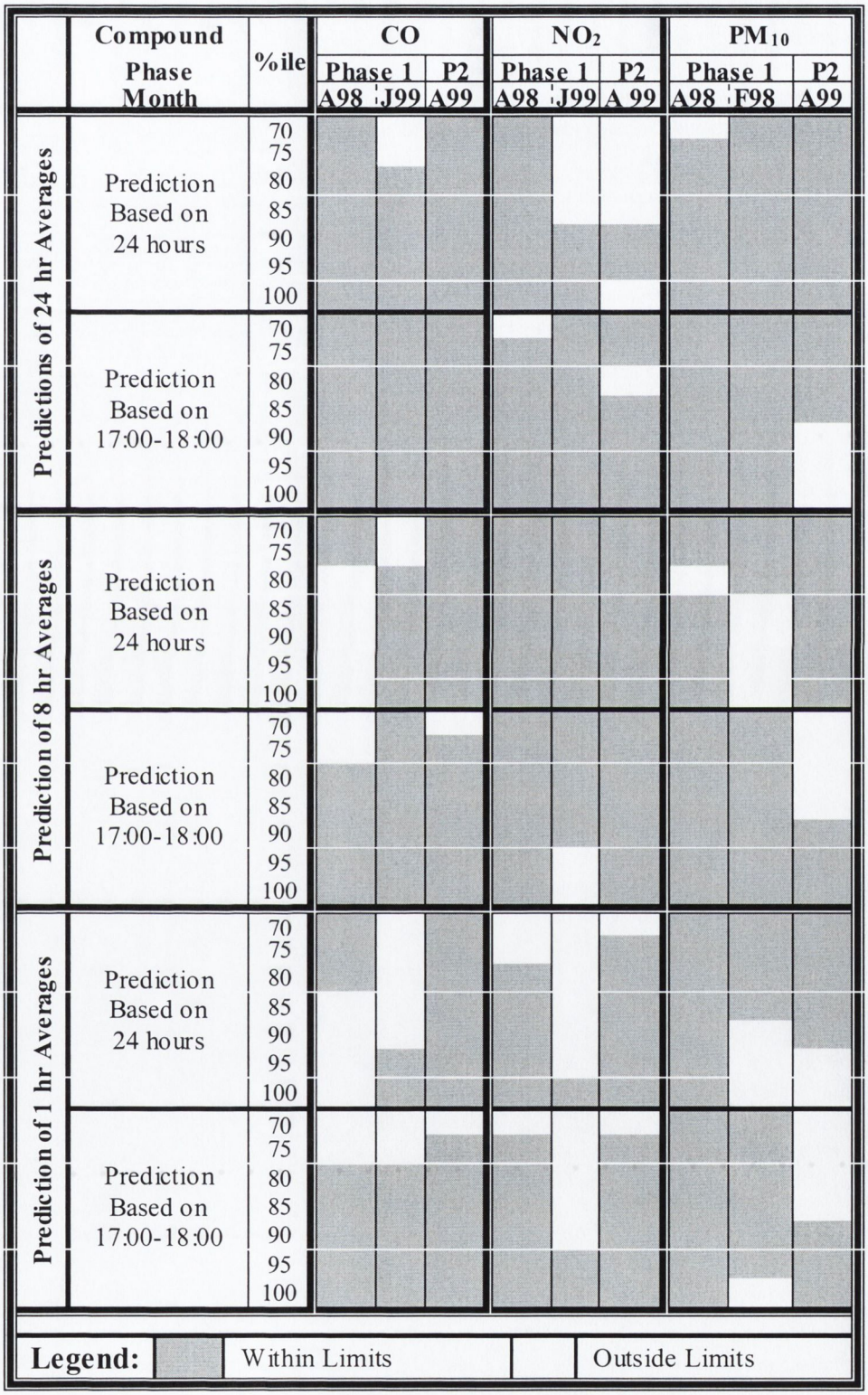

8. EXTENSION AND APPLICATION OF ALGORITHM TO OTHER SITES AND POLLUTANTS

8.1 INTRODUCTION

The accuracy of the prediction algorithm and the application of frequency distributions were established in Chapter 7. Chapter 8 examines the extension of this methodology to other sites and pollutants. The application of the algorithm to roadside and street canyon sites is investigated. The algorithm is also applied to other pollutants measured at the Pearse Street/Westland Row junction (Site A). Finally, a combination of both extensions is investigated by performing NO concentration estimations at the street canyon site. The structure of this chapter is shown diagrammatically in Figure 8.1.

The transferability of the prediction algorithm to other urban roadside sites is analysed and discussed in Section 8.2, using the data recorded at Pearse Street (Site B).

The application of the methodology to street canyons is analysed in Section 8.3 using NO_2 data measured at Westland Row (Site C). The adjustments factors for Westland Row were calculated using only one week of data, randomly selected, to investigate if the algorithm is viable when a large amount of historical data are not available.

Section 8.4 discusses the application of the prediction algorithm to acetylene, 1,3,5-trimethylbenzene, and benzene concentrations at the Pearse St./Westland Row intersection (Site A), again using one week of data for calculation of the adjustment factors.

Section 8.5 covers the extension of the algorithm to other pollutants using nitrogen monoxide at the street canyon (Site C) as an example; as before, one week of data are used to calculate the adjustment factors.

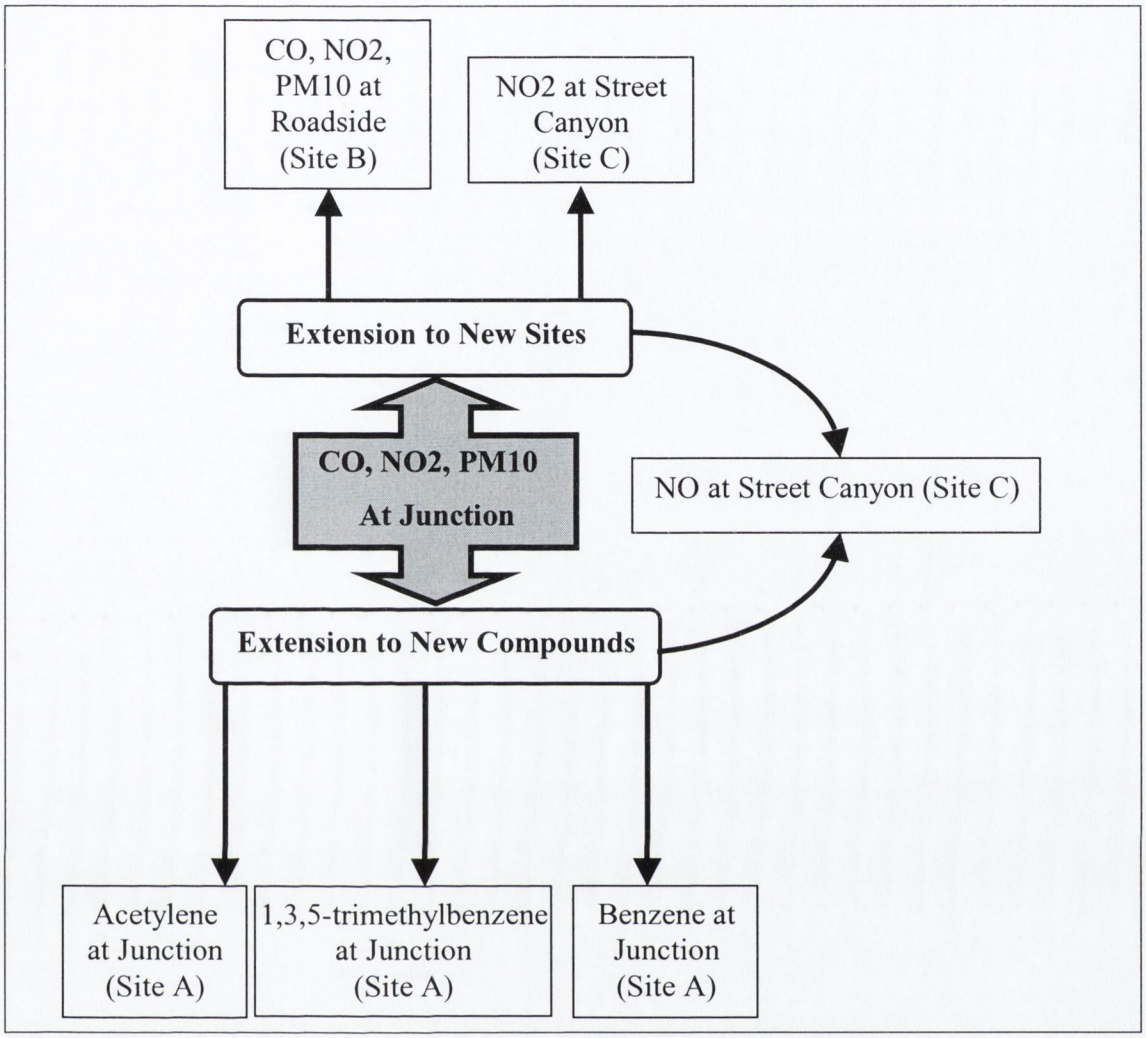

Figure 8.1 Schematic diagram of extensions to prediction algorithm

8.2 Application of Algorithm to Roadside Site

The transferability of the prediction algorithm was analysed first by examining its performance at a roadside site. Site B (Pearse Street) differed from Site A, in that it was not situated at a junction. Further details are given in Section 3.2.

8.2.1 Calculation of Monthly Averages

As for Site A, adjustment factors for the estimation of the 30-day average were calculated using all available data. The average errors in the prediction of the 30-day averages are

tabulated in Table 8.1. As can be seen from Table 8.1, the errors in the predicted estimate of the monthly average for each compound tend to be of a similar magnitude regardless of the input data; the majority of the predictions are more accurate or of a similar accuracy to the equivalent predictions in Phase 1, (Section 7.1). Although r-values are generally very low, in all but very few cases the predicted average is more accurate than the value calculated by simply using the arithmetic average of the measured data. In many cases, however, the observed improvement is only marginal.

Table 8.1 Summary of average errors for CO, NO_2 and PM_{10} 30-day average prediction

		CO Arith. Ave.	**CO Pred.**	**NO_2 Arith. Ave.**	**NO_2 Pred.**	**PM_{10} Arith. Ave.**	**PM_{10} Pred.**
24 hours	Pearson's r	0.18	0.25	0.31	0.33	0.38	0.46
	RMSE (%)	22.6	20.1	4.1	4.2	17.1	16.8
	σ_{RMS} (%)	25.6	21.7	5.1	5.7	18.4	19.3
	MAE (%)	18.5	17.5	3.3	3.0	14.3	13.4
	σ_{MAE} (%)	13.3	10.2	2.6	2.9	9.6	10.4
10:00 – 16:00	Pearson's r	0.12	0.11	-0.04	-0.03	0.04	0.05
	RMSE (%)	22.6	19.1	5.6	6.4	38.5	15.7
	σ_{RMS} (%)	31.0	24.3	6.4	6.8	31.9	14.9
	MAE (%)	15.8	15.4	4.7	5.4	35.2	13.9
	σ_{MAE} (%)	16.6	11.7	3.2	3.5	16.0	7.3
10:00 – 11:00	Pearson's r	0.42	0.39	-0.23	-0.26	-0.03	-0.05
	RMSE (%)	11.5	11.9	9.3	9.4	36.7	22.8
	σ_{RMS} (%)	14.3	17.7	11.5	9.5	44.5	24.0
	MAE (%)	9.1	8.5	7.0	8.0	29.7	19.4
	σ_{MAE} (%)	7.2	8.7	6.3	5.0	22.4	12.5
13:00 – 14:00	Pearson's r	-0.05	-0.06	-0.18	-0.19	0.20	0.16
	RMSE (%)	28.5	24.2	9.3	10.1	35.8	23.2
	σ_{RMS} (%)	39.1	26.8	10.1	11.8	35.1	23.9
	MAE (%)	18.0	20.8	7.9	7.8	31.5	19.1
	σ_{MAE} (%)	22.6	12.7	5.2	6.5	17.6	13.6
17:00 – 18:00	Pearson's r	0.59	0.58	0.23	0.22	0.53	0.53
	RMSE (%)	72.8	33.3	22.1	9.4	57.9	43.8
	σ_{RMS} (%)	30.4	28.3	16.1	10.0	42.2	59.9
	MAE (%)	72.5	30.6	21.3	8.2	55.0	32.7
	σ_{MAE} (%)	6.6	13.5	6.1	4.7	18.4	30.1
Note: See Table 7.1 for explanation of symbols and acronyms							

8.2.2 24-Hour Averages – Carbon Monoxide

Sample results are shown for March 1999 in Figure 8.2 and Figure 8.3. Data measured on the 5th, 15th and 25th were used to calculate the predicted frequency distributions for all pollutants. Figure 8.2 shows the predicted frequency distributions calculated using three days of 24 hours of data, while Figure 8.3 shows the same distribution calculation with three days of data collected between 17:00 and 18:00. The sampling period 17:00 – 18:00 was chosen to evaluate the algorithm, as the unadjusted concentrations measured during this period are the least representative of the long-term average concentration. The confidence intervals calculated using 24 hours of measured data for each of the three days bound the observed frequency distributions. The confidence intervals calculated using the data measured between 17:00 and 18:00 are accurate for the higher percentiles.

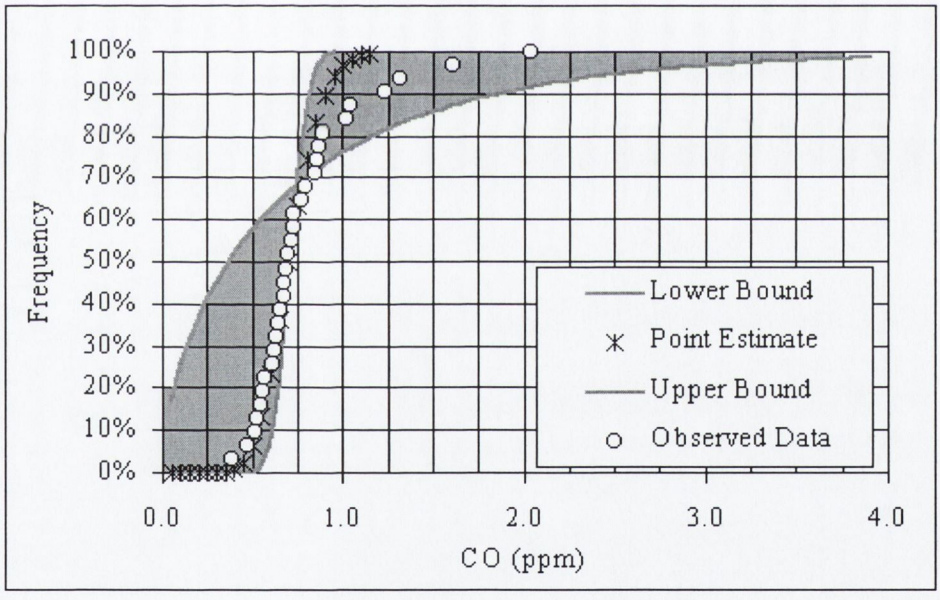

Figure 8.2 Predicted frequency distribution of 24-hour CO averages for March 1999 (Site 2), calculated using 3 complete days of monitoring.

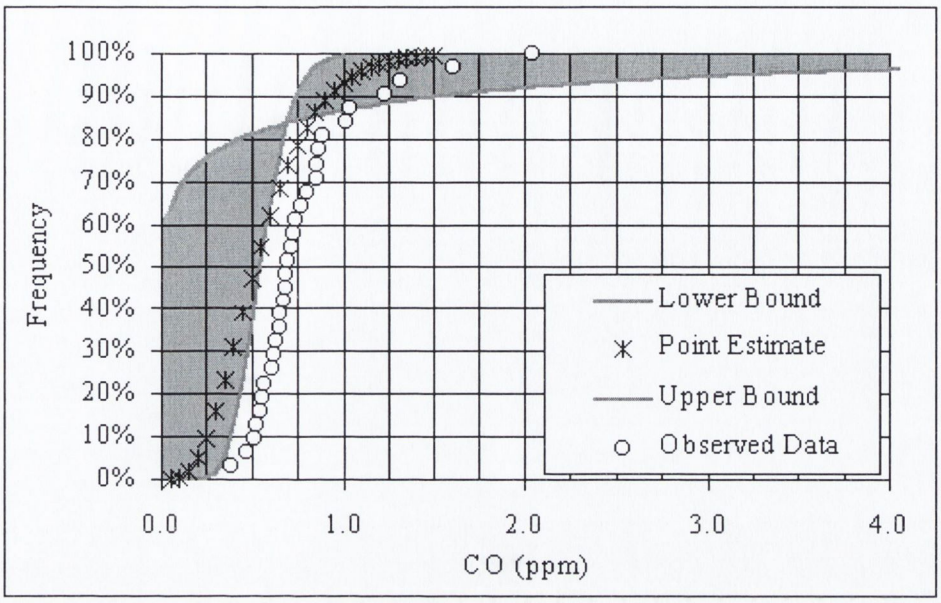

Figure 8.3 Predicted frequency distribution of 24-hour CO averages for March 1999 (Site 2), calculated using 3 days with data collected between 17:00 and 18:00

8.2.3 24-Hour Averages – Nitrogen Dioxide

The predicted and observed NO_2 frequency distributions are graphed in Figure 10.37 and Figure 10.38 in Appendix D. The observed values follow the values predicted using the point estimate of the standard deviation (based on a 24-hour sampling period) closely. However, the observed values lie outside the confidence intervals when concentrations measured between 17:00 and 18:00 are used. This is largely attributable to the overprediction of the monthly average by 9.6%.

8.2.4 24-Hour Averages – PM_{10}

Figure 10.39 and Figure 10.40, in Appendix D, show the observed and predicted frequency distributions for PM_{10} 24-hour averages for the sample month of March 1999. The observed distributions are seen to be within the calculated confidence intervals for both sampling periods, and there is a good degree of agreement between the observed distribution and the distribution calculated with the point estimate of the standard deviation.

8.2.5 8-Hour Averages – Carbon Monoxide

The equivalent results for 8-hour concentrations are given in Figure 8.4 and Figure 8.5. The 85th percentile and upwards lies within the calculated bounds for both sets of calculations. The better estimate is again given by the prediction using 24-hours of data each day, with the observed frequency distribution falling within the two bounds limits at all percentiles.

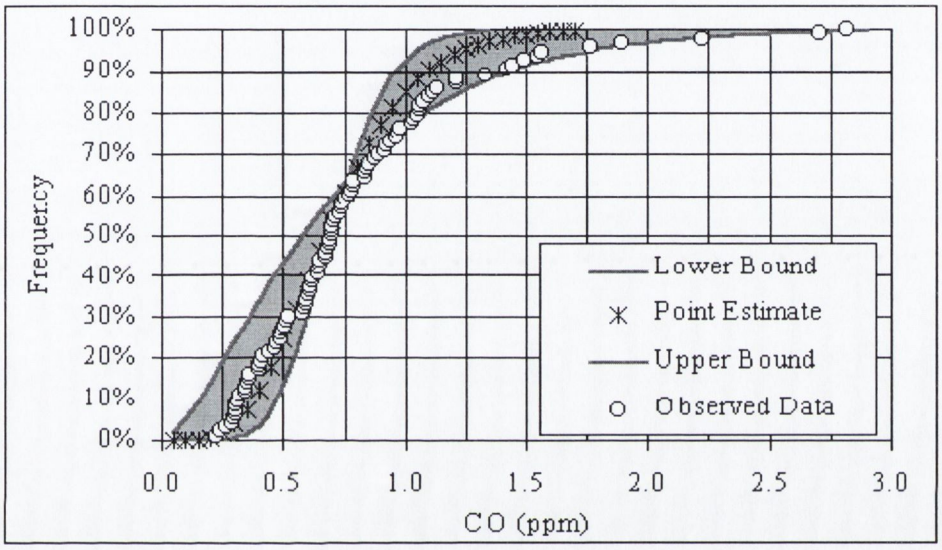

Figure 8.4 Predicted frequency distribution of 8-hour CO averages for March 1999 (Site 2), calculated using 3 complete days of monitoring.

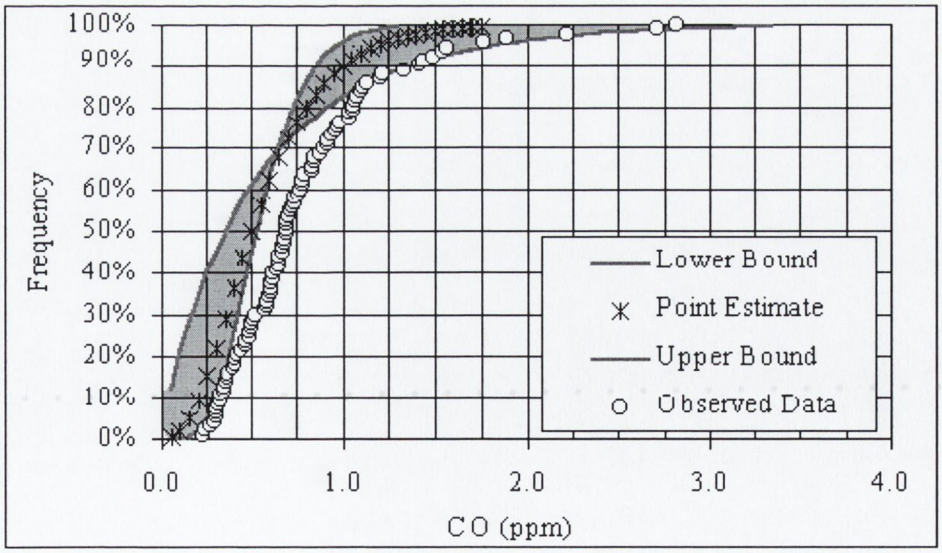

Figure 8.5 Predicted frequency distribution of 8-hour CO averages for March 1999 (Site 2), calculated using 3 days of monitoring data between 17:00 and 18:00

8.2.6 8-Hour Averages – Nitrogen Dioxide

The results for the average 8-hour frequency distributions (Figure 10.41 and Figure 10.42) are similar to those seen for 24-hour averages in Section 8.2.3. Predictions calculated using 24-hour sampling periods reflect the observed frequency distribution closely, in particular the predicted frequency distribution based on the point estimate of the standard deviation. The predicted frequency distributions based on concentrations measured between 17:00 and 18:00 overestimate the observed distribution due to the overestimation of the monthly average.

8.2.7 8-Hour Averages – PM_{10}

For predictions based on 24-hour sampling periods there is a good agreement between the observed frequency distribution and the predicted distribution based on the point estimate of the standard deviation, and for all percentiles the observed distribution is within the calculated confidence intervals (Figure 10.43). Predicted distributions based on concentrations measured between 17:00 and 18:00 do not agree with the observed distribution as well as those predictions calculated using complete days of monitoring data, especially for the higher percentiles, where the observed distributions fall slightly outside the predicted confidence intervals (Figure 10.44).

8.2.8 1-Hour Averages – Carbon Monoxide

Calculated and observed 1-hour CO concentrations are shown in Figure 8.6 and Figure 8.7. Predictions using 24 hours of data for each of the three days used in the estimation are again very effective, with only the 100^{th} percentile beyond the upper bound. However, all percentiles between the 85^{th} and 100^{th} are within the predicted bounds when the calculation is based on short-term data measured between 17:00 and 18:00.

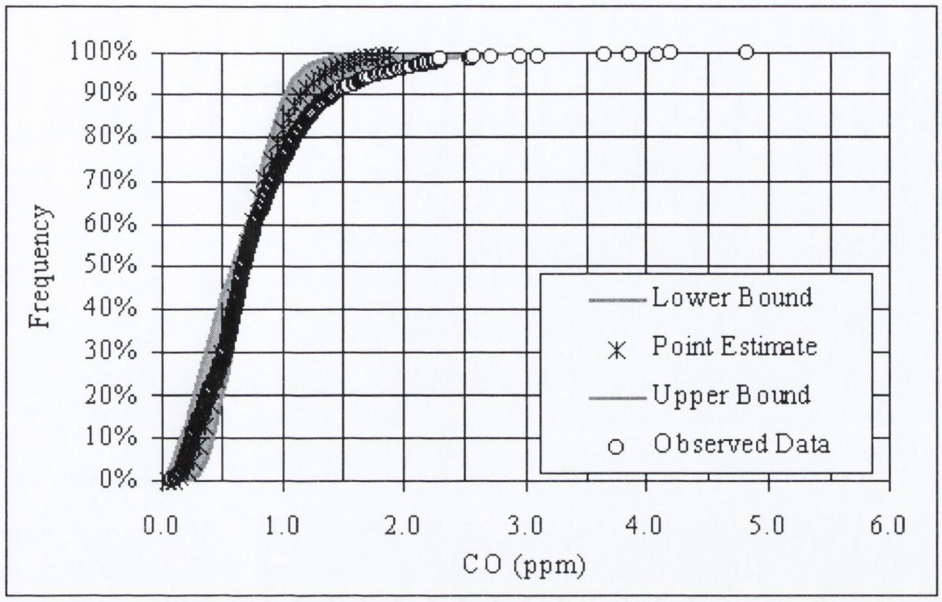

Figure 8.6 Predicted frequency distribution of 1-hour CO averages for March 1999 (Site 2), calculated using 3 complete days of monitoring.

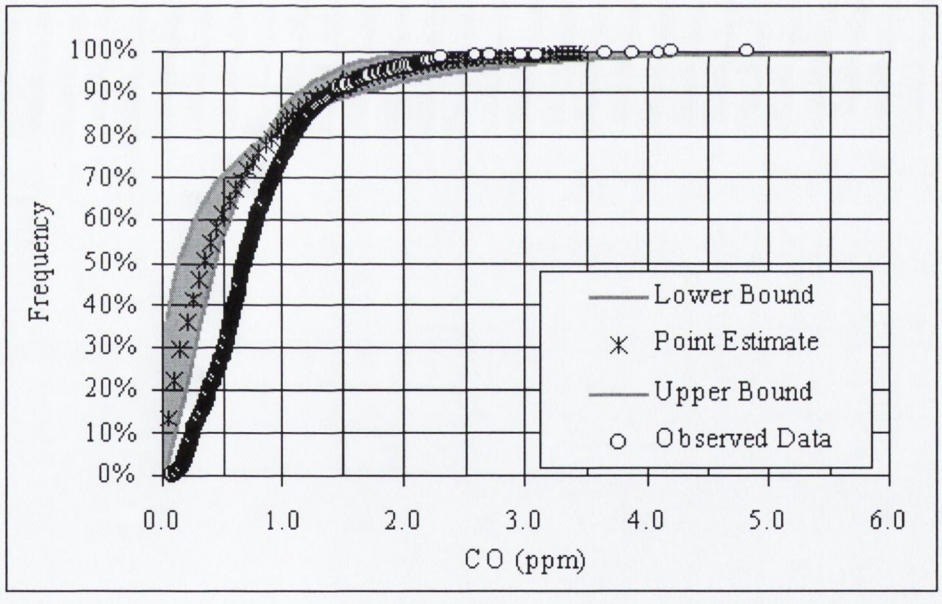

Figure 8.7 Predicted frequency distribution of 1-hour CO averages for March 1999 (Site 2), calculated using 3 days of monitoring data between 17:00 and 18:00

8.2.9 1-Hour Averages – Nitrogen Dioxide

Again, as with the 1-hour NO_2 averages measured at the Pearse Street/Westland Row junction, the frequency distribution has a stepped effect rather than a smooth curve, caused by the poor resolution of the instrument, and the rate of recurrence of a small number of values (see Section 4.3.4). However, for both predictions the upper end of the observed distribution (which is not affected to the same degree by the dominance of the mid-range values) is within the confidence intervals (Figure 10.45, Figure 10.46).

8.2.10 1-Hour Averages – PM_{10}

Again, there is very good agreement between the observed and predicted distributions when 24 hours of data each day is used, with the 100^{th} percentile being the only point not within the predicted confidence intervals (Figure 10.47). The predicted distribution calculated using concentration data measured between 17:00 and 18:00 overestimates the 70^{th} to 95^{th} percentiles slightly (Figure 10.48).

8.2.11 Prediction of Exceedences

Table 8.2 summarises the results of the prediction of the numbers of exceedences of reference values during March 1999 at the Pearse St. monitoring site. Again, the limit value concentrations for CO, NO_2 and PM_{10} are used, along with a second reference value for each. The observed numbers of exceedences of the reference CO values are within the predicted range with one exception – the number of times the hourly average exceeds 4.0 ppm is underestimated by one, using 24-hour sampling period. The number of exceedences of the 35 ppb reference NO_2 concentration was underestimated twice, due to the monthly average being underpredicted. The numbers of exceedences of reference PM_{10} concentrations were also not within the predicted bounds on two occasions (17%).

Table 8.2 Comparison of measured and predicted concentration exceedences at Pearse St. monitoring site.

	Ave. Period	Conc ppm	Predictions based on 24 hours			Predictions based on 17:00-18:00			Measured
			Lower Bound	Point Estimate	Upper Bound	Lower Bound	Point Estimate	Upper Bound	
CO	24hr	8.7	0	0	0	0	0	0	0
		4.0	0	0	3	0	0	2	1
	8hr	8.7	0	0	0	0	0	0	0
		4.0	0	0	3	0	0	3	3
	1hr	8.7	0	0	0	0	0	0	0
		4.0	0	2	21	8	29	54	30
NO_2	24hr	104	0	0	0	0	0	0	0
		35	0	0	9	0	4	11	0
	8hr	104	0	0	0	0	0	0	0
		35	3	10	22	17	24	31	3
	1hr	104	0	0	0	0	0	0	0
		35	77	134	192	159	206	243	90
PM_{10}	24hr	50	0	0	6	0	2	6	0
		40	1	3	8	2	6	7	4
	8hr	50	2	7	16	7	13	19	4
		40	14	20	26	21	25	26	14
	1hr	50	13	47	104	96	134	154	50
		40	107	156	197	193	202	209	126

8.2.12 Conclusions of Application of Algorithm to Roadside Site

The prediction algorithm and methodology was seen to be transferable to a second roadside site, for all three compounds, CO, NO_2, and PM_{10}. For each of the three averaging periods there was a good level of agreement between the predicted and observed distributions, with the observed distributions lying between the estimated confidence intervals in most cases. Also, for all compounds, distributions calculated using point estimates of the standard deviation tend to be good indicators of the observed frequency distributions. The numbers of exceedences of concentration values were also estimated with a reasonable level of accuracy.

8.3 Application of Algorithm to Street Canyon (Westland Row)

Having successfully applied the prediction algorithm to an urban junction site and a roadside site (as discussed in Chapter 7 and Section 8.2), the performance of the prediction methodology at an urban canyon site is of importance. The majority of urban roadside sites can be classified as either junction sites, semi-open roadside sites or urban canyons. The successful application of the algorithm to an urban canyon would demonstrate that short-term results from the majority of urban sites can be improved through use of the algorithm.

NO_2 is used to investigate the accuracy of the algorithm as only oxides of nitrogen were monitored at this site. Results of the application of the algorithm to NO_2 24-hour, 8-hour and 1-hour averages are discussed in Sections 8.3.3, 8.3.4, and 8.3.5. One week of data was used to calculate the adjustment factors, to investigate the performance of factors calculated over short term periods.

8.3.1 Calculation of Adjustment Factors for Nitrogen Dioxide

The week starting 19th July 1999 was used to calculate the NO_2 adjustment factors. The ability of factors calculated using relatively short monitoring period to effectively improve short-term or indicative monitoring results is important, as it will enable more sites to be characterised in a fixed period of time, or with a limited amount of monitoring equipment.

8.3.2 Calculation of NO_2 Monthly Averages

The errors in the 30-day average NO_2 concentration predictions using the arithmetic average of the recorded data and the predictions calculated using the algorithm are summarised in Table 8.3. The lowest error is for predictions using the arithmetic average of concentrations collected during 24-hour monitoring periods. The prediction algorithm is seen to predict the 30-day NO_2 average with a high level of accuracy, and limits the magnitude of the error when shorter monitoring periods are used. All average errors (both RMSE and MAE) are below

16% (compared to over 40% for the arithmetic average), a higher level of accuracy than was achieved at either of the other two sites.

Table 8.3 Summary of errors in the predictions of the 30-day NO_2 average using the arithmetic average of the recorded data and the prediction algorithm

			Arithmetic Average	Prediction
24 hours	Pearson's r		0.38	0.23
	RMSE	%	10.9	12.8
	σ_{RMS}	%	12.0	17.1
	MAE	%	9.0	9.7
	σ_{MAE}	%	6.2	8.4
10:00 – 16:00	Pearson's r		0.43	0.18
	RMSE	%	36.0	12.0
	σ_{RMS}	%	32.4	17.9
	MAE	%	32.4	9.1
	σ_{MAE}	%	15.8	7.9
10:00 – 11:00	Pearson's r		0.45	0.31
	RMSE	%	40.5	15.3
	σ_{RMS}	%	40.1	23.9
	MAE	%	35.8	10.7
	σ_{MAE}	%	19.2	11.0
13:00 – 14:00	Pearson's r		0.31	0.12
	RMSE	%	28.6	14.4
	σ_{RMS}	%	26.1	16.0
	MAE	%	25.0	11.7
	σ_{MAE}	%	14.1	8.4
17:00 – 18:00	Pearson's r		0.31	0.10
	RMSE	%	37.6	12.0
	σ_{RMS}	%	35.2	12.8
	MAE	%	33.9	10.1
	σ_{MAE}	%	16.5	6.7

8.3.3 24-Hour Averages– Nitrogen Dioxide

The standard deviations for all compounds are calculated using methods discussed in Section 6.12. Figure 8.8 and Figure 8.9 show the predicted and observed frequency distributions for 24-hour NO_2 averages. The distributions calculated using point estimates of the standard deviation match the observed distribution very closely.

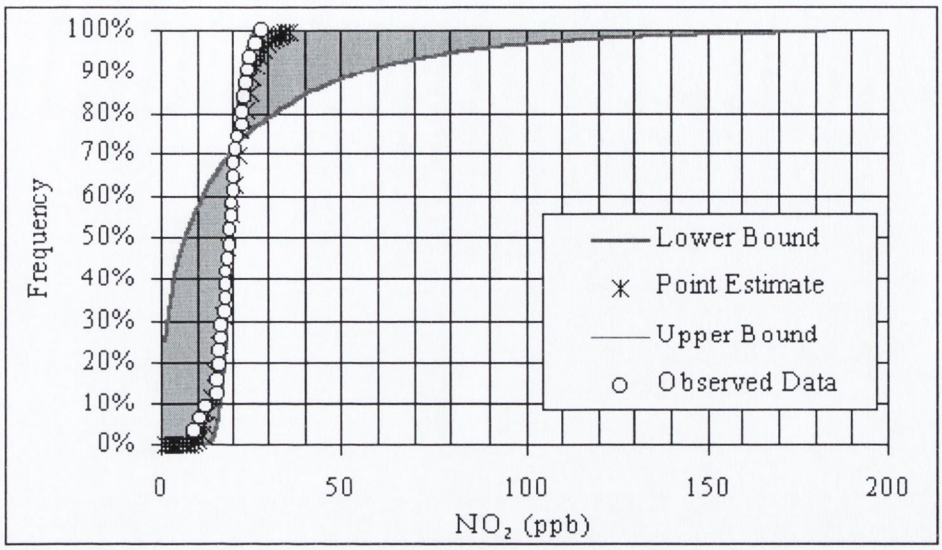

Figure 8.8 Predicted frequency distribution of 24-hour NO_2 averages for August 1999 (street canyon), calculated using 3 complete days of monitoring.

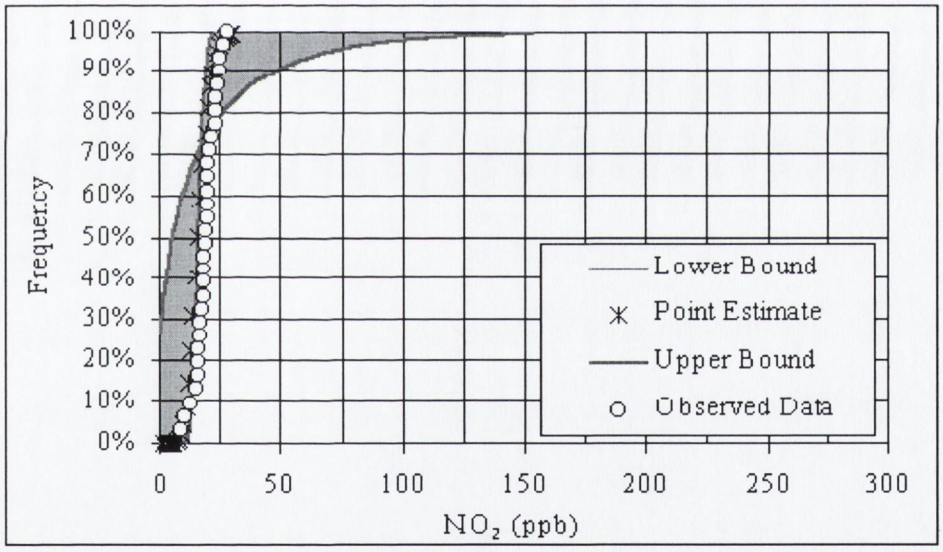

Figure 8.9 Predicted frequency distribution of 24-hour NO_2 averages for August 1999 (street canyon), calculated using 3 days of monitoring data between 17:00 and 18:00

8.3.4 8-Hour Averages – Nitrogen Dioxide

Figure 8.10 and Figure 8.11 show the corresponding graphs of the results for 8-hour NO_2 predictions. Again, there is a good degree of agreement between the observed and predicted distributions calculated using the point estimate of the standard deviation.

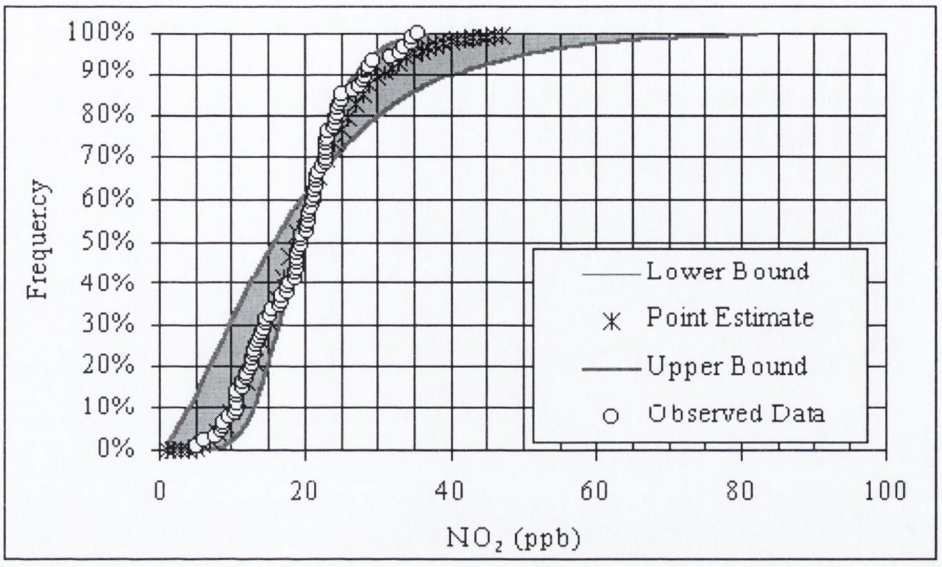

Figure 8.10 Predicted frequency distribution of 8-hour NO_2 averages for August 1999 (street canyon), calculated using 3 complete days of monitoring

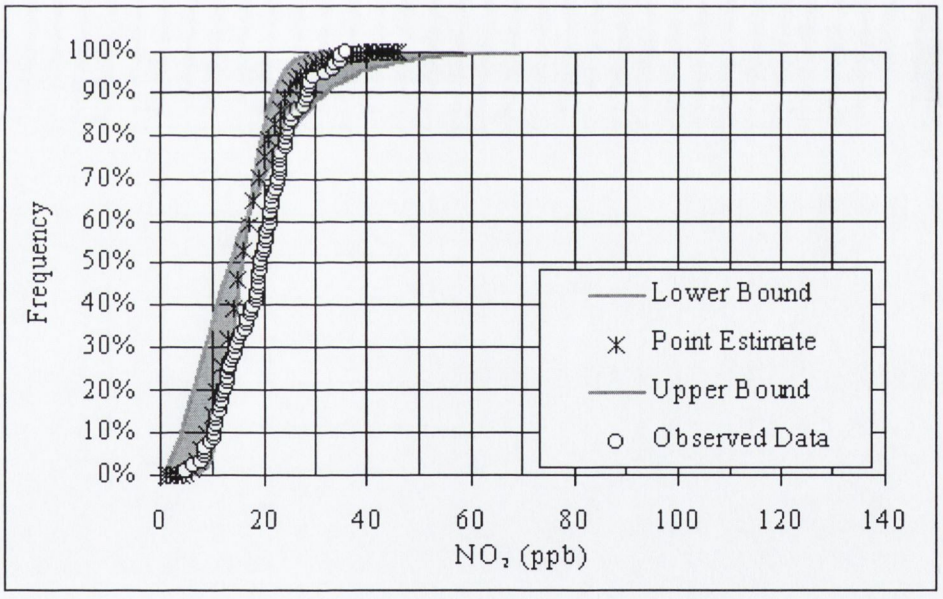

Figure 8.11 Predicted frequency distribution of 8-hour NO_2 averages for August 1999 (street canyon), calculated using 3 days of monitoring data between 17:00 and 18:00

8.3.5 1-Hour Averages – Nitrogen Dioxide

The predicted and observed distributions for 1-hour NO_2 averages are shown in Figure 8.12 and Figure 8.13. As for the 24-hour and 8-hour distributions, the predicted 1-hour distributions calculated using the point estimate of the standard deviations follow the observed distributions closely.

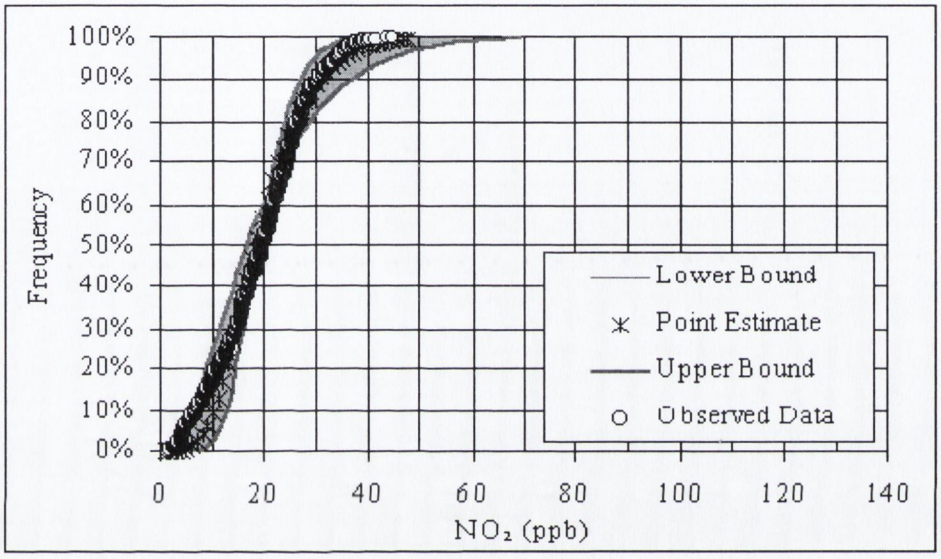

Figure 8.12 Predicted frequency distribution of 1-hour NO_2 averages for August 1999 (street canyon), calculated using 3 complete days of monitoring.

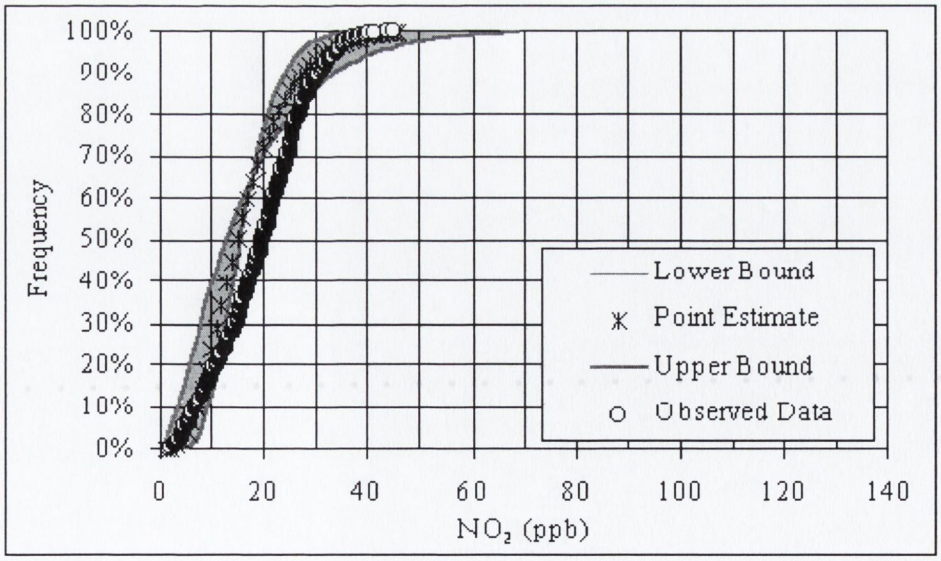

Figure 8.13 Predicted frequency distribution of 1-hour NO_2 averages for August 1999 (street canyon), calculated using 3 days of monitoring data between 17:00 and 18:00

8.3.6 Prediction of Exceedences

Predicted and observed numbers of exceedences of two reference NO_2 concentrations (the limit value of 104 ppb, and 40 ppb) are compared in Table 8.4. The observed numbers of exceedences are, in each case, within the calculated intervals.

Table 8.4 Comparison of predicted and measured numbers of exceedences of sample NO_2 values at Westland Row, during August 1999.

	Ave. Period	Conc ppb	Predictions based on 24 hours			Predictions based on 17:00-18:00			Measured
			Lower Bound	Point Estimate	Upper Bound	Lower Bound	Point Estimate	Upper Bound	
NO_2	24hr	104	0	0	2	0	0	2	0
		40	0	3	5	1	4	4	1
	8hr	104	0	0	1	0	0	1	0
		40	4	9	17	4	10	18	9
	1hr	104	0	0	6	0	0	4	0
		40	48	93	135	48	94	138	103

8.3.7 Conclusions on Application of Algorithm to Street Canyon.

As seen in Sections 8.3.3, 8.3.4, and 8.3.5, the observed frequency distributions are matched very closely by the predicted distributions calculated using point estimates of the standard deviation. The algorithm and prediction methodology are seen to work effectively under street canyon conditions as demonstrated by the high level of accuracy in the NO_2 predictions. The predicted numbers of exceedences of specific reference concentrations were also predicted with a high degree of accuracy.

8.4 Application of Model to Other Pollutants (At Original Location – Site A)

The prediction algorithm has been demonstrated to work effectively at urban roadside, junction and street canyon sites for CO, NO_2 and PM_{10}. The transferability of the prediction algorithm and methodology has been established with regard to location, therefore the next step is to examine the transferability of the methodology with respect to compounds. This has been investigated using acetylene, 1,3,5-trimethylbenzene and benzene at the original Pearse Street/Westland Row junction site.

As the adjustment factors for NO_2 levels at the street canyon were calculated using 1 week of data and were shown to work effectively, one week of data was also used to calculate adjustment factors for acetylene, 1,3,5-trimethylbenzene and benzene. For this purpose, data from the first week in April 1998 were used, and sample results are shown here for March 1998.

8.4.1 24-Hour Averages – Acetylene

The observed and predicted distributions (based on 24 hours and 1 hour of measured data between 17:00 and 18:00) are shown in Figure 8.14 and Figure 8.15. For the predictions based on 24 hours of data, the distribution calculated using the point estimate of the standard deviation matches the observed distribution closely, and the confidence intervals bound the measured distributions for virtually all percentiles. The distributions calculated using the data collected between 17:00 and 18:00 underestimate the observed distribution between the 30^{th} and 90^{th} percentiles.

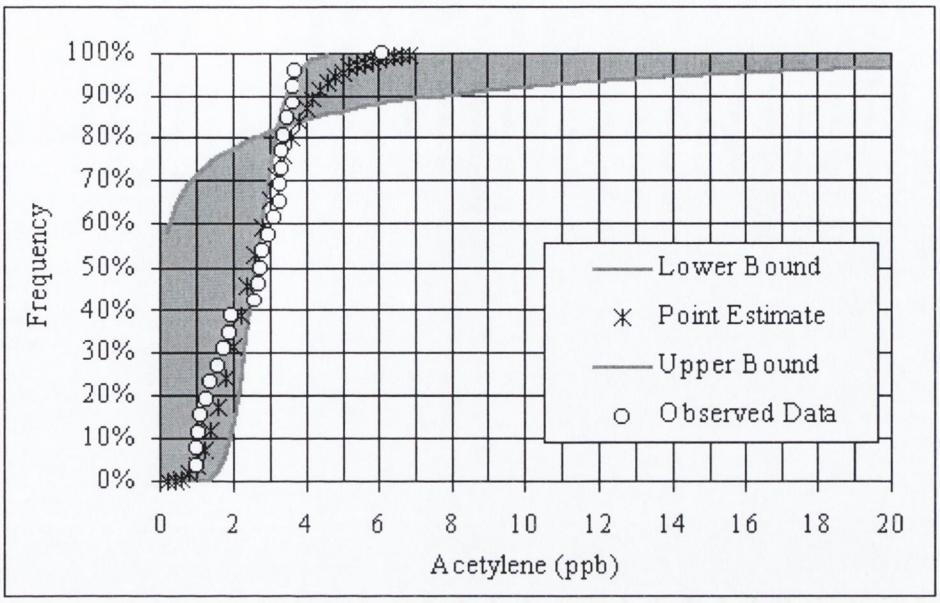

Figure 8.14 Predicted frequency distribution of 24-hour acetylene averages for March 1998 (Site A), calculated using 3 complete days of monitoring.

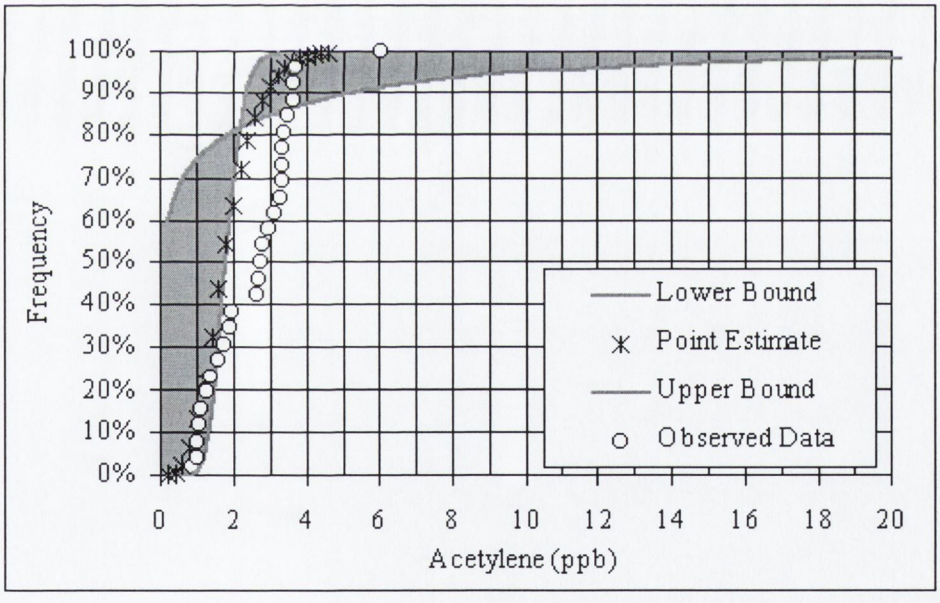

Figure 8.15 Predicted frequency distribution of 24-hour acetylene averages for March 1998 (Site 1), calculated using 3 days of monitoring data between 17:00 and 18:00

8.4.2 24-Hour Averages – 1,3,5-Trimethylbenzene

As for acetylene, the predicted distribution calculated using 24-hour data is more accurate than that calculated using only data measured between 17:00 and 18:00. The observed distribution (based on a 24-hour sampling period) is seen to closely follow the distribution calculated using the point estimate of the standard deviation. For predictions calculated using data measured between 17:00 and 18:00, the observed distribution lies outside the predicted confidence intervals below the 90th percentile. The observed and predicted distributions are graphed in Figure 10.49 and Figure 10.50 in Appendix D.

8.4.3 8-Hour Averages – Acetylene

The corresponding results for the 8-hour acetylene averages are shown in Figure 8.16 and Figure 8.17. Again, the predictions using the 24 hours of data each day predict the observed distributions well. The predicted distributions calculated using the point estimate of the standard deviation show a very high level of agreement with the observed data.

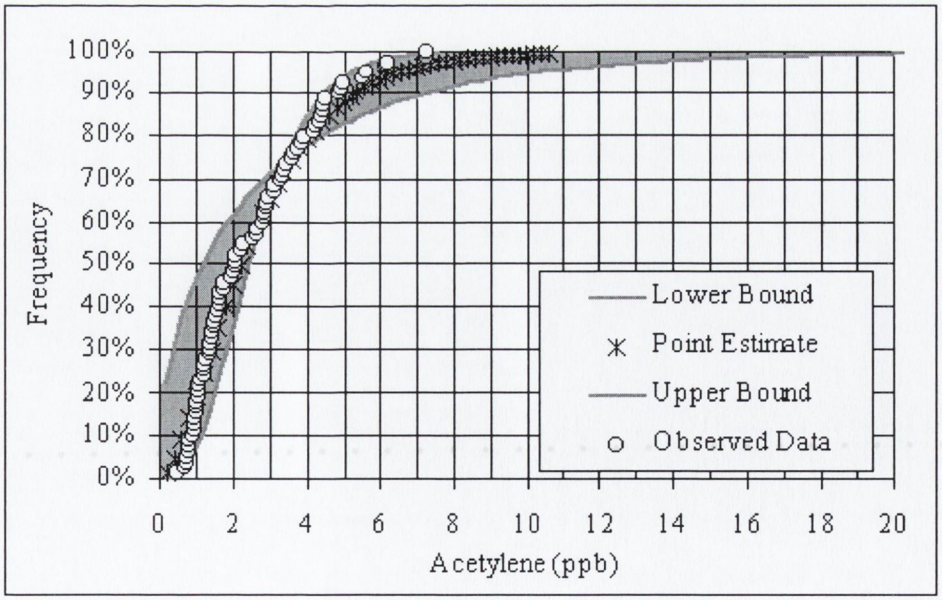

Figure 8.16 Predicted frequency distribution of 8-hour acetylene averages for March 1998 (Site 1), calculated using 3 complete days of monitoring.

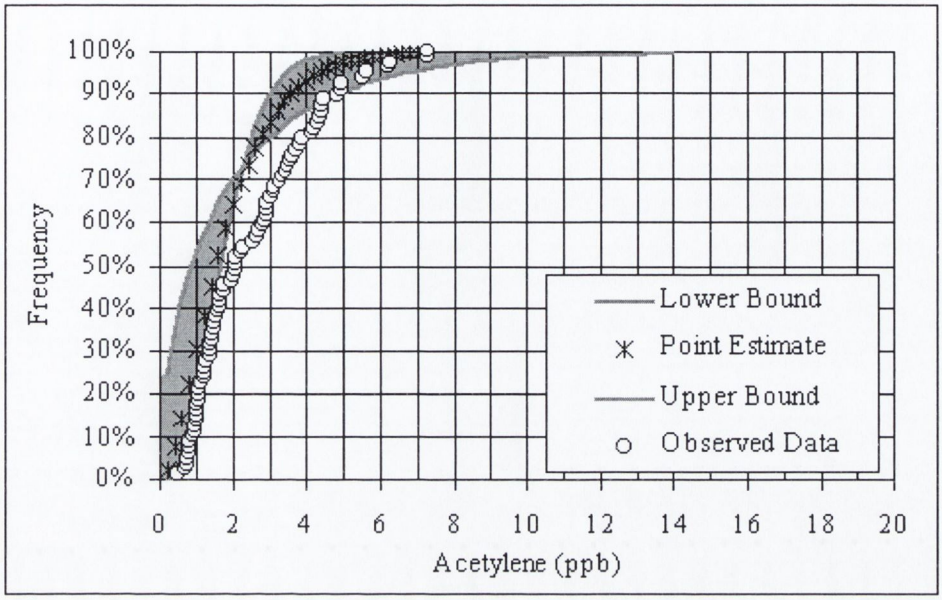

Figure 8.17 Predicted frequency distribution of 8-hour acetylene averages for March 1998 (Site 1), calculated using 3 days of monitoring data between 17:00 and 18:00

8.4.4 8-Hour Averages – 1,3,5-Trimethylbenzene

Observed 1,3,5-trimethylbenzene concentrations follow the distribution calculated using the point estimate of the standard deviation (based on 24-hour sampling periods) very closely, and the observed distribution is within the predicted confidence intervals at all times (Figure 10.51). The distributions calculated using data measured between 17:00 and 18:00 slightly underestimate the measured distributions for percentiles lower than the 90^{th} percentile (Figure 10.52).

8.4.5 1-Hour Averages – Acetylene

Figure 8.18 and Figure 8.19 compare the observed and predicted frequency distributions of the 1-hour acetylene concentrations. The distributions based on the 24-hour monitoring periods predict the observed distribution well for all percentiles except the 100^{th} percentile. The

confidence intervals calculated using the data collected between 17:00 and 18:00 bound the 100th percentile, but underpredict the measured data below the 90th percentile.

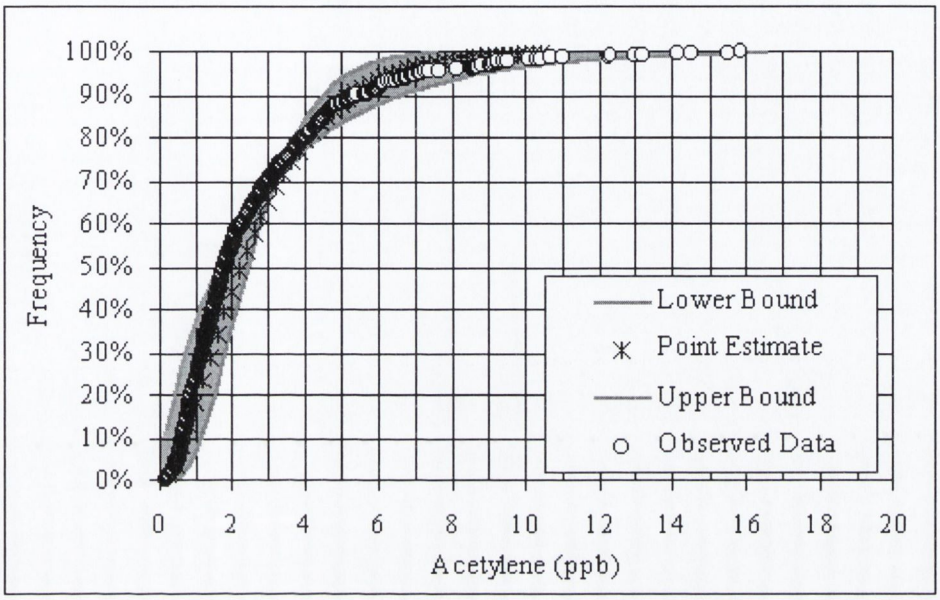

Figure 8.18 Predicted frequency distribution of 1-hour acetylene averages for March 1998 (Site 1), calculated using 3 complete days of monitoring.

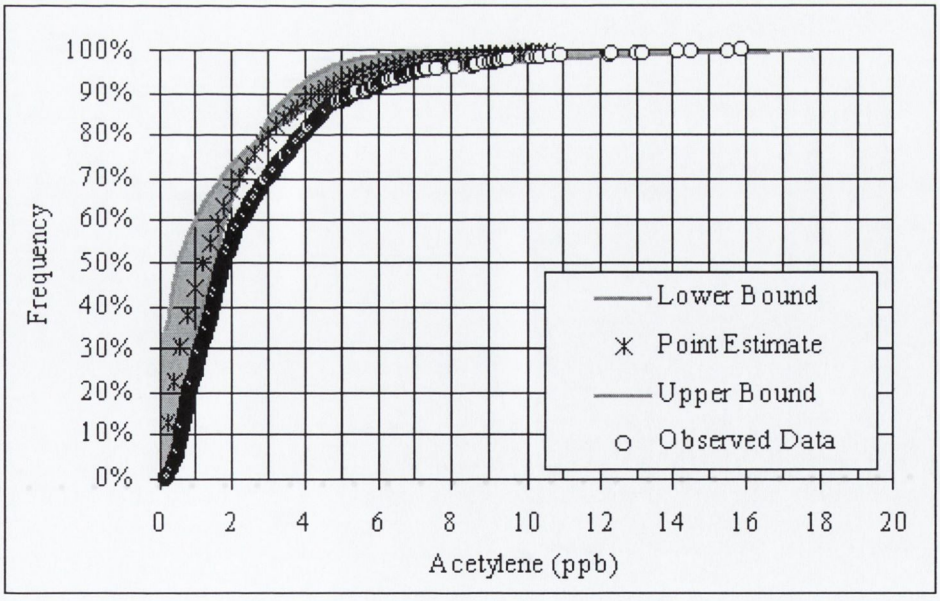

Figure 8.19 Predicted frequency distribution of 1-hour acetylene averages for March 1998 (Site 1), calculated using 3 days of monitoring data between 17:00 and 18:00

8.4.6 1-Hour Averages – 1,3,5-Trimethylbenzene

Good agreement was found between the predicted and observed values for all values, except the 100th percentile, which is underestimated by the prediction based on 24-hour sampling periods (Figure 10.53). The observed 90th to 100th percentiles are within the bounds predicted using data measured between 17:00 and 18:00, although concentrations are underpredicted below the 90th percentile (Figure 10.54).

8.4.7 Prediction of Benzene Concentrations

The performance of the prediction algorithm with respect to benzene was also investigated. The algorithm predicted the monthly average to within 2%, compared to an error of 39% for the arithmetic average, based on 24-hour monitoring periods. However, for data collected between 17:00 and 18:00, the algorithm did not result in a significant improvement over the arithmetic average, with errors of 70% and 83% respectively.

As benzene concentrations, particularly 8-hour and 1-hour averages, were found not to conform to either the gamma or lognormal distributions, the algorithm based on the gamma distribution failed to effectively predict short-term peak concentrations. This can be observed in Figure 8.20, where, although the mean predicted and observed concentrations are seen to agree, the predicted and observed frequency distributions of the 8-hour concentrations follow different patterns. The failure of the algorithm to predict peak concentrations accurately is in conflict with the common view that CO and benzene are closely correlated. The results would indicate that the behaviour of the CO and benzene at peak concentrations are dissimilar.

However, the accuracy of long-term average concentration predictions is not dependent upon the frequency distribution, and as limits for benzene are framed in terms of long-term averages, the failure of the algorithm to accurately predict short-term peak concentrations is not of critical importance for this compound.

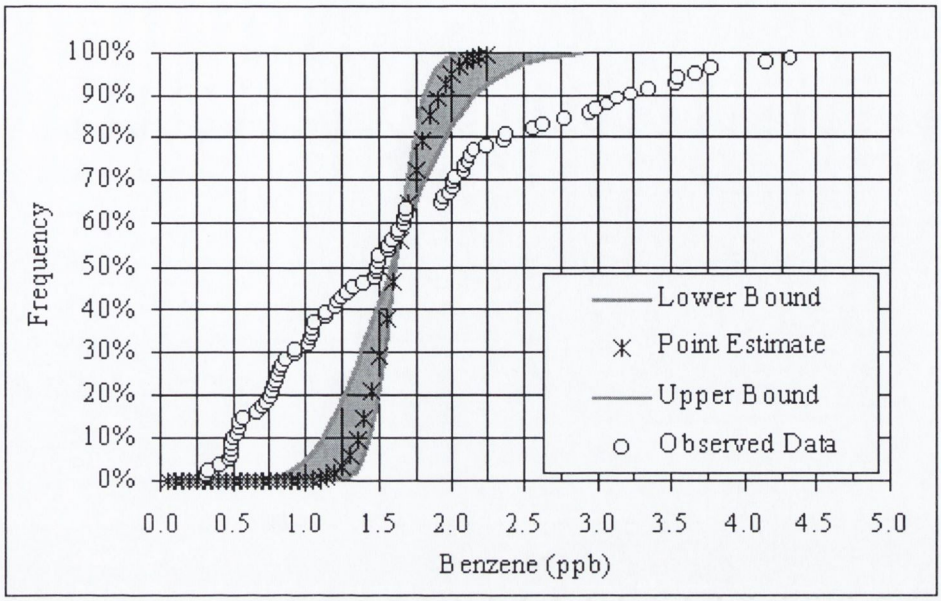

Figure 8.20 Predicted and observed frequency distributions of 8-hour benzene concentrations for March 1998

8.4.8 Prediction of Exceedences

As there are no limit or guideline values for these acetylene and 1,3,5-trimethylbenzene, two reference values from the upper end of the frequency distribution were selected for each compound and the predicted and measured numbers of exceedences of these compounds compared (Table 8.5). The observed numbers of exceedences were within the predicted range for the 24-hour and 8-hour averages, but the 1-hour average values were slightly underpredicted.

Table 8.5 Comparison of measured and predicted number of exceedences of VOC concentrations at the Pearse St./Westland Row junction monitoring site.

	Ave. Period	Conc ppb	Predictions based on 24 hours			Predictions based on 17:00-18:00			Measured
			Lower Bound	Point Estimate	Upper Bound	Lower Bound	Point Estimate	Upper Bound	
Acetylene	24hr	8	0	0	3	0	0	2	0
		6	0	0	4	0	0	3	1
	8hr	8	0	2	8	0	0	3	0
		6	2	6	12	0	1	6	4
	1hr	8	2	15	47	2	12	35	28
		6	17	48	87	10	32	59	55
1,3,5-Trimethylbenzene	24hr	1.5	0	0	2	0	0	0	0
		1	0	0	3	0	0	1	0
	8hr	1.5	0	0	2	0	0	3	1
		1	0	1	8	0	2	6	1
	1hr	1.5	0	1	14	12	26	34	35
		1	2	16	53	35	49	49	55

8.4.9 Conclusions of Application of Algorithm to New Compounds at Pearse Street/Westland Row Junction

The prediction algorithm and methodology was seen to be quite effective for the prediction of acetylene and 1,3,5-trimethylbenzene at the junction of Pearse Street and Westland Row. Long-term average predictions of benzene were predicted with a good degree of accuracy when 24-hour sampling periods were used. Table 8.6 and Table 8.7 summarise whether or not the observed acetylene and 1,3,5-trimethylbenzene concentrations were between the predicted confidence intervals for percentiles between 70 and 100. The results for both compounds are very similar, with a high degree of accuracy displayed when predictions are based on 24 hours of data on each sample day.

Table 8.6 Summary of prediction accuracy for prediction of acetylene levels for March 1998 (Site A)

Percentile	24-hour Averages		8-Hour Averages		1-Hour Averages	
	3x24 hours	**3x17:00-18:00**	**3x24 hours**	**3x17:00-18:00**	**3x24 hours**	**3x17:00-18:00**
70	Within Limits	*Outside Limits*	Within Limits	*Outside Limits*	Within Limits	*Outside Limits*
75	Within Limits	*Outside Limits*	Within Limits	*Outside Limits*	Within Limits	*Outside Limits*
80	Within Limits	*Outside Limits*	Within Limits	*Outside Limits*	Within Limits	*Outside Limits*
85	Within Limits	*Outside Limits*	Within Limits	*Outside Limits*	Within Limits	*Outside Limits*
90	Within Limits	Within Limits	Within Limits	Within Limits	Within Limits	Within Limits
95	Within Limits	Within Limits	Within Limits	Within Limits	Within Limits	Within Limits
100	Within Limits	Within Limits	Within Limits	Within Limits	*Outside Limits*	Within Limits

Table 8.7 Summary of prediction accuracy for prediction of 1,3,5-trimethylbenzene levels for March 1998 (Site A)

Percentile	24-hour Averages		8-Hour Averages		1-Hour Averages	
	3x24 hours	**3x17:00-18:00**	**3x24 hours**	**3x17:00-18:00**	**3x24 hours**	**3x17:00-18:00**
70	Within Limits	*Outside Limits*	Within Limits	*Outside Limits*	Within Limits	*Outside Limits*
75	Within Limits	*Outside Limits*	Within Limits	*Outside Limits*	Within Limits	*Outside Limits*
80	Within Limits	*Outside Limits*	Within Limits	*Outside Limits*	Within Limits	*Outside Limits*
85	Within Limits	*Outside Limits*	Within Limits	*Outside Limits*	Within Limits	*Outside Limits*
90	Within Limits	Within Limits	Within Limits	Within Limits	Within Limits	Within Limits
95	Within Limits	Within Limits	Within Limits	Within Limits	Within Limits	Within Limits
100	Within Limits	Within Limits	Within Limits	Within Limits	*Outside Limits*	Within Limits

8.5 Application of Algorithm to New Compound at Street Canyon Location

As shown in Section 8.4, the prediction algorithm and methodology can be used to predict the frequency distributions of different compounds at the original site. Sections 8.2 and 8.3 discussed the application of the prediction algorithm to new sites, for the prediction of the original compounds, CO, NO_2 and PM_{10}. In this section, both of these extensions are combined, and the algorithm is applied to a new compound, NO, at a new site, the street canyon site (Westland Row). This site is described in Section 3.2.

8.5.1 Calculation of Factors

The adjustment factors for the prediction of the monthly average are again calculated using one week of measured data. The week beginning July 19th 1999 is used for this purpose.

8.5.2 Calculation of Monthly Averages

Using the method previously described, the 30-day average concentration was predicted from monitoring data collected over both 24-hour and short-term periods over three separate days. The average errors in the predicted values and the arithmetic average of the data for each of the monitoring periods are given in Table 8.8. The 30-day averages predicted using the algorithm are seen to have quite similar errors regardless of the input data, unlike the arithmetic averages. The magnitudes of the prediction algorithm errors are also, in all cases, less than the errors associated with the arithmetic averages.

Table 8.8 Summary of average errors for NO and 30-day average prediction

			Arithmetic Average	Prediction
24 hours	Pearson's r		0.79	0.69
	RMSE	%	24.3	20.5
	σ_{RMS}	%	27.2	24.3
	MAE	%	19.9	15.7
	σ_{MAE}	%	14.2	13.4
10:00 - 16:00	Pearson's r		0.81	0.72
	RMSE	%	45.5	21.9
	σ_{RMS}	%	49.5	23.7
	MAE	%	37.7	17.8
	σ_{MAE}	%	25.7	13.0
10:00 - 11:00	Pearson's r		0.81	0.75
	RMSE	%	66.2	23.3
	σ_{RMS}	%	72.7	26.3
	MAE	%	54.3	18.7
	σ_{MAE}	%	38.2	14.1
13:00 - 14:00	Pearson's r		0.75	0.68
	RMSE	%	35.1	31.7
	σ_{RMS}	%	36.8	37.2
	MAE	%	29.5	25.2
	σ_{MAE}	%	19.3	19.4
17:00 - 18:00	Pearson's r		0.76	0.58
	RMSE	%	39.3	25.1
	σ_{RMS}	%	40.5	27.1
	MAE	%	33.8	20.8
	σ_{MAE}	%	20.3	14.3

8.5.3 24-Hour Averages – Nitrogen Monoxide

Figure 8.21 and Figure 8.22 compare observed and predicted 24-hour average frequency distributions. For both monitoring periods, the observed distribution is seen to be closely matched by the prediction calculated using the point estimate of the standard deviation.

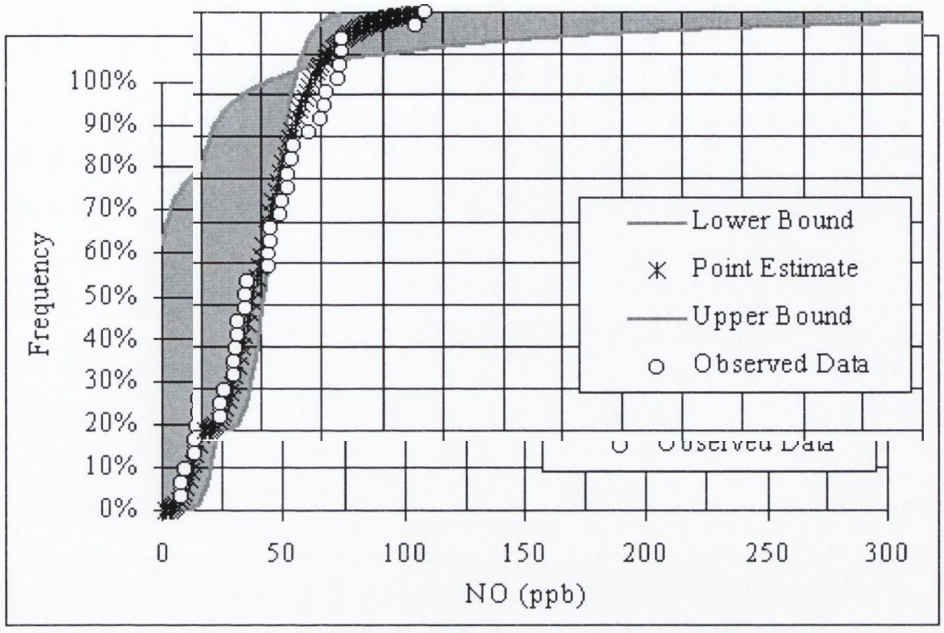

Figure 8.21 Predicted frequency distribution of 24-hour NO averages for August 1999 (street canyon), calculated using 3 complete days of monitoring.

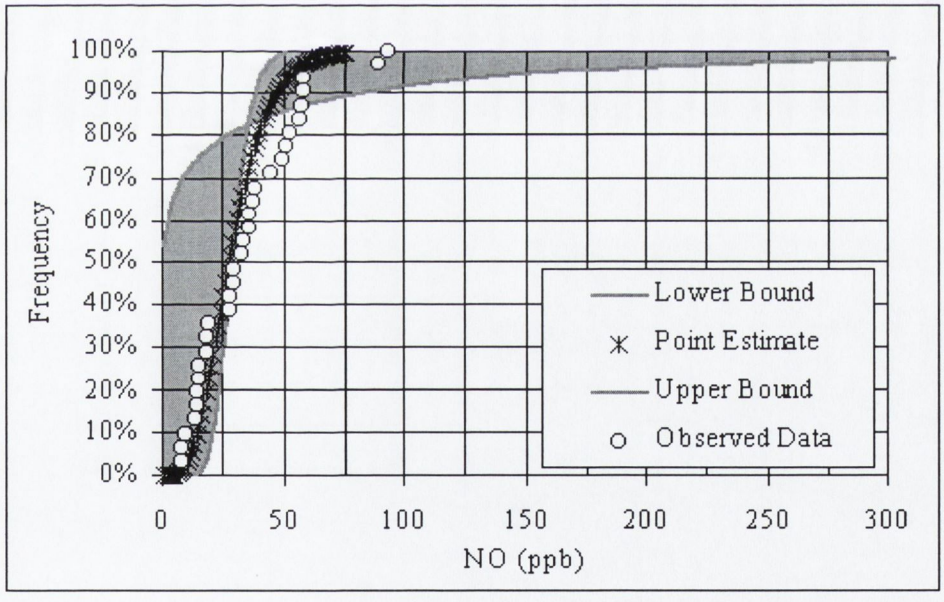

Figure 8.22 Predicted frequency distribution of 24-hour NO averages for August 1999 (street canyon), calculated using 3 days of monitoring data between 17:00 and 18:00

8.5.4 8-Hour Averages – Nitrogen Monoxide

Figure 8.23 and Figure 8.24 show the equivalent graphs for the 8-hour average NO concentrations. Again the observed distribution is within the calculated confidence intervals at most percentile values, and there is good agreement between the observed distribution and the distributions calculated using the point estimate of the standard deviation.

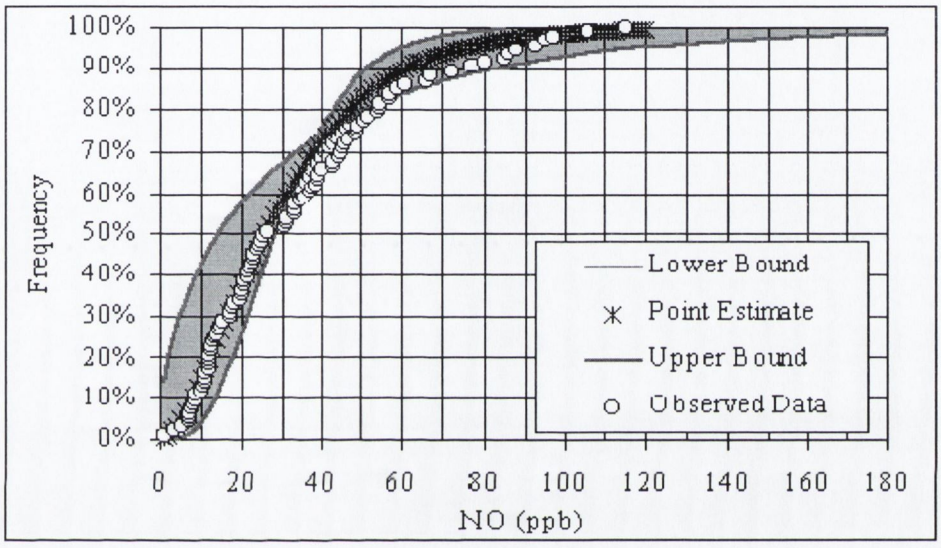

Figure 8.23 Predicted frequency distribution of 8-hour NO averages for August 1999 (street canyon), calculated using 3 complete days of monitoring.

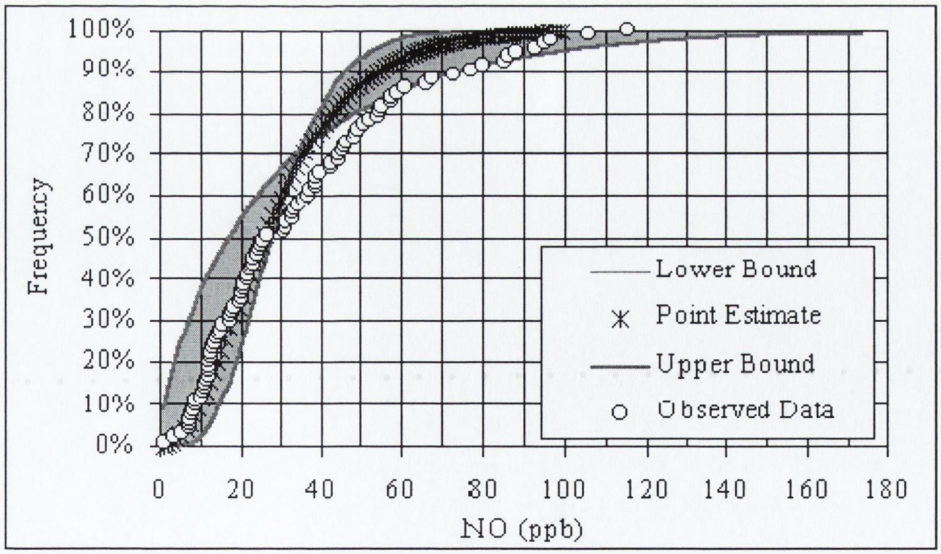

Figure 8.24 Predicted frequency distribution of 8-hour NO averages for August 1999 (street canyon), calculated using 3 days of monitoring data between 17:00 and 18:00

8.5.5 1-Hour Averages – Nitrogen Monoxide

The observed and estimated distributions of the hourly NO concentrations (Figure 8.25 and Figure 8.26) also show good agreement between the observed and predicted distributions. However, the 100^{th} percentile is slightly underestimated by the predicted distributions calculated using the 24 hours of data.

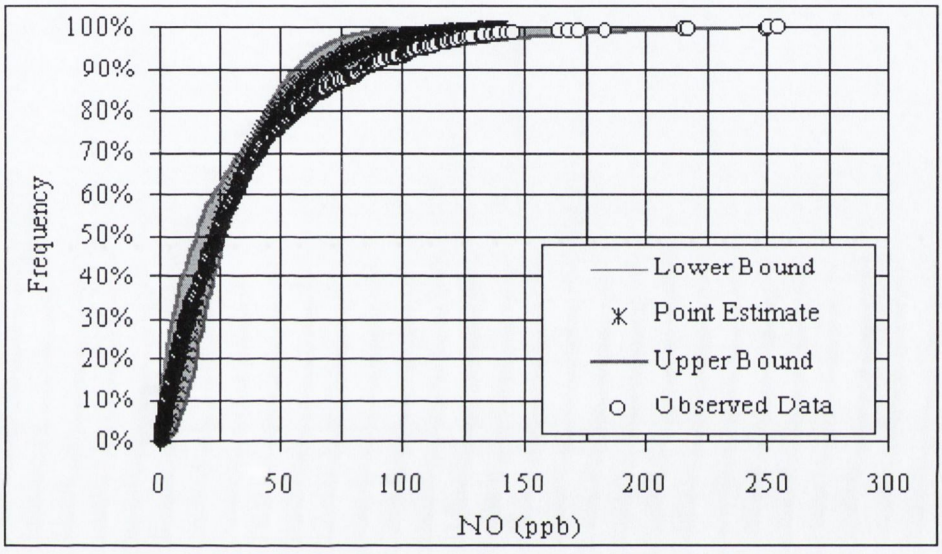

Figure 8.25 Predicted frequency distribution of 1-hour NO averages for August 1999 (street canyon), calculated using 3 complete days of monitoring.

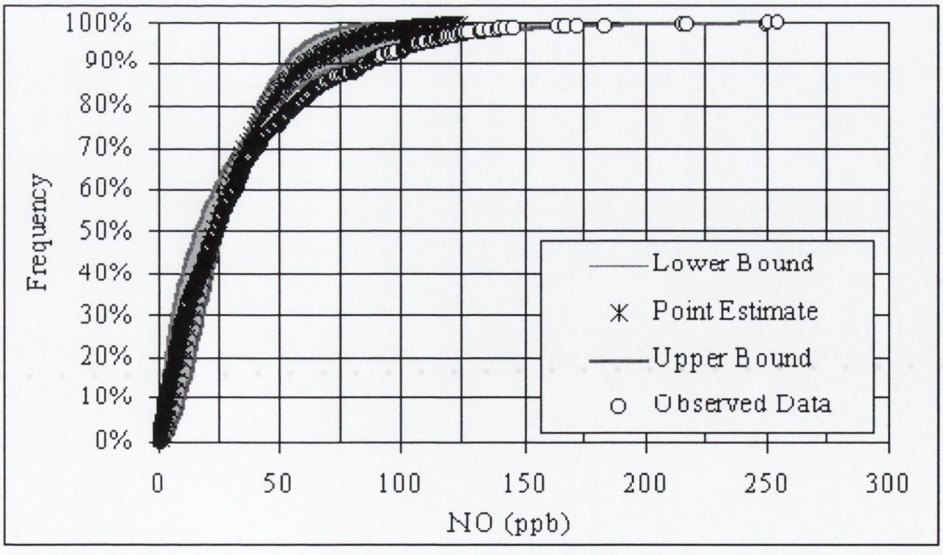

Figure 8.26 Predicted frequency distribution of 1-hour NO averages for August 1999 (street canyon), calculated using 3 days of monitoring data between 17:00 and 18:00

8.5.6 Prediction of Exceedences

As seen in Table 8.9, the numbers of exceedences of 100 ppb and 90 ppb reference values are within the predicted intervals for 8-hour and 24-hour concentrations, although for three out of four cases, the number of 1-hour exceedences is underpredicted.

Table 8.9 Comparison of predicted and measured numbers of exceedences for NO at the Westland Row monitoring station

Ave. Period	Conc ppb	Predictions based on 24 hours			Predictions based on 17:00-18:00			Measured
		Lower Bound	Point Estimate	Upper Bound	Lower Bound	Point Estimate	Upper Bound	
24hr	100	0	0	3	0	0	3	0
	90	0	0	3	0	0	3	1
8hr	100	0	1	6	0	0	5	2
	90	0	2	8	0	1	6	5
1hr	100	3	19	50	1	11	40	50
	90	7	28	61	3	18	51	63

8.6 Conclusions on Transferability of Methodology with respect to Locations and Compounds

The prediction algorithm was applied to three different types of urban roadside site:

- junction
- semi-open roadside
- street canyon

For each of these sites the algorithm was seen to perform well, indicating that the same methodology can be applied with similarly successful results at most urban roadside locations.

The prediction algorithm was used to estimate the frequency distributions of a number of different pollutants, both primary and secondary:

- Carbon monoxide
- Nitrogen dioxide
- PM_{10}
- Nitrogen monoxide
- Acetylene
- 1,3,5-trimethylbenzene
- Benzene

The prediction algorithm was seen to work comparably well with all these compounds, with the exception of benzene, demonstrating a high level of flexibility and transferability.

In all cases, the prediction algorithm was tested for an input of three days of 24 hours of data, and three days with data measured only between 17:00 and 18:00 (to test the algorithm with the most unrepresentative data). The predictions calculated with the 24-hour inputs outperformed the predictions using only data measured between 17:00 and 18:00 for acetylene and 1,3,5-trimethylbenzene, but otherwise neither input resulted in consistently better predictions.

9. DISCUSSION

9.1 Introduction

This section considers the algorithm in the context of existing methods of air pollution modelling. Section 9.2 introduces categories of various air quality models and examples of each are discussed. The main similarities and dissimilarities between the commonly used models and the algorithm are then presented in Section 9.3. Section 9.4 summarises the conclusions to this chapter.

9.2 Categories of Air Quality Models

The first step in modelling air pollution is the definition of the pollutants and the time and spatial scales of interest. Only then can an appropriate model be chosen. Models are formulated in a number of ways. Each formulation has certain strengths and certain limitations.

A schematic diagram of different model types is given in Figure 9.1. Mathematical air quality models are of one of two types: empirical/statistical or deterministic. Empirical/statistical models attempt to predict concentrations by establishing a relationship between historically observed air quality and the corresponding emissions. Deterministic air quality models describe in a fundamental manner the individual processes that affect the evolution of pollutant concentrations. These models are based on solving the atmospheric diffusion/reaction equation, which is, in essence, a conservation of mass principle for each pollutant species (Russell, 1988).

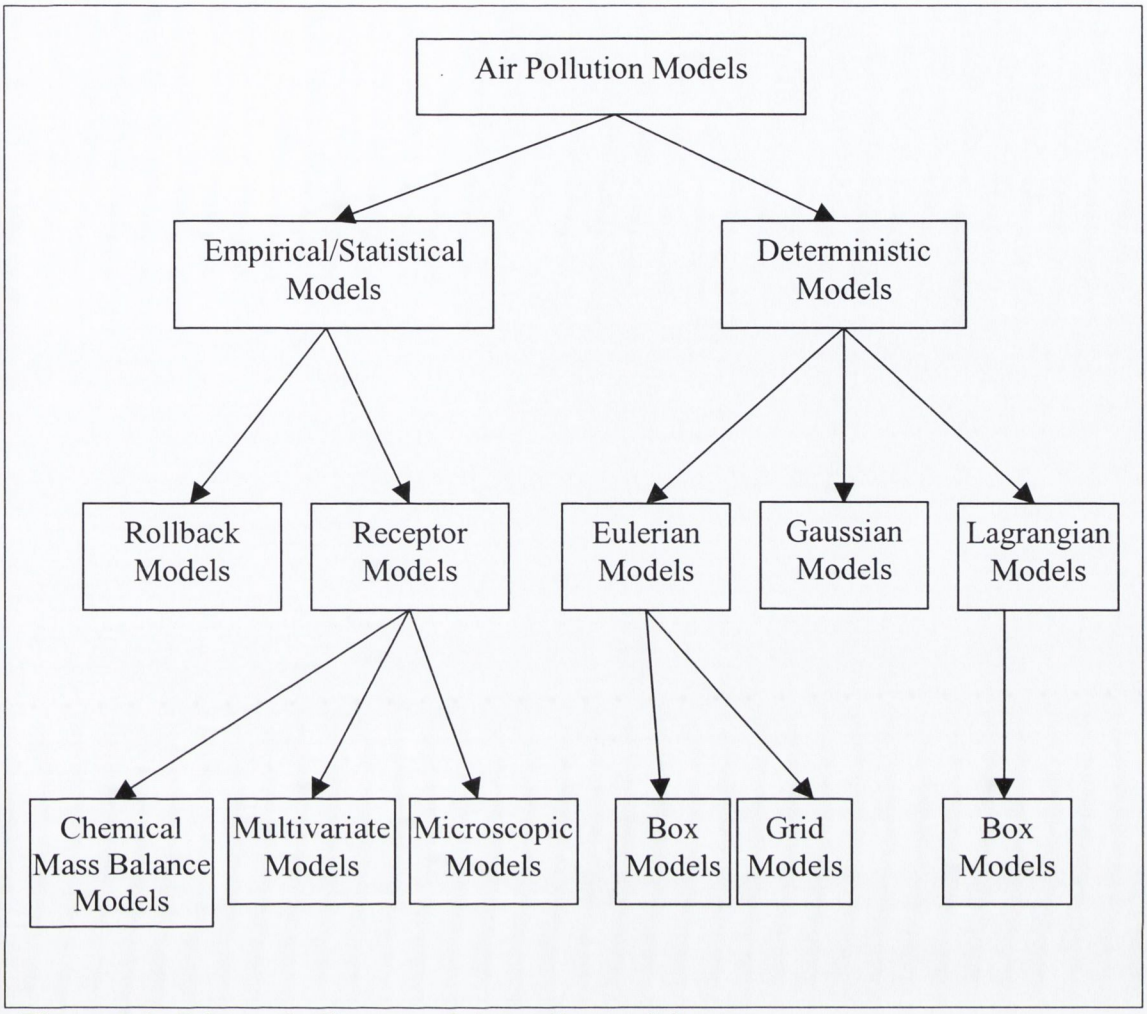

Figure 9.1 Schematic diagram of air quality model types

Air pollution models also vary from very simple methods with very few parameters, to complex ones, with a large number of parameters. The larger the number of parameters, the smaller the errors in the model's representation of the physical reality. However, this is counteracted by a larger input error. While complex models can be 'tuned' or calibrated to fit the available measurements (Zannetti, 1990), this can result in the models becoming highly location-specific, requiring extensive recalibration for application to each new site. A number of different model types are identified in the following paragraphs.

9.2.1 Empirical/Statistical Models

Empirical/statistical models, such as receptor-oriented and roll-back models, are based on establishing a statistical relationship between observed air quality and calculated emissions.

Linear Rollback Model

The linear rollback model is simple and requires relatively few inputs, and for those reasons has been widely used. Linear rollback models assume that the highest measured pollutant concentration is proportional to the basin-wide emission rate, plus the background value according to equation Equation 9.1.

$$C_{max} = aE + c_b \qquad \text{Equation 9.1}$$

where C_{max} is the maximum measured pollutant concentration, E is the emission rate, c_b is the background concentration due to sources outside the modelling region, and *a* is the constant of proportionality. The constant, *a,* accounts for the dispersion, transport, deposition, and chemical reactions of the pollutant. Thus, the allowable emission rate, E_a, necessary to reach a desired ambient concentration can be calculated from Equation 9. 2.

$$\frac{E_a}{E_t} = \frac{c_d - c_b}{c_{max} - c_b} \qquad \text{Equation 9. 2}$$

where

E_t is the emission rate at time t

C_d is the desired ambient concentration

This is a very much simplified approach and as a consequence its application is limited in terms of scope and accuracy. Nonlinear processes such as chemical reactions and spatial or temporal changes in the emission patterns are not accounted for specifically in this type of model (Russell, 1988).

Receptor Models

This type of model is used for estimating the source contributions to particulate matter concentrations. Non-reactive gases have also been tracked using the same methods. Receptor models compare the measured chemical composition of emissions from the major sources to identify the source contributions at ambient monitoring sites. They can generally be categorised into chemical mass balance or multivariate models, although hybrid analytical and receptor (or combined source/receptor) models have also been used (Russell, 1988).

Receptor models are powerful tools for source apportionment where particulate species characterisation data are collected. At a sampling (or receptor) site, the aerosol mass concentration of each species *i* is:

$$Ci = \sum_{j=1}^{n} a_{ij} S_j \qquad i=1,2,\ldots m \qquad \text{Equation 9.3}$$

(Russell, 1988)

where C_i is the mass concentration of species *i* at the receptor site; S_j is the total mass concentration of all species emitted by source category *j* as found at the receptor site; a_{ij} is the fraction of the total mass from source *j* emitted as species *i* arriving at the sampling site; m is the total number of species measured and n is the total number of sources. The mass concentration C_i measured at the receptor site of interest and the coefficient a_{ij} that describes the chemical composition for the major sources are the inputs from which S_j, the mass apportioned to source *j*, is determined. As the parameter a_{ij} characterises the source, it is unique to the source and can therefore be referred to as the source fingerprint. This method works best when the sources are not alike as when the chemical composition of the emissions from two source categories are similar, it is extremely difficult for receptor models to distinguish between the sources. The categories of the models are differentiated by the techniques used to determine *Sj*.

Chemical Mass Balance Methods:

If the source fingerprints, $a_{ij,}$ for each of n sources are known, and the number of sources is less than or equal to the number of species measured, an estimate for the solution to Equation 9.3 can be obtained. If the number of sources is greater than the number of species measured then least-squares or linear programming methods must be used to solve for S_{ij}.

Multivariate Models

Multivariate models rely on finding the underlying structure of large sets of air quality data in order to determine the source of the pollutant. Multivariate techniques identify groups of pollutants whose concentrations fluctuate together, and whose concentrations are correlated, implying that these come from the same source.

Synoptic Class

Meteorological synoptic class has been linked to pollution levels, and the synoptic class alone can be used as a location-specific approximate indicator of relative pollution levels (Sánchez *et al.*, 1990), although fine temporal or spatial resolution is not possible.

9.2.2 Deterministic Models

Deterministic models are based on solving the atmospheric diffusion/reaction equation, which is in essence the conservation-of-mass principle for each pollutant species, and can be divided into two main categories, Eulerian and Lagrangian models. Eulerian models are best suited to situations when the numerical methods employed are sufficiently accurate, computational requirements are not excessive, and fine discretization is required. Conversely, Lagrangian models are used when high accuracy or fine discretization is not required (Zanetti, 1998). Eulerian modelling is generally used for modelling in three dimensions, and Lagrangian modelling for two-dimensional cases with no diffusion processes.

Eulerian Models

In Eulerian modelling the coordinate system is fixed at the earth's surface, and a succession of air parcels is viewed as being carried past an observer.

Box Models

The box model is the simplest form of Eulerian modelling which can be used to estimate pollutant concentrations from an area source. Box models are based on an approximate solution of the diffusion-convection equation (Würtz and Haastrup, 1996). The area to be modelled is viewed as a well-mixed box (Russell, 1988). Pollutants are assumed to be mixed instantly and completely, so that concentrations are always uniform. In general, box models can be used to obtain order-of-magnitude estimates of pollution levels (Lettau, 1970). However, these models do not account for changes of wind with height, and the simplifying assumptions do not closely reflect the real processes of transport and diffusion.

Grid Models

Eulerian grid models are more complex, but potentially more powerful, and involve less restrictive assumptions. They are, however, more computationally intensive. Grid models divide the area of interest into a large number of cells, both horizontally and vertically. These cells interact with each other through a simulation of diffusion, advection and sedimentation (for particles) processes. Eulerian grid models predict pollutant concentrations throughout the entire airshed over successive time periods.

Gaussian Models

Gaussian plume modelling is one of the more widely used forms of air pollution modelling. Gaussian plume models are easy to use, require relatively few input data, and are very quick computationally, although previous studies have shown that it is unrealistic to expect Gaussian models to predict real-world dispersing plume concentrations consistently to within a factor of two or three (Misstear *et al.*, 2000). Models are based on Equation 9.4.

$$C(x,y,z) = \frac{Q}{2\pi u \sigma_y \sigma_z} \exp\frac{-y^2}{2\sigma_y^2}\left[\exp\left(\frac{-(z-H)^2}{2\sigma_z^2}\right) + \exp\left(\frac{-(z-H)^2}{2\sigma_z^2}\right)\right]$$ Equation 9.4

where

C is the pollutant concentration (g/m^3);

x is the downwind distance (m);

y is the crosswind distance from the plume centreline (m);

z is the vertical distance (m);

Q is the source emission rate (g/sec);

u is the mean wind speed (m/sec);

H is the effective height of the source above ground level (m);

δ_y is the standard deviation of a statistically normal plume concentration in the lateral direction (m); and

δ_z is the standard deviation of a statistically normal plume concentration in the vertical direction (m).

Prediction of a single source contribution to ambient pollutant concentrations requires a precise knowledge of dispersion in complex flows (Sini *et al.*, 1996). The estimation of source strength is of prime importance (Singh *et al.*, 1990). Gaussian plume modelling is one of the more basic and commonly used forms of modelling (Curtiss and Rabl, 1996; Russell, 1988), although gaussian plume models do not have an adaptive structure and require costly and well-defined data (Lee *et al.*, 1997).

Multiple sources are modelled by superimposing the calculated contributions of individual sources to ambient concentrations at a given receptor site. It is possible to include the first-order chemical decay of pollutants within the Gaussian plume framework, although for chemically more complex situations the model fails to give an acceptable solution.

Dispersion models can also be combined with chemistry and photochemical models, to model the concentrations of chemically reactive species, such as NO_x (Owen *et al.*,

2000). However, the accuracy of these models can be limited by the extreme complexity of NO_x chemistry and photochemistry, which play an important role in determining NO_x concentrations (Uno *et al.*, 1996).

The following assumptions are made when applying the basic Gaussian model (Zanetti, 1998)

- Emission times equal to or greater than travel times to the downward position of interest pertain so that diffusion in the direction of travel can be ignored.
- The material diffused is a stable gas or aerosol (<20 μm diameter), which remains suspended in the air over long periods of time.
- The plume concentrations have a normal distribution in the cross-wind and vertical directions.
- No material is removed from the plume. This is not the case in the event of wet deposition where a precipitation event removes material via diffusion, adsorption, or absorption. To avoid dry deposition, there must be complete reflection at the ground; this is usually satisfied if the plume is far from a significant body of water.
- Steady-state conditions pertain during the time interval for which the model is used. Meteorological conditions remain constant for this condition to be fulfilled.
- Constant wind speed is assumed. As wind speed is dependent upon height, the plume rise must be small for this approximation to remain valid.
- Constant wind direction is assumed. A change in wind direction results in a larger spread of pollutants and a deviation of the centre-line concentration on the ground.
- No allowance is made for the wind shear effect on horizontal diffusion. This approximation is not valid at distances greater than about 10 km.
- The dispersion parameters are assumed to be independent of altitude and to be functions of downwind distance (and hence windspeed) alone.
- The averaging times for all quantities (u, δ_y, δ_y, and C) are assumed to be equal.

The methods for obtaining the certain parameters used in Gaussian models are also subject to many assumptions and constraints (Pasquill and Smith, 1983), such as those for

- obtaining atmospheric stability classifications, which, in turn, characterise the degree of turbulence;
- determining profiles of wind speed versus emission height;
- converting short-term ground-level concentrations from one averaging period to another.

Lagrangian Models

Lagrangian models are so called because they use a Lagrangian reference frame, in which the reference frame moves with the flow of air. This, is effect, maintains the observer in contact with the same air parcel over extended periods of time.

Mathematically, the Lagrangian models calculate pollutant diffusion, transformation and removal, in a moving frame of reference tied to each of a number of air 'parcels' as they are transported by the calculated or observed wind field. The calculations can be performed using the ordinary differential equation system (Tran, 1981):

$$\delta C_s / \delta t = -(k_{1,s} + k_{2,s}) C_s(x, y, z, t) + E_s(x, y, z, t) + R_s(C_1, C_2, ..., C_q) \quad \text{Equation 9.5}$$

where

$k_{1,s}$ and $k_{2,s}$ are the dry and wet deposition of species S;

E_s is emission rate;

C_s, C_1, C_2, ,…,C_q are pollutant concentrations;

R_s is the chemical transformation of pollutant S; and

q is the number of pollutants involved.

Lagrangian Box Models

Unlike Eulerian Box models where the box remains stationary, in Lagrangian models the box is advected horizontally according to the local time-varying average wind speed and direction. Lagrangian box models are often used for photochemical modelling (Drivas *et al.,* 1997) where the models provide average time-varying concentration estimates along the box trajectory. The major shortcoming of this

approach is the assumption that wind speed and direction are constant throughout the planetary boundary layer. However, Lagrangian box models are less computationally expensive than Eulerian box models as calculations are carried out on a smaller number of moving cells rather than a larger number of fixed cells.

Since ideal model application conditions are seldom found, air quality models are often used beyond their theoretical and practical limits of applicability (Zannetti, 1990). Several model validation studies have, therefore, shown unsatisfactory levels of performance, especially when steady-state representations are used to simulate complex, time-dependent atmospheric phenomena (Zannetti, 1990). It has also been acknowledged that the ability of deterministic models to predict extreme events is limited (Pasquill and Smith, 1983).

9.3 Discussion of algorithm

Investigations of air quality can be divided into two main categories, modelling and measurement. Air pollution models quantitatively simulate factors affecting the fate of pollutants in the atmosphere through mathematical characterisation of pollutant emissions, advection, diffusion, deposition, chemical reactions. Model input data include emission inventories with spatial and temporal variations, meteorological data (such as wind speed, mixing height, and diffusion coefficients), site characteristics (such as details of the terrain) and removal processes. The accuracy of a model is dependent upon the accuracy of the input data; incorrect characterisation of any one of the input variables will result in inaccurate output regardless of how well the model simulates the processes to which the pollutants are subjected. Numerical models have only recently been able to simulate flow patterns accurately on the meso-scale level and micro-scale conditions can still not be accurately modelled.

The alternative approach is to physically measure the concentrations of the pollutants under consideration at the site of interest. This guarantees that the concentrations will be known exactly. However, for predictions of how a change in conditions will affect the air quality at a site, a measurement strategy is obviously not appropriate.

The algorithm previously discussed has similarities with both modelling and measurement, although is fundamentally different from pure modelling in that the starting point for the algorithm is physical measurement of the pollutant concentrations, albeit over short periods of time. The algorithm also differs from pure measurement approaches in that the measurements are refined by applying factors based on observed relationships between ambient concentrations and influencing factors.

As the adjustment factors used in the algorithm are based on observed relationships between ambient concentrations and factors such as wind speed and direction it has more in common with empirical models than deterministic models. This approach is very different to that used for deterministic models which take the atmospheric diffusion/reaction equation as a starting point. However, a problem with empirical models is the lack of transportability; a model designed for one location can rarely be transferred to another. It is hoped that the algorithm presented will enable greater ease of transportability but further work is required to evaluate its potential.

The algorithm also differs from a modelling approach in that source details, such as emission inventories, and traffic flow details are not used. These are replaced instead by short term measurement of the pollutant concentrations at the site of interest and characterisation of the daily pattern at the site of interest. An advantage of this is that a significant proportion of the information needed for traditional modelling is not necessary for input into the model, although the corresponding disadvantage is that the algorithm can then not be used to predict how changes in the emissions would affect air quality.

However, as the effects of the variables such as wind speed, wind direction, and time of measurement are mathematically characterised in terms of their effect on ambient concentration levels, the algorithm shares characteristics with statistical models.

For some models, statistics on the frequency of different meteorological conditions are required, while for others, time series of meteorological conditions are needed. For all modelling, therefore, pre-processing of meteorological data is required. This is

true of the algorithm also, where information on average meteorological conditions is required.

9.4 Conclusions

Categories of various air quality models are introduced and examples of empirical and deterministic models are discussed in Section 9.2. The algorithm is then analysed in the context of the two air quality investigation approaches of modelling and measurement. The algorithm combines elements of both measurement and modelling. The algorithm differs from the pure measurement approach in that the measurements are adjusted using calculated factors. However, in terms of the two main approaches of modelling, empirical and deterministic, the algorithm has more in common with statistical models, as the adjustment factors are calculated using the observed relationships between the pollutant concentrations and the influencing factors.

10.CONCLUSIONS

10.1 SUMMARY

The research project involved the commissioning and application of the Trinity College Mobile Air Monitoring Unit for the investigation of urban air quality. There were two main objectives: 1) to add to the limited information on the state of the atmospheric environment in Dublin, and 2) to formulate a methodology to maximise the efficiency and effectiveness of future air monitoring equipment and programmes.

Pollutant concentration data from a number of monitoring sites were collected and analysed to ascertain the theoretical frequency distributions which best characterised the observed distributions over different averaging periods. The effects of temporal and meteorological factors on ambient concentrations of individual compound were then investigated. These relationships were used to calculate adjustment factors to compensate for local conditions at the time of sampling. With these adjustment factors, short-term monitoring data (between 1 hour and 24 hours) collected over the course of three days were used to predict the mean monthly concentration. Short-term peak concentrations over the course of the month were predicted from the chosen theoretical frequency distribution, the predicted monthly concentration and the estimated standard deviation. These predictions were compared with actual measured concentrations and assessed in terms of the limit values defined under the EU Framework Directive 96/62/EC on Ambient Air Quality Assessment and Management (CEC, 1996).

10.2 CONCLUSIONS

The main conclusions of this research are:

Ambient Air Quality

a) Pollutant concentrations measured at three urban sites (intersection, roadside, and street canyon) by Trinity College Dublin, the Environmental Protection Agency and the Electricity Supply Board were presented. All monitoring equipment was located along the northern and eastern boundary of Trinity College, adjacent to streets with heavy traffic congestion. None of the pollutant concentrations breached limits specified under the EU Framework Directive 96/62/EC of 27th September 1996 (CEC, 1996) on ambient air quality assessment and management.

Pollutant Measurement

b) When compared with simultaneous PM_{10} measurement by the EPA, using a light scattering method, the TEOM was found to record lower values, reflecting the volatilisation of compounds such as ammonium nitrate. Good results were achieved for CO measurements using the RPM, although, the resolution of the NO_2 measurements was lower than that necessary for good characterisation of urban roadside NO_2 concentrations.

Pollutant Variability

c) The underlying frequency distributions of the recorded concentration data were analysed. The observed distributions of CO 15-minute averages and PM_{10} 30-minute averages were characterised equally well by both the lognormal and gamma distributions, and the observed distributions of NO_2 15 minute averages were best represented by the normal distribution. The monthly data sets of 1-hour, 8-hour and 24-hour average concentrations for CO, and PM_{10} were also found to conform to both the lognormal and gamma distributions.

d) CO, NO_2 and PM_{10} were all found to exhibit pronounced temporal patterns on a daily and weekly scale, although no seasonal trends could be distinguished from the data. When diurnal patterns displayed by CO, NO_2 and PM_{10} were normalised, all compounds exhibited similar patterns, with the exception of an increased peak in CO concentrations during the evening rush-hour, associated with congestion.

e) Concentrations of CO, NO_2, and PM_{10} were found to be influenced by wind speed, and power relationships with good correlation coefficients were established for CO and PM_{10}. Concentrations of CO and PM_{10} were observed to be influenced by the wind direction. In contrast, NO_2 concentrations were largely independent of wind direction. Pollutant concentrations were not significantly influenced by temperature, relative humidity or sunshine hours.

f) Concentrations of nitrogen oxides were measured at two sites simultaneously. NO_2 displayed a higher degree of spatial variability than NO.

g) CO was found to be very strongly correlated (with Pearson's correlation coefficients over 0.9) with several VOCs: 1,3,5-trimethylbenzene, ethylbenzene, m+p-xylene, o-xylene, 1,3-butadiene, propylene, benzene and ethylene. The strongest correlation between NO_2 and the measured VOCs was with 3-methylpentane, with a Pearson's correlation coefficient of 0.63. The strongest correlation between PM_{10} and the measured VOCs was with 1,2,4-trimethylbenzene, with a Pearson's correlation coefficient of 0.64. Correlation coefficients of 0.92, 0.60, and 0.62 were calculated for benzene with CO, NO_2 and PM_{10}, respectively.

h) One week of data was used to calculate the ratios between CO and VOC concentrations. Predictions of individual hourly concentrations of VOCs based on concentrations of CO displayed substantial errors, but a reasonable accuracy for longer-term average predictions was observed, with the exceptions of cis-2-butene and toluene.

i) Diurnal fluctuations of NO and NO_2 were found to differ, reflecting their natures as primary and secondary pollutants, respectively. A correlation coefficient of 0.77 was calculated for NO and NO_2. NO_2 was found to have a stronger correlation with total

NO_x, with a correlation coefficient of 0.87. A correlation coefficient of 0.98 was calculated for NO and NO_x.

j) The ratio of NO to NO_2 was found to be related to concentrations of NO. The increase in this ratio with NO concentrations was found to follow a power relationship.

k) $PM_{2.5}$ and PM_1 were found to follow similar diurnal patterns to PM_{10}, with less pronounced peaks. PM_{10} concentrations were very strongly correlated with measured concentrations of total particulates ($r = 0.95$). PM_1 and $PM_{2.5}$ were also very strongly correlated ($r = 0.92$). PM_{10} was also correlated with $PM_{2.5}$ and PM_1, although to a slightly lesser degree, with correlation coefficients of 0.69 and 0.62, respectively.

l) SO_2 was moderately correlated with CO, NO_2, and PM_{10}, with correlation coefficients of 0.63, 0.58, and 0.42, respectively.

Prediction of Pollutant Concentrations

m) An algorithm for the prediction of monthly averages based on short-term monitoring was formulated. The convergence of the adjustment factors was found to suggest that factors could be calculated over a sufficiently short period (one week) to be of use in short-term monitoring programmes."

n) It was demonstrated that, using the algorithm, predictions of the 30-day averages can be made from short monitoring periods with, in many cases, some degree of accuracy, for a wide range of primary and secondary pollutants, by correcting the recorded data for the time of sampling and local conditions during sampling. The choice of monitoring period was seen to affect the accuracy of the 30-day averages to a much lesser extent for the prediction algorithm than for the arithmetic averages.

o) A methodology for the prediction of 1-hour, 8-hour and 24-hour concentrations using the theoretical frequency distributions, and the estimated standard deviation combined with either the predicted or measured monthly average or a long-term average, was formulated.

p) 1-hour, 8-hour and 24-hour extreme concentrations of CO, NO_2, PM_{10}, NO, acetylene, and 1,3,5-trimethylbenzene over 30-day periods were predicted with a good degree of accuracy in many cases. On average, 73%, 72%, 77%, of the analysed predictions for CO, NO_2, and PM_{10}, respectively, were within the predicted limits. 57%, 67% and 67% of the predicted upper percentiles of NO, acetylene, and 1,3,5-trimethylbenzene, respectively, were within the predicted limits. The numbers of exceedences of reference concentrations were also predicted with a reasonable degree of accuracy in many cases.

q) The adjustment factors and frequency distributions used in the prediction algorithm have been found to be stable with respect to time for the period over which monitoring was carried out.

r) The prediction algorithm was applied to three different types of urban roadside site, junction, semi-open roadside and street canyon. For each of these sites the algorithm was seen to perform well; this would appear to suggest that the same methodology can be applied with similarly successful results at many urban locations.

s) The prediction algorithm was seen to work comparably well with all compounds investigated other than benzene (due to benzene not conforming to a gamma distribution), demonstrating a high level of flexibility and transferability.

10.3 Recommendations for Further Research

Recommendations for further research include:

(i) An independent assessment of the prediction algorithm at another urban site using data monitored over one week to calculate the adjustment factors, which could then be assessed with respect to the concentration data recorded over one month;

(ii) The continuation of the study at more urban sites;

(iii) An investigation into whether adjustment factors for an individual site can be used at other sites of a similar nature, without recalculating the adjustment factors;

(iv) The inclusion of rainfall and precipitation adjustment factors in the algorithm for prediction of PM_{10} concentrations;

(v) The application and investigation of the performance of the algorithm to rural sites;

(vi) The extension of the algorithm to compounds not characterised by the lognormal or gamma distributions, such as benzene;

(vii) The use of NO_2 monitoring equipment capable of finer resolution for analysis of ambient concentrations;

(viii) The monitoring of pollutant concentrations over longer periods to investigate seasonal variability at the site;

(ix) Further investigation of the spatial (both horizontal and vertical) variability of pollutant concentrations, in the vicinity of road sources;

11.APPENDICES

11.1 APPENDIX A

r Pearson's correlation coefficient. This describes how strongly the x and y values in a sample of pairs are related to one another.

R^2 Coefficient of determination,
where (correlation coefficient)^2 = (coefficient of determination).
This gives the proportion of variation that is attributable to the linear relationship between the two variables.

r is defined using Equation 10.1.

$$r = \frac{\sum(x_i - \bar{x})(y_i - \bar{y})}{\sqrt{\sum(x_i - \bar{x})^2}\sqrt{\sum(y_i - \bar{y})^2}}$$

Equation 10.1

where

(x_1,y_1), (x_2,y_2), …, (x_n,y_n) denote a sample of (x,y) pairs, and $\bar{x}, \bar{y}$ are the averages of the x samples and y samples.

11.2 APPENDIX B

Sample Calculation of Wind Direction Factors for February 1998

The 15-minute average CO concentration (including data from all directions) for February 1998 was calculated to be 1.58 ppm. The average wind speed was 2.47 m/s. As the wind speed was higher than usual, the CO concentration was lower than might otherwise have been expected. Using Equation 6.6 (from Section 6.6.1), this CO concentration was converted to an equivalent value at a wind speed of 2 m/s. When the same operation is carried out on the averages in each direction this allows like to be compared with like, negating the effect of the wind speed.

As complete days are being used in the calculation, the wind speed does not need to be corrected for the time of sampling.

$$fac(u) = \frac{100}{245.17 \times (u)^{-1.07}}$$ Equation 6.6

$$fac(u) = \frac{100}{245.17 \times (2.47)^{-1.07}}$$

$fac(u) = 1.07$

$$C_{adj,u} = \overline{c} \times fac(u)$$ Equation 6.1

$C_{adj,u} = 1.58 \times 1.07$

$C_{adj,u} = 1.69$ ppm

The data for February 1998 were split up into the eight directions already defined, and then averaged to give the values shown in Table 10.1.

Table 10.1 Measured and corrected CO concentrations in individual directions for February 1998.

	WR	WR/PW	PW	PW/L	L	L/PE	PE	PE/WR
$\bar{c}$ (ppm)	1.23	1.45	1.28	1.78	3.77	4.27	2.85	1.97
u (m/s)	2.61	2.65	2.24	1.96	1.19	1.37	1.14	1.26
fac(u)	1.14	1.16	0.97	0.84	0.49	0.57	0.47	0.52
C_{adj} (ppm)	1.40	1.68	1.24	1.43	1.85	2.44	1.34	1.02

These corrected values can then be expressed as a fraction of the monthly average in Table 10.2.

Table 10.2 CO concentrations as a fraction of the monthly average for February 1998

Direction	WR	WR/PW	PW	PW/L	L	L/PE	PE	PE/WR
CO as fraction of monthly average	0.83	0.99	0.73	0.85	1.09	1.44	0.79	0.60

The same calculations were carried out for each month of data and then averaged to give the factors in Table 10.3.

Table 10.3 Average CO concentrations as a fraction of the monthly average and corresponding adjustment factor

Direction	WR	WR/PW	PW	PW/L	L	L/PE	PE	PE/WR
CO as a fraction of monthly average	0.92	0.97	1.07	1.31	1.19	1.16	1.23	1.18
$Fac_{dir}(\theta)$	1.09	1.03	0.93	0.76	0.84	0.86	0.81	0.85

11.3 APPENDIX C

24-Hour Averages – Phase 1

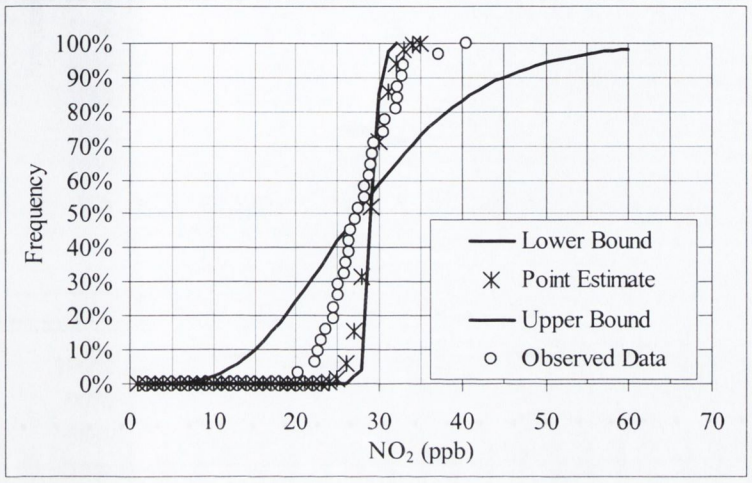

Figure 10.1
Predicted frequency distribution of 24-hour NO_2 averages for August 1998, calculated using 3 complete days of monitoring.

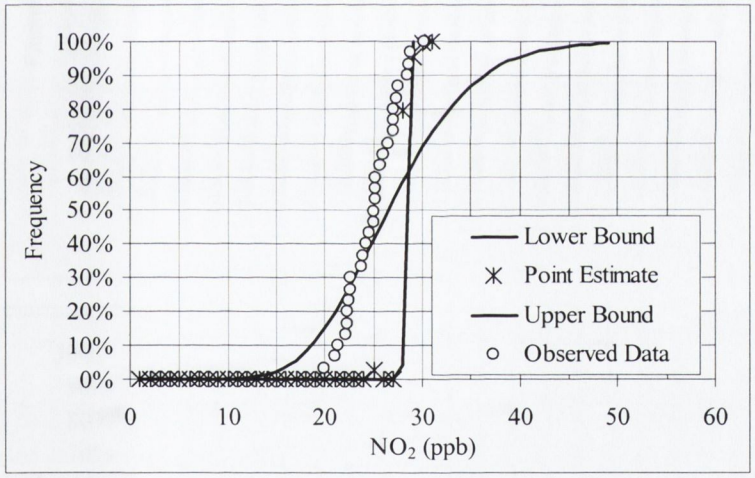

Figure 10.2
Predicted frequency distribution of 24-hour NO_2 averages for January 1999, calculated using 3 complete days of monitoring.

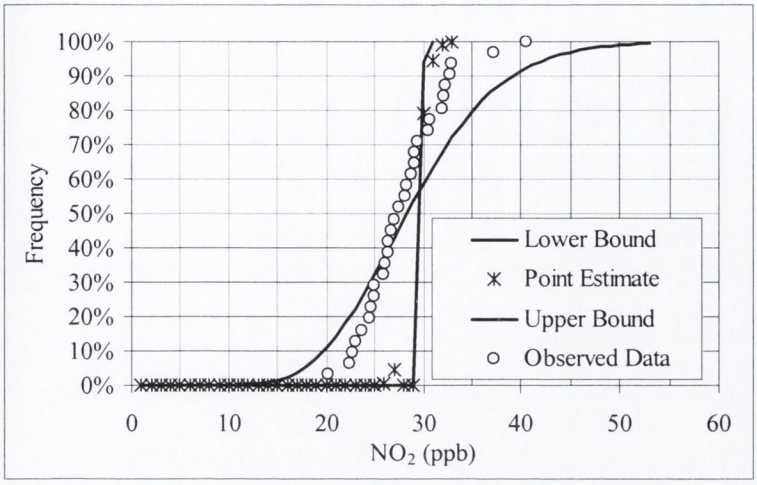

Figure 10.3
Predicted frequency distribution of 24-hour NO_2 averages for August 1998, calculated using 3 days of data collected between 17:00 and 18:00.

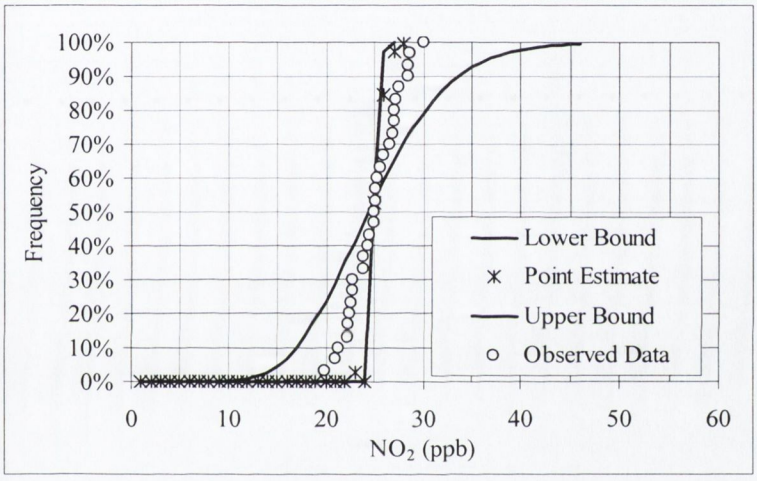

Figure 10.4
Predicted frequency distribution of 24-hour NO_2 averages for January 1999, calculated using 3 days of data collected between 17:00 and 18:00.

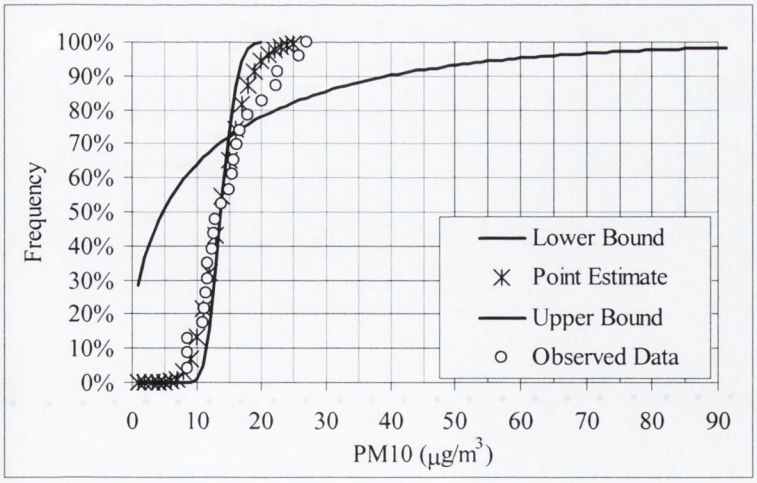

Figure 10.5
Predicted frequency distribution of 24-hour PM_{10} averages for August 1998, calculated using 3 complete days of monitoring.

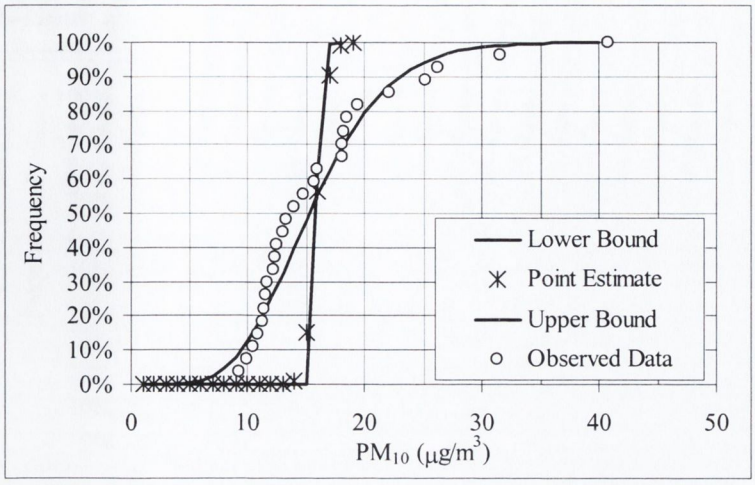

Figure 10.6
Predicted frequency distribution of 24-hour PM_{10} averages for February 1998, calculated using 3 complete days of monitoring

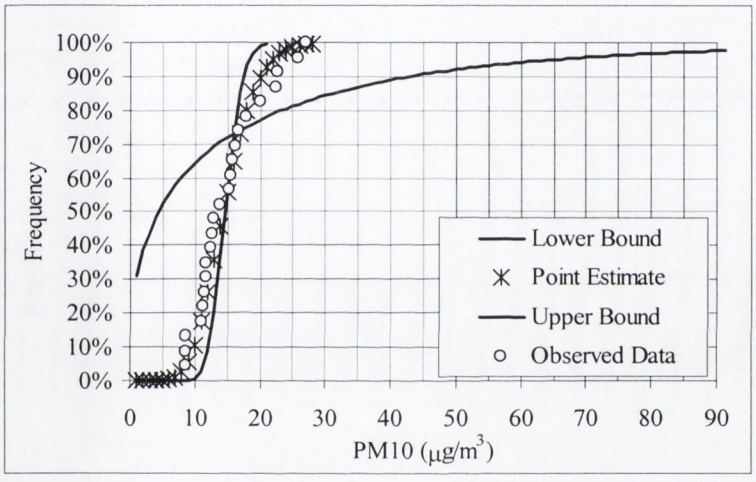

Figure 10.7
Predicted frequency distribution of 24-hour PM_{10} averages for August 1998, calculated using 3 days with data collected between 17:00 and 18:00

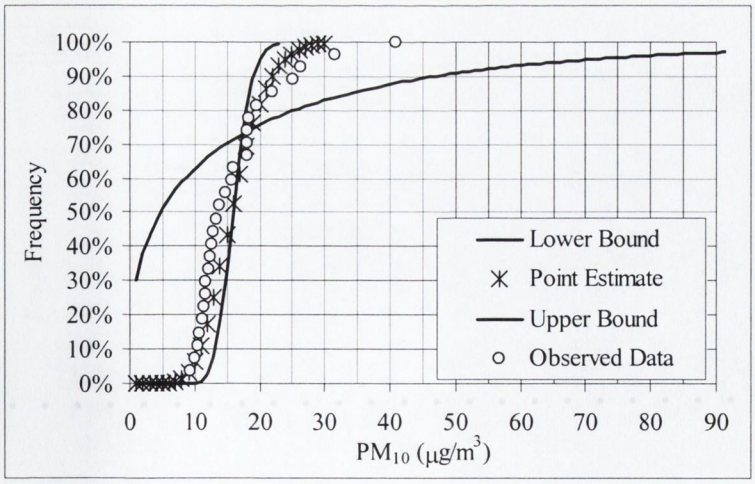

Figure 10.8
Predicted frequency distribution of 24-hour PM_{10} averages for February1998, calculated using 3 days with data collected between 17:00 and 18:00

8-Hour averages Phase 1.

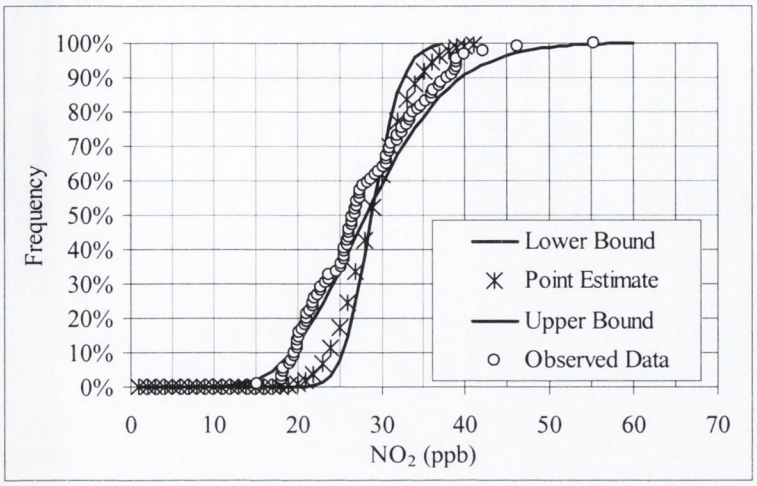

Figure 10.9
Predicted frequency distribution of 8-hour NO_2 averages for August 1998, calculated using 3 complete days of monitoring.

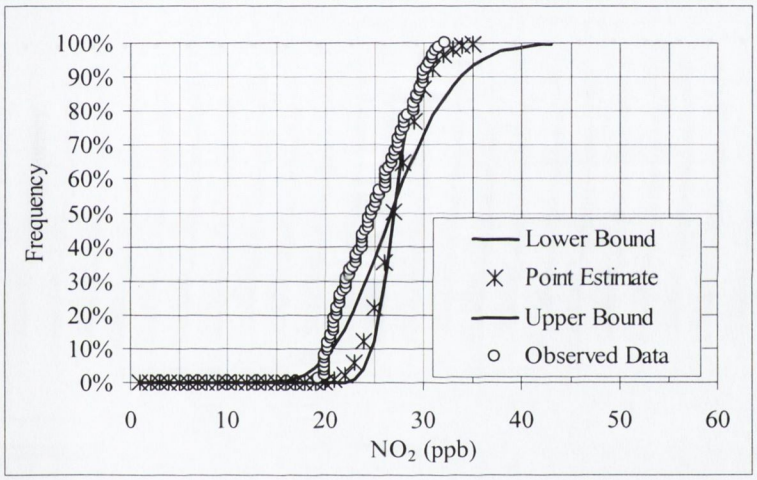

Figure 10.10
Predicted frequency distribution of 8-hour NO_2 averages for January 1999, calculated using 3 complete days of monitoring.

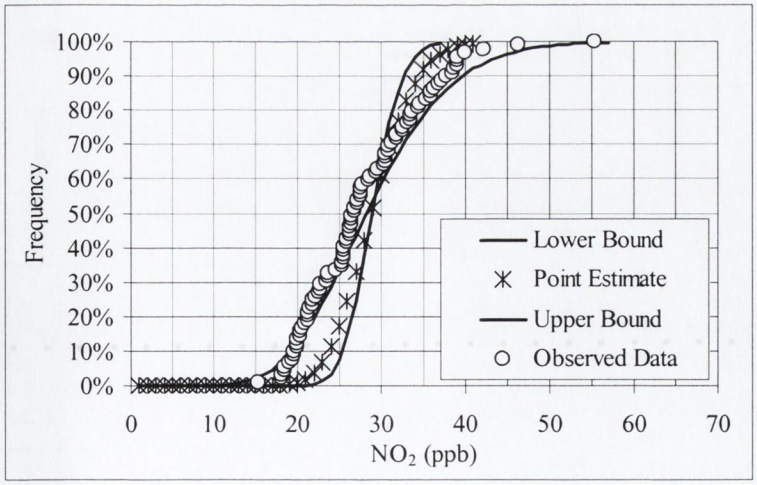

Figure 10.11
Predicted frequency distribution of 8-hour NO_2 averages for August 1998, calculated using 3 days of data collected between 17:00 and 18:00.

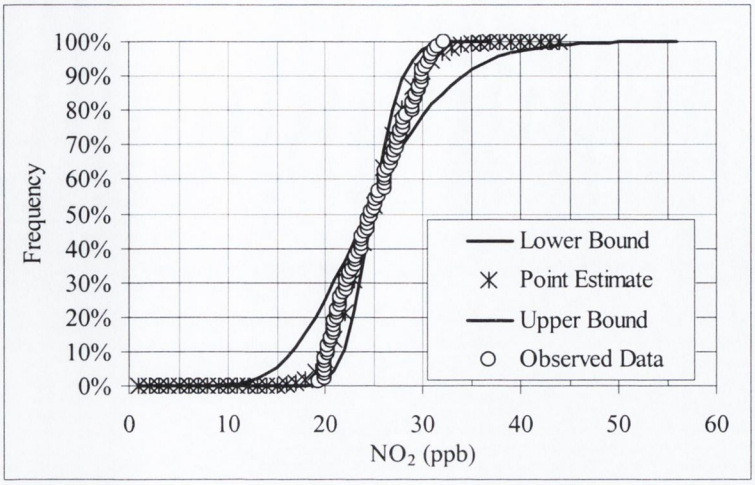

Figure 10.12
Predicted frequency distribution of 8-hour NO_2 averages for January 1999, calculated using 3 days of data collected between 17:00 and 18:00.

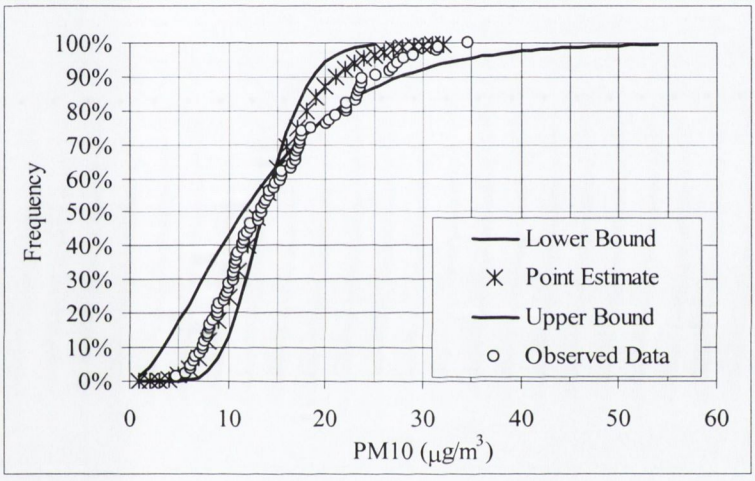

Figure 10.13
Predicted frequency distribution of 8-hour PM_{10} averages for August 1998, calculated using 3 complete days of monitoring.

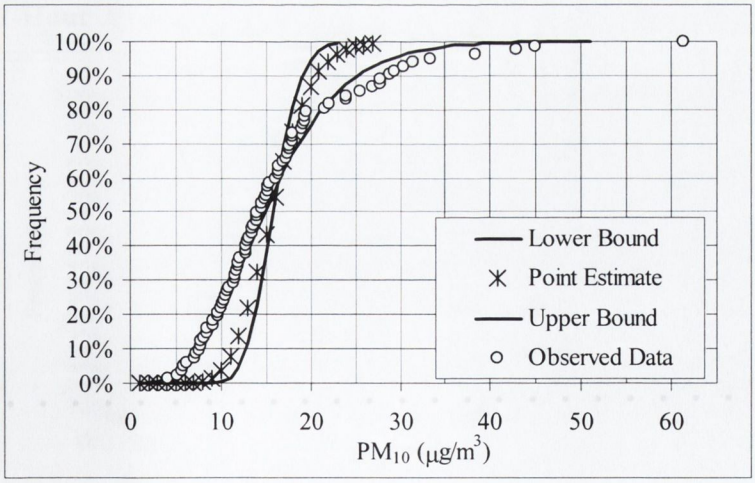

Figure 10.14
Predicted frequency distribution of 8-hour PM_{10} averages for February 1998, calculated using 3 complete days of monitoring.

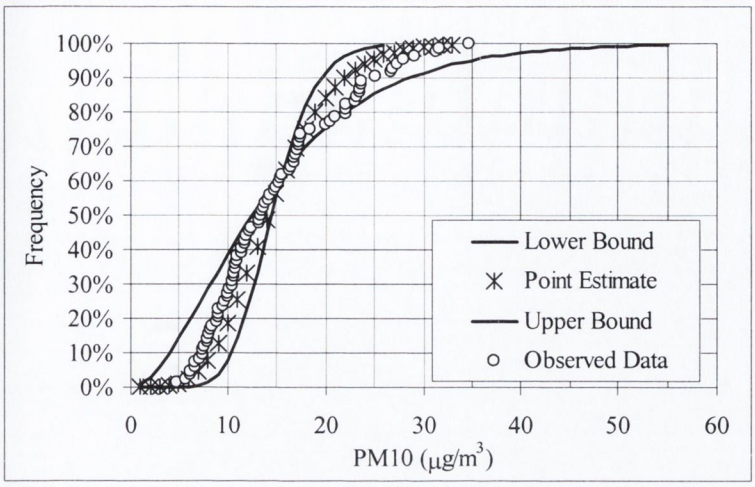

Figure 10.15
Predicted frequency distribution of 8-hour PM_{10} averages for August 1998, calculated using 3 days with data collected between 17:00 and 18:00

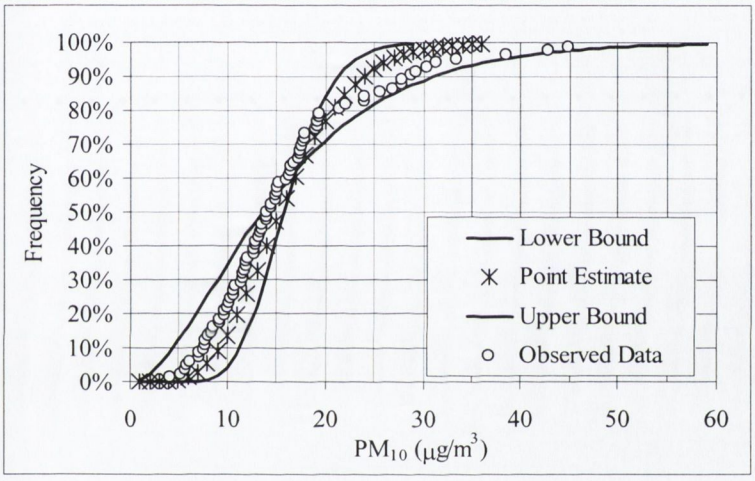

Figure 10.16
Predicted frequency distribution of 8-hour PM_{10} averages for February 1998, calculated using 3 days with data collected between 17:00 and 18:00

1-Hour Averages – Phase 1

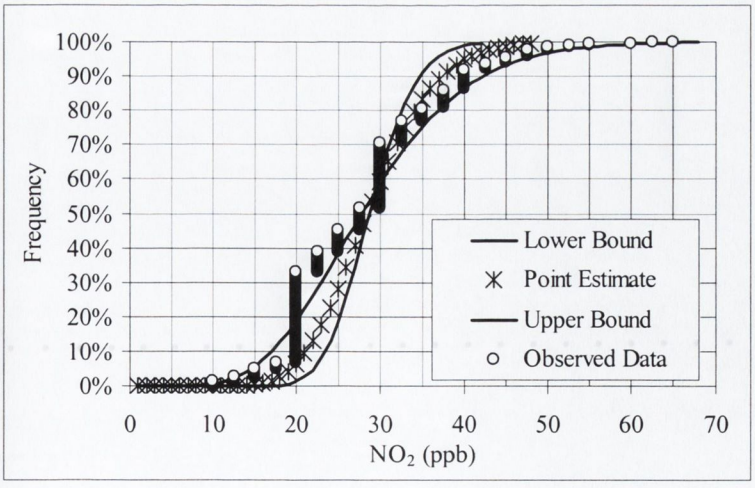

Figure 10.17
Predicted frequency distribution of 1-hour NO_2 averages for August 1998, calculated using 3 complete days of data

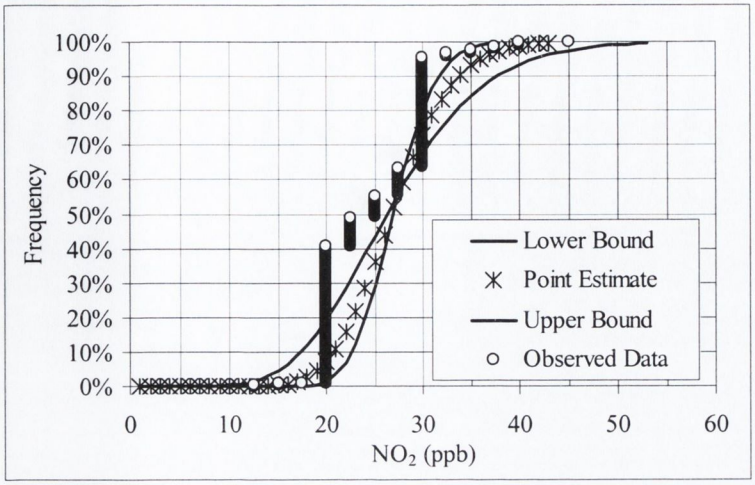

Figure 10.18
Predicted frequency distribution of 1-hour NO_2 averages for January 1999, calculated using 3 complete days of data.

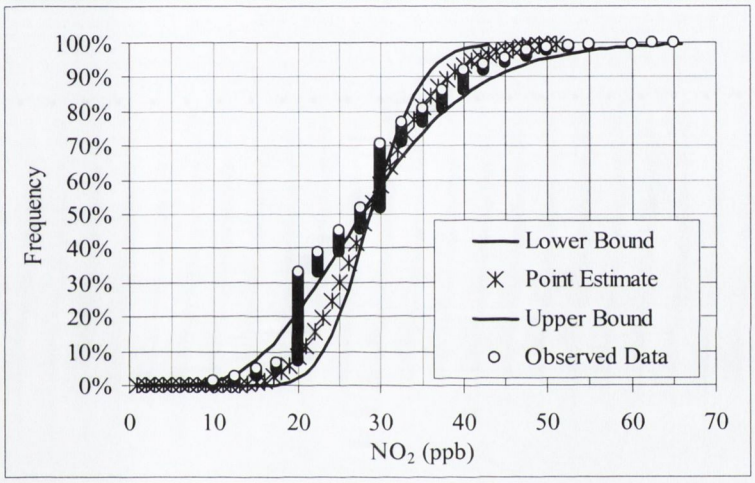

Figure 10.19
Predicted frequency distribution of 1-hour NO_2 averages for August 1998, calculated using 3 days of data collected between 17:00 and 18:00.

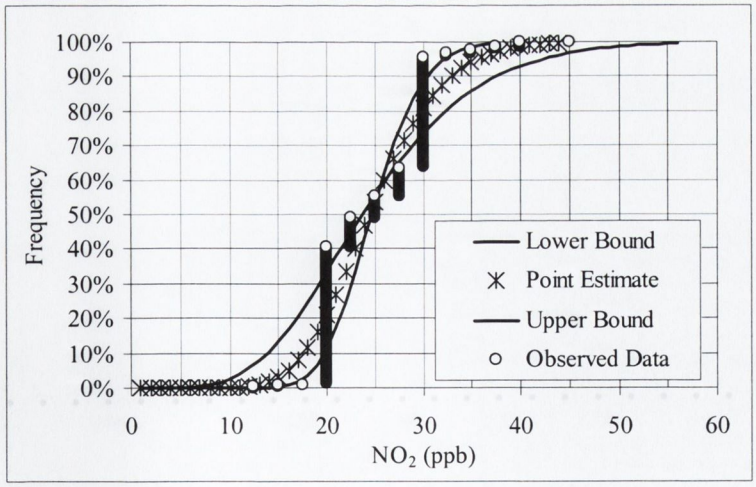

Figure 10.20
Predicted frequency distribution of 1-hour NO_2 averages for January 1999, calculated using 3 days of data collected between 17:00 and 18:00.

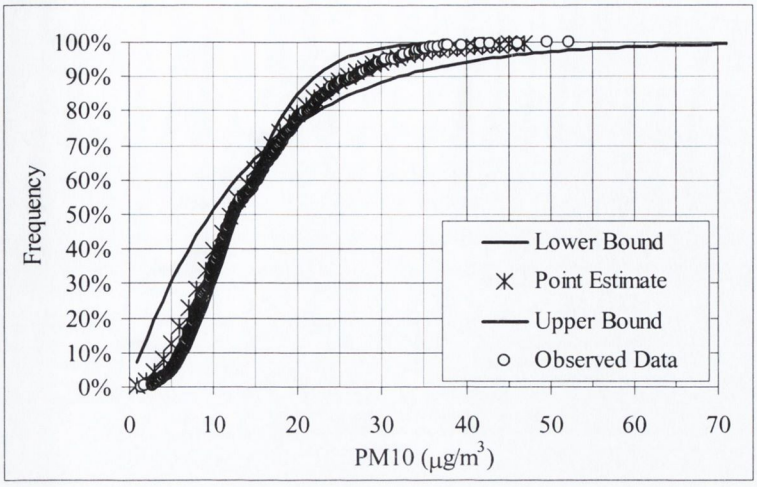

Figure 10.21

Predicted frequency distribution of 1-hour PM_{10} averages for August 1998, calculated using 3 complete days of monitoring.

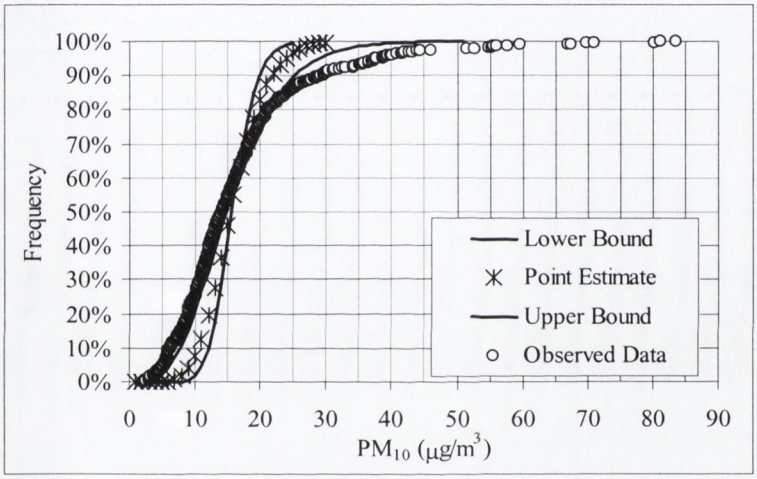

Figure 10.22

Predicted frequency distribution of 1-hour PM_{10} averages for February 1998, calculated using 3 complete days of monitoring.

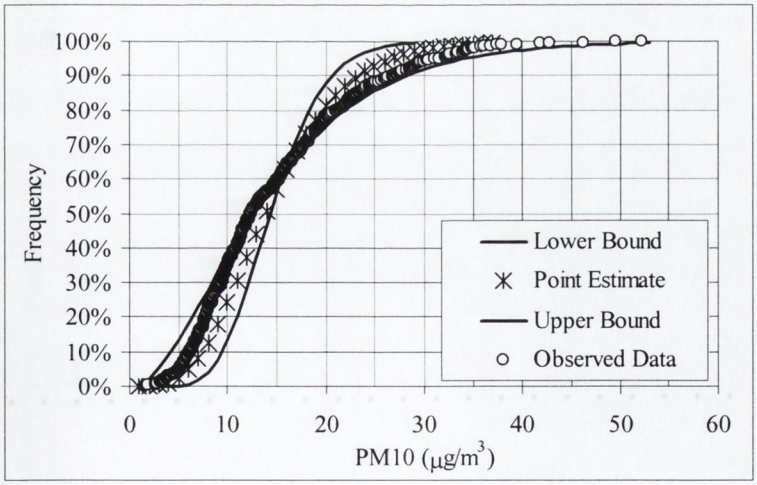

Figure 10.23

Predicted frequency distribution of 1-hour PM_{10} averages for August 1998, calculated using 3 days with data collected between 17:00 and 18:00

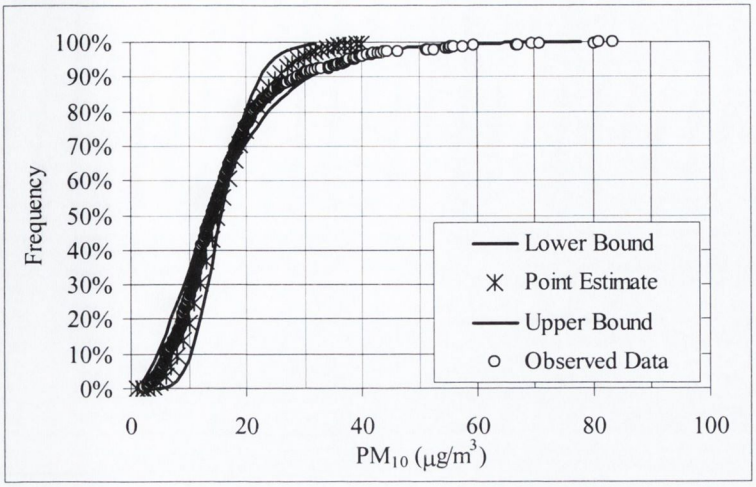

Figure 10.24
Predicted frequency distribution of 1-hour PM_{10} averages for February1998, calculated using 3 days with data collected between 17:00 and 18:00

24-Hour Averages – Phase 2

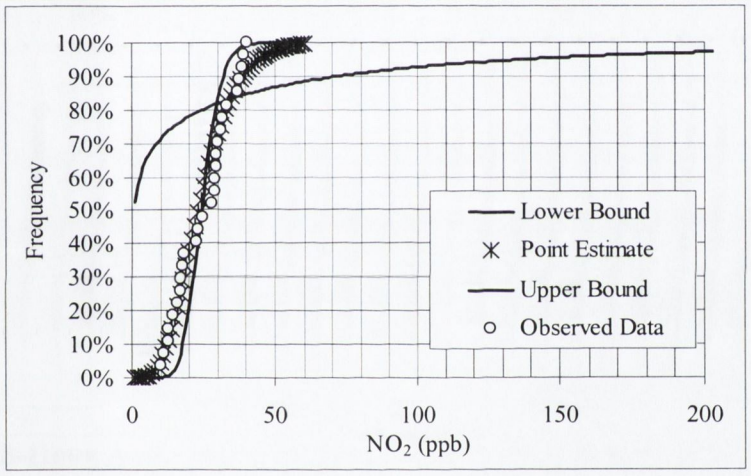

Figure 10.25
Predicted frequency distribution of 24-hour NO_2 averages for August 1999, calculated using 3 complete days of monitoring.

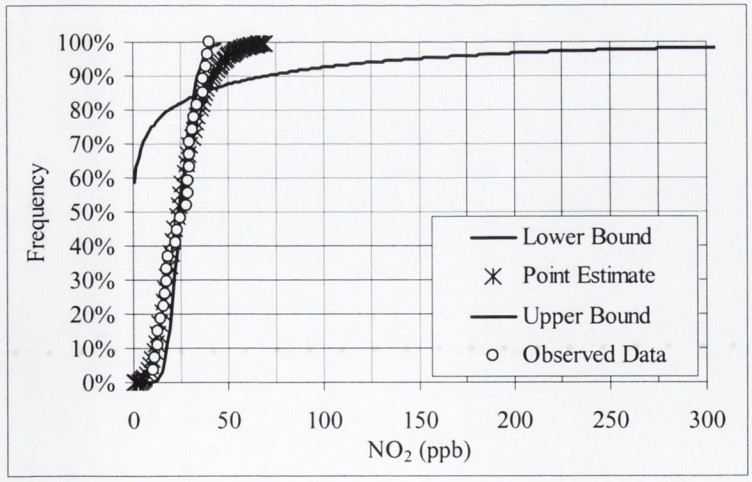

Figure 10.26
Predicted frequency distribution of 24-hour NO_2 averages for August 1999, calculated using 3 days with data collected between 17:00 and 18:00

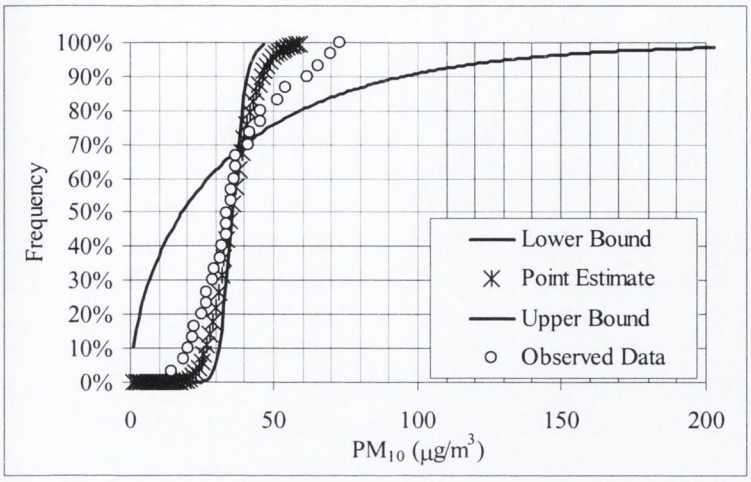

Figure 10.27
Predicted frequency distribution of 24-hour PM_{10} averages for November 1999, calculated using 3 complete days of monitoring.

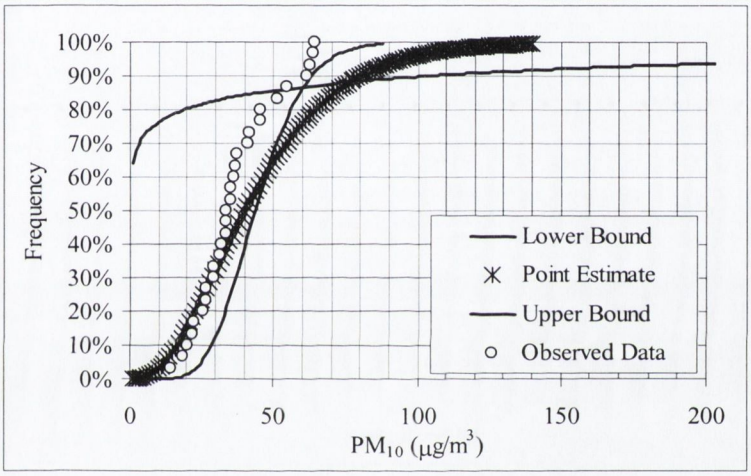

Figure 10.28
Predicted frequency distribution of 24-hour PM_{10} averages for November 1999, calculated using 3 days with data collected between 17:00 and 18:00

8-Hour Averages – Phase 2

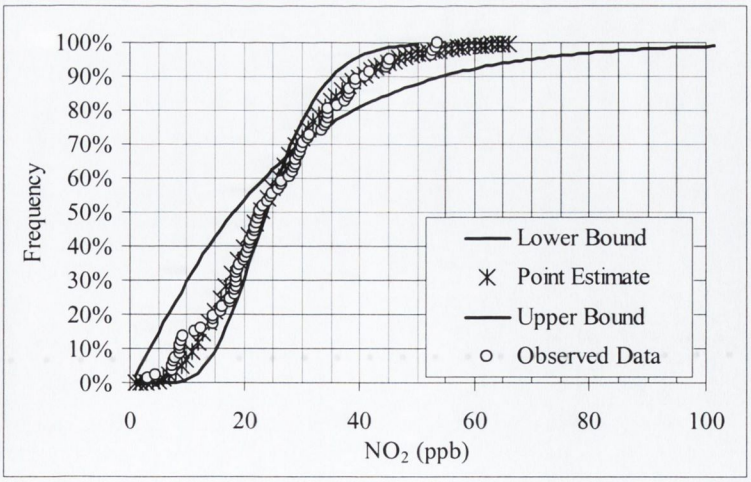

Figure 10.29
Predicted frequency distribution of 8-hour NO_2 averages for August 1999, calculated using 3 complete days of monitoring.

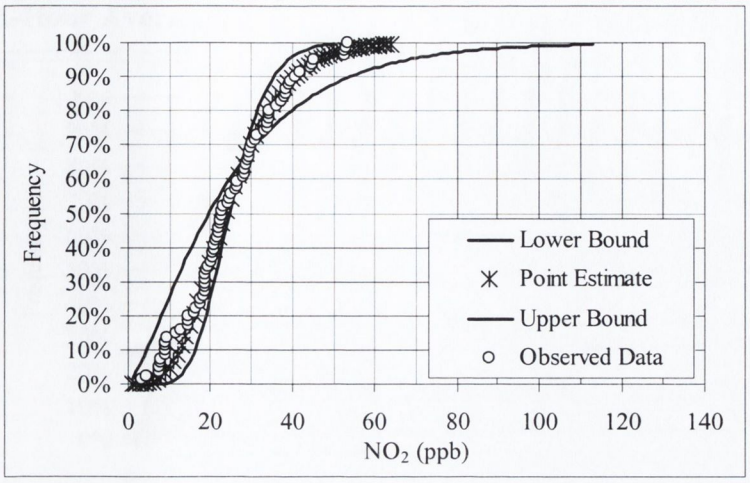

Figure 10.30
Predicted frequency distribution of 8-hour NO_2 averages for August 1999, calculated using 3 days with data collected between 17:00 and 18:00

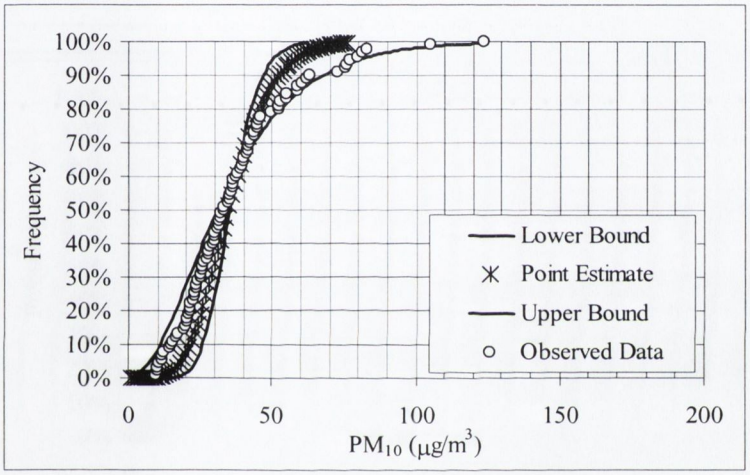

Figure 10.31
Predicted frequency distribution of 8-hour PM_{10} averages for November 1999, calculated using 3 complete days of monitoring.

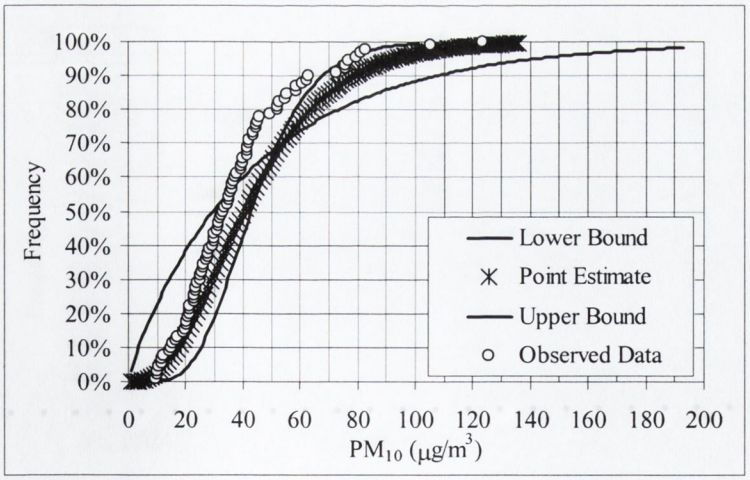

Figure 10.32
Predicted frequency distribution of 8-hour PM_{10} averages for November 1999, calculated using 3 days with data collected between 17:00 and 18:00

1-Hour Averages – Phase 2

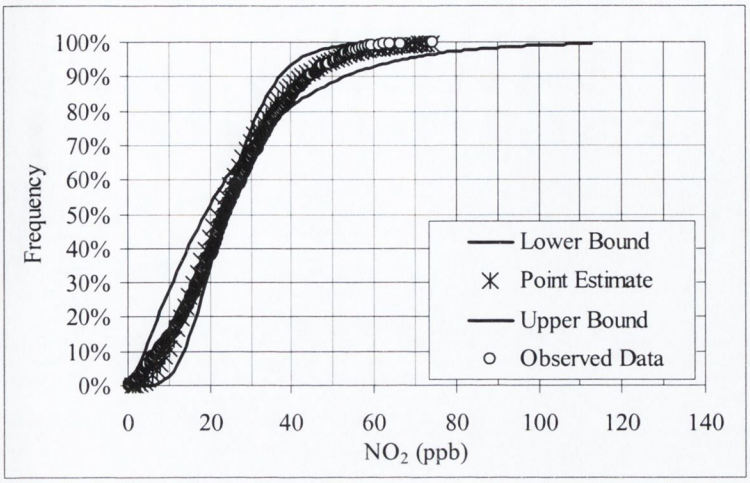

Figure 10.33
Predicted frequency distribution of 1-hour NO_2 averages for August 1999, calculated using 3 complete days of monitoring.

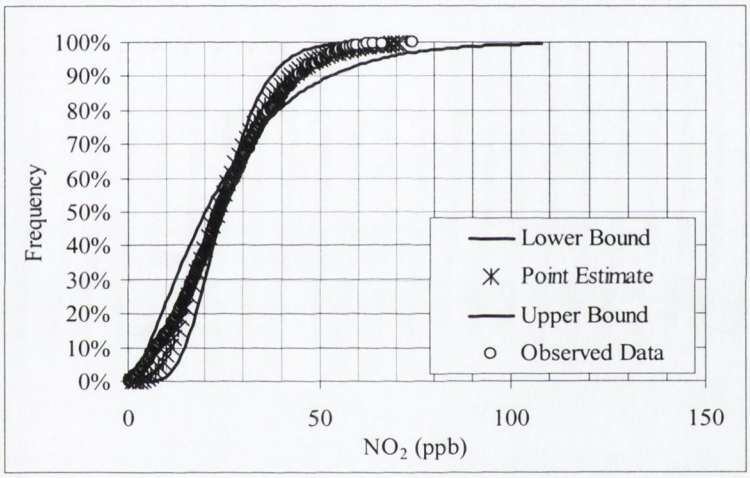

Figure 10.34
Predicted frequency distribution of 1-hour NO_2 averages for August 1999, calculated using 3 days with data collected between 17:00 and 18:00

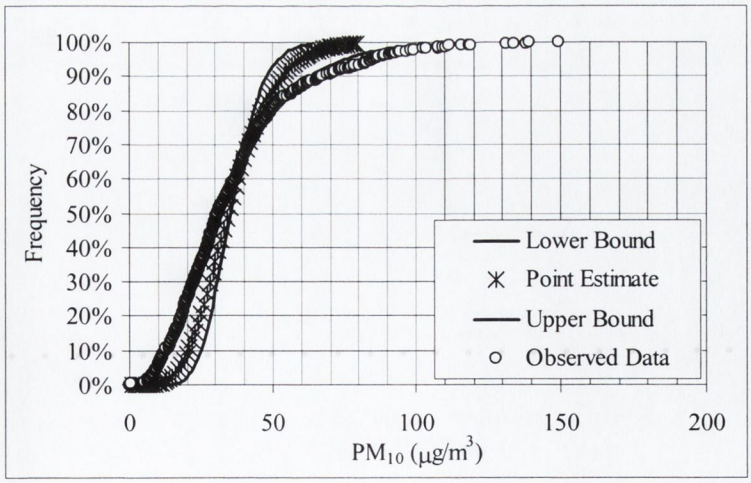

Figure 10.35
Predicted frequency distribution of 1-hour PM_{10} averages for November 1999, calculated using 3 complete days of monitoring.

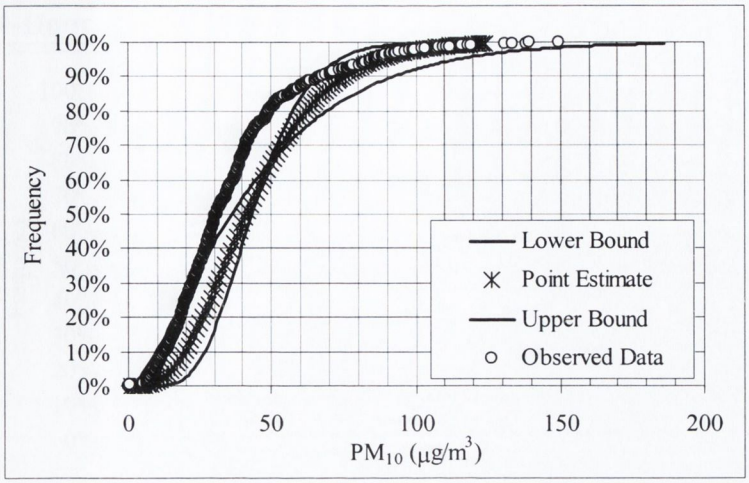

Figure 10.36
Predicted frequency distribution of 1-hour PM_{10} averages for November 1999, calculated using 3 days with data collected between 17:00 and 18:00

11.4 APPENDIX D

24-Hour Averages – Roadside Site (Pearse St.)

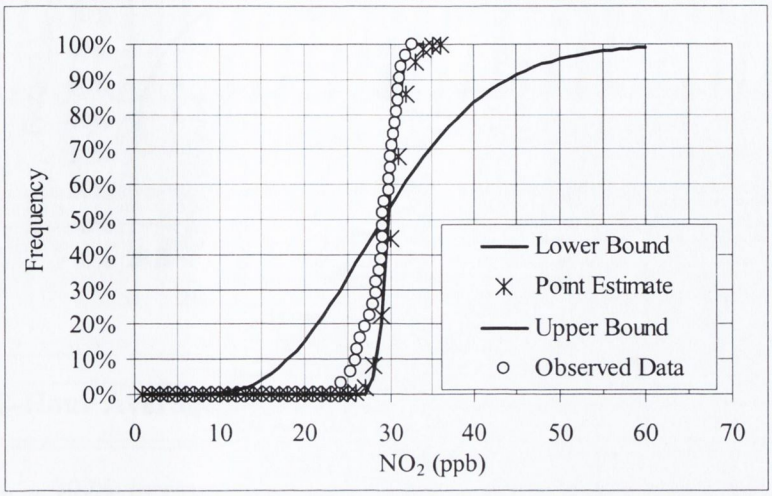

Figure 10.37
Predicted frequency distribution of 24-hour NO_2 averages for March 1999, calculated using 3 complete days of monitoring.

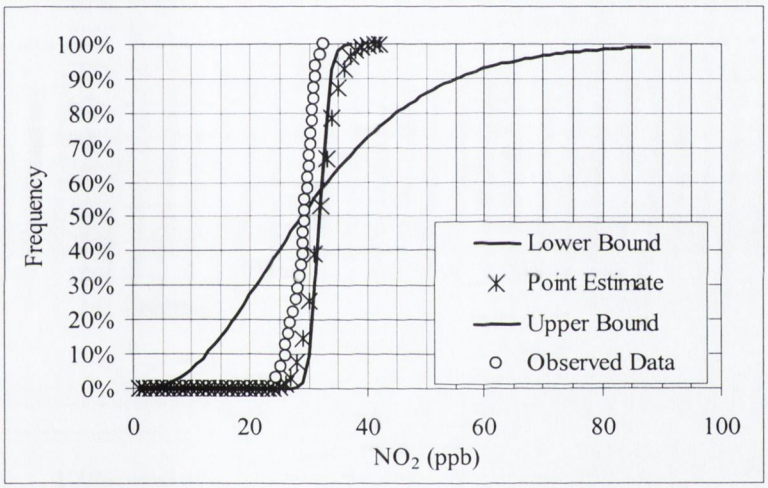

Figure 10.38
Predicted frequency distribution of 24-hour NO_2 averages for March 1999, calculated using 3 days with data collected between 17:00 and 18:00

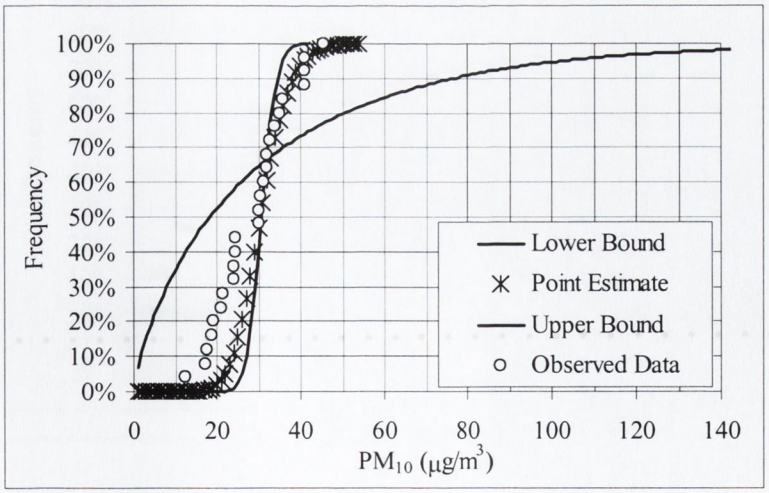

Figure 10.39
Predicted frequency distribution of 24-hour PM_{10} averages for March 1999, calculated using 3 complete days of monitoring.

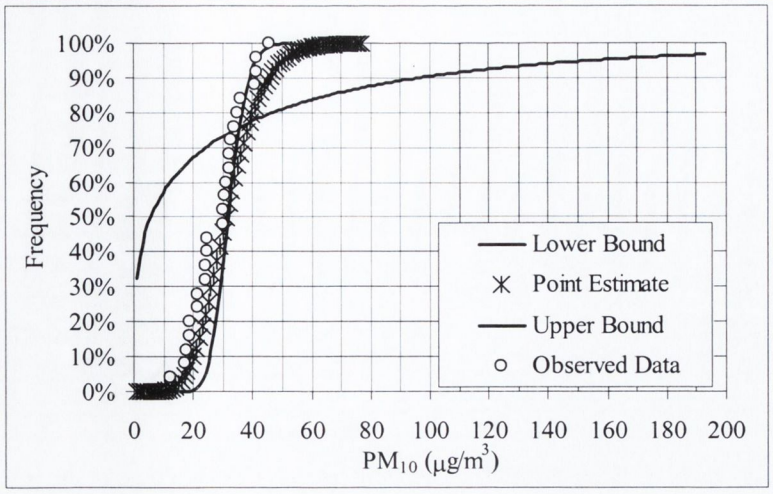

Figure 10.40
Predicted frequency distribution of 24-hour PM_{10} averages for March 1999, calculated using 3 days with data collected between 17:00 and 18:00

8-Hour Averages – Roadside Site (Pearse St.)

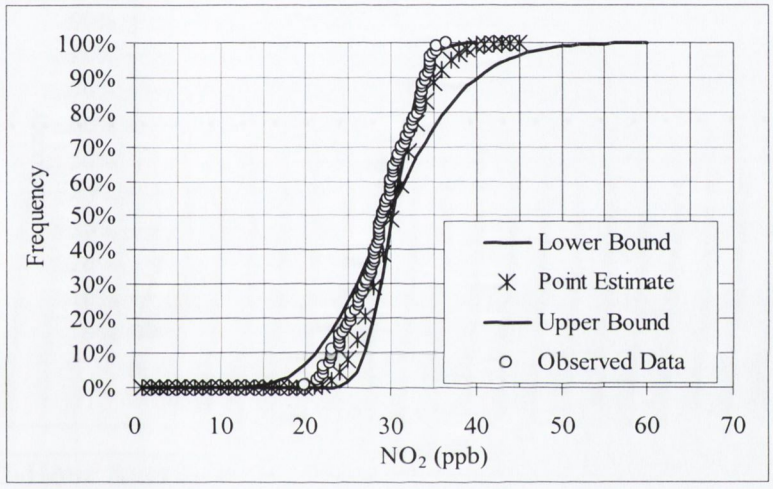

Figure 10.41
Predicted frequency distribution of 8-hour NO_2 averages for March 1999, calculated using 3 complete days of monitoring.

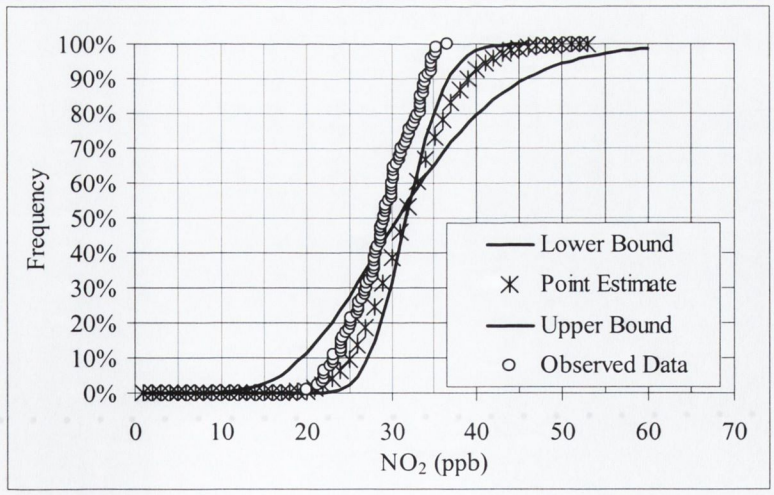

Figure 10.42
Predicted frequency distribution of 8-hour NO_2 averages for March 1999, calculated using 3 days with data collected between 17:00 and 18:00

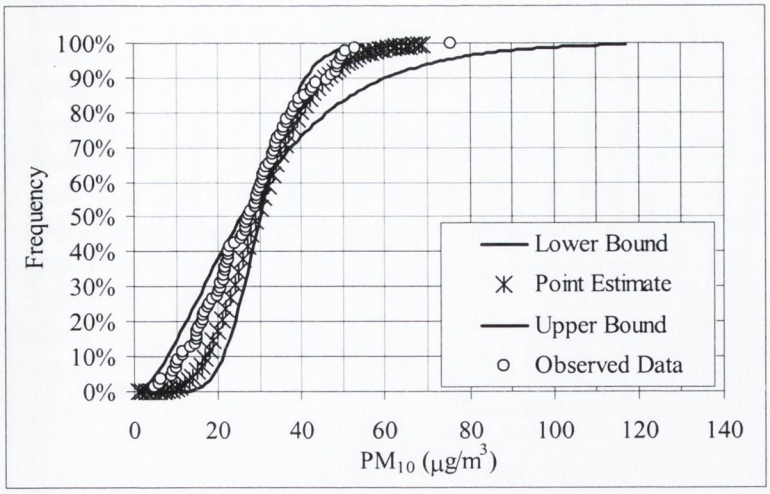

Figure 10.43 Predicted frequency distribution of 8-hour PM_{10} averages for March 1999, calculated using 3 complete days of monitoring.

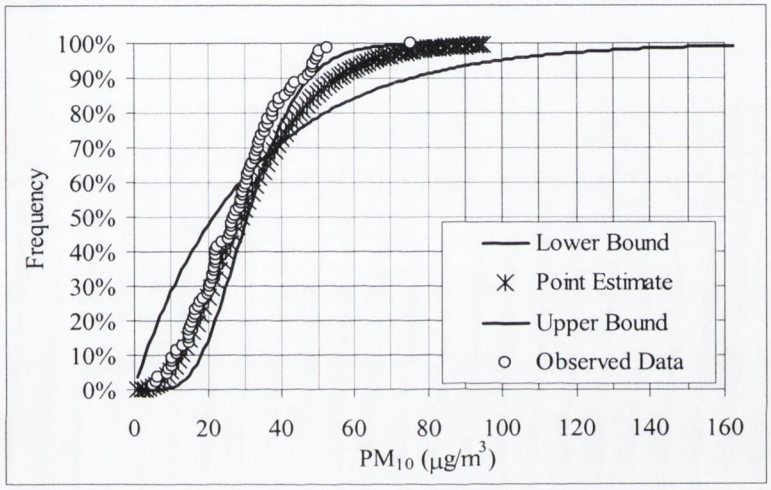

Figure 10.44 Predicted frequency distribution of 8-hour PM_{10} averages for March 1999, calculated using 3 days with data collected between 17:00 and 18:00

1-Hour Averages – Roadside Site (Pearse St.)

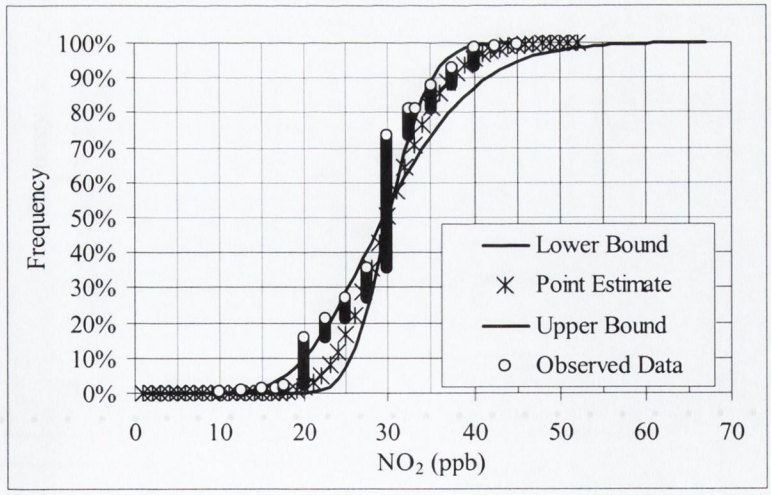

Figure 10.45 Predicted frequency distribution of 1-hour NO_2 averages for March 1999, calculated using 3 complete days of monitoring.

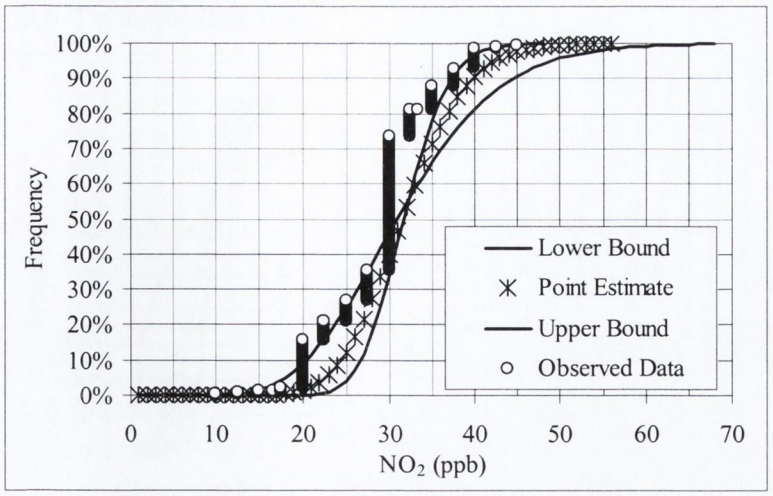

Figure 10.46 Predicted frequency distribution of 1-hour NO_2 averages for March 1999, calculated using 3 days with data collected between 17:00 and 18:00

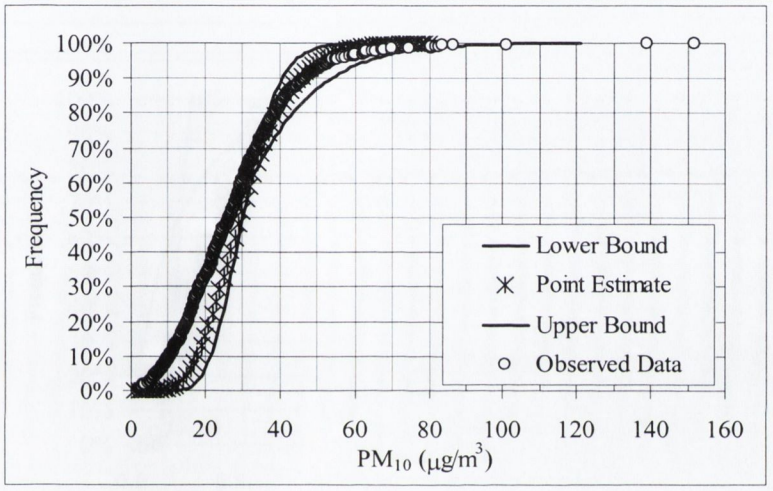

Figure 10.47 Predicted frequency distribution of 1-hour PM_{10} averages for March 1999, calculated using 3 complete days of monitoring.

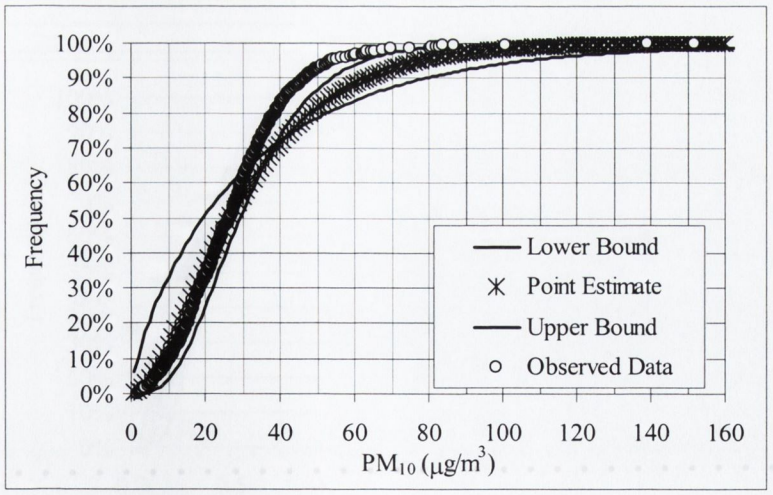

Figure 10.48 Predicted frequency distribution of 1-hour PM_{10} averages for March 1999, calculated using 3 days with data collected between 17:00 and 18:00

1,3,5-Trimethylbenzene (Pearse St./Westland Row Jnc)

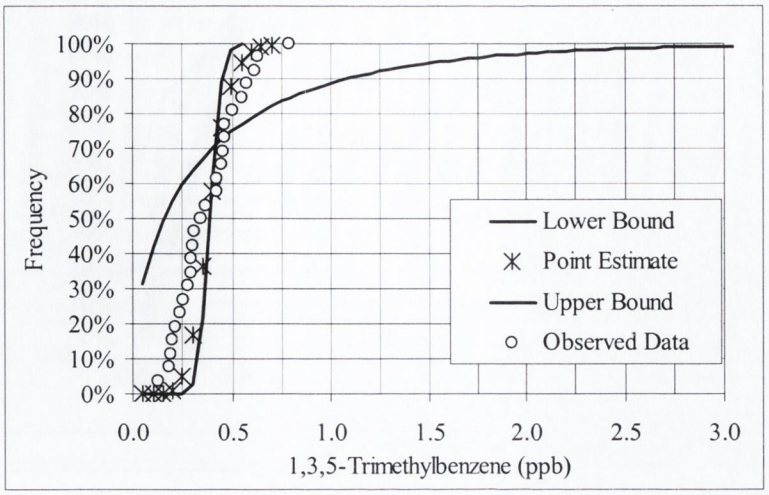

Figure 10.49
Predicted frequency distribution of 24-hour 1,3,5-trimethylbenzene averages for March 1998, calculated using 3 complete days of monitoring.

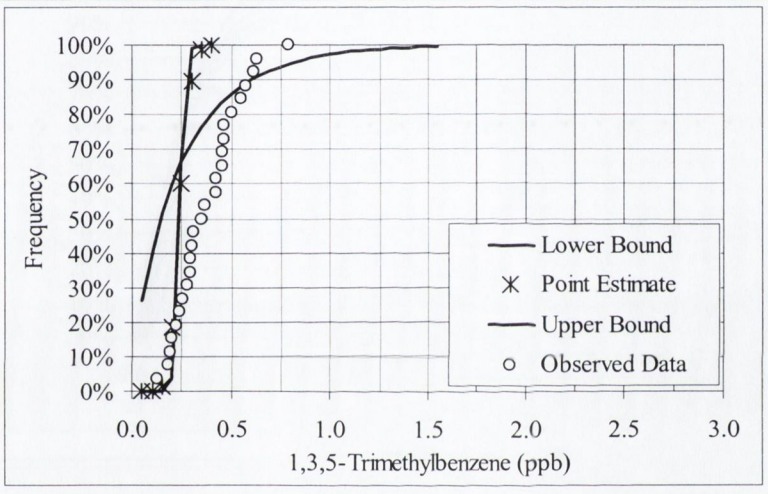

Figure 10.50
Predicted frequency distribution of 24-hour 1,3,5-trimethylbenzene averages for March 1998, calculated using 3 days with data collected between 17:00 and 18:00

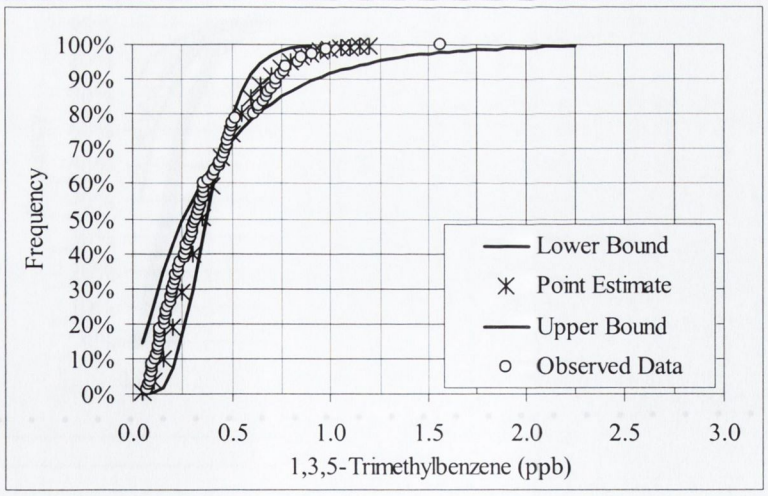

Figure 10.51
Predicted frequency distribution of 8-hour 1,3,5-trimethylbenzene averages for March 1998, calculated using 3 complete days of monitoring.

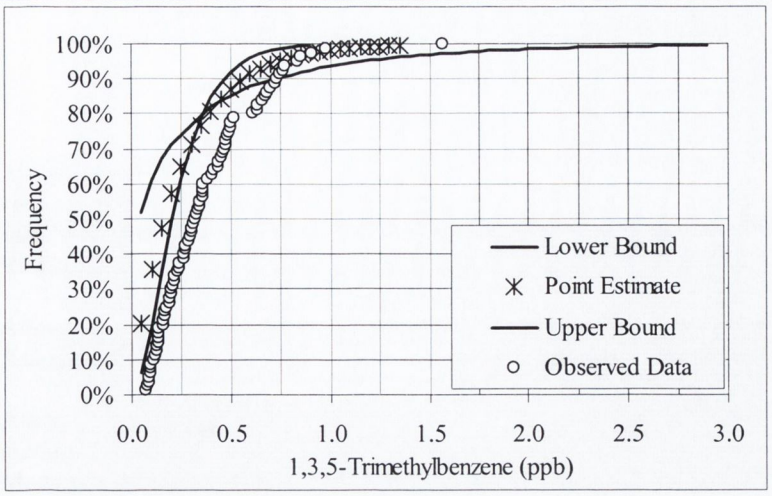

Figure 10.52
Predicted frequency distribution of 8-hour 1,3,5-trimethylbenzene averages for March 1998, calculated using 3 days with data collected between 17:00 and 18:00

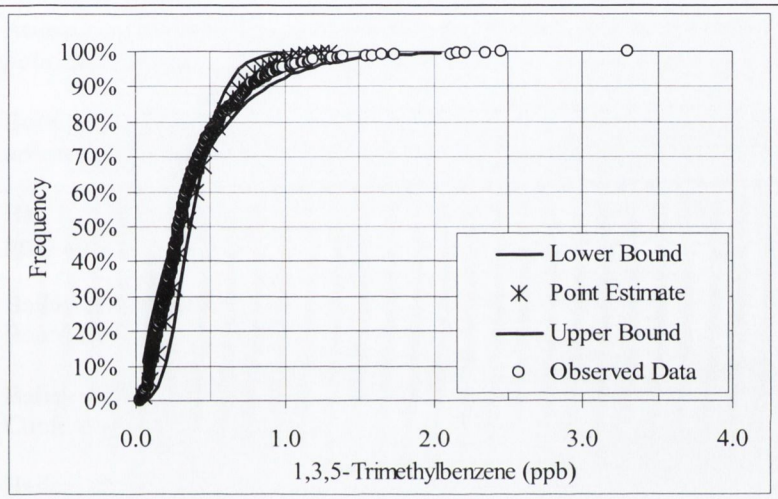

Figure 10.53
Predicted frequency distribution of 1-hour 1,3,5-trimethylbenzene averages for March 1998, calculated using 3 complete days of monitoring.

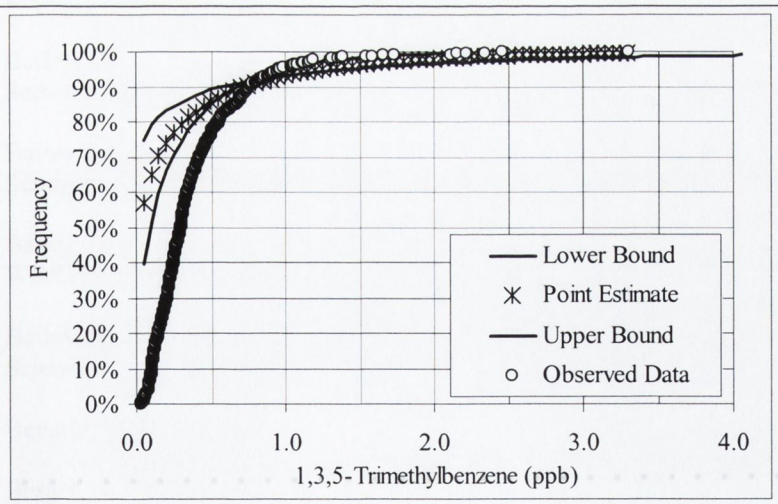

Figure 10.54
Predicted frequency distribution of 1-hour 1,3,5-trimethylbenzene averages for March 1998, calculated using 3 days with data collected between 17:00 and 18:00

12.REFERENCES

Akeredolu, F.A., Oluwole, A.F., Betiku, E.A., Ogunsola, O.J. (1994*) Modelling of carbon monoxide concentration from motor vehicles travelling near roadway intersections in Lagos, Nigeria.* Second International Conference on Air Pollution: Pollution Control and Monitoring, Ed. Baldasano, J.M., Brebbia, C.A., Power, H., Zannetti, P., Computational Mechanics Publications

Allen, G. (1998) Letters to the Editor *'Author's Response'* Journal of the Air and Waste Management Association Vol. 48 pp. 197-199

Allen, G., Sioutas, C., Koutrakis, P., Reiss, R., Lurmann, F., Roberts, P.T. (1997*) Evaluation of the TEOM method for measurement of ambient particulate mass in urban areas* Journal of the Air and Waste Management Association Vol. 47 pp. 682-689

Atimtay, A.T., Emri, S., Bagci, T., Demir, A.U. (2000*) Urban CO exposure and its effects on traffic policemen in Ankara* Environmental Research, Vol.82 (3) pp. 222-130

Baek, S.O., Kim, Y.S., Perry, R. (1997) *Indoor air quality in homes, offices and restaurants in Korean urban areas, indoor/outdoor relationships* Atmospheric Environment Vol.31, No. 4, pp. 529 – 544

Bai, J., Jakeman, A.J., McAleer, M. (1995) *Empirical models for evaluating errors in fitting extremes of a probability distribution*, Mathematics and Computers in Simulation Vol.39, pp.1-7

Bailey M.L., Walsh, J.J. (1980) *An inventory of smoke and sulphur dioxide emissions for Dublin.* National Board for Science and Technology, Shelbourne Road, Dublin

Bailey, M.L. (1981) *Air pollution monitoring and control experience in Ireland.* Proceedings of First Conference on the Scientific Basis for Environmental Regulatory Action, Rome, Italy

Bailey, M.L. (1983) *Air quality in Ireland – recent trends in atmospheric emissions and concentrations.* Report No. WR/C85, Environmental Services Section, An Foras Forbartha, Dublin

Bailey, M.L. (1984) *Air quality in Ireland – the present position.* Report No. WR/G12, Environmental Services Section, An Foras Forbartha, Dublin

Bailey, M.L. (1988) *Air quality in Ireland – the present position.* Proceedings of Air Pollution in Ireland Seminar, Royal Dublin Society, Dublin, pp.20-30

Bailey, M.L., Bowman, J.J., O'Donnell, C. (1986) *Air quality in Dublin, the present position*, Report No. WR/G13, Environmental Services Section, An Foras Forbatha, Dublin

Bailey, M.L., Walsh, J.J., Kevany, J.P. (1978) *A study of Dublin air quality 1970-1975.* National Board for Science and Technology, Shelbourne Road, Dublin

Benarie, M.M. (1980) *Urban air pollution modelling* Macmillan Press, London

Berger, A., Melice, J.L., Demuth, C.I. (1982) *Statistical distributions of daily and high atmosphere SO2 concentrations.* Atmospheric Environment Vol.16, pp.2863-2877

Berkowicz, R., Palmgren, F., Hertel, O., Vignati, E. (1996) *Using measurements of air pollution in streets for evaluation of urban quality – meteorological analysis and model calculations.* The Science of the Total Environment Vol. 189/190 pp.259-265

Boddy, R.E., (1999) *Study of spatial and temporal variations in pollutant levels*, PhD thesis, University of Nottingham

Bogo, H., Negri, R.M., San Roman, E. (1999) *Continuous measurements of gaseous pollutants in Buenos Aires City.* Atmospheric Environment Vol.33 pp.2587-2598

Boubel, R.W. (1994) *Fundamentals of air pollution,* 3rd Ed., Academic Press, London

Bower, J.S., Broughton, G.F.J., Dando, M.T., Lees, A.J., Stevenson, K.J., Lampert, J.E., Sweeney, B.P., Parker, V.J., Driver, G.S., Waddon, C.J., Wood. A.J. (1991) *Urban NO2 Concentrations in the U.K. in 1987.* Atmospheric Environment 25b (2) pp. 267-283

Brimblecombe, P. (1996) *Air composition and chemistry*, Cambridge Environmental Chemistry Series 6, Cambridge University Press

British Lung Foundation, (1996) *The Lung Report, Lung Disease: A Shadow over the Nation's Health.* The British Lung Foundation, London

Brook, J.R., Wiebe, A.H., Woodhouse, S.A., Audette, C.V., Dann, T.F., Callaghan, S., Piechowski, M., Dabek-Zlotorzynska, E., Dloughy, J.F. (1997) *Temporal and spatial relationships in fine particulate strong acidity, sulphate, PM10, and PM2.5 across multiple Canadian locations* Atmospheric Environment Vol.31, No. 24, pp. 4223-4236

Cabot, D. (1985) *The state of the environment.* Report prepared for the Minister of the Environment by An Foras Forbartha, Dublin.

Cadle, S.H. (1985*) Seasonal variation in nitric acid, nitrate, strong aerosol acidity and ammonia in an urban area* Atmospheric Environment Vol.19, No. 1, pp. 181-188

Casimiro, A.P., Castro, L.M., Cerqueira, M.A., Santos, I.M., Belchior, F., Salgueiro (1996) *Source assessment of particulate air pollutants measured at the southwest European coast* Atmospheric Environment Vol.30, No. 19, pp. 3309 – 3320

CEC (Council of the European Communities) (1996*) Council Directive 96/62/ of 27 September on ambient air quality assessment and management.* O.J.L296, 11 November 1998

CEC (Council of the European Communities) (1999) *Council Directive 1999/30/EC of 22 April 1999 relating to limit values for sulphur dioxide, nitrogen dioxide, and oxides of nitrogen, particulate matter, and lead in ambient air.* O.J.L163, 29 June 1999

Chan, L.Y., Lam, K.S. (1985*) Methane, Non-methane hydrocarbon carbon monoxide and oxides of nitrogen concentration in roadside ambient air*, Pollution in the Environment – POLMET '85, Ed. Chan, M.W.H., Hoare, R.W.M., Holmes, P.R., Law, R.J.S., Reed, S.B. pp.184 – 189

Chang, T.Y., Norbeck, J.M., Weinstock, B. (1980*) Ambient temperature effect on urban CO air quality* Atmospheric Environment Vol.14, No. 9, pp.603-608

Chapman, T.T. (1965*) Air Pollution and forced expiratory volume in chronic bronchitis.* Irish Journal of Medical Science Vol.4, pp.24-32

Chow, J.C., Liu, C.S., Cassmassi, J., Watson, J.G., Lu, Z., Pritchett, L.C. (1992*) A neighbourhood-scale study of PM10 source contributions in Rubidoux, California* Atmospheric Environment Vol.26a, No. 4, pp. 693-706

Claggett, M., Shrock, J., Noll, K.E. (1981) *Carbon monoxide near an urban intersection* Atmospheric Environment Vol.15, No. 9, pp.1633-1642

Clifford, M.J., Clarke, R., Riffat, S.B. (1997) *Drivers' exposure to carbon monoxide in Nottingham, U.K.* Atmospheric Environment Vol.31, No. 7, pp. 1003-1009

Comrie, A.C., Diem, J.E. (1999) *Climatology and forecast modeling of ambient carbon monoxide in Phoenix, Arizona* Atmospheric Environment Vol.33, pp. 5023-5036

Cooper, C.D. (1988) *Eight hour carbon monoxide persistence factors.* Report No. FL/DOT/BMR-88/325; FL-ER-39-88, College of Engineering, University of Central Florida, Orlando, Florida, USA

Cooper, C.D. (1989) *Persistence factors for mobile source (roadway) carbon monoxide modelling.* Journal of the Air Pollution Control Association Vol.39 (5) 714-720.

Cooper, C.D., Malone, L.C., Liu, P.S. (1992) *Identifying worst case persistence factors for carbon monoxide modeling near intersections in Orlando, Florida.* Journal of the air and waste management association Vol.42 (11) pp.1461-1465

Croxford, B., Penn, A., (1998) *Siting considerations for urban pollution monitors* Atmospheric Environment Vol.32, No. 6, pp. 1049-1057

Croxford, B., Penn, A., Hillier, B. (1995) *Spatial distribution of urban air pollution: civilizing urban traffic.* Paper presented at the fifth symposium in highway and urban pollution, May 1995.

Cuhadaroglu, B., Demirci, E. (1996) *Influence of some meteorological factors on air pollution in Trabzon* city. Energy and Buildings Vol.25, pp.179-184

Curtiss, P.S., Rabl, A. (1996) *Impacts of air pollution: general relationships and site dependence* Atmospheric Environment Vol.30, No. 19, pp. 3331-3347

Dawson, F.E. (1963) *Measurement of air pollution 1961.* Department of Local Government, Dublin

Dawson, F.E. (1964) *Measurement of air pollution 1962 and 1963.* Department of Local Government, Dublin

Dawson, F.E. (1966) *Measurement of air pollution 1964.* Department of Local Government, Dublin

De Wytt, C. Kevany, J.P. (1971) *Air Pollution in Ireland.* Irish Journal of Medical Science Vol.3. pp.108-117

Dean, G. (1988) *Air Pollution – Health Implications.* Air Pollution in Ireland: Dublin – A Case Study, Royal Dublin Society, Dublin, pp.31-36

Delaney, D., Dowling, P. (1988) *The relationship between extreme nitrogen oxide (NOx) concentrations in Dublin's atmosphere and meteorological conditions.* Environmental Monitoring and Assessment Vol.52 (1-2), pp.159-172

Demirci, E., Cuhadaroglu, B. (2000) *Statistical analysis of wind circulation and air pollution in urban Trabzon.* Energy and Buildings Vol.31, pp.49-53

Derwent, R.G., Middleton, D.R., Field, R.A., Goldstone, M.E., Lester, J.N., Perry, R. (1995) *Analysis and interpretation of air quality data from an urban roadside location in central London over the period from July 1991 to July 1992* Atmospheric Environment Vol.29, No. 8, pp. 923-946

Devore, J., and Farnum, N., (1999) *Applied statistics for engineers and scientists*, Duxbury Press, London

Dobbins, R.A. (1979) *Atmospheric motion and air pollution*, Wiley-Interscience, New York

Dockery, D. (1999) *Smoke: health effects of airborne particles.* Presented at the Institute of Physics Seminar Programme, NUI, Galway.

DoE (Department of the Environment and Local Government) (1999) *Environmental Protection Agency Act, 1992 (Ambient Air Quality Assessment and Management) Regulations, 1999.* S.I. No.244 of 1987

Drivas, P.J., Chan, M.W., Wayne, L.G. (1977) 'Validation of an improved photochemical air quality simulation model', *Proc. AMS joint conference on Applications of Air Pollution Meteorology,* Salt Lake City, Utah

Dublin Corporation (1998) *Atmospheric pollution and noise control unit annual report.* Environmental Health Section, Environment and Culture Department, Civic Offices, Dublin.

Dublin County (1999) *Dublin county air quality and noise report.* Air Quality and Noise Control Unit, April, 1999

Dye, A., Rhead, M., Trier, C. (1998) *The physical nature of airborne particulate matter (PM10) in Plymouth UK* International Journal of Vehicle Design Vol. 20, Nos 1-4 (Special Issue) pp. 3-9

EC, (European Commission) (1998) *Proposal for a European Parliament and Council Directive relating to limit values for benzene and carbon monoxide in ambient air.* COM (1998) 591

El-Fadel, M., Massoud, M. (2000) *Particulate matter in urban areas, health based economic assessment.* The Science of the Total Environment, Vol. 257, pp. 133-146

ENFO (1992*) Air quality data.* Fact Sheet No 13, ENFO, Environmental Information Service, Dublin

Envirocon (1995) *Dublin air quality management plan: phase 1.* Prepared by ENVIROCON, Clifton House, Fitzwilliam St., Dublin

Envirocon (1996) *Dublin air quality management plan: phase II.* Prepared by ENVIROCON, Clifton House, Fitzwilliam St., Dublin

Fenger, J. (1999) *Urban air quality* Atmospheric Environment Vol.33, pp. 4877-4900

Fischer, P.H., Hoek, G., van Reeuwijk, H., Briggs, D.J., Lebret, E., van Wijnen, J.H., Kingham, S., Elliot, P.E. (2000) *Traffic related differences in outdoor and indoor concentrations of particles and volatile organic compounds in Amsterdam.* Atmospheric Environment Vol.34 pp.3713-3722

Flachsbart, P.G., Yo, C.Ah. (1987*) Microenvironmental models of commuter exposure to carbon monoxide from vehicle exhaust.* Final report under contract no. 68-02-4084, U.S. EPA, Environmental Monitoring Systems Laboratory, Research Triangle Park, North Carolina

Flanagan, P.J., O'Donnell, C., Callan, B., Bailey, M.L., Horan, H. (1988) *Irish participation in the common measurement programme.* Environmental Services Section, An Foras Forbartha, Dublin

Freedomchannel (2000) *Pennsylvania: fourteenth district,* www.freedomchannel.com/img/2000/states/pa/pa14.cfm, 1233 20th St., NW, Suite 302, Washington, DC, 20036

Fukino, H., Mimura, S., Inque, K., Yamane, Y. (1984) *Correlations among atmospheric elements, airborne particulate matter, benzene extracts, benzo(a)pyrene, NO, NO2, and SO2 concentrations in Japan* Atmospheric Environment Vol.18, No. 5, pp. 983-988

Georgopoulos, P.G. and Seinfeld J.H. (1982) *Statistical distributions of air pollutant concentrations* Environmental Science and Technology, Vol. 16, No. 7, pp. 401a-416a

Glen, W.G., Zelenka, M.P., Graham, R.C. (1996) *Relating meteorological variables and trends in motor vehicle emissions to monthly urban carbon monoxide concentrations* Atmospheric Environment Vol.30, No. 24, pp. 4225-4232

Goodman, P.G., Sinclair, H., Clancy, L., Dockery, D.W. (1999) *Evidence of a cumulative effect of particulate air pollution on mortality in Dublin.* American Journal of Respiratory and Critical Care Medicine Vol.159 (3), A322.

Hao, J., He, D., Wu, Y., Fu, L., He, K. (2000) *A study of the emission and concentration distribution of vehicular pollutants in the urban area of Beijing* Atmospheric Environment Vol.34, pp. 453-465

Hargreaves, P.R., Leidi, A., Grubb, H.J., Howe, M.T., Mugglestone, M.A. (2000) *Local and seasonal variations in atmospheric nitrogen dioxide levels at Rothamsted, UK, and relationships with meteorological conditions* Atmospheric Environment Vol.34, pp. 843-853

Härkönen, J., Kukkonen, J., Valkonen, E., Karppinen, A. (1998) *The influence of vehicle emission characteristics and meteorological conditions on urban NO2 concentrations* International Journal of Vehicle Design Vol. 20, Nos 1-4 (Special Issue) pp. 125-130

Harrison, R.M. Ed. (1996) *Pollution, causes, effects and control*, 3rd Ed. The Royal Society of Chemistry, Cambridge, U.K.

Harrison, R.M. Ed. (1999) *Understanding our environment, an introduction to environmental chemistry and pollution,* 3rd Ed. Royal Society of Chemistry, Cambridge, U.K.

Harrison, R.M., Deacon, A.R., Jones, M.R., Appleby, R.S. (1997) *Sources and processes affecting concentrations of PM10 and PM2.5 particulate matter in Birmingham, (U.K.)* Atmospheric Environment Vol.31, No. 24, pp. 4103-4117

Haynes, R. (editor) (1982) *Environmental Science Methods*, Chapman and Hall, London

Healy, D., Dowling, P. (1997) *Personal exposure to PM10 of cyclists in Dublin.* Proceedings of the 7th Irish Environmental Researchers Colloquium, University of Limerick, Paper no.74 (abstract)

Healy, D., Dowling, P. (1998) *Exposure of cyclists to particulate air pollution in Dublin.* Proceedings of the 8th Irish Environmental Researchers Colloquium, Sligo Institute of Technology, Sligo, Paper No.41, (abstract)

Hegner, H., Monn, Ch., Stahel, W., Ackermann, U., Leuenberger, Ph., and SAPALDIA Team (1996) *Kleinraumige verteilung von sticksdoff-dioxid.* Gesundsheit und Umwelttechnik 4., pp. 3-7

Henderson, E., Jennings, S.G., Keary, J., Lee, M., McManus, B., O'Connor, T.C., Shanahan, I. (1997) *A baseline study on the concentrations of volatile organic compounds and PM10 in Dublin city.* Environmental Protection Agency, Ardcavan, Wexford.

Jakeman, A.J., Bai, J., Miles, G.H. (1991) *Prediction of seasonal extremes of one hour average urban CO concentrations* Atmospheric Environment 25b (2) pp. 219-229

Jo, W.K., Yoon, I.H., Nam, C.W. (2000*) Analysis of air pollution in two major Korean cities: trends, seasonal variations, daily 1-hr maximum versus other hour based concentrations, and standard exceedances*. Environmental Pollution Vol.110 (2000) pp.11-18

Kahn, H.D. (1973) *Note on the Distribution of Air Pollutants* Journal of the Air Pollution Control Association Vol.23 (11) pp.973

Karpinnen, A., Kukkonen, J., Elolähde, T., Kontinnen, M., Koskentalo, T. (2000*) A modelling system for predicting urban air pollution: comparison of model predictions with the data of an urban measurement network in Helsinki.* Atmospheric Environment Vol.34 pp.3735-3743

Kartal, S., Özer, (1998) *Determination and Parameterization of some air pollutants as a function of meteorological parameters in Kayseri, Turkey* Journal of the Air and Waste Management Association Vol. 48 pp. 853-859

Kassomenos, P. Kotroni, V., Kallos, G. (1995) *Analysis of climatological and air quality observations from greater Athens area.* Atmospheric Environment Vol.29, No.24, pp.3671-3688

Keary, J. (1997) *PM10 concentration measurements in Dublin city.* Proceedings of the 7th Irish Environmental Researchers Colloquium, University of Limerick, Paper no.75

Keary, J., Jennings, S.G., O'Connor, T.C., McManus, B., Lee, M. (1998) *PM10 concentration measurements in Dublin city*. Environmental Monitoring and Assessment Vol.52, (1-2), 3-18.

Kelly, F. (1993) *The evaluation and application of an air dispersion model in Dublin.* M.Sc. Thesis, Department of statistics, Trinity College, Dublin.

Kelly, I., Clancy, L. (1984) *Mortality in a general hospital and urban air pollution.* Irish Medical Journal Vol.77 (10) pp.322 – 324

Kevany, J.P., Rooney, R., Kennedy, J. (1975) *Health effects of air pollution in Dublin.* Irish Journal of Medical Science Vol.3, pp.102-115

Kiely, G. (1997) *Environmental Engineering*, McGraw Hill, London

Kleeman, M.J., Cass, G.R. (1998) *Source contributions to the size and composition distribution of urban particulate pollution.* Atmospheric Environment, Vol.32, pp. 2803-2816

Kleeman, M.J., Schauer, J.J., Cass, G.R. (2000*) Size and composition distribution of fine particulate matter emitted from motor vehicles.* Environmental Science and Technology Vol.34 (7) pp. 1132-1142

Lam, G.C.K., Leung, D.Y.C., Niewiadomski, M., Pang, S.W., Lee, A.W.F., Louie, P.K.K. (1999) *Street-level concentrations of nitrogen dioxide and suspended particulate matter in Hong Kong* Atmospheric Environment Vol.33, pp. 1-11

Lebret, E., Briggs, D., vanReeuwijk, H., Fischer, P., Smallbone, K., Harssema, H., Kriz, B., Gorynski, P., Elliott, P. (2000) *Small area variations in ambient NO2 concentrations in four European Areas* Atmospheric Environment Vol.34, pp. 177-185

Lee, J.K., Ro, K.K., Yu, P.I., (1997) *Knowledge based prediction model – A case study of urban air pollutant concentrations* Journal of Environmental Management 51, pp. 29-42

Lee, K., Yanagiswa, Y., Hishunima, M., Spengler, J.D., Billick, I.H. (1992) *Passive sampler for measurement of carbon monoxide using a solid adsorbent* Environmental Science and Technology Vol. 26 (4) pp.697-702

Leonard, A.G.G., McVerry, B.P., Crowley, D. (1940*) Atmospheric pollution in Dublin during the year 1939.* Scientific Proceedings of the Royal Dublin Society 25, pp.57-265

Leonard, A.G.G., McVerry, B.P., Crowley, D. (1941) *Atmospheric pollution in Dublin during the year 1940.* Scientific Proceedings of the Royal Dublin Society 41, pp.398-404

Leonard, A.G.G., McVerry, B.P., Crowley, D. (1950) *Atmospheric pollution in Dublin during the years 1944-1950.* Scientific Proceedings of the Royal Dublin Society 112, 116-122

Lettau, H.H., (1970) 'Physical and meteorological basis for mathematical models of urban diffusion processes', *Proc. Symp. On Multiple-Source Urban Diffusion Models,* US EPA Publication, No. AP-86

Linkaritakis, K.N. (1988) *Factors affecting traffic related air pollutant levels in urban streets,* PhD, Imperial College, University of London

Lipfert, F.W., (1994) *Air Pollution and Community Health, A critical review and sourcebook*, Van Nostrand Reinhold, New York

Lodge, J.P. Jr., Waggoner, A.P., Klodt, D.T., Crain, C.N., (1981) *Non-health effects of airborne particulate matter* Atmospheric Environment Vol.15, pp. 431-482

Maffeis, G. (1999) *Prediction of carbon monoxide acute air pollution episodes. Model formulation and first application in Lombardy* Atmospheric Environment Vol.33, pp. 3859-3872

Mage, D., Ozolins, G., Peterson, P., Webster, A., Orthofer, R., Vandeweerd, V., Gwynne, M., (1996) *Urban air pollution in the megacities of the world* Atmospheric Environment Vol.30, No. 5, pp. 681-686

Magellan Geographix (1993) www.cnn.com/TRAVEL/CITY.GUIDES/WORLD/Europe/dublin.html, Magellan Geographix: Santa Barbara, CA, USA

Marnane, I. (2000) *Online Hydrocarbon Monitoring* Ph.D. thesis, Trinity College, Dublin

Martin, A., Barber, F.R. (1985*) Particulate sulphate and ozone in rural air: preliminary results from three cities in central England* Atmospheric Environment Vol.19, No. 7, pp. 1091-1102

Mayer, H. (1999) *Air pollution in cities* Atmospheric Environment Vol.33, pp. 4029-4037

McGettigan, M. (2000) *Air Quality Monitoring Annual Report 1998.* Environmental Protection Agency, Wexford.

McGettigan, M.F., O'Donnell, C. (1995) *Air Pollutants in Ireland – emissions depositions and concentrations 1984 – 1994.* Environmental Protection Agency, Ardcavan, Wexford.

McGettigan, M.F., O'Donnell, C., Bowman, J.J. (1993) *Air quality in Ireland – a review 1981 – 1991.* Environmental Research Unit, St. Martins House, Waterloo Road, Dublin

McManus, B. (1998) *Air pollution monitoring in Dublin city.* Proceedings of Seminar on LPG as an Alternative Fuel, Dublin

McManus, T. (1975) *National survey of air and water pollution, 1974.* Report to the Industrial Development Authority, prepared by the Chemical Engineering Department, Institute for Industrial Research and Standards, Dublin.

McManus, T., O'Reilly, P.M. (1976) *Air pollution standards.* Proceedings of 2nd Pollution Conference on Monitoring Industrial Pollution , Dublin, pp. 165-190

McMurray, P.H., Stolzenburg, M.R. (1989*) On the sensitivity of particle size to relative humidity for Los Angeles aerosols* Atmospheric Environment Vol.23, No. 2, pp. 497-507

McNair, L.A., Harley, R.A., Russell, A.G., (1996*) Spatial inhomogeneity in pollutant concentrations, and their implications for air quality model evaluation* Atmospheric Environment Vol.30, No. 24, pp. 4291-4301

Miles, G.H., Jakeman, A.J., Bai, J. (1991) *A method for predicting the frequency distribution of air pollution from vehicle traffic, basic meteorology and historical concentrations to assist urban planning* Environment International. Vol. 17, pp 575-580

Misstear B.D. Misstear, Broderick, B.M., Jennings S.G., Marnane, I.S. (2000) 'Optimal monitoring of air quality in the vicinity of point sources, phase one report' Trinity College Dublin, NUI Galway, NETCEN (AEA Technology)

Mondal, R., Sen, G.K., Chatterjee, M., Sen, B.K., Sen, S. (2000*) Ground-level concentration of nitrogen dioxides (NOx) at some traffic intersection points in Calcutta* Atmospheric Environment Vol.34, pp. 629-633

Monn, Ch., Carabias, V., Junker, M., Waeber, R., Karrer, M., Wanner, H.U., (1997) *Small-scale spatial variability of particulate matter < 10μm (PM10) and nitrogen dioxide* Atmospheric Environment Vol.31, No. 15, pp. 2243-2247

Morawska, L., Thomas, S., Jamriska, M., Johnson, G. (1999*) The modality of particle size distributions of environmental aerosols.* Atmospheric Environment Vol.33 pp.4401-4411

Morel, B., Yeh, S., Cifuentes, L. (1999*) Statistical distributions for air pollution applied to the study of the particulate problem in Santiago*, Atmospheric Environment 33 pp. 2575-2585

Moser, R., Lee, J.S., Phalen, R.F., (1996) *Recent research studies of particulate air pollution and health.* Paper presented at the second colloquium on particulate air pollution and health, May 1996.

Murray, F. (1997) *Urban air pollution and health effects*, Chap.33 The Global Environment, Science, Technology and Management, Volume 1. Ed. Brune, D., Chapman, D.V., Gwynne, M.D., Pacyna, J.N. VCH, A Wily Company, New York

Namdeo, A., Baker, C., Colls, J. (1998) *Particulate pollution from motor vehicles in an urban street canyon in Nottingham (UK)* International Journal of Vehicle Design Vol. 20, Nos 1-4 (Special Issue) pp. 10-20

Neave, H.R. and Worthington, P.L. (1988) *Distribution-free tests*, Unwin Hyman, London

Nevalainen, J., Pekkanen, J. (1998) *The effect of particulate air pollution on life expectancy.* The Science of the Total Environment Vol.217, pp.137-141

Nielson, T. (1996) *Traffic contribution of polycyclic aromatic hydrocarbons in the center of a large city* Atmospheric Environment Vol.30, No. 20, pp. 3481-3490

Nolan, S. (1979) *Operational experiences in air pollution monitoring in Dublin.* Proceedings of Seminar: Air Pollution Impacts and Control, Galway, pp.97-101

Nosal, M., Legge, A.H., Krupa, S.V. (2000) *Application of a stochastic, weibull probability generator for replacing missing data on ambient concentrations of gaseous pollutants.* Environmental Pollution Vol.108 pp.439-446.

O'Keefe, J. (1997) *Monitoring and modelling of nitrogen dioxide in urban areas*, PhD thesis, Imperial College of Science, Technology and Medicine

O'Regan, F.A. (1996) *Vehicular air pollution and the use of traffic management in its control,* MSc. thesis N.U.I.

Osborn, P.D. (1989) *The engineers' clean air handbook*, Butterworths, London

Ostro, B.D., Hurley, S., Lipsett, M.J. (1999) *Air pollution and daily mortality in the Coachella valley, California: A study of PM10 dominated by coarse particles.* Environmental Research Vol.81, (3) pp. 231-238

Ott W.R (1990) *A physical explanation of the lognormality of pollutant concentrations* Journal of the air and waste management association Vol. 40 pp.1378-1383

Owen, B., Edmunds, H.A., Carruthers, D.J., Singles, R.J., (2000) *Prediction of oxides of nitrogen and nitrogen dioxide concentrations in a large urban area using a new generation urban scale dispersion model with integral chemistry model* Atmospheric Environment Vol.34, pp. 397-406

Palmgren, F., Berkowicz, R., Ziv, A., Hertel, O. (1999) *Actual car fleet emissions estimated from urban air quality measurements and street pollution models.* The Science of the Total Environment, Vol. 235, pp.101-109

Pasquill F. Smith F.B. (1983) *Atmospheric diffusion* 3rd edition. Ellis Horwood, Chichester

Patashnick, H., (1998a) *Letters to the Editor 'The TEOM system'* Journal of the Air and Waste Management Association Vol. 48 pp. 195-197

Patashnick, H., (1998b) *Letters to the Editor 'Rebuttal'* Journal of the Air and Waste Management Association Vol. 48 pp. 199-200

Patashnick, H., Rupprecht, E.G. (1991) *Continuous PM10 measurements using the tapered element oscillating microbalance.* Journal of Air and Waste Management Vol.41 1079-1083

Penn, A., and Croxford, B., (1998) *Fingerprinting urban kerbside CO concs: interaction between street grid configuration, vehicle flows and local wind effects* International Journal of Vehicle Design Vol. 20, Nos 1-4 (Special Issue) pp. 60-70

Pisano, J.T., McKendry, I., Steyn, D.G., Hastie, D.R., (1997) *Vertical nitrogen dioxide and ozone concentrations measured from a tethered balloon in the lower Fraser Valley* (1997) Atmospheric Environment Vol.31, No. 14, pp. 2071-2078

Reilly, M. (1986) *Air Pollution in Dublin.* Air Pollution Unit, Department of the Environment, Dublin

Reynolds, A.W. (2000) *Development and application of an integrated air quality modelling system for traffic related pollution in urban areas* Ph.D. thesis, Trinity College, University of Dublin

Reynolds, S.A. (1996) *Monitoring and prediction of air pollution from traffic in the urban environment.* Ph.D. Thesis, University of Nottingham

Richter, D.A.U., Williams, W.P. (1998) *Assessment and management of air quality in Europe.* European Environment Agency, Copenhagen, Denmark

Rohatgi, V.K. (1984) *Wiley Series in probability and mathematical statistics: Statistical Inference,* John Wiley & Sons, Inc, New York

Romero, H., Ihl, M., Rivera, A., Zalazar, P., Azocar, P. (1999) *Rapid urban growth, land-use changes and air pollution in Santiago, Chile.* Atmospheric Environment Vol.33, pp.4039-4047

Russell, A.G. (1988) *Mathematical Modeling of the effect of emission sources on atmospheric pollutant concentrations*, Air Pollution, the Automobile and Public Health, ed. Watson, A.Y., Bates, R.R., Kennedy, D., National Academy Press, Washington.

Sachs, L. (1984) *Applied statistics, A handbook of techniques*, 2nd ed, Springer Series in statistics, Springer-Verlag, New York

Salter, L.F., Parsons, B. (1999) *Field Trials of the TEOM and Partisol for PM10 monitoring in the St Austell china clay area, Cornwall, UK* Atmospheric Environment Vol.33 pp. 2111-2114

Samson, P.J. (1988) *Atmospheric transport and dispersion of air pollutants, associated with vehicular emissions air pollution, the automobile and public health* Ed. Watson, A.Y., Bates, R.R., Kennedy, D. National Academy Press, Washington

Sánchez, M.L., Pascual, D., Ramos, C., Pérez, I. (1990) *Forecasting particulate pollutant concentrations in a city from meteorological variables and regional weather patterns* Atmospheric Environment Vol.24a, No. 6, pp. 1509-1519

Scaperdas, A., Colville, R.N. (1999*) Assessing the representativeness of monitoring data from an urban intersection in central London, UK* Atmospheric Environment Vol.33, pp. 661-674

Seinfeld, J.H., (1986) *Atmospheric Chemistry and Physics of Air Pollution*, Wiley-Interscience, New York

Sen, I., Prabhashanker, V, (1980) *Journal of Quality Technology* 12 (1980), pp.138-143

Shanahan, I., McManus, B., Lee, M. (1997) *Baseline survey of VOCs in Dublin city.* Proceedings of the 7th Irish Environmental Researchers Colloquium, University of Limerick, Paper no.75

Shi, J.P., Harrison, R.M. (1997*) Regression modelling of hourly NOx and NO2 concentrations in urban air in London* Atmospheric Environment Vol.31, No. 24, pp. 4081-4094

Simpson, R.W. (1984) *Predicting frequency distributions for ozone, NO2 and TSP from restricted data sets* Atmospheric Environment, Vol.18, No.2, pp. 353-360

Sinclair, H., Goodman, P.G., Clancy, L.J., Dockery, D.W. (1997*) Effects of particulate air pollution control on mortality in Dublin.* Respiratory and Critical Care Medicine Vol.55 (4) A426

Singh, H.B., Salas, L.J., Cantrell, B.K., Redmond, R.M. (1985*) Distribution of aromatic hydrocarbons in the ambient air* Atmospheric Environment Vol.19, No. 11, pp. 1911-1919

Singh, M.P., Goyal, P., Basu, S., Agarwal, P., Nigam, K., Kumari, M., Panwar, T.S. (1990*) Predicted and measured concentrations of traffic carbon monoxide over Delhi* Atmospheric Environment Vol.24a, No. 4, pp. 801-810

Sini, J.F., Anquetin, S., Mestayer, P.G., (1996*) Pollutant dispersion and thermal effects in urban street canyons* Atmospheric Environment Vol.30, No. 15, pp. 2659-2677

Sivacoumar, R., Thanasekaran K. (1999*) Line source model for vehicular pollution prediction near roadways and model evaluation through statistical analysis.* Environmental Pollution Vol.104, pp.389-395

Spanton, A.M., McInnes, G. (1993) *Monitoring network assessment for the Dublin area.* Report Non. LR-555(AP)M, Warren Spring Laboratory, Stevenage, Hertfordshire, UK.

Spicer, C.W., Buxton, B.E., Holdren, M.W., Smith, D.L., Kelly, T.J., Rust, S.W., Pate, A.D., Sverdrup, G.M., Chuang, J.C. (1996*) Variability of hazardous air pollutants in an urban area* Atmospheric Environment Vol.30, No. 20, pp. 3343 – 3456

Stapleton, L. (1996) *State of the environment in Ireland.* Environmental Protection Agency, Wexford

Stein, A.F., Toselli, B.M. (1996) *Street level air pollution in Córdoba city, Argentina* Atmospheric Environment Vol.30, No. 20, pp. 3491-3495

Steiner, D., Burtscher, H., Gross, H., (1992) *Structure and disposition of particles from a spark-ignition engine* Atmospheric Environment Vol.26a, No. 6, pp. 997-1003

Stern, A.C. (Ed.) (1976) *Air pollution 3rd Ed.*, Academic Press, New York – London

Straub, C.P. (1989) *Practical handbook of environmental control,* C.R.C. Press, Boca Raton (Fla.) U.S.

Strauss, W., Mainwaring, S.J. (1984) *Air pollution.* Edward Arnold, London

Stump, F., Tejada, S., Ray, W., Dropkin, D., Black, F., Crews, W., Snow, R., Siudak, P., Davis, C.O., Baker, L., Perry, N. (1989) *The influence of ambient temperature on tailpipe emissions from 1984-1987 model year light-duty gasoline motor vehicles* Atmospheric Environment Vol.23, No. 2, pp. 307-320

Sweeney, J.C. (1991) *Modelling Dublin smoke pollution – An epilogue?* Proceedings of Environment and Development Seminar, The Environmental Institute, University College, Dublin, pp.232-239.

Tarrant, N. (1999) *Mean annual NO2 in Dublin.* Electricity Supply Board, Fitzwilliam Street, Dublin.

Theurer, W. (1999) *Typical building arrangements for urban air pollution modelling.* Atmospheric Environment, Vol.33, pp.4057-4066

Tombach, I. (1985) *Ambient air pollution measurements: from black smoke to photochemistry,* Pollution in the Environment – POLMET '85, Ed. Chan, M.W.H., Hoare, R.W.M., Holmes, P.R., Law, R.J.S., Reed, S.B., Elsevier Applied Science, London

Torvela, H. (1994) *Measurement of Atmospheric Emissions*, Springer-Verlag, London

Tran, K. (1981) *TRACE user's guide*, Applied Modelling Inc., Report 81/003, California.

UK-DETR (1998) *Selection and use of dispersion models.* Report No.LAQM.TG3(98), Department of the Environment, Transport and the Regions, London, UK.

Uno, I., Ohara, T., Wakamatsu, S. (1996) *Analysis of wintertime NO2 pollution in the Tokyo metropolitan area* Atmospheric Environment Vol.30, No. 5, pp. 703-713

US-EPA (1992) *Screening procedures for estimating the air quality impact of stationary sources.* Report no. EPA-454/R-92-005. US Environmental Protection Agency, Research Triangle Park, North Carolina, USA

VanCuren, T. (1999) *Spatial factors influencing winter primary particle sampling and interpretation* Journal of the Air and Waste Management Association Vol. 49 pp. PM3 – PM15

Viles, H.A. (1997)*Urban air pollution and the deterioration of buildings and monuments,* Chap.34 The Global Environment, Science, Technology and Management, Volume 1. Ed. Brune, D., Chapman, D.V., Gwynne, M.D., Pacyna, J.N. VCH, A Wiley Company, New York

Walsh, J. (1976) *Air pollution monitoring in Ireland.* Proceedings of 2nd Pollution Conference on Monitoring Industrial Pollution, Dublin pp.133-145

Walsh, J. (1988) *The nature of air pollution.* In: Proceedings of Seminar: Air Pollution – Impacts and Controls, Galway, pp.9-13

Wanta, R.C., Lowry, W.P. (1976) *The meteorological setting for dispersal of air pollutants.* In Air Pollution, Stern, A.C.

Ward, J.B., Keeley, C., Dean, G. (1978) *Urban/rural mortality in the Republic of Ireland.* Journal of the Irish Medical Association Vol.71 (3) pp.73-80

Watkins, L.H. (1981) *Environmental impact of roads and traffic* Applied Science Publishers, London

Weingartner, E., Keller, C., Stahel, W.A., Burtscher, H., Baltansperger, U. (1997) *Aerosol emission in a road tunnel* Atmospheric Environment Vol.31, No. 3, pp. 451 – 462

Williams, M.L., Maughan, R.A. Roberts, G.H. (1983) *The impact on air quality of power station development in Dublin.* Report No. LR-440(AP), Warren Spring Laboratory, Stevenage, Hertfordshire, UK.

WHO (2000) Guidelines for Air Quality, Geneva

Wilson, W.E., Suh, H.H., (1997) *Fine particles and coarse particles: concentration relationships relevant to epidemiologic studies* Journal of the Air and Waste Management Association Vol. 47 pp. 1238-1249

Wolff, G.T., Korsog, P.E. (1985) *Estimates of the contributions of sources to inhalable particulate concentarions in Detroit* Atmospheric Environment Vol.19, No. 9, pp. 1399-1409

Würtz, J., Haastrup, P. (1996) *The use of dispersion modeling for urban air pollution management,* Presented to TIEME96 Conference, the International Emergency Management and Engineering Society, May 1996

Zannetti, P. (1990) *Air pollution modeling, theories, computational methods and available software,* Van Nostrand Reinhold, New York

Zannetti, P. (1998) *Air Pollution Modelling Lecture Notes,* Wessex Institute of Technology, Southampton